This is to certify that the

dissertation entitled

Development and Mechanical Characterization of Carbon Fiber Reinfoced Cement Composites & Mechanical Properties and Structural Applications of Steel Fiber Reinforced Concrete

presented by

Mohamad Ziad Bayasi

has been accepted towards fulfillment
of the requirements for

Doctor of ~~Philosophy~~ degree in ~~Civil Engineering~~

Dr. Parviz Soroushian

Major professor

Date 5/15/89

DEVELOPMENT AND MECHANICAL CHARACTERIZATION OF CARBON FIBER REINFORCED CEMENT COMPOSITES

&

MECHANICAL PROPERTIES AND STRUCTURAL APPLICATIONS OF STEEL FIBER REINFORCED CONCRETE

by

Mohamad Ziad Bayasi

A DISSERTATION

Submitted to
Michigan State University
in partial fulfillment of the requirements
for the degree of

DOCTOR OF PHILOSOPHY

Department of Civil and Environmental Engineering

1989

DEVELOPMENT AND MECHANICAL CHARACTERIZATION OF CARBON FIBER REINFORCED CEMENT COMPOSITES

by

Mohamad Ziad Bayasi

Volume I of

A DISSERTATION

Submitted to

Michigan State University

in partial fulfillment of the requirements

for the degree of

DOCTOR OF PHILOSOPHY

Department of Civil and Environmental Engineering

ABSTRACT

DEVELOPMENT AND MECHANICAL CHARACTERIZATION OF CARBON FIBER REINFORCED CEMENT COMPOSITES

By

Mohamad Ziad Bayasi

Based on a comprehensive experimental study on carbon fiber reinforced cement composites incorporating the Ashland's industrial grade carbon fibers (Carboflex), the optimum mix variables and processing techniques were decided. The types and proportions of different mix constituents, the fiber lengths and volume fractions, and the mixing and curing procedures which produce desirable fresh mix properties and superior hardened material performance were decided. A comprehensive experimental data set on the performance characteristics of carbon fiber reinforced cement was also generated. The research was performed in three phases:

(1) Establishment of the mixing procedure and mix proportions for achieving desirable fresh mix characteristics;

(2) Assessment of the trends in the effects of different mix variables on the strength of air cured specimens and further optimization of the mix proportions for achieving superior strength characteristics in addition to the desirable fresh mix workability; and

(3) Optimization of the curing condition and full mechanical characterization for carbon fiber reinforced cement composites with some optimum values of fiber length and volume fraction.

The fresh mix in this investigation was characterized by flow, and also subjective measures of workability and fiber dispersability. The hardened material was characterized by tensile, flexural and compressive strength, energy obsorption and toughness and initial stiffness; and also by impact resistance. The rate of strength development with time was another criterion for the evaluation of carbon fiber reinforced cement composites.

To my ever loving and caring mother and father

Ghada Bazarbashi and Fayez Bayasi

ACKNOWLEDGMENTS

The work presented here was conducted under the guidance of Dr. Parviz Soroushian. The author deeply appreciates the contributions of Dr. Soroushian to this work. His great effort and very helpful supervision and advise will never be forgotten, and the author wishes to hope that Dr. Soroushian will continue to be his mentor.

The author also would like to thank Dr. William C. Taylor, Dr. Lawrence T. Drzal and Dr. George Mase for their help during his doctoral program.

Table of Contents

List of Figures

Figure Page

Figure Page

Figure Page

Figure

Page

Figure

Page

Figure Page

List of Tables

CHAPTER 1

INTRODUCTION

1.1. General

World use of hydraulic cement is close to 1 billion tons per year, and this figure is proposed to double by the end of this century.[1,2] The low cost and low production energy demand of portland cement (see Table 1.1), and the ready availability of its raw materials (limestone, clay, etc.) provide the incentives for optimizing the strength, toughness and durability of hydraulic cement for its conventional use and new applications as replacements for plastics and metals.

Table 1.1: Cost and production energy demand of portland cement vs. other materials.

Material	Specific Gravity (lbs/ft^3)	Approximate Price ($/Kips)	Energy of Production (GJ/Kips)
Portland Cement	154	34	3.7
Polyester	80	688	45.9 - 68.8
Polyethylene	62	459	45.9 - 68.8
Glass	154	972	9.2 - 11.5
Steel	488	211	23.6
Aluminum	167	734	91.8

1 in. = 25.4 mm, 1 lb = 458.7 g

In order to optimize cement-based materials, measures should be taken to overcome their brittle manner of failure under tensile and impact loads. Fiber reinforcement is an effective method for improving the toughness and ductility of portland cement products.[3] Broadly, the reason why brittle cementitious matrices are strengthened by uniformly dispersed short fibers is that cracks are stopped or deflected by the presence of fibers.

Failure in fiber reinforced cementitious composites emanates from defects (e.g. microcracks, matrix flaws, etc.) in the material. Figure 1.1 shows the mechanisms of crack arrest by short fibers.

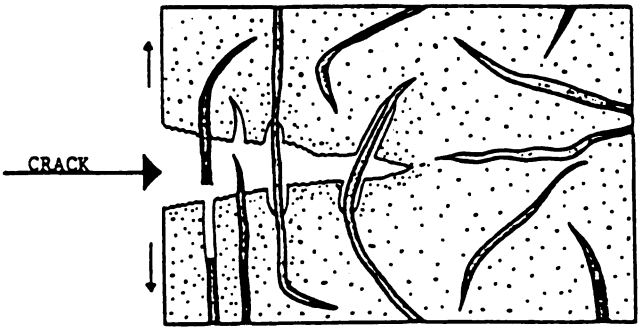

Figure 1.1: Schematic representation of a crack traveling through a composite material.

In 1970, 4 million tons of asbestos fibers were used worldwide to reinforce cement in the production of corrugated roofing panels, side panels and pipes.[4] The health hazards associated with the use of asbestos fibers, however, has led to sudden drop in the application of this enormously successful cement reinforcement. Various types of fibers are now under serious consideration to substitute asbestos. Low-modulus carbon, glass, and Kevlar[5-8] are the fibers that, from the points of view of price and effectiveness in brittle cement matrices, are now considered as prime candidates to substitute asbestos in cement. Among these, low-modulus carbon fiber is the only one which provides sufficiently durable cementitious composites at a reasonable cost, while glass fibers and also Kevlar are prone to deterioration in the alkaline environment of cement. The relative cost-effectiveness low-modulus carbon fibers, together with their superior durability, show the important potentials of carbon fibers for substituting

asbestos in cement products. Carbon fiber reinforced cement, due to the desirable durability characteristics of carbon fibers, may also find applications in repair and rehabilitation projects. This could provide this material with a vast market that is growing rapidly (more than 40% of the construction spendings in developed countries is on repair and rehabilitation rather than new construction projects).[1,9]

1.2. Background

The use of continuous high modulus carbon fibers for reinforcing cement was considered during the 1960's and early 1970's for the production of structural elements, such as floor planks and corrugated panels.[10,11] The development of low-cost, low-modulus carbon fibers in the recent years provided the incentives for commercializing cement products reinforced with short uniformly dispersed carbon fibers in Japan.[12-17] Current applications of carbon fiber reinforced cement in Japan include cladding panels free access floor panels, repair and protective coating of structural elements in aggressive environments, and light-weight decorative frames (see Figure 1.2 for some of these applications).[5] These applications have been encouraged by the cost effectiveness of low-modulus carbon fibers, and also by their durability and high efficiency as reinforcement for cement.

The key reasons for efficiency of carbon fibers in cement, noting that hey are inert in the alkaline environment of cementitious matrices, are the relatively close spacing of fibers (small fiber dimensions lead to high fiber counts at a specific volume fraction of fibers) and also their strong and durable bonding to cementitious matrices. When cracks start to propagate in between internal flaws of

a. Cladding panels of a high-rise office building

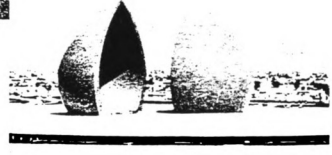

b. Tile panels for Al-Shaheed Monument.

Figure 1.2: Some applications of carbon fiber reinforced cement in Japan.[5]

matrix and the microcracks of aggregate-matrix interface, it is important to have fibers located in between the flaws and microcracks in order to stop or deflect the propagating cracks. Steel fibers, at typical spacings of about 0.2 in. (5 mm), are too far apart to effectively interact with microcracks (Figure 1.3.a), and thus are only moderately effective in increasing the tensile strength of cement-based materials. Carbon fibers with typical spacings of about 0.004 in. (0.1 mm), encounter the propagating microcracks more frequently and thus efficiently stop or deflect the microcracks (Figure 1.3.b). This is the main reason for the efficiency of carbon fibers in increasing the tensile strength of cement-based materials. Desirable bonding of carbon fibers to cementitious matrices also contributes to the tensile strength and post-peak ductility of carbon fiber reinforced cement composites (due to the energy absorbed during pull-out of the well-bonded fibers from the matrix, as shown in Figure 1.3). The effective microcrack arrest action of carbon fibers not only increases the ductility and strength of cement-based materials under direct tension, but also improves the general performance of the material under external load and environmental effects, noting that most external effects damage cement-based materials is the appearance and growth of microcracks.[1]

An important factor to be considered in the comparison of steel and carbon fibers is the difference in the type of cementitious matrices which generally incorporate them. Carbon fibers, with their relatively small dimensions, can be conveniently dispersed in matrices incorporating relatively small volume fractions of fine aggregates with maximum particle sizes of about 0.04 in. (1 mm). Steel fibers, however, are generally dispersed in concretes incorporating relatively high volume fractions of coarse aggregates with maximum sizes of the

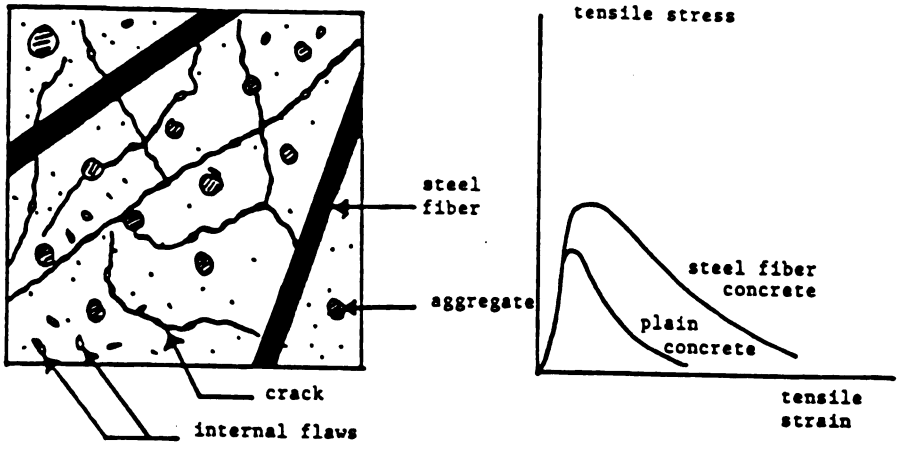

a. Steel fiber reinforced concrete

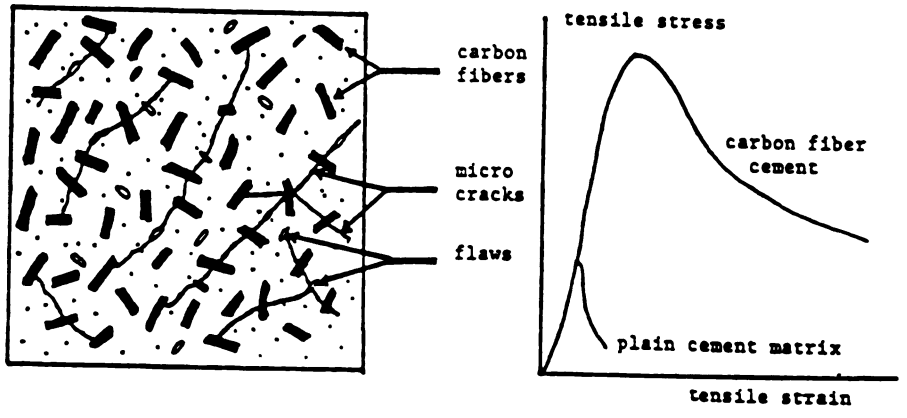

b. Carbon fiber reinforced cement

Figure 1.3: Carbon fiber vs. steel fiber spacing in cement matrices and it's effect on tensile behavior of cement-based materials.

order of 0.8 in. (20 mm). The differences in matrix type also lead to differences in application fields. While carbon fiber reinforced cement composites find applications in products consisting of relatively thin sheets (wall panels, floor and roof corrugated sheets, pipes, etc.) or in repair applications at small thicknesses, steel fibers are generally used in relatively thick overlays and pavements.

Research at Michigan State University on carbon fiber reinforced cement composites was initiated in 1986 with the support of the Ashland Carbon Fiber Division. This activity later received major supports from the U.S. Department of Housing and Urban Development, and the Research Excellence and Economic Development Fund of the State of Michigan to establish itself as a major research program in the area of fiber reinforced cement composites. The accomplishments of the carbon fiber reinforced cement research team at Michigan State University during the past few years include: (a) Optimization of the cementitious matrix, fiber reinforcement properties and processing techniques for achieving desirable fresh and hardened material properties at low cost; (b) Characterization of the mechanical, shrinkage and durability properties of carbon fiber reinforced cement; (c) Development of light-weight carbon fiber reinforced cement materials; (d) Resolving the practical and theoretical problems related to the application of carbon fiber reinforced cement to thin panels; and (e) Introduction of latex to carbon fiber reinforced cement for the development of a high-performance repair material. The fundamental approach taken at Michigan State University to the refinement of carbon fiber reinforced cement as and development of methodologies for its application in different fields has led to a situation where the cement products and repair industries can efficiently benefit from the new material. The sound basis developed

at Michigan State University for carbon fiber reinforced cement will also facilitate future investigations for further refining the material and introducing it to new application fields.

This dissertation summarizes a fraction of the research performed in Michigan State University on carbon fiber reinforced cement. It deals with the more basic aspects of the research program on material developments, but leaves out the work on light-weight carbon fiber cement, introduction of latex, application to cladding panels, and the use of carbon fiber reinforced cement as a repair material. These aspects of research will be covered in other reports and publications.

The first part of Chapter 2 in this report summarizes the work on fresh mix properties, which led to the development of a cementitious matrix and a corresponding processing methodology for uniform dispersion of carbon fibers and achievement of a workable mix. The second and last part of Chapter 2 investigates the effects of matrix mix proportions and fiber reinforcement properties on the strength of carbon fiber reinforced cement under different loading conditions. The test data generated in Chapter 2 provided the basis for optimizing the fiber reinforcement and matrix properties of the composite. The work summarized in the remaining chapters of this report was performed on the optimum matrix incorporating different fiber lengths and volume fractions, cured in different conditions. The experimental program for the remainder of this research is sumarized in Chapter 3. Chapters 4,5,6 and 7 deal with the flexural, tensile, compressive, and impact properties of carbon fiber reinforced cement, respectively. The effects of fiber reinforcement properties and curing methodologies on strength, stiffness and energy absorption properties of the composite materials under these loading conditions

are discussed. Chapter 8 summarizes the findings of this research program on carbon fiber reinforced cement.

CHAPTER 2

OPTIMIZATION OF MIX PROPORTIONS FOR FRESH MIX WORKABILITY AND HARDENED MATERIAL STRENGTH

2.1. Introduction

Carbon fiber reinforced cement composites which are suitable for manufacturing by conventional mortar mixer should be proportioned carefully. Some necessary constituents of the mix include: dispersant, superplasticizer, cementitious materials, water and, of course, carbon fibers. The optimization of mix proportions involves selecting the specific proportions of each of these components which, in the presence of a certain volume fraction of fibers a certain length, provide a fresh mix with acceptable workability and fiber dispersability which hardened to a cementitious composite with desirable performance characteristics.

In order to facilitate the process of mix optimization in this investigation, the trends in the effects of different mix variables on the fresh mix workability and fiber dispersability, and the hardened material flexural, tensile and compressive strength have been established. These trends are presented in this chapter following a review of the related literature.

2.2. Review of the Literature

A variety of mix proportions have been used in the construction of carbon fiber reinforced cement composites. A key consideration in the manufacture of carbon fiber reinforced cement

composites is the achievement of a workable fresh mix with uniformly dispersed fibers.

A uniform dispersion of carbon fibers is generally achieved by using special dispersing additives and/or special manufacturing techniques. Different dispersants (e.g., methyl cellulose, silica fume and fly ash) have been used in carbon fiber reinforced cement,[12-17] some of which may have adverse effects on the air content and workability of the material. These problems caused by dispersants have been overcome by the use of other admixtures such as defoaming agents and superplasticizers.

While conventional mixing techniques (using mortar mixers) have been successfully applied to properly proportioned carbon fiber reinforced cement composites,[6,12,13] many investigators have used Omni mixers for the construction of the material (see Figure 2.1).[5,14-18] Omni mixer is capable of applying greatly varying accelerations to the mix particles and fibers in many different directions, forcing all materials to come into intimate contact with the cement-water mixture in a very short time; hence, eliminating the possibility of dry fiber balls forming in the mixture. The use of an Omni mixer results in more flexibility in the selection of the mix proportions.

Table 2.1 presents typical ranges of mix proportions used by different investigators for carbon fiber reinforced cement composites. Fine aggregates may also be incorporated in the mix. These aggregates may be normal-or light weight (e.g. microballoon), with maximum particle size of about 0.2 in (5 mm), and up to 50% of the total volume of the composite material may be occupied by the aggregates. Some detailed information about the dispersants and aggregates used in the mixtures of Table 2.1 are presented in Table 2.2. The previous

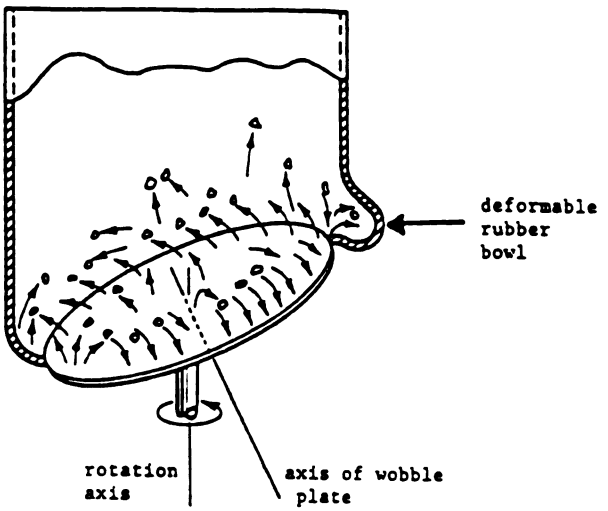

Figure 2.1: Schematic drawing of Omni mixer.[18]

Table 2.1: Typical mix proportions used for carbon fiber reinforced cement composites (Note: Ratios are by weight).[5,6,12-17]

water cement	dispersant type	dispersant cement	water reducer cement	fiber length (mm)	maximum fiber volume fraction (%)	other ingredients (%of cement)	mixer type
0.3	silica fume	0.2-0.5	0.02-0.10	3-10	5	--	mortar mixer
0.3-0.6	fly ash	0.5	--	3	2	foaming agent(0-0.3),latex (0-5)	mortar mixer
0.3-0.5	methyl cellulose	0.00-0.01	0.005	10	3	defoaming agent (0-0.5)	Omni mixer
0.6-1.15	methyl cellulose	0.01-0.015	0.01	10	4	micro-balloon (20-70)	Omni mixer
0.45-0.7	methyl cellulose	0.00-0.0	0.01-0.02	3-10	5	silica powder (20-50)	Omni mixer
0.5	methyl cellulose	0.005	--	10	3	defoaming agent(0.05) silica sand of size 0.0018-2.5 mm(10-80)	Omni mixer

1in = 25.4 mm

Table 2.2: Chemical and physical properties of carbon fiber dispersants or aggregates in cementitious matrices.[5,6,12-17]

dispersant or aggregate	chemical composition	physical properties
silica fume	90-95% $SiO2$; 1% Al_2O_3; others	specific gravity = 2.26; particle size = 0-8 microns specific surface = 200,000 cm^2/g
fly ash	60% $SiO2$; 24% Al_2O_3; 4% Fe_2O_3; 3% CaO; others	specific gravity - 2.10; particle size = 0-40 microns
silica powder	95% $SiOz$; 2% Al_2O_3; 1% Fe_2O_3; others	specific gravity = 2.70, particle size = 0-18 microns; specific surface = 3500 cm^2/g
microballoon	67% SiO_2; 14% Al_2O_3; others	specific gravity = 2.10, particle size = 0-150 microns
Silica sand	Mainly SiO_2 crystals	specific gravity = 2.65 size = 0.0018 - 2.5 mm
methyl cellulose	Cellulose ether-based polymer	White powder specific gravity = 0.4-0.5

1 in. = 25.4 mm, 1 lb = 0.46 Kg

investigations in this area had been conducted using the Kureha (Japanese) carbon fibers.[19] Table 2.3 presents some physical and mechanical properties of the Kureha pitch-based carbon fibers used in past investigations.

Table 2.3: Physical and mechanical properties of the Kureha pitch-based carbon fiber.[19]

Diameter	Specific Gravity	Tensile Strength	Modulus of Elasticity	Elongation
4-7 x 10^{-4} in. (10-18 microns)	1.6-1.63	60-110 Ksi (400-750 MPa)	4,000-8,000 Ksi (27,000-55,000 MPa)	1.4-2.4%

a. Fresh Mix Properties

Workability is a comprehensive measure representing the ease of handling, placing, compacting and finishing of the material. A single test can hardly give a reliable measure of all these aspects of workability. A flow table test is usually used to assess the mobility (under repeated blows) of fresh carbon fiber reinforced cement composites. The flow table test results provide information on the mechanical effort required for the compaction of the material.

Figure 2.2 presents a comprehensive set of the flow table test data, performed in accordance to the Japanese standard JIS R 5201, [5,6,12-17] produced for different carbon fiber volume fractions in a variety of matrices. From this figure it may be concluded that the flow, as a representative of workability, decreases almost linearly as the fiber volume fraction increases. Another important factor influencing the workability of fresh carbon fiber reinforced cement mixes in the presence of water reduces (superplasticizers). The effect of dispersants on fresh mix flowability seems to depend on the type of dispersant. Silica fume damages workability, while silica powder and microballoons have no significant effects on the measured flow of fresh mix.[5,6,12-17]

A more clear indication of the effects of water reducing agents and silica fume on the flow of fresh mix is given in Figure 2.3.[13] Figure 2.3.a shows that at zero fiber volume fraction, the water reducing agent content has a major effect on flow, but this effect tends to be much smaller at 5% carbon fiber volume fraction. The effect of silica fume content on flow, shown in Figure 2.3.b, also seems to be more important in plain matrices than in fibrous composites with 5% carbon fiber volume content. It is also worth mentioning that the increase in fiber length is expected to damage the

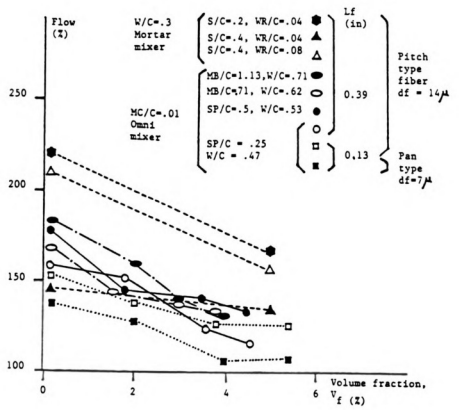

Figure 2.2: Effects of carbon fiber volume fraction on the flow of carbon fiber reinforced cement.[5,12-17] (1 in = 25.4 mm) W = water, C = cement, S = silica fume, SP = silica powder, MB = microballoon, MC = methyl cellulose, WR = water reducer, L_f = fiber length, V_f = fiber volume fraction.

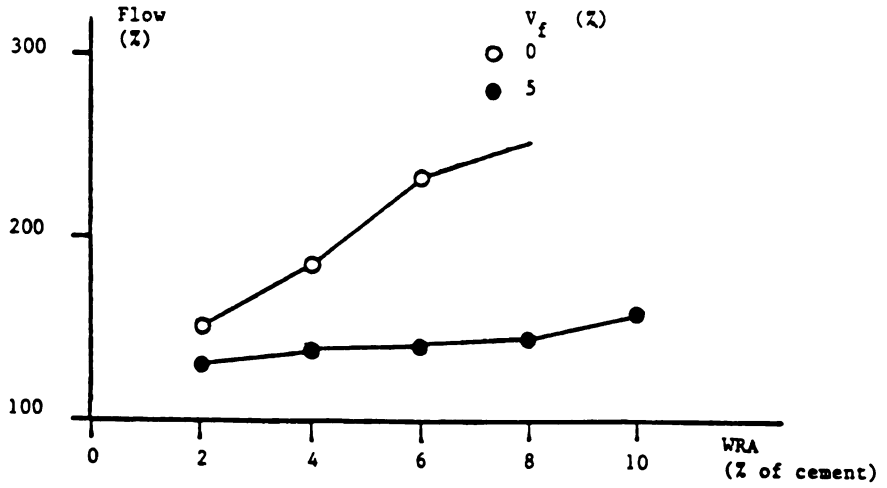

a. Water reducing agent (WRA) (silica fume/cement = 0.3)

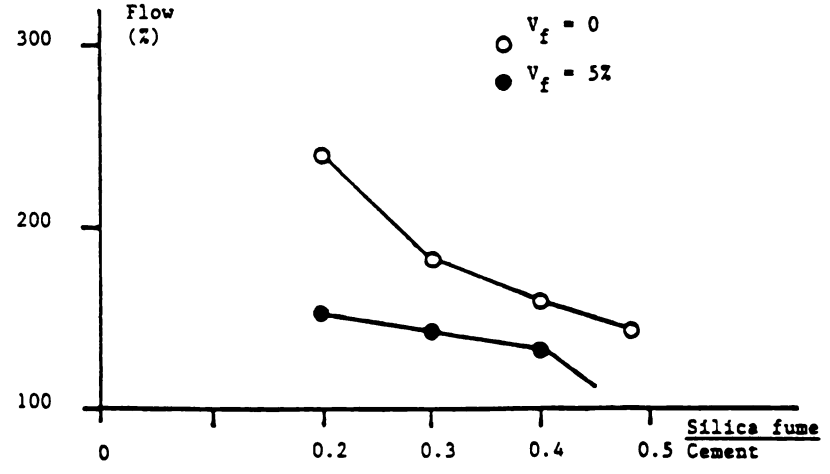

b. Silica fume (water reducing agent/cement = 0.04)

Figure 2.3: Effects of water reducing agent (WRA) and silica fume on the flow of carbon fiber reinforced cement.[13] (water/cement = 0.3, fiber length (L_f) = 10 mm = 0.4 in, fiber volume fraction (V_f) = 0 and 5%, and mixing in mortar mixer)

workability of fresh fibrous mixes. There is, however, insufficient test data reported in the literature for quantifying this effect.

b. Hardened Material Strength

A major contribution of carbon fibers to the behavior of cementitious materials is the increase in flexural strength. The relationships between fiber volume fraction and flexural strength in different cementitious matrices are shown in Figure 2.4.a.[4,5,12-17] The tensile strength of cement-based materials also increases significantly in the presence of carbon fibers (Figure 2.4.b). Carbon fiber reinforcement, however, does not have a significant effect on the compressive strength of cementitious materials. There may actually be a slight drop in compressive strength in the presence of carbon fibers (see Figure 2.4.c). A comprehensive review of the literature on the load-deformation behavior and strength of carbon fiber reinforced cement composites will be presented in later chapters devoted specifically to those topics.

It should be noted that the curing condition is also an important factor influencing the strength of carbon fiber reinforced cement. The preliminary phase of this research was concerned with establishing the trends in the effects of different mix variables on fresh mix workability and hardened material strength. In the preliminary phase summarized in this chapter, curing was performed solely in air at the ambient temperature. Optimization of the curing conditions was the subject matter of investigations in the later phases of this project, as described in the following chapters.

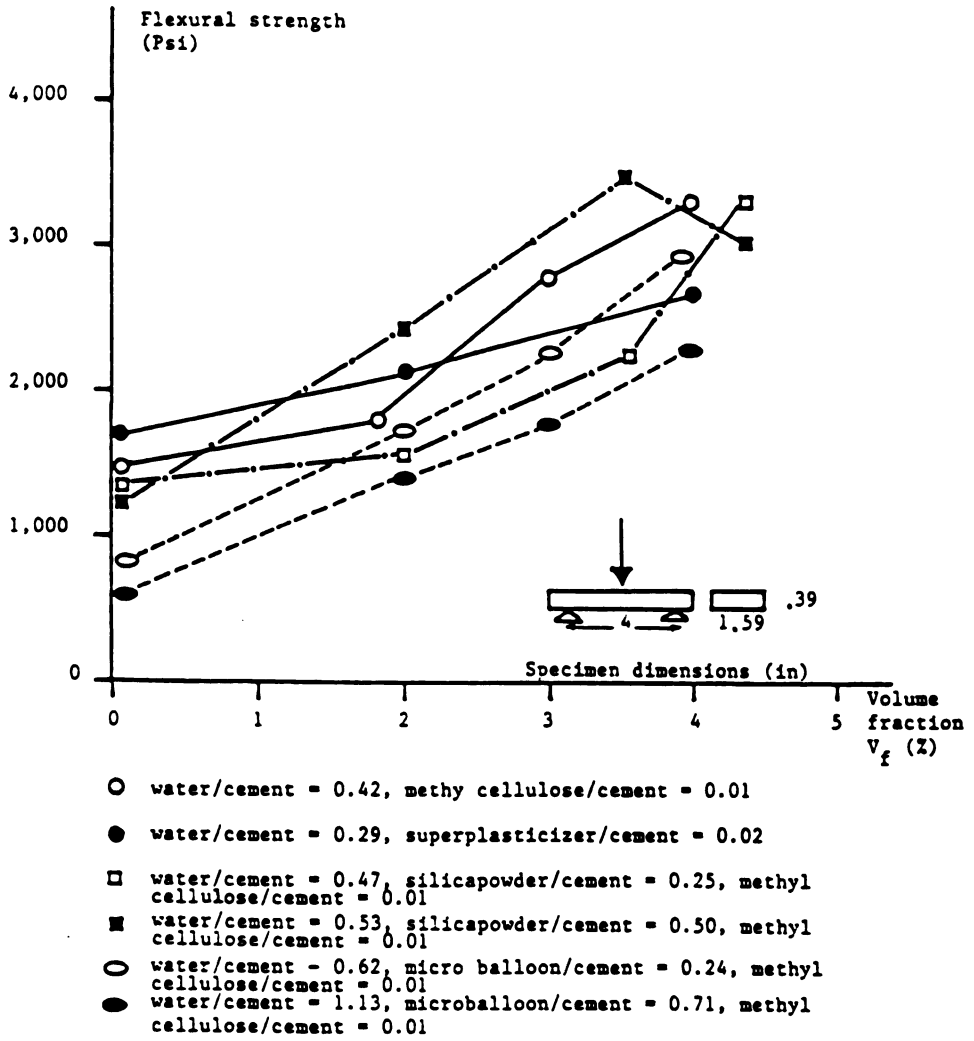

a. Flexural strength

Figure 2.4: Effects of carbon fiber volume fraction on the flexural, tensile and compressive strength of cementitious materials with different matrix mix proportions[5,6,12-17] (Fiber length (L_f) = 10 mm = 0.4 in, mixing by Omni mixer and 7 days curing in air) (Ksi = 6.9 MPa, 1 in = 25.4 mm

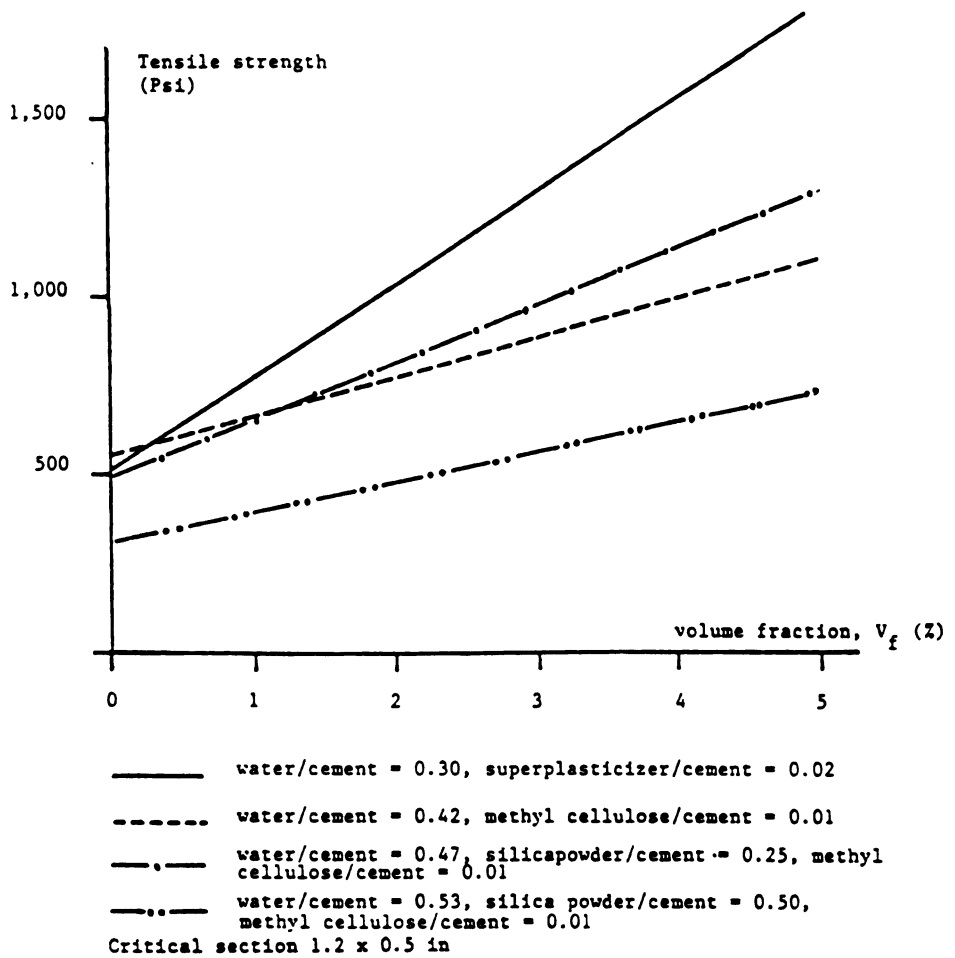

b. Tensile strength

Figure 2.4 (continued)

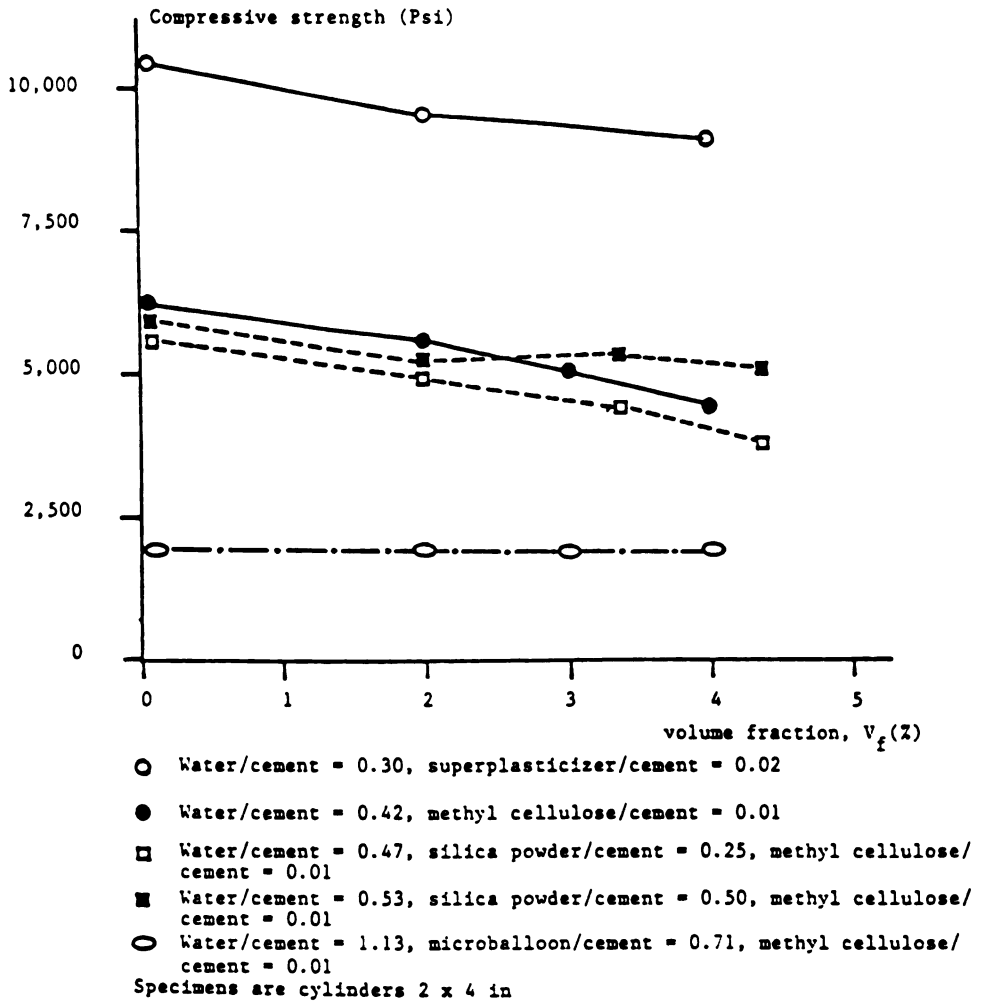

c. Compressive strength

Figure 2.4 (continued)

2.3 Experimental Program on Fresh Mix Properties

This section introduces the mix ingredients, mix proportions, manufacturing techniques and material test procedures used in studies on the effects of different factors on carbon fiber reinforced cement properties in the fresh state.

a. Mix Ingredients

The carbon fiber reinforced cement composites constained carbon fibers and a cementitious matrix incorporating portland cement, silica fume, superplasticizer and water.

The carbon fiber used in this study was Ashland's industrial grade type called "Carboflex."[11,20] Carboflex is made from a pitch produced from a residue of an oil refining process. The heavy, viscous pitch is transformed into a fiber product through a specially developed spinning process followed by application of high tempratures. The finished product is a non-woven mat which can be chopped into fibers varying in length from .004 in. (100 microns) to 2 in. (51 mm) or more.[20] This investigation is concerned with the use of chopped fibers as randomly distributed reinforcement for cementitious matrices. Some physical and mechanical properties of the Ashland's pitch-based carbon fibers are presented in Table 2.4. From a comparison between Tables 2.3 and 2.4 it may be concluded that the Ashland's fibers are smaller in diameter and specific gravity, and have a lower elongation but higher tensile strength and modulus of elasticity when compared with Kureha fibers. Carbon fibers incorporated in cementitious matrices typically range in length from 1/16 to 7/16 in. (1.5 to 10 mm).

The cementitious matrices incorporating carbon fibers should be capable of uniformly dispersing the fibers using the specified

Table 2.4: Ashland's pitch-based carbon fiber.[26]

Diameter	Specific Gravity	Tensile Strength	Modulus of elasticity	Elongation
4×10^{-4} in. (10 microns)	1.6	100 Ksi (690 MPa)	8,000 Ksi (55,000 MPa)	1.4%

manufacturing technique, but should also maintain a reasonable degree of workability in the presence of fibers. In order to achieve a cementitious matrix capable of uniformly dispersing fibers, it is important to increase the fineness of the particles inside the matrix and to increase the cohesiveness of the matrix such that the fibers can be sufficiently coated with the paste and the fiber balls can be broken during the mixing process.

Table 2.5 presents the typical properties of the type I regular portland cement used in the matrix.[21] It is important to note that the particle size in portland cement is of the order of the carbon fiber diameter and therefore typical cement particles cannot effectively coat the low-diameter carbon fibers. It was thus decided to substitute a fraction of type I portland cement with silica fume. The physical and chemical properties of silica fume used in this study (a product of Elkem Chemicals)[22], are presented in Table 2.6, indicate that the spherical particles of this highly reactive pozzolan are small enough to produce a paste that can effectively coat carbon fibers. With their high pozzalanic reactivity, the fine silica fume particles convert the less useful calcium hydroxile crystals into the useful CSH-jel binder,[23] and results in an abundance of ultra fine particles that are dispersed in spaces around and between the cement grains, leading to a uniform distribution of the hydration products

Table 2.5: Typical properties of type I regular portland cement.[21]

Chemical composition

Chemical Compound	CaO	SiO_2	Al_2O_3	Fe_2O_3	MgO	SO_3	K_2O
%	63	21	6	3	2	2.5	1

Physical properties

Specific Gravity	Specific Surface
3.15	16,00 cm^2/g

1 in. = 25.4 mm, 1 lb = 0.45 Kg

Table 2.6: Chemical and physical properties of grade EMS 960 silica fume.[22]

Physical properties

Specific Gravity	Bulk Density	Specific Surface	Average Particle Size	Particles smaller than 45 microns (0.018 in.)
2.3	14 lb/ft^3 (225 Kg/m^3)	200,000 cm^2/g (14 x 106 in. /lb)	0.14 microns (6×10^{-3} in.)	99.5%

Chemical composition

Chemical Compound	SiO_2	C	Fe_2O_3	M_gO	Al_2O_3	K_2O	$N_{a2}O$
%	96.5	1.4	0.15	0.20	0.15	0.04	0.20

and a dense micro structure inside the paste and especially in the vicinity of fibers. Silica fume also increases the cohesiveness of the cementitious matrix which is another factor contributing to the dispersability of fibers in the composite. Besides being a fiber dispersant, silica fume also enhances many properties of the hardened material.[23]

Application of silica fume improves the fiber dispersability properties of the matrix but adversely influences the workability of

the fresh mix. The increase in water content of the matrix is not a desirable approach to improve the workability of carbon fiber reinforced cement composites due to its detrimental effects on the hardened matrix and the nature of interaction between the cementitious paste and carbon fibers. The approach taken in this study to improve the workability of fresh carbon fiber cement mixes involved the use of superplasticizers (high rangewater reducers).[24] The superplasticizer used in this study was Daracam 100, a Naphthalene-Formaldahyde-Sulfonate based compound produced by of W.R. Grace and Company.[25] This superplasticizer improves the mix fluidity and maintains this fluidity over time for successful placing. The water used in this study was the regular water used in concrete production.

b. Mix Proportions

The main objective of the fresh mix experimental program was to assess the effects of all the mix variables on the workability and fiber dispersability of the fresh carbon fiber reinforced cement composites. In order to reliably achieve this objective, about 150 fibrous and plain mixes with different proportions were manufactured and tested in fresh state. Table 2.7 presents the ranges of the fibrous mix variables used with each fiber length investigated in this study. It should be noted that the mix proportions in Table 2.7 are used to determine the trends in the effects of different variables on fresh mix properties, and are not necessarily the optimum carbon fiber reinforced cement mix proportions.

c. Manufacturing Technique

A major objective in this phase of the research was to develop carbon fiber reinforced cement mixes which could be manufactured by

Table 2.7: Ranges of mix proportions in the fresh mix experimenal program

Fiber Length in (mm)	V_f (%)	w/(c+s)	s/(c+s)	sp/(c+s)
1/16 (1.5)	2-17.5	0.34-0.45	0.17-0.29	0.012-0.020
1/8 (3)	1-6	0.25-0.45	0.17-0.29	0.010-0.20
1/4 (6)	1-4	0.26-0.45	0.17-0.29	0.10 -0.20
1/2 (13)	1-3	0.41	0.23	0.018
Plain	0	0.24-0.54	0.0 -0.29	0.008-0.020

w = water
c = cement
s = silica fume
sp = superplasticizer (Note: mix design is based on the solid weight of superplasticizer; the water in superplasticizer is considered as part of the mixing water).

conventional mixing techniques. This is an important consideration facilitating the introduction of new materials for practical applications.

Carbon fiber reinforced cement was mixed in this study using a regular 12 liter three-phase mortar mixer, Hobart model A200 (Fig. 2.5),[26] following to ASTM C-305 procedures.[27]

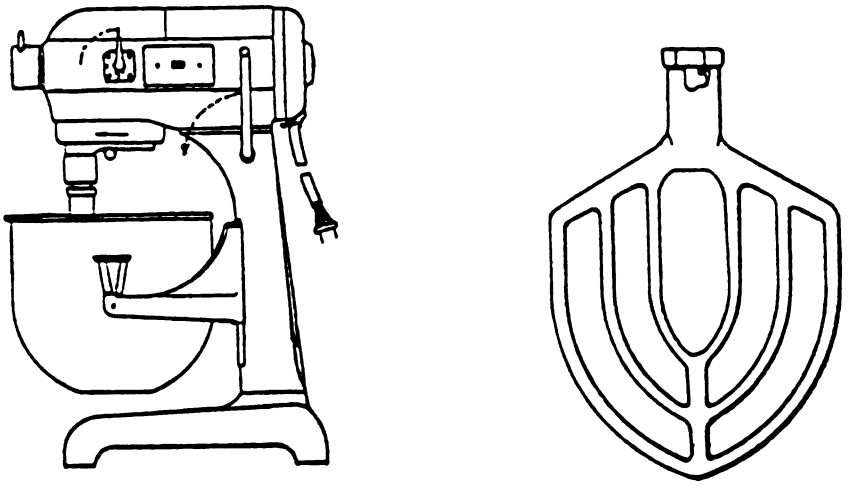

a. Overall view b. Mixing blade.

Figure 2.5: Mortar mixer.[26]

The following mix procedure was chosen, based on a number of trials, for application to carbon fiber reinforced cement:

1. Add all the silica fume and about 2/3 of the water-superplasticizer mixture;
2. Start mixing at low speed (53 RPM) and mix for about 30 seconds until a uniform mixture is achieved;
3. Gradually add fibers while the mixer is running, over a period of about 3 minutes;
4. Gradually add the remainder of water-superplasticizer mixture followed by the cement so that the flowability and uniformity of the mixture are maintained. This process takes approximately 3 minutes; and
5. Continue mixing for 1 minute at low speed. Turn to the medium speed (99 RPM) and mix for another one minute.

The above mixing procedure gives optimum results as far as the workability and fiber dispersability of the fresh mix are concerned. Desirable fresh mix properties will have positive effects on the hardened material performance.

Compaction of carbon fiber reinforced cement was achieved in this study by external vibration (using a vibration table).

d. Assessment of the Workability and Fiber Dispersability of Fresh Mixes

The two important aspects of the fresh fibrous mix characteristics are workability at different time periods after mixing, and fiber dispersability.

Workability is a representative of the plastic material flowability, placeability, compactibility and finishability. A single test result can hardly provide information on all these aspects of workability. Following some trial applications of different

workability test techniques, the flow table test (ASTM C-230)[27,28] together with a subjective measure were used to assess the workability of fresh carbon fiber reinforced cement mixtures. The flow table test measures the percentage increase in diameter of a specified volume of fresh material subjected to a specific number of drops under standard conditions. A 10 in. (254 mm) flow table (ASTM C109 and ASTM C230) was used in this investigation (Fig. 2.6)[27,28]. A flow of 50% was judged to be the minimum acceptable value, and flows above 70% were judged to represent desirable workability conditions in carbon fiber reinforced cement. The flow table tests were performed at 1, 4 and 10 min. after the completion of mixing, in order to assess the drop in workability with time.

The flow table test results are partial representatives of fresh mix flowability, but provide limited information on the placeability and finishability of carbon fiber reinforced cement mixtures. In order to make a more comprehensive assessment of the fresh mix workability, a subjective measure was used. In this approach, the flowability, placeability, compactibility and finishability of the fresh mix were each catagorized from 1 to 5, with 1 being the worst, 5 the best, and 2 the minimum acceptable value. The average of these subjective measures of different aspects of workability was used as a quantitative representative of the fresh mix workability.

The dispersability of carbon fibers in cement matrix was also assessed subjectively in this study. A ranking of 1 to 5 was used for fiber dispersability, with 1 referring to a poor fiber dispersion with balling, and 5 to an excellent dispersion of fibers. A subjective fiber dispersion measure of 3 was considered to be the minimum acceptable level for manufacturing carbon fiber reinforced cement.

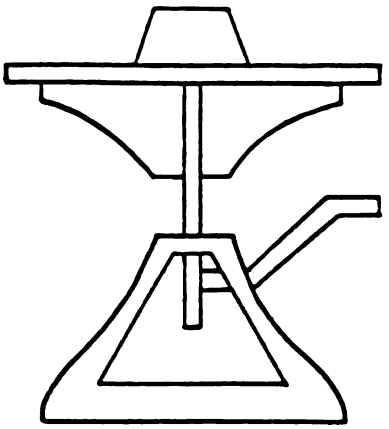

Figure 2.6: Schematic drawing of flow table.[27]

2.4. Fresh Mix Test Results

The results of flow table test and subjective assessments of workability and fiber dispersability are presented in Figures 2.7 through 2.13. In the evaluation of flow table test results it should be noted that the maximum measurable flow is 146%. This value represents a very fluid mix. The judgment criteria for categorizing the flow, workability and dispersability measures as poor, acceptable and desirable are given in Table 2.8.

Table 2.8: Criteria for qualitative expressions of fresh mix test results

Test	Poor range	Acceptable range	Desirable range
flow table	0-40%	40-70%	70-146%
workability	1-2	2-3	3-5
fiber dispersability	1-3	3-4	4-5

The conclusions which may be derived from the generated test results regarding the effects of different variables on the properties of fresh carbon fiber reinforced cement mixtures are described in the following sections. It can be noticed that in Figures 2.7 to 2.13, the matrix mix proportions are expressed in terms of the cementitious (binding) materials by weight. Where the binder in those figures is the weight of cement and silica fume.

a. Fiber Volume Fraction

Figure 2.7 indicates that the flow, workability and fiber dispersability of fresh fibrous mixes are all adversely influenced by the increase in fiber volume fraction. This adverse influence is more pronounced for longer fibers. Figure 2.7 also indicates that a reasonably workable mix does not necessarily give a desirable dispersion of fibers. It should be noted that carbon fiber reinforced cement is not as finishable as conventional mortar and care should be taken in finishing the material.

b. Fiber Length

The effects of fiber length on fresh mix properties are presented in Figure 2.8. At a constant fiber volume fraction, the increase in fiber length has adverse effects on the flow, workability and fiber dispersability of fresh fibrous mixes. For each fiber length, there is a maximum volume fraction beyond which problems in fresh mix start to appear. This maximum limit increases as fiber length decreases.

c. Silica Fume Content

Figure 2.9 presents test results related to the effects of

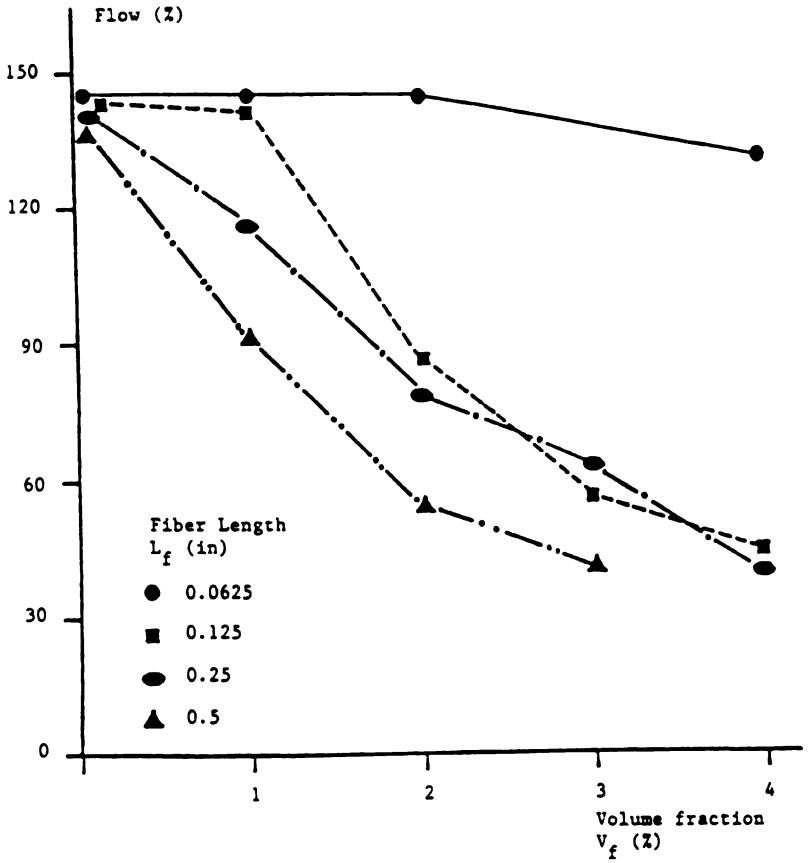

a. Flow

Figure 2.7: Effects of fiber volume fraction (V_f) on fresh mix characteristics (water/binder = 0.41, silica fume/binder = 0.23, and superplasticizer/binder = 0.018)1in = 25.4 mm

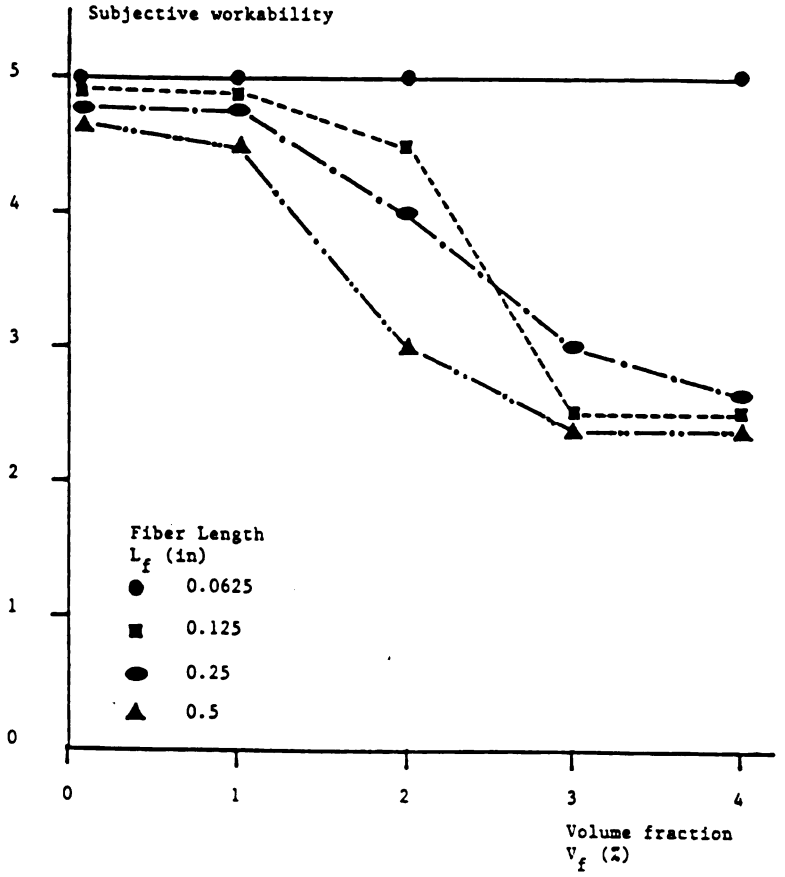

b. Subjective workability

Figure 2.7: (continued)

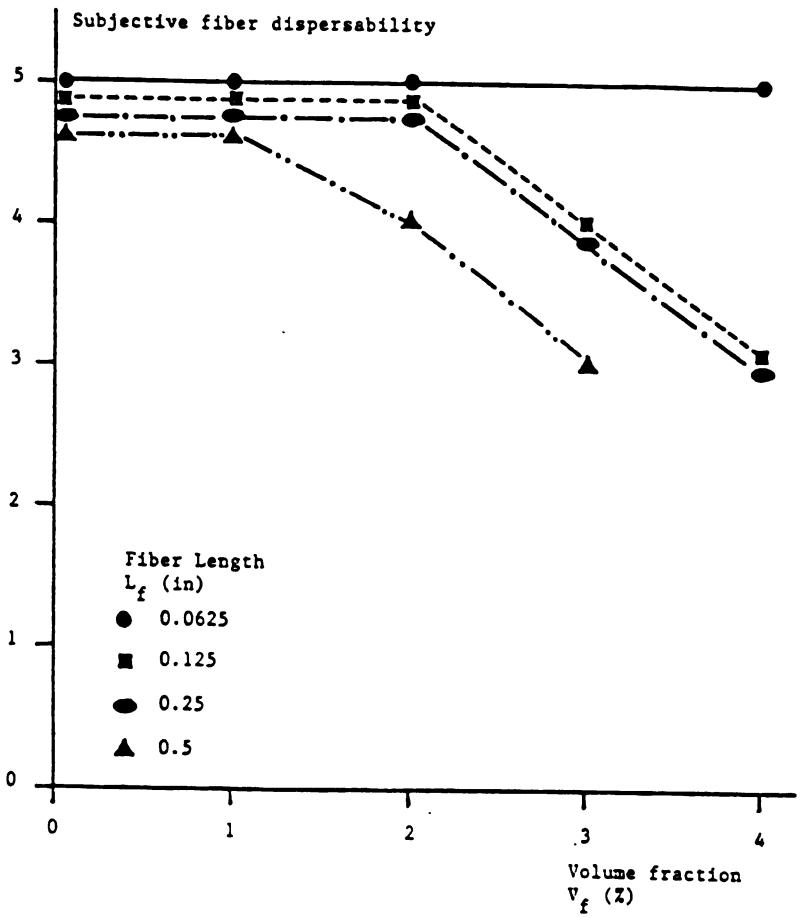

c. Subjective fiber dispersability.

Figure 2.7: (continued)

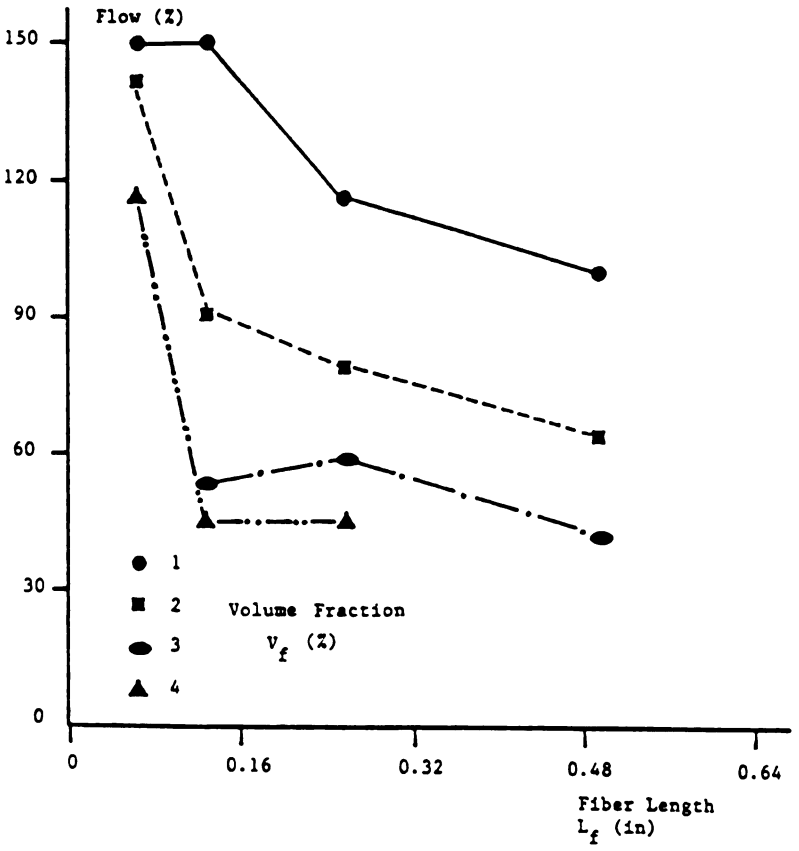

a. Flow

Figure 2.8: Effects of fiber length (L_f) on fresh mix characteristics (water/binder = 0.41, silica fume/binder = 0.23, and superplasticizer/binder = 0.018) 1 in = 25.4 mm

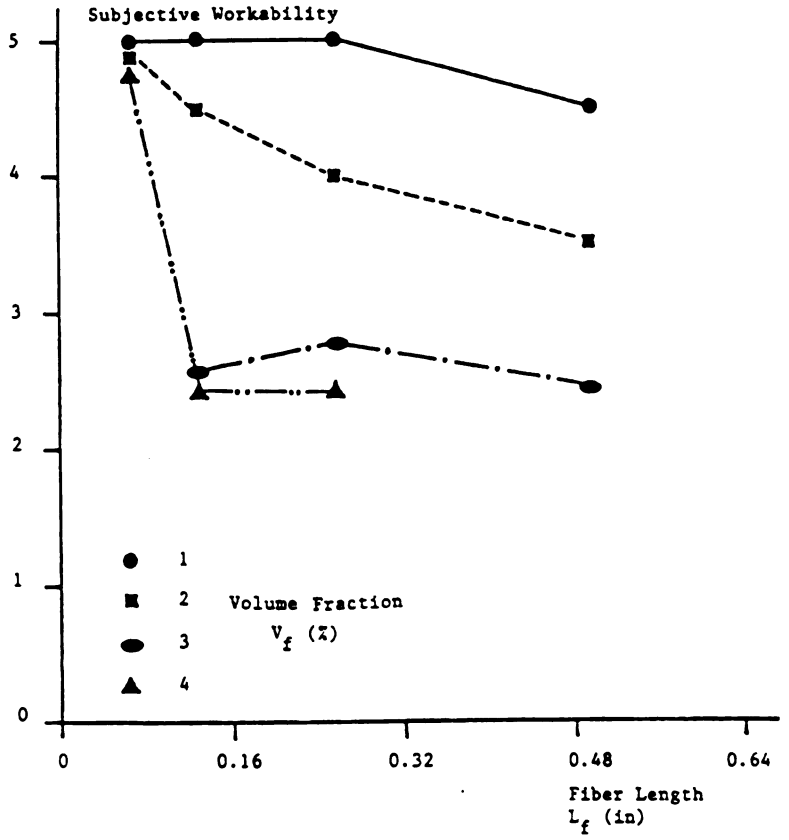

Figure 2.8: (continued)

b. Subjective workability

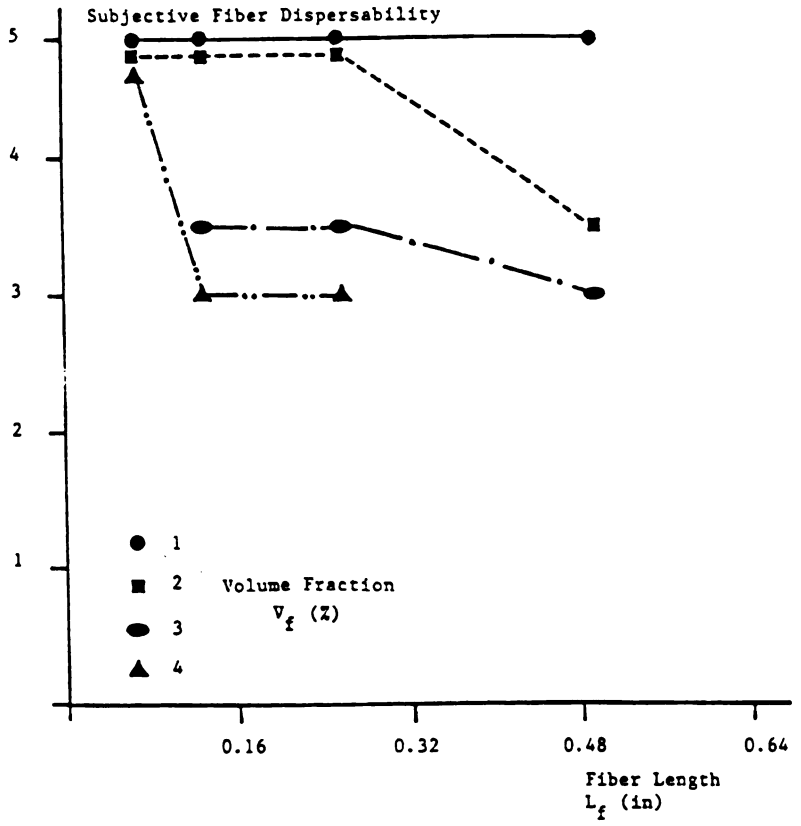

c. Subjective fiber dispersability

Figure 2.8: (continued)

silica fume on fresh mix characteristics. The increase in silica fume content is observed to damage the flow and workability of fresh mix but to improve the dispersability of fibers in cementitious matrices. The flow and workability of fresh fibrous mix drop at increasing rates with the increase in silica fume content. In mix proportioning of carbon fiber reinforced cement (to be constructed using conventional mortar mixer), due considerations should be given to the optimization of silica fume content for achieving a reasonably workable mix which is capable of uniformally dispersing fibers.

d. Water Content

The increase in water binder ratio is observed in Figure 2.10 to improve the flow and workability of the fresh fibrous mixes, but to have no significant effects on fiber dispersability. The improvements in flow and workability generally take place at a decreasing rate with increasing water content.

e. Superplasticizer Content

Figure 2.11 presents the effects of superplasticizer-binder ratio on the properties of fresh carbon fiber reinforced cement mixes. The increase in superplasticizer content is observed in Figures 2.11.a and 2.11.b to significantly improve the flow and especially the subjective workability of fresh fibrous mixes. As far as the dispersability of carbon fibers is concerned, the increase in superplasticizer content up to a certain level is observed in Figure 2.11.c to have some positive effects on the uniform dispersion of fibers. Beyond this limit, however, fiber dispersability seems to be independent of the superplasticizer content.

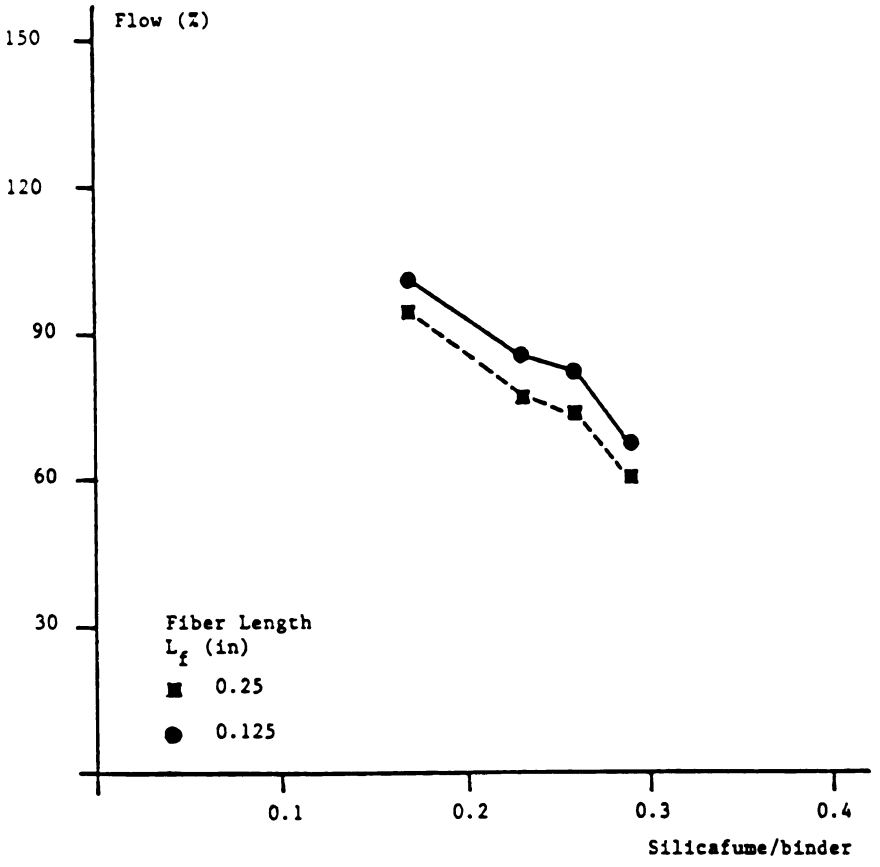

a. Flow

Figure 2.9: Effects of silica fume content on fresh mix characteristics (water/binder = 0.41, superplasticizer/binder = 0.018, and fiber volume fraction (V_f) = 2%) 1 in = 25.4 mm

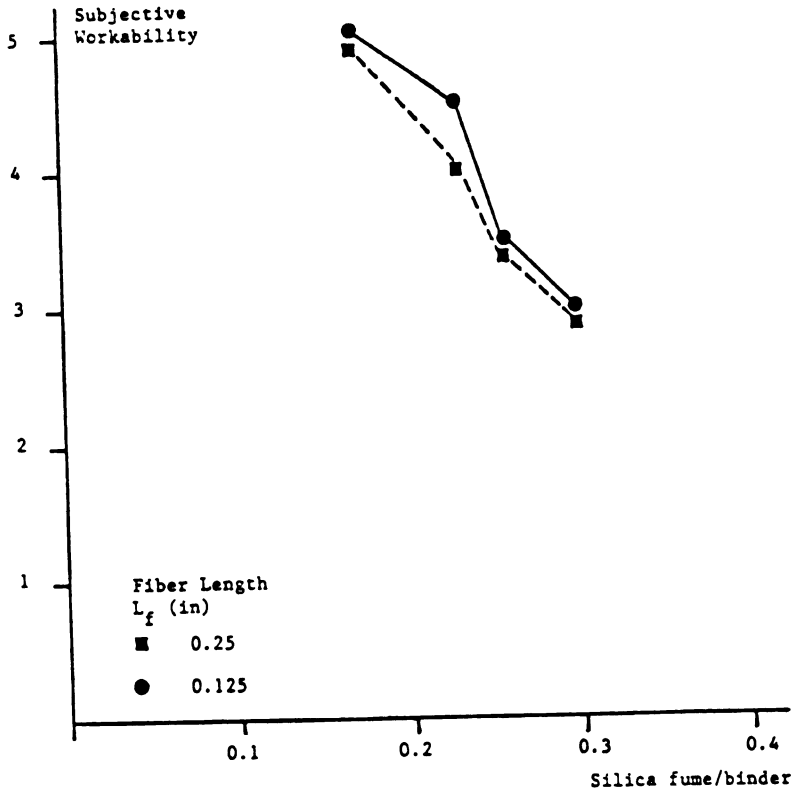

b. Subjective workability

Figure 2.9: (continued)

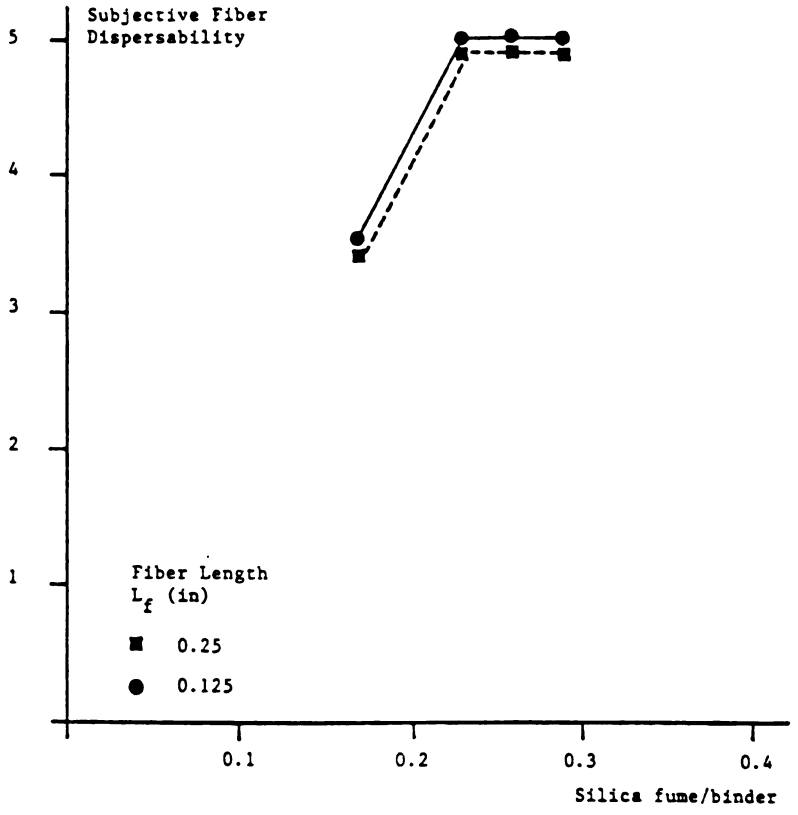

c. Subjective fiber dispersability.

Figure 2.9: (continued)

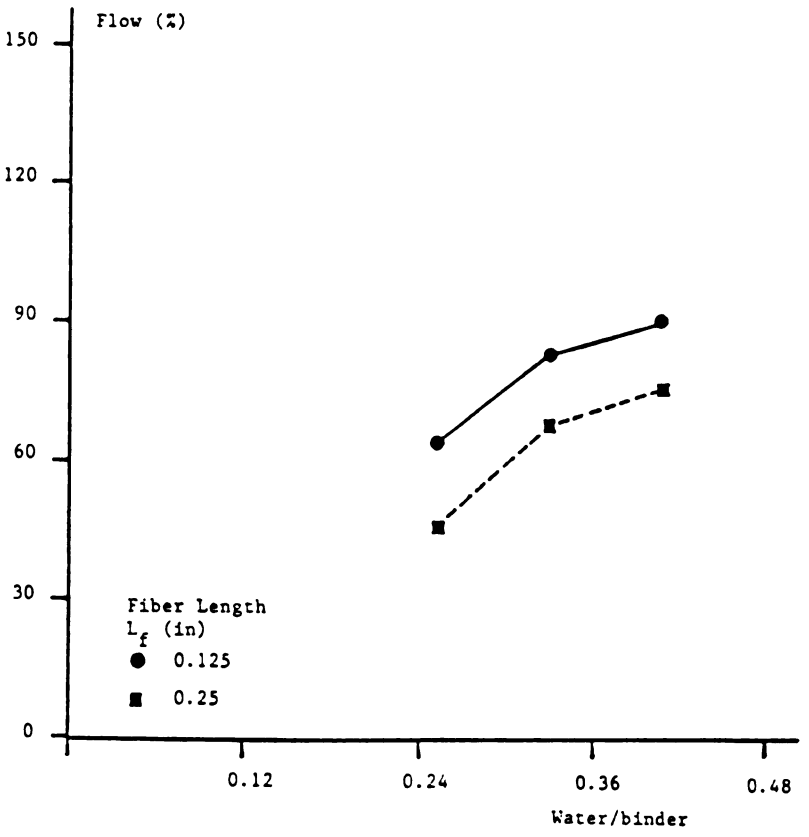

a. Flow

Figure 2.10: Effects of water content on fresh mix characteristics (silica fume/binder = 0.23, superplasticizer/binder = 0.018, and fiber volume fraction (V_f) = 2%) 1 in = 25.4 mm

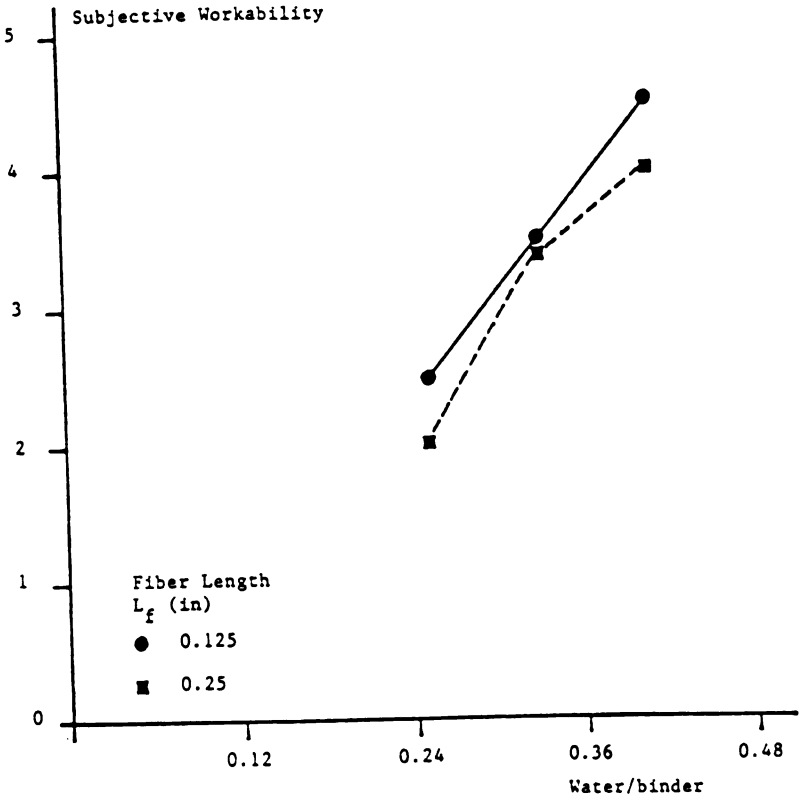

b. Subjective workability

Figure 2.10: (continued)

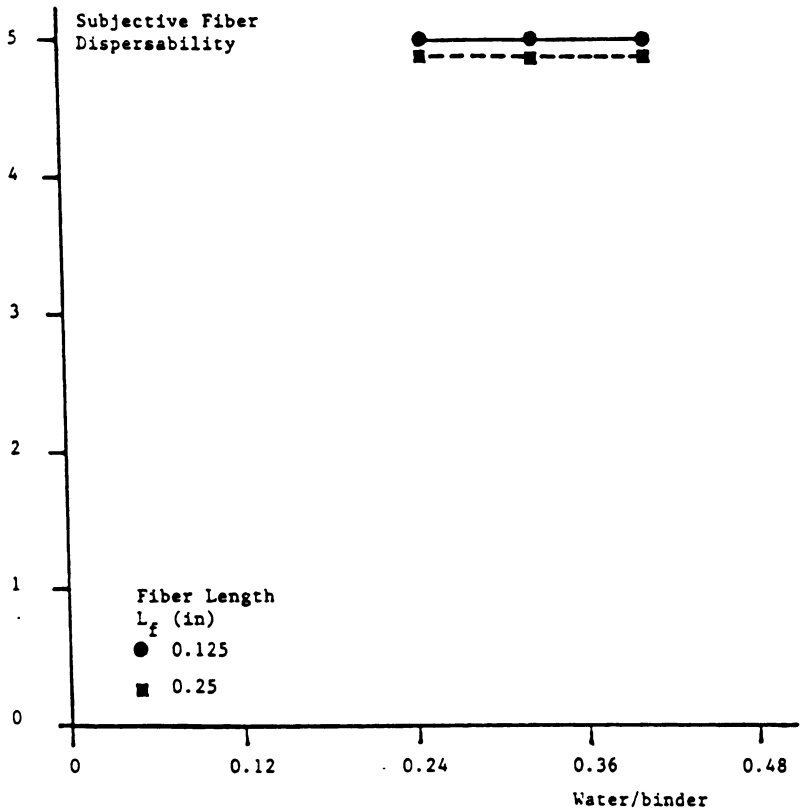

c. Subjective fiber dispersability

Figure 2.10: (continued)

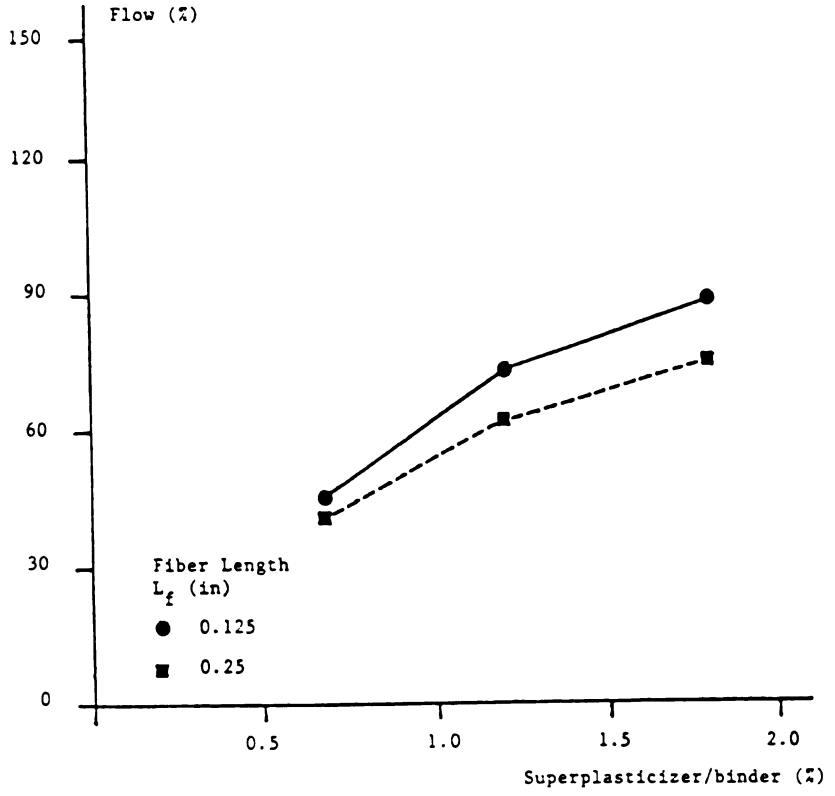

a. Flow

Figure 2.11: Effects of superplasticizer content on fresh mix characteristics (water/binder = 0.41, silica fume/binder = 0.23, and fiber volume fraction = 2%) 1 in = 25.4 mm

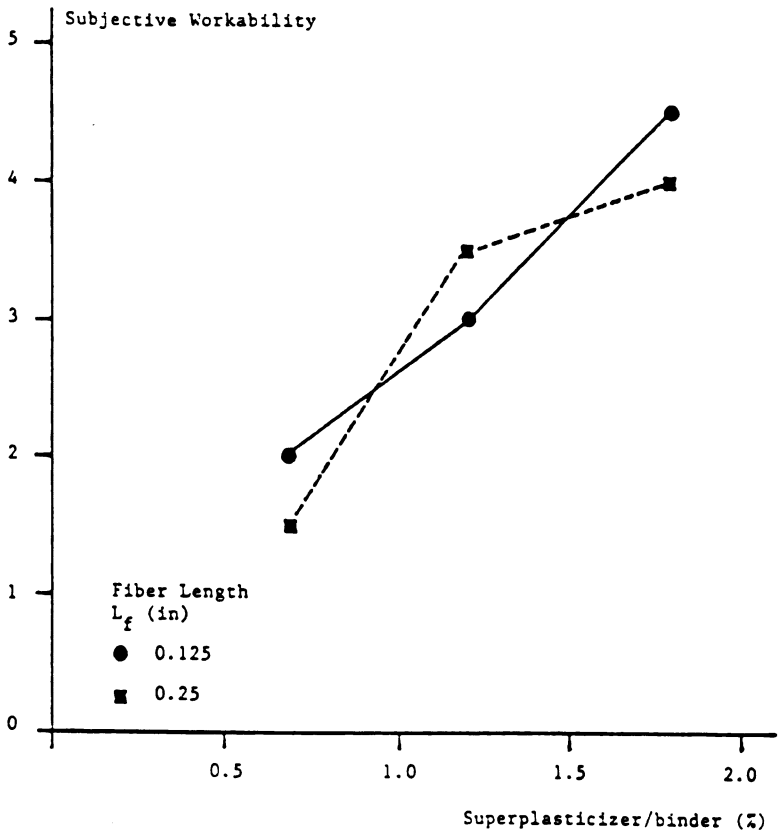

b. Subjective workability

Figure 2.11: (continued)

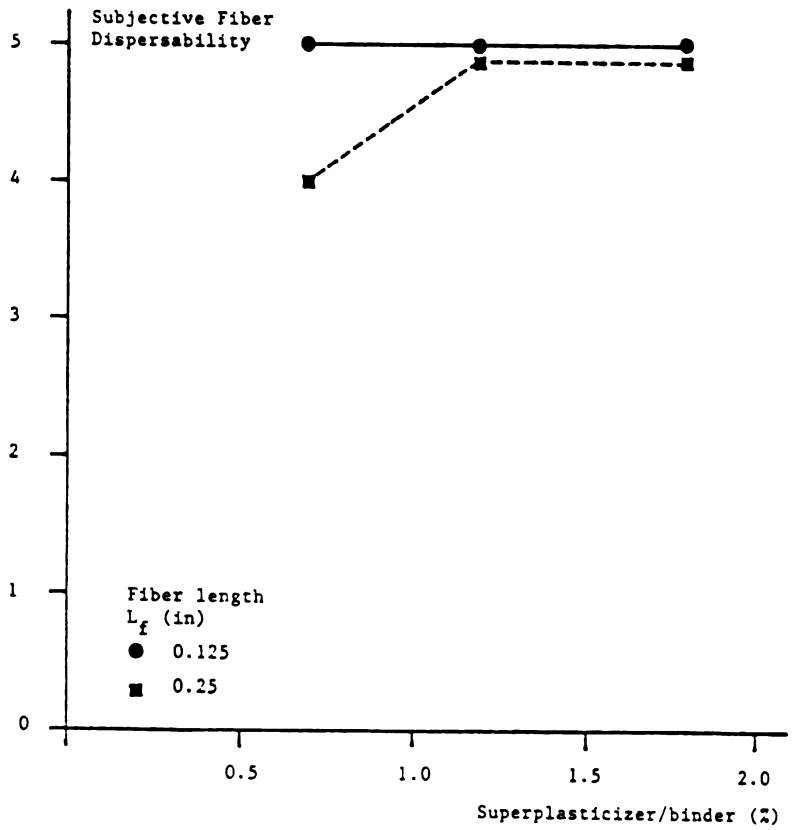

c. Subjective fiber dispersability

Figure 2.11: (continued)

f. Variability of Fiber Length

Ashland's pitch-based carbon fibers show variations in the actual average length. This is observed in Figure 2.12 to generate some important variations in the flow, workability and fiber dispersability of comparable carbon fiber reinforced cement mixtures.

g. Effect of Time on Fresh Mix Flowability

Carbon fiber reinforced cement mixes with silica fume generally tend to lose workability rather rapidly. Figure 2.13 presents the flow test results for typical carbon fiber reinforced cement mixes at 1,4, and 10 minutes after the completion of mixing. Similar tendencies were observed irrespective of the specific mix proportions. On the average, the fresh mix flows at 4 and 10 minutes after mixing were 85% and 70%, respectively, of the flow at 1 minute after mixing.

The fast hardening characteristics of carbon fiber reinforced cement is an advantage in application by the spraying technique, but it also may be a disadvantage in some applications in the sense that it reduces the time available after mixing for application of the material. The rate of hardening of carbon fiber reinforced cement can be controlled through the use of set retarders.

2.5. Experimental Program on the Hardened Material Strength

An experimental program was conducted to investigate the effects of fiber length and volume fraction, and the matrix mix proportions, on the flexural, direct tensile and compressive strengths of carbon fiber reinforced cement. The objective in this phase of the

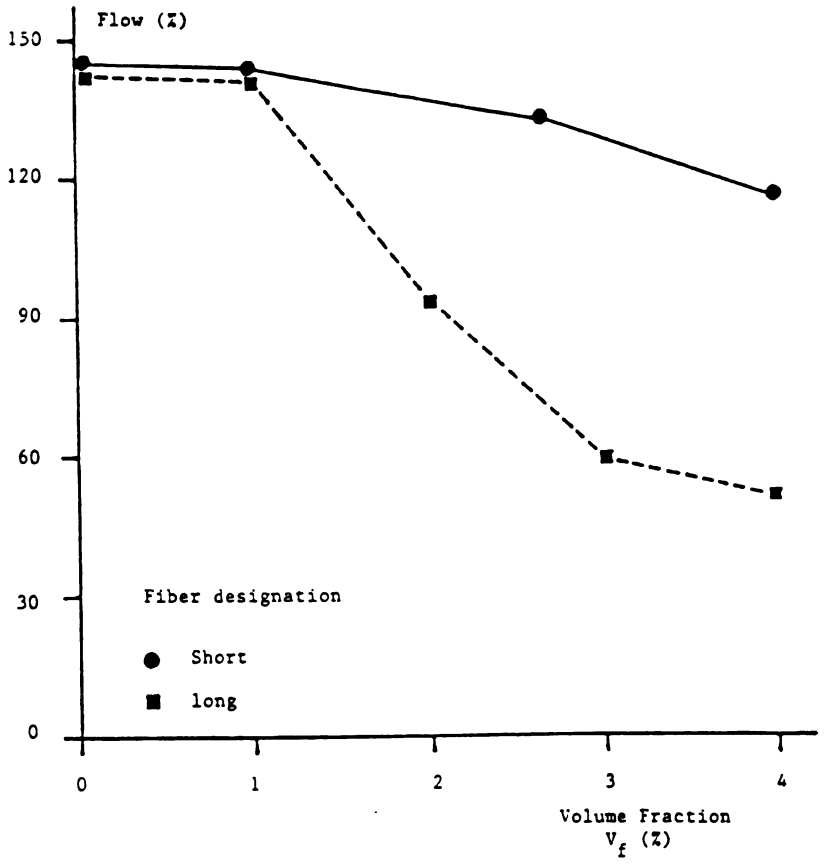

a. Flow

Figure 2.12: Typical variations in fresh mix characteristics of carbon fiber reinforced cement due to variations in fiber length (water/binder = 0.41, silica fume/binder = 0.23, superplasticizer/binder = 0.018, and fiber length = 0.125 in)1in=25.4 mm·

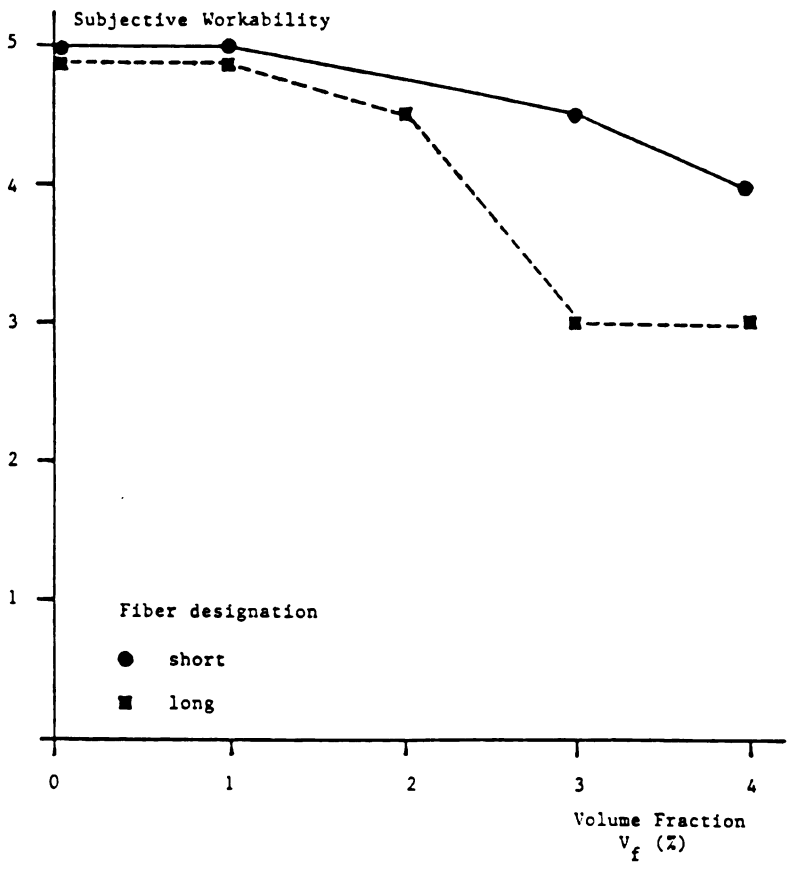

b. Subjective workability

Figure 2.12: (continued)

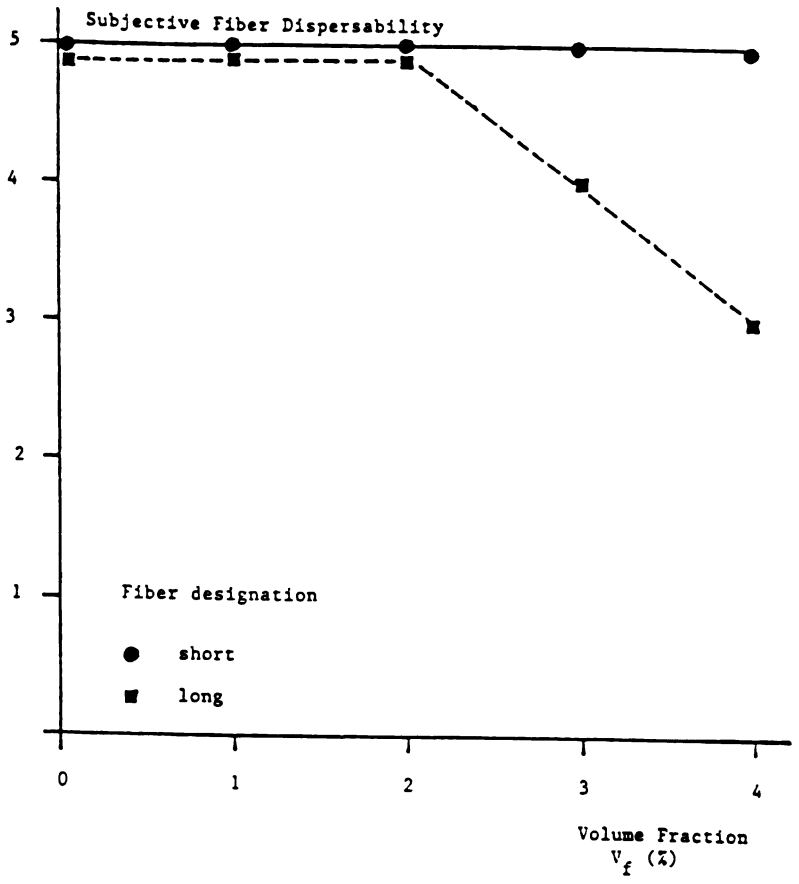

c. Subjective fiber dispersability

Figure 2.12: (continued)

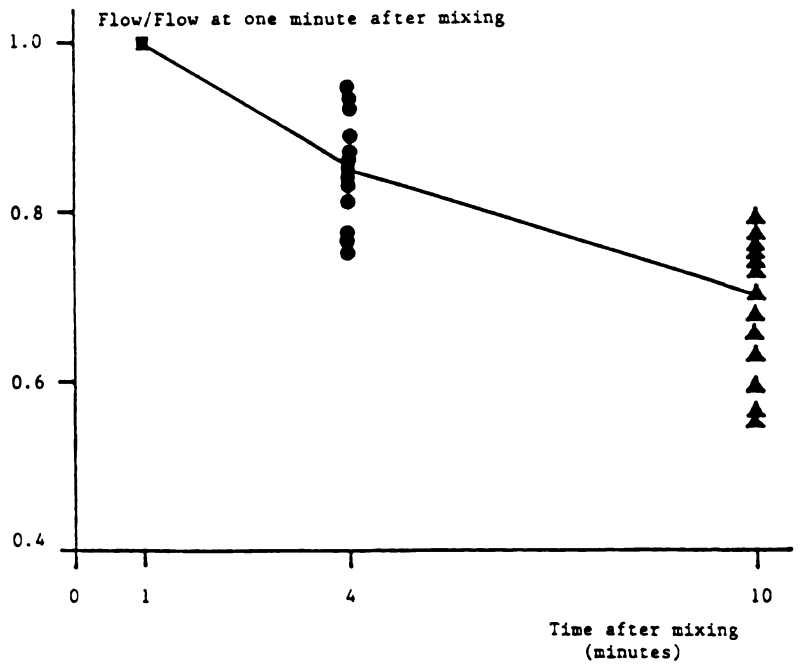

Figure 2.13: Effect of time on flow of fresh carbon fiber reinforced cement.

experimental study was to optimize the mix composition. Comprehensive experimental data on the load-deformation characteristics of the optimized material under different stress systems, and its impact strength were generated at later stages of this investigation. The optimum curing condition for carbon fiber reinforced cement was also decided at later stages for the optimized mix composition.

It is worth mentioning that the test program presented in this section is based on a preliminary investigation. This preliminary work revealed some problems with the expansion of carbon fiber reinforced cements with normal water contents, which led to severe cracking of the material at early ages. This problem could be attributed to the coating of carbon fibers by water and the surface tension of water on carbon fiber surfaces. After recognizing the source of the problem, the solution was found by reducing the water content of the mixture and simultaneously increasing its superplasticizer content in order to maintain workability. The preliminary results indicated that the water-binder ratio should be kept below 0.33 (for manufacturing with mortar mixer) if expansion and excessive cracking is to be avoided. At such low water-binder ratios, superplasticizer-binder ratios of the order of 3.2% are needed for enhancing the workability of fresh mix to desirable levels. It should be noted that the superplasticizer used in this investigation consisted of 40% solids and 60% water. The water in superplasticizer was added to the mixing water, and the superplasticizer weight is based on its solid constituents.

Table 2.9 presents the fiber lengths and volume fractions, and the matrix mix proportions used in this phase of the project. All the specimens were cured in air (at about 72°F and 60% RH) following

Table 2.9: Mix proportions for the experimental program on strength of carbon fiber reinforced cement.

w/(c+s)	sp/(c+s)	L_f in (mm)	V_f(%)	s/(c+s)
		1/4(6)	3	0.23
0.30	0.03	1/8(3)	0	0.23
			3	0.17 0.23 0.26 0.29
			5	0.23
		1/16(1.5)	3	0.23
			5	0.23 0.29
			7	0.23
		1/64(0.4)	5	0.23
			7	0.23
0.27	0.03	1/16(1.5)	5	0.23

w = water
c = cement
s = silica fume
sp = superplasticizer
L_f = fiber length
V_f = fiber volume fraction

demolding at the age of 24 hours. While in molds, the specimens were covered by a plastic sheet.

For each mix proportion given in Table 2.9, 9 flexural specimens: 1.5 x 1.5 x 6.5 in. (38.1 x 28.1 x 165.1 mm) prisms (ASTM C348), 9 direct tensile specimens: 1 in. (25.4 mm) thick briquetts (ASTM C190), and 6 compression specimens 2 in. (51 mm) diameter by 4 in. (102 mm) high cylinders (ASTMC 109) were constructed. The specimens were cast in one layer and compacted externally on a vibration table. The flexural tests were performed according to ASTM C348 with three-point loading and a span of 4.8 in. (122 mm).

Tests on specimens were performed at ages of 4, 12 and 28 days, with one-third of the specimens tested at each age. This was done to establish not only the strength of the material under different stress systems, but also the development of strength with time.

2.6. Test Results on the Hardened Material Strength

The generated test results are presented in this section. The format followed in this presentation is to give strength as a function of different mix variables. This format helps in establishing the trends in the effects of mix proportions on strength, which is the information needed for determining the optimum mix compositions. The mix variables considered were: fiber volume fraction, fiber length, microsilica content, and water-binder ratio. The standard test age used in this investigation was 12 days. The effects of age on strength of carbon fiber reinforced cement is presented at the end of this section.

a. Effects of Carbon Fiber Volume Fraction

The increase in volume fraction of fibers with different lengths substantially increases the flexural and tensile strengths but reduces the compressive strength of the composite (see Figure 2.14 for the average tendencies). The increase is flexural and tensile strengths resulting from carbon fiber reinforcement may be attributed to the role of fibers in arresting microcracks and delaying their propagation. The loss in compressive strength resulting from carbon fiber reinforcement could possibly be due to the increase in entrapped air content in the presence of carbon fibers. The rate of increase in flexural and tensile strengths with increasing fiber volume fraction tends to drop as the fiber volume fraction exceeds 4%, due to the problems with fresh mix workability and fiber dispersability at high fiber contents (which result in excessive entrapped air content and fiber balls in the material). The rate of decrease in compressive strength with increasing fiber content, however, slows down at higher fiber volume fraction, possibly due to the increase in the confinement provided by fibers. It is worth mentioning that, as shown in later phases of the study, major improvements in the compressive strength of carbon fiber reinforced cement can be achieved through optimizing the curing conditions of the material.

b. Effects of Fiber Length

The flexural and tensile strengths of carbon fiber reinforced cement composites incorporating 3 and 5 % fiber volume fractions increase at a decreasing rate as the fiber length increases up to about 1/8 in. (3 mm). Thereafter, the flexural and tensile strengths start to drop as the fiber length increases (see Figures 2.15.a and

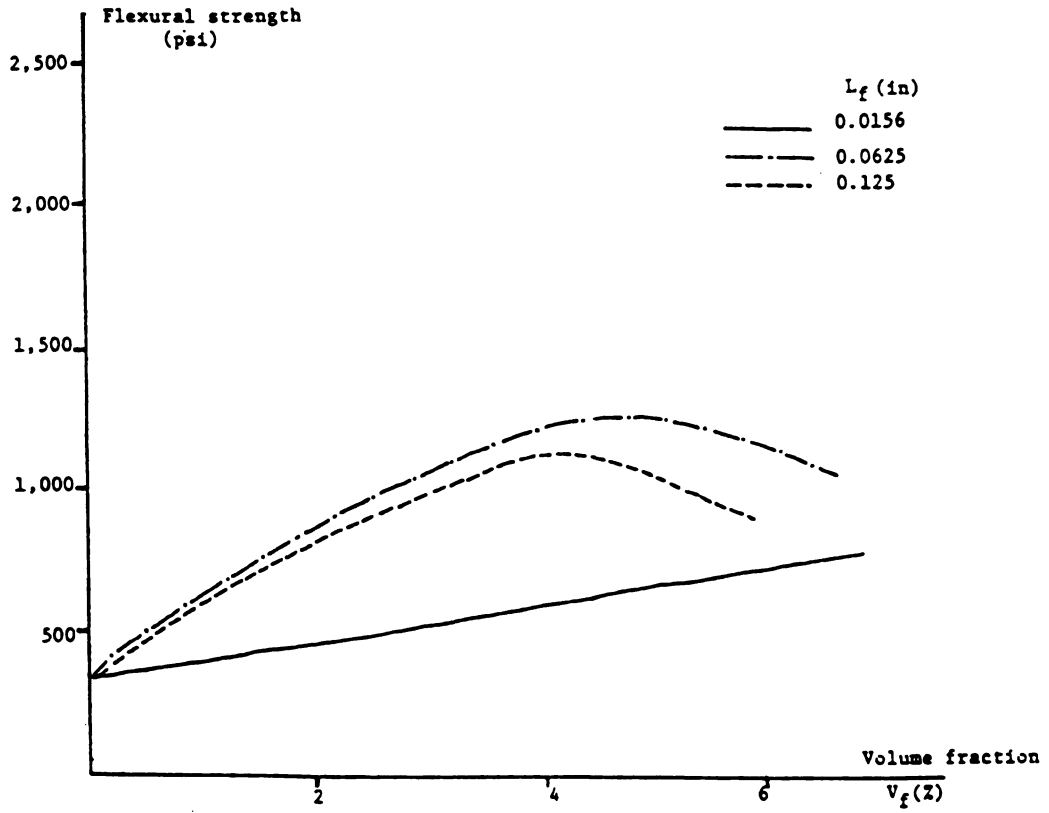

a. Flexural strength

Figure 2.14: Average trends in the effects of fiber volume fraction on the strength of carbon fiber reinforced cement (water/binder = 0.30, silica fume/binder = 0.23, and superplasticizer/binder = 3.4%) 1 in = 25.4 mm, 1 Ksi = 6.9 MPa

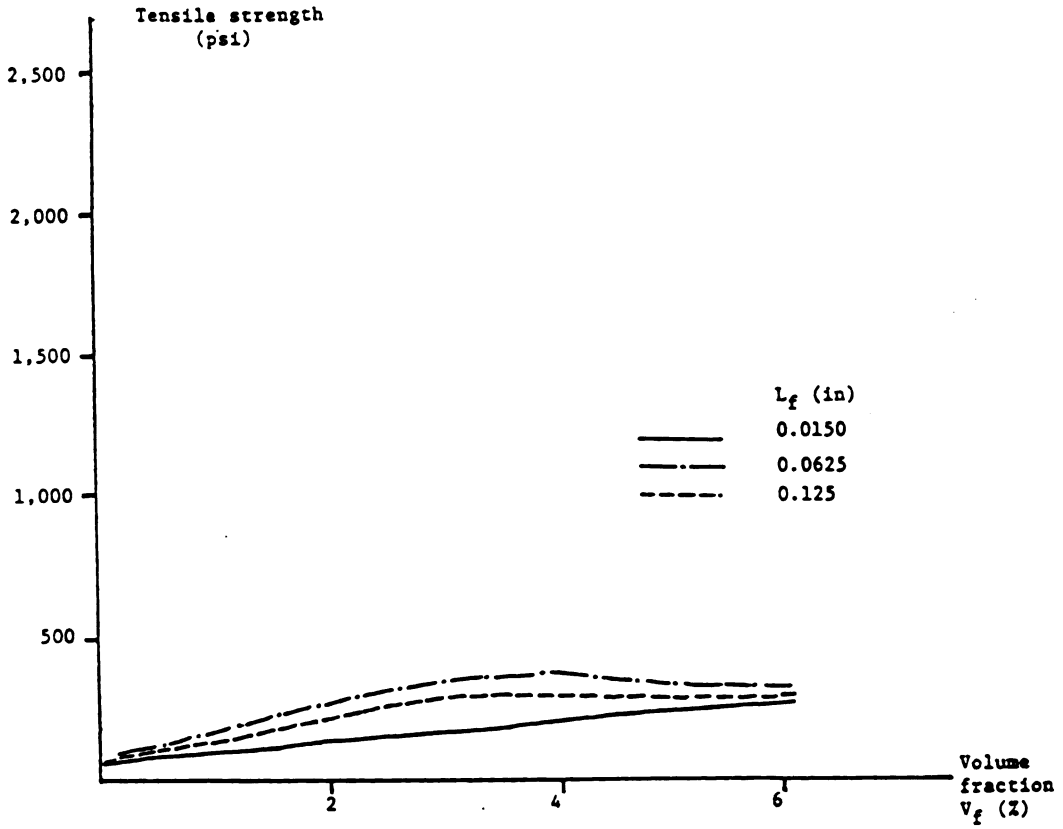

b. Tensile strength

Figure 2.14: (continued)

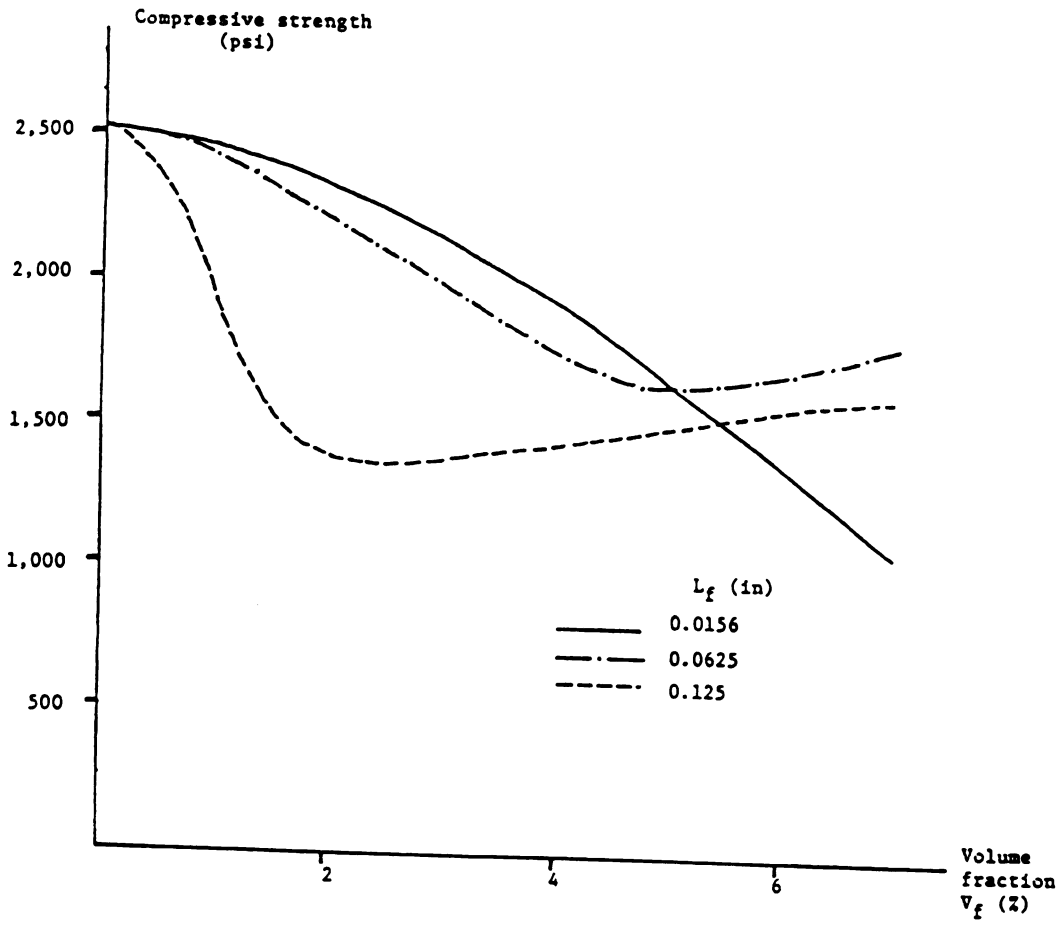

c. Compressive strength

Figure 2.14: (continued)

2.15.b). The compressive strength of fibrous composites with 3 and 5% fiber volume fractions decreases with increasing fiber length, but this tendency slows down or even reverses at higher fiber lengths (Figure 2.15.c). The effect of fiber length on compressive strength can be illustrated, as mentioned in the discussion on volume fraction, by the damage to workability and the consequent increase in entrapped air resulting from the increase in fiber length on one hand, and on the other hand, by the higher efficiency of longer fibers in confining cement composites.

c. Effects of Microsilica Content

Microsilica improves the properties of carbon fiber reinforced cement composites in the hardened state by uniformly dispersing the fibers and enhancing the fiber-matrix interfacial bond. The workability of fresh mix is, however, damaged by the presence of microsilica. This may have adverse effects on the hardened material properties. As shown in Figures 2.16.a and 2.16.b, the flexural and tensile strengths of the fibrous composite tend to increase with the increase in microsilica-binder ratio up to a microsilica-binder ratio of about 0.23. Thereafter, this tendency starts to reverse due to the workability problems associated with the use of more than 3% volume fraction of 1/8 in. (3 mm) fibers. Composites with 0.23 microsilica-binder ratio have roughly 25% more flexural and tensile strengths than the ones with 0.17 microsilica-binder ratio. The compressive strength of carbon fiber cement composites consistentcy increases with the increase in microsilica-binder ratio from 0.17 to 0.26 (see Figure 2.16.c for average tendencies).

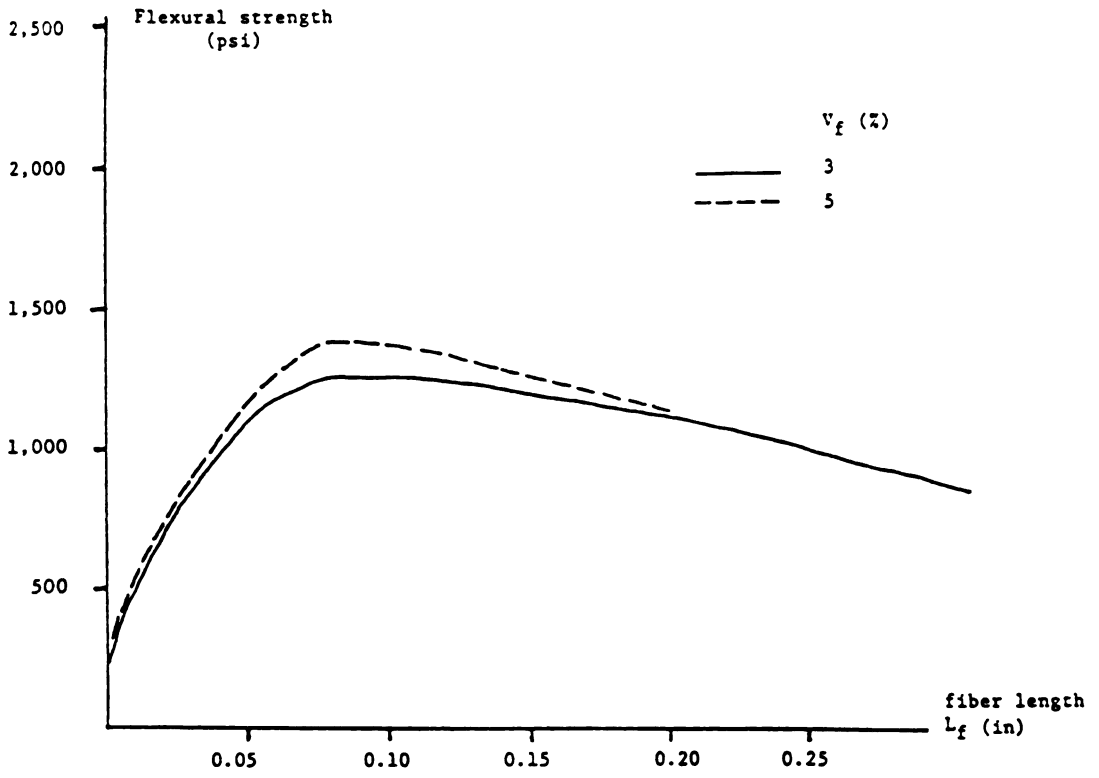

a. Flexural strength

Figure 2.15: Average trends in the effects of fiber length on the strength of carbon fiber cement (water/binder = 0.30, silica fume/binder = 0.23, and superplasticizer/binder = 3.4%) 1 in = 25.4 mm, 1 Ksi = 6.9 MPa

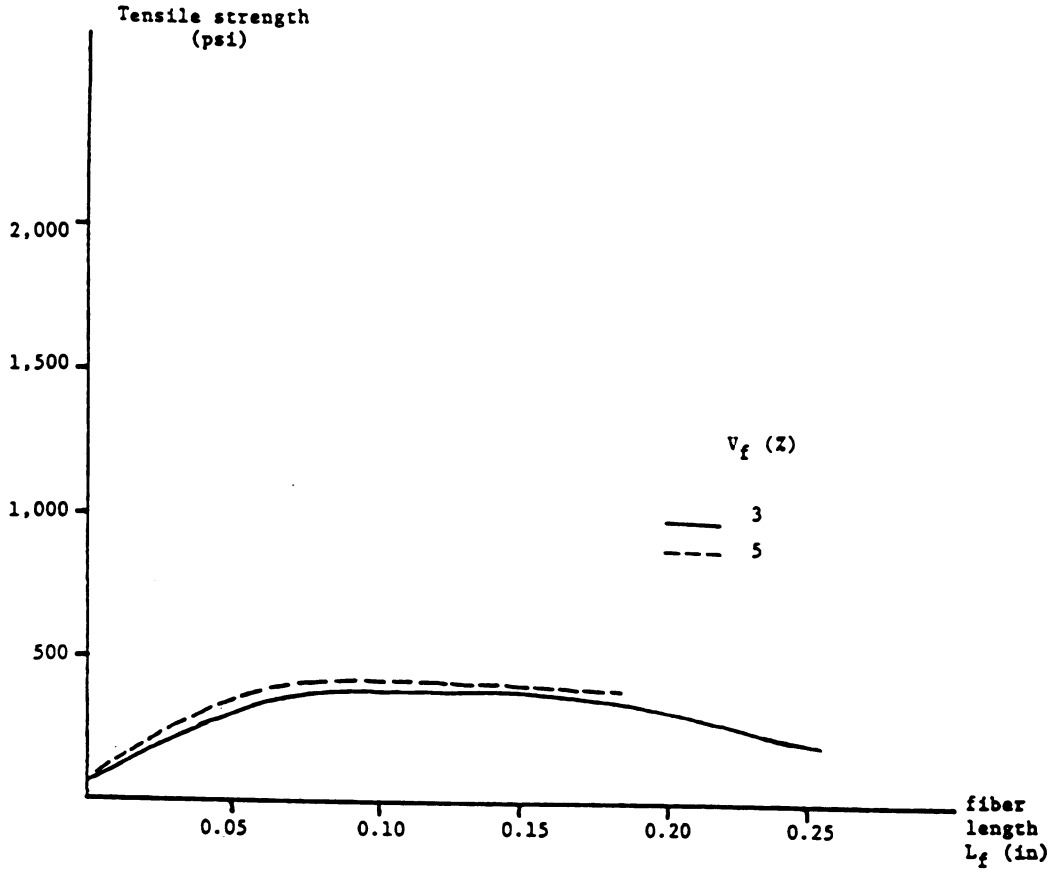

b. Tensile strength

Figure 2.15: (continued)

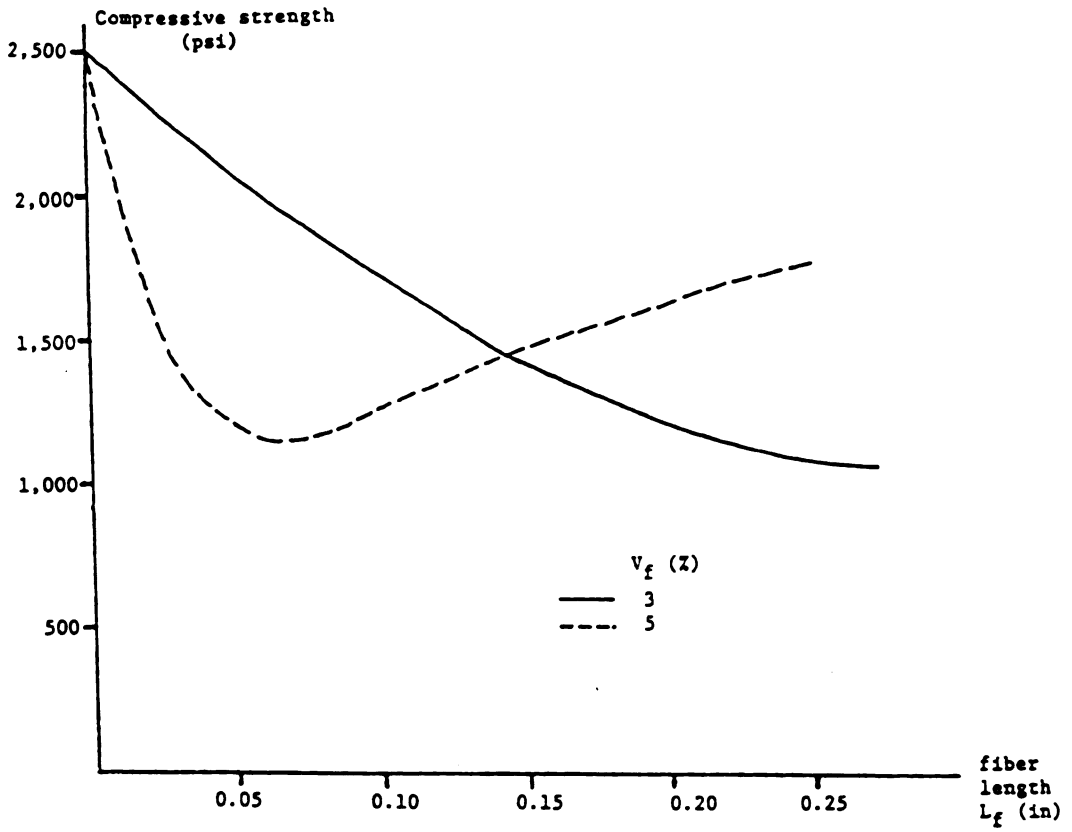

c. Compressive strength

Figure 2.15: (continued)

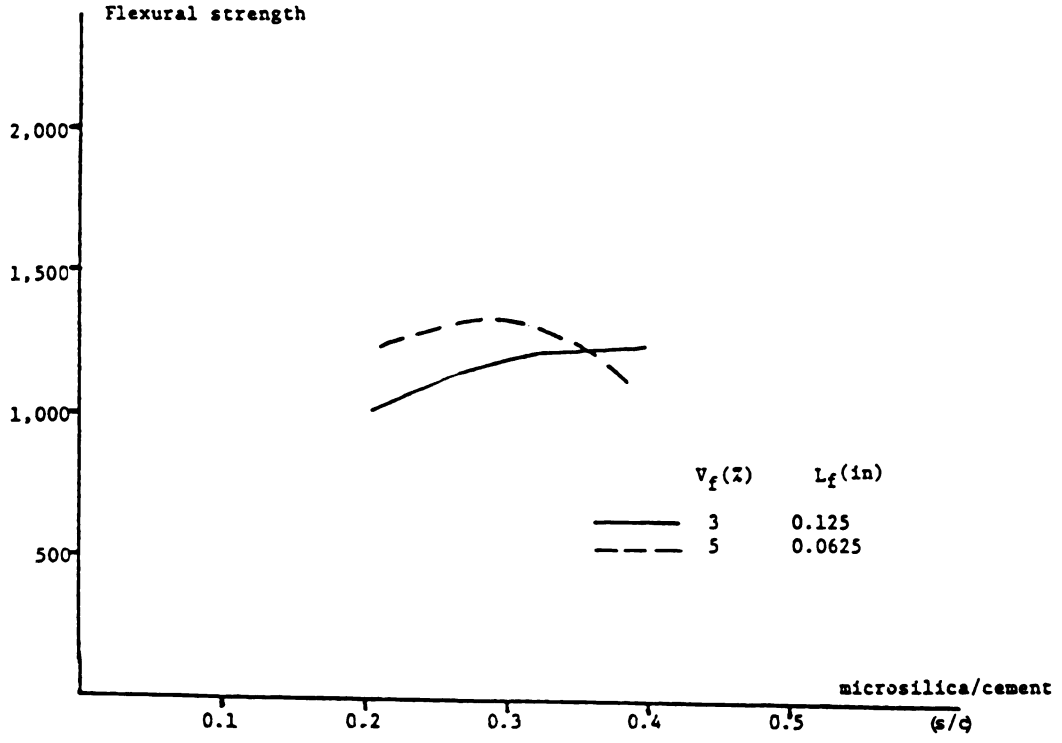

a. Flexural strength

Figure 2.16: Average trends in the effects of microsilica content on strength of carbon fiber cement (water/binder = 0.30, superplasticizer/binder = 3.4%, fiber length = 1/8 in, and fiber volume fraction = 3%) 1 in = 25.4 mm, 1 Ksi = 6.9 MPa

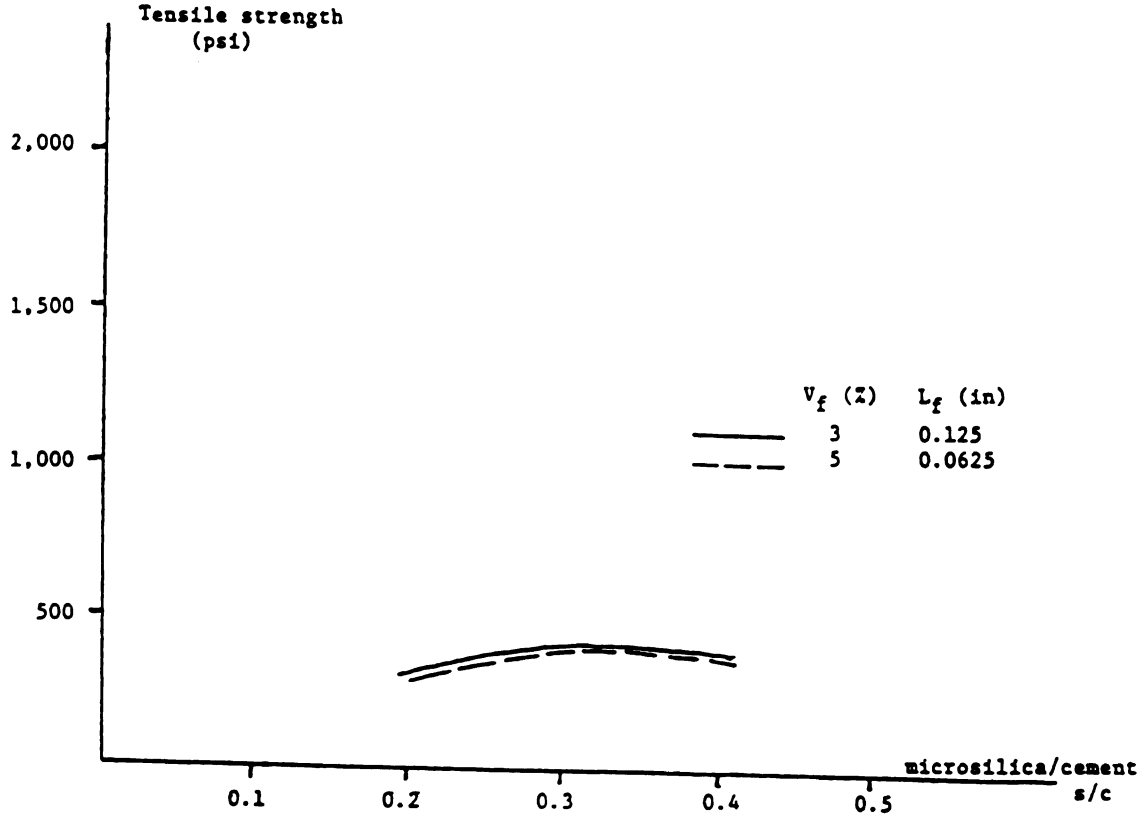

b. Tensile strength

Figure 2.16: (continued)

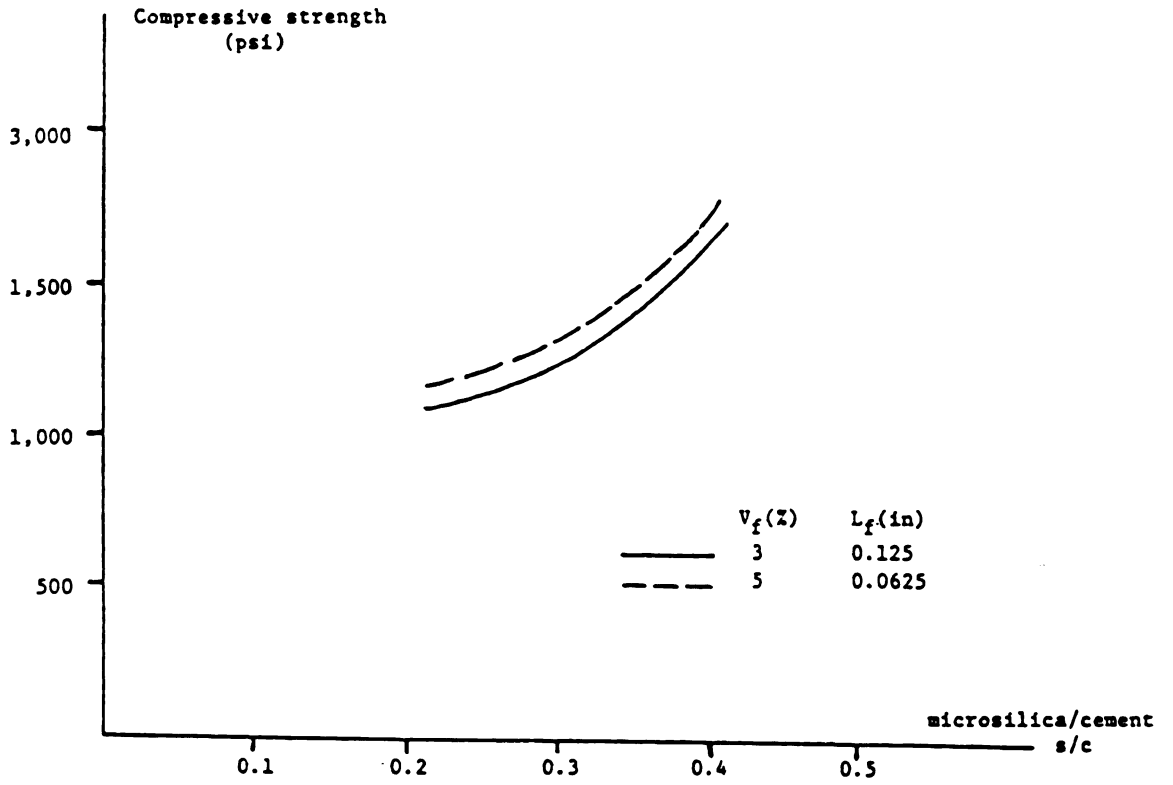

c. Compressive strength

Figure 2.16: (continued)

d. Effects of Water Content

The flexural, the tensile, and especially the compressive strength of carbon fiber reinforced cement were observed to increase with decreasing water-binder ratio. Figure 2.17 presents the average trends in the effects of water content on the strength fibrous composite under different stress systems.

e. Effects of Age on the Strength of Air-Cured Specimens

After 4, 7 and 12 days of air curing, the flexural strength of carbon fiber reinforced cement was 40%, 50% and 95% of the 28-day flexural strength. The corresponding values for direct tensile strength were 60%, 90% and 100% . The compressive strengths of carbon fiber reinforced cement after 7 and 12 days of air curing were 60% and 90% of the full compressive strength which was reached at the age of 18 days. Figure 2.18 presents the average trends in strength development of air-cured specimens with time. Compared to conventional concrete, the gain in strength of air-cured carbon fiber reinforced cement seems to be more rapid. In general, 12 days of air curing was sufficient for the material to develop more than 90% of its strength.

f. Relative Values of Strength Under Different Stress Systems

The flexural strength of air-cured carbon fiber reinforced cement can get very close to the compressive strength of the material. The flexural strength is also substantially greater than the tensile strength in carbon fiber cement. At 5% fiber volume fraction, the flexural strength ranges from 70% to 100% of the compressive strength depending on the fiber length, while the direct tensile strength is

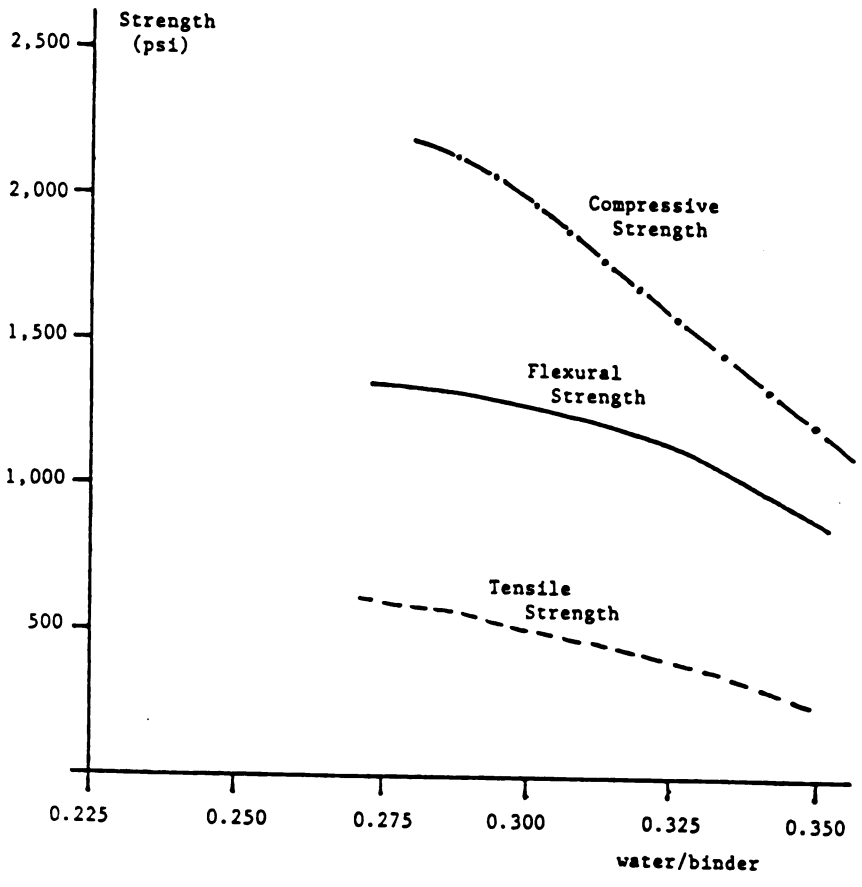

Figure 2.17: Average trends in the effects of water content on strength of carbon fiber reinforced cement (silica fume/ binder = 0.23, superplasticizer/binder = 3.4%, fiber length = 1/8 in, fiber volume fraction = 3%) 1 in = 25.4 mm, 1 Ksi = 6.9 MPa

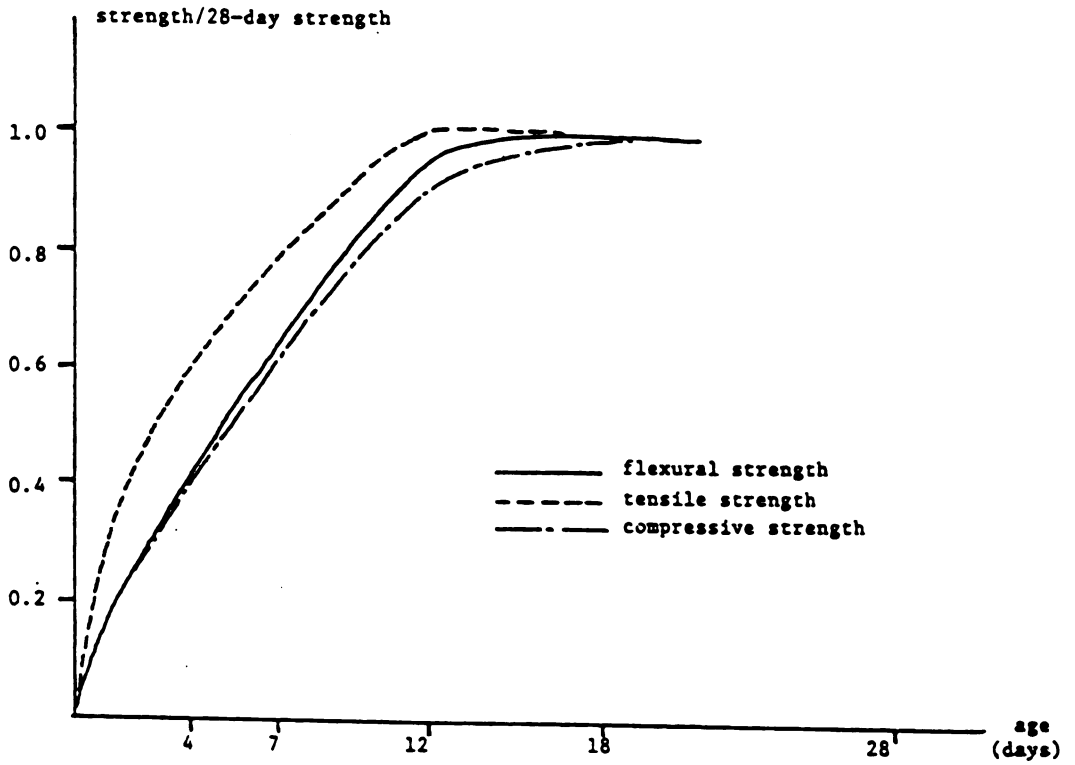

Figure 2.18: Average trends in strength development for air-cured carbon fiber reinforced cement.

only about 25% of the compressive strength. The relatively high ratio of flexural to compressive strength. The relatively high ratio of flexural to compressive strength may be attributed to the effects of fibers on increasing the flexural strength and decreasing the compressive strength. The efficiency of fibers in increasing flexural strength, when compared with tensile strength, could be due to the inelastic stress distribution at ultimate load under flexural loads, which provides a condition for effective use of the ductility of fibrous material behavior in increasing flexural strength.

g. Scatter of Test Results

Relatively large scatters was observed in strength test results of carbon fiber reinforced cement. This was especially true for the flexural and compressive strengths. This scatter could be caused by the dependence of fiber efficiency on some highly variable factors including: fiber dispersability, bonding of fibers to the cementitious matrix, and fiber effects on pore system characteristics of the matrix. The variations in carbon fiber length is another factor contributing to the variability of test results. Thus, it is no surprise that carbon fiber reinforced cement shows more variations in strength test results than plain concrete.

2.7. Summary and Conclusions

An experimental research was conducted to establish the trends in the effects of different mix variables on the properties of fresh carbon fiber reinforced cement mixes. The variables considered in this study were: fiber volume fraction, fiber length, silica fume-

binder ratio, water-binder ratio, superplasticizer-binder ratio, variability in fiber length, and time elapsed after mixing. The fresh mix properties investigated were: flow, subjective workability and subjective fiber dispersability. All mixes were manufactured in a conventional mortar mixer.

The following conclusions could be derived from test results:

1. Silica fume is an effective additive in cementitious matrices for improving the ability of uniformly dispersing fibers. The addition of silica fume, however, damages the flowability and workability of fresh carbon fiber reinforced cement mixtures.

2. In order to solve the workability problems caused by the addition of silica fume and fibers in cementitious mixes, it is essential to use relatively large dosages of superplasticizer. The increase in superplasticizer content up to a certain limit also improves fiber dispersability of cementitious matrices.

3. The increase in water content improves the flowability and workability of fibrous mixes at a gradually decreasing rate, but does not influence fiber dispersability.

4. The flowability, workability and fiber dispersability of fresh carbon fiber reinforced cement are adversely influenced by the increase in fiber volume fraction. This effect is more pronounced for longer fibers.

5. The fresh mix workability tends to be damaged, at a generally decreasing rate, with increasing fiber length. The dispersability of fibers in cementitious matrices also tends to be damaged as the fiber length increases. The variability in carbon length generates relatively large variations in the fresh mix properties of carbon fiber reinforced cement.

6. Carbon fiber reinforced cement mixes with silica fume have relatively short setting times. Their flow drops by about 15% and 30% at 4 and 10 minutes after mixing, respectively, compared to their flow at 1 minute after mixing.

An experimental study was also conducted on the flexural, direct tensile and compressive strengths of air-cured carbon fiber reinforced cements. The results indicated that:

1. The flexural the and direct tensile strengths of carbon fiber reinforced cement increase, at a decreasing rate, with the increase in fiber volume fraction up to an optimum value beyond which this tendency starts to reverse. The compressive strength, however, decreases with increasing fiber volume fraction up to a point beyond which the compressive strength tends to either stay constant or increase as the fiber volume fraction increases.

2. The tendencies in the effects of fiber length on strength are comparable to those caused by fiber volume fraction. The flexural and tensile strengths increase and then decrease with increasing fiber length, while the reverse is true for compressive strength.

3. Microsilica, due to its positive effects on dispersability and bonding of carbon fibers, improves the material strength. At a certain microsilica content, however, its negative effects on fresh mix workability start to overshadow the advantages obtained by the use of microsilica.

4. The limited test data obtained on the effects of water content indicated that the strength of carbon fiber cement generally increases with decreasing water-binder ratio.

5. Air-cured carbon fiber reinforced cement develops strength at a higher rate than conventional concrete. After 12 days of air curing, carbon fiber reinforced cement gains more than 90% of its full

strength.

6. Carbon fiber reinforced cement has distinctly high flexural-to-compressive and flexural-to-tensile strength ratios. There is generally a relatively large scatter in test results of carbon fiber reinforced cement.

CHAPTER 3

EXPERIMENTAL PROGRAM

3.1. Introduction

In Chapter 2, Phase I (the preliminary phase) of the experimental program on carbon fiber reinforced cement was presented. The goals of Phase I were to optimize the material mix proportions and fiber reinforcement properties for achieving desirable fresh mix workability and hardened material strength. A large number of mixes were tested for fresh mix flowability and hardened material strength under different loading conditions. Air curing was employed throughout Phase I of the experimental project as a basic curing condition for optimizing the hardened material strength. The optimum mix proportions for achieving desirable fresh mix flowability and optimum hardened material strength were derived in Chapter 2. Phase II (the final phase) of the experimental program, described in this chapter, was performed on the optimum carbon fiber reinforced cement mixes selected using the results of Phase I. The hardened material, in this phase of the experimental program, was characterized by its strength and ductility under flexural, tensile, compressive and impact loading conditions. Five different curing conditions were experimented in Phase II in order to explore the effects of curing environment on the material load-deformation diagrams under flexure, tension and compression.

The objective of this final phase of the experimental program was to derive fiber reinforcement parameters and curing conditions required for achieving the optimum mechanical properties of carbon fiber reinforced cement.

3.2. Materials, Manufacturing and Curing

Materials used in Phase II of the experimental program were obtained from the same sources of materials in Phase I. Therefore, the material properties of cement, silica fume, superplasticizer and carbon fibers introduced in Chapter 2 also represent the materials used in Phase II. This also applies to the manufacturing process of carbon fiber reinforced cement.

Curing conditions have significant effects on the material strength and ductility in the hardened state. One of the objectives of this study was to optimize the curing process of carbon fiber reinforced cement composites for achieving superior hardened material mechanical properties. Five different curing conditions were employed in this experimental investigation as follows:

1. Following the mixing and casting processes described in Chapter 2, the molded materials were kept under a plastic sheet for 24 hours;

2. The specimens were demolded at the age of 24 hours, and were air dried for 12 hours (this precautionary measure prevents the surface deterioration of young specimens in moist environments);

3. The specimens were then exposed to the prospective curing environments for 24 hours. These environments were:

   a. Laboratory environment with a temperature of 75 ± 5°F and a relative humidity of about 50%;
   b. Under water at a temperature of 75°F;
   c. Under hot water at 175°F;
   d. In steam room at 140°F and 100% relative humidity; and
   e. In moist room at 74°F and close to 100% relative humidity; and

4. The specimens after exposure to any of the curing conditions described in step 3 for 24 hours, were moved to a regular laboratory environment, with a temperature of about 75°F and humidity of about 50% until the testing age.

3.3. Test Plan

a. Mechanical Properties of Hardened Carbon Fiber Reinforced Cement

The first part of the plan was to study the effects of carbon fiber length and volume fraction, and the curing procedure, on the mechanical properties of carbon fiber reinforced cement under flexural, compressive, tensile and impact loading conditions. The mix proportions adopted here were derived from the first phase of research on fresh mix workability and the strength of carbon fiber reinforced cement cured in air (curing condition "a" in section 3.2). These mix proportions were found to produce maximum flexural, tensile and compressive strengths. The mixes used in this phase of the research contain 3% and 5% volume fractions of 1/16 in. (1.5 mm) long fibers, and 3% of 1/8 in. (3 mm) fibers. In addition to that, a control mix (containing no fibers) was also included in the test program. The matrix mix proportions used in this investigation are: silica fume-binder ratio (by weight) = 0.23, water-binder ratio = 0.30, and superplasticizer-binder ratio = 0.032.

All the mixes were cured in the five different conditions introduced earlier, and were tested in flexure, tension, compression and impact at an age of 28 days. The load-deformation diagrams were determined in flexure, tension and compression tests. Based on the

generated test results, the optimum mix design and the optimum curing condition can be determined.

For each mix cured in a specific condition, the following material test specimens were constructed:

1. Six prismatic flexural specimens 1.5 x 1.5 x 6.5 in. (38.1 x 28.1 x 165.1 mm) according to ASTM C 348, for center point loading on a span of 4.8 in. (122 mm). The flexure test was performed using a servo- controlled hydraulic test machine with a constant quasi-static displacement rate;

2. Six tension briquets with a 1 in x 1 in (25.4 mm x 25.4 mm) critical cross-section (ASTM C190). The test was performed on a hydraulic test machine, with a quasi-static rate of load application, and two transducers were used for displacement (strain) measurements over a gage length of 1 in. (25.4 mm);

3. Four cylinders 2 in. (50.8 mm) in diameter by 4 in. (101.6 mm) in height (ASTM C190). Displacement rate was quasi-static, and two transducers were used for displacement (strain) measurements over a gage length of 4 in. (101.6 mm) which is the cylinder's height; and

4. Three 6 in. (152 mm) diameter by 2 1/2 in. (61.5 mm) height cylindrical impact specimens[29]. The number of blows from a standard 10 lb (4.6-Kg) mass dropping a distance of 18 in. (454.2 mm) required to cause the first visible crack and to cause ultimate failure are, by definition, the first crack and ultimate impact strengths of the material.

An outline of the test plan for this part of the investigation on carbon fiber reinforced cement is shown in Table 3.1.

Table 3.1: Test plan for hardened material mechanical properties (1 in. = 25.4 mm)

Matrix	Fiber	Curing Condition
water/binder = 0.30 silica fume binder = 0.23 superplasticizer/binder = 0.032	V_f=5%, L_f=0.0625 in	in water in air in hot water in steam room in moisture
	V_f=3%, L_f=0.0625 in	in water in air in hot water in steam room in moisture
	V_f=3%, L_f=1.125 in	in water in air in hot water in steam room in moisture
	V_f = 0%	in water in air in hot water in steam room in moisture

ratios are by weight
binder = cement + silicafume
V_f = fiber volume fraction
L_f = fiber length

b. Development of Strength with Time

In order to establish the trends in the development of strength in carbon fiber reinforced cement with time, an experimental study was performed in which a standard mix (silica fume-binder ratio = 0.23, water-binder ratio = 0.30, superplasticizer binder ratio = 0.032, fiber length = 1/16 in. = 1.5 mm, and fiber volume fraction = 5%) was cured in all five different curing conditions and tested for flexural strength at the ages of 1, 4, 7, 10, 15 and 28 days (3 specimens at each age) for every curing procedure. The flexural strength was used here to represent the strength characteristics of carbon fiber reinforced cement, noting that flexural behavior dominates the performance of the service performance of the material in its popular applications (panel-type elements).

CHAPTER 4

FLEXURAL PERFORMANCE CHARACTERISTICS

4.1. Introduction

Carbon fiber reinforced cement, as a substitute for asbestos cement, has found important applications in thin-walled floor and wall panels which act dominantly in flexure under service conditions.[5,6,12-17] Unreinforced cementitious composites have relatively low flexural strengths and fail in a brittle manner under flexural loads. Fiber reinforcement (carbon fiber reinforcement in particular) is an effective technique for improving the ultimate strength and energy absorption capacity of cementitious composites under flexural loads. Fibers improve the tensile strength, and enhance the tensile and compressive ductility of cement-based materials. The combined action of these factors results in major improvements in the performance of fiber reinforced cement composites under flexural loads.

In this chapter, first a comprehensive review of the literature on the flexural performance characteristics of carbon fiber reinforced cement composites is presented, and then the flexural test results generated in this study are discussed.

4.2. Background

The flexural strength of carbon fiber reinforced cement is influenced by the volume fraction, dimensions and type (mechanical properties) of fibers, and the matrix mix proportions. Manufacturing procedures (mixing and curing) and the geometry of test specimens are

also among the factors with important effects on the flexural behavior of the material. The following sections will review the effects of these critical factors on the flexural load-deformation characteristics and modulus of rupture of carbon fiber reinforced cement composites.

a. Fiber Volume Fraction

Typical flexural load-deflection diagrams obtained for plain cementitious matrices and fibrous cement composites with different volume fractions of carbon fibers are compared in Figure 4.1.a[14]. the dramatic improvements in flexural behavior are obvious in this figure. It is worth mentioning that the improvements in flexural behavior of cementitious composites due to carbon fiber reinforcement tend to occur at a decreasing rate with increasing carbon fiber volume fraction (this could possibly be due to potential workability problems at high fiber volume fractions).

Some important aspects of the test data in Figure 4.1.a are presented in Figures 4.1.b and 4.1.c[14]. Figure 4.1.b shows the effects of carbon fiber volume fraction on the flexural strength (modulus of rupture) of cementitious materials, and Figure 4.1.c summarizes the effects of carbon fiber volume fraction on the total flexural energy absorption capacity of the composite.

According to Figure 4.1.b, at a fiber volume fraction of about 3%, the flexural strength increases by about 120% over that of the plain matrix. The corresponding increase in flexural energy absorption capacity is about 30 times. The percentage improvements in strength and energy absorption capacity will be higher at fiber volume fractions greater than 3%.

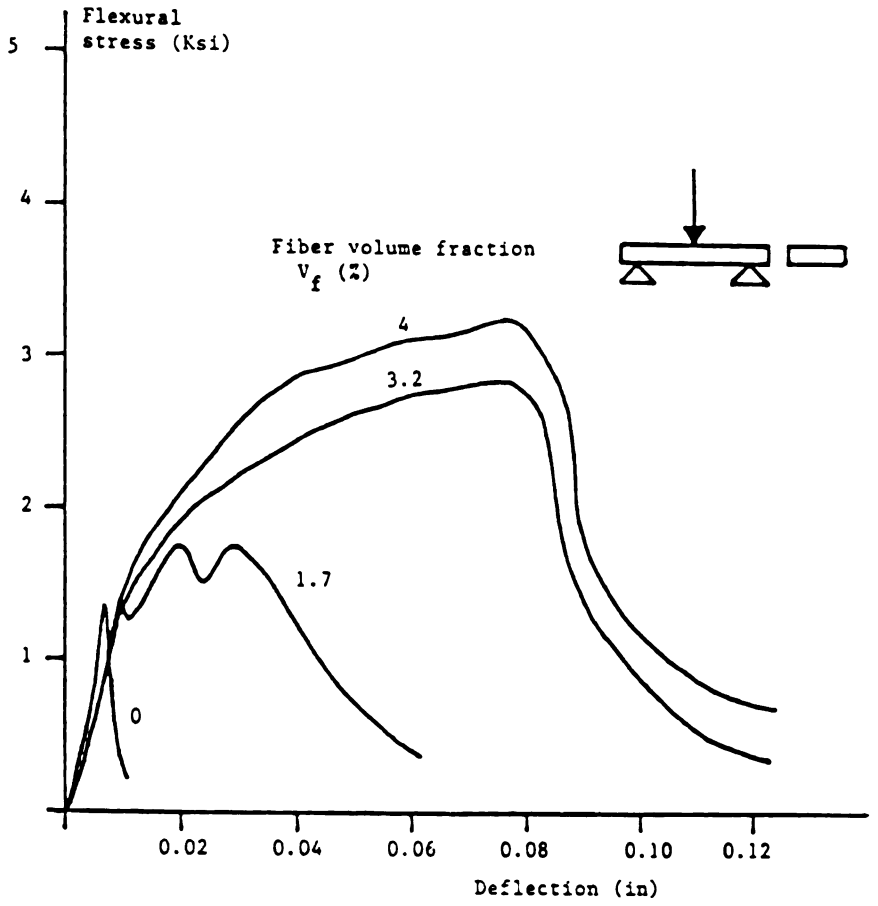

a. Flexural stress-deflection relationships

Figure 4.1: Effects of carbon fiber volume fraction on the flexural behavior of cement composites.[14] (water/cement = 0.42, methyl cellulose/cement = 0.01, fiber length = 0.4 in = 10 mm, mixing by Omni mixer, specimen dimensions = 0.4 x 1.6 x 4 in and 7 days air-curing) 1 in = 25.4 mm, 1 Ksi = 6.9 MPa, 1 lb. in = 114 N.mm

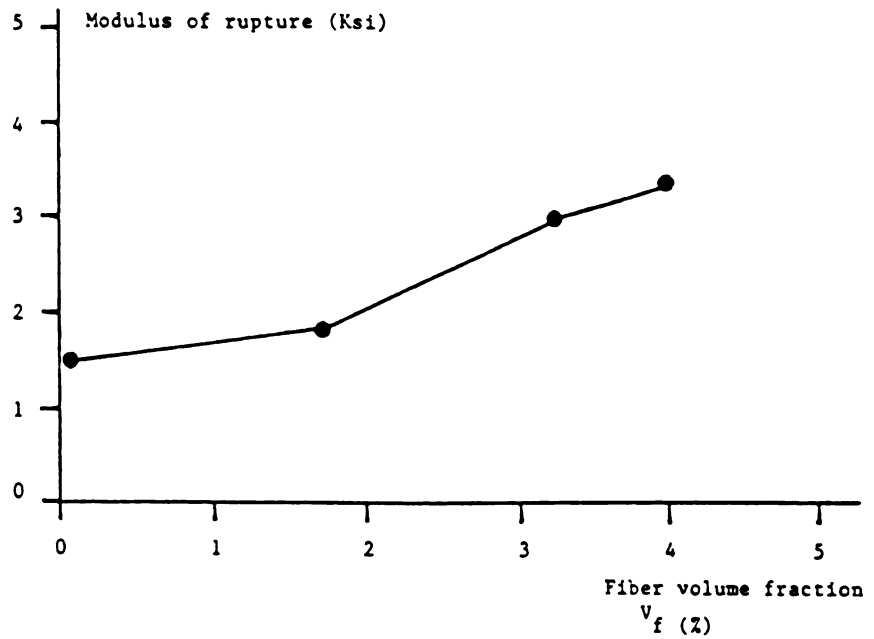

b. Flexural strength (modulus of rupture)

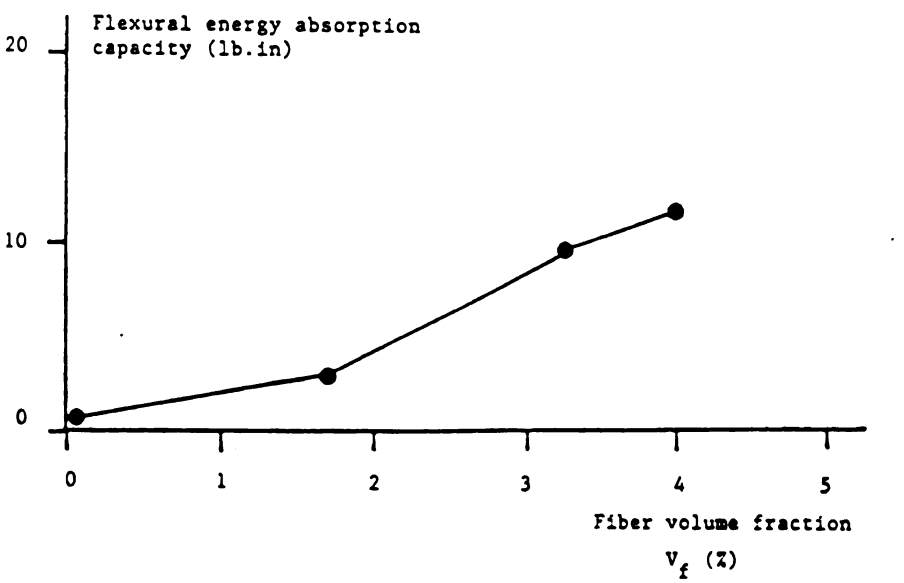

c. Flexural energy absorption capacity.

Figure 4.1 (continued)

b. Fiber Length

Figures 4.2.a, b and c show typical effects of fiber length at different volume factions on the overall flexural load-deflection relationships, and flexural strength and energy absorption capacity of carbon fiber reinforced cement composites.[12] The fiber lengths shown in Figure 4.2 range from 3 mm (0.125 in.) to 10 mm (0.4 in.), covering practiaclly all the fiber lengths used in the past. It may be concluded from Figure 4.2 that the 3 mm carbon fibers are more effective than the 10 mm ones in increasing the ultimate strength and energy absorption of cement-based materials under flexural loading. Shorter fibers are more effective, possibly because they develop less fresh mix workability problems and thus result in a better compaction of the composite. The desirable bond between carbon fibers and cementitious matrices, which results in fiber rupture prior to pull-out at relatively short embedment lengths under tension, might be another factor for the damaging effects of longer fibers on their effectiveness in improving the flexural behavior of cementitious composites.[15]

c. Fiber Tensile Strength

The effect of fiber tensile strength (or in general fiber quality) on the flexural performance of carbon fiber reinforced cement was investigated in Reference 17. As shown in Figure 4.3, the first crack strength of the fibrous composite is only slightly affected by the tensile strength of carbon fibers, and it exceeds the flexural strength of the matrix by about 10% to 50%. However, the flexural strength of carbon fiber reinforced cement as well as the deflection at maximum flexural load significantly increase as a result of the increase in fiber tensile strength (see Figures 4.3.a and b). This

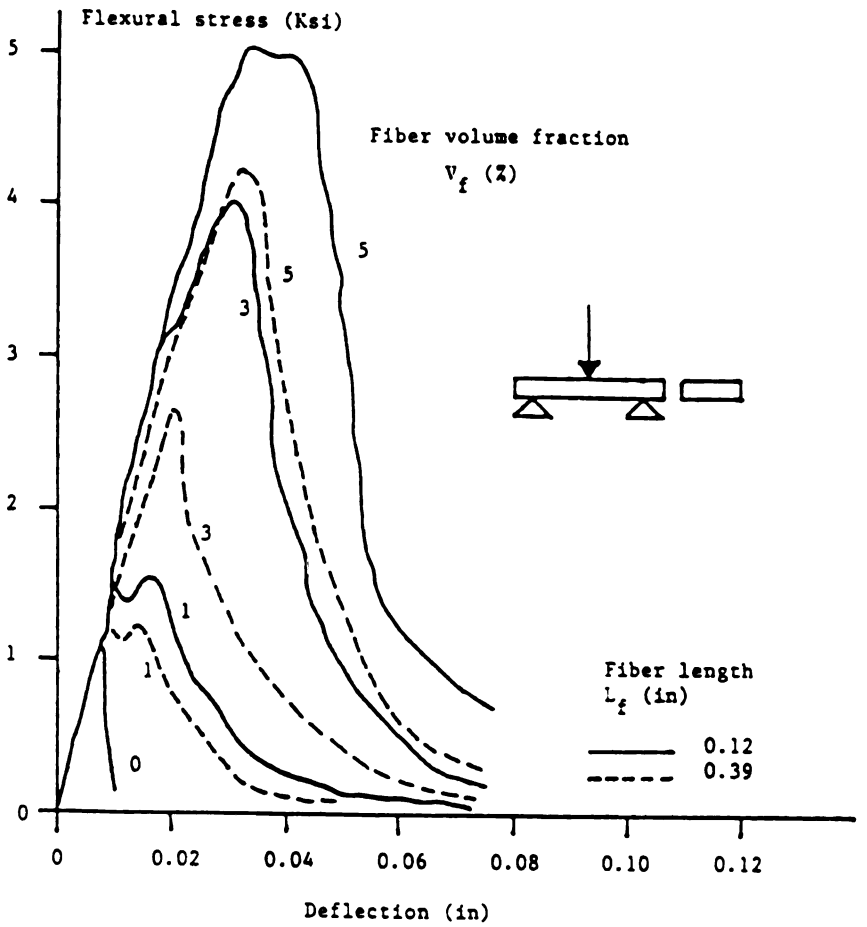

a. Flexural stress - deflection curves.

Figure 4.2: Effects of carbon fiber length on the flexural behavior of carbon fiber reinforced cement.[12] (water/cement = 0.3, silica fume/cement = 0.4, superplasticizer/cement = 0.06, mixing by mortar mixer, specimen dimensions = 0.4 x 1.6 x 4 in and autoclave curing) 1 in = 25.4 mm, 1 Ksi = 6.9 MPa, 1 lb. in = 114 N.mm

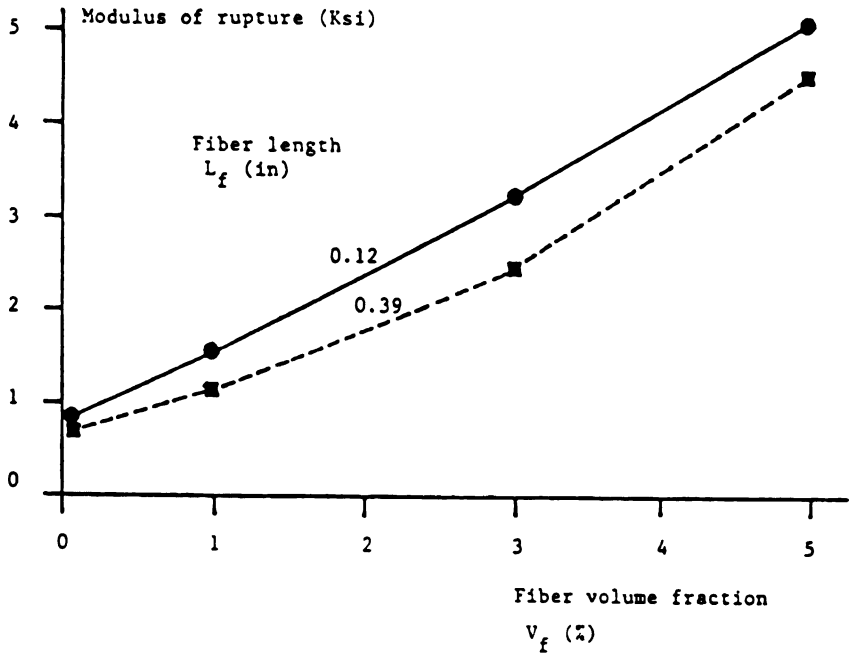

b. Flexural strength (modulus of rupture)

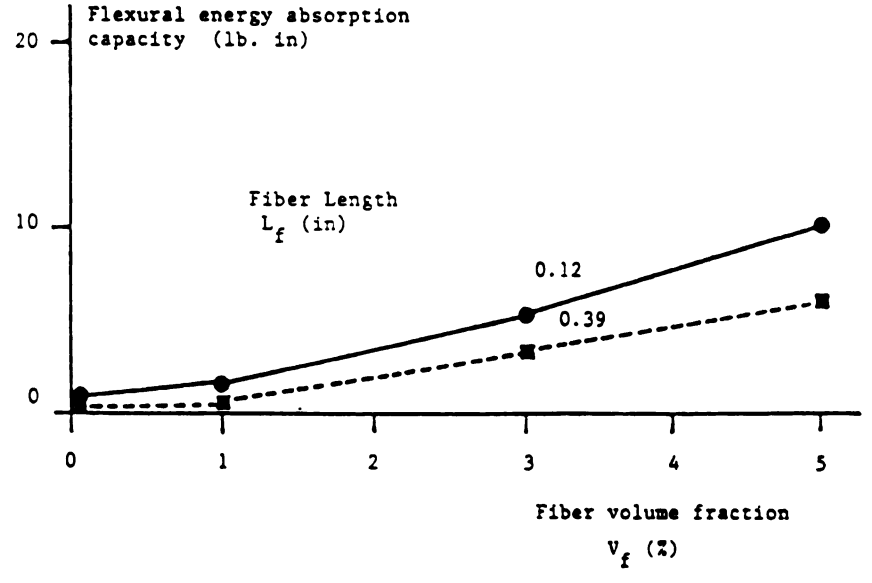

c. Flexural energy absorption capacity

Figure 4.2 (continued)

could be explained by the fact that the first crack strength of the composite is strongly related to the spacing of fibers inside the matrix. However, the ultimate flexural strength of carbon fiber reinforced cement is partly dependent on the fiber pull-out behavior and tensile strength (as well as fiber spacing). It may also be concluded from Figure 4.3 that failure of carbon fiber reinforced cement with the mix proportions of Reference 17 and fiber length of 10 mm (0.4 in.) occured dominantly by the rupture of fibers. The flexural energy absorption capacity of carbon fiber reinforced cement composite is also observed in Figure 4.3.c to increase significantly as a result of the increase in fiber tensile strength.

d. Carbon Fiber Type

Reference 15 experimented with two 3 mm (0.125 in.) long carbon fiber types, pitch type and pan type. Whereas pitch type is the common carbon fiber type used in cement composites, the pan type is a high-quality carbon fiber with higher tensile strength, higher modulus of elasticity in tension and lower diameter (or higher aspect ratio), when compared with the pitch type carbon fibers. Pan type carbon fibers are, however, more expensive than the pitch type fibers. It can be noted from Figure 4.4.a that pan type carbon fibers are significantly more effective than the pitch type ones in improving the flexural strength of carbon fiber reinforced cement. This was expected because of the higher strength and tensile modulus of elasticity of the pan type fibers. Another important factor that leads to the superior performance of pan type fibers is their higher aspect ratio (due to a smaller diameter) compared to pitch type fibers. The above mentioned conclusions indicate that the flexural failure of the composite material occurs dominantly by the rupture of

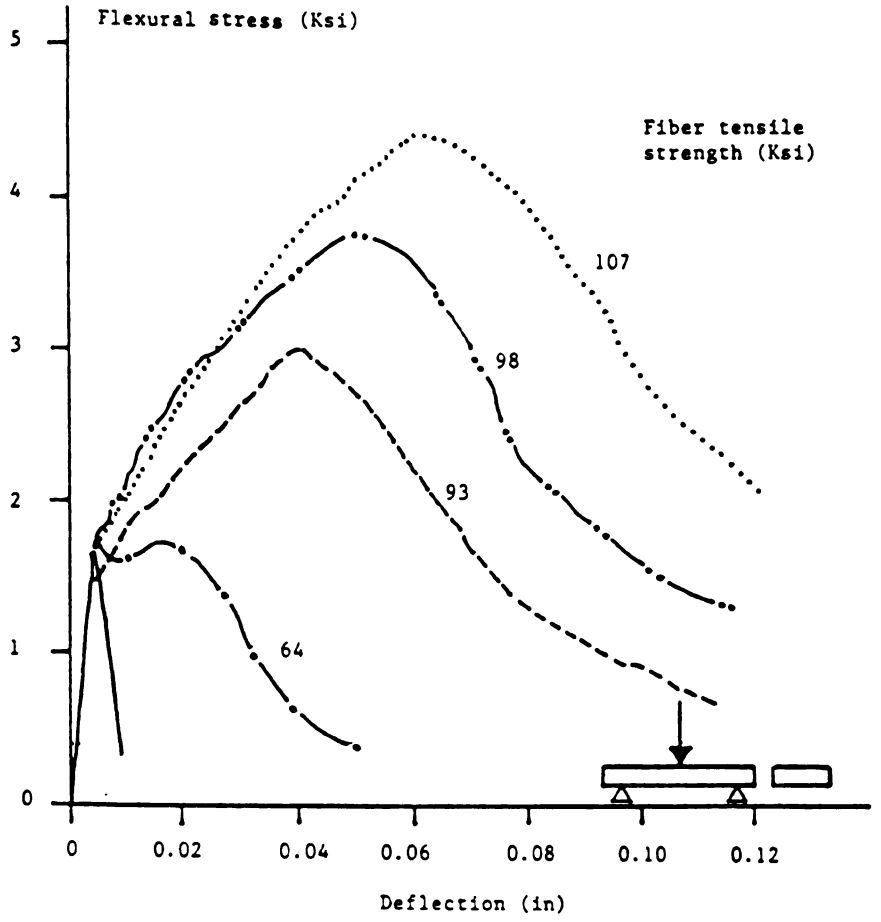

a. Flexural stress - deflection curves

Figure 4.3: Effects of fiber tensile strength on the flexural behavior of carbon fiber reinforced cement.[17] (water/cement = 0.50, silica sand/cement = 0.5, methyl cellulose/cement = 0.005, defoaming agent/cement = 0.001, fiber length = 0.4 in = 10 mm, fiber volume fraction = 3%, mixing by Omni mixer, specimen dimensions = 0.4 x 1.6 x 4 in and autoclave curing) 1 in = 25.4 mm, 1 Ksi = 6.9 MPa, 1 lb. in = 114 N. mm

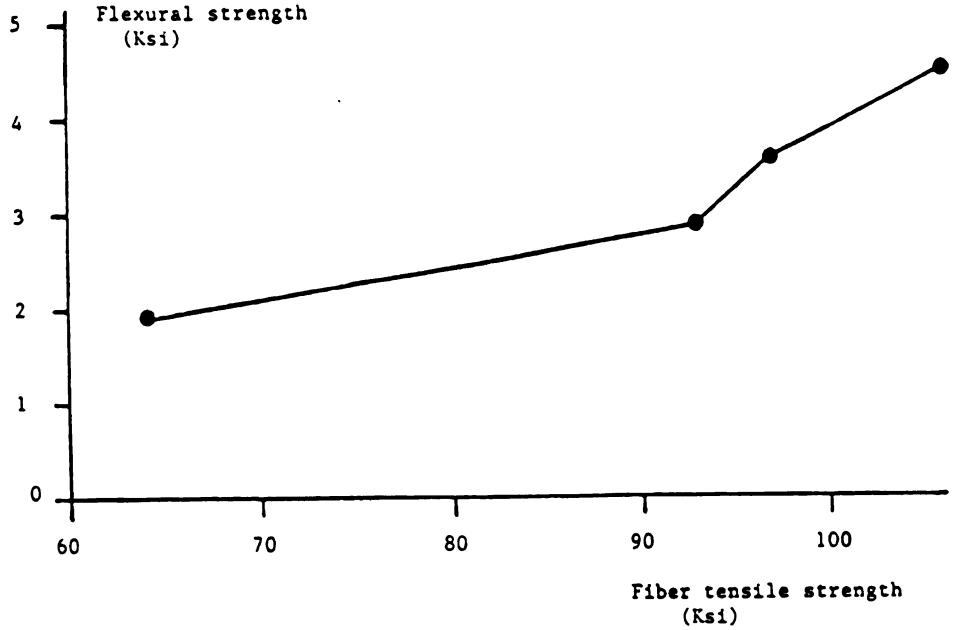

b. Flexural strength (modulus of rupture)

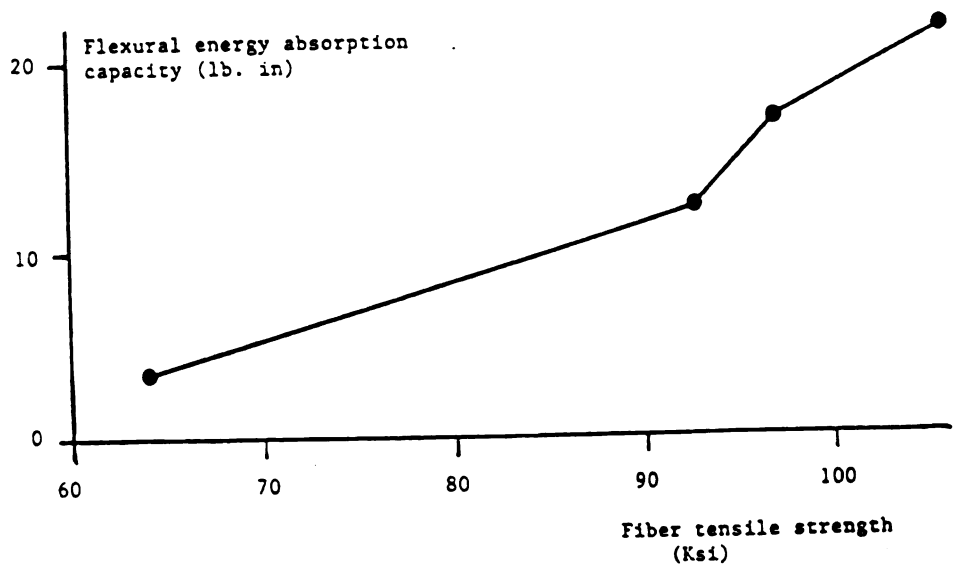

c. Flexural energy absorption capacity.

Figure 4.3 (continued)

fibers (and not by fiber pull-out).[15] Figure 4.4.b indicates that the use of pan type fibers usually reduces the toughness of the material below the values obtained for the composites with pitch type fibers. Toughness in Figure 4.4b is defined as the total energy absorption capacity (in flexure) divided by the pre-cracking flexural energy absorption. The effect of pan type fibers on toughness is especially obvious at higher fiber volume fraction. The adverse effects of pan type fibers on toughness may abe attributed to their superior bond to cementitious matrices and also to their small diameter (and consequently high surface area for bond stress). These two factors strongly encourage the more brittle type failure caused by fiber rupture. Pitch type fibers, however, especially at larger fiber volume fractions, where the bond strength is expected to be smaller, might have increased the role of fiber pull-out in flexural failure, thereby improving the material toughness.

e. Matrix Mix Proportions

The matrix of carbon fiber reinforced cementitious composites consists of the following ingredient:[5,6,12-17]

1) Dispersing agents for uniform dispersion fibers (e.g., methyl cellulose, silica fume, silica powder, or fly ash). Dispersing agents may also increase the bond between the fibers and the matrix.[30] Hence, dispersants tend to increase the flexural (tensile) strength of carbon fiber cement. In some cases, when Omni mixer is used, uniform carbon fiber cement mixtures can be achieved without the use of a dispersant; however, this may have an adverse effect on flexural strength;[14]

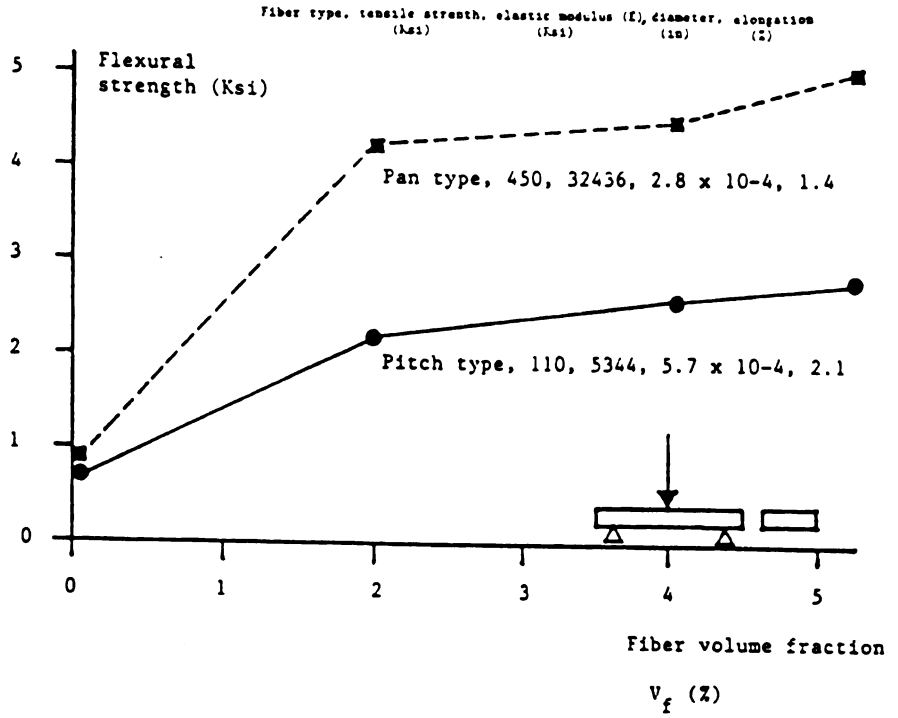

a. Flexural strength (modulus of rupture)

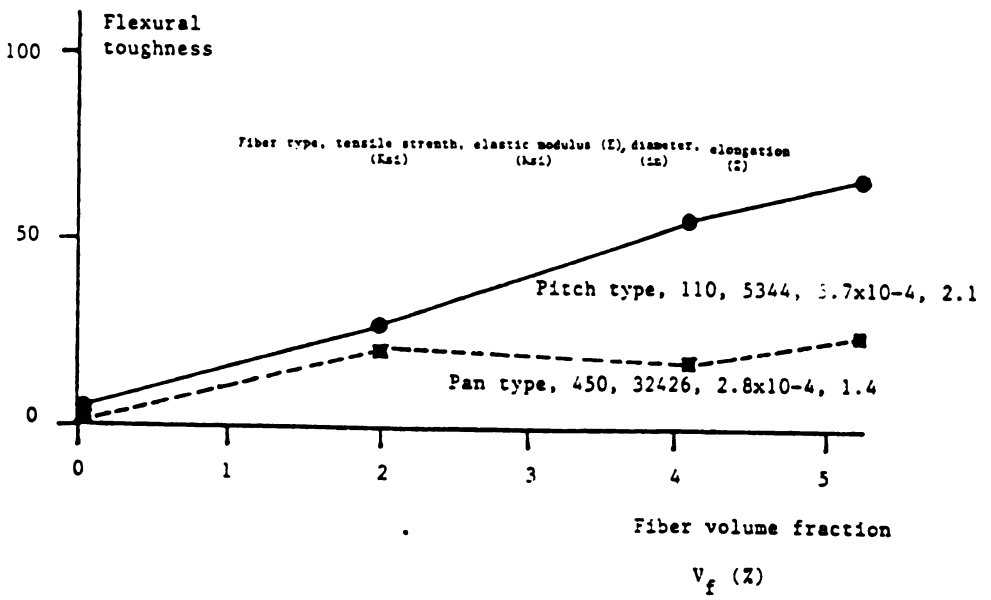

b. Flexural toughness.

Figure 4.4: Effect of carbon fiber type on the flexural performance of carbon fiber cementitious composite.[15] (water/cement = 0.47, silica powder/cement = 0.25, methylcellulose/cement = 0.01, fiber length = 0.12 in = 3 mm, mixing by Omni mixer, specimen dimensions = 0.4 x 1.6 x 4 in and 7 days air curing) 1 in = 25.4 mm, 1 Ksi = 6.9 MPa

2) Plasticizing agent or superplasticizers to improve the plasticity of the mix and consequently the compaction and strength of the composite;

3) Aggregates which can be normal-weight (e.g., silica sand) or light weight (e.g., micro-balloons which are hollow spheres of SiO_2);

4) Cement;

5) Polymers; and

6) Water.

Some ranges of the mix proportions (by weight) used by different investigators are as follows: water/cement = 0.3-0.6, superplasticizer/cement = 0.04-0.06, silica fume (or fly ash)/cement = 0-0.4, methyl cellulose/cement = 0-0.1, fiber length = 3 mm to 10 mm (0.13 in. to 0.40 in.), fiber volume fraction = 0 to 5.5%, aggregate content by volume = 0 to 50%, aggregate size up to 10 mm (0.40 in.), and polymer (latex)/cement = 0-10%. Other additives (e.g., foaming agent) can also be used with carbon fiber reinforced cement.[5,6,12-17]

The matrix mix proportion is an important factor in determining the characteristics of carbon fiber reinforced cement composites. Among the the matrix variables with important effects on the composite material performance, the following play specially important roles: 1) Strength of the matrix is a major factor deciding of the strength of the resulting composite; 2) Interfacial bond between fibers and matrix (with important effects in composite properties) is affected to a large extent by the matrix mix proportions; and 3) Aggregates, when used in the matrix, affect the distribution and spacing of fibers in the matrix and may adversly influence the strength and ductility of the composite material.

In Figures 4.5.a, b and c,[14] the flexural load-deflection diagrams, and flexural strengths and energy absorption capacities, respectively, of carbon fiber reinforced cements with different mix proportions are presented. It can be concluded from Figure 4.5 that, in the absence of a dispersing agent, the use of low water-cement ratios can lead to a relatively brittle behavior of carbon fiber cement composites. This may be explained by the damaging effect of water-cement ratio on fresh mix workability. On the other hand, the use of high water-cement ratios and high volumes of light-weight aggregates (micro balloons) lead to a reduction in flexural strength paired by an improvement in ductility (see Figure 4.5). This might be due to the adverse effects of water-cement ratio and possibly aggregates on bond between carbon fibers and the cementitious matrix.

Reference 13 has concluded that the increase in silica fume content, up to a silica fume-cementitious ratio of 0.4, tends to increase the flexural strength of carbon fiber reinforced cement (see Figure 4.6). This is due to the fineness of silica fume particles which favorably affect the coating of fibers with the cementitious matrix, and thus imrpove the fiber matrix interfacial bond strength. Silicafume-binder ratios in excess of 0.40, however, start to have some adverse effects on the composite material behavior, mainly due to the damage to fresh mix properties.

In Reference 6, the use of fly ash ("a low quality dispersant") in the mix has limited the volume fraction of carbon fibers of 3 mm (0.13 in.) long to a maximum of about 2%, and has led to a relatively low flexural strength (see Figure 4.7). It is worth mentioning that the mixes of Figure 4.7 contained 30% by volume of light-weight aggregates of an average particle size of 2 mm (0.08 in),

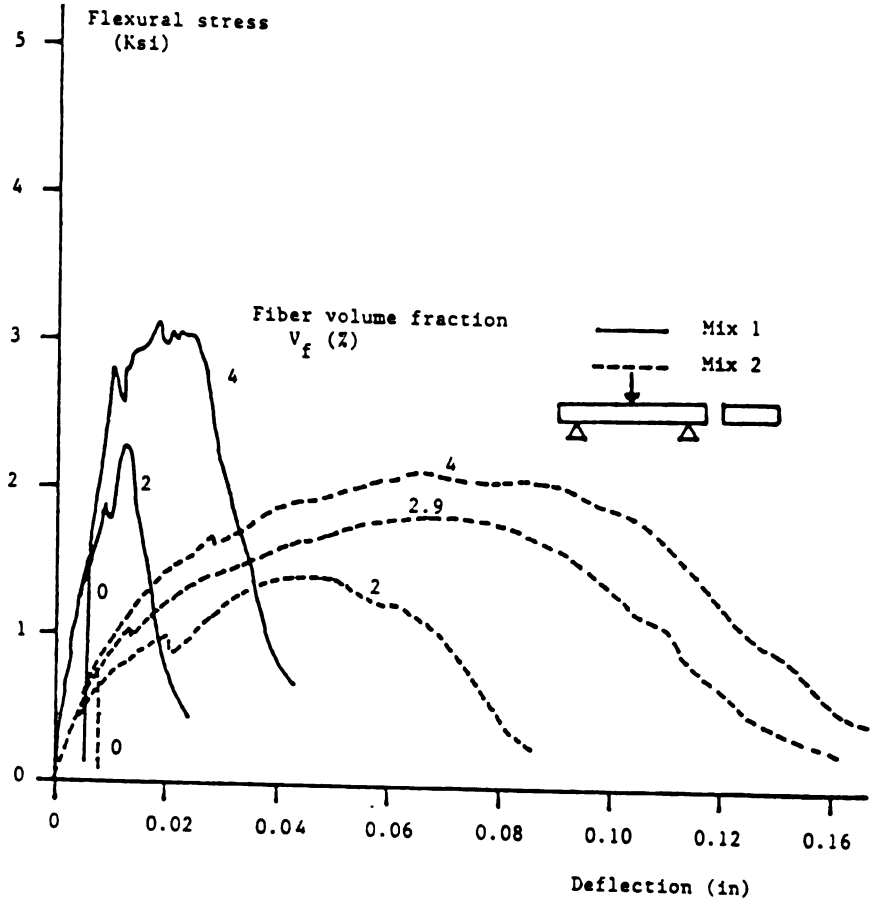

a. Flexural stress - deflection relationships.

Figure 4.5: Effects of matrix mix proportions on the flexural behavior of carbon fiber cement.[14] (fiber length = 0.4 in = 10 mm, mixing by Omni mixer, specimen dimensions = 0.4 x 1.6 x 4 in and 7 days air curing; Mix 1: water/cement = 0.30 and water reducer/cement = 0.02; and Mix 2: water/cement = 1.13, microballoon/cement = 0.7 and methyl cellulose/cement = 0.009) 1 in = 25.4 mm, 1 Ksi = 6.9 MPa, 1 lb. in = 114 N. mm

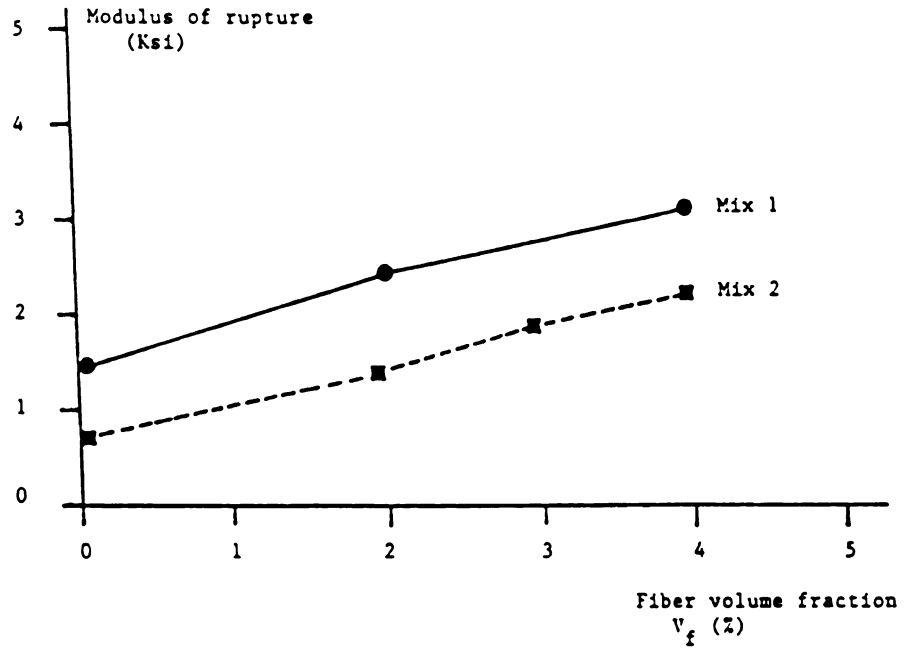

b. Flexural strength (modulus of rupture)

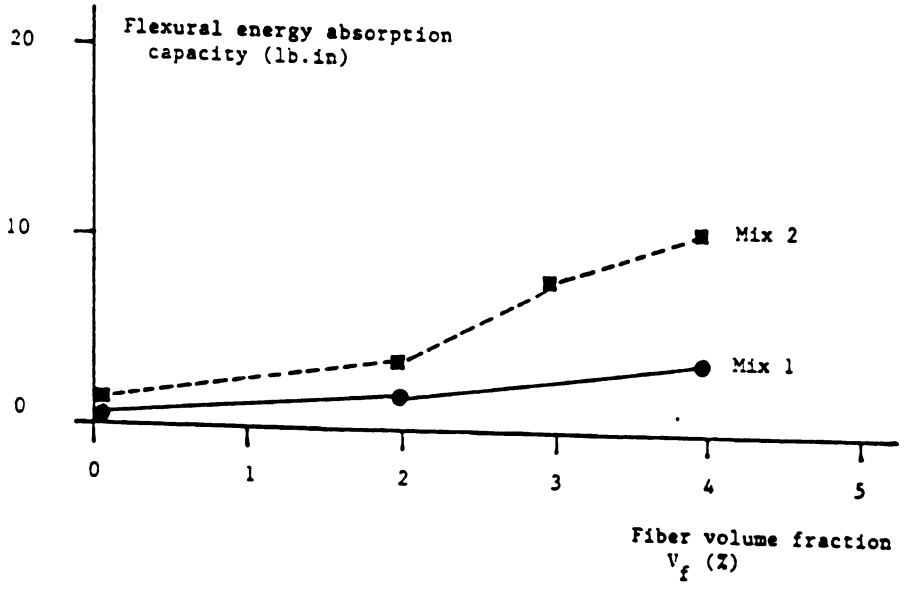

c. Flexural energy absorption capacity.

Figure 4.5 (continued)

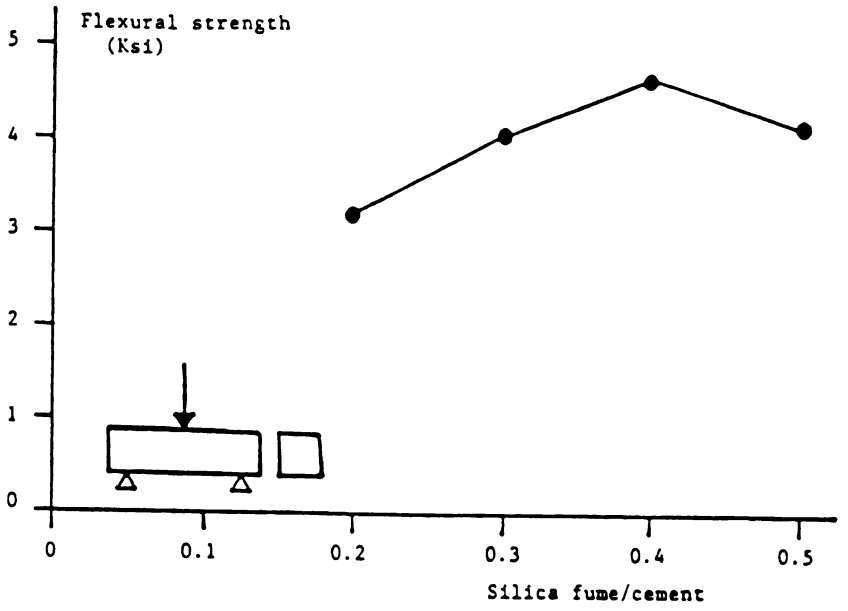

Figure 4.6: Effects of silica fume contents on the flexural strength of carbon fiber reinforced cement.[13] (water/cement = 0.3, water reducing agent/cement = 0.08, fiber length = 0.4 in = 10 mm, fiber volume fraction = 5%, mixing by mortar mixer, specimen dimensions = 1.6 x 1.6 x 4 in and autoclave curing) 1 in = 25.4 mm, 1 Ksi = 6.9 MPa

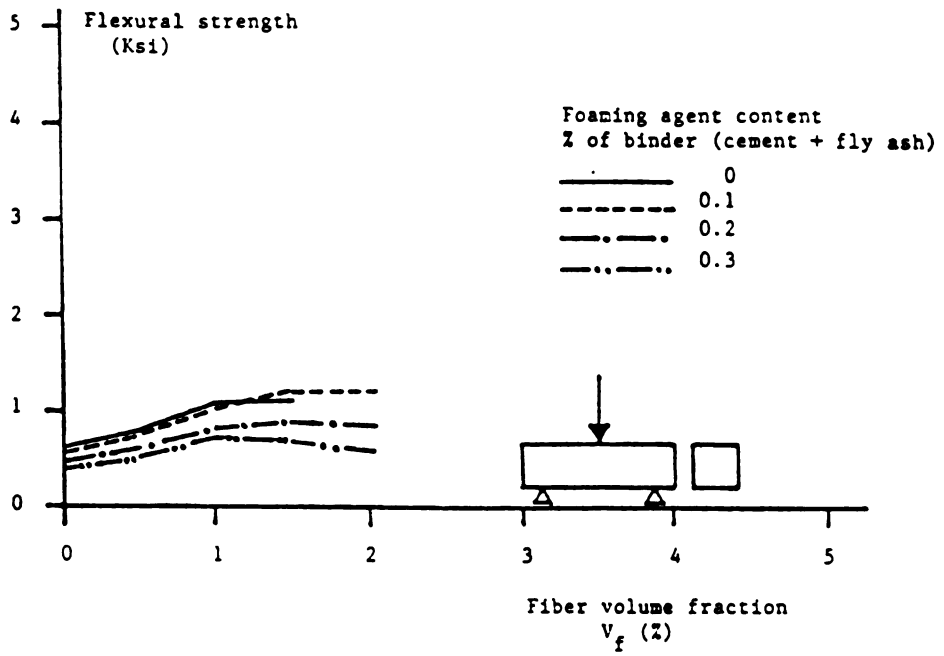

Figure 4.7: Effects of fly ash and foaming agent contents on the flexural strength of lightweight carbon fiber reinforced cement.[6] (fly ash/cement = 1 light-weight aggregate content (by volume of cement + flyash) = 0.3 and size = 0.05-0.1 in = 1.2 - 2.5 mm, fiber length = 0.12 in = 3 mm, mixing by mortar mixer, specimen dimensions = 1.6 x 1.6 x 4 in and autoclave curing) 1 in = 25.4 mm, 1 Ksi = 6.9 MPa.

and their water-cement ratios were selected to give comparable workabilities (flows) for all mixes.

The superplasticizer content had limited effects on the flexural strength of carbon fiber cements tested in Reference 13 (see Figure 4.8). However, an increase in superplasticizer-cement ratio beyond 8% had some adverse effects on the flexural strength of the composite. The use of foaming agents in Reference 6 has generally led to reductions in the flexural strength of carbon fiber cement composites due to the increase of air voids see Figure 4.7).

The use of 5% latex (by weight of binder) in carbon fiber cement mixtures has led to higher flexural strengths, higher flexural stiffness, and lower ductilities (see Figure 4.9).[6] The use of latex improves the bond strength between fibers and matrix. This would lead to increased strength and would encourage failure modes involving the rupture of fibers. Modification of the matrix by latex seemed to be an effective technique for improving the flexural strength and other properties of carbon fiber reinforced cement composites.[6] The hardened polymer in latex improves the material perofrmance by filling the material voids and improving the microstructure of the material. Strength, shrinkage, and impermeability properties can also be improved effectively through polymer modification of cement composites.

In order to study the effects of the fine aggregate size and content in carbon fiber reinforced cement composites, Reference 17 has tried 3 artificial silica sands at sand-cement ratio varying from 0.1 to 0.8. The grain sizes of the silica sand ranged from 0.0018 to 0.15 mm (0.00007 to 0.006 in.) for the finer sand, from 0.3 to 1.3 mm (0.012 to 0.05) in. for the sand with medium fineness and from 0.6 to 2.25 mm (0.24 to 0.089 in.) for the coarser sand. The average grain

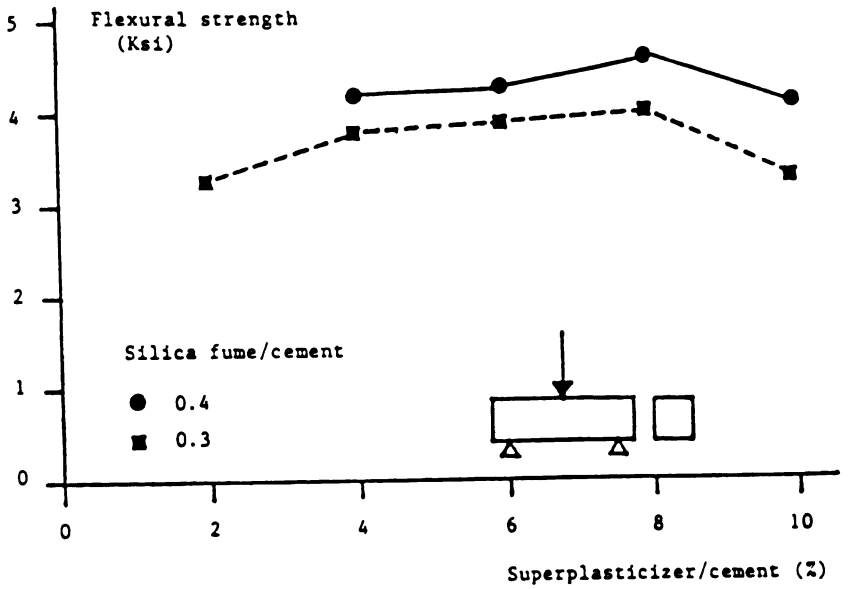

Figure 4.8: Effects of superplasticizer content on the flexural strength of carbon fiber reinforced cement.[13] (water/cement = 0.3, fiber length = 0.4 in 10 mm, fiber volume fraction = 5%, mixing by mortar mixer, specimen dimensions = 1.6 x 1.6 x 4 in and autoclave curing) 1 in = 25.4 mm, 1 Ksi = 6.9 MPa

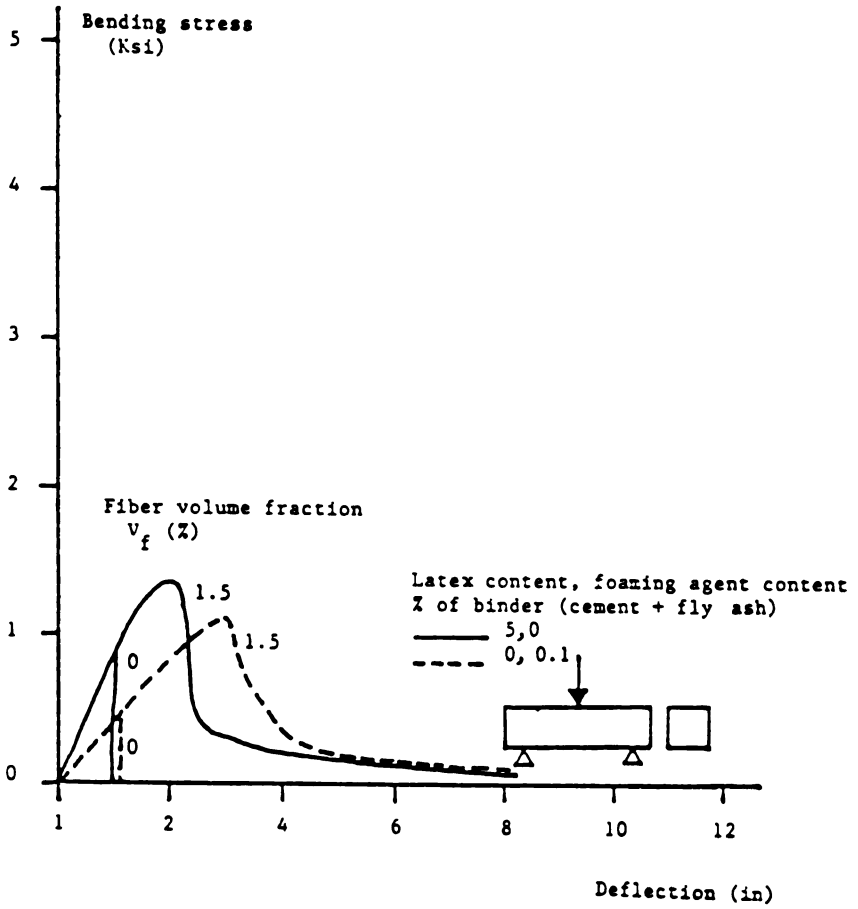

a. Flexural stress - deflection relationships.

Figure 4.9: Effects of latex on the flexural performance of carbon fiber reinforced cement.[6] (water/cement was varied to obtain a constant workability for all mixes, fly ash/ cement = 1, light-weight aggregate content (by volume of cement + flyash) = 30% and size = 0.05 - 0.1 in = 1.2 - 2.5 mm, fiber length = 0.12 in = 3 mm, mixing by mortar mixer, specimen dimensions = 1.6 x 1.6 x 4 in and autoclave curing) 1 in = 25.4 mm, 1 Ksi = 6.9 MPa, 1 lb. in = 114 N. mm

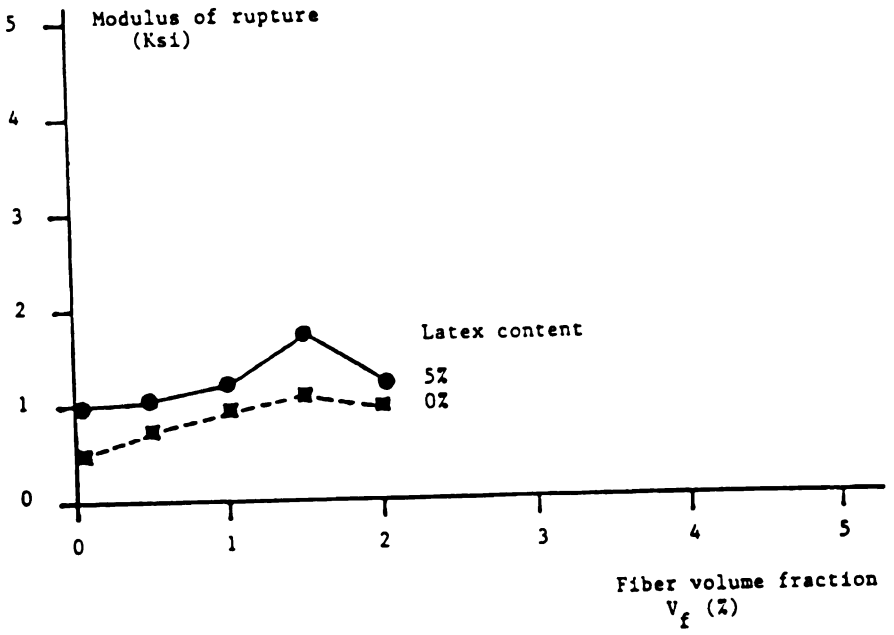

b. Flexural strength (modulus of rupture)

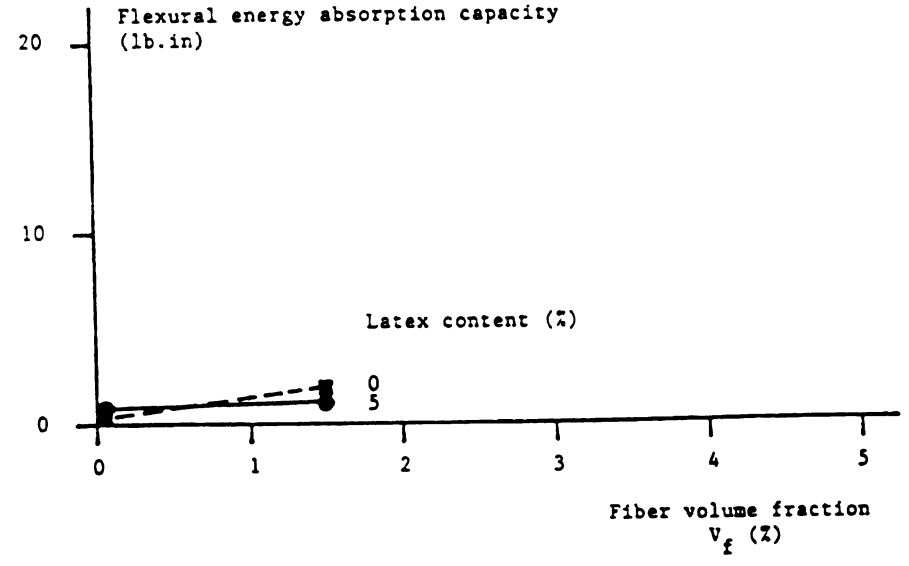

c. Flexural energy absorption capacity

Figure 4.9: (continued)

sizes were 0.05, 0.5 and 1.2 mm (0.002, 0.02 and 0.05 in.), respectively. The carbon fibers used were 3 mm (0.12) long. It is shown in Figure 4.10 that the increase in the grain size of silica sand tends to damage the flexural performance of carbon fiber reinforced cement. It can also be seen from Figure 4.10 that the increase in silica sand content also has some damaging effects on the ultimate flexural strength of the composite.

It should be noted that the average spacing of typical carbon fibers in a fibrous mix with 3% volume fraction of carbon fibers is of the order of 0.1 mm (0.004 in).[31]. Hence, aggregates with particle sizes substantially greater than 0.1 mm tend to damage fiber dispersability and reduce the positive effects of fibers on strength and ductility of the composite material. It should also be mentioned that the presence of very fine silica sand (0.05 mm = 0.002 in average grain size) might enhance the hydration process of portland cement and produce a better binder during autoclave curing.[17] It is also interesting to note that the flexural deflection at maximum flexural load decreases as the aggregate size and content increase. Some factors illustrating the effects of aggregates on the overall behavior of the composite are: 1) Aggregates with particle sizes larger than the fiber spacing tend to damage the fiber-matrix interaction by bundling the fibers during mixing, and 2) Carbon fibers are more easily broken into smaller pieces during mixing in the Omni mixer by aggregates. On the other hand, the use of aggregates in carbon fiber cement is necessary for producing a more economical material with reduced shrinkage movements.

It is worth mentioning that the background literature on carbon fiber reinforced cement consists of different mixes with broad ranges of mix variables. It is thus rather difficult to draw general

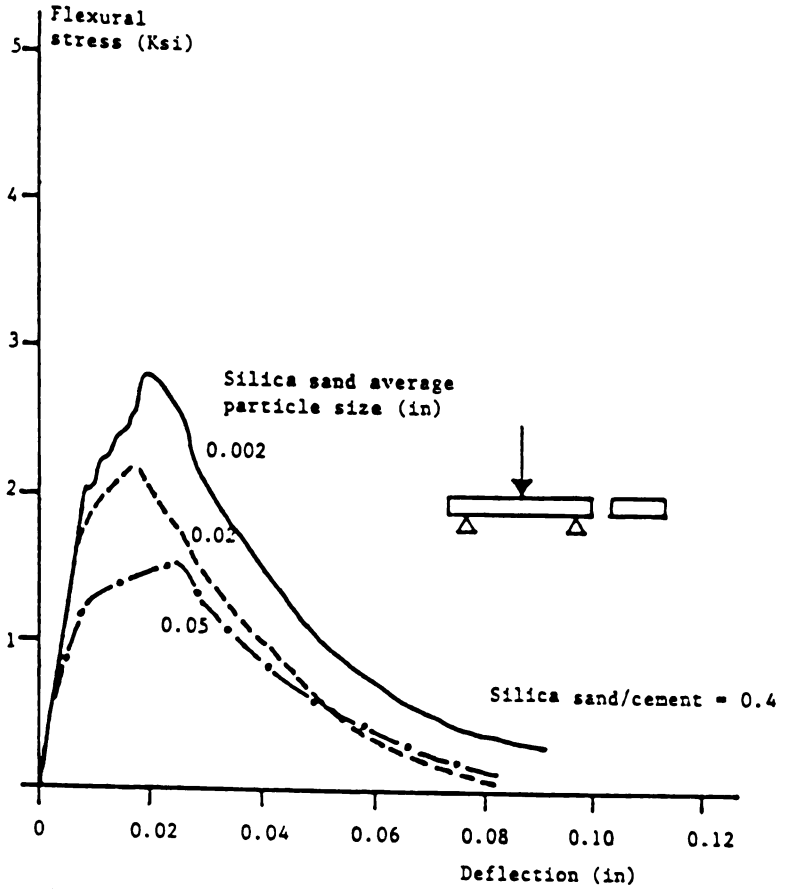

a. Flexural stress - deflection relationships

Figure 4.10: Effects of silica sand size and content on the flexural behavior of carbon fiber reinforced mortar.[17] (water/cement = 0.50, methyl cellulose/cement = 0.005, defoaming agent/cement = 0.0005, fiber length = 0.12 in = 3 mm, fiber volume fraction = 0.03, mixing by Omni mixer, specimen dimensions = 0.4 x 1.6 x 4 in and autoclave curing) 1 in = 25.4 mm, 1 Ksi = 6.9 MPa, 1 lb. in = 114 N. mm

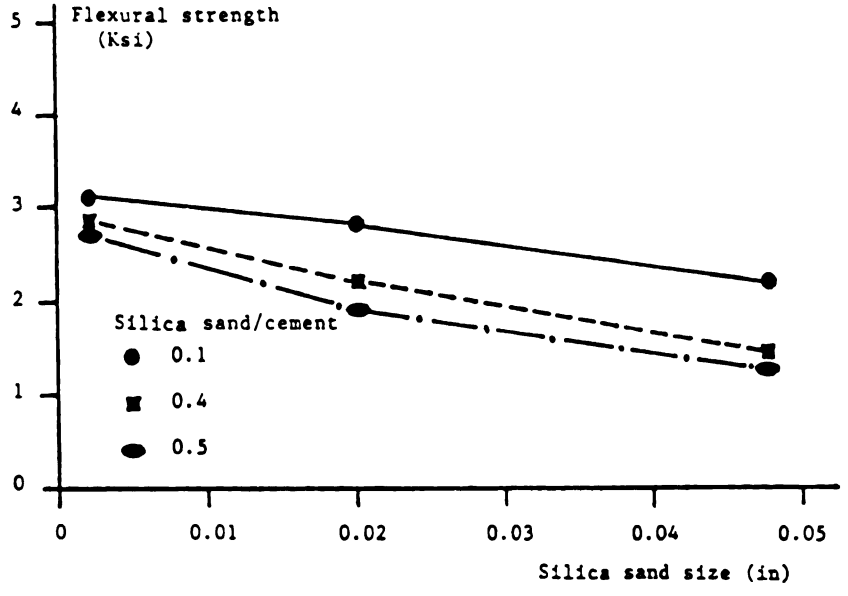

b. Flexural strength (modulus of rupture)

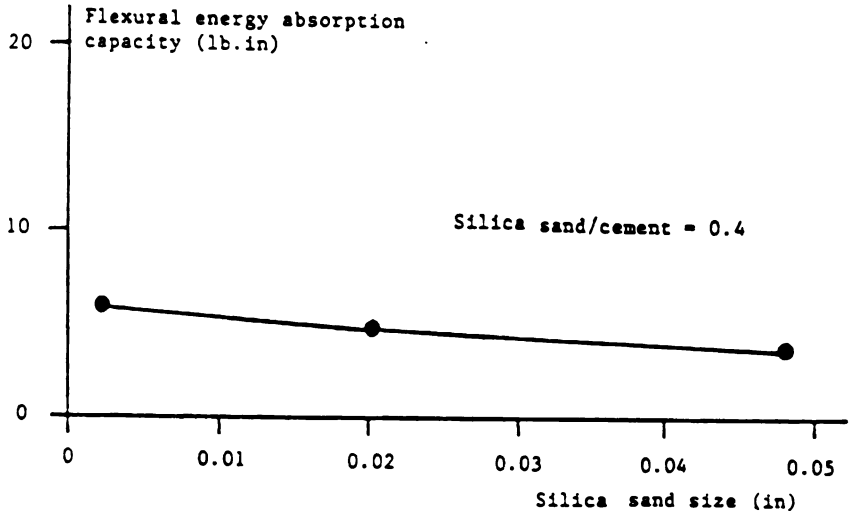

c. Flexural energy absorption capacity

Figure 4.10: (continued)

conclusions about the effects of some mix variables on the flexural characteristics of the composite material. Figure 4.11 presents flexural strengths of carbon fiber reinforced cement composites with different mix proportions.[5,6,12-17]

f. Mixing Procedure

Two mixing procedures have been examined in the literature:[5,6,12-17] 1) Mixing by Omni mixer, and 2) Mixing by mortar mix. Due to the high efficiency of Omni mixer, it can provide a significantly better coating of the mix ingredients (especially fibers) with the cementitious matrix, when compared with other mixer types. This would lead to a better bonding of the paste to carbon fibers, leading to reduced significance of the use of dispersants (e.g., silica fume or fly ash). However, very high strengths and energy absorption capacities have been achieved using both Omni and mortar mixers. An obvious advantage of mortar mixer, when compared with Omni, mixer is its worldwide availability, low price, and ease of operation.

g. Curing Procedure

Reference 14 has reported a comparison between carbon fiber reinforced cement (with a high water-cement ratio and a large fraction of micro balloons) cured in air and in autoclave. Autoclaving, which accelerates the strength gain in cementitious materials, is observed in Figure 4.12 to have a relatively small effect on the flexural strength, and to adversely influence the flexural toughness of light-weight carbon fiber reinforced cement.

Reference 15, on the other hand, experimented with three different curing procedures as follows: 1) Air curing; 2) Autoclaving;

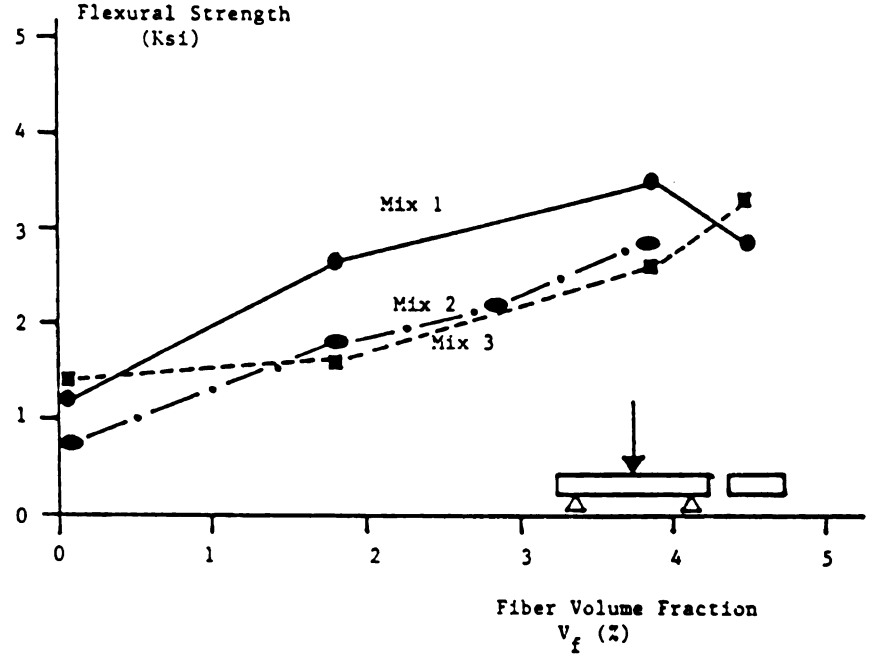

Figure 4.11: Flexural strength of carbon fiber reinforced cements with different matrix mix proportions.[14] (fiber length = 0.4 in = 10 mm, mixing in Omni mixer, specimen dimensions = 0.4 x 1.6 x 4 in and 7 day air curing; Mix 1: water/cement = 0.53, silica powder/cement = 0.5, and methyl cellulose/cement = 0.01; Mix 2: water/cement = 0.62, microballoon/cement = 0.24 and methyl cellulose/cement = 1.6%; and Mix 3: water /cement = 0.47, silica powder = 0.25, and methyl cellulose/cement = 0.01). 1 in = 25.4 mm, 1 Ksi = 6.9 MPa.

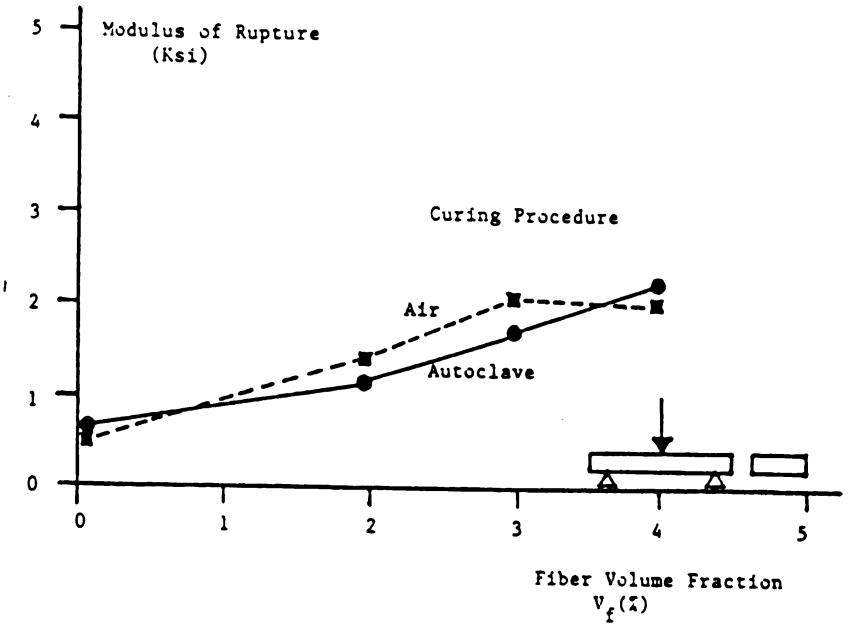

a. Flexural strength

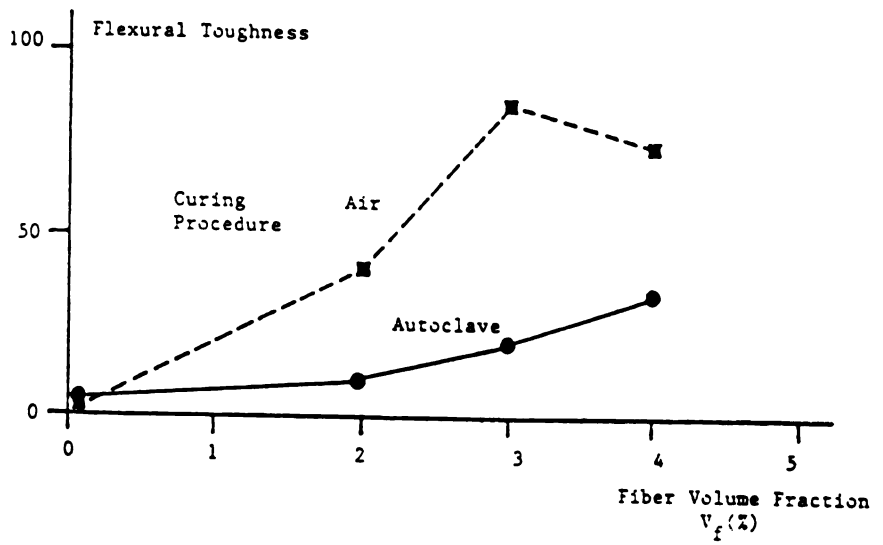

b. Flexural toughness

Figure 4.12: Effects of different curing procedures on the flexural strength and toughness of light-weight carbon fiber reinforced mortar.[14] (water/cement = 1.13, microballoon/cement = 0.71, methyl cellulose/cement = 0.009, fiber length = 0.4 in = 10 mm, mixing by Omni mixer and specimen dimensions = 0.4 x 1.6 x 4 in) 1 in = 25.4 mm, 1 Ksi = 6.9 MPa

and 3) Autoclaving followed by polymer impregnation. Autoclaving (as shown in Figure 4.13) significantly improves the flexural behavior (strength and toughness) of carbon fiber reinforced cement. These effects are possibly due to the improvements in interfacial bond strength and also in matrix properties (autoclaving in the presence of silica fume improves the matrix mechanical properties)[32]. Furthermore, polymer impregnation after autoclaving can significantly increases the flexural strength of the composite material as shown in Figure 4.13.[15] However, polymer impregnation after autoclaving can seriously damage the flexural toughness of the material (Figure 4.13.b). The effect of polymer impregnation after autoclaving can be explained by the improvements in bond due to polymer impregnation after autoclaving, which encourage failure by fiber rupture (rather than by fiber pull out) and could lead to high flexural strengths paired with low toughness characteristics.

h. Specimen Geometry

Figure 4.14 shows the effects of specimen geometry (specimen cross-section and span length) on the flexural strength of carbon fiber cement.[16] The adverse effects of the increase in size on flexural strength can justified considering by the effects of the following factors: 1) The increase in specimen size tends to increase the number of internal flaws and microcracks from which failure usually initiates; and 2) The increase in specimen size tends to change the fiber distribution and orientation to more closely resemble a three-dimensional orientation which may reduce fiber efficiency.

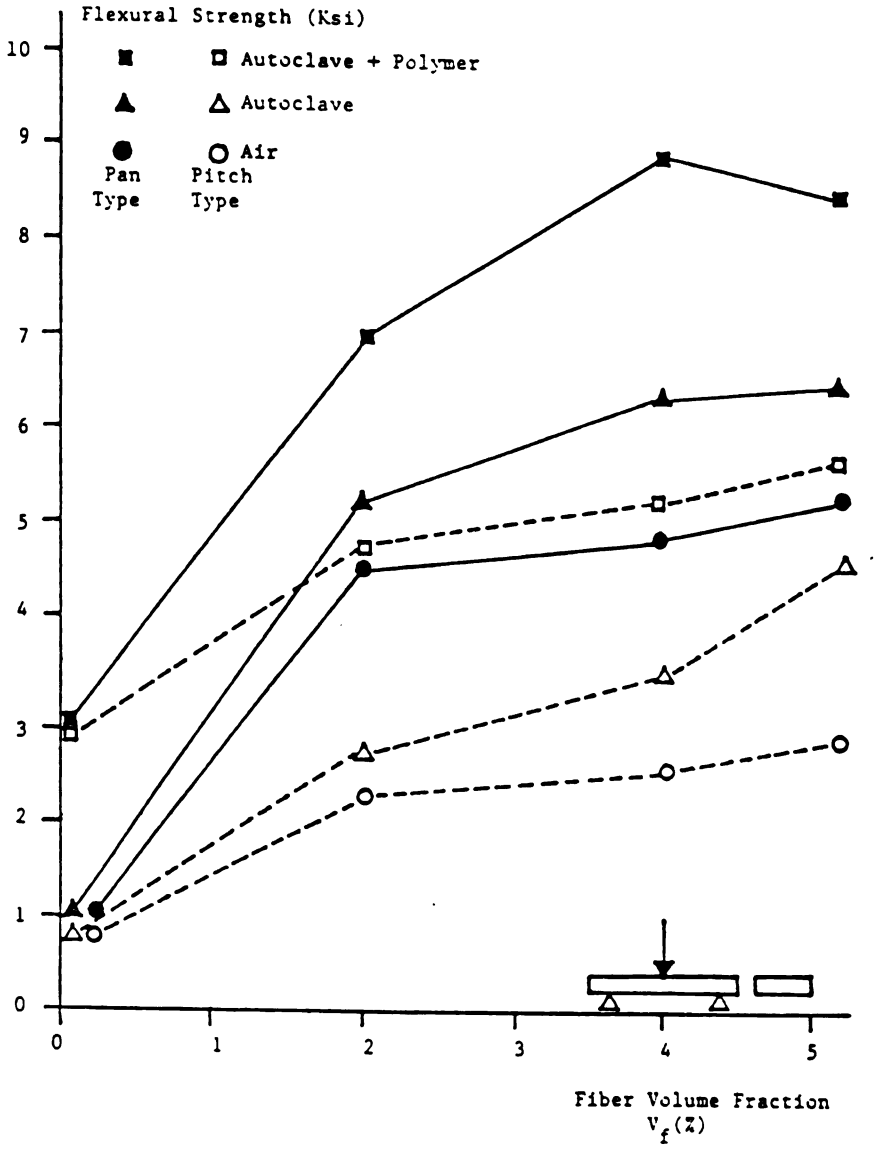

a. Flexural strength (modulus of rupture)

Figure 4.13: Effects of different curing procedures on the flexural strength and toughness of carbon fiber reinforced cement.[15] (water/cement = 0.47, silica powder/cement = 0.25, methyl cellulose/cement = 0.01, fiber length = 0.12 in = 3 mm, mixing by Omni mixer and specimen dimensions = 0.4 x 1.6 x 4 in; pitch - based fibers: tensile strength = 110 Ksi, elastic modulus (E) = 5344 Ksi, diameter = 14.5 microns and elongation = 2.1 %; and pan-based fibers: tensile strength = 450 Ksi, elastic modulus (E) = 32,436 Ksi, diameter = 7 microns and elongation = 1.4%) 1 in = 25.4 mm, 1 Ksi=6.9 MPa

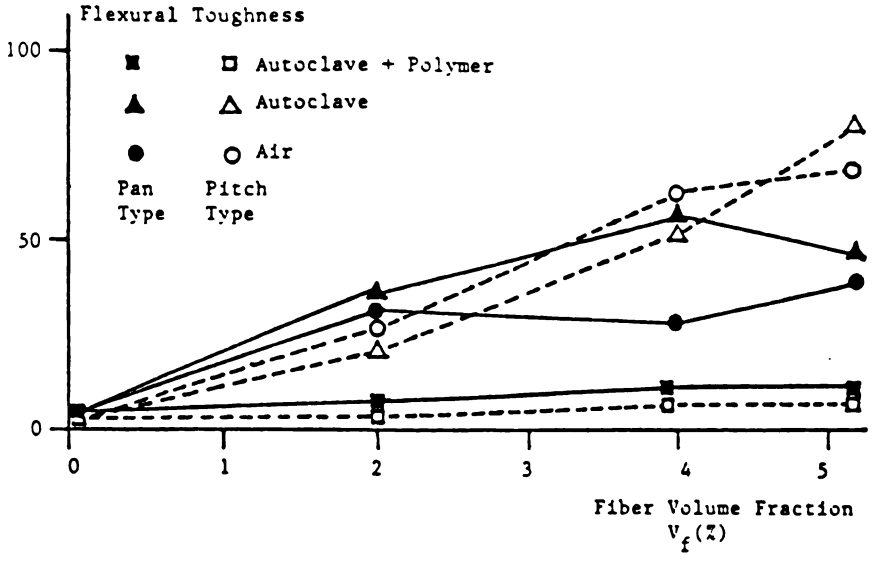

b. Flexural toughness.

Figure 4.13: (continued)

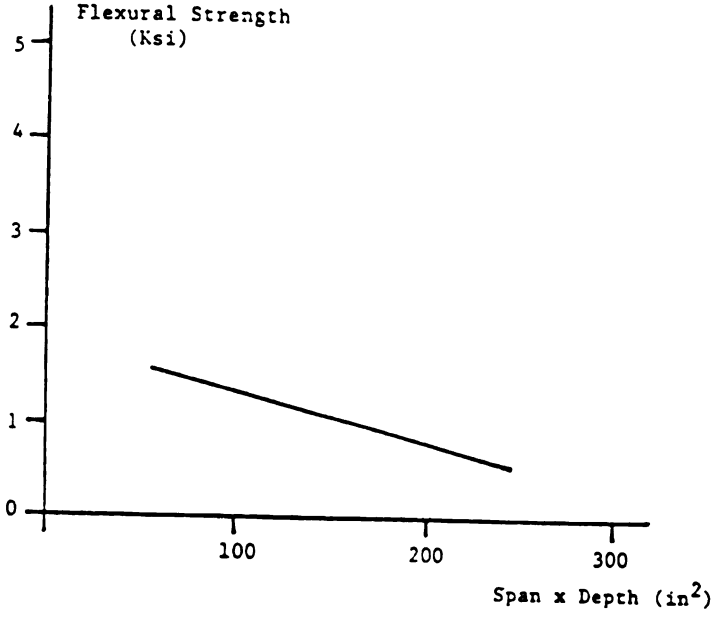

Figure 4.14: Effects of specimen size on the flexural strength of carbon fiber reinforced cement.[16] 1 in = 25.4 mm, 1 Ksi = 6.9 MPa.

4.3. Experimental Results Generated in this Study

Figures 4.15.a through 4.15.d show the flexural load-deformation relationships for the plain cementitious matrix, and the matrices reinforced with 3% volume fraction of 1/8 in. (13 mm) fibers, 3% volume fraction of 1/16 in. (1.5 mm) fibers, and 5% volume fractions of 1/16 in. (1.5 mm) fibers, respectively, cured in different conditions. Using the experimental flexural load-deflection curves presented in Figure 4.15, information on the first crack and ultimate strengths, toughness, energy absorption capacity, and stiffness of the plain and fibrous materials tested in this study after curing in different conditions was derived. This information is given in Figures 4.16 through 4.18. In these figures, energy absorption capacity is the area underneath flexural load-deflection curve up to a deflection twice that at first crack (at this deflection, the flexural load generally drops close to zero), and toughness is defined as the ratio of this energy absorption capacity to the energy absorbed up to the cracking load.

The ultimate flexural strength of carbon fiber reinforced cement composites is shown in Figure 4.16 to increase significantly as a result of carbon fiber reinforcement. With curing in air, water and moist room, comparable improvements are obtained by the use 1/8 in. fibers at 3% volume fraction, or 1/16 in fibers at 3% and 5% volume fractions. Steam curing does not produce any significant effects on the ultimate flexural strength of fibrous specimens with 3% volume of 1/8 in. or 1/16 in. fibers. With 5% volume fraction of 1/16 in. fibers, steam curing provides roughly 50% more ultimate flexural strength when compared with air, water or moist curing conditions. Hot water curing seems to give the best results as far as the ultimate flexural strength is concerned. This method of curing when applied to

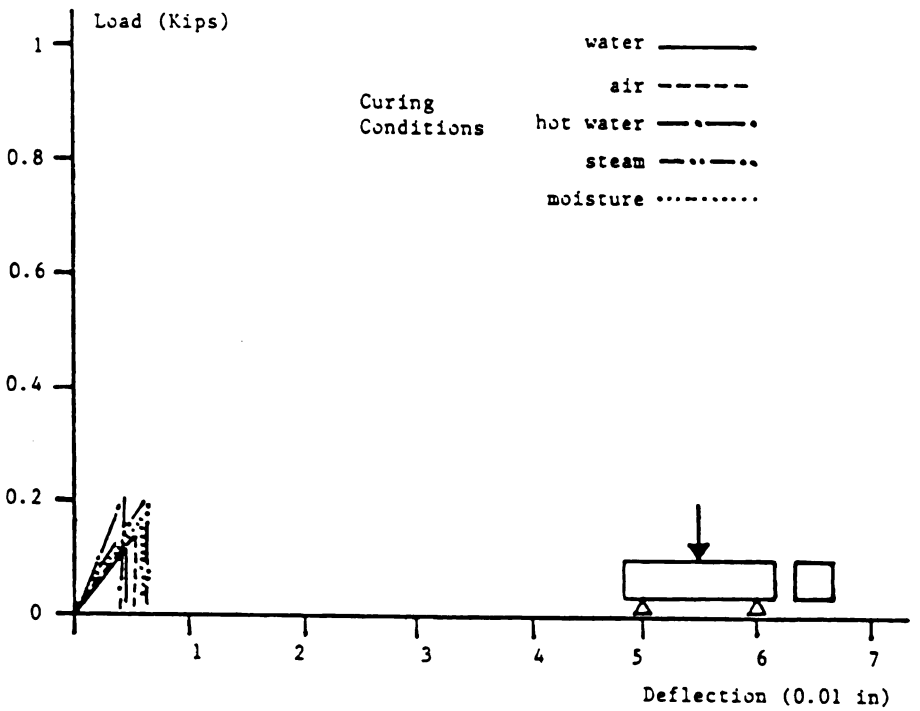

a. Plain cementitious matrix

Figure 4.15: Flexural load-deflection relationships of different carbon fiber reinforced cement mixes cured in different conditions. (water/binder = 0.3, silica fume/binder = 0.23, superplasticizer/binder = 0.032, mixing by mortar mixer and specimen dimensions = 1.5 x 1.5 x 4.8 in) 1 in = 25.4 mm, 1 Kip = 4.5 KN.

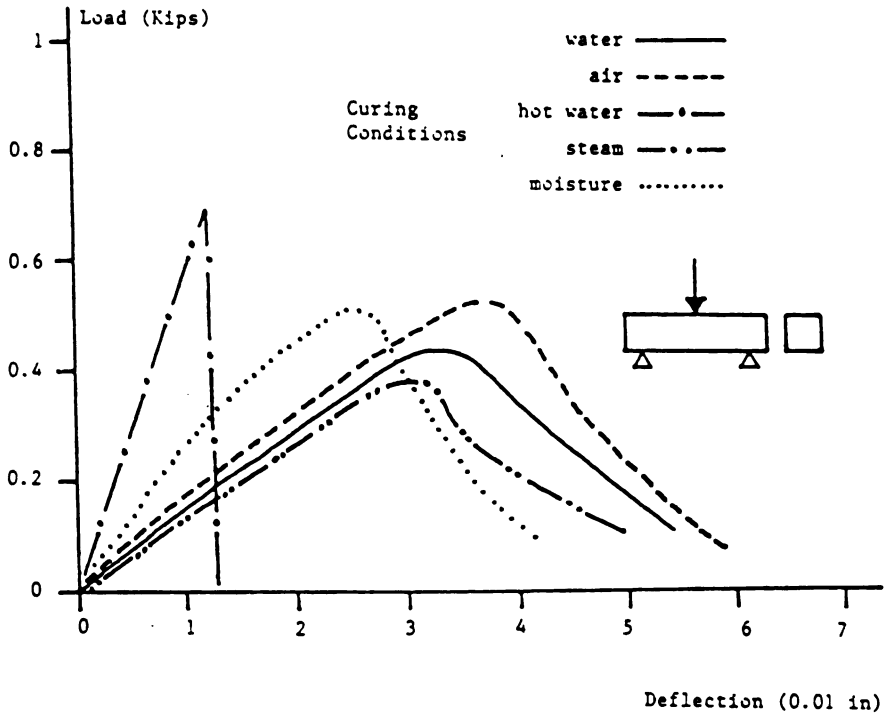

b. Fiber volume fraction (V_f) = 3%, fiber length (L_f) = 1/8 in

Figure 4.15 (continued)

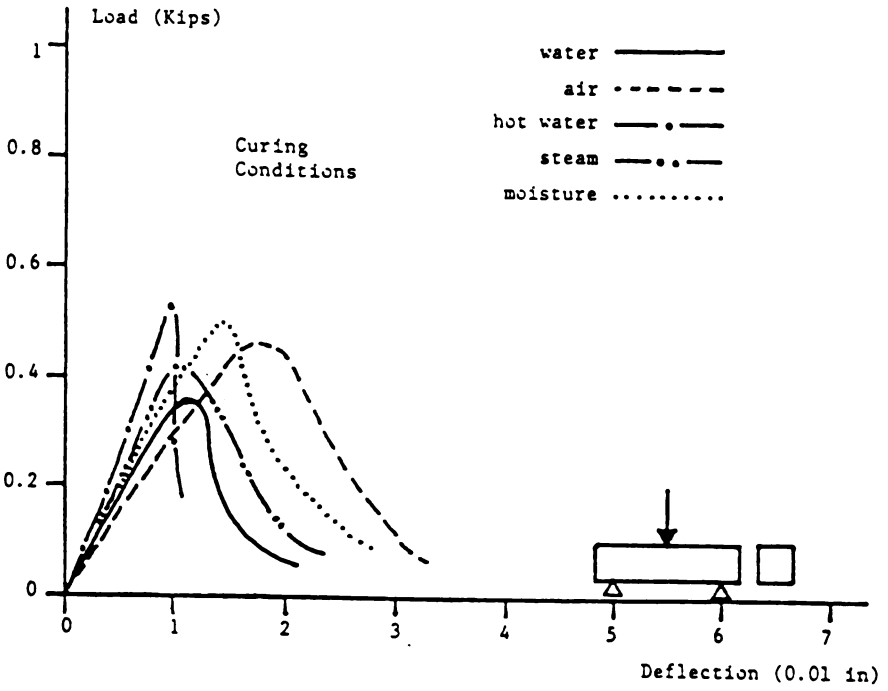

c. Fiber volume fraction (V_f) = 3%, fiber length (L_f) = 1/16 in

Figure 4.15 (continued)

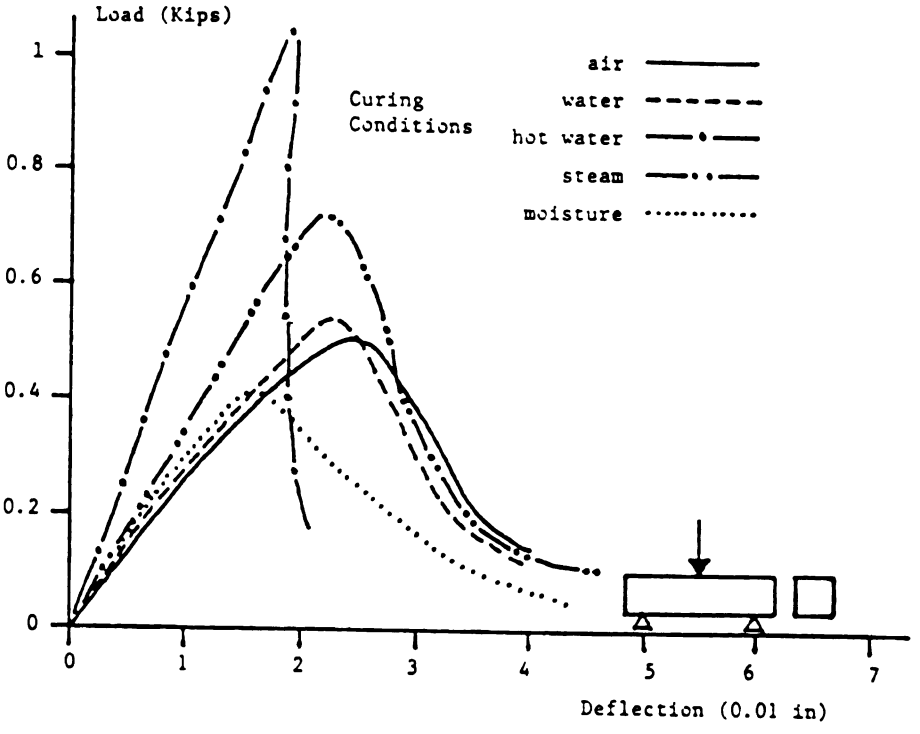

d. Fiber volume fraction (V_f) = 5%, fiber length (L_f) = 1/16 in

Figure 4.15 (continued)

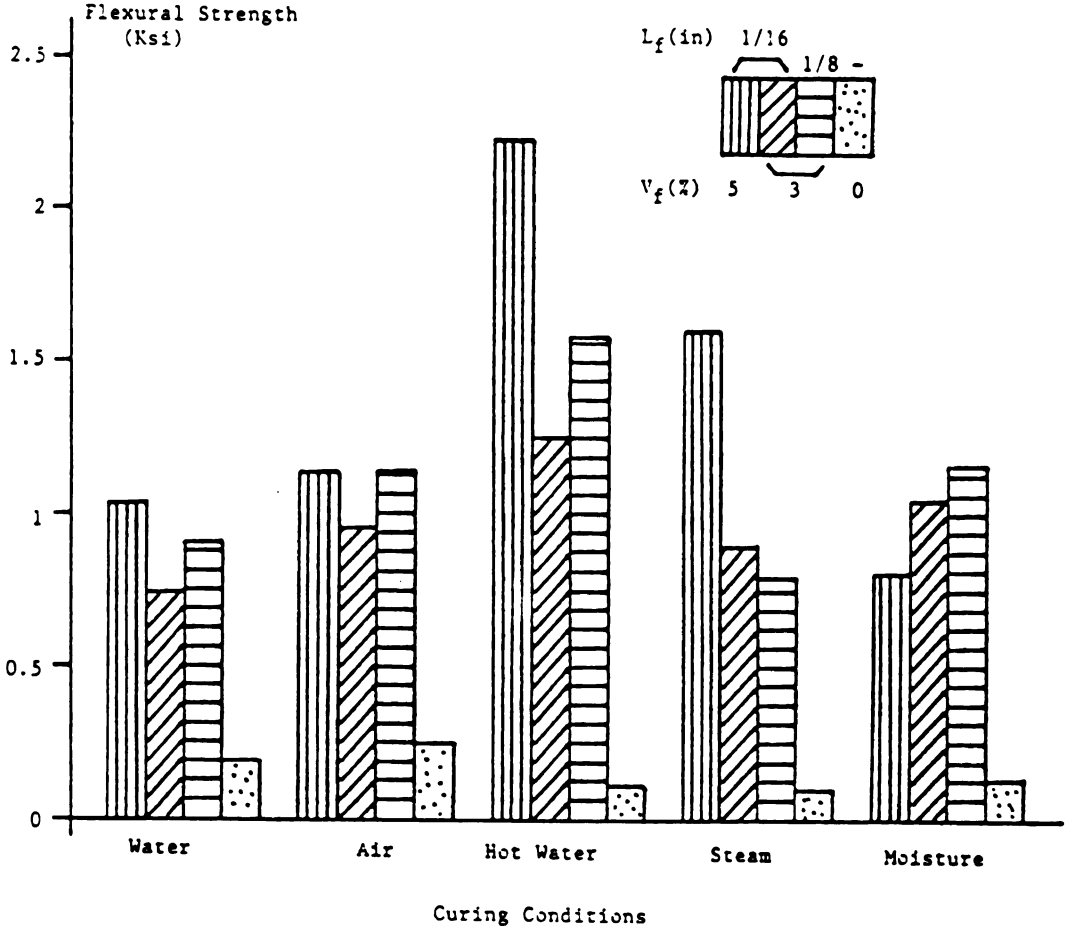

Figure 4.16: Effects of fiber reinforcement properties and curing conditions on the ultimate flexural strength (modulus of rupture) 1 in = 25.4 mm, 1 Ksi = 6.9 MPa.

specimens with 3% volume fraction of 1/8 in. and 1/16 in. fibers give roughly 50% and 30% more ultimate flexural strengths, respectively, than what could be obtained using any of the other curing conditions. Hot water curing turned out to be especially effective in application to the fibrous material incorporating 5% volume fraction of 1/16 in fibers. In this case, the ultimate flexural strength for hot water curing was about 100% more than the values obtained in air and water or by moist curing, and roughly 35% more than the ultimate strength after steam curing.

The fact that after curing in air, water or moist environment, the increase in fiber volume fraction from 3 to 5% has insignificant effects on flexural strength might be attributed to the loss in bond and material compactibility resulting from the increase in fiber volume fraction. These negative factors would reduce the benefits that could result from the increase in fiber volume fraction. Steam and especially hot water curing, however, seem to improve the fiber-matrix bond strength providing better conditions for the composite to benefit from the positive effects of the increase in fiber content.

Energy absorption is a critical aspect of the flexural behavior of cement composites which can be improved by carbon fiber reinforcement. This property is usually measured in the form of:[33] a) the total area underneath the flexural load-deformation curve up to a certain deflection (two times the cracking deflection in this study) which represents the overall energy absorption capacity of the material; and b) toughness index defined as the total energy absorption capacity divided by the pre-cracking energy absorption capacity, representing the ability of the material to absorb energy after cracking (a toughness index close to 1 is indicative of a small post-peak energy absorption capacity).

The effects of carbon fiber reinforcements and curing condition on the energy absorption capacity and toughness index of cementitious materials are shown in Figures 4.17.a and b, respectively. It should be noted that the plain cementitious materials are very brittle with minimal energy absorption capacity and toughness. Figure 4.17.a indicates that at 3% fiber volume fraction the longer 1/8 in. fibers generate, on the average, about 40% more energy absorption capacity in cement composites than the 1/16 in. fibers. The increase in volume fraction of 1/16 in. carbon fibers from 3 to 5% does not significantly change the energy absorption capacity of the composite cured in moist room, but increases the energy absorption capacity in other curing conditions (about 30% increase in air curing, and more than 100% increase in water, hot water, and stream curing). When 3% volume fraction of 1/16 in. and 1/8 in. fibers are used, steam curing and hot water curing basically reduce the energy absorption capacity of carbon fiber reinforced cement composites below the values obtained for air, water, and moist room curing. The increase in the ultimate flexural strength of composites cured in steam or under hot water tends to compensate for the negative effect of these curing conditions on post-peak behavior. The best energy absorption capacity at 5% fiber volume content is obtained for the steam-cured specimens. Specimens with 5% volume fraction cured in hot water generally have smaller energy absorption capacities than the comparable specimens cured in other conditions.

The trends in the effects of fiber reinforcement properties and curing conditions on the toughness index observed in Figure 4.17.b indicate that comparable toughnesses are obtained for composites with 3% volume fraction of 1/16 in. and 1/8 in. carbon fibers and 5% volume fraction of 1/16 in. fibers cured in air, water, moist room or steam

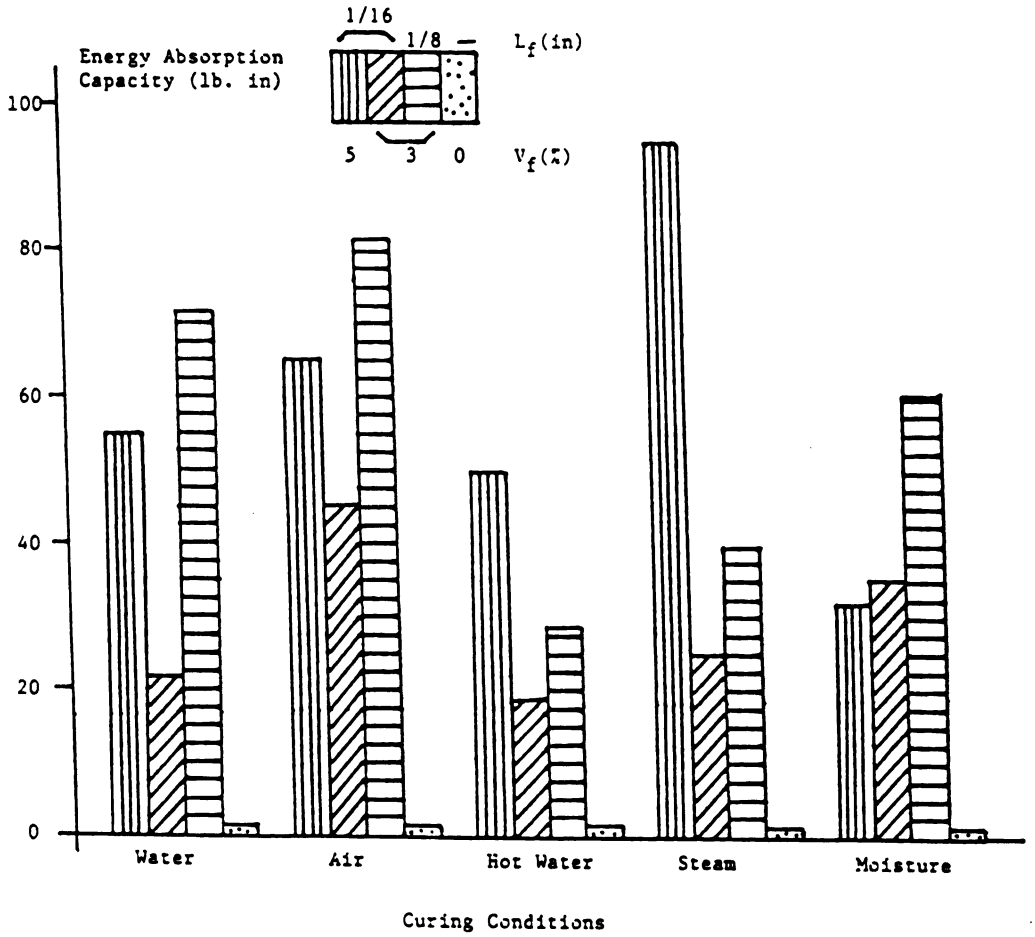

a. Energy absorption capacity

Figure 4.17: Effects of fiber reinforcement properties and curing conditions on the energy absorption capacity and toughness index under flexural loading conditions. 1 in = 25.4 mm, 1 lb. in = 114 N. mm

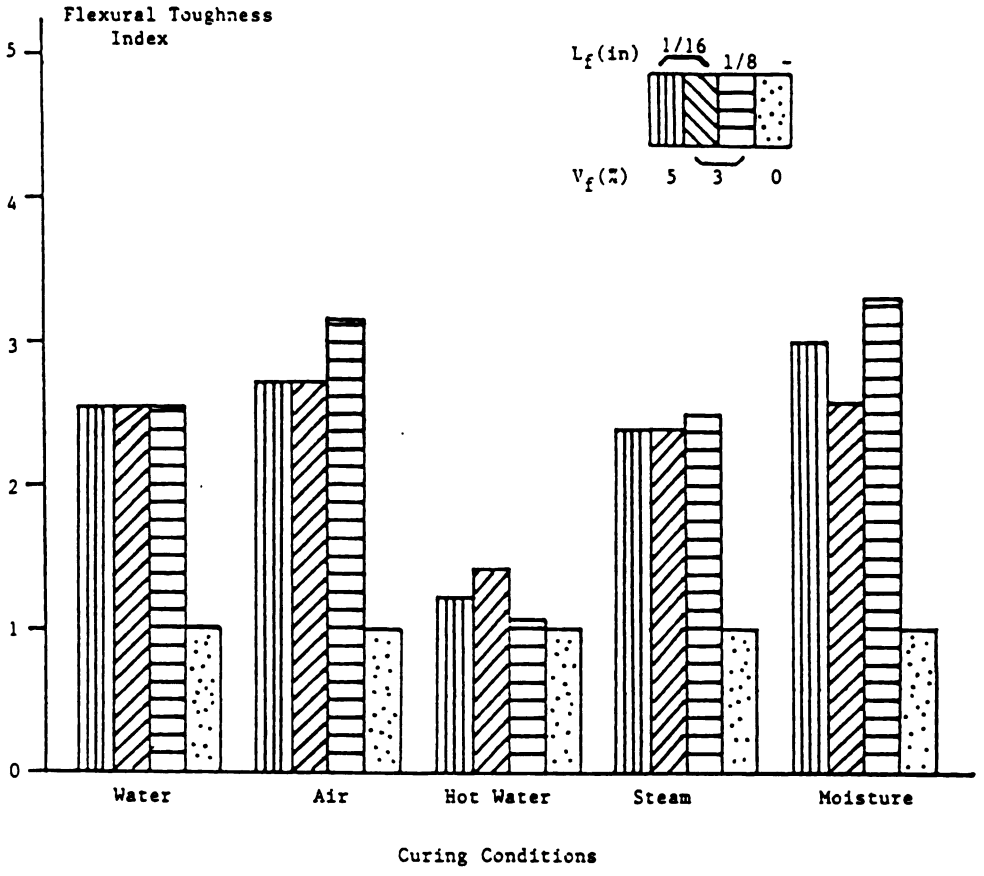

b. Toughness

Figure 4.17 (continued)

(with 1/8 in. fibers generally giving slightly better results than 1/16 in. fibers). The toughness index obtained for the fibrous specimens cured in hot water, however, is only about half the corresponding values in other curing conditions. This indicates that the fibrous composites cured in hot water are relatively brittle and absorb flexural energy dominantly prior to cracking.

Two other important aspects of the flexural behavior of fibrous cement composites are the initial stiffness and the first-crack strength of the material. Figure 4.18.a indicates that (considering the scatter of test results on initial flexural stiffness) carbon fiber reinforcement has a relatively small effect on the initial flexural stiffness of cementitious materials. Among the curing conditions, hot water curing gives consistently higher flexural stiffness values than other curing conditions.

Test results on the ratio of first crack to ultimate flexural strengths of carbon fiber reinforced cement composites presented in Figure 4.18.b indicate that this ratio is about 0.8 for fibrous composites cured in air, water, moist room and steam and it is 1.0 for fibrous specimens cured in hot water and also for plain specimens irrespective of the curing condition.

In order to investigate the development of flexural strength with time in carbon fiber reinforced cement subjected to different curing environments, flexural strength tests were performed on the material incorporating 5% volume fraction of 1/16 in fibers at ages of 1, 3, 7, 12, 20 and 30 days. Following 1 day of curing underneath a plastic sheet inside the molds, the specimens were air-dried for half a day and then were cured in air, steam, hot water, water and moist room. Figure 4.19 presents the average tendencies in flexural strength development with time under different curing conditions. The

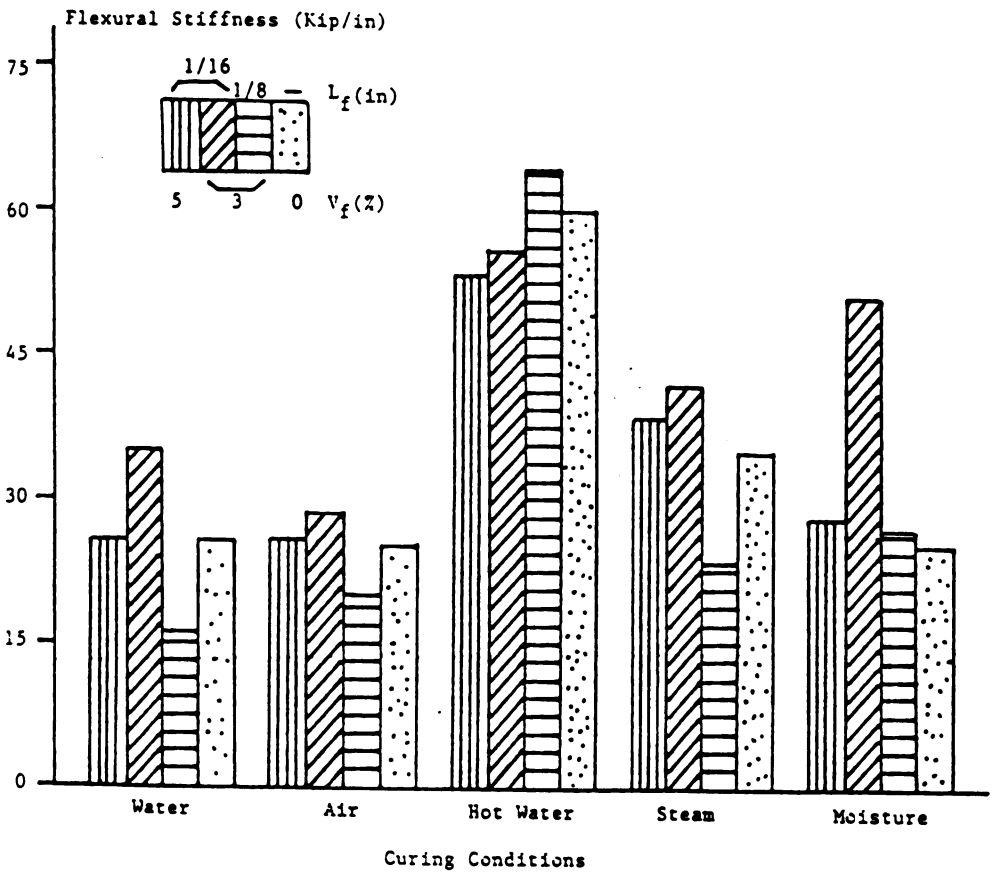

a. Initial flexural stiffness

Figure 4.18: Effects of fiber reinforcement properties and curing conditions on the intial flexural stiffness and the ratio of first-crack flexural strength-to-ultimate flexural strength. 1 in = 25.4 mm, 1 lb. in = 114 N. mm

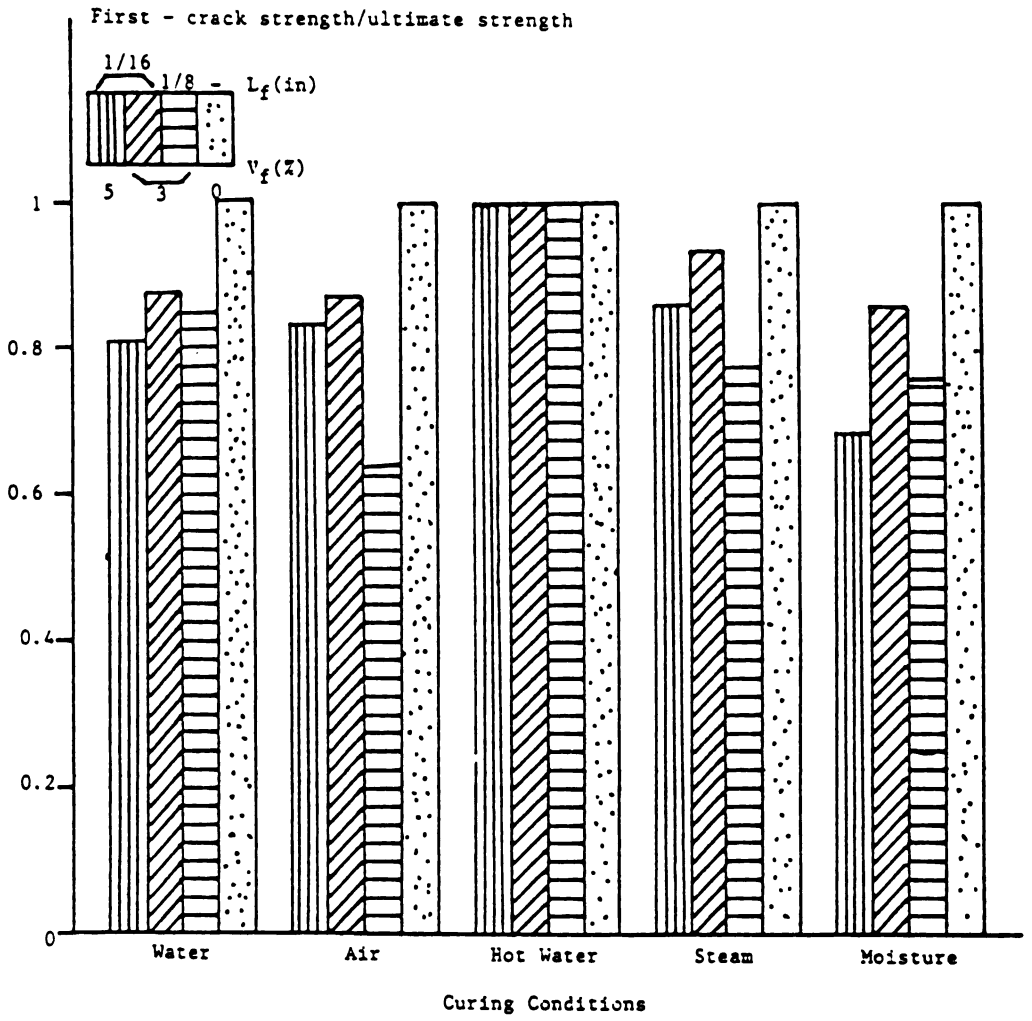

b. First-crack strength/ultimate strength

Figure 4.18 (continued)

figure indicates that hot water curing accelerates the gain in strength such that the specimens practically reach their full strength at the ages of 7 days. Other curing conditions produce similar tendencies in flexural strength development with time, and require about 14 days to provide the material with its full strength.

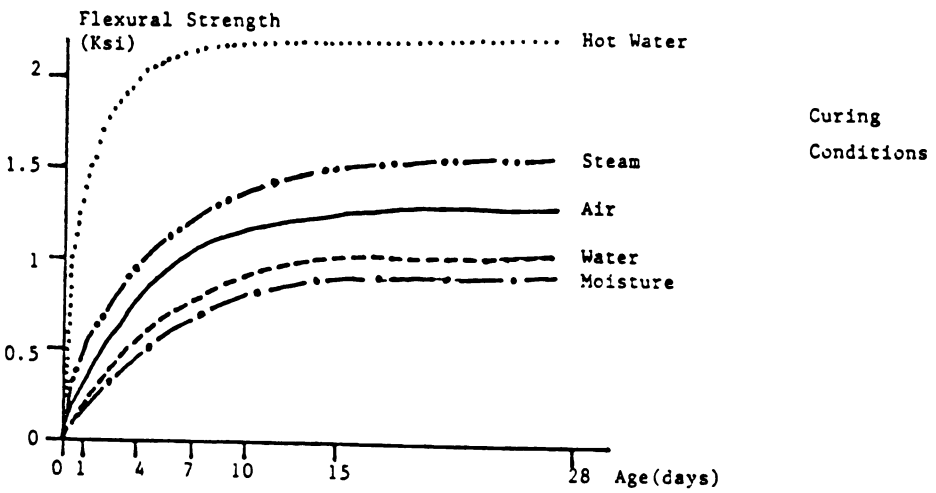

Figure 4.19: Flexural strength development with time of carbon fiber reinforced cement cured in different environments 1 Ksi = 6.9 MPa.

4.4. Summary and Conclusions

An experimental study was performed on the flexural behavior of carbon fiber reinforcd cement. The effects of fiber length and volume fraction, and curing condition on the flexural load-deformation characteristics were investigated. Two fiber lengths (1/8 in. = 3 mm and 1/16 in. = 1.5 mm), two volume fractions (3% for both fiber lengths and 5% for shorter fibers), and five curing conditions (in air, water, hot water, moist room or steam for one day and then in

air) were included in the experimental program. The flexural load-deformation relationships were characterized by ultimate flexural strength, total energy absorption capacity, toughness (representing post-peak energy absorption), initial stiffness, and first crack-to-ultimate strength ratio. The following conclusions could be derived from the experimental results generated in this study:

1. Carbon fiber reinforcement results in significant improvements in the flexural strength of cement materials. Different fiber lengths and volume fractions considered in this study produced composites with comparable flexural strengths, except for conditions with hot water and steam curing where fibers at 5% volume fraction were more effective in increasing flexural strength than those at 3% volume fractions. Hot water curing results in carbon fiber cement composites with highest flexural strength (typically about 40% more than what would be obtained by the second best curing condition which is usually in steam);

2. Carbon fiber reinforcement substantially increases the energy absorption capacity of cement-based materials. Longer fibers are more effective in increasing energy absorption. The increase in fiber volume fraction, except for the moist curing condition, also has a positive effect on energy absorption. Steam and especially hot water curing damage the ductility of material behavior and reduce its energy absorption capacity. At 5% value fraction, however, the superior flexural strength obtained by hot water and steam curing tends to provide a significant pre-peak energy absorption capacity which, to a certain extent, compensate for the negative effects of steam and hot water curing on post-peak ductility;

3. Fiber reinforcement generally increases the toughness

(post-peak energy absorption capacity) of cement composites, noting that small toughness is a deficiency of plain cementitious materials. Different fiber lengths and volume fractions considered in this investigation generate composites with comparable toughness characteristics, except that fibrous composites cured in hot water have practically zero post-peak energy absorption;

4. Carbon fiber reinforcement has a small effect on the initial flexural stiffness of cementitious materials. Hot water curing produces plain and fibrous cements with distinctly high flexural stiffnesses;

5. The ratio of first crack to ultimate flexural strength is 1.0 for plain matrices, about 0.8 for fibrous composites cured in other than hot water conditions, and 1.0 for fibrous composites cured in hot water. It should be noted that the pre-peak behavior of carbon fiber reinforced cement under increasing flexural loads involves a gradual process of micro crack propagation, and thus a distinct cracking load can be hardly distinguished.

CHAPTER 5

TENSILE PERFORMANCE CHARACTERISTICS

5.1. Introduction

Unreinforced cementitious composites are usually weak and brittle under tensile stress systems, mainly due to the relative ease of propagation and interconnection of microcracks that lead to the formation of an unstable microcrack system that grows catastrophically and causes macrocracking.[1-3] These macrocracks cannot be restrained in plain cementitious materials and thus failure in these materials is brittle. Fibers, especially the low-diameter ones like carbon, when uniformly dispersed in cementitious materials, can arrest and deflect microcracks (thus increasing the tensile strength and ductility of cementitious materials). Fibers also bridge the macrocracks in cement-based matrices and provide some restraint against their opening, thus increasing the post-peak energy absorption of the material under direct tension.

This chapter deals with the behavior of carbon fiber reinforced cementitious composties under direct tension. A comprehensive review of the literature on this topic is presented followed by the tensile test results produced in this research project.

5.2. Background

The direct tensile strength and ductility of cementitious materials increase as a result of carbon fiber reinforcement (Figure 5.1.a).[5,14]

The increase in direct tensile strength is almost proportional to the fiber volume fraction (Figure 5.1.b). Figure 5.1.a indicates that there is a significant increase in the ductility of carbon fiber reinforced cement with increasing fiber volume up to a certain limit. Thereafter, the rate of increase in ductility decreases. This can be illustrated by the potential damage to fresh mix workability and fiber dispersability (and consequently strength and especially ductility) of cementitious materials at excessively high fiber volume fractions.

Factors influencing the direct tensile behavior of carbon fiber reinforced cement, besides fiber volume fraction, include fiber geometry and material properties, matrix composition, curing conditions, and specimen size.

Reference 15 has compared the tensile behavior of carbon fiber reinforced cements containing two different types of carbon fibers. These were pitch-type and pan-type carbon fibers with diameters of 14.5 microns and 7.0 microns (5.7×10^{-4} in. and 2.8×10^{-4} in.), aspect ratios of 207 and 429 (both having a length of 3 mm = 0.125 in.), tensile strengths of 780 and 3,200 MPa (110 and 450 Ksi), elastic moduli of 3.8×10^{4} and 230×10^{4} MPa (5,400 and 32,400 Ksi), and elongations of 2.1% and 1.4%, respectively. Figure 5.2.a compares the tensile stress-strain diagrams of similar cementitious matrices reinforced with these two types of fibers. Figure 5.2.b presents the increase in the fibrous composite tensile strength resulting from the increase in volume fraction of the two fiber types.

The tensile strength of cementitious materials reinforced with pan type carbon fibers is observed, in Figure 5.2, to be more than that of comparable matrices reinforced with pitch-type fibers. This can abe attributed to the higher tensile strength and elastic modulus, and also higher aspect ratio (and consequently higher interfacial

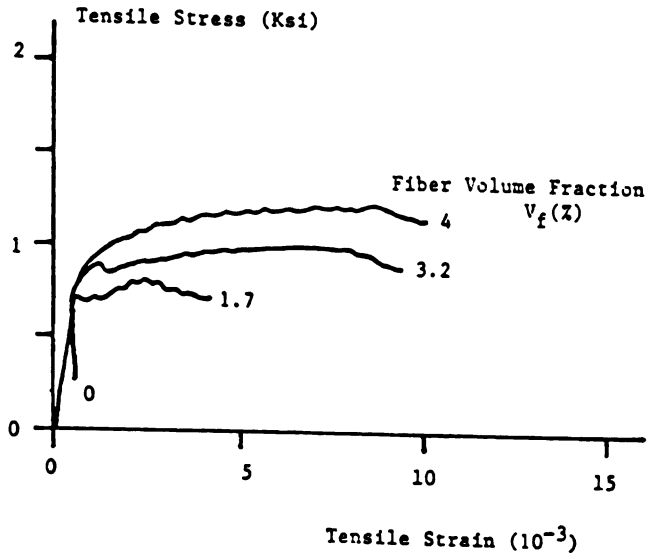

a. Overall stress-strain relationships

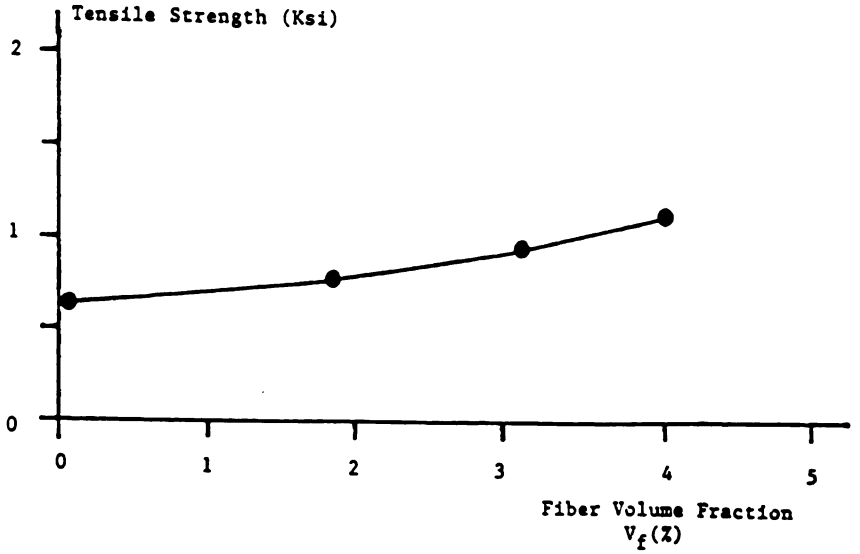

b. Direct tensile strength.

Figure 5.1: Effects of carbon fiber reinforcement on the direct tensile behavior of cementitious materials.[14] (water/cement = 0.42, methyl cellulose/cement = 0.01, fiber length = 0.4 in = 10 mm, mixing by Omni mixer, specimen's cross section = 0.47 x 1.18 in and 7 days air-curing). 1 in = 25.4 mm, 1 Ksi = 6.9 MPa

area) of the pan type fibers. Beyond a certain fiber volume percentage, however, the problems with uniform dispersion of pan-type carbon fibers (having higher aspect ratios than pitch-type fibers) in cementitious materials start to reduce their superiority over pitch-based carbon fibers. Figure 5.2.a also indicates that pitch-based carbon fibers generate cementitious composites with a better post-peak ductility, when compared with pan-based carbon fibers. This could be due to the higher elongation and lower pull-out strength (due to lower interfacial area) of pitch-based fibers compared to pan-based ones. The lower pull-out strength would encourage pull-out of fibers instead of their rupture at cracks under tensile stress systems. Fiber pull-out is an effective means of absorbing energy and providing ductility.

Reference 12 has presented the results of an experimental study on the effects of fiber length on the tensile strength of carbon fiber reinforced cement. As shown in Figure 5.3, the 3 mm (0.125 in.) carbon fibers seem to be more effective than the 10 mm (0.394 in.) fibers in increasing the direct tensile strength of cementitious composites. This can be interpreted by the fact that the longer carbon fibers tend to have some balling problems which tend to reduce their effectiveness in enhancing the tensile characteristics of cementitious materials.

Matrix composition is another important factor influencing the direct tensile behavior of carbon fiber reinforced cementitious composites. This is clearly shown in Figure 5.4[5,6,12-17] which presents the tensile strengths for different carbon fiber reinforced cementitious composites with different matrix mix proportions. Figure 5.4 indicates that the incorporation of high volume fractions of light-weight aggregates (71% by weight of cement), and the consequent increase in water-cement ratio (113% by weight) for preserving the

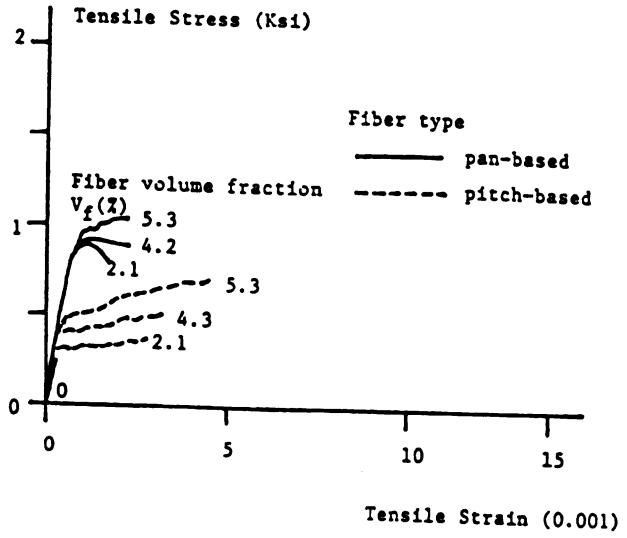

a. Overall stress-strain curves

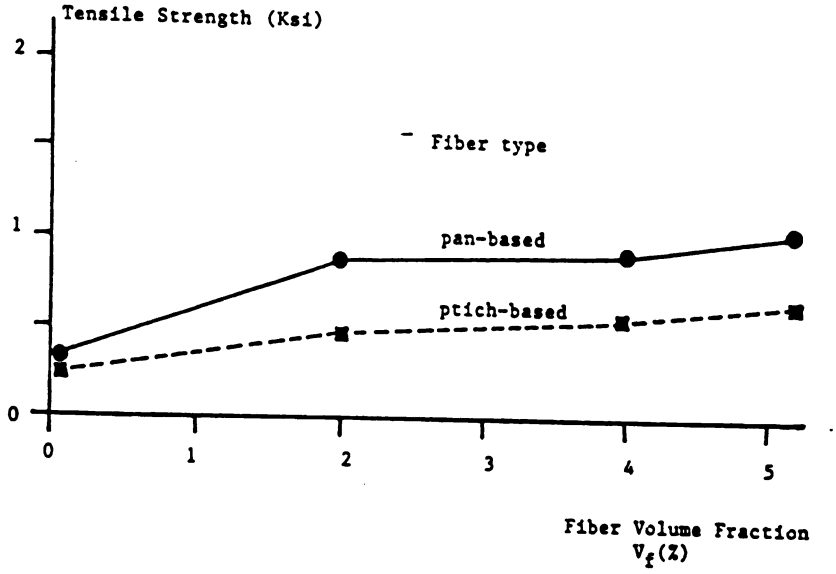

b. Direct tensile strength.

Figure 5.2: Effects of carbon fiber type (material and geometric properties) on the direct tensile behavior of carbon fiber reinforced cement.[15] (water/cement = 0.47, silica powder/cement = 0.25, methyl cellulose/cement = 0.01, fiber length = 0.12 in = 3 mm, mixing by Omni mixer, specimen's cross section = 0.24 x 1.18 in and autoclave curing). 1 in = 25.4 mm, 1 Ksi = 6.9 MPa

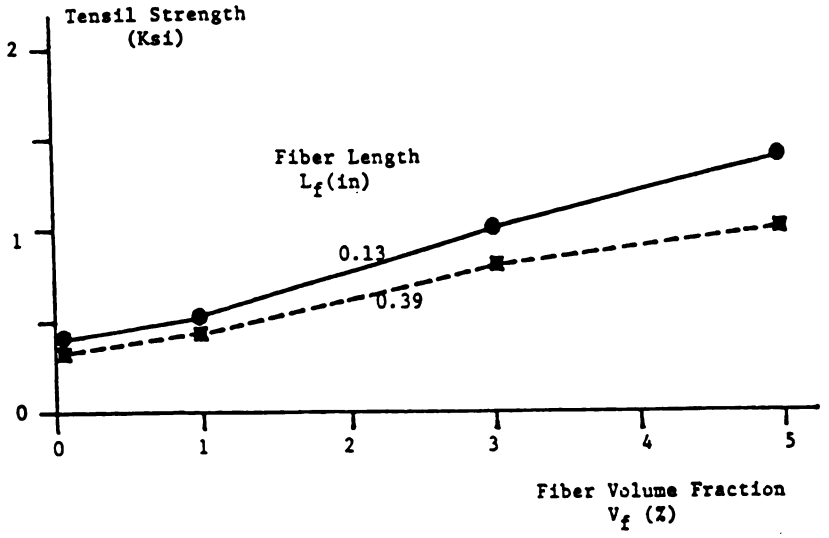

Figure 5.3: Effects of carbon fiber length on the direct tensile strength of carbon fiber reinforced cement.[12] (water/cement = 0.3, silica fume/cement = 0.4, superplasticizer/cement = 0.06, mixing by mortar mixer, specimen's cross section = 0.47 x 1.18 in and autoclave curing). 1 in = 25.4 mm, 1 Ksi = 6.9 MPa

flowability of fresh mix, have significantly lower tensile strengths than carbon fiber reinforced cement with no aggregates. However, the use of microballoons at 24% volume fraction does not necessarily lead to a composite with low tensile strength. It can also be concluded from Figure 5.4[5,6,12-17] that the increase in silica powder-cement ratio from 25% to 50% tends to have a negative effect on the tensile strength of carbon fiber reinforced cement. The damaging effect on tensile strength of silica powder and microballoons can be explained by the fact that aggregates in carbon fiber cement tend to disturb the uniform dispersion of fibers and reduce the bond strength between the matrix and fibers.

The use of class F fly ash as a dispersant (low-quality dispersant) at 50% of the weight of cement with light-weight aggregates (parlite) occupying 30% of the total volume of the composite tended in Reference 6 to limit the carbon fiber volume fraction that could be practically incorporated in the composite (by the use of a conventional mortar mixer) to a maximum of 2%. Also, the tensile strength of light-weight fly ash carbon fiber reinforced cement was significantly lower than carbon fiber reinforced cement mixes with silica fume (silica fume has a lower particle size and higher pozzolanic activity than fly ash) as shown in Figure 5.4. The use of latex as a mix ingredient (at 5% by weight of cement) in light weight carbon fiber cement with fly ash can significantly improve the tensile strength of the composite. This is due to the improved microstructure of the composite and the consequent increase in bond strength between the fibers and the matrix due to the incorporation of latex.[6] It is worth mentioning that in Reference 6, different water-binder ratios were used with different mixes to obtain a constant workability for all mix proportions.

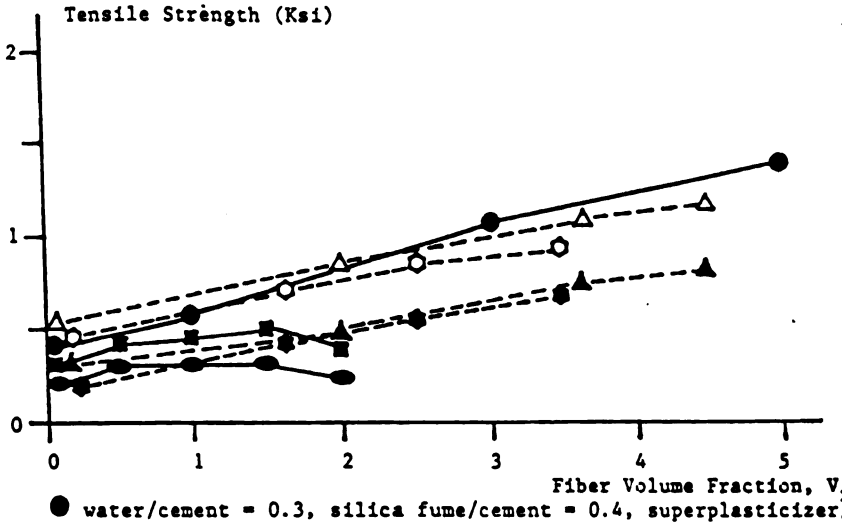

● water/cement = 0.3, silica fume/cement = 0.4, superplasticizer/cement = 0.06

■ flyash/cement = 1, light-weight sand/binder = 0.3 by volume, foaming agent/binder = 0.001

⬬ flyash/cement = 1, light-weight sand/binder = 0.3 by volume, latex/binder = 0.05

Fiber length = 0.12 in, mixing by mortar mixer and autoclave curing.

△ water/cement = 0.47, silica powder/cement = 0.25, methyl cellulose/cement = 0.01

▲ water/cement = 0.53, silica powder/cement = 0.50, methyl cellulose/cement = 0.01

⬡ water/cement = 0.62, microballoon/cement = 0.24, methyl cellulose/cement = 0.016

⬢ water/cement = 1.13, microballon/cement = 0.71, methyl cellulose/cement = 0.009

Fiber length = 0.39 in, mixing by Omni mixer and 7 days air curing.

Figure 5.4: Effects of matrix mix proportions on the direct tensile strength of carbon fiber cementitious composites.[6,12,14] (specimen's cross section = 0.47 x 1.18 in) 1 in = 25.4 mm, 1 Ksi = 6.9 MPa

The decrease in water-cement ratio leads to an increase in tensile strength and a decrease in ductility of carbon fiber reinforced cement composites under direct tension as shown in Figure 5.5.[5,14] This is probably due to the increase in strength of the matrix and the consequent increase in interfacial bond strength which may lead to the rupture of fibers prior to their pull-out.

The curing condition is another factor significantly affecting the tensile behavior of carbon fiber reinforced cement. Autoclave curing (as shown in Figure 5.6)[5,14,15] improves the tensile strength of carbon fiber reinforced cementitious composites. Autoclaving, however, tends to damage the ductility and energy absorption capacity of the material (see Figure 5.7). These effects of autoclave curing may be due to the improvements in fiber-matrix bond characteristics resulting from curing in autoclave, which encourage fiber rupture with low energy absorption.

Polymer impregnation has also been applied to autoclaved carbon fiber reinforced cement composites.[15] This approach to the modification of the matrix and interface properties is effective in further increasing the tensile strength of the composite. Polymer impregnation, however, damages the ductility and energy absorption capacity of carbon fiber reinforced cement, possibly due to the increase in bond strength which encourages fiber rupture before pull-out (see Figure 5.8).

It is worth mentioning that an increase in tensile strength (due to autoclaving) does not necessarily lead to an increase in flexural strength. Post-peak ductility in tension (which is damaged due to autoclaving) is an important factor deciding the flexural strength of carbon fiber reinforced cement.

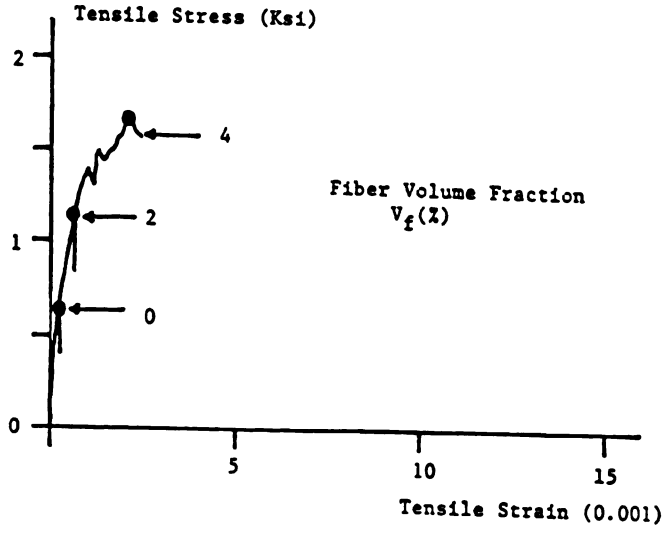

a. Direct tensile stress-strain relationships

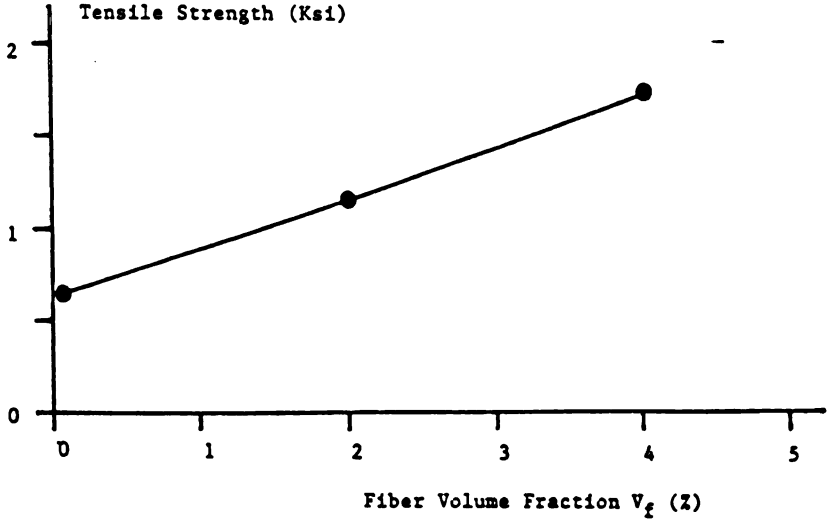

b. Direct tensile strength

Figure 5.5: Tensile performance of carbon fiber reinforced cement with low water - cement ratio.[14] (water/cement = 0.30, water reducer/cement = 0.02, fiber length = 0.39 in, mixing by Omni mixer, specimen's cross-section = 0.47 x 1.18 in and 7 days air curing. 1 in = 25.4 mm, 1 Ksi 6.9 MPa

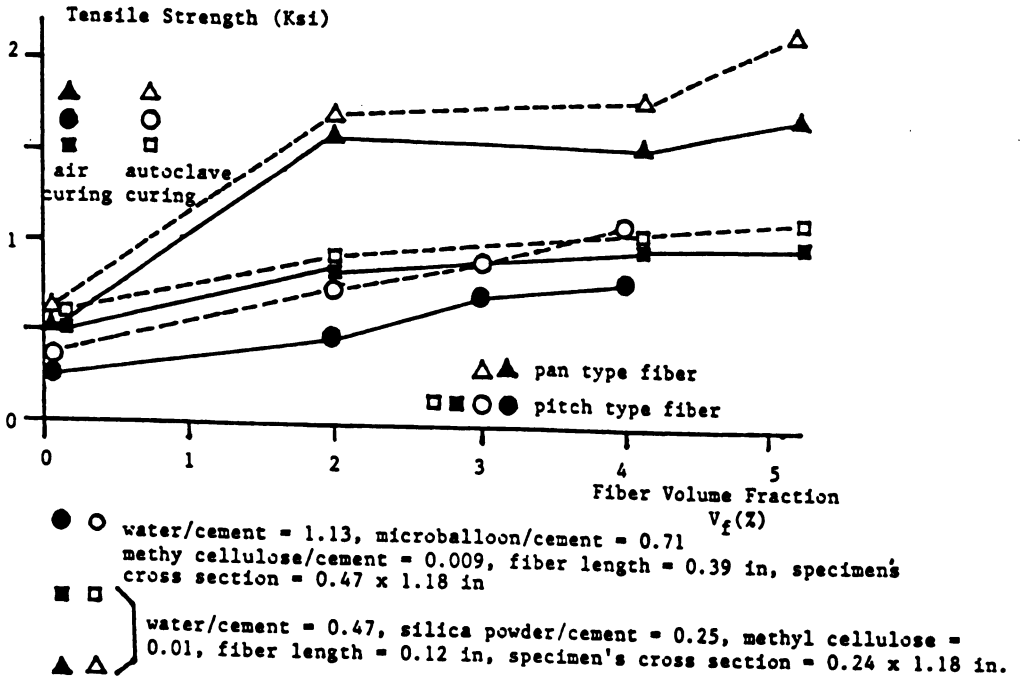

Figure 5.6: Effect of autoclave curing on the direct tensile strength of carbon fiber reinforced cement.[14,15] (Mixing in Omni mixer) 1 in = 25.4 mm, 1 Ksi = 6.9 MPa.

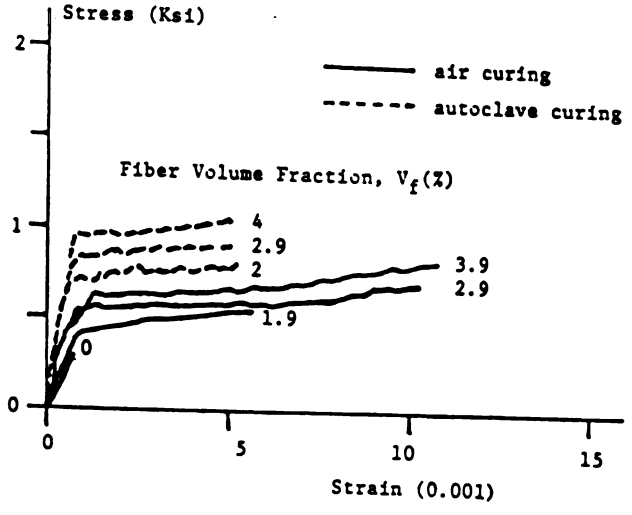

Figure 5.7: Effects of autoclave curing on the tensile stress-strain relationship of carbon fiber cement compossites.[14](water/cement = 1.13, microballoon/cement = 0.71, methyl cellulose/cement = 0.009, fiber length = 0.39 in, mixing by Omni mixer, specimen's cross-section = 0.47 x 1.18 in). 1in = 25.4 mm, 1 Ksi = 6.9 MPa

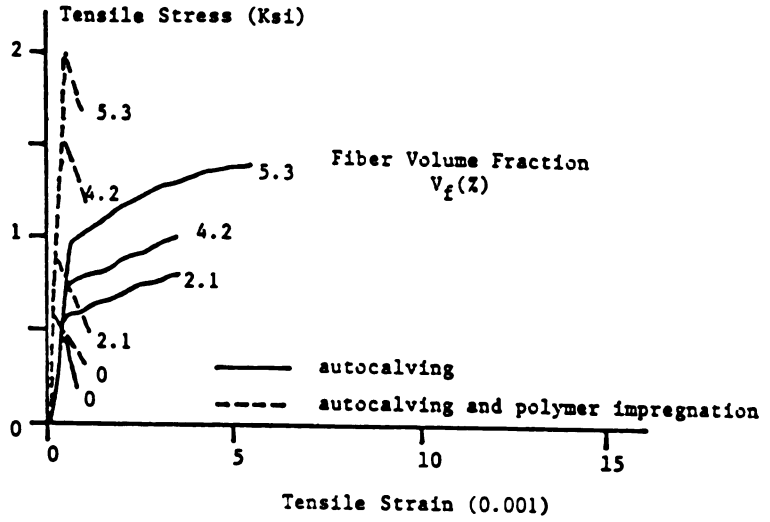

a. Stress-strain relationships

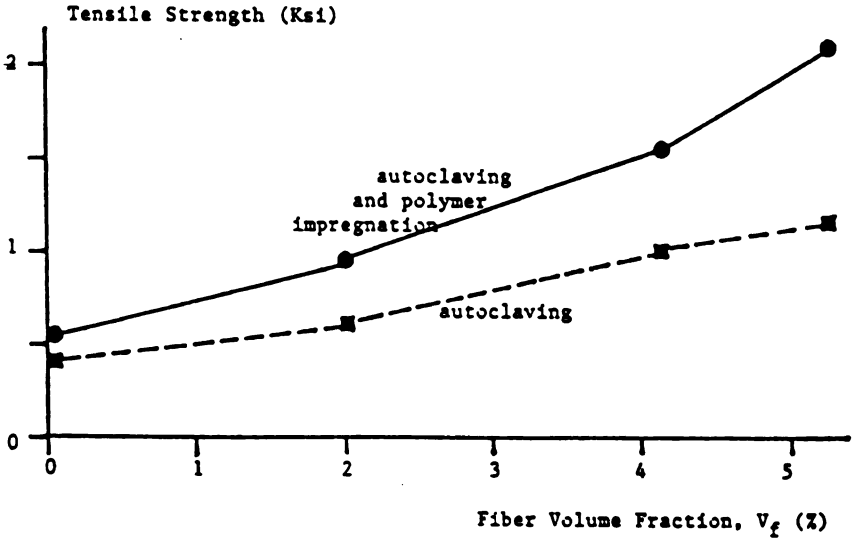

b. Tensile strengths.

Figure 5.8: Effects of polymer impregnation on the tensile performance characteristics of autoclaved carbon fiber reinforced cement.[15] (water/cement = 0.47, silica powder/cement = 0.25, methyl cellulose/cement = 0.01, fiber length = 0.39 in, mixing by Omni mixer and specimen's cross-section = 0.24 x 1.18 in). 1 in = 25.4 mm, 1 Ksi = 6.9 MPa.

5.3. Experimental Results

Figures 5.9.a through 5.9.d show the tensile stress-strain relationships of the plain cementitious matrix, and also those for matrices reinforced with 3% volume fraction of 1/8 in. (3 mm) fiber, 3% volume fraction of 1/16 in. (1.5 mm) fibers, and 5% volume fraction of 1/16 in. (1.5 mm) fibers, respectively, cured in different conditions. The trends observed in Fig. 5.9 regarding the effects of fiber reinforcement properties and curing conditions on the composite material performance will be discussed in this section.

In order to quantify the toughness and energy absorption properties of carbon fiber reinforced cement under direct tension, in the evaluation of stress-strain measurements given in Figure 5.9, the total area underneath the tensile stress-stress curve up to a strain of 0.006 was defined as a measure of energy absorption, and the ratio of this value to the area underneath stress-strain curve prior to cracking was chosen to represent toughness.[27]

Figure 5.10 summarizes the first crack and ultimate strength test results for cementitious composites with different carbon fiber reinforcement properties and curing conditions, subjected to direct tension. It can be concluded form Figure 5.10 that hot water curing results in distinctly higher tensile strengths especially at higher fiber volume fractions. The other curing conditions give comparable tensile strengths, and different fiber reinforcement properties produce similar improvements in tensile strengths after curing in water at ambient temperature, in steam or moist room. Hot water curing, when compared with air curing, increases the tensile strength by about 40% at a fiber volume fraction of 3% (1/16 or 1/8 in. fibers), and by about 100% at a fiber volume fraction of 5% (1/16 in.).

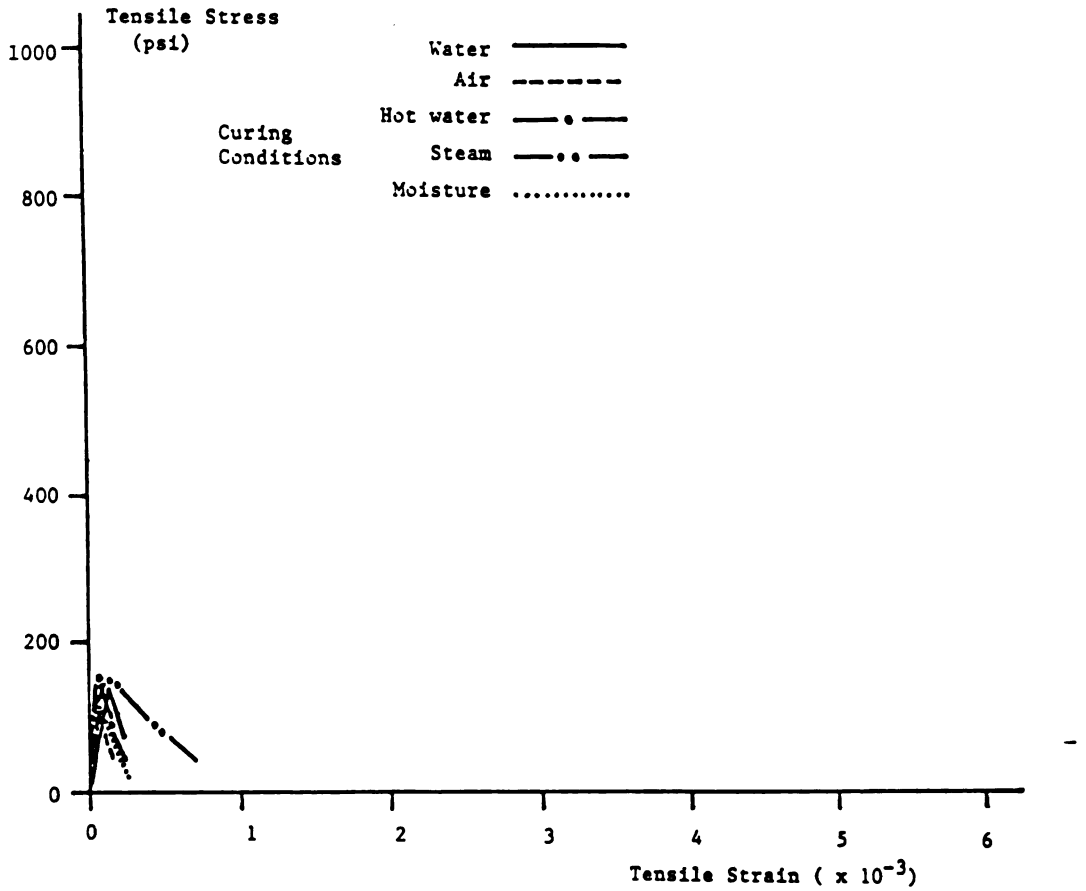

a. Plain cementitious matrix

Figure 5.9: Tensile stress-strain relationships for carbon fiber reinforced cement composites with different fiber reinforcement properties and curing conditions. (water/ binder = 0.3, silica fume/binder = 0.23, superplasticizer /binder = 0.032, mixing by mortar mixer and specimen's cross section = 1 x 1 in) 1 in = 25.4 mm, 1 Ksi = 6.9 MPa

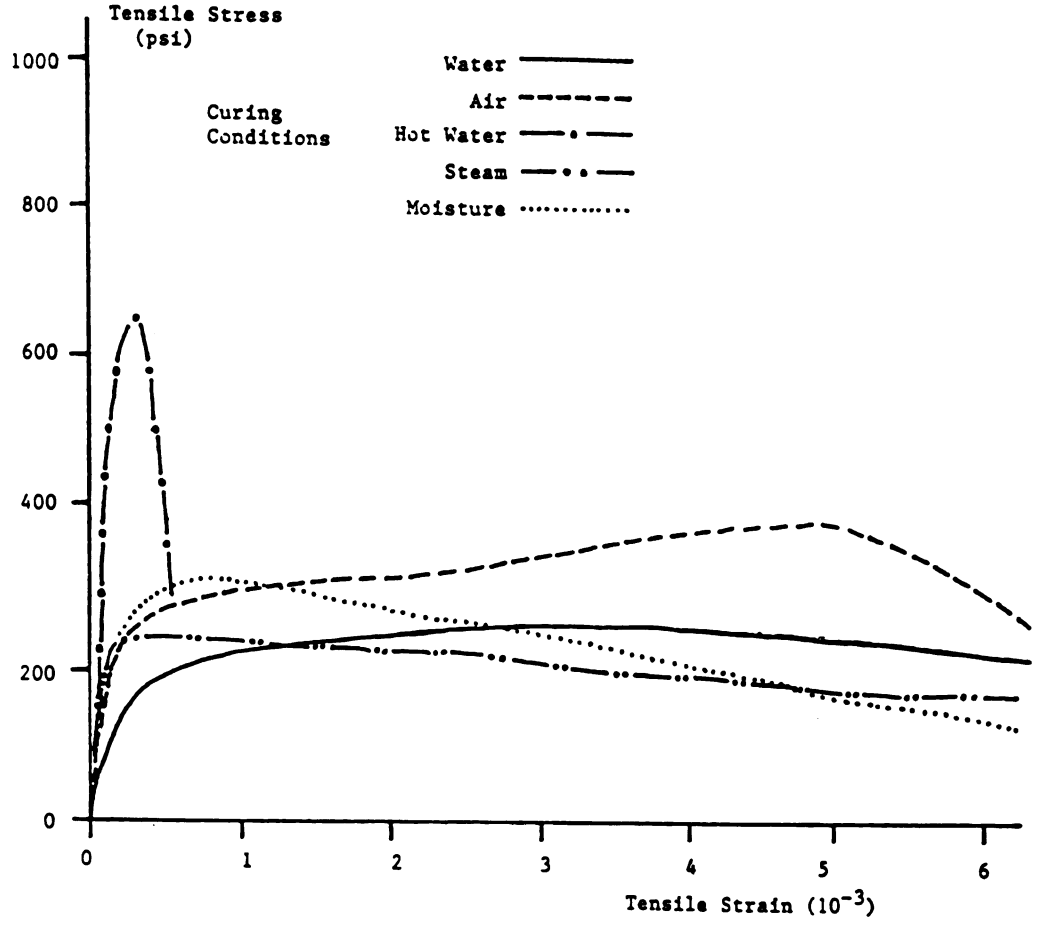

b. Fiber volume fraction (V_f) = 3%, fiber length (L_f) = 1/8 in

Figure 5.9: (continued)

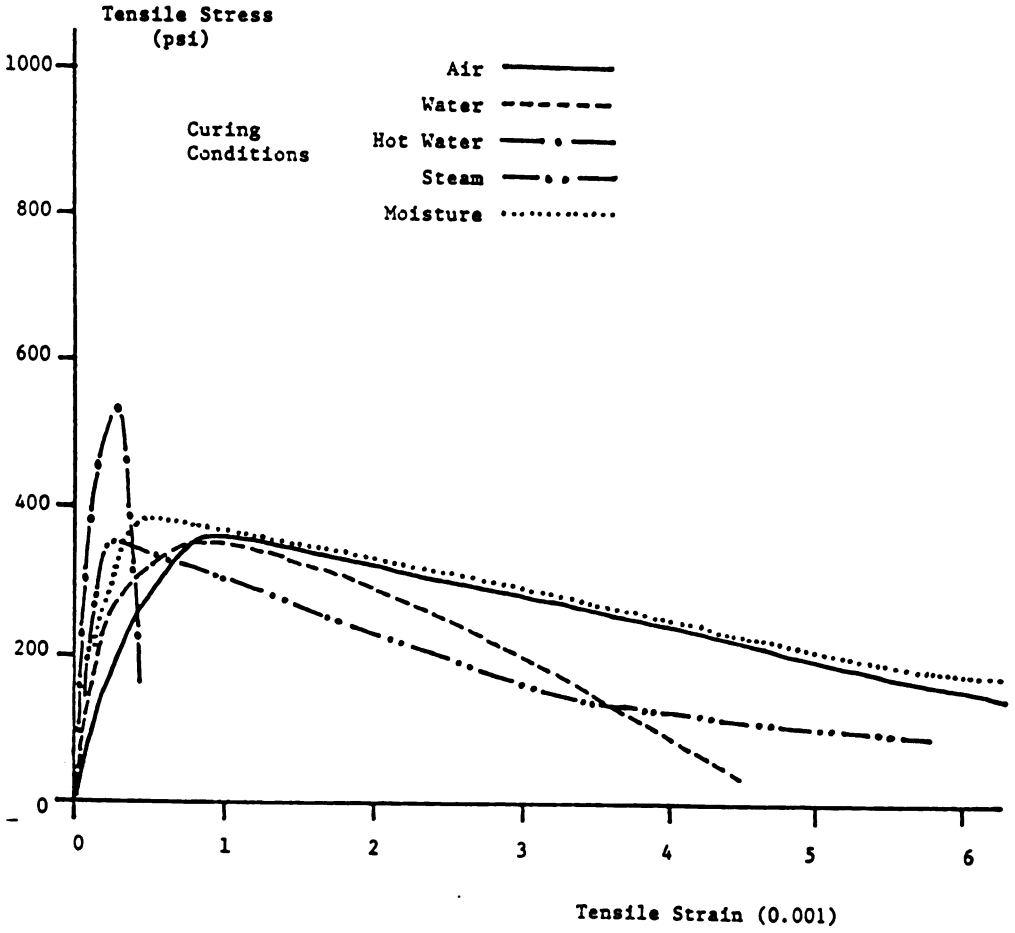

c. Fiber volume fraction (V_f) = 3%, fiber length (L_f) = 1/16 in

Figure 5.9: (continued)

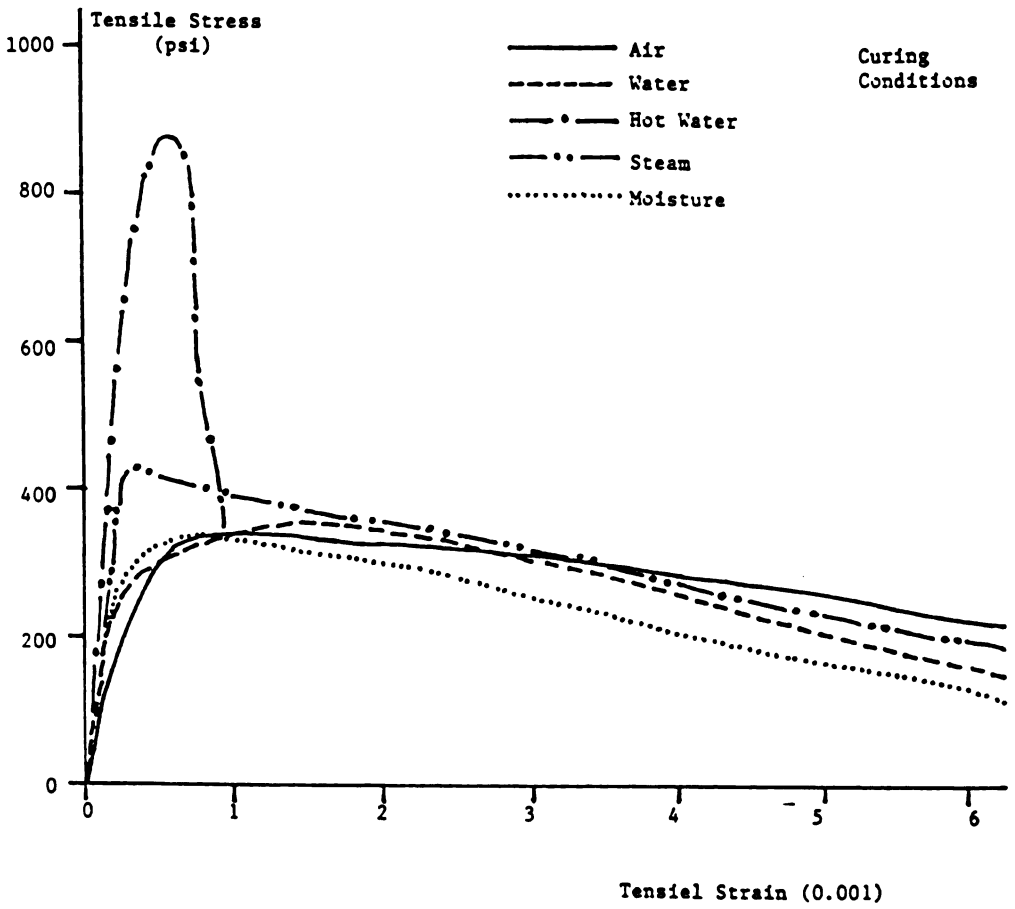

d. Fiber volume fraction (V_f) = 5%, fiber length (L_f) = 1/16 in

Figure 5.9 (continued)

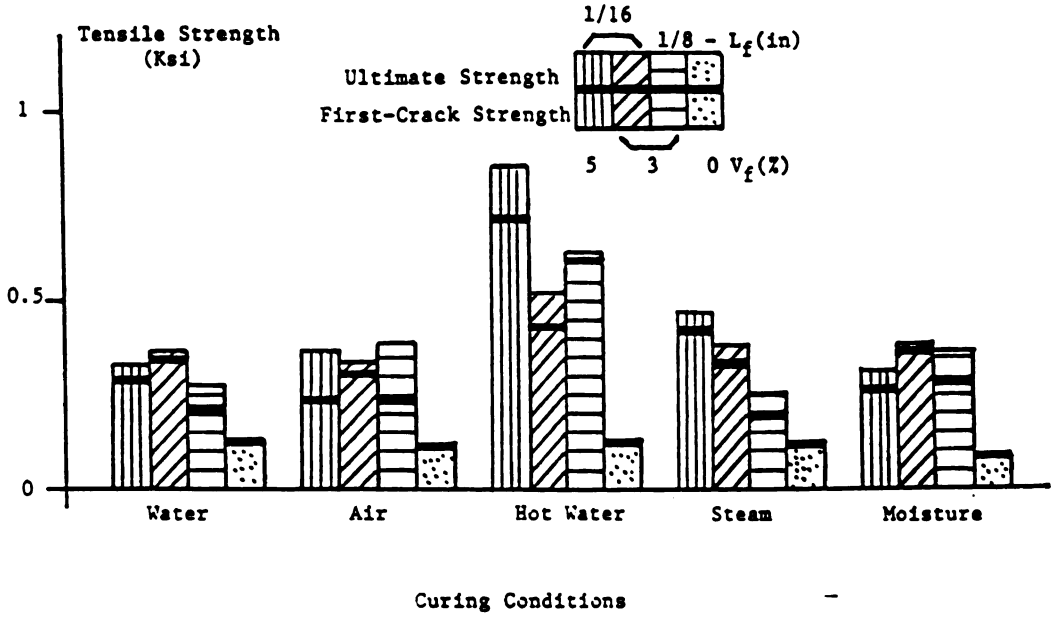

Figure 5.10: Effects of fiber reinforcement properties and curing conditions on the ultimate and first-crack tensile strengths. 1 in = 25.4 mm, 1 Ksi = 6.9 MPa

Test results on energy absorption capacity of carbon fiber reinforced cement composites under direct tension are summarized in Figure 5.11. While plain cementitious materials show negligible energy absorption, the fibrous ones are capable of absorbing significant amounts of energy under direct tension. Considering the variations in test results, it may be concluded from Figure 5.11 that, except for the specimens cured in hot water, carbon fiber reinforced cementitious composites considered in this study have similar energy absorption capacities. The hot water cured specimens were relatively brittle, and absorb energy mainly prior to cracking capacity which is associated with fiber pull-out.

The measured initial stiffness of plain and fibrous cementitious materials under direct tension are shown in Figure 5.12. Compared to the effects of curing condition, carbon fiber reinforcement seems to have an insignificant influence on the tensile stiffness of cement-based materials. Curing in steam and especially in hot water are effective in increasing the tensile stiffness of plain and fibrous materials.

5.4. Summary and Conclusions

The results of an experimental study on the performance of carbon fiber reinforced cement under direct tension are presented. The effects of carbon fiber length and volume fraction, and curing condition, on the tensile behavior of cement-based materials are described. The test program covered plain cementitious composites and fibrous ones with 3% and 5% volume fraction of 1/16 in. (1.5 mm) fibers, and with 3% of 1/8 in. (3 mm) fibers. The test specimens were cured in air, moist room, water, hot water, and steam.

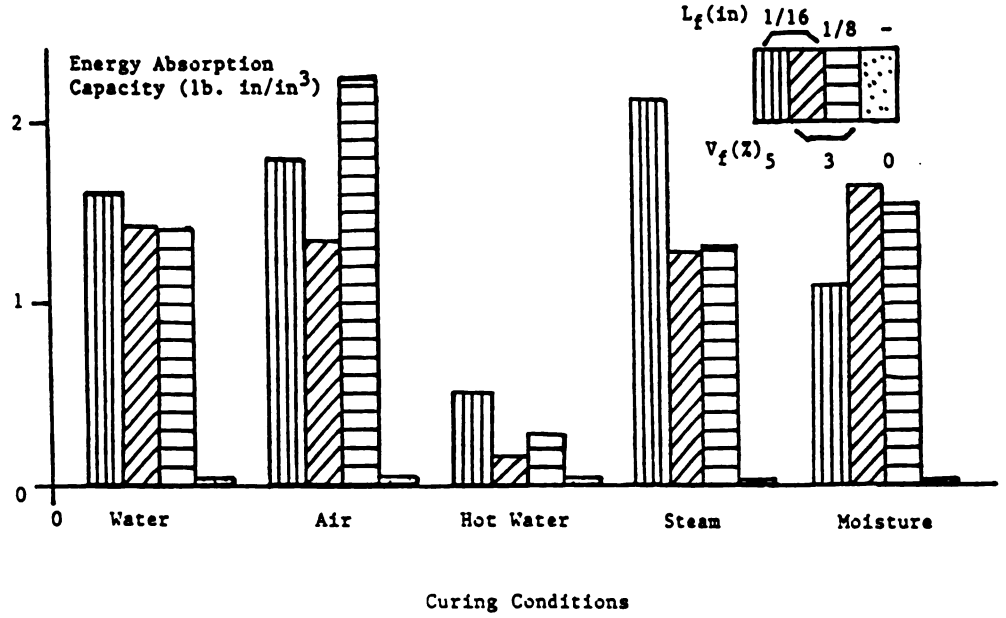

Figure 5.11: Effects of fiber reinforcement properties and curing conditions on the energy absorption capacity under tensile loading conditions. 1 in = 25.4 mm, 1 lb. in/in ^{3} = 0.007 N. mm/mm^3

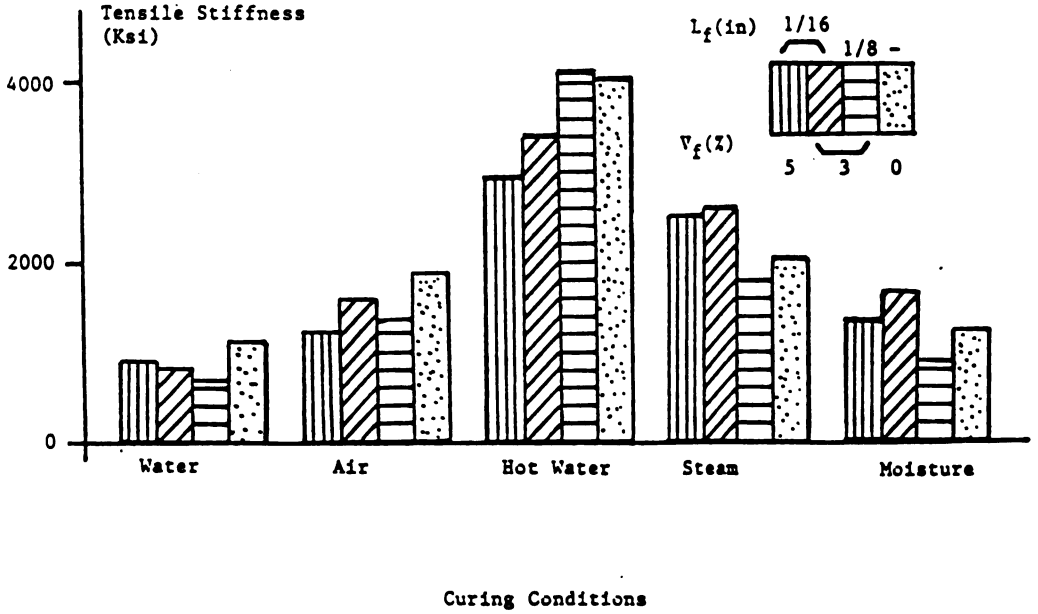

Figure 5.12: Effects of fiber reinforcement properties and curing conditions on the intial stiffness under direct tension. 1 in = 25.4 mm, 1 Ksi = 6.9 MPa

Toughness (a representative of post-peak energy absorption) is generally defined as the ratio of total energy absorption capacity (measured up to a strain of 0.006) to the energy absorbed by the material prior to cracking. Figure 5.13 summarizes the measured values of toughness in tension tests performed in this study. The plain specimens have a toughness value close to 1.0, indicating negligible post-peak energy absorption. Carbon fiber reinforcement, except for curing in hot water, provides cementitious materials with a substantially improved toughness. There seems to be a tendency in the toughness of carbon fiber reinforced cement composites to increase with increasing fiber length and volume fraction. The damage to toughness resulting from hot water curing may be attributed to the improvements in the bonding of cementitious matrices to carbon fibers resulting from hot water curing. An excessively strong bond encourages the rupture of fibers prior to their pull-out. This eliminates the major fraction of energy absorption by fiber pull-out action. The test data generated in this investigation indicate that:

1. Carbon fiber reinforcement results in major improvements in the tensile stress-strain behavior of cementitious materials. The highly brittle nature of failure in plain cement matrices is changed, except after hot water curing, to a desirable performance with major post-peak ductility.

2. Important improvements in the first crack and ultimate tensile strength of cement-based materials can be achieved through carbon fiber reinforcement. Different fiber reinforcement properties lead to comparable tensile strengths after air, water, steam and moist curing. Hot water curing, especially at 5% fiber volume fraction, results in relatively high tensile strengths.

3. Major improvements in the total energy absorption capacity of cementitious materials can be achieved by carbon fiber reinforcement. Hot water curing, through generating excessive interfacial bond strength between fibers and matrix, and by eliminating the pull-out action of fibers before rupture, reduces the efficiency of fibers in enhancing the energy absorption capacity of cement-based materials.

4. Toughness, a representative of post-peak energy absorption capacity, is significantly higher in carbon fiber reinforced cement than in plain cement, except after hot water curing. The increase in fiber length and volume fraction generally improves the toughness of fibrous cement.

5. The initial tensile stiffness of cementitious materials seems to be more dependent on curing condition than on carbon fiber reinforcement properties. Steam and especially hot water curing give higher stiffnesses for both plain and fibrous materials.

CHAPTER 6

COMPRESSIVE BEHAVIOR

6.1. Introduction

The reported investigations on compressive characteristics of carbon fiber reinforced cement composites have been mainly concerned with the compressive strength of the material.[5,6,12-17] Some test results are also available on the strain at peak compressive stress and the compressive modulus of elasticity of carbon fiber cement.[14,15] Compressive stress-strain relationships have not been recorded in the literature.[5,6,12-17] Carbon fibers, due to their crack-arresting properties, are anticipated to have significant effects on the post-peak ductility and energy absorption capacity of cement-based materials under compression.

The compressive behavior of carbon fiber reinforced cement is characterized by:

1. The matrix provide the main fraction of the composite strength under compressive stresses, and fibers, in general, tend to have a relatively small effect on the compressive behavior of the material;

2. Carbon fibers, due to their damaging effect on the fresh mix workability, tend to increase the air content of the composite material, thereby having potentially negative effects on the compressive performance; and

3. Fibers, due to their crack arresting properties, have some potentials for improving the compressive behavior of cement-based materials, especially in the post-peak region.

This chapter includes a review of the available literature on the compressive performance of carbon fiber reinforced cement, followed by the presentation of followed by the presentation of test results generated in this investigation, on the compressive behavior of carbon fiber reinforced cement composites.

6.2. Background

The compressive strength of cementitious materials generally tend to decrease with increasing carbon fiber volume fraction (see Figure 6.1.a).[6,14] Similar trends are also observed for the compressive modulus of elasticity of the composite (Figure 6.1.b). However, no consistent effects were observed in Reference 14 of carbon fiber reinforcement on the strain at peak compressive stress as shown in Figure 6.1.c.

-The effects of incorporating carbon fibers in light-weight matrices (with hight volume percentage of light-weight aggregates and relatively high water-cement ratios) on the compressive strength and modulus of elasticity seem to be negligible (Figures 6.2.a and 6.2.b).[14] Carbon fibers, however, increase the strain at peak compressive stress of light-weight carbon fiber reinforced cement (Figure 6.2.c).[14] The mode of failure in compression tends to be ductile in carbon fiber cement.

Matrix mix proportions, curing conditions, fiber length, fiber type and size of specimens are among the factors that affect the compressive characteristics of carbon fiber reinforced cement.

Reference 6 has studied the effects of adding a foaming agent to cementitious matrices incorporating carbon fibers. The results indicate that the increase in the foaming agent content (which leads

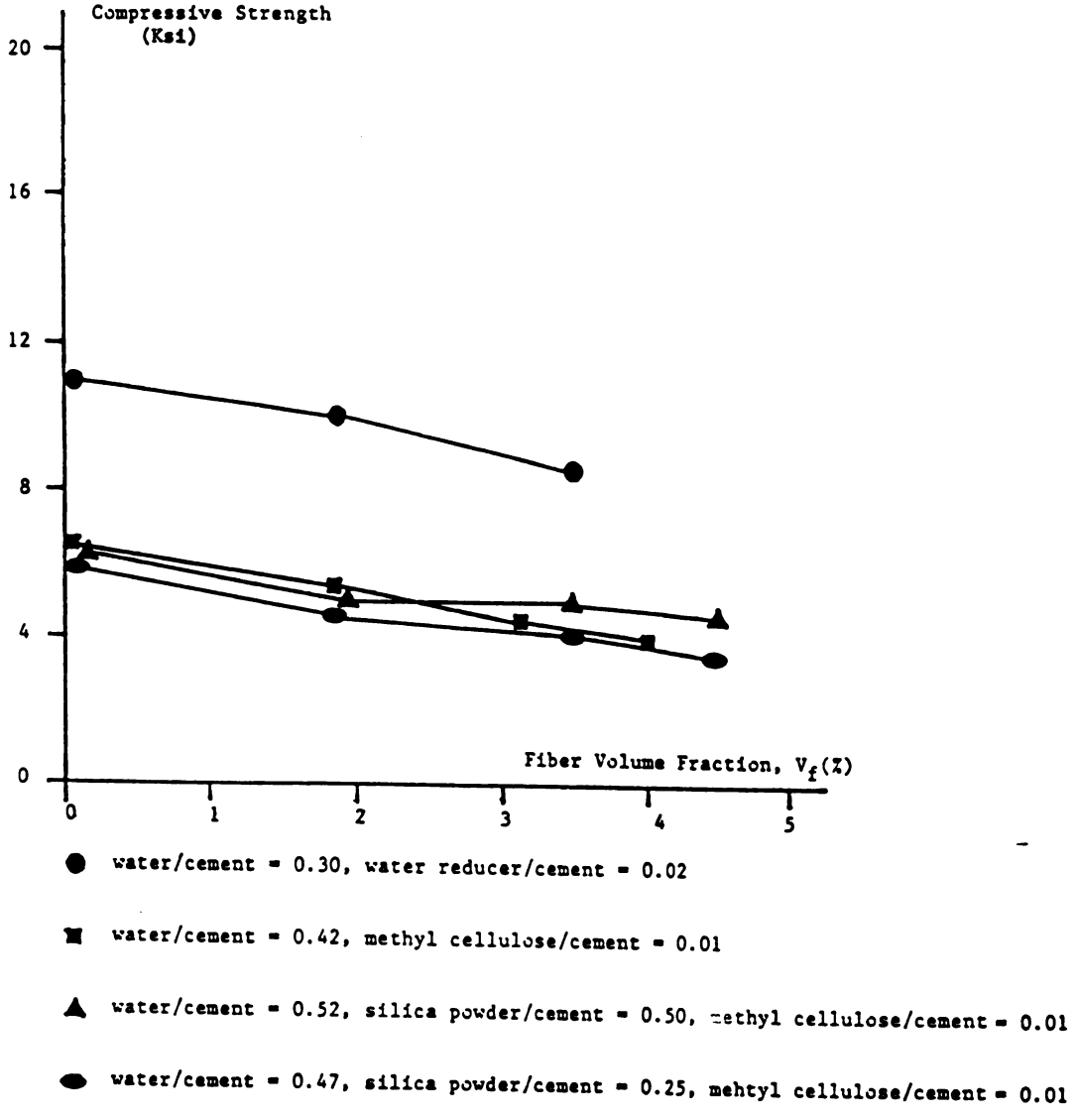

a. Compressive strength

Figure 6.1: Effects of carbon fiber reinforcement on the properties of cement-based materials under compression.[14] (fiber length = 0.4 in = 10 mm, mixing by Omni mixer, cylinderical specimens 2 x 4 in and 7 days air curing). 1 in = 25.4 mm, 1 Ksi = 6.9 MPa

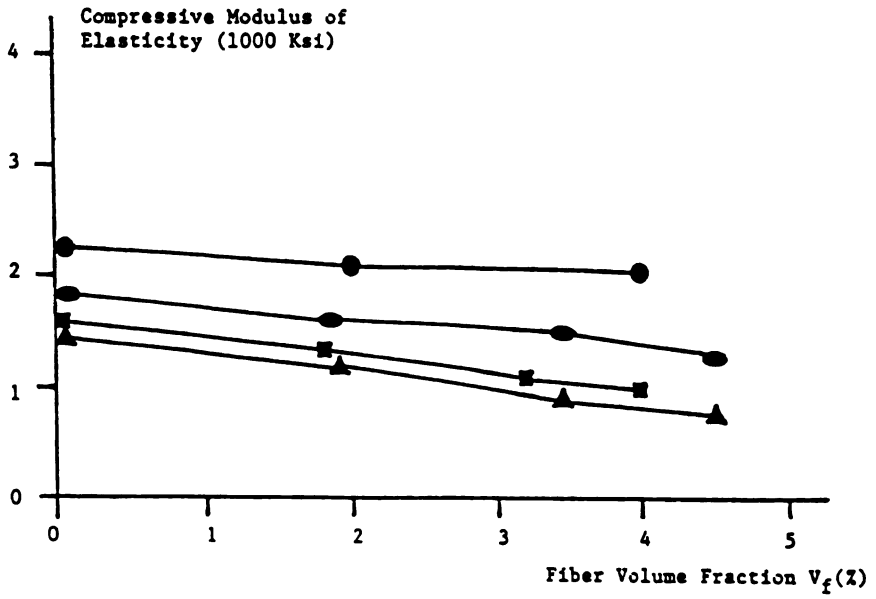

b. Compressive modulus of elasticity.

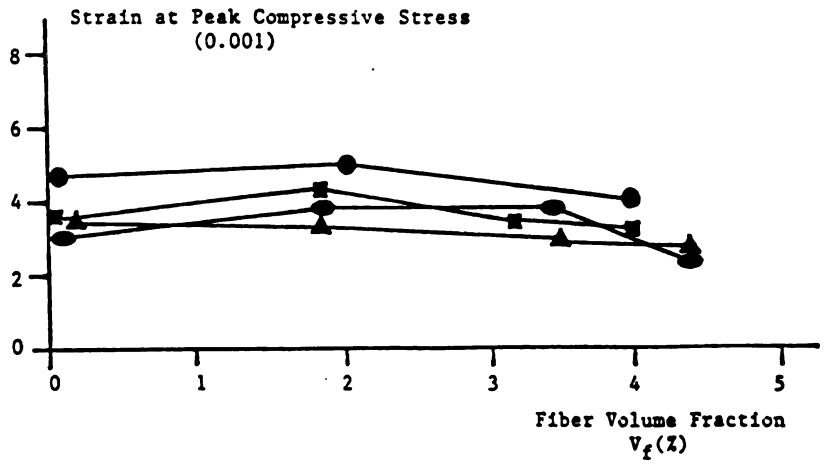

c. Strain at peak compressive stress

Figure 6.1: (continued)

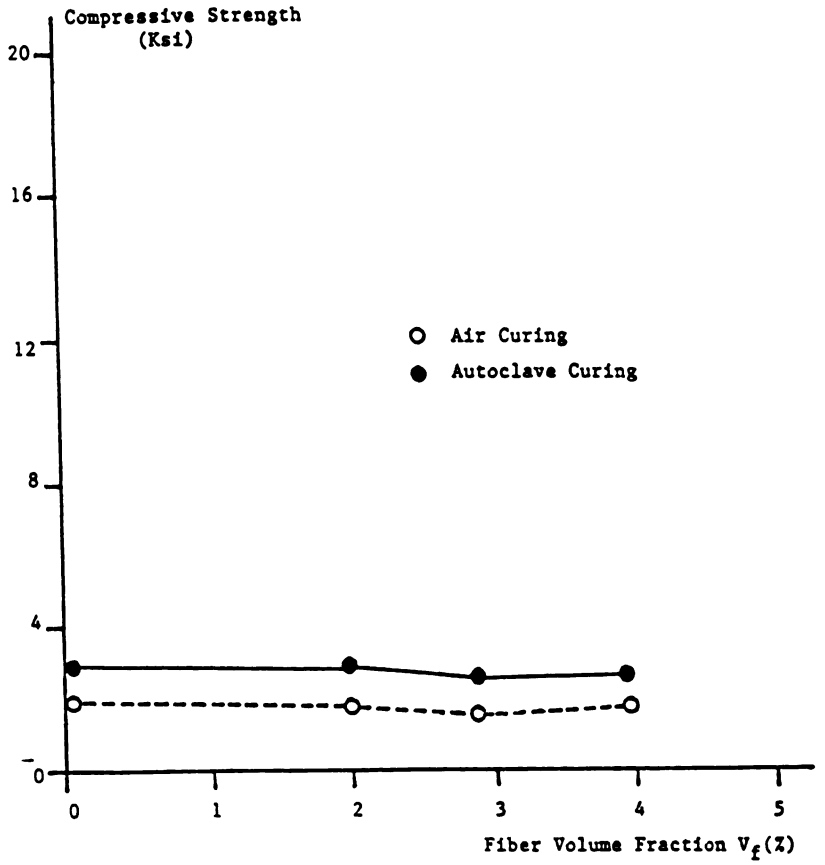

a. Compressive strength

Figure 6.2: Effects of carbon fiber reinforcement on the properties of light-weight cement-based materials under compression.[14] (water / cement = 1.13, micro balloon/cement = 0.71, methyl cellulose/cement = 0.01, fiber length = 0.39 in, mixing by Omni miter and cylindrical specimens 2x4 in) 1 in = 25.4 mm, 1 Ksi = 6.9 MPa.

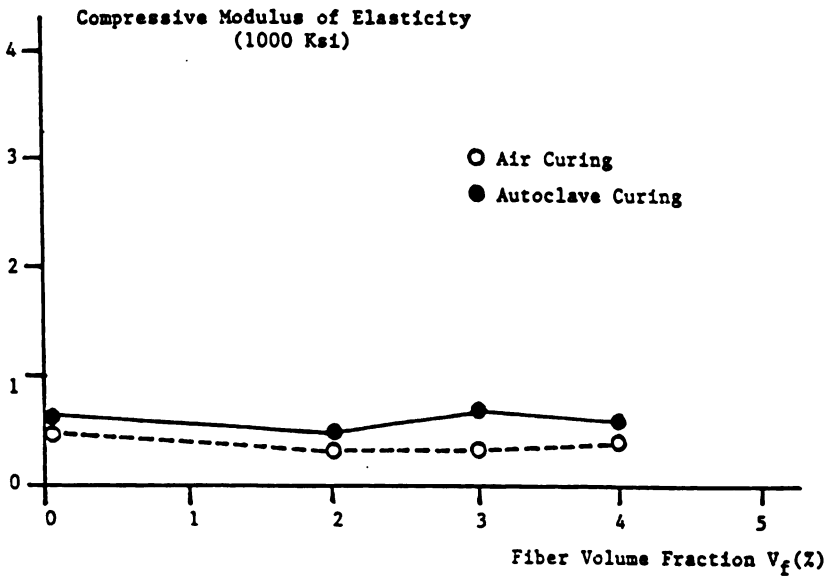

b. Compressive modulus of elasticity

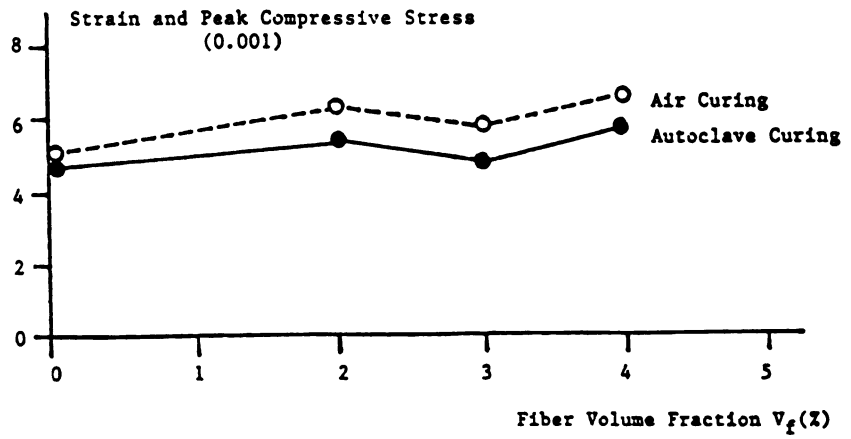

c. Strain at peak compressive stress.

Figure 6.2: (continued)

to an increase in air content of the material) tends to damage the compressive strength of material at a decreasing rate (Figure 6.3). It is worth mentioning that the mix proportions of Reference 6 were distinguished by a high volume percentage (30%) of light-weight aggregates and also by 50% replacement of cement with fly ash. These distinct aspects of matrix mix proportions led to a relatively low compressive strength. In another experiment, Reference 6 used a latex polymer at 5% of the binder (cement and fly ash) weight. Polymers tend to fill the voids inside matrix, and also bond the mix constituents and fibers in the composite, and thus increase the compressive strength of the composite material, as shown in Figure 6.4. The test results of Reference 6 have indicated that carbon fibers, especially at higher volume fractions, have a negative effect on the compressive strength of cementitious materials. It is worth mentioning that the cement composites tested in Reference 6, with different fiber volume fractions, have comparable workabilities. This was achieved in Reference 6 simply by increasing the water content at higher fiber volume fractions.

The use of silica fume, up to a certain limit, tends to improve the uniform dispersion of carbon fibers, and also the overall properties of cementitious matrices. This leads to a favorable effect on the compressive strength, of carbon fiber cement composites, as shown in Figure 6.5.[13] Beyond a silicafume/binder ratio of 40%, however, there are adverse effects on the compressive strength of the composite material resulting from an increase in silicafume content, possibly due to the damage to workability.

The use of superplasticizers in cement matrices fresh mix tends to improve the distribution of carbon fibers in the cement matrix, thereby improve in the compressive strength of carbon fiber

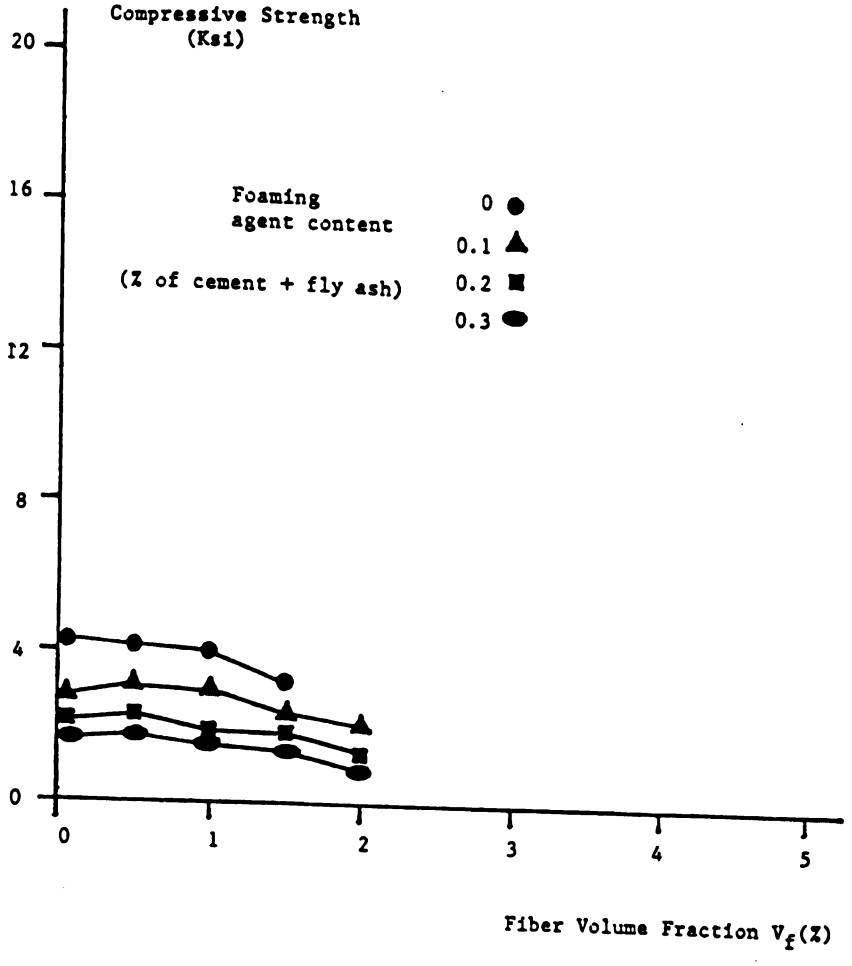

Figure 6.3: Effects of foaming agent on the compressive strength of carbon fiber reinforced cement.[6] (fly ash/cement = 1, light-weight sand/cement +fly ash= 0.3 (by volume), fiber length = 0.12 in = 3 mm, mixing by mortar mixer, broken flexural specimens 1.6 x 1.6 x 4 in were used for compressive strength tests and autoclave curing was employed). 1 in = 25.4 mm, 1 Ksi = 6.9 MPa

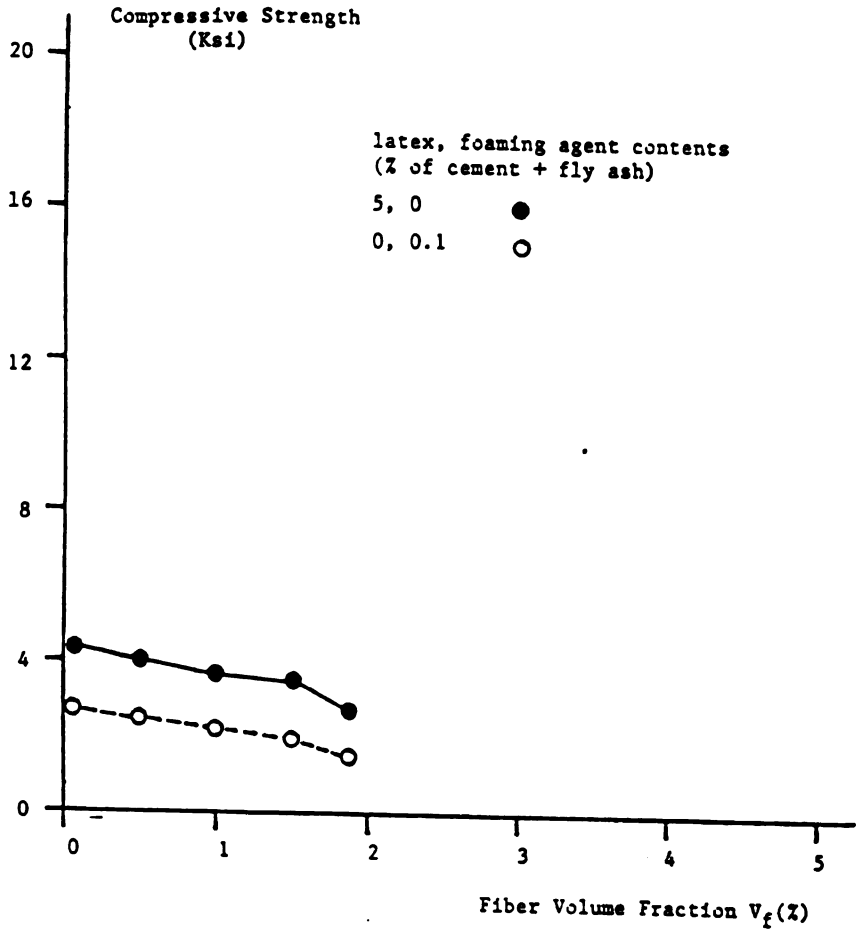

Figure 6.4: Effects of latex on the compressive strength of carbon fiber reinforced cement.[6] (fly ash/cement = 1, light weight sand/cement + fly ash = 0.3 (by volume), fiber length = 0.12 in = 3 mm, mixing by mortar mixer, cylinderical specimens 2 x 4 in and autocalve curing) 1 in = 25.4 mm, 1 Ksi = 6.9 MPa

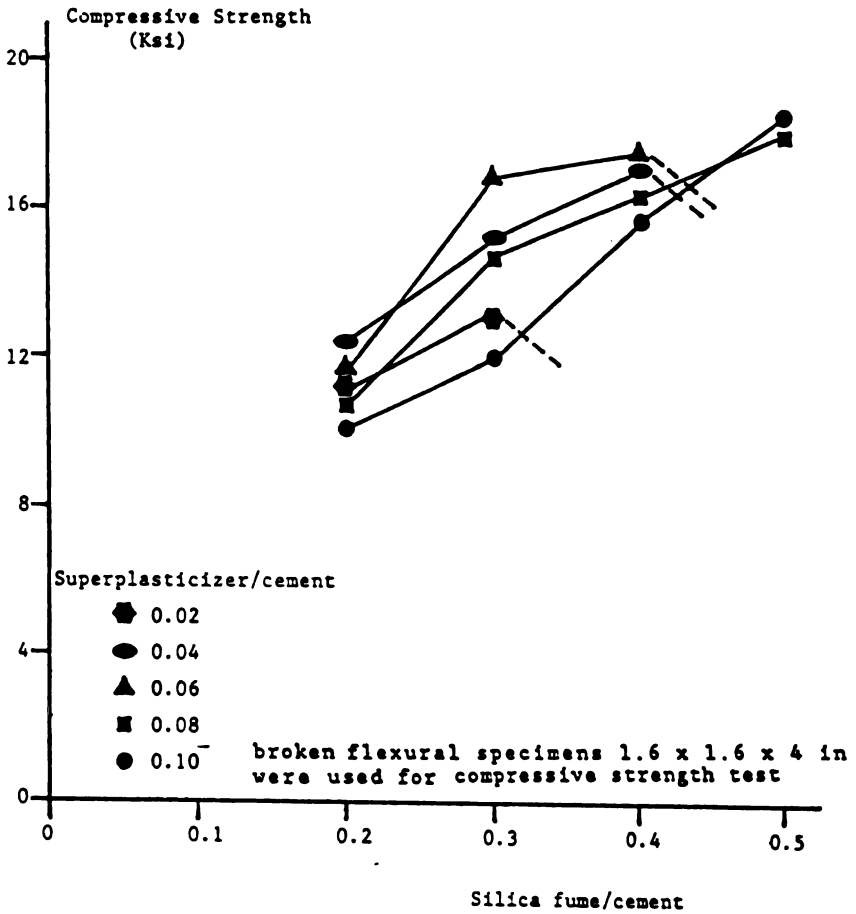

Figure 6.5; Effects of silica fume content on the compressive strength of carbon fiber reinforced cement.[13] (water/cement = 0.3, fiber length = 0.39 in = 10 mm, mixing by mortar mixer and autoclave curing) 1 in = 25.4 mm, 1 Ksi = 6.9 MPa.

reinforced cement (Figure 6.6).[13] Excessive amounts of superplasticizer however, (as shown in Figure 6.6), may actually lead to unfavorable effects on workability. This could be due to the increase in air content of the material resulting from the addition of large dosages of superplasticizer.

As far as the fiber length effects on compressive properties of carbon fiber reinforced cement is concerned, the strength test results reported in Reference 12 indicate that the 3 mm (0.125 in.) fibers are generally more effective than the 10 mm (0.390 in.) ones in increasing the compressive strength of cementitious materials (see Figure 6.7).

Reference 15 has conducted an experimental study on the compressive strength and modulus of elasticity of carbon fiber reinforced cement (see Figures 6.8 and 6.9). Two types of carbon fiber were incorporated in the cementitious matrix of Reference 15: (a) low-modulus, low-tensile strength, pitch-based carbon fibers with relatively large diameters; and (b) high-modulus, high-tensile strength pan-based carbon fibers with relatively small diameters. Three different curing conditions were used in this reference: a) curing in air, b) autoclave curing, and c) autoclave curing followed by polymer impregnation. Carbon fibers, as expected, had relatively small effects on the compressive strength of cementitious materials. Pitch-based fibers were more effective in improving the compressive strength of the cementitious composite; probably due to the higher aspect ratio of pan-based fibers and the consequent damage to workability. In the test results of Reference 15, carbon fiber reinforcement generally resulted in an increase in the compressive strength of cement-based materials as far as the fiber volume fraction of did not exceed a certain limit (about 3%).[15] Beyond that, the

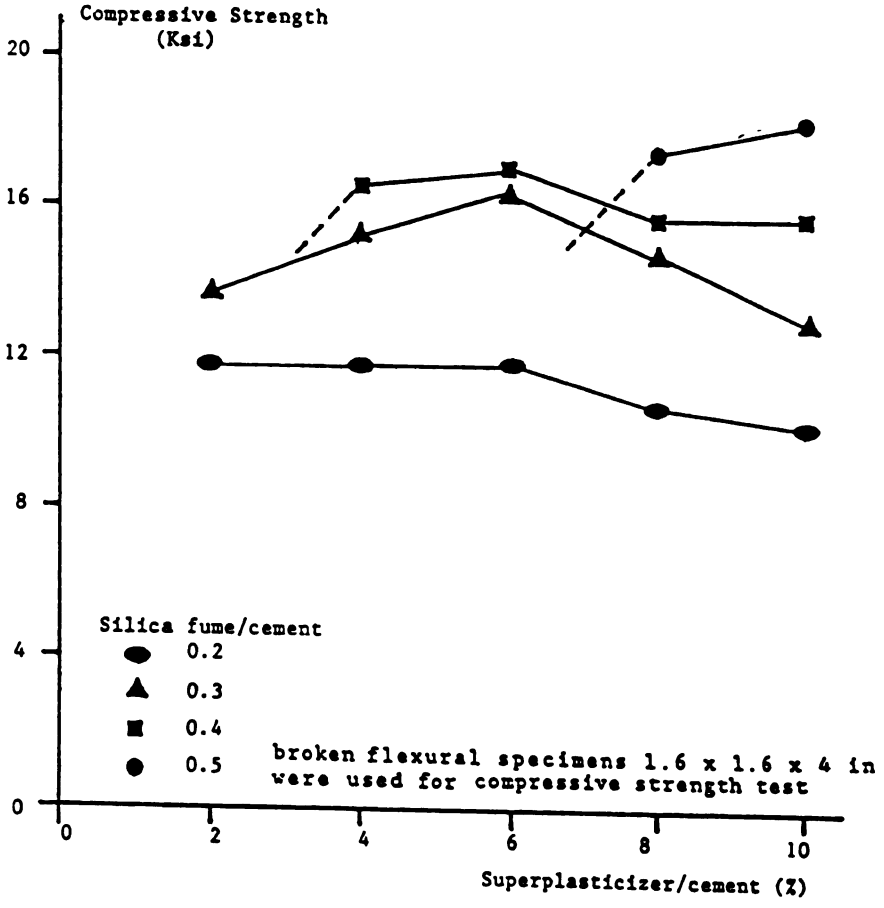

Figure 6.6: Effects of superplasticizer content on the compressive strength of carbon fiber reinforced cement.[13] (water/cement = 0.3, fiber length = 0.39 in = 10 mm, mixing by mortar mixer and autoclave curing). 1 in = 25.4 mm, 1 Ksi = 6.9 MPa.

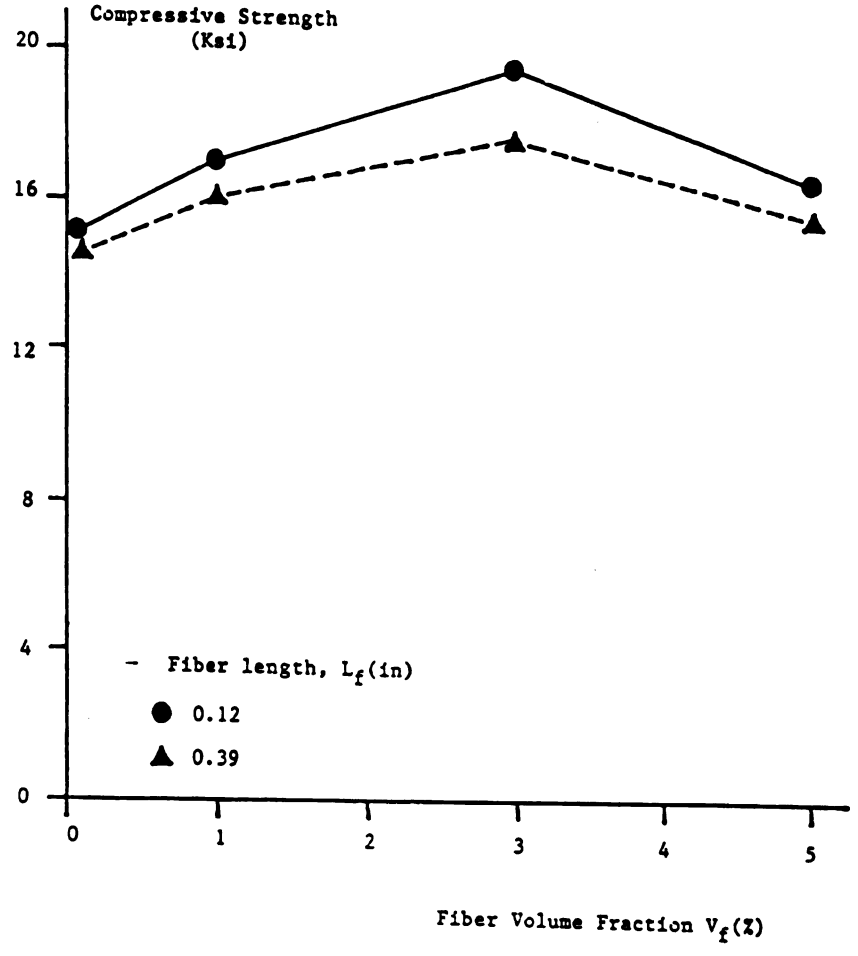

Figure 6.7: Effects of fiber length on the compressive strength of carbon fiber reinforced cement.[12] (water/cement = 0.3, silica fume/cement = 0.4, superplasticizer/cement = 0.06, mixing in mortar mixer, cylinderical specimens 2 x 4 in and autoclave curing). 1 in = 25.4 mm, 1 Ksi = 6.9 MPa

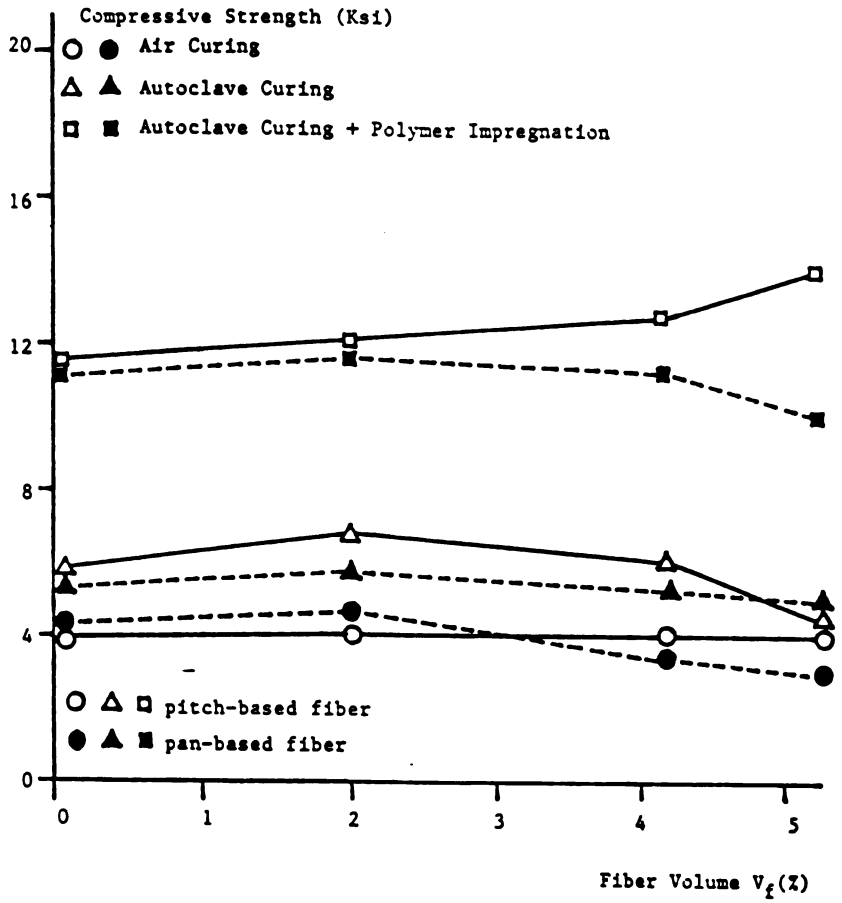

Figure 6.8: Effects of fiber type and curing conditions on the compressive strength of carbon fiber reinforced cement.[15] (water/cement = 0.47, silica powder/cement = 0.25, methyl cellulose/cement = 0.01, fiber length = 0.12 in = 3 mm, mixing in Omni mixer, cylinderical specimens 2 x 4 in). 1 in = 25.4 mm, 1 Ksi = 6.9 MPa

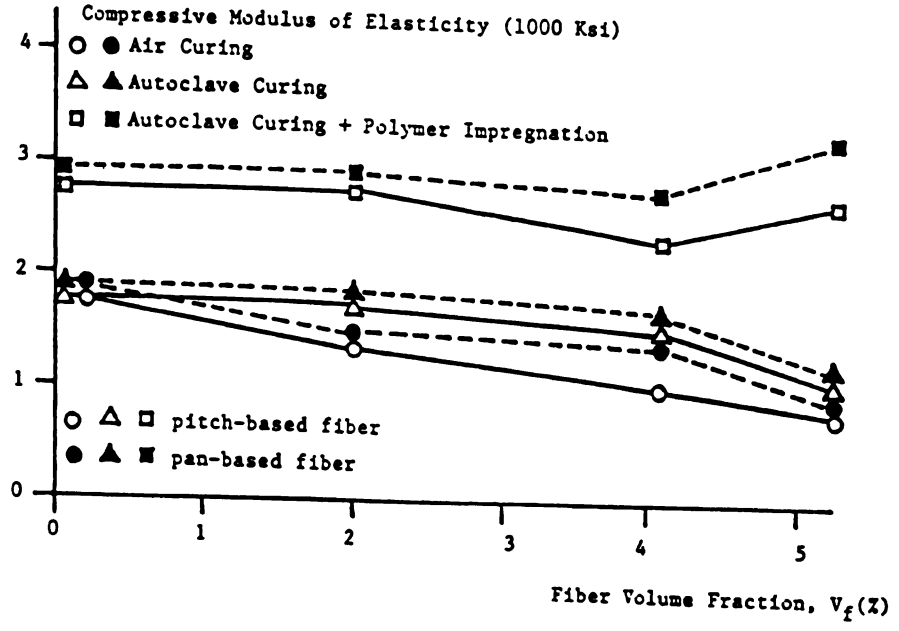

Figure 6.9: Effects of fiber type and curing conditions on the compressive modulus of elasticity of carbon fiber cement.[15] (water/cement = 0.47, silica powder/cement = 0.25, methyl cellulose/cement = 0.01, fiber length = 0.12 in = 3 mm, mixing in Omni mixer and cylinderical specimens 2 x 4 in) 1 in = 25.4 mm, 1 Ksi = 6.9 MPa.

damaging effect of fibers on workability seemed to dominate the behavior and damage the compressive strength. Polymer impregnation after autoclaving was (according to Reference 15) the best curing condition for producing carbon fiber cement composites with high compressive strengths. Autoclave curing was the next effective caring procedure and the least effective one was air curing (see Figure 6.8).

Figure 6.9 indicates that carbon fiber cement composites cured in air and autocalve have lower compressive moduli of elasticity when compared with plain cementitious matrices. In the case of composites that were polymer impregnated after atuoclaving, no consistent effects of pitch-based carbon fibers on compressive modulus of elasticity were detected. High volume fractions of pan-based carbon fibers, however, were observed to increase the modulus of elasticity of the material under compression (see Figure 6.9).

The increase in specimen size tends to increase the possibility of flaws occuring in the specimen cross-section. Hence, the compressive strength of carbon fiber reinforced cement is adversely influenced by the increase in specimen size (see Figure 6.10).[16]

6.3. Experimental Results

Figures 6.11.a through 6.11.d show the compressive stress-strain relationships for the plain cementitious matrix, and the matrices reinforced with 3% volume fraction of 1/8 in. (3 mm) fibers, 3% volume fraction of 1/16 in. (1.5 mm) fibers and 5% volume fraction of 1/16 (1.5 mm) fibers, respectively, cured in different conditions. The trends observed in Figure 6.11 regarding the effects of fiber

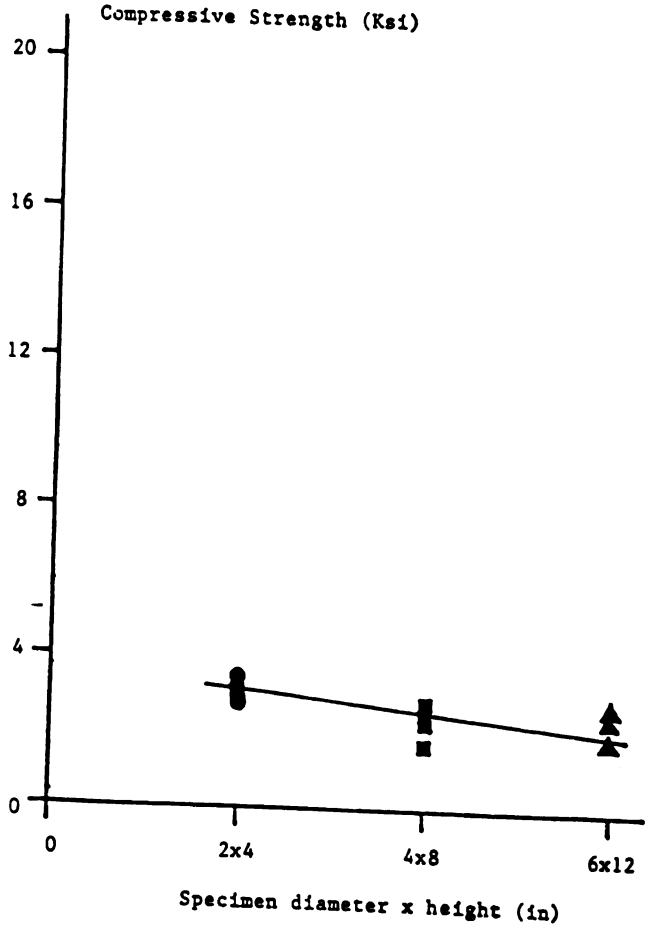

Figure 6.10: Effects of specimen geometry on the compressive strength of carbon fiber reinforced cement.[16] 1 Ksi = 6.9 MPa

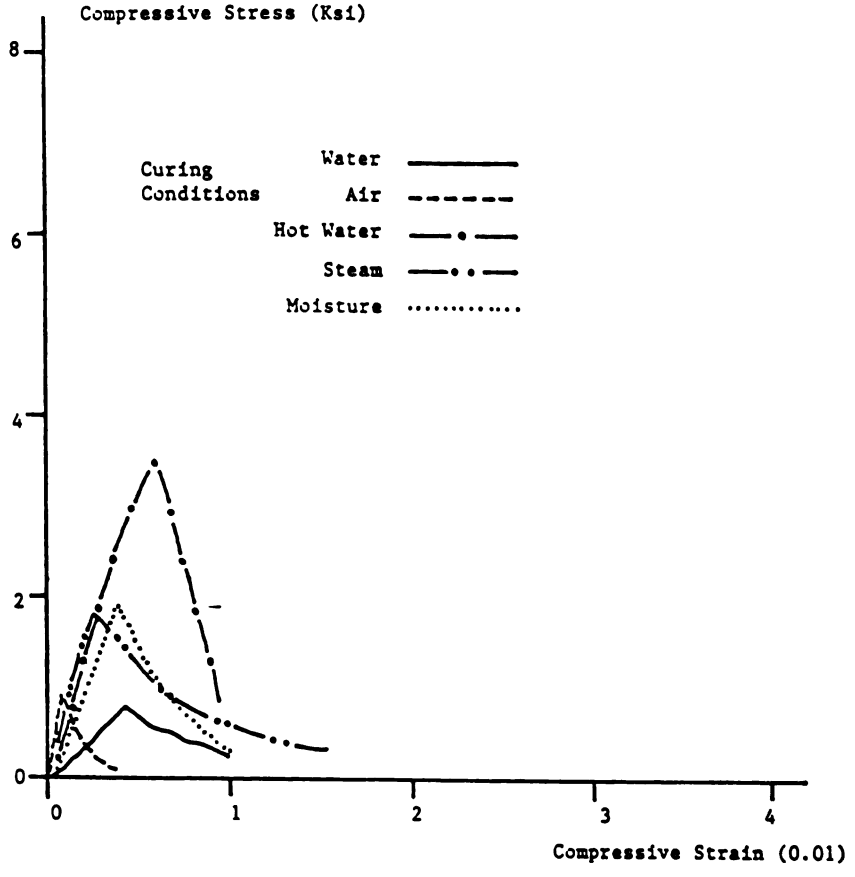

a. Plain cementitious matrix

Figure 6.11: Compressive stress-strain relationships for carbon fiber reinforced cement composites with different fiber reinforcement properties and curing conditions (water/binder = 0.3, silica fume/binder = 0.23, superplasticizer /binder = 0.032, mixing by mortar mixer and cylinderical specimens 2 x 4 in) 1 in = 25.4 mm, 1 Ksi = 6.9 MPa

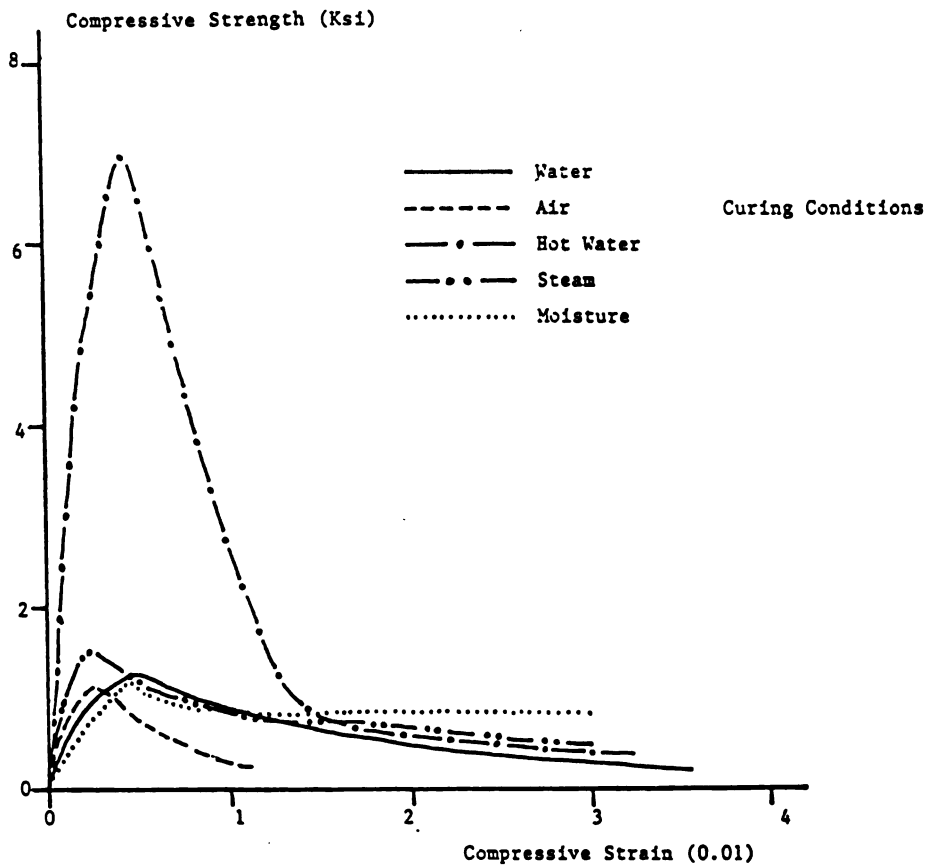

b. Fiber volume fraction (V_f) = 3%, fiber length (L_f) = 1/8 in

Figure 6.11: (continued)

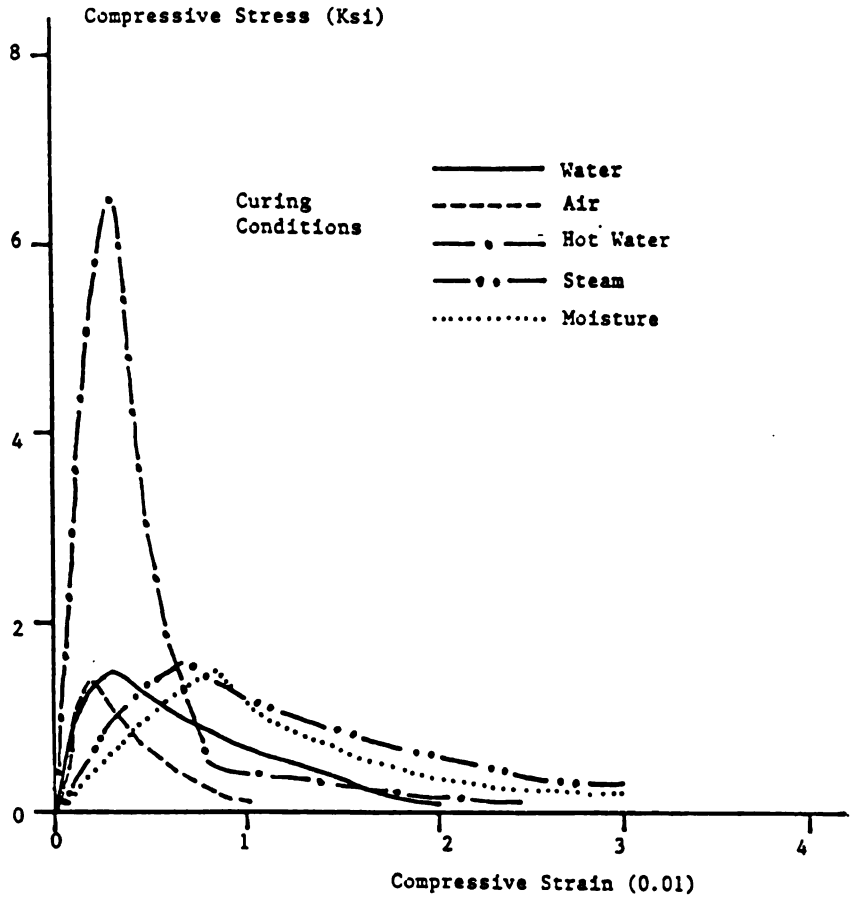

c. Fiber volume fraction (V_f) = 3%, fiber length (L_f) = 1/16 in

Figure 6.11: (continued)

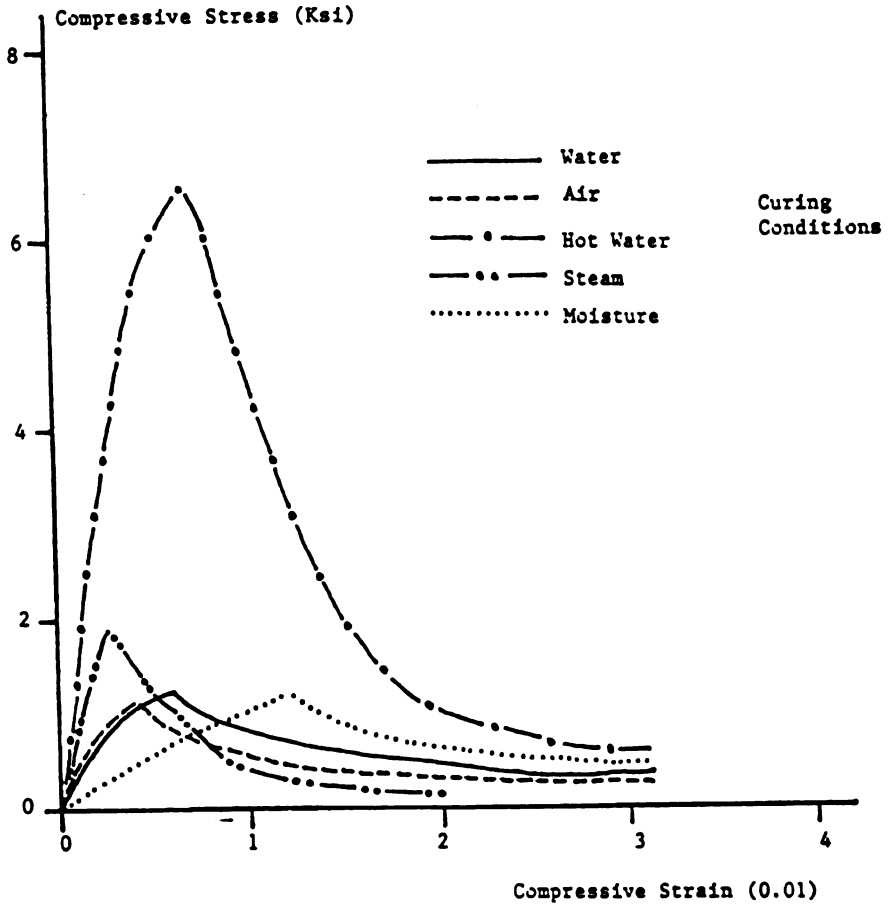

d. Fiber volume fraction (V_f) = 5%, fiber length (L_f) = 1/16 in

Figure 6.11: (continued)

reinforcement properties and curing conditions on the composite material performance are described below.

In quantifying the compressive energy absorption properties of carbon fiber reinforced cement, the total area underneath the compressive stress-strain curve up to a strain of 0.03 was defined as energy absorption capacity. Figure 6.12 presents the compressive strength of plain and carbon fiber cements cured in different conditions. Except for the hot water-cured specimens, the others show relatively low compressive strengths (in the order of 1,500 psi = 10.3 MPa), with carbon fiber reinforcement having no consistent effects on strength. Hot water curing, however, results in significant improvements in the compressive strength of plain and especially fibrous materials. The compressive strength of the plain matrix cured in hot water is about 3,500 psi (24.1 MPa), and those of fibrous mixes are of the order of 6,500 psi (44.8 MPa). Different fiber reinforcement conditions (3% volume fraction of 1/8 in. fibers, and 3% and 5% volume fraction of 1/16 in. fibers) produce comparable compressive strengths in all curing conditions, and result in specifically high compressive strengths after hot water curing.

Figure 6.13 summarizes the test results on compressive energy absorption capacity of plain and fibrous materials cured in different conditions. In all curing conditions, carbon fiber reinforcement results in improved energy absorption capacity of cement-based matrices. In spite of some loss of the post-peak energy absorption at relatively large strains resulting from hot water curing, the experimental information presented in Figure 6.13 indicates that the plain and especially fibrous specimens cured in hot water, mainly due to their superior compressive strength, provide desirable total energy absorption capacities in compression when compared with plain and

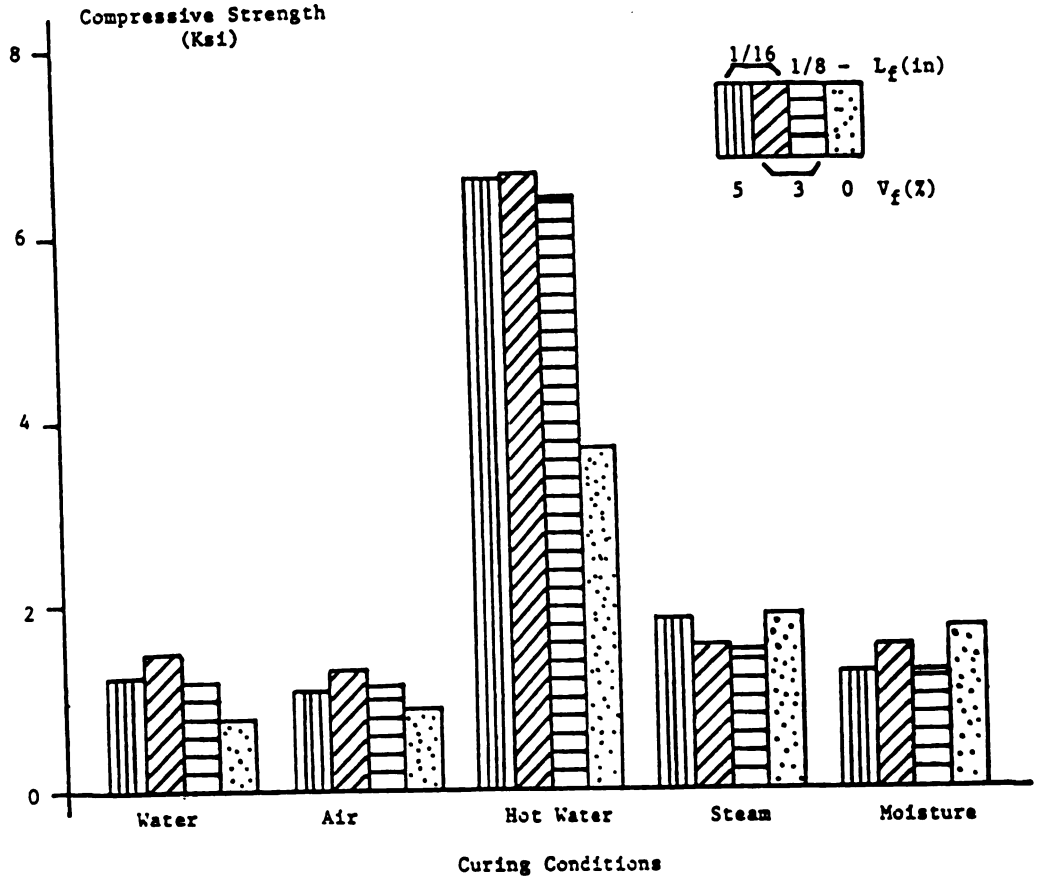

Figure 6.12: Effects of carbon fiber reinforcement on compressive strength of cementitious materials cured indifferent conditions. 1 in = 25.4 mm, 1 Ksi = 6.9 MPa.

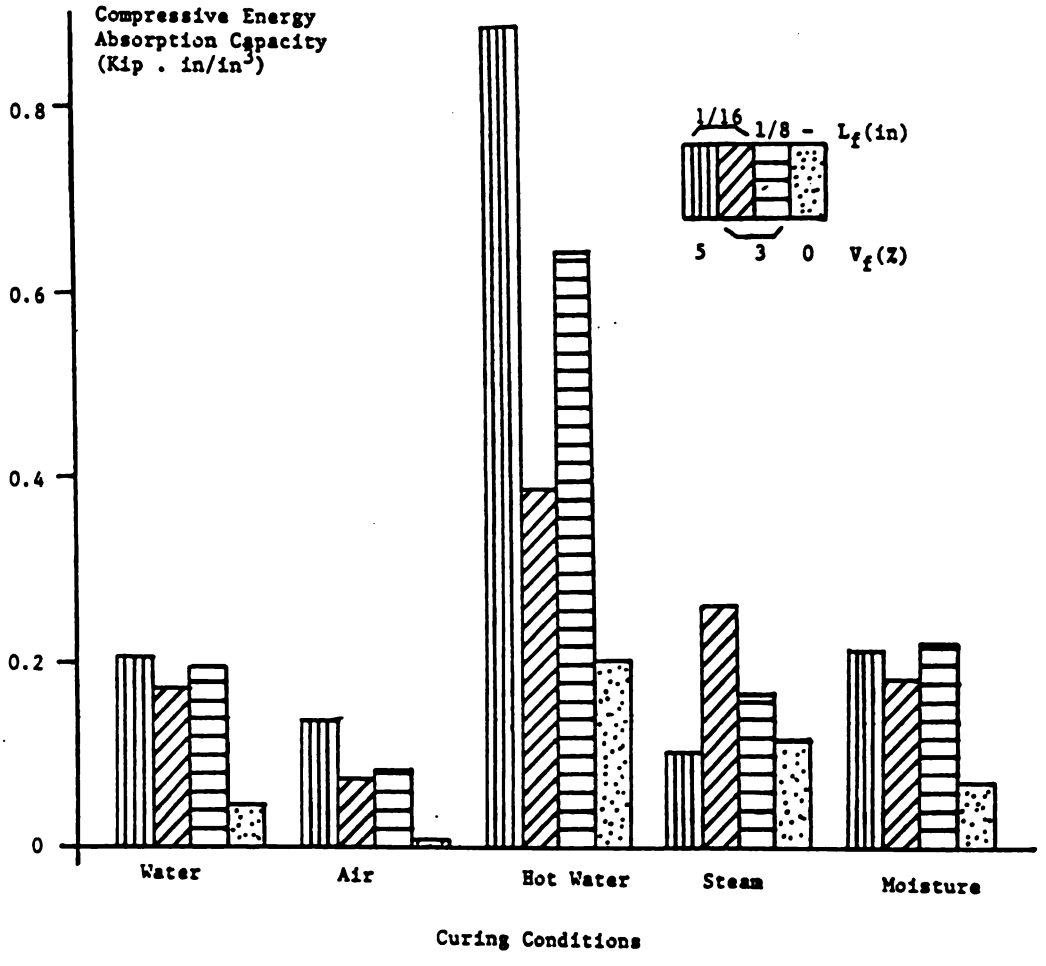

Figure 6.13: Effects of carbon fiber reinforcement on energy obsorption capacity of cementitious materials cured indifferent conditions. 1 in = 25.4 mm, 1 lb. in/in^3 = 0.007 N. mm/mm^3

fibrous materials cured in other conditions. The increase in fiber length and volume faction seem to improve the energy absorption properties of carbon fiber reinforced cement composites.

6.4. Summary and Conclusions

The constitutive behavior, strength and energy absorption properties of the composite material under compression were studied experimentally. The generated test data indicated that:

a) Unless the curing condition of carbon fiber rinced cement is optimized, there is practically no increase in compressive strength and only moderate improvements in energy absorption capacity of cement-based materials under compression resulting from carbon fiber reinforcement. Desirable curing conditions for carbon fiber cement generally involve hot and humid environments (hot water or high pressure steam); and

b) Hot water curing produces significant improvements in the compressive strength and energy absorption capacity of plain and especially carbon fiber reinforced cement-based materials. Carbon fibers, at different lengths and volume fractions considered in this study (3% of 1/8 in. (3 mm), and 3% and 5% of 1/16 in. (1.5 mm)), produce comparable effects on the compressive strength of cement, but the increase in length and volume fraction of fibers seems to improve their efficiency in enhancing the energy absorption capacity of hot water-cured cementitious materials subjected to compressive stresses.

CHAPTER 7

IMPACT RESISTANCE

7.1. Introduction

In many field applications, concrete materials are subjected to impact loading.[33,34] For example, in hydraulic structures, the positive and negative pressures caused by imploding air bubbles in high-velocity flows induce repeated impacts. Likewise, the continuous pounding of cobbles, boulders, and other debries in the stilling basing of dams and along the invert of large box culverts would produce an impact loading condition which can easily cause erosion in brittle material. Impact loading is also an important design factor in air field pavements which should survive repeated landing of airplains, and in protective structures under the impact of projectiles and blasts.[33] Overlays and industrial floor systems should also be capable of resisting the impact loads caused by the falling objects. Impact resistance as a measure of the energy absorption capacity of material is also an important property in applications such as siesmic resistant structures where energy absorption is a prime design criterion.[33-41]

Under repeated impact loads, tough materials capable of absorbing the impact energy input are preferred over a harder but more brittle material. Under the impact loading conditions, the full reliance on compressive strength of concrete as the only design criterion is insufficient, and in some cases misleading.[33] A material with high compressive strength can be very brittle and may easily fail due to impact, whereas a more resilient material with much less compressive strength would perform better. Impact resistance is a key

design factor in applications involving impact loading, for the selection of the optimum material.

Plain concrete is a rather brittle material, and it might be shattered soon under impact loading conditions.[1,2] The impact resistance of concrete can be improved considerably through the application of randomly oriented short fibers. These fibers are effective in arresting the propagation of microcracks, and in delaying the formation of macrocracks and major internal damage under repeated impacts.[1-3,35-42] Small-diameter fibers (such as carbon) are expected to be more effective than the large-diameter ones (such as steel) in arresting the microcrack propagation (see Figure 1.3) and in improving the toughness and impact resistance of concrete.[33]

The study reported in this chapter has been concerned with the effects of carbon fiber reinforcement on the impact resistance of cementitious materials. The effects of different fiber parameters (volume fraction and length) and curing conditions on the impact resistance of carbon fiber reinforced cement are investigated. A comparative study is also performed on the effectiveness of different fiber types, including carbon fibers, in improving concrete performance under impact loading.[12,33,34,43,44]

7.2. Background

Fiber reinforcement is especially effective in improving the impact resistance of cementitious materials[12,33-44] (as measured by the number of drops of a 10-lb hammer onto a steel ball resting on a standard test specimen, needed for cracking and failure of the specimen[29,34]). For steel fiber reinforced concrete (Figure 7.1.a), the number of blows to failure is typically several hundreds compared to 30 to 50 for plain concrete.[33,43] Carbon fibers, with their

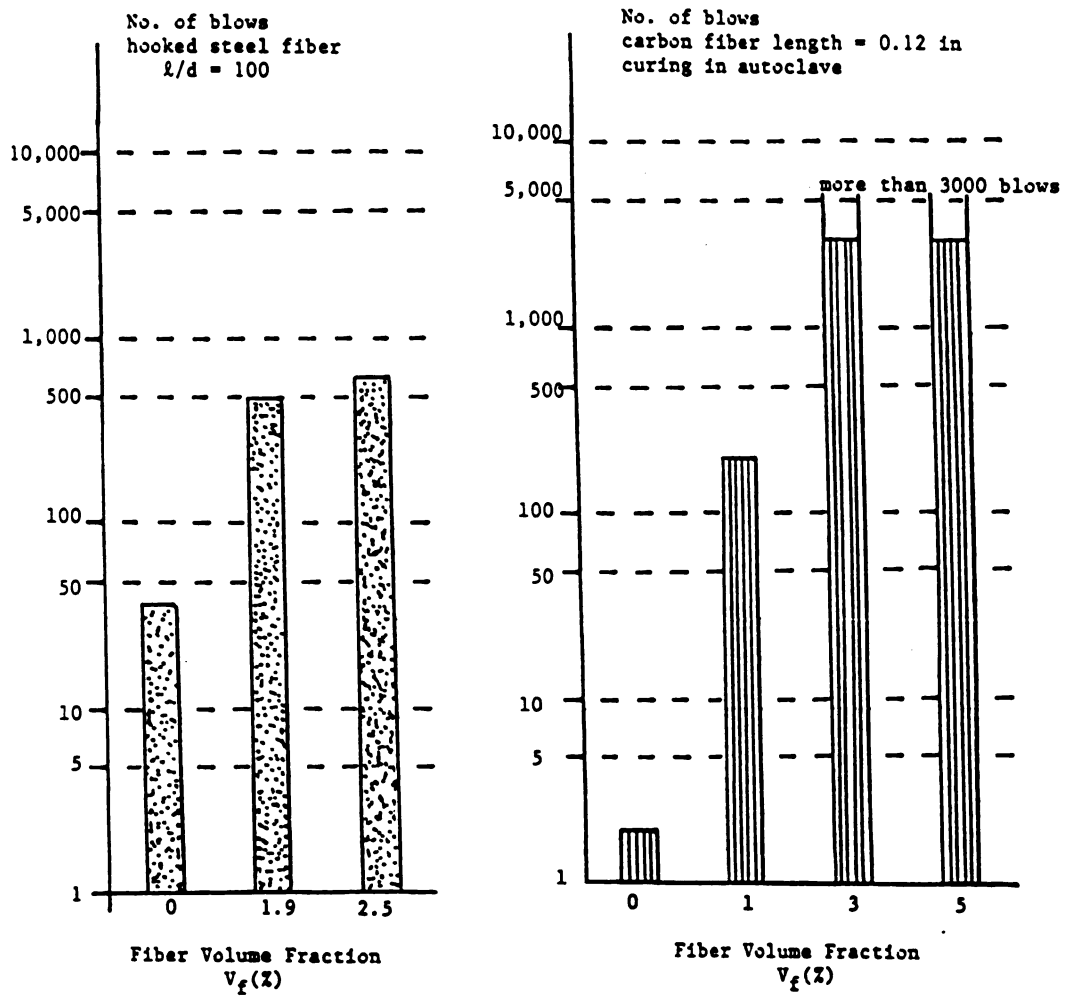

a. Steel fiber Concrete

b. Carbon fiber cement.

Figure 7.1: Effect of fiber reinforcement on impact resistance of cementitious matrices.[12,43] 1 in = 25.4 mm

relatively small diameter and consequently close spacing at a specific volume fraction, are even more efficient than steel fibers in improving the impact resistance of cementitious materials (Figure 7.1.b, noting that the test on carbon fiber cement was stopped after a maximum of 3000 blows).[12] The high efficiency of carbon fibers in improving the impact resistance of cementitious composites can abe illustrated by their relatively close spacing which is essential in arresting the microcracks,[31] nothing that the propagation of microcracks under repeated impact loads is the factor enventually leading to cracking and failure of the material.

It is worth mentioning that in spite of the fact that in many field applications of fiber reinforced concrete impact resistance is a key design factor, there are limited experimental data available in the literature on this important property of fiber reinforced concrete.

7.3. Test Procedure

The impact test equipment is shown in Figure 7.2.[45] A 6-in. diameter and 2 1/2-in. high cylindrical specimen is made by casting and external vibration. After curing, the specimen is placed on the base plate of the impact test device (see Figure 7.2). The specimen should be free to move horizontally 3/16 in. off center before touching the four positioning legs. A bracket is placed over the test specimen which contains a cylindrical sleeve that positions a hardened 2 1/2-in. diameter steel ball on the top of the test specimen. The ball is free to move vertically within the sleeve and ASTM B-1557 drop hammer (modified compacction hammer, which is used for compaction of asphalt and soil samples) is then placed on top of the ball. The number of blows from this standard 10-lb mass, dropping from an

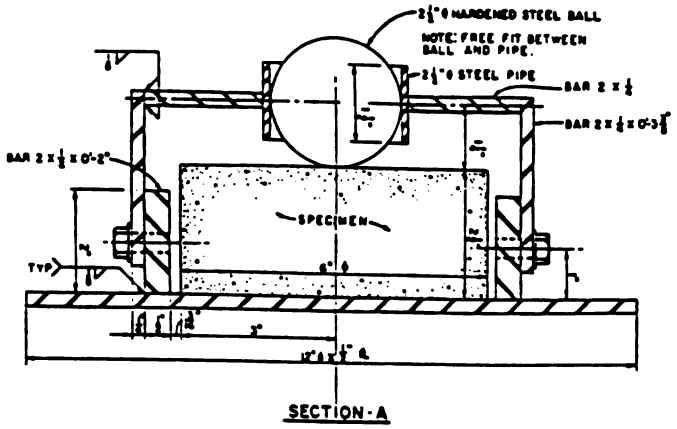

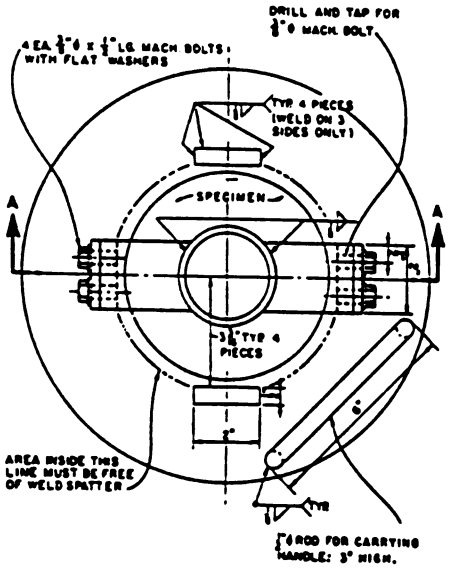

Figure 7.2: Impact test device.

established height of 18 in., required to cause the first visible crack and to cause ultimate failure are recorded. By definition, ultimate failure occurs when sufficient impact energy has been supplied to spread cracks sufficiently so that three of the four steel logs are touched by the test specimen. If desired, the "blow count" test results can be put in more scientific terminology by converting them to units of energy. Since the drop hammer weighs 10 lbs and falls 1.5 ft. per blow, each blow represents 15 ft.-lb of energy.

The impact test is popularly used to compare the relative merits of different fiber concrete mixes or to demonstrate the improved performance of a fiber mix when compared with a conventional concrete mix.[45]

There is a relatively large scatter in the impact test results of fiber reinforced concrete.[45,46] It was decided in this study that a minimum of three specimens should be used for each mix in order to assess a reasonably accurate average value for impact resistance. Comprehensive experimental studies are needed in order to establish the statistical variations, and consequently the minimum number of specimens and rejection criteria for off test results.

7.4. Test Results

The experimental data in terms of the number of blows up to first crack and failure in the impact test are presented in Table 7.1 for different carbon fiber reinforced cements cured in different conditions. The trends in the effects of different fiber volume fractions and lengths and different curing conditions, on the average cracking and ultimate impact strengths are demonstrated in Figure 7.3.

Table 7.1: Impact Test Results

Curing Condition	V_f(%), l_f(in)	First Crack Resistance				Ultimate Resistance			
		Test 1	Test 2	Test 3	Average	Test 1	Test 2	Test 3	Average
Air	5, 0.0625	13	103	27	48	25	120	30	58
	3, 0.0625	7	42	9	19	9	53	15	26
	3, 0.125	69	12	12	31	85	33	71	63
	0, 0	1	1	1	1	2	2	2	2
Water	5, 0.0625	19	14	11	15	25	39	19	28
	3, 0.0625	13	16	3	11	17	25	10	17
	3, 0.125	21	67	33	40	90	96	113	99
	0, 0	1	1	1	1	1	2	2	2
Hot Water	5, 0.0625	>3000	1829	1068	1966	>3000	1829	1133	1987
	3, 0.0625	18	80	100	66	21	84	110	72
	3, 0.125	63	417	86	188	83	425	90	199
	0, 0	1	1	1	1	2	2	2	2
Steam	5, 0.0625	684	383	156	408	1042	440	331	604
	5, 0.0625	3	48	10	20	5	55	14	25
	3, 0.125	11	7	4	7	13	10	7	10
	0, 0	1	1	1	1	1	1	1	1
Moisture	5, 0.0625	336	33	14	28	46	50	39	45
	3, 0.0625	17	15	23	18	29	29	25	28
	3, 0.125	37	11	40	29	102	23	89	71
	0, 0	1	1	1	1	1	1	1	1

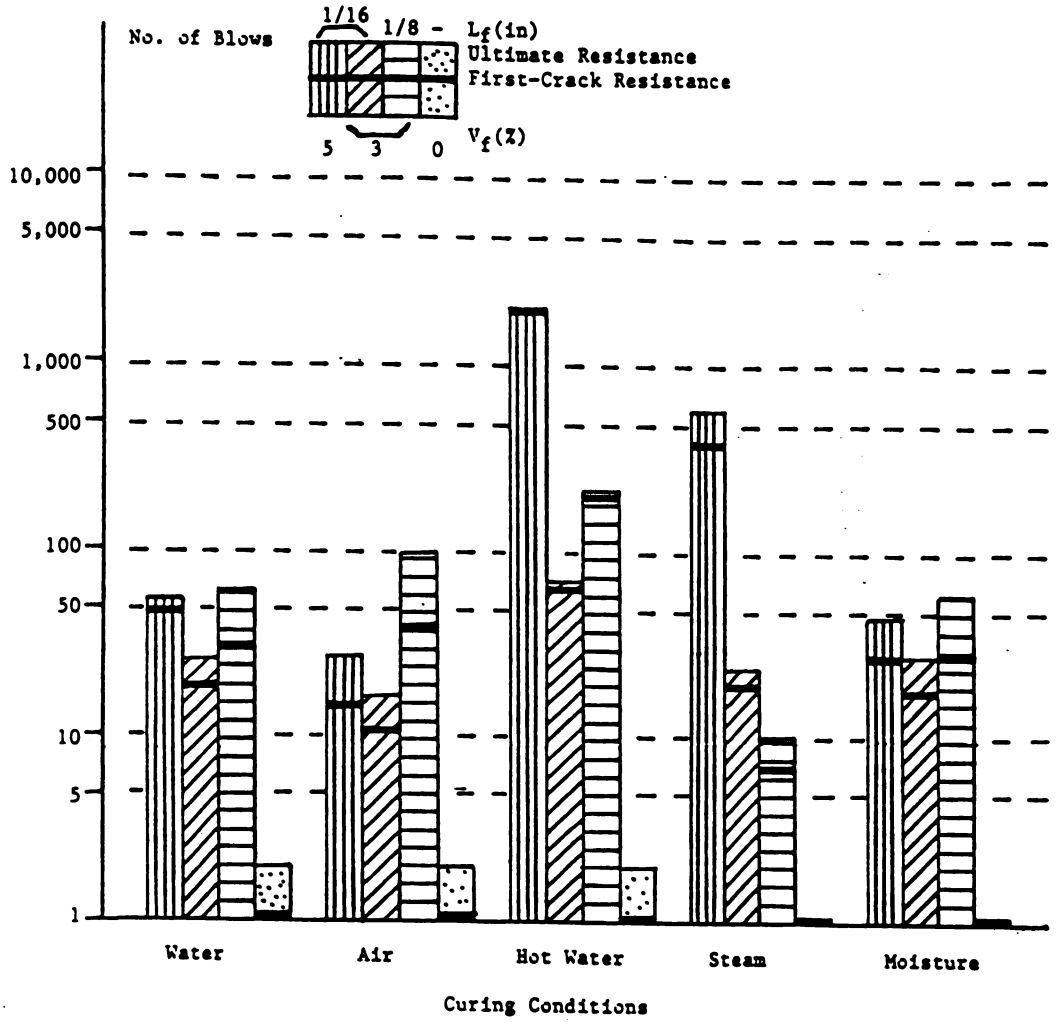

Figure 7.3: Impact resistance test results (1 blow = 15 lb. ft impact energy) 1 in = 25.4 mm, 1 lb. in = 114 N. mm

The individual test results presented in Table 7.1 are indicative of the relatively large scatter of impact test results on fibrous cement, especially for the first crack impact resistance and for curing in air. The average trends of Figure 7.3, regarding the effects of fiber volume fraction and length on impact test data, show that the impact resistance increases with increasing fiber length and volume fraction. The significance of these effects is, however, strongly dependent on the curing condition. At 3% fiber volume fraction, the increase in fiber length from 0.0625 in. to 0.125 in. increases the ultimate impact resistance of carbon fiber reinforced cement by 140%, 480%, 180%, and 150% for curing in air, water, hot water, and moist environment, respectively, and decreases the ultimate impact resistance by 60% in the case of steam curing. This data indicates that the fiber length is an important factor in deciding the impact resistance of water-cured materials. In the case of hot water and steam curing, however, the length is a less significant factor (considering both the average values and the variations in test results) in deciding the impact resistance, at least at the 3% fiber volume fraction considered in this investigation. It might be hypothesized that the hot water and steam curing conditions improve the fiber-matrix interfacial bond to an extent that both the 0.625 in. and 0.125 in. fibers dominantly fracture at cracks rather than being pulled out. In other curing conditions, however, the interfacial bond level seems to encourage the pull-out of 0.0625 in. fibers, while the 0.125 in. fibers might still have sufficient embedment length to fracture.

The increase in volume fraction of 0.0625 in. fibers from 3% to 5 % tends to increase the average ultimate impact resistance of cementitious composites by 120%, 70%, 2700%, 2300%, and 60%, for curing in air, water, hot water, steam, and moist environment, respectively. The tremendous effects of fiber volume fraction for the hot water- and steam-cured composites might be attributed to the effects of curing conditions on the matrix microstructure and carbon fiber-matrix interfacial bond characteristics.

In regard to the effects of curing conditions on impact resistance, the data presented in Table 7.1 and Figure 7.3 indicate that the hot water and steam curing conditions, at the higher 5% fiber volume fraction, are highly superior to the air, water, and moist curing conditions in improving the impact resistance of cementitious composites. Another effect of the curing condition is in regard to the ratio of the first crack to ultimate impact resistance. This ratio is 0.68, 0.53, 0.95, 0.73, and 0.56 for curing in air, water, hot water, steam, and moist environment, respectively. Hot water and steam curing conditions seem to reduce the difference between the first crack and ultimate impact strengths. This could be due to the better interfacial bond characteristics in these curing conditions, which encourage the fracture of fibers at cracks and thus eliminates the post-cracking resistance associated with the pull-out of fibers.

Non-fibrous cementitious composites are generally brittle with a very low impact resistance. This is especially true in the case of the cementitious matrix used in this study which, due to the lack of aggregates, could be damaged by shrinkage cracking when used without fibers.

7.5. Summary and Conclusions

The impact resistance of concrete is a prime property of the material in a variety of applications, including the hydraulic structures, airfield pavements, overlays and industrial floor systems, protective shelters, and siesmic-resistant structures. Impact resistance is a measure of the energy absorption capacity of the material, and it can abe improved considerably by fiber reinforcement. Fibers arrest the microcracks propagation and consequently control the damage to concrete under repeated impact loads. This is especially true for the smaller-diameter fibers which are closely spaced at a specific volume fraction; and are thus more effective in arresting the microcracks.

An experimental program was performed in this study on the effectiveness of carbon fibers in improving the impact resistance of cementitious materials. This study quantified the effects of carbon fiber volume fraction and length as well as the curing procedure on the impact resistance of cementitious materials.

Carbon fiber reinforced cementitious composites have a water-cementitious ratio of 0.25, a silica fume-cementitious ratio of 0.23, and superplasticizer-cementitious ratio of 0.08. The fiber volume fraction and lengths considered were 5% and 3% of 0.0625 in. fibers, and 3% of 0.125 in. fibers. A control plain matrix was also tested without fibers. The materials were either air-cured, moist-cured, steam-cured, or cured in water at ambient and also high temperatures.

The impact test basically consisted of the application of repeated blows of a standard mass from a specific height to a standard ball positioned on a 6 in. diameter x 2 1/2 in. high cylinder specimen, according to ASTM B-1557. The number of blows required for the appearance of the first visible crack and ultimate failure are

defined as the first-crack and ultimate impact resistances of the fibrous concrete. The impact test data can be represented either by the number of blows or by the energy associated with the application of these blows.

The test data generated in this investigation indicated that, in spite of the relatively large scatter in results, the impact resistance of cementitious materials tends to increase with increasing fiber length and fiber volume fraction. The curing condition heavily influenced the effects of fiber variables. AT 3% fiber volume fraction, the increase in length from 0.0625 in. to 0.125 in. increased the ultimate impact resistance by about 150% for curing in air, hot water, and moist environment, and by about 500% for curing in water, while reduced the impact resistance by 60% in the case of steam curing.

The increase in fiber volume fraction from 3% to 5% for the 0.0625 in. fibers increased the ultimate impact resistance of cementitious composites by about 60% for curing in water and moist environment, by about 100% for curing in air, and by about 2500% for the hot water and steam curing conditions. The difference between the first crack and ultimate impact strengths was smaller for the composites with 5% fiber volume fraction. Basically, the hot water and steam curing conditions were far superior to the other curing procedures for composites with 5% fiber volume fraction. This superiority was less significant at 3% fiber volume fraction. Based on these test results it may be hypothesized that the hot water and steam curing conditions lead to major improvements in the interfacial fiber-matrix bond characteristics, and also produce some improvements in the matrix pore system. These seem to be the key factors contributing to the high efficiency of carbon fibers in increasing the

impact resistance of cementitious composites cured in steam and hot water.

CHAPTER 8

SUMMARY AND CONCLUSIONS

8.1. General

A comprehensive experimental study was performed on mix proportioning, manufacturing techniques, and fresh and hardened material properties of carbon fiber reinforced cement composites. The study was performed in two stages. The first stage was concerned with characterizing carbon fiber reinforced cement in the fresh and hardened states by establishing the variations in fresh mix workability and air cured hardened material strength resulting from changing the matrix mix proportions and carbon fiber reinforcement properties. The results of this phase of study were used to decide the optimum matrix mix proportions and the desirable ranges of carbon fiber length and volume fraction for achieving a satisfactory fresh mix workability with superior hardened material strength.

In the second stage of this research, which was performed on carbon fiber reinforced cement composites with optimum matrix mix proportions and selected values of fiber length and volume fraction, a comprehensive experimental study was performed on the hardened material characteristics obtained after the curing of material in different conditions. In this stage, the complete flexural load-deflection relationships, compressive and tensile stress-strain properties, impact resistance and strength development of the material with time were investigated. A comprehensive review of the available literature on these aspects of the material behavior were also presented. A summary of the activities and findings of different phases of the investigation are given below.

8.2. Fresh Mix Properties

An experimental research was conducted to establish the trends in the effects of different mix variables on the properties of fresh carbon fiber cement mixes. The variables considered in this study were: fiber volume fraction and length, silica fume-binder ratio, water-binder ratio, superplasticizer-binder ratio, variability in fiber length, and time elapsed after mixing. The fresh mix properties investigated were: flow, subjective workability, and subjective fiber dispersability. All mixes were manufactured in a conventional mortar mixer.

The following conclusions could be derived from test results.

1. Silica fume is an effective additive in cementitious matrices for improving their ability of uniformly dispersing fibers. The addition of silica fume, however, damages the flowability and workability of fresh carbon fiber reinforced cement mixtures.

2. In order to solve the workability problems caused by the addition of silica fume and fibers in cementitious mixes, it is essential to use relatively large dosages of superplasticizers. The increase in superplasticizer content up to a certain limit also improves the fiber dispersability of cementitious matrices.

3. The increase in water content improves the flowability and workability of fibrous mixes at a gradually decreasing rate, but does not influence fiber dispersability.

4. The flowability, workability and fiber dispersability of fresh carbon fiber reinforced cement are adversely influenced by the increase in fiber volume fraction. This effect is more pronounced for longer fibers.

5. The fresh mix workability tends to be damaged at a generally decreasing rate with increasing fiber length. The

dispersability of fibers in cementitious matrices also tends to be damaged as the fiber length increases. The variability of carbon fiber length generates relatively large variations in the fresh mix properties of carbon fiber reinforced cement.

6. Carbon fiber reinforced cement mixes with silica fume have relatively short setting times. Their flow drops by 15% and 30% at 4 and 10 minutes after mixing, respectively, compared to their flow at 1 minute after mixing.

8.3. Hardened Material Strength

An experimental program was also conducted on the flexural, direct tensile and compressive strengths of air-cured carbon fiber reinforced cement. The results indicated that:

1. The flexural and direct tensile strength of carbon fiber reinforced cement increase, at a decreasing rate, with the increase in fiber volume fraction of fibers up to an optimum value beyond which this tendency starts to reverse. The compressive strength, however, decreases with increasing volume fraction of fibers up to a point beyond which the compressive strength tends to either stay constant or increase as the fiber volume fraction increases.

2. The tendencies in the effects of fiber length on strength are comparable to those of fiber volume fraction. The flexural and tensile strengths first increase and then decrease with increasing fiber length, while the reverse is true for compressive strength.

3. Microsilica, due to its positive effects on dispersability and bonding to carbon fibers, improves the material strength. Beyond a certain microsilica content, however, its negative effects on fresh

mix workability start to overshadow the advantages obtained through the use of microsilica.

4. The limited test data obtained on the effects of water content indicate that the strength of carbon fiber cement generally increases with decreasing water-binder ratio.

5. Air-cured carbon fiber reinforced cement develops strength at a higher rate than conventional concrete. After 12 days of air curing, carbon fiber reinforced cement gains more than 90% of its full strength.

6. Carbon fiber reinforced cement has distinctly high flexural-to-compressive and flexural-to-tensile strength ratios. There is generally a relatively large scatter in test results obtained for carbon fiber reinforced cement.

8.4. Flexural Characteristics

An experimental study was performed on the flexural behavior of carbon fiber reinforced cement. The effects of fiber length and volume fraction, and curing condition on the flexural load-deformation characteristics were investigated. Two fiber lengths (1/8 in. = 3 mm and 1/16 in. = 1.5 mm), two volume fractions (3% for both fiber lengths and 5% for shorter fibers), and five curing conditions (in air, water, hot water, moist room and steam for one day and then in air) were included in the experimental program. The development of flexural strength in carbon fiber reinforced cement composites subjected to different curing conditions was also studied. The overall flexural load-deformation relationships were characterized by the ultimate flexural strength, total energy absorption capacity, toughness (representing the post-peak energy absorption), initial

stiffness, and first crack-to-ultimate strength ratio. The following conclusions can be derived from the experimental results generated in this study:

1. Carbon fiber reinforcement results in significant improvements in the flexural strength of cement materials. Different fiber lengths and volume fractions considered in this study produced composites with comparable flexural strengths, except for conditions involving hot water and steam curing where fibers at 5% volume fraction were more effective than at 3% volume fractions in increasing the flexural strength. Hot water curing results in carbon fiber cement composites with highest flexural strengths (typically about 40% more than what could be obtained by the second best curing condition, which is usually in steam).

2. Carbon fiber reinforcement substantially increases the energy absorption capacity of cement-based materials. Longer fibers are more effective in increasing energy absorption. The increase in fiber volume fraction, except for the moist room curing condition, also has a positive effect on energy absorption. Steam and especially hot water curing damage the ductility of the material behavior and reduce its energy absorption capacity. At 5% volume fraction, however, the superior flexural strength obtained by hot water and steam curing tends to provide a significant pre-peak energy absorption capacity which, to a certain extent, compensates for the negative effects of steam and hot water curing on post-peak ductility.

3. Fiber reinforcement generally increases the toughness (post-peak energy absorption capacity) of cement composites, noting that the toughness of plain cementitious materials is negligible. Different fiber lengths and volume fractions considered in this investigation generated composites with comparable toughness

characteristics except that fibrous composites cured in hot water have practically zero post-peak energy absorption.

4. Carbon fiber reinforcement has a small effect on the initial flexural stiffness of cementitious materials. Hot water curing produces plain and fibrous cements with distinctly high flexural stiffnesses.

5. The ratio of first crack to ultimate flexural strength is 1.0 for plain matrices, about 0.8 for fibrous composites cured in other than hot water conditions, and 1.0 for fibrous composites cured in hot water. It should be noted, however, that the pre-peak behavior of carbon fiber reinforced cement under increasing flexural load involves a gradual process of microcrack propagation, and thus a distinct cracking load can hardly be distinguished.

6. Carbon fiber reinforced cement composites generally have a higher rate of strength development with time than conventional concrete materials. The material, when cured in air, steam, water and moist environments, practically reaches its full flexural strength at an age of 16 days. Hot water curing tends to accelerate the development of flexural strength, producing practically the full strength at an age of about 7 days.

8.5. Tensile Characteristics

The results of an experimental study on the performance of carbon fiber reinforced cement under direct tension are presented. The effects of carbon fiber length and volume fraction, and curing condition, on the tensile behavior of cement-based materials are described. The test program covered plain cementitious composites and fibrous ones with 3% and 5% of 1/16 in. (1.5 mm) fibers, and with 3%

of 1/8 in. (0.125 mm) fibers. The test specimens were cured in air, moist room, water, hot water, and steam.

Toughness (a representative of post-peak energy absorption) is generally defined as the ratio of the total energy absorption capacity (measured up to a strain of 0.006) to the energy absorbed by the material prior to cracking. The plain specimens was observed to have a toughness value close to 1.0, indicating no post-peak energy absorption. Carbon fiber reinforcement, except for curing in hot water, provides cementitious materials with a substantially improved toughness. There seems to be a tendency in the toughness of carbon fiber reinforced cement composites to increase with increasing fiber length and volume fraction. The damage to toughness resulting from hot water curing may be attributed to the improvements in the bonding of cementitious matrices after hot water curing to carbon fibers. An excessively strong bond encourages the rupture of fibers prior to pull-out. This eliminates the major fraction of energy absorption associated with fiber pull out. The test data generated in this investigation indicated that:

1. Carbon fiber reinforcement results in major improvements in the tensile stress-strain behavior of cementitious materials. The highly brittle nature of failure in plain cement matrices is changed, except after hot water curing, to a desirable performance with major post-peak ductility.

2. Important improvements in the first crack and ultimate tensile strengths of cement-based material can be achieved through carbon fiber reinforcement. Different fiber reinforcement properties lead to comparable tensile strengths after air, water, steam and moist curing. Hot water curing, especially at 5% fiber volume fraction, results in relatively high tensile strengths.

3. Major improvements in the total energy absorption capacity of cementitious materials can be achieved by carbon fiber reinforcement. Hot water curing, through generating excessive interfacial bond strength between fibers and matrix and eliminating fiber pull-out before rupture, reduces the efficiency of fibers in enhancing the energy absorption capacity of cement materials.

4. Toughness, a representative of post-peak energy absorption capacity, is significantly higher in carbon fiber reinforced cement when compared to plain cementitious materials, except after hot water curing. The increase in length and volume fraction of fibers generally improve the toughness of fibrous cements.

5. The initial tensile stiffness of cementitious materials seems to be more dependent on curing condition than carbon fiber reinforcement properties. Steam and especially hot water curing give higher stiffnesses for both plain and fibrous materials.

8.6. Compressive Behavior

The constitutive behavior, strength and energy absorption properties of carbon fiber reinforced cement composites under compression were studied experimentally.

The overall conclusions that could be derived from the test data generated in this study are as follows.

a) Unless the curing conditions of carbon fiber reinforced cement are optimized, there are practically no increase in compressive strength and only moderate improvements in the compressive energy absorption capacity of cement-based materials resulting from carbon fiber reinforcement. Desirable curing conditions require hot and humid environments (e.g. hot water or high pressure steam); and

b) Hot water curing produces significant improvements in the compressive strength and energy absorption capacity of plain and especially carbon fiber reinforced cement materials. Carbon fibers at different lengths and volume fractions considered in this study (3% of 1/8 in. (3 mm) and 3% and 5% of 1/16 in. (1.5 mm)) produce comparable improvements in the compressive strength of cement, but the increase in length and volume fraction of fibers seems to improve the efficiency of fibers in enhancing the energy absorption capacity of hot water-cured cementitious materials subjected to compressive stresses.

8.7. Impact Characteristics

The impact resistance of concrete is a prime property of the material in a variety of applications, including the hydraulic structures, airfield pavements, overlays and industrial floor systems, protective shelters, and siesmic-resistant structures. Impact resistance is a measure of the energy absorption capacity of the material, and it can be improved considerably by fiber reinforcement. Fibers arrest the propagation of microcracks and consequently control the damage to concrete under repeated impact loads. This is especially true about the smaller-diameter fibers which are closely spaced at a specific volume fraction; and are thus more effective in arresting the microcracks.

An experimental program was conducted in this study on the effectiveness of carbon fibers in improving the impact resistance of cementitious materials. The study quantified the effects of carbon fiber volume fraction and length, and the curing procedure, on the impact resistance of the composite.

Carbon fiber reinforced cementitious composites had a water-cementitious ratio of 0.25, a silica fume-cementitious ratio of 0.23,

and superplasticizer-cementitious ratio of 0.08. The fiber volume fractions and lengths considered were 3% and 5% of 0.0625 in. (1.5 mm) fibers, and 3% of 0.125 in. (3 mm) fibers. A control plain matrix was also tested without fibers. The materials were either air-cured, moist-cured, steam-cured, or cured in water at ambient and also high temperatures.

The impact test basically consisted of the application of repeated blows of a standard mass from a specific height to a standard ball positioned on a 6 in. (150 mm) diameter x 2 1/2 in. (63 mm) high cylindrical specimen, according to ASTM B-1556. The number of blows required to cause the first visible crack and the ultimate failure are the first crack and ultimate impact resistances of fibrous concrete. The impact test data can be represented either by the number of blows or by the energy associated with the application of these blows.

The test data generated in this investigation indicated that, in spite of the relatively large scatter in results, the impact resistance tends to increase with increasing fiber length and fiber volume fraction, with the curing conditions heavily influencing the effects of these variables. At 3% fiber volume fraction, the increase in length from 0.0625 in. (1.5 mm) to 0.125 in. (3 mm) increases the ultimate impact resistance by 60% in the case of steam curing.

The increase in fiber volume fraction from 3% to 5% for the 0.0625 in. (1.5 mm) fibers increases the ultimate impact resistance of cementitious composites by about 60% for curing in water and moist environment, by about 100% for curing in air, and by about 2500% for the hot water and steam curing conditions. The difference between the first crack and ultimate impact strengths was smaller for composites cured in hot water and steam. Basically, the hot water and steam curing conditions were far superior to the other curing procedures for

composites with 5% fiber volume fraction. This superiority was less significant at 3% fiber volume fraction. From these test results it may be hypothesized that the hot water and steam curing conditions lead to major improvements in the interfacial fiber-matrix bond characteristics and some improvements in the matrix pore system. These factors seem to illustrate the high efficiency of carbon fibers in increasing the impact resistance of cementitious composites cured in steam and in hot water.

REFERENCES

1. Mehta, P.K., "Concrete Structure, Properties and Materials," Printice-Hall, Inc., 1986, 450 pp.

2. Mindess, S. and Young, J.F., "Concrete," Printice Hall, Inc., 1981, 671 pp.

3. Visalvanich, K. and Naaman, A., "Fracture Model for Fiber Reinforced Concrete," ACI Journal, Vol. 80, No. 2, March-April 1983, pp. 128-138.

4. Krenchel, H. and Hejgaard, O., "Can Asbestos Be Completely Replaced One Day?," Proceedings, RILEM Symposium on Fiber Reinforced Cement and Concrete, (London), Vol. 1, September 1975, pp. 335-346.

5. Akihama, S., Suenaga, T. and Nakagawa, H., "Carbon Fiber Reinforced Concrete," Concrete Vol. 10, No. 1, January 1988, pp. 40-47.

6. Ohama, Y., Demura, K. and Sato, Y., "Development of Lightweight Carbon Fiber Reinforced Fly Ash-Cement Composites," Proceedings, International Symposium on Fiber Reinforced Concrete, (Madras) Vol. 1, December 1987, pp. 3.23-3.31.

7. Neelamegam, M. and VenKateswardu, B., "Properties of Glass Fiber Reinforced Cement Composites with an without Polymer Impregnation," Proceedings, International Symposium on Fiber Reinforced Concrete (Madras), Vol. 1, December 1987, pp. 3.67 - 3.81.

8. Konczalski, P. and Piekarski, P., "Tensile Properties of Portland Cement Reinforced with Kevlar Fibers," Journal of Reinforced Plastics and Composites, Vol. 1, October 1982, pp. 378-384.

9. Soroushian, P. and Nagi, M., "Durability of Carbon Fiber Reinforced Cement," Report MSU-ENGR-87-07, Michigan State University, June 1987, 60 pp.

10. Ali, M.A., Majumdar, A.J. and Rayment, D.L., "Carbon Fiber Reinforcement of Cement, "Vol. 2, No. 2, 1972, pp. 201-212.

11. Waller, J.A., "Carbon Fiber Reinforced Cement Composites," ACI Publication SP 44: Fiber Reinforced Concrete, 1974, pp. 143-161.

12. Ohama, Y., Amano, M. and Mitshuhiro, E., "Properties of Carbon Fiber Reinforced Cement with Silica Fume," Concrete International, Vol. 7, No. 3, March 1985, pp. 58-62.

13. Ohama, Y. and Amano, M., "Effects of Silica Fume and Water Reducing Agent on Properties of Carbon Fiber Reinforced Mortar," Proceedings, 27th Japan Congress on Materials Research, Kyoto, 1984, pp. 187-191.

14. Akihama, S., Suenaga, T., and Banno, T., "Mechanical Properties of Carbon Fiber Reinforced Cement Composite and the Application to Large Domes," KICT Report No. 53, Kajima Institute of Construction Technology, Tokyo, July 1984, 97 pp.

15. Akihama, S., Suenaga, T., Nakagawa, H. and Suzuki, K., "Influence of Fiber Strength and Polymer Impregnation on the Mechanical Properties of Carbon Fiber Reinforced Cement Composites," Proceedings, RILEM Symposium on Developments in Fiber Reinforced Cement and Concrete (Sheffield), Vol. 1, July 1986.

16. Akihama, S., Kobayashi, M., Suenaga, T., Nakagawa, H. and Suzuki, K., "Effect of CFRC Specimen Geometry on Flexural Behavior," Proceedings, RILEM Symposium on Developments in Fiber Reinforced Cement and Concrete (Sheffield), Vol. 1, July 1986.

17. Nishioka, K., Yamakawa, S. and Shirakawa, K., "Properties and Applications of Carbon Fiber Reinforced Cement Composite," Proceedings, RILEM Symposium on Developments in Fiber Reinforced Cement and Concrete (Sheffield), Vol. 1, July 1986.

18. Garlinghouse, L.H. and Garlinghouse, R.E., "The Omni Mixer- A New Approach to Mixing Concrete," ACI Journal, Vol. 69, No. 4, April 1972, pp. 220-223.

19. "Kureha Carbon Fiber," product information brochure, Kureha Chemical Industry Company, Tokyo, 1986, 16 pp.

20. "Carboflex," production information sheets, Ashland Petroleum Company, Ashland, 1986, 5 pp.

21. "Huron Cement," product information brochure, Huron Cement, Southfield, 1985, 6 pp.

22. "Microsilica - Typical Analysis," product information sheets, Elkem Chemicals, Pittsburgh, 1984, 2 pp.

23. Wolsiefer, J., "Ultra High-Strength Field Placeable Concrete with Silica Fume Admixture," Concrete International, Vol. 6, No. 4, April 1984, pp. 25-31.

24. Ramakrishnan, V. and Srinivasan, V., "Silicafume in Fiber Reinforced Concrete," Indian Concrete Journal, Vol. 56, No. 12, December 1982, pp. 326-334.

25. "The Daracem Advantage," product information brochure, Grace Construction Products, Cambridge, 1986, 6 pp.

26. Instruction Manual for Hobart Model A-200 Mixer, The Hobart Manufacturing Company, Troy, 1977, 8 pp.

27. "1986 Annual Book of ASTM Standards," Section 4: Construction, Vol. 4.01: Cement, Lime, Gypsum; ASTM, Philadelphia, 1986.

28. Operation and Service Instruction for Model CT-21 10-in Flow Table, Soil Test Incorporated, Evanston, 1985, 4 pp.

29. ACI Committee 544, "Measurement of Properties of Fiber Reinforced Concrete," ACI Journal, Vol. 75, No. 7, July 1978, pp. 283-289.

30. Larson, B., "Carbon Fiber-Cement Adhesion in Carbon Fiber Reinforced Cement," M.S. Thesis, Michigan State University, East Lansing, 1988, 55 pp.

31. Romualdi, J.P. and Mandel, J.A., "Tensile Strength of Concrete Affected by Uniformly Distributed and Closely Spaced Short Lengths of Wire Reinforcement," ACI Journal, Vol. 61, No. 6, June 1964, pp. 657-670.

32. Ohama, Y. and Muranishi, R., "Relation Between Curing Conditions and Strength of Silica Fume Modified Concrete," Proceedings, 27th Japan Congress on Materials Research, Kyoto, 1984, pp. 199-202.

33. ACI Committee 544, "State-of-the-Art Report on Fiber Reinforced Concrete," Report No. ACI 544.1R-82, ACI, May 1982, 16 pp.

34. Schrader, E.K., "Impact Resistance and Test Procedure for Concrete," ACI Journal, Vol. 78, No. 2, March - April 1981, pp. 141-146.

35. Kavyrchine, M. and Astruc, M., "Impact Testing Equipment for Structural Elements," Proceedings, RILEM Symposium on Testing and Test Methods of Fiber Cement Composites (Sheffield), 1978, pp. 129-138.

36. Verhagen, A.H., "Impact Testing of Fiber Reinforced Concrete: Reflection on Possible Test Methods," Proceedings, RILEM Symposium on Testing and Test Methods of Fiber Cement Composites (Sheffield), 1978, pp. 99-106.

37. Hibbert, A.P. and Hannant, D.J., "The Design of an Instrumented Impact Test Machine for Fiber Concretes," Proceedings, RILEM Symposium on Testing and Test Methods of Fiber Cement Composites, (Sheffield), 1978, pp. 107-120.

38. Jamrozy, Z., "Lightweight Aggregate Concrete with Steel Fiber Admixture," Proceedings, RILEM Symposium on Testing and Test Methods of Fiber Cement Composites (Sheffield), 1978, pp. 121-127.

39. Suaris, W. and Shah, S.P., "Properties of Concrete Subjected to Impact," ASCE Journal of Structural Engineering, Vol. 109, No. 7, July 1983, pp. 1727-1741.

40. Naaman, A.E., "Fiber Reinforced Concrete Under Dynamic Loading," ACI Publication SP-81: Fiber Reinforced Concrete, 1984, pp. 169-186.

41. Lakshmipathy, M. and Santhakumar, A.R., "Experimental Verification of the Behavior of Reinforced Fibrous Concrete Frames Subjected to Seismic Type of Loading," Proceedings, RILEM Symposium on Developments in Fiber Reinforced Cement and Concrete (Sheffield), Vol. 2, No. 8.15, 1986.

42. Bentur, A., Gary, R.J. and Mindess, S., "Cracking and Pull-Out Processes in Fiber Reinforced Cementitious Materials," Proceedings, RILEM Symposium on Developments in Fiber Reinforced Cement and Concrete (Sheffield), Vol. 2, No. 6.2, 1986.

43. Ramakrishnan, V., Brandshaug, T., Coyle, W.V. and Schrader, E.K., "A Comparative Evaluation of Concrete Reinforced Straight Steel Fibers and Fibers with Deformed Ends Glued Together into Bundles," ACI Journal, Vol. 77, No. 3, May-June 1980, pp. 135-143.

44. Ramakrishnan, V., Coyle, W.V., Kulandaisamy, V. and Schrader, E.K., "Performance Characteristics of Fiber Reinforced Concretes with Low Fiber Contents," ACI Journal, Vol. 78, No. 5, September - October 1981, pp. 388-394.

45. Schrader, E.K., "Formulating Guidance for Testing of Fiber Concrete in ACI Committee 544, "Proceedings, RILEM Symposium on Testing and Test Methods of Fiber Cement Composites (Sheffield), 1978, pp. 9-21.

46. Zollo, R.F., "Collated Fibrillated Polypropylene Fibers in FRC," ACI Publication SP-81: Fiber Reinforced Concrete, 1984, pp. 397-409.

MECHANICAL PROPERTIES AND STRUCTURAL APPLICATIONS OF STEEL FIBER REINFORCED CONCRETE

By

Mohamad Ziad Bayasi

Volume II of

A DISSERTATION

Submitted to

Michigan State University

in partial fulfillment of the requirements

for the degree of

DOCTOR OF PHILOSOPHY

Department of Civil and Environmental Engineering

1989

ABSTRACT

A comprehensive investigation was performed on the material properties and structural applications of steel fiber reinforced concrete. The effects of fiber reinforcement properties and concrete matrix mix variables on the fresh mix workability and hardened material mechanical characteristics were assessed. The fiber reinforcement properties considered in this investigation were: (a) volume fraction; (b) length and cross-sectional dimensions; and (c) type of mechanical deformation. The matrix variables considered were: (a) content of pozzolanic materials (fly ash and silica fume); (b) binder content; (c) superplasticizer dosage; (d) water-binder ratio; (e) maximum aggregate size; (f) aggregate gradation; and (g) dosage of air entraining agent. The trends established in the effect of fiber and matrix variables on the material performance can be helpful in proportioning of steel fiber reinforced cement mixtures which has been traditionally performed based on experience. The experimental studies were concluded by establishing the statistical variation in the fresh and hardened steel fiber reinforced concrete properties.

In studies on the application of steel fiber reinforced concrete a load bearing structural elements, the effects of steel fibers on improving the strength and dictility of concrete footings under bearing pressure, and enhancing bond between deformed bars and concrete were investigated.

Finally, through a critical investigation of the available analytical techniques

simulating the steel fibre reinforced concrete performance under tensile stress systems, the mechanism of action if steel fibers in concrete was investigated.

To my wife

ACKNOWLEDGEMENTS

The present work was performed under the supervision of Dr. Parviz Soroushian. Throughout this work, Dr. Soroushian was a sincere friend more than any thing else. The author is indebted to Dr. Soroushian for the achievements that could not be possible without his great leadership, selflessness and sacrifices. Dr. Soroushian's priceless contributions to this work will never be forgotten and the author wishes him to always be his mentor.

The author also would like to thank Dr. William C. Taylor, Dr. Lawrence T. Drazal and Dr. George Mase for their help and precious advice during his Ph.D. Program.

TABLE OF CONTENTS

Page

LIST OF FIGURES

LIST OF TABLES

CHAPTER 1

Introduction

1.1 General

Steel fiber reinforced concrete is generally constructed by adding short fibers of small cross-sectional size to the fresh mix (Figure 1.1.a). The idea is to reinforce the concrete with uniformly dispersed and randomly oriented steel fibers (Figure 1.1.b). There are numerous advantages that can be achieved by reinforcing concrete with short randomly distributed steel fibers. There are also some precautions needed for construction with fiber reinforced concrete.

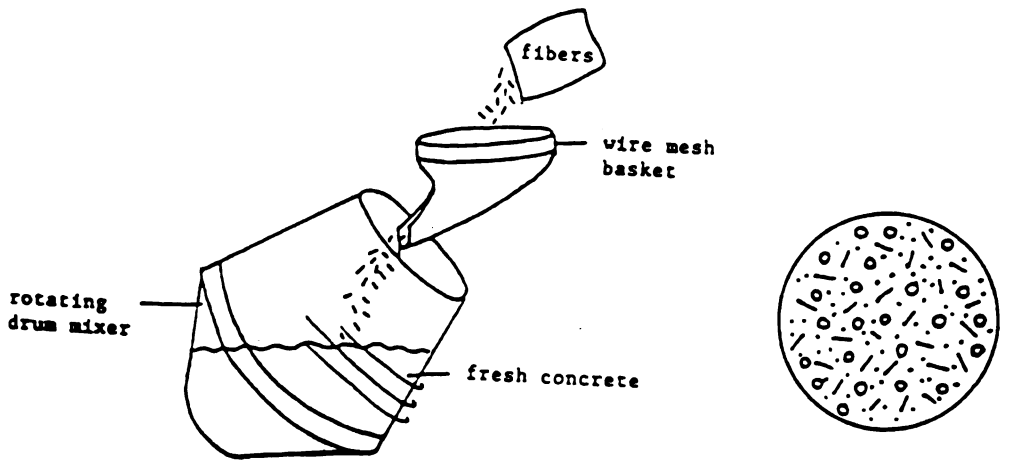

a. Fibers being added during mixing

b. Fiber reinforced concrete

Figure 1.1: Addition of steel fibers to concrete.

1.2 Advantages

The properties of concrete that can be improved by steel fiber reinforcement include:[1-5] (a)ductility; (b) impact resistance; (c) tensile and flexural strengths; (d) fatigue life; (e) shrinkage; and (f) durability and erosion resistance. These improvements and some of their practical implications are discussed in the following:

1.2.a Ductility: One of the problems of cement-based materials is their inherently brittle type of failure under tensile stress systems. Fibers enable the composite to absorb energy and behave effectively as a ductile material.[1-5] The gains in ductility resulting from fiber reinforcement are obvious in Figures 1.2.a and 1.2.b which qualitatively compare the compressive stress-strain diagrams and flexural load-deflection relationships, respectively, of plain and steel fiber reinforced concretes. Failure of plain concrete is brittle, while fiber reinforced concrete is capable of sustaining a major portion of its capacity at large deformations.

The improvements in ductility resulting from fiber reinforcement are of extreme significance in seismic- and blast-resistant reinforced concrete srtuctures. Such structures should be capable of absorbing severe energy inputs through large inelastic deformations without collapse.[1,4,6] Fiber reinforcement, by improving ductility, can also promote application of high strength concretes and steels which generally suffer from brittle modes of failure.[1,4,7] Figure 1.3 shows the

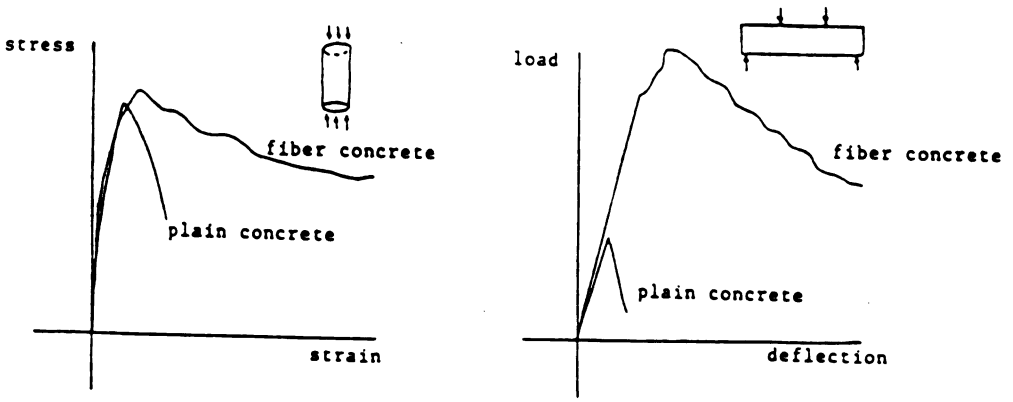

a. Compression b. Flexure

Figure 1.2: Improvements in ductility resulting from steel fiber reinforcement.

improvement in the behavior of an exterior beam-column connection under cyclic loads resuting from steel fiber reinforcement.[6] The fibrous joint is more stable under cyclic loads and fails in a ductile manner.

1.2.b Impact Resistance: Cement-based materials can not resist impact loads satisfactorily. Tremendous improvements in their impact resistance and shock absorbance can be achieved through fiber reinforcement (Figure 1.4).[8] Such improvements are advantageous in applications such as airfield pavements and protective structures.

1.2.c Tensile and flexural strengths: Low tensile strength is a major weakness of cementitous materials. This shortcoming can be overcome to some extent by fiber

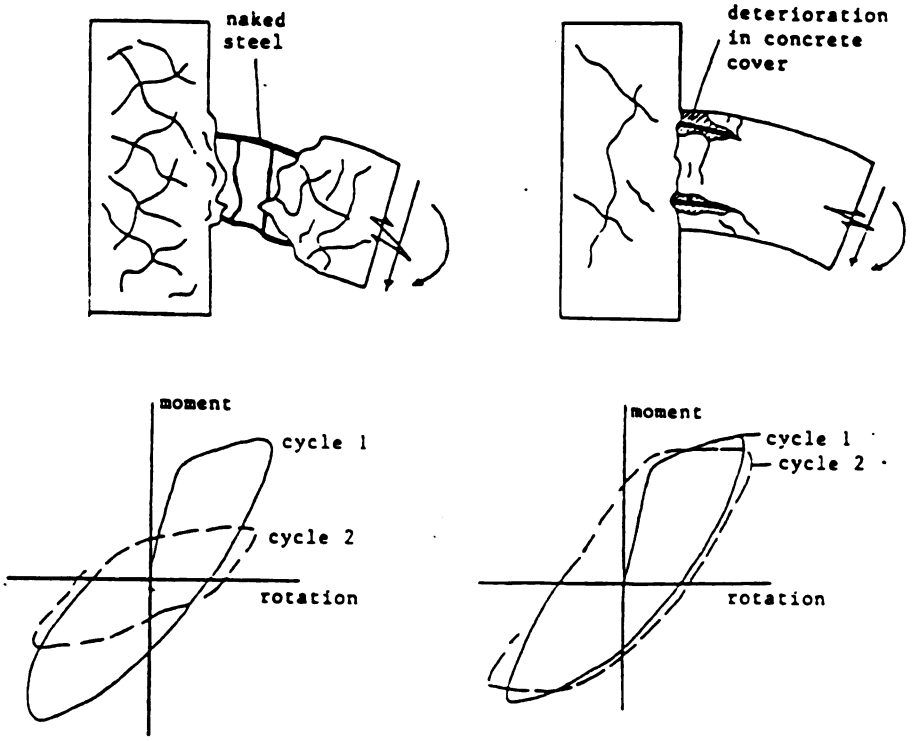

a. Conventional concrete

b. Fibrous concrete

Figure 1.3: Improvements in joint behavior resulting from steel fiber reinforcement.[6]

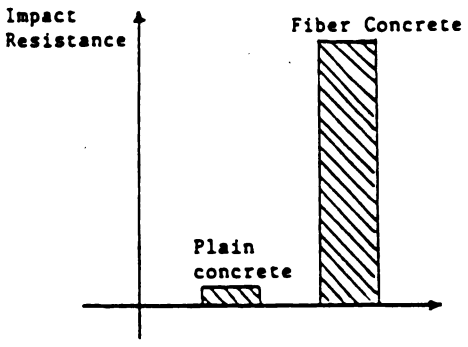

Figure 1.4: Improvement in impact resistance resulting from steel fiber reinforcement.[8]

reinforcements. Figure 1.5 compares typical stress-strain diagrams of plain and fiber reinforced mortars obtained in direct tension tests.[1-10] A similar comparison is made in Figure 1.2.b for flexural tests. A major effect of steel fiber reinforcement is seen to be the improvement in ductility. The tension and flexural strengths are also observed to increase in the presence of steel fibres.

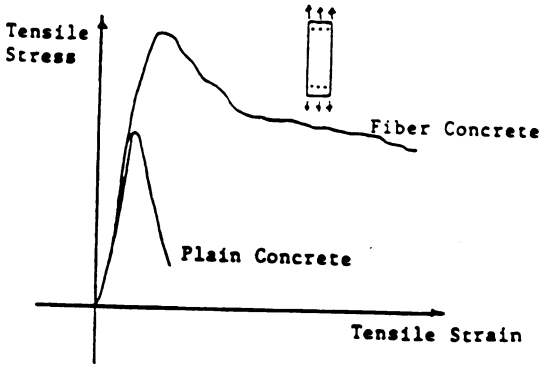

Figure 1.5: Improvements in direct tensile behavior resulting from steel fiber reinforcement.[1-10]

The increased tensile strength makes fiber reinforced concrete an attractive alternative material for many applications such as pavements, water tanks, and pipes. The higher tensile strength of fibrous concrete also enhances the behavior and strength under shear stresses in structural components such beams, slabs and beam-column connections. Figure 1.6 shows some applications of fiber reinforced concrete encouraged by its improved tensile strength.

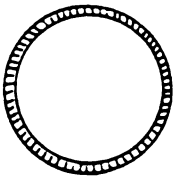

a. Concrete pipes.[11]

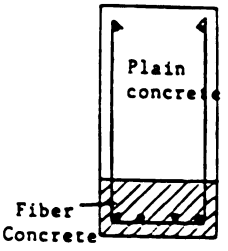

b. Tensile skin in reinforced concrete beams.[12]

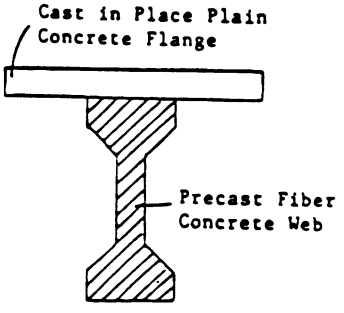

c. Precast web in composite beams.[13]

Figure 1.6: Applications of steel fiber reinforced concrete encouraged by its improved tensile (flexural) strength.[11-13]

1.2.d Fatigue Life: Test results have indicated significant increases in fatigue strength with increasing percentage of steel fibers. Addition of steel fibers also decreases crack widths and deflections under fatigue loading. The improvements in fatigue life resulting from steel fiber reinforcement have encouraged the application of steel fiber reinforced to pavements and bridges. With steel fiber concrete, the pavement thickness can be as low as 50% that of conventional concrete pavements.[4]

1.2.e Shrinkage: Some of the cracking which occurs in reinforced concrete results from the restraint to free shrinkage provided the continuity of structures, reinforcing bars and moisture gradient in concrete. Experiments on fibre reinforced concrete have indicated that the presence of steel fibers reduces the free shrinkage and controls shrinkage cracks.[14,15] Figure 1.7 presents a typical comparison between drying shrinkage of plain and fiber reinforced concretes. There are numerous areas of concrete applications that can benefit from the reduced shrinkage resulting from fiber reinforcements.

Applications of steel fibers also improves a number of other properties of concrete, including their durability, erosion resistance, thermal properties, friction and skid resistance, fragmentation and spalling resistance, and certain rheological characteristics.[1,4] Table 1.1 summarizes some applications of reinforced concrete and those advantages of fiber reinforcement that are of particular significance in each application.[1]

Table 1.1: Some applications of steel fiber reinforced concrete.[1-17]

APPLICATIONS \ IMPROVEMENTS	Ductility (Energy Absorption)	Dynamic Stiffness and Strength	Impact Resistance	Tensile (Flexural) Strength	Shear Strength	Serviceability (Cracking & Deflec.)	Fatigue Properties	Reduced Size and Weight	Abrasion & Corrosion Resistance	Cavitation Resistance	Multi-Axial Strength	Behavior under High Temperature	Reduced Water Absorption
Seismic-Resistant Structures	•	•		•	•	•		•			•		
Airfield and Highway Pavements			•	•			•	•	•				
Thin Shells				•	•	•		•			•		
Frames, Beams, and Flat Slabs	•			•	•	•		•			•		
Bridge Structures	•	•		•	•	•	•	•			•		
Blast-Resistant Structures	•	•	•	•	•	•		•			•		
Water Tanks				•		•		•					•
Hydraulic Structures				•		•	•	•	•	•	•		•
Precast and Prestressed Concrete Structures	•			•	•	•		•			•		
High-Strength Concrete and High-Strength Steel	•			•		•					•		
Overlay in Industrial Environments						•			•				
Refractory Structures									•			•	
Patching, and Repair with Shotcrete				•		•							
Rock Slope Stabilization				•		•		•	•	•			•
Concrete Pipes				•		•		•	•	•	•		•
Nuclear Reactors	•	•	•	•	•	•		•	•	•	•	•	•
Mine Tunneling				•	•	•				•	•		•

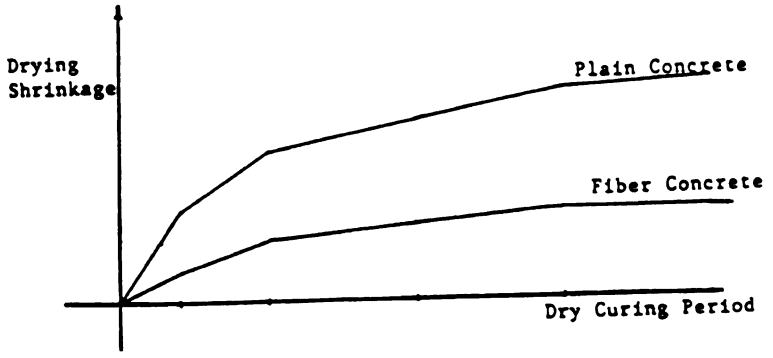

Figure 1.7: Drying shrinkage of plain vs.fiber reinforced concrete.[14,15]

1.3 Precautions

In order to take full advantage of the fiber reinforcement technique, attention should be paid to resolving some problems associted with its use; the main ones being related to fiber dispersion and workability of fresh mix.[14,16] It is important that the fibers be dispersed uniformly throughout the mix. This might require some modifications in the proportions (e.g. use of some additives), and mixing technique (e.g., the sequence of adding different mix constituents). Additions of fibers also reduces mix workability, and certain modifications should be made in the mix design to overcome this problem. Use of superplasticizers in the mix is a popular approach to enhancing the fibrous mix workability.[1,16] It is worth mentioning that both the dispersion and workability problems of fiber reinforced concrete are strongly influenced by type and especially the aspect ratio of steel fibers (length of fiber divided by its nominal diameter, 1/d). A general rule is that the fresh mix properties deteriorate as the aspect ratio of fibers

increases. Typical effects of the fiber volume fraction and aspect ratio of steel fibers on the workiability of fresh mix are presented qualitatively in Figures 1.8.a and 1.8.b, respectively.[16,17]

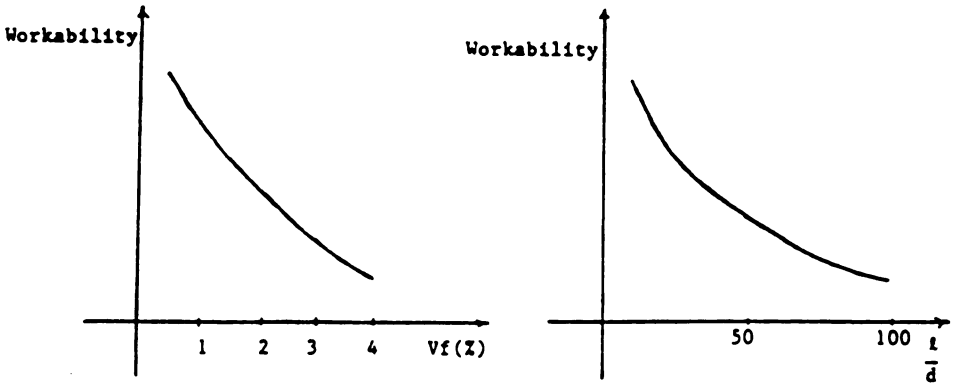

a. Volume fraction, V_f b. Aspect ratio, l/d

Figure 1.8: Effects of steel fiber volume fraction and aspect ratio on workability.[1-17]

Insofar as the corrosion of steel fibers in cementitious matrices due to the environmental effects is concerned, the experience with steel fiber reinforced concrete has revealed that the concrete is capable of effectively protecting fibers under severe long-term exposure condition.[4]

1.4 Steel Fiber Properties

Short steel wire is currently the most common fiber type. Basic characteristics of steel fibers are presented in Table 1.2. Steel fibers might be round or rectangular

in cross-section, and they are produced in the following forms: straight-smooth (Figure 1.9.a), straight-deformed (ordinary duoform shown in Figure 1.9.b and double duoform shown in Figure 1.9.c), crimped end (Figure 1.9.e), hooked-end (Figure 1.9.f), irregularly shaped (Figure 1.9.g), and paddeled (Figure 1.9.h). Steel fibers have relatively large strength and modulus of elasticity, they are inert in the alkaline environment of the cementitious matrix, and their bond to the matrix can be enhanced by mechanical anchorage. Long-term loading does not adversely influence the mechanical properties of steel fibers, and their price is also comparable with those of the other fibers. They are, however, prone to corrosion if not protected by the matrix, and relatively heavy. They can not also be impregnated in the cement-based matrices at high volume fractions.

Table 1.2: Basic properties of steel fibers.[1-17]

Specific Gravity=7.86	Tensile Strength=100-300 ksi
Young's Modulus=$30x10^3$ ksi	Elongation at Failure=up to 30%
Common Volume Fraction=0.5-3%	Common Diameters=0.01-0.04 in
Common Length=0.5-2 in	
1 in=25.4 mm, 1 ksi=6.9 MPa	

1.5 Trends in Steel Fiber Reinforced Concrete Applications

During the 1970's and 1980's extensive research and development work, together with a wide range of practical applications, have transferred steel fiber concrete

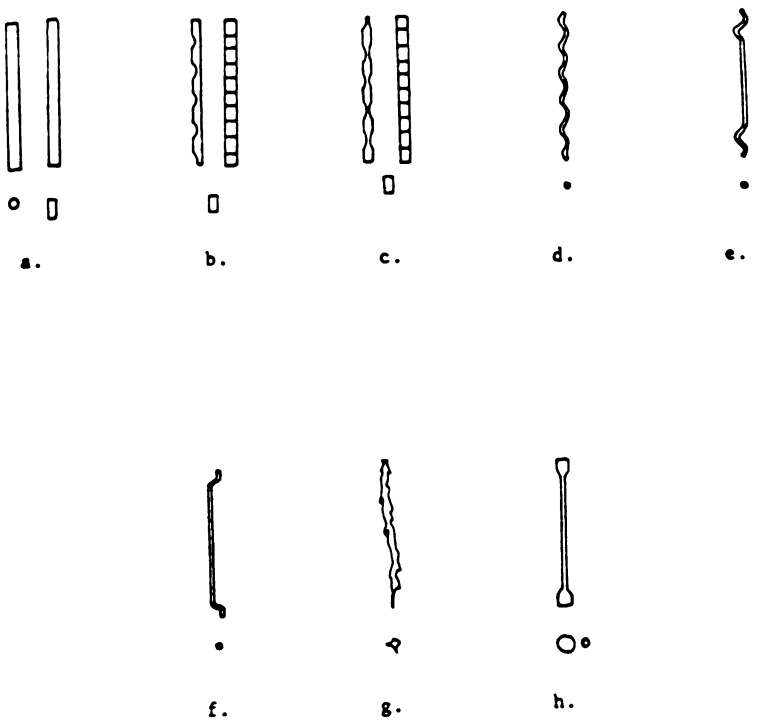

Figure 1.9: Examples of various steel fiber types.

materials from a laboratory curiosity into a reliable construction material in practical applications. Steel fibrous concretes possess better performance characteristics than conventional concrete, and they have opened up a new class of construction materials.

Several advances have recently been made in understanding the mechanics of fiber reinforcement, the performance characteristics of fiber reinforced concrete, and the conditions that enhance or deteriorate their long-term stability. These findings, together with the experience in actual field applications of the material, are expected to create confidence and facilitate development of standard techniques for mix proportioning, construction and design with fiber concrete. These will undoubtedly lead to increased applications of the material.

In the 1970's research on fiber concrete was heavily aimed at standardizing the applicable test techniques and establishing the basic engineering properties of the fresh and hardended material (e.g. workability of the fresh mix, strength and toughness in tension and compression, impact resistance, shrinkage and durability). This major research trend of the 1970's continued to be very in the 1980's. However, the following research areas also gained increasing popularity: (a) Devlopment of a theoretical basis for predicting the fracture process and mechanical properties of steel fiber concrete; and (b) Resolving practical and theoretical problems with field applications of the material and exploring new areas of application.

1.6 Organisation of Chapters

The results of a comprehensive experimental study on steel fiber reinforced concrete materials and structural applicantions are presented in the following chapters. The effects of fiber volume fraction and aspect ratio on steel fiber reinforced concrete in the fresh and hardended states are presented in Chapter 2. Steel fiber types are commercially produced in a variety of forms with deformations meant to improve their mechanical bonding to concrete. An evaluation of different steel fiber types is made in Chapter 3. The effectiveness of steel fiber in concrete strongly depends on the mix proportions of the matrix. The effects of some basic concrete mixture variables and the introduction of pozzolanic materials (fly ash and silica fume) to the mix are discussed in Chapters 4 and 5, respectively.

The introduction of steel fibers to concrete is expected to modify the statistical variations of the fresh and hardened material properties of steel fiber reinforced concrete. This issue is treated in Chapter 6.

Applications of steel fiber reinforced concrete to primary load-bearing structures is a promising area where such research is needed before steel fiber concrete can be accepted as an alternative to conventionally reinforced concrete. Chapters 7 and 8 are concerned with the applications of steel fiber reinforced concrete to footing and beam- column connections, respectively. A critical evaluation of some basic

theoretical concepts which have found popularity in analytical treatments of steel fiber reinforced concrete is presented in Chapter 9. Chapter 10 summarises the activities and findings of this research program.

CHAPTER 2

Effects of Steel Fiber Reinforcement on the Performance Characteristics of Concrete

2.1 Introduction

Steel fiber reinforcement is an effective technique for overcoming the problems related to the brittle nature of concrete failure and its low tensile strength. There are two important fiber reinforcement properties which decide the degree of improvements in concrete material performance achieved by fiber reinforcement: volume fraction and length-to-diameter (aspect) ratio.[1-10] Generally, the increase in the volume fraction and aspect ratio of fibers, up to certain limits, results in improved material properties. Beyond these limits, however, at relatively high fiber volume fractions and/or aspect ratios, problems with fresh mix workability and fiber balling start to damage the compactibility of the fibrous mix and the uniform dispersion of fibers, thus adversely influencing the hardened material properties.[5,8,19,20] Considering the similar effects of fiber volume fraction and aspect ratio on the material properties of concrete in the fresh and hardened states, it has been proposed that the multiplication of these two parameters (fiber volume fraction times aspect ratio) provides a single variable representing the effectiveness of a certain steel fiber reinforcement condition in a specific concrete mixture.[7,8,17,22-24]

The work reported in this chapter has been concerned with quantifying the trends

in the effects of steel fiber volume fraction and aspect ratio on the fresh and hardened concrete material properties. This objective was achieved through a comprehensive review of the available literature on this topic and by the performance of an extensive experimental study.

2.2 Background

This section presents test results reported in the literature on the effects of fiber volume fraction and aspect ratio on the fresh mix and hardened material properties of steel fiber reinforced concrete.

2.2.a Fresh Mix Workability: Workability of the fresh mix decides the ease of handling, placing, compacting and finishing of the mix (with a minimum loss of homogenity), its stabiliaty and, therefoere, the hardened material propeerties. When fibers are added to a cementitious matrix, their long thin shape and large surface area automatically reduce the workability of the mix. The shape of fibers creates interlocking, which stiffens the matrix, whereas their large surface area adsorbs water immediately and results in the reduction of the free water available for workability of fresh mix. Another factor damaging the workability of fresh fibrous mix is the interparticle friction between fibers and aggregates. The damage to workability resulting from fiber reinforcement depends, in large part, on fiber volume fraction and fiber aspect ratio. [1, 4-9,16,19-22,25,26]

In regard to the effect of fiber addition on workability, it should be mentioned that

although fibers bond together and resist movement and adsorb part of the mixing water in a static condition, vibration results in more mobility of fibers and releases the adsorbed water.[16] Hence, a fibrous mix that appears very stiff and unworkable might be placed and compacted easily under vibration.[2,4,5,8,16-22]

Because of the distinct properties of steel steel fiber reinforced concrete, a comprehensive assessment of its workability can not be achieved through the slump test which is popularly applied to conventional concrete .[4-26] Stiffness of the fibrous mix in static conditions results in relatively low slumps. The slump can not represent the capability of a fibrous mix to compact under vibration.[4,9,16] Considering the fact that compaction of steel fiber concrete is normally carried out by vibration, those workability techniques that involve vibration and shaking of the fresh mix are more applicable to fiber reinforced mortar and concrete. Such tests include the inverted slump cone and Vebe consistometer tests. However, since the slump test is widely used and very convenient for field applicationsit is still applied to to steel fiber reinforced concrete for checking the consistency of the mix from batch to batch.[4,9,16]

Inverted slump cone test (Figure 2.1.a) is devised especially for fibrous concrete, and it has found to be an effective measure of workability that is also convenient for field use. [4,8,9,16,21] In this method an inverted slump mold is loosely filled with concrete without compaction. An internal vibrator is then started, inserted into the centre of the cone and allowed to fall freely (approximately a few seconds

being required for immersion of the vibrator). The vibrator is held vertically with its end just resting on the bottom of the bucket. The time for the initial immersion of the vibrator untill the slump mold is empty is recorded as the test time. The test primarily measures the mobility or fluidity of the mix and takes into account the effects of aggregate size, shape and gradation, cement content, admixtures and surface friction of fibers.[4,9,16]

The British standard Vebe test (Figure 2.1.b)[5,8,19,20,25] is another way to determine workability of fiber reinforced concrete. The procedure of Vebe test is similiar to that of inverted slump cone, except that vibration is applied externally through a vibration table on which the slump cone is installed in a cylindrical mold. The slump cone is filled similar to the procedure of the standard slump test, the vibrating table is then started and the time needed for the concrete to remold (with a flat surface) in the cylindrical mold is the Vebe time. Many investigators[5,7,8,19,20,25,26] have indicated that the Vebe test is quite capable of simulating the compaction of fiber reinforced concrete by vibration in practice. It is applicable to mortar and concrete and it also takes account the effect of aggregate shape, gradation, air content, admixture effect, and surface friction of fibers. The Vebe time can identify quite positively a critical fiber volume for a given fiber type with a specified geometry above which compaction is unlikely to be possible using normal site compaction procedures.[5,7,8,19,20,25,26] The difficulty with Vebe test apparatus is that it is not convenient for field placement.[5,8,19,20]

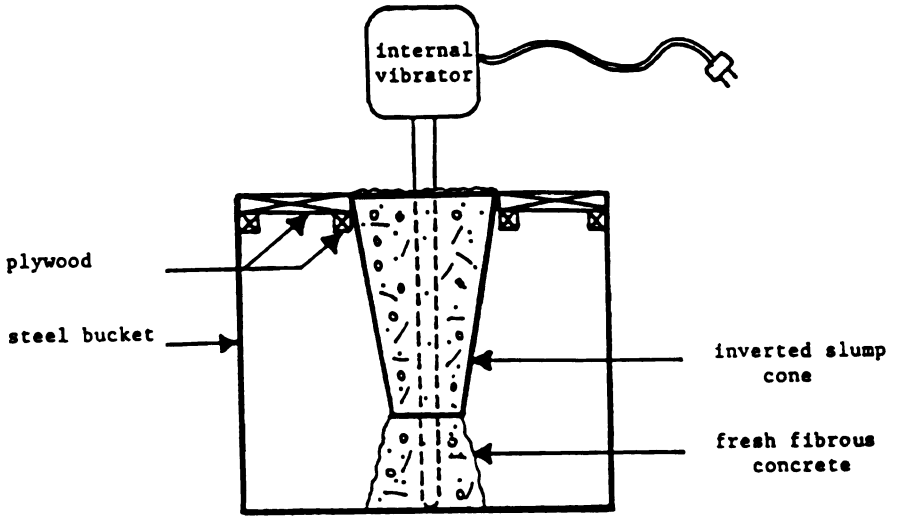

a. Inverted slump cone apparatus

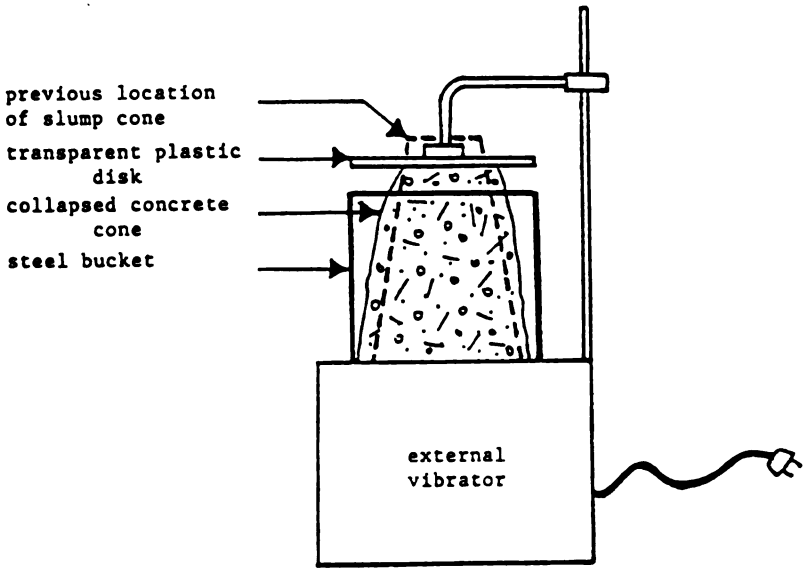

b. Vebe apparatus

Figure 2.1:

Both the Vebe and the inverted slump cone test techniques have shortcomings when applied to fiber concrete. For stiff mixtures both of these techniques lack an end point,[5,16,19,20] that is excessively large times are heeded for remolding stiff mixes and the results do not indicate the relative workability of these mixes. Also neither of these test is applicable to very flowable concretes.[5,16,19,20]

The remainder of this section deals with the background information available on fresh mix workability (measured by either of techniques described above) as influenced by steel fiber reinforcement properties.

Based on a comprehensive experimental study, Reference 19 has concluded that the slump of fresh fiber mixes decreases and their Vebe time increases proportionally with the increase in aspect ratio and square root of volume fraction, and proportionally with the increase in the power two of aspect ratio and volume fraction of steel fibers of the same type, respectively, (see Figure 2.2) noting that a lower Vebe time represents better compactibility under vibration. At the same fiber volume fraction and aspect ratio, the limited test data of Reference 19 indicate that crimped fibers result in more workable mixes (with higher slumps and lower Vebe times) than straight round, duoform and hooked steel fibers (see Figure 2.3).

Reference 5 provides further evidence of the adverse effects of the increase in fiber volume fraction on the fresh mix Vebe time (see Figure 2.4). Assuming a

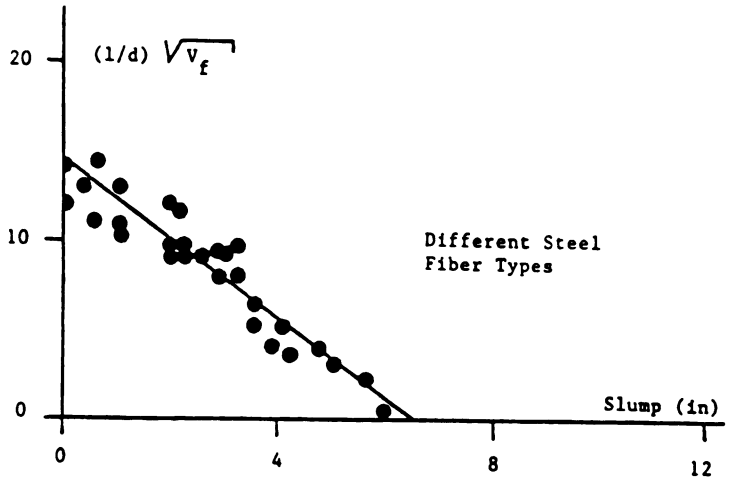

a. Slump. 1 in = 25.4 mm

Figure 2.2: Effects of fiber volume fraction and aspect ratio on the workability of fresh mix reinforced with straight-round fibers.[19] (water-cement ratio = 0.60, aggregate-cement ratio = 5.0, fine-to-coarse aggregate ratio = 0.67 and maximum aggregate size = 3/8 in (10mm)).

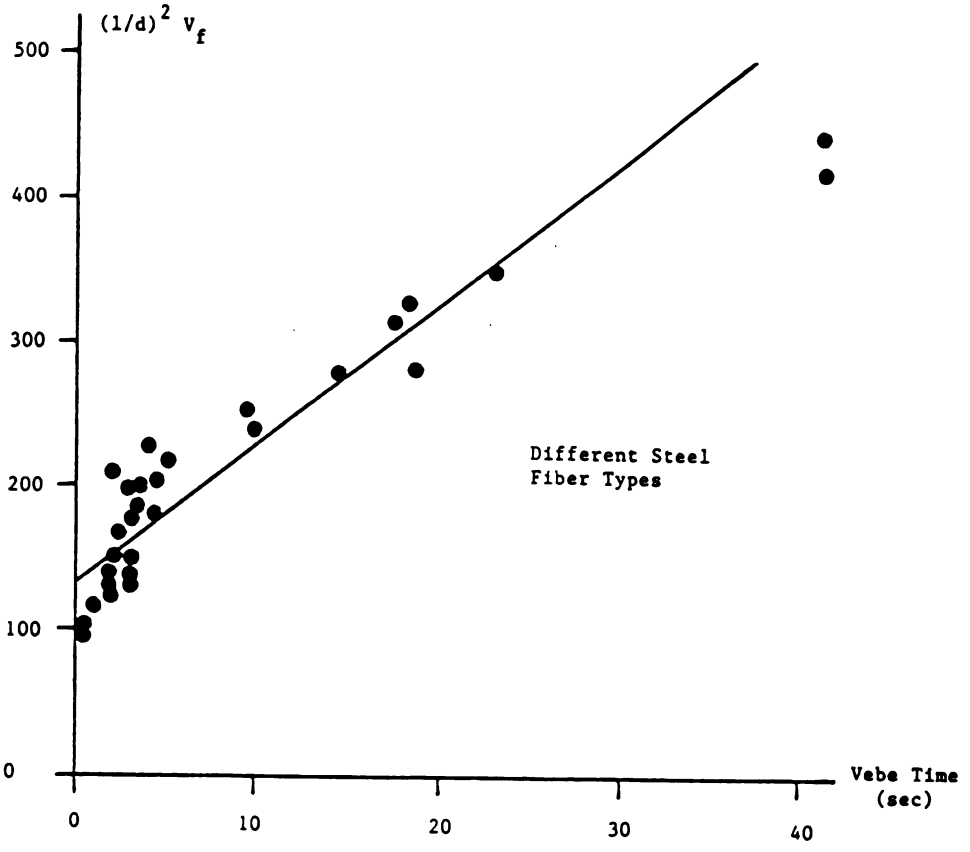
$(1/d)^2 V_f$
500
400
300
200
100
0
0
10
20
30
40
Vebe Time
(sec)
Different Steel
Fiber Types

b. Vebe time

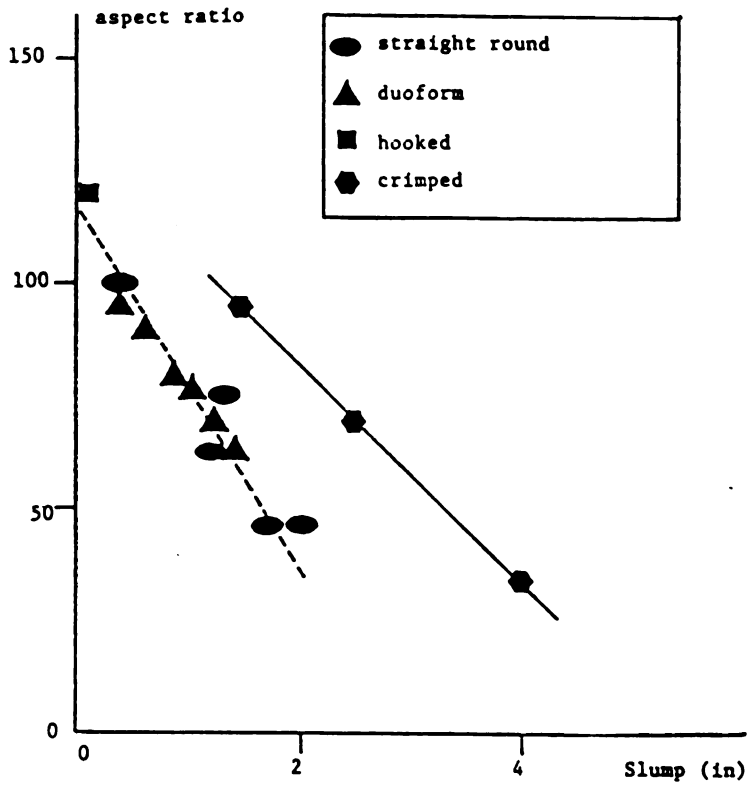

a. Slump. 1 in = 25.4 mm

Figure 2.3: Effects of fiber type on fresh mix workability at a fiber volume fraction of 1.5% and different fiber aspect ratios.[19](water-cement ratio = 0.49, aggregate-cement ratio = 4.0, fine-to-coarse aggregate ratio = 0.6 and maximum aggregate size = 3/8 in (10 mm)).

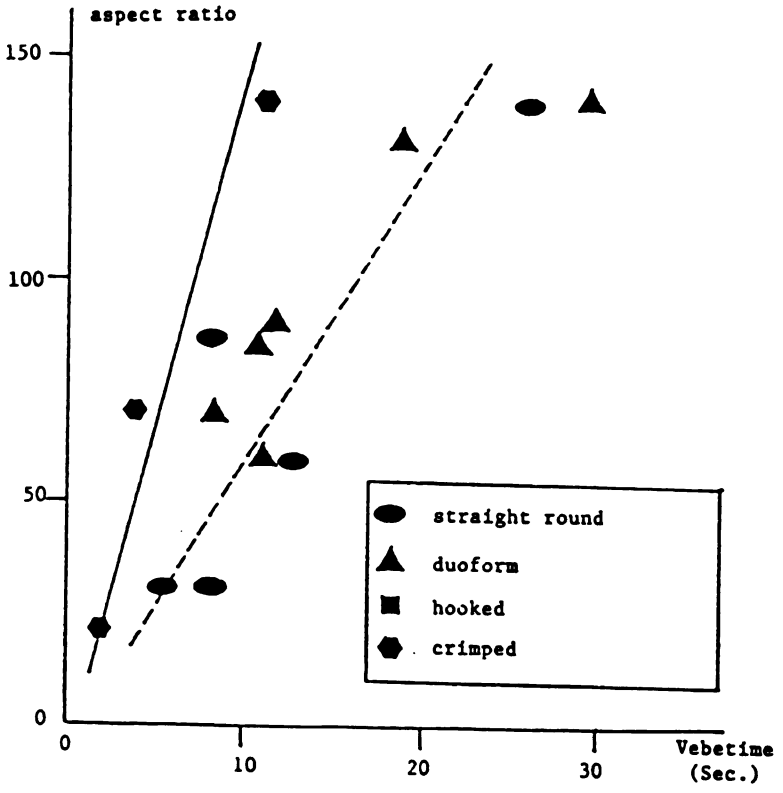
aspect ratio
150
100
50
0
0
10
20
30
Vebetime
(Sec.)
straight round
duoform
hooked
crimped

b. Vebe time

maximum Vebe time of 20 second as the acceptable limit for relatively easy compaction, Figure 2.4 indicates that an aspect at ratio of 100, a maximum fiber volume fraction of 1.7% can be incorporated into mortar. A simple empirical equation is given in Reference 5 for approximately estimating the maximum fiber volume fraction that can be incorporated in concrete matrices containing aggregate of normal density:

$$Vf(\%) \leq \frac{200(1-Ag)}{l/d} \qquad (2.1)$$

Where:

V_f = fiber volume fraction in the concrete matrix which can be compacted with normal field techniques;

A_g = volume fraction of coarse aggregates (particle size geater than 5 mm = 3/16 in) of the total volume of the concrete;

l = length of fibers; and

d = (nominal) diameter of fibers.

The effects of fiber volume fraction on the Vebe time and slump of fresh steel fibrous mixes of References 26 are shown in Figures 2.5.a and 2.5.b, respectively. It can be noted from Figure 2.5 that increasing the volume fraction of steel fibers tends to damage the fresh mix workability.

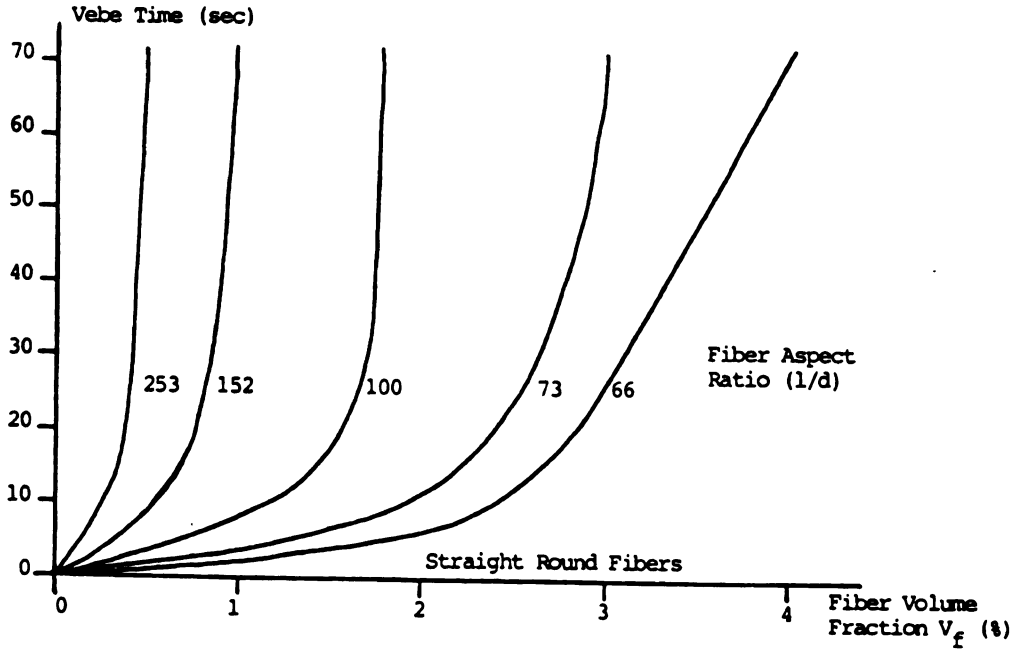

Figure 2.4: Effects of fiber aspect ratio and volume fraction on Vebe time of steel fiber reinforced mortar.[5]

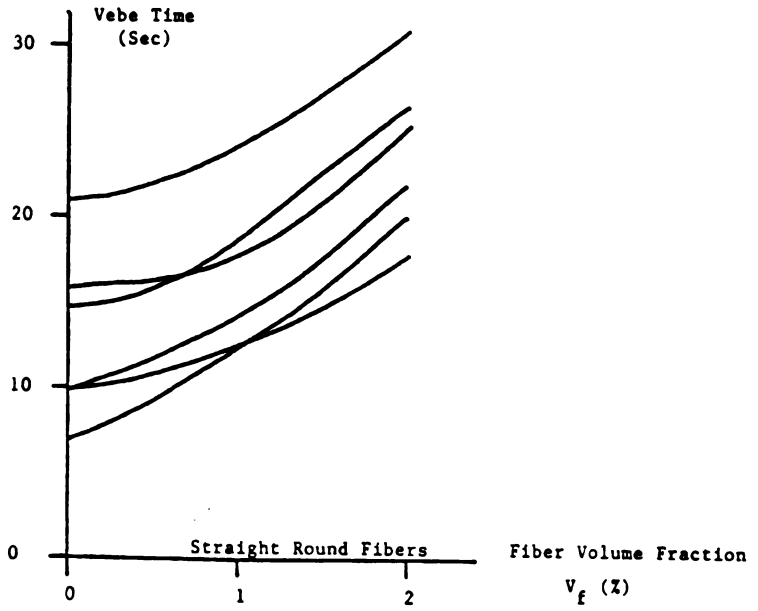

a. Vebe time

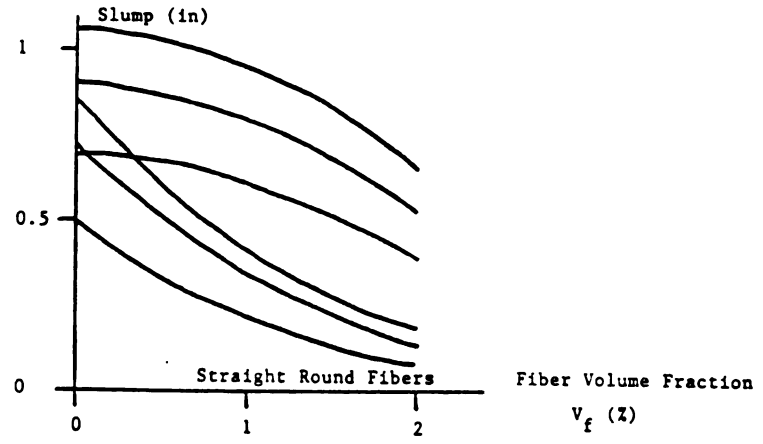

b. Slump. 1 in = 25.4 mm

Figure 2.5: Effects of fiber volume fraction on workability of steel fiber reinforced concrete with different matrix mix proportions.[26]

The test data generated in Reference 17 indicates that the relationship between Vebe time and fiber reinforcement index (V_f l/d) is not unique, but depends on fiber geometry (see Figure 2.6.a). According to this reference, for each fiber length, an empirical relationship can be derived to represent the Vebe time as a decreasing function of fiber spacing (see Figure 2.6.b), with fiber spacing (from Reference 10 spacing $=13.8\ d\ (1/V_f(\%))^{0.5}$) representing the average distance between fiber centroids. Figure 2.6.c further shows that at a constant fiber spacing (i.e. for a given diameter and volume fraction of fibers), the Vebe time increases linearly with increasing fiber length, and the rate of increase is higher at smaller value of fiber spcing (corresponding to smaller fiber diameters).

Besides Vebe time, the other common measure of fresh fibrous mix compactibility under vibration is the inverted slump cone time.[9,27] The inverted slump cone time is generally longer than the Vebe time, but the influence of fiber reinforcement properties on the Vebe and inverted slump cone times are expected to show similar trends. The test results presented in Figure 2.7 are representative of the proportioality of the inverted slump cone and Vebe times.[8]

Reference 5 suggests that the long thin fibers with an aspect ratio greater than 100 tend to interlock and form a mat, from which it is very difficult to disperse in concrete matrices. Short stubby fibers with aspect ratios less than 50, however, are not able to interlock and can easily be dispersed by vibration.[5]

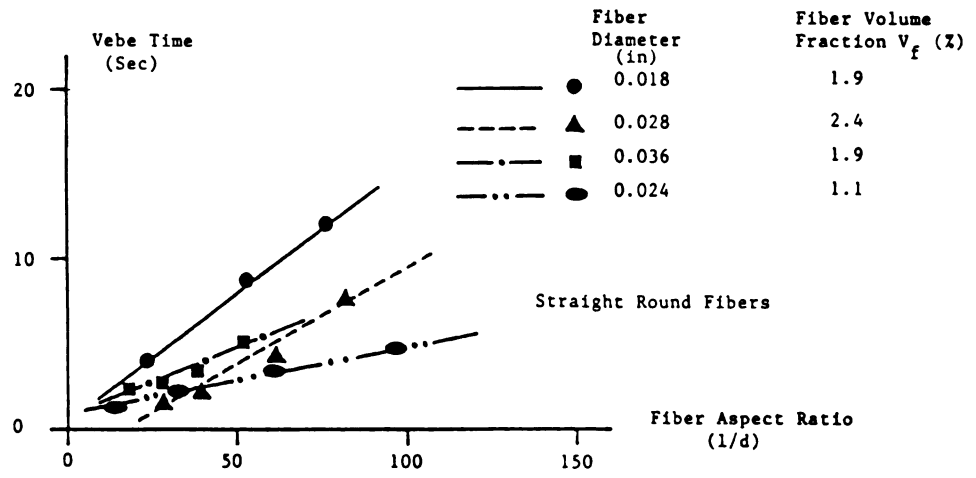

a. Fiber reinforcement index

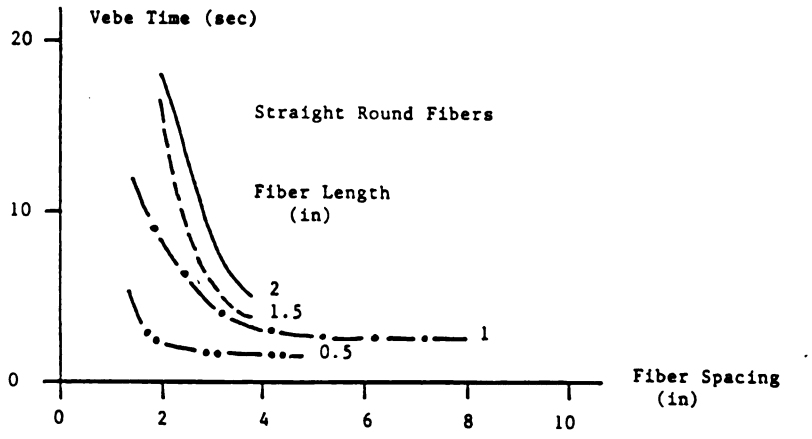

b. Fiber spacing at different fiber lengths

Figure 2.6: Effects of fiber reinforcement properties and fiber spacing on Vebe time.[17] (water-cement ratio = 0.55, aggregate-cement ratio = 4.4, fine-to-coarse aggregate ratio = 1.30 and maximum aggregate size = 3/8 in (10 mm)). 1 in = 25.4 mm.

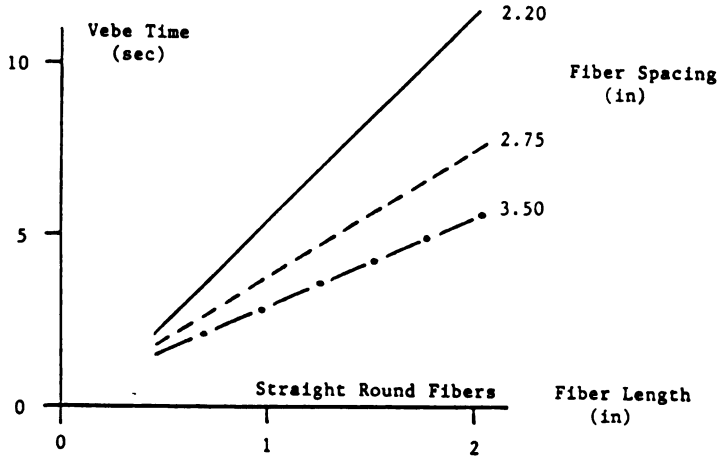

c. Fiber length at different fiber spacing

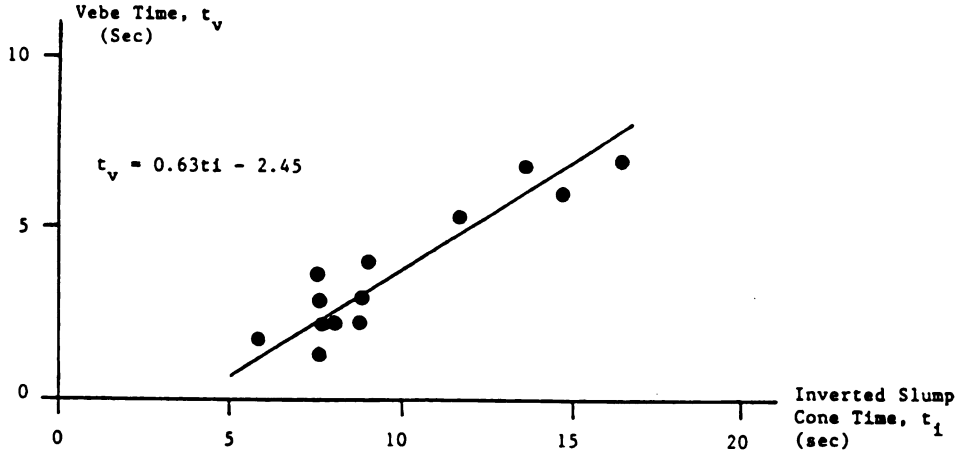

Figure 2.7: Correlation between the inverted slump cone and Vebe times for steel fiber reinforced concrete with different matrix mix proportions.[8]

Considering the desireable effects of reducing the aspect ratio of fibers in fresh concrete matrices, a technique involving the use of water soluable glue to produce fiber bundles has been developed.[8] These bundles have low equivalent aspect ratios and thus generate desirable workability and fiber dispersability at the time of fiber addition to the fresh mix. During the mixing process, following the dispersion of fiber bundles, the solution of the glue results in the separation of individual fibers which are dispersed inside the mix by the continuation of the mixing process. Reference 8 presented test results which are indicative of the improvements in the dispersability of hooked fibers resulting from the use of fiber bundles with water soluable glue.

Reference 21 has studied the effects of mixing time on the separation of individual

fibers from the bundles (with water soluable glue) in steel fiber concrete. It has been concluded that shorter mixing times are not effective in dispersing the individual fibers (which result from the solution of the glue binding the bundles). Total separation of the fibers is required for utilizing the advantages of steel fiber reinforcement. Figure 2.8 (Reference 21) shows the short mixing times result in better workability of the mix reflecting the incomplete separation of fibers. Reference 21 also suggests that 15 to 20 minutes of mixing time is required for full separation of fiber bundles.

2.2.b Flexural Behavior: The improvements in flexural strength and energy absorbtion capacity of concrete resulting from steel fiber reinfircement (see Figure 2.9.a)[5] depend on the fiber volume fraction and the geometry of fibers. As shown in Figure 2.9.b,[1] the increase in flexural strength per unit volume of fiber seems to be higher for fibers with aspect ratios.[1]

From Figure 2.9.c,[1] which represents the effects of fiber aspect ratio on flexural strength, it may be concluded that there is a relatively large scatter in the test data, perhaps indicating that other factors like fiber length or diameter also might influence the results. Another conclusion from Figure 2.9.c is that beyond a certain aspect ratio, at a specific fiber volume fraction, the problems with fresh mix workability and fiber dispersability start to damage the hardened material performance.[1,5]

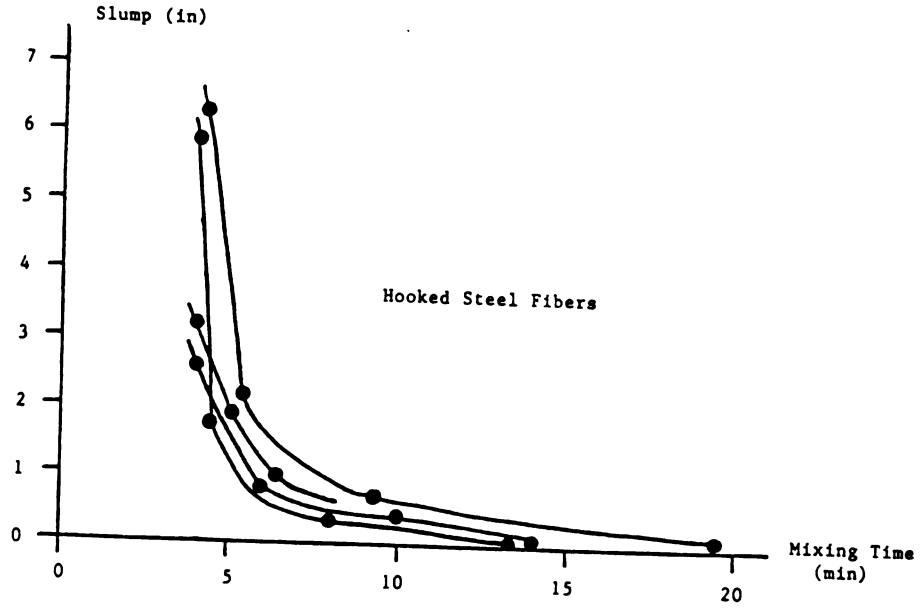

a. Slump. 1 in = 25.4 mm

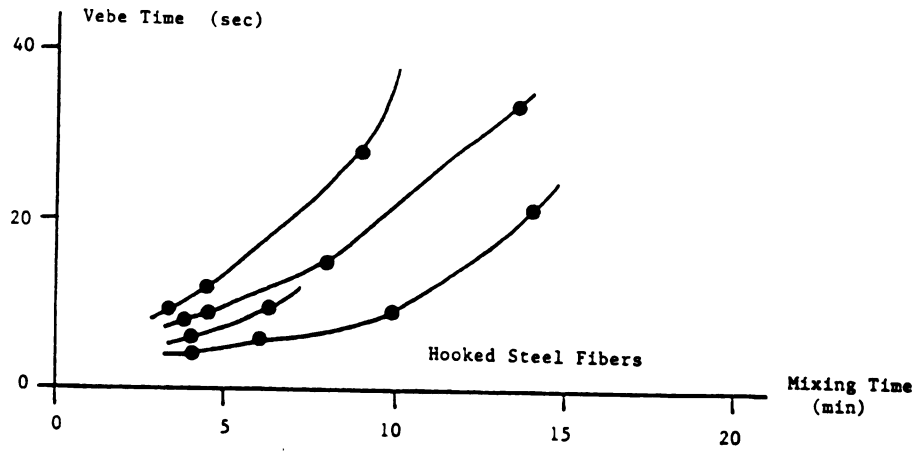

b. Inverted slump cone time

Figure 2.8: Typical effects of mixing time on slump and inverted slump cone time of fresh fibrous mixtures with collated steel fibers.[21] (water-cement ratio = 0.40).

The combined effects of fiber volume fraction and aspect ratio on concrete flexural strength are shown in Figure 2.9.d.[1] Although there is a definite tendency in flexural strength to increase with the fiber reinforcement index (V_f l/d), but the relatively large scatter in test results of Figure 2.9.d suggests that V_f and l/d are not necessarily the only fiber rerinforcement properties influencing the flexural strength of fiber concrete. This scatter is further evident in Figure 2.9.e[1] which presents empirical relationships between flexural strength and fiber reinforcement index derived by different investigators.

Reference 26 has studied the effect of fiber volume fraction on the flexural strength of steel fiber reinforced concrete. The results show dramatic improvement in flexural strength with increasing fiber volume fraction (see Figure 2.10).

In addition to increasing the flexural strength, a cosiderable increase in energy absorbtion capacity is also imparted by steel fibers. Figures 2.11.a and 2.11.b show that the areas underneath the flexural load deflection curve (for the complete curve, and up to the peak load, respectively) tend to increase with increasing fiber reinforcement index.[1,5]

Considering the scatter in the relationship between (V_f l/d) and flexural properties of fiber concrete, some investigators have suggested the relationship

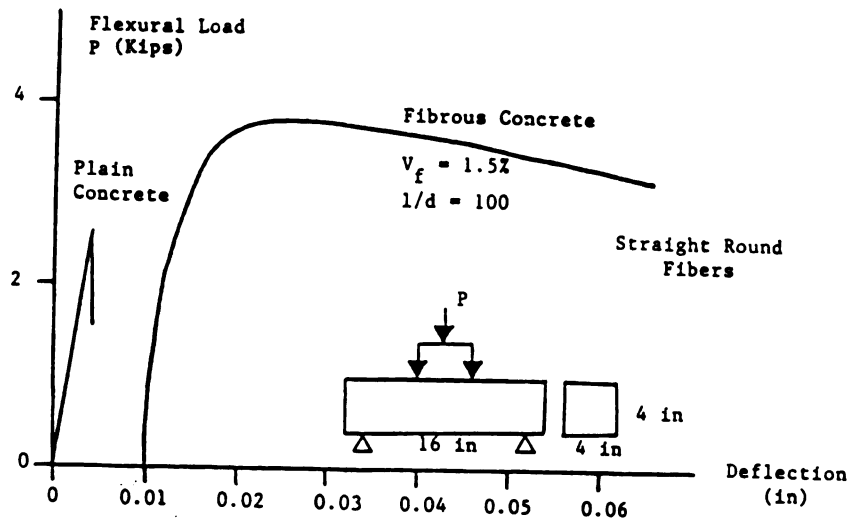

a. Plain vs. fibrous concrete

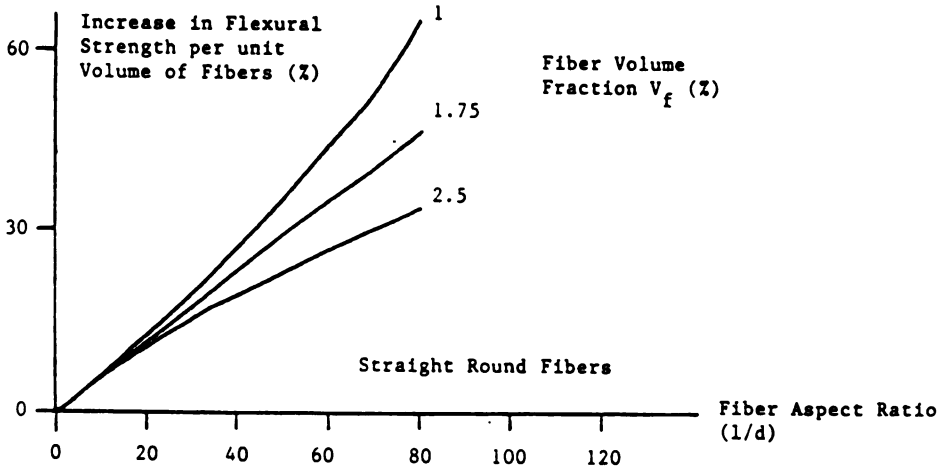

b. Effects of volume fraction and aspect ratio of circular fibers (water-cement = 0.45 - 0.65, and fiber diameter - 0.018 = 0.064 in)

Figure 2.9: Effects of fiber reinforcement properties on the flexural behavior of fiber reinforced mortar and concrete. [1,5] 1 in = 25.4 mm, 1 Kip = 4.5 KN, 1 Ksi = 6.9 N/mm^2.

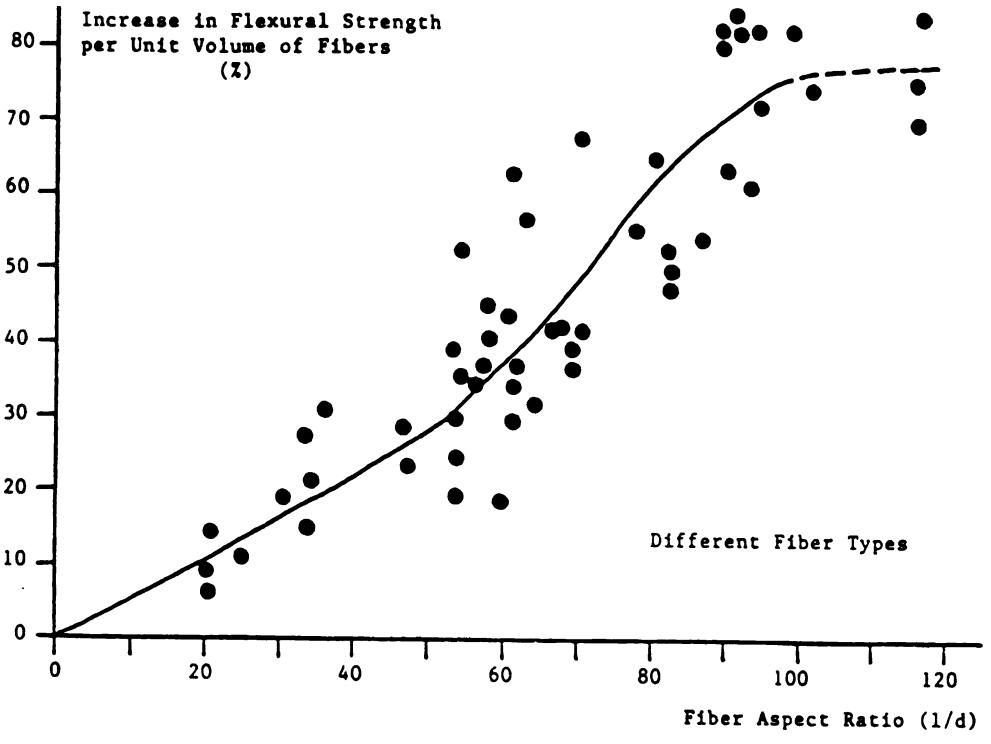

c. Effects of fiber aspect ratio

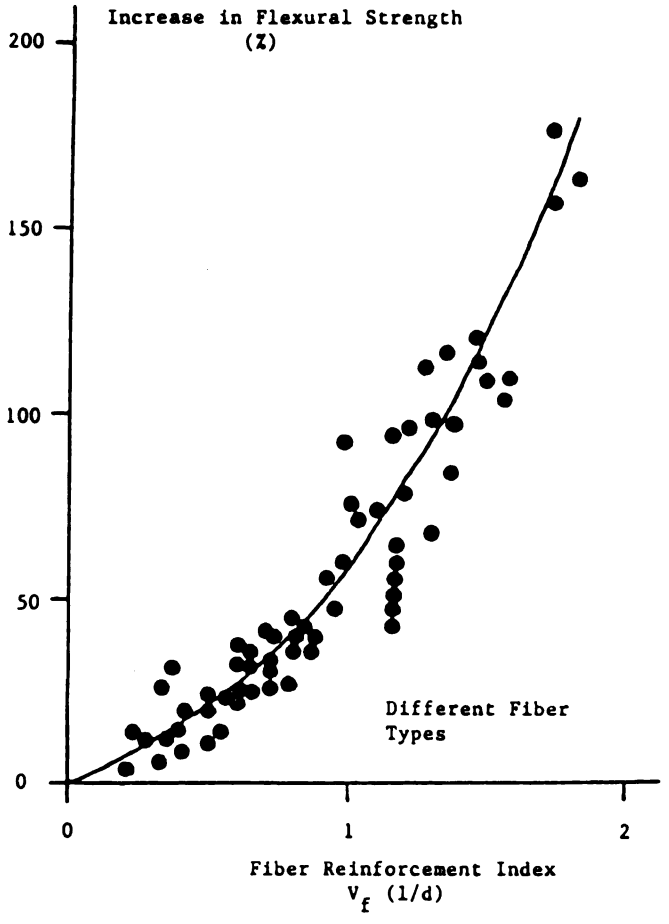

d. Effect of fiber reinforcement index (mortar)

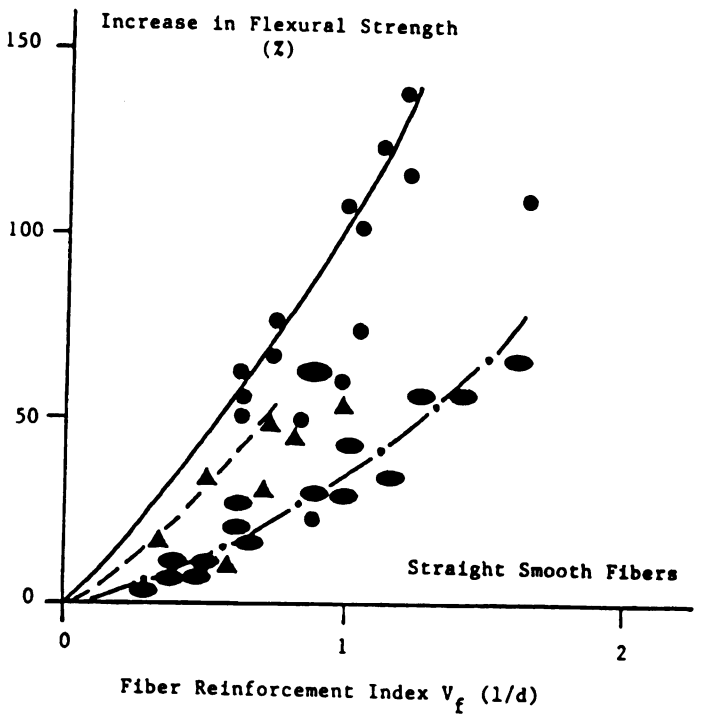

e. Scatter in the effect of fiber reinforcement index (concrete)

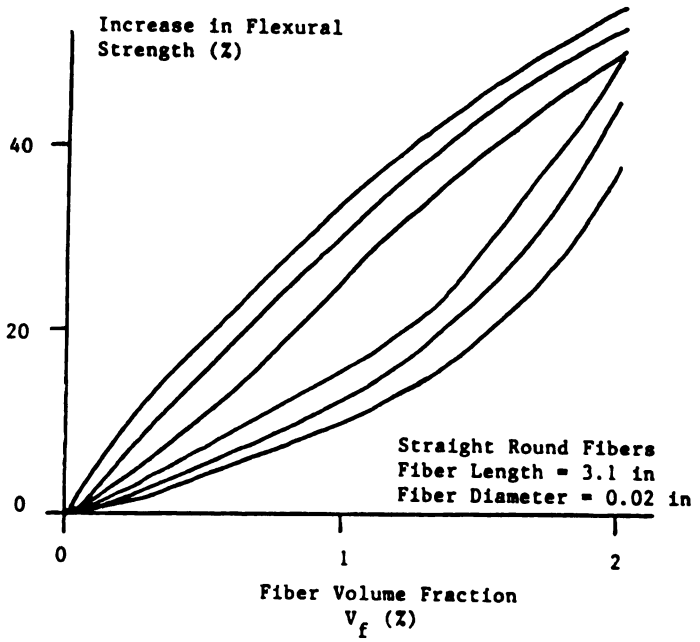

Figure 2.10: Increase in flexural strength of steel fiber reinforced concrete with increasing fiber volume fraction with different matrix mix proportions.[26]

1 in = 25.4 mm

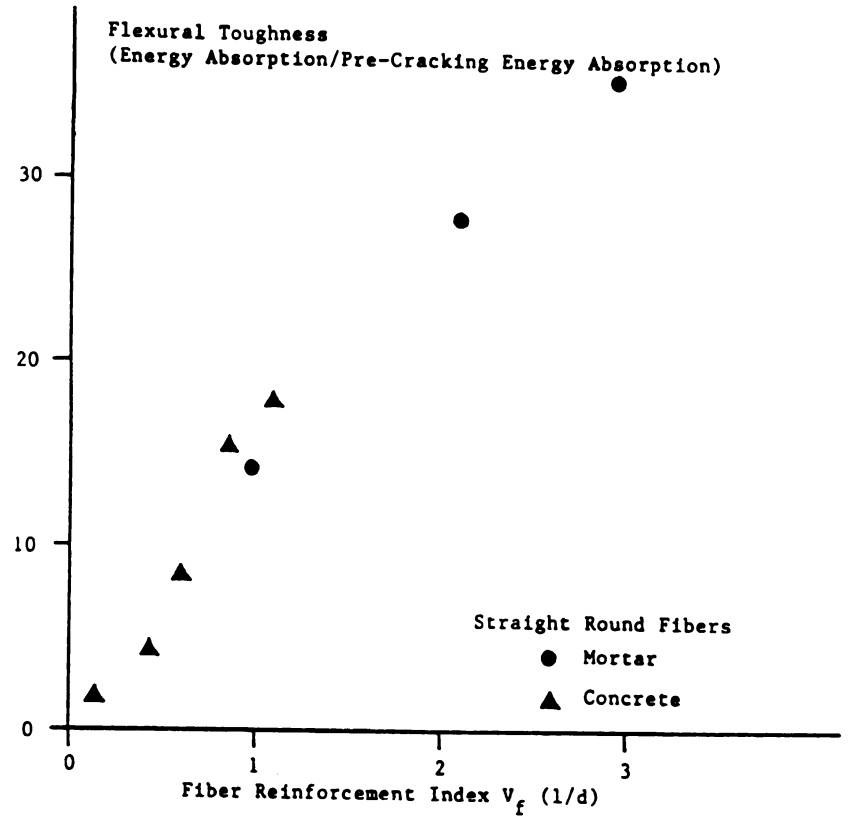

a. Based on total area (concrete mixes: water-cement ratio = 0.6, aggregate-cement ratio = 5.0 and fine-to-coarse aggregate ratio = 0.67; and mortar mixes: water-cement ratio = 0.5 and sand-cement ratio = 2.4)

Figure 2.11: Influence of fiber reinforcement index on the flexural toughness. [1,5]

1 in = 25.4 mm.

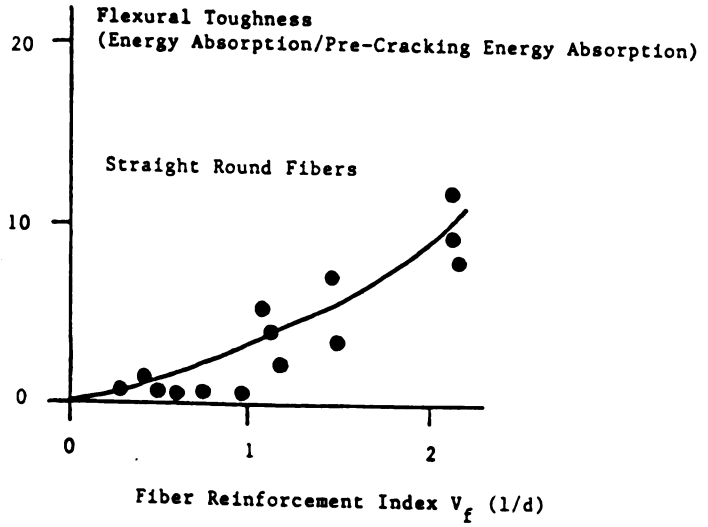

b. Based on area up to peak load (water-cement ratio = 2.4)

between fiber aspect ratio and flexural properties is dependent on fiber volume fraction and fiber diameter.[3,17] For example, Figure 2.12.a (from Reference 17) indicates that the relationship between flexural strength and aspect ratio differs depending on the fiber volume fraction and fiber diameter. The flexural load-deflection curves shown in Figure 2.12.b[3] also indicate that the increase in aspect ratio (at resonable workabilities) does not necessarily improve the flexural performance of fiber reinforced concrete.[3] Shorter fibers having higher aspect ratios might actually have inferior flexural properties when compared with longer fibers of lower aspect ratios, for similar fiber types and volume fractions.[3] The data presented in Reference 22 on hooked fibers also confirms that at a constant aspect ratio and volume fraction, shorter fibers tend to be less effective in improving the flexural properties of concrete.

Fiber type is another important factor influencing the flexural strength of fiber concrete.[1,3,4,28] The trends in the effects of volume fraction and aspect ratio of different fiber types on flexural properties of concrete are, thus, expected to be different. Figure 2.13.a presents the trends in the effects of fiber volume fraction on the total energy absorption capacity (up to 3/8 in =10mm central deflection of 4x4x20 in =102x102x508 mm specimens of two months of age loaded at one third points)[23] of concretes reinforced with hooked and crimped fibers all having an aspect ratio of 100. Figures 2.13.b and 2.13.c provide further evidence indicating that the effects of fiber aspect ratio on flexural strength and energy absorbtion capacity are dependent on the types of steel fibers.[3,23]

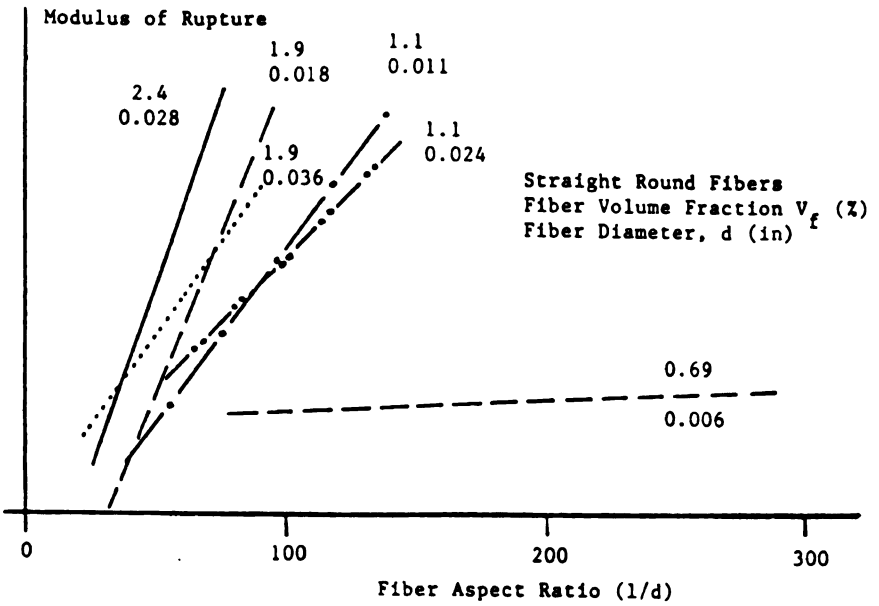

a. Strength[17]

Figure 2.12: Effects of fiber aspect ratio on flexural properties at different fiber diameters (length).[3,17] 1 in = 25.4 mm, 1 Kip = 4.5 KN

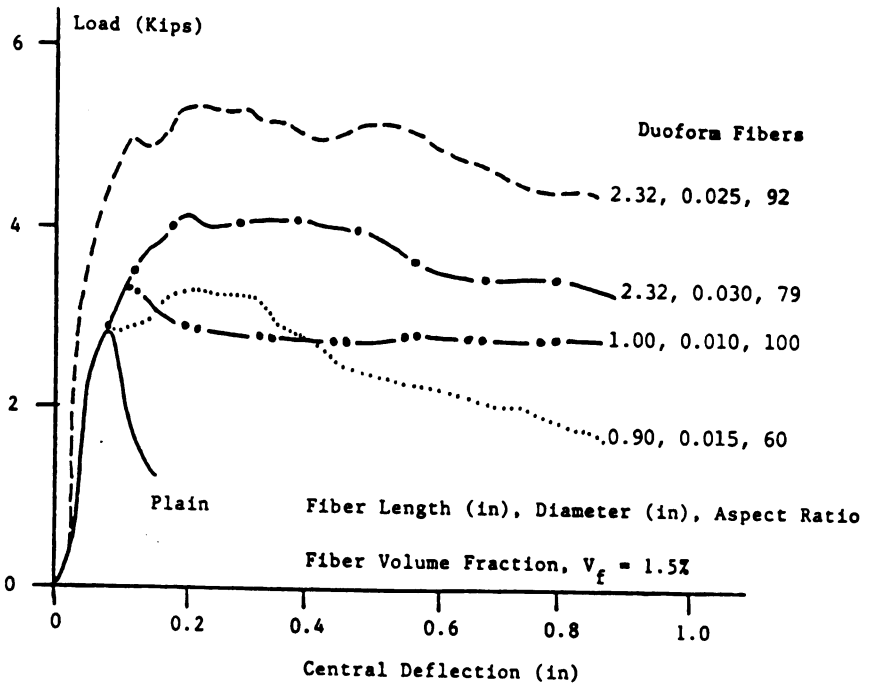

b. Load - deflection curve.[3] (water-cement ratio = 0.49, aggregate-cement ratio = 4.0, fine-to-coarse aggregate ratio = 0.6, maximum aggregate size = 3/8 in (10 mm)), centrally loaded specimens of 4x4x20 in (102x102x508 mm) and span = 16 in (406 mm))

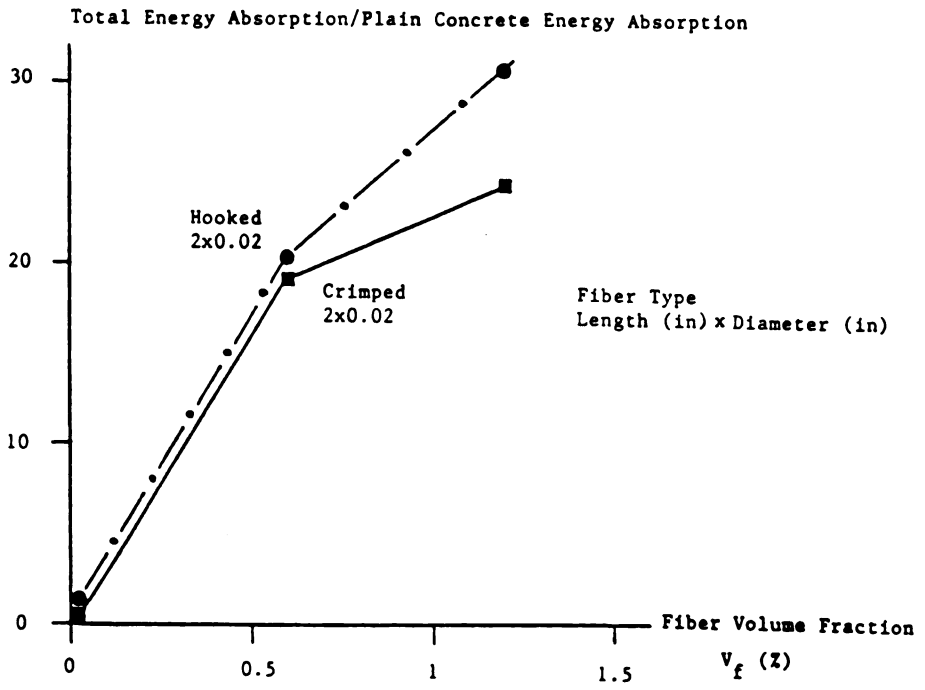

a. Energy absorption capacity.[23]

Figure 2.13: Effects of fiber volume fraction and aspect ratio on the flexural performance of concrete reinforced with different steel fiber types.[3,23] 1 in = 25.4 mm, 1 Kip = 4.5 KN, 1 Ksi = 6.9 N/mm^2

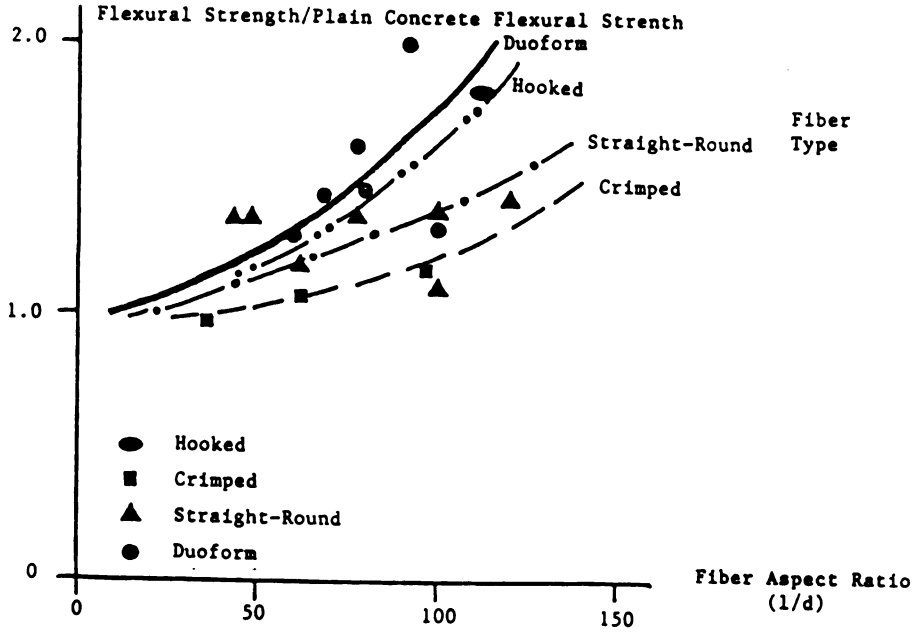

b. Flexural strength.[3] (V_f = 1.5%, water-cement ratio = 0.49, aggregate-cement ratio = 4, fine-to-coarse aggregate ratio = 0.6, maximum aggregate size = 3/8 in (10 mm), centrally loaded specimens of 4 x 4 x 20 in (102 x 102 x 508 mm) and span = 16 in (406mm))

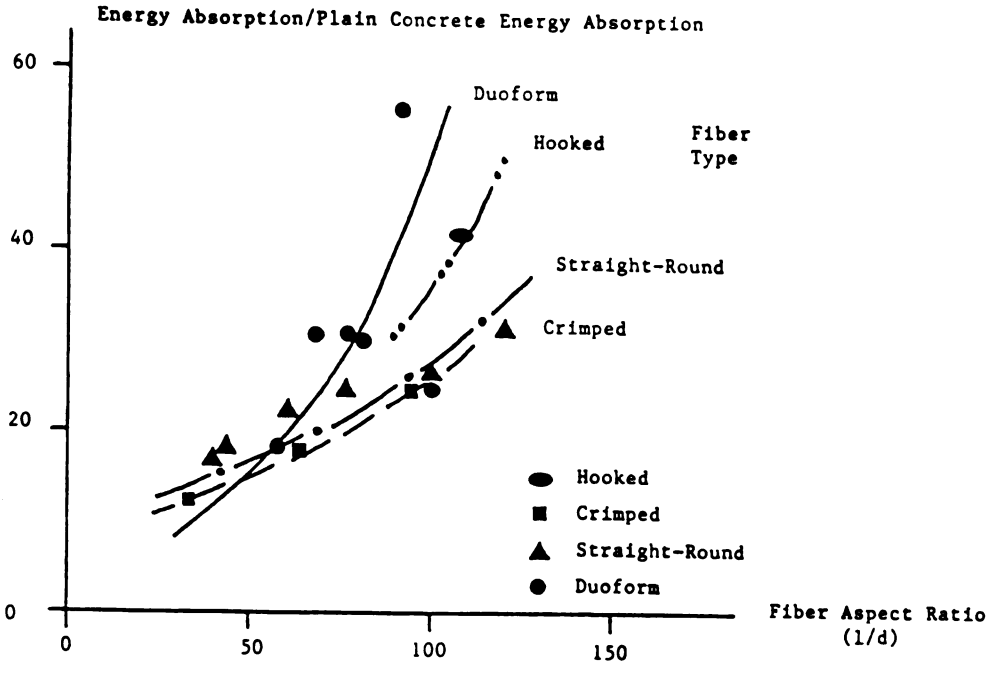

c. Energy absorption capacity.[3] (V_f = 1.5%, water-cement ratio = 0.49, aggregate-cement ratio = 4, fine-to-coarse aggregate ratio = 0.6, maximum aggregate size = 3/8 in (10 mm), centrally loaded specimens of 4 x 4 x 20 in (102 x 102 x 508 mm) and span = 16 in (406 mm))

2.2.c Compressive Behavior: Reinforcement of concrete and mortar by randomly oriented short steel fibers improves their compressive ductility and energy absorbtion capacity (Figure 2.14).[2,29] Steel fiber reinforced concrete also has a slightly higher strength than plain concrete (Figure 2.14.a).[29] This, however, is not always true in the case of fiber reinforced mortar (Figure2.14.b).[2]

An increase in fiber volume fraction leads to improvements in post-peak ductility and energy absorbtion capacity of concrete under compression (Figure 2.14). The compressive strength of concrete also increases with fiber volume fraction, but that of mortar may stay constant or even decreases.[2,29-31]

For both steel fiber reinforced concrete and mortar, there is an upper limit of fiber volume fraction, beyond which higher fiber contents tend to adversely influence the hardened material properties, the damage has been consistently correlated with the reduction in density of the material.[2] The damage to material properties at excessive fiber contents is shown in Figure 2.15. This figure indicates that the toughness index of steel fiber first increases and then decreases with fiber volume fraction (toughness index is defined here as the ratio of fiber concrete energy absorbtion capacity to that of plain concrete).

References 26 and 31 have generated test results on the effects fiber volume fraction on compressive strength of concrete and mortar. The results shown in Figure 2.16[26,31] indicate that the compressive strength of concrete increases while that of mortar decreases slightly with the increase in volume fraction of

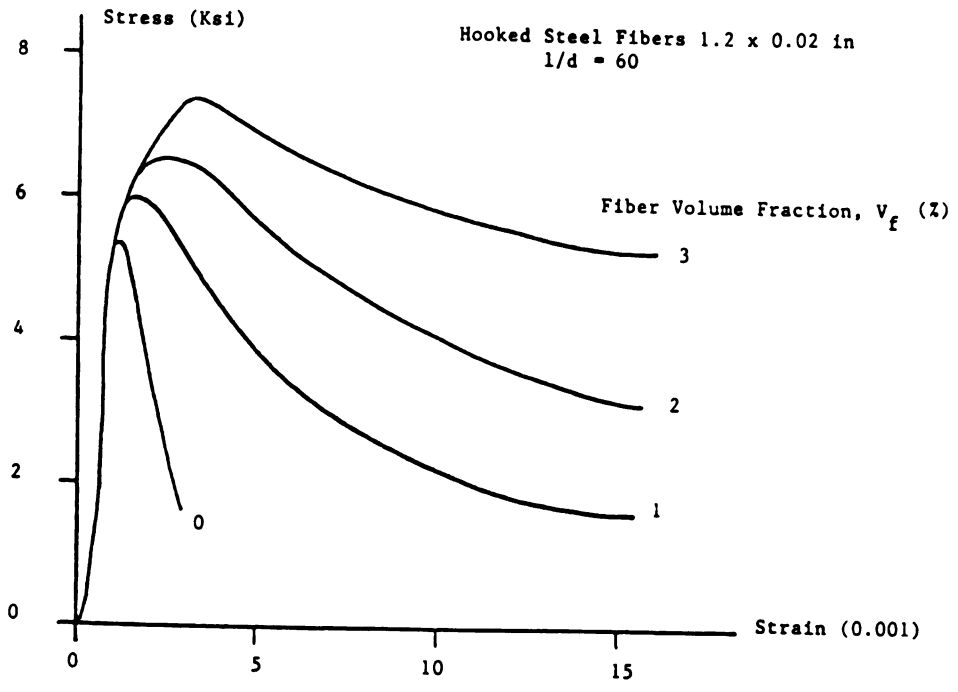

a. Concrete .[29] (water -cement ratio = 0.6, aggregate-cement ratio = 4.6, fine-to-coarse aggregate ratio = 1.2, maximum aggregate size = 3/4 in (19 mm) and cylindrical specimens 4 x 8 in (100x200 mm) of 1 year of age)

Figure 2.14: Effects of fiber reinforcement on the compressive stress-strain charactristics of concrete and mortar.[2,29] 1 in = 25.4 mm, 1 Ksi = 6.9 N/mm^2

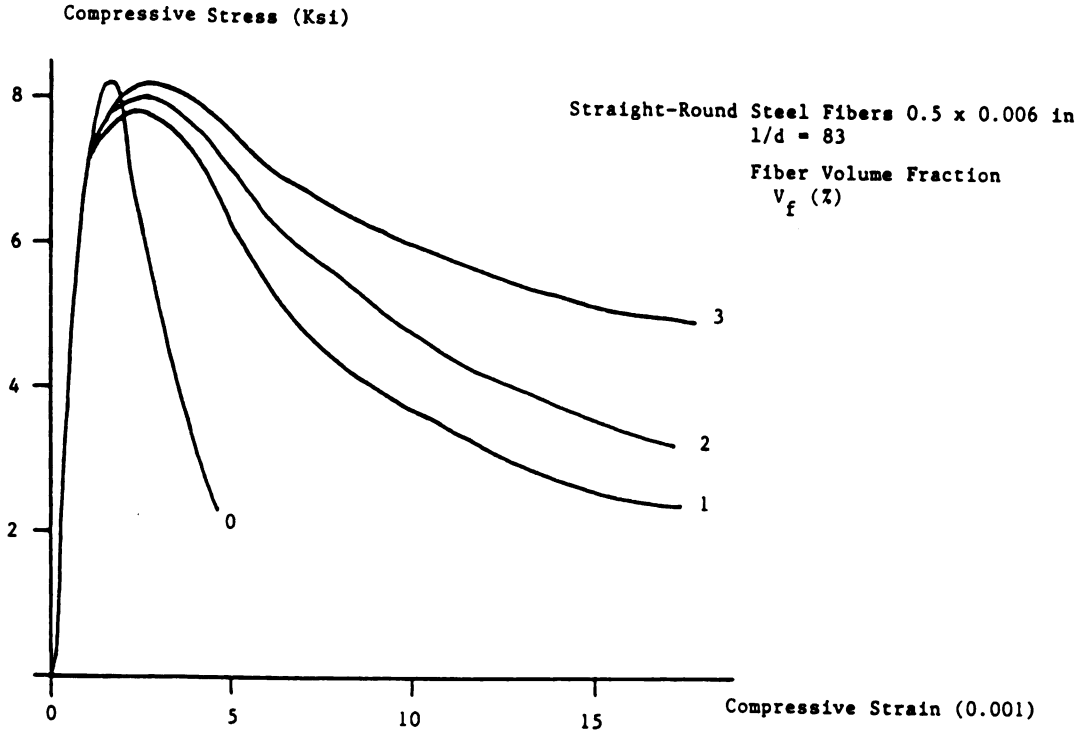

b. Mortar.[2] (water-cement ratio = 0.5, sand-cement ratio = 3 and cylindrical specimens 3 x 6 in (75 x 150 mm))

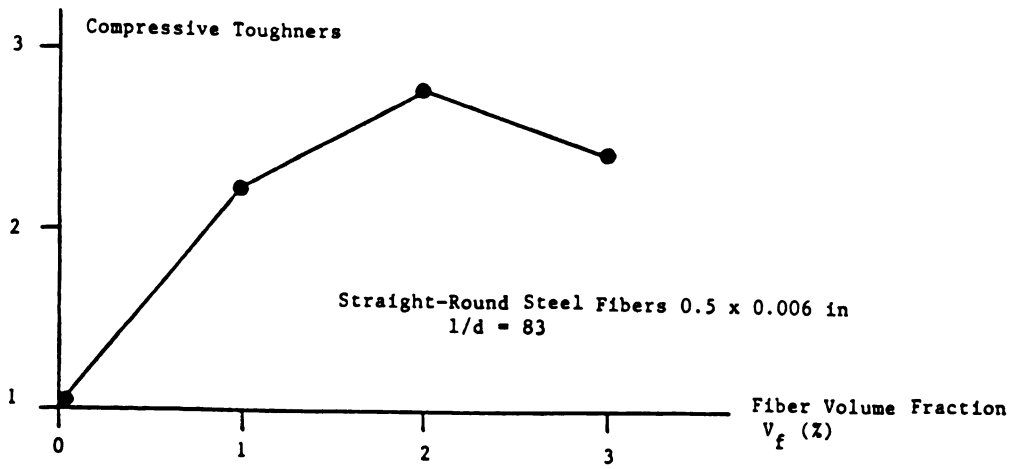

Figure 2.15: Effect of fiber volume fraction on toughness index of mortar with different matrix mix proportions.[2] 1 in = 25.4 mm

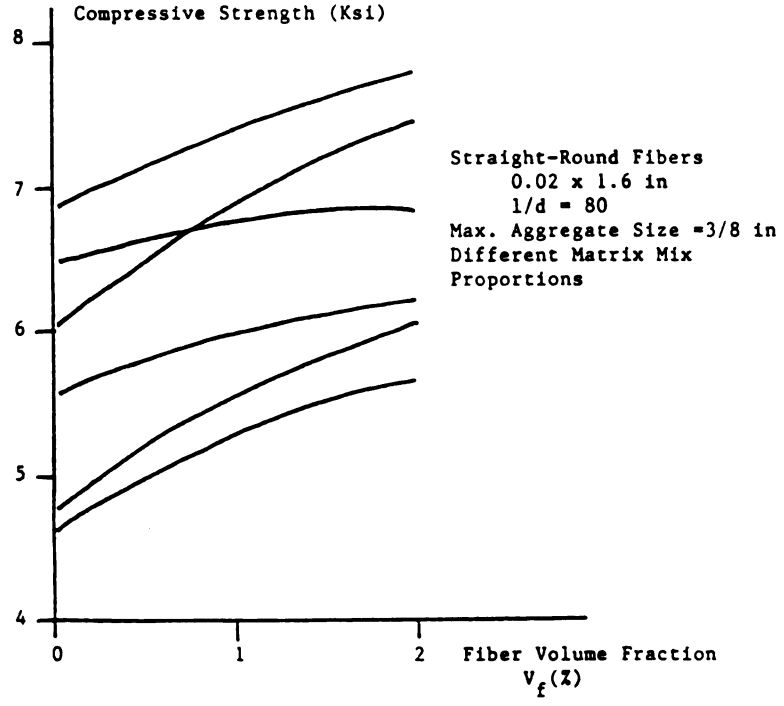

a. Reference 26 test results (concretes with different mix proportions, water-cement ratio = 0.35-0.50 and cylindrical specimens 6 x 12 in (150 x 300 mm))

Figure 2.16: Effect of fiber volume fraction on compressive strength of concrete and mortar.[26,31] 1 in = 25.4 mm, 1 Ksi = 6.9 N/mm^2

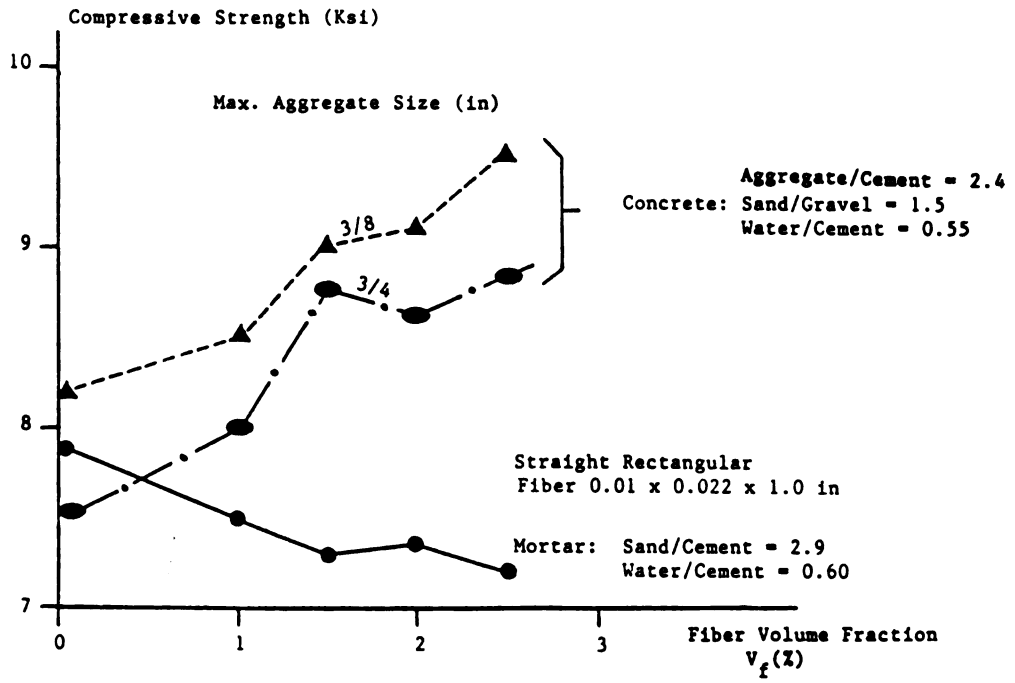

b. Reference 31 test results (water-cement ratio = 0.55-0.60 and cylindrical specimens 6 x 12 in (150 x 300 mm))

fibers. These references suggest that the lower effectiveness of steel fibers in mortar could be due to the unfavorable effects of the increase in sand content on the bonding of cement paste to mix inclusions. References 2 and 29, on the other hand, attribute this effect to the reduction in shear-friction effect in mortar caused by the removal of the coarse aggregates which tend to roughen the crack surface in concrete.

An increase in the aspect ratio of steel fibers at a constant volume fraction has an important effect on improving the post-peak ductility and energy absorbtion capacity of fibrous concrete under compression (Figure 2.17.a).[24,30] The compressive strength of fiber reinforced concrete, however, shows only slight (if any) improvement with the increase in aspect ratio (see Figure 2.17.b). According to Reference 17, the variation in compressive strength with aspect ratio is usually below 10%, and it may be considered insignificant.

The trends in the effects of fiber aspect ratio on compressive energy absorbtion capacity may be reversed beyond a certain maximum limit of aspect ratio. Fibers with excessively high aspect ratio start to increase the harshness of fresh mix, leading to high entrapped air contents and inferior hardened material performance. For example, Figure 2.18[29] shows that the increase in aspect ratio from 60 to 80 at a 2% volume fraction of smooth straight steel fibers actually reduces the post-peak resistance of concrete at compressive strains greater than 0.01.[29]

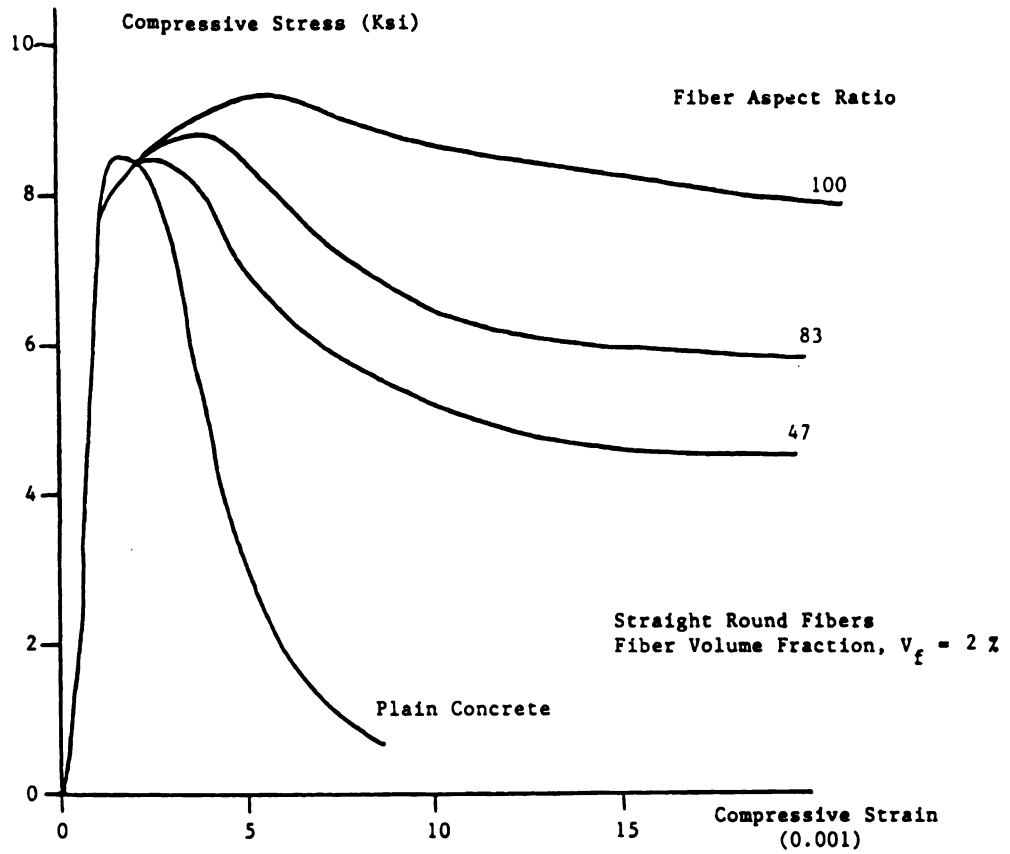

a. Compressive stress-strain relationships (water-cement ratio = 0.5, sand-cement ratio = 3.0 and cylindrical specimens 3 x 6 in (75 x 150 mm))

Figure 2.17: Effect of fiber apsect ratio on compressive behavior of steel fiber mortar and concrete.[2,17,29,30] 1 in = 25.4 mm, 1 Ksi = 6.9 N/mm^2

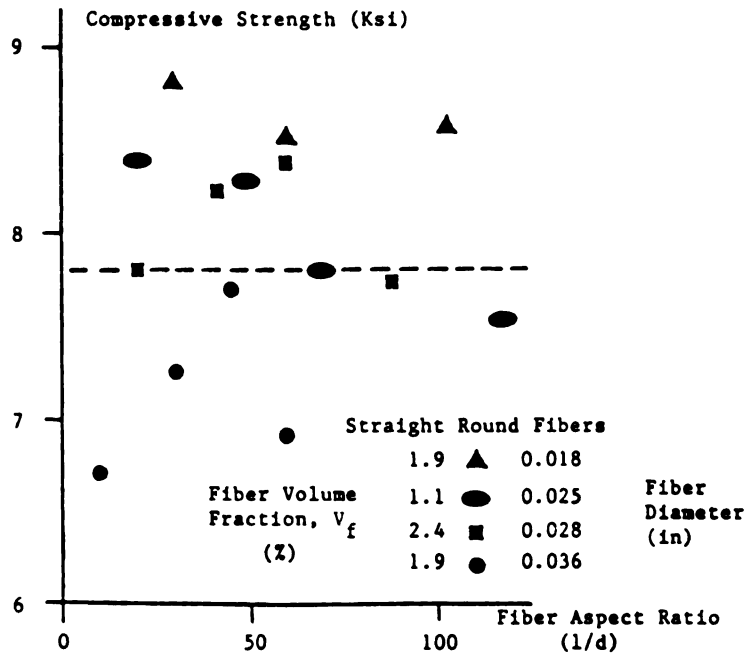

b. Compressive strength (water-cement ratio = 0.55, aggregate-cement ratio = 4.4, fine-to-coarse aggregate ratio = 0.76, maximum aggregate size = 3/8 in (10 mm) and cubical specimens 4 x 4 in (100 x 100 mm))

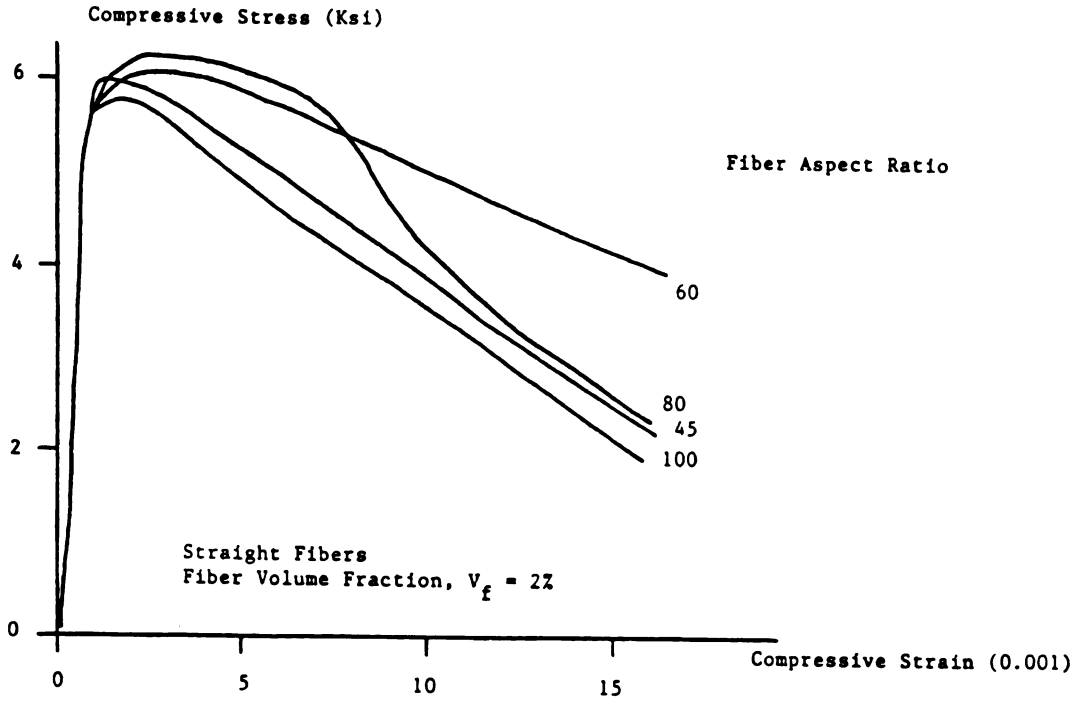

Figure 2.18: Reversal of the fiber aspect ratio effect resulting from workability problems.[29] (water-cement ratio = 0.6, aggregate-cement ratio = 4.6, fine-to-coarse aggregate ratio = 1.2, maximum aggregate size = 3/4 in (19 mm) and cylindrical specimens 4 x 8 in (100 x 200 mm) of 1 year of age)

Considering the comparable effects of fiber volume fraction and aspect ratio on the compressive performance of steel fiber reinforced concrete, some investigators have proposed that their multiplication (V_f l/d) acts as a single variable representing fiber reinforcement properties. Figure 2.19.a confirms that the normalized post-peak stress-strain relationships of steel fiber reinforced mortar are positively influenced by the increase in fiber reinforcement index, and Figure 2.19.b shows that there is also an increase in toughness index (defined as the ratio of fibrous concrete energy absorbtion capacity of that of plain concrete) resulting from the increase in fiber reinforcement index.[2] References 29 and 30 suggest that beyond a fiber reinforcement index value of about 2, the difficulties in mixing and uniform dispersion of fibers start to damage the compressive strength and energy absorbtion capacity of steel fiber reinforced concrete.

Reference 31 has shown that the incorporation of steel fibers tend to increase the modulus of elasticity of mortar under compression. However, fibers decrease the compressive modulus of elasticity of concrete (see Figure 2.20).[31]

It is worth mentioning that test results presented in References 2,29-32 indicate that the strain at peak compressive stress in fiber concrete is significantly larger than that of plain concrete. Also, increasing the fiber volume fraction and aspect ratio, or the fiber reinforcement index, would increase the value of strain at peak compressive stress. This is especially true for hooked steel fibers.[24] The increase in strain at peak compressive stress of concrete resulting from fiber

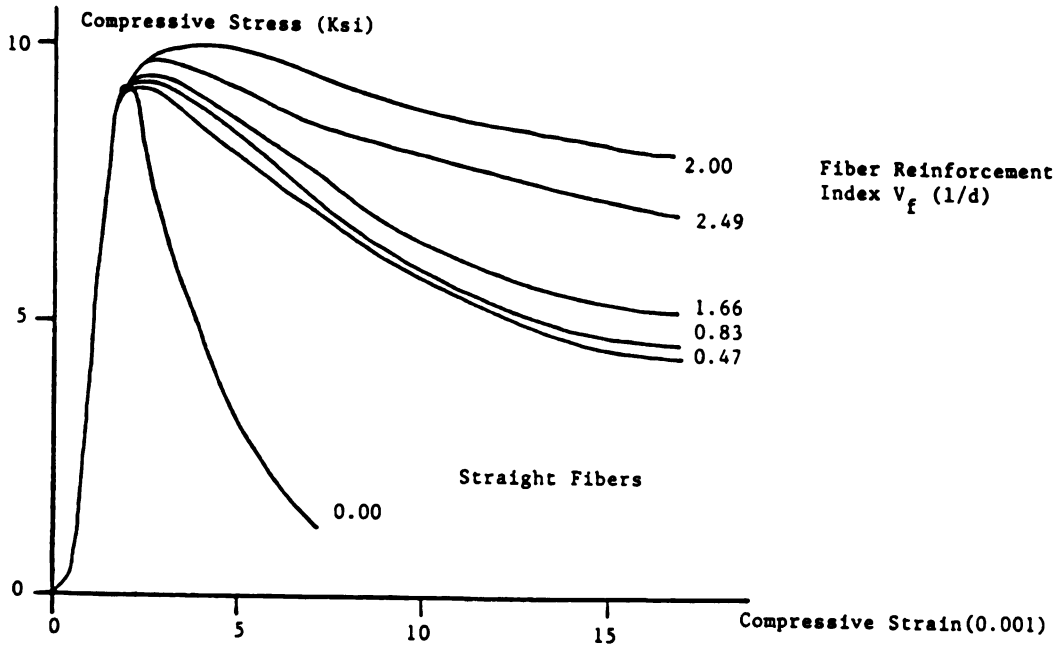

a. Compressive stress-strain relationships

Figure 2.19: Effects of fiber reinforcement index on the compressive properties of mortar.[2] (water-cement ratio = 0.5, sand-cement ratio = 3 and cylindrical specimens 3 x 6 in (75 x 150 mm)). 1 in = 25.4 mm, 1 Ksi = 6.9 N/mm^2

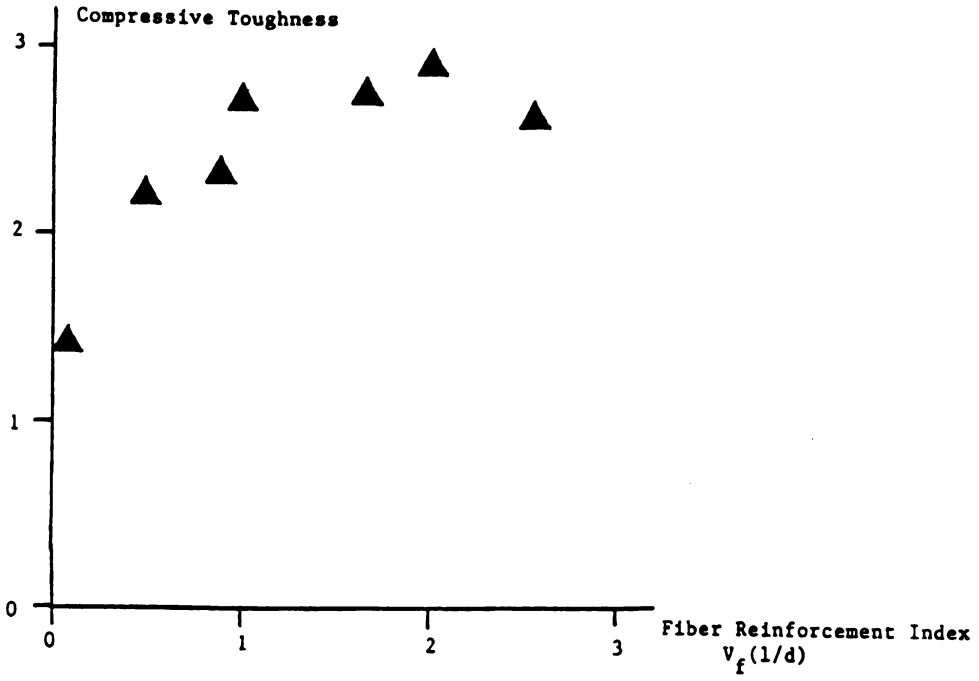

b. Compressive toughness

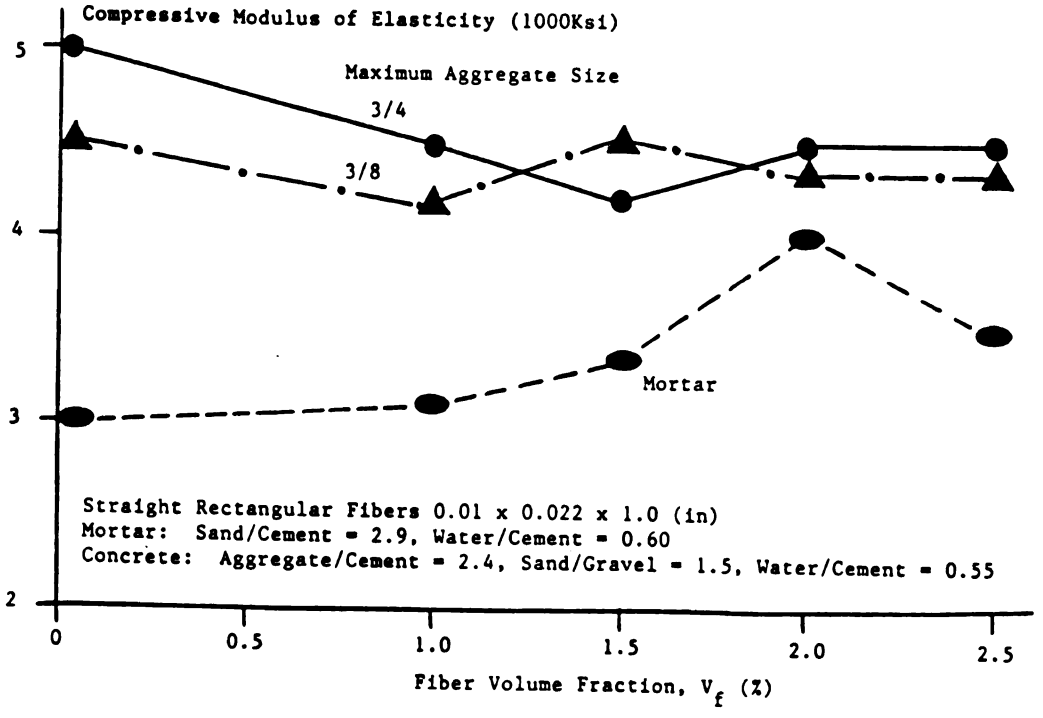

Figure 2.20: Effect of steel fibers on the compressive modulus of elasticity of concrete.[31] (water-cement ratio = 0.55 - 0.60 and cylindrical specimens 6 x 12 in (150 x 300 mm)) 1 in = 25.4 mm, 1 Ksi = 6.9 N/mm^2

reinforcement is mainly due to the drop in tangent modulus of elasicity of fiber reinforced concrete near peak (see Figures 2.14 to 2.20). [2,29-32]

2.2.d Tensile Behavior: Typical tensile stress-strain relationships resulting from tests on plain and fibrous mortar matrices are shown in Figure 2.21.[32] The specimens were rectangular and prismatic (3x3/4x12 in =76x19x305 mm), and the fibers were brass coated and straight-round with a length of 1 in (25 mm) and diameter of 0.016 in (0.4 mm).[32]

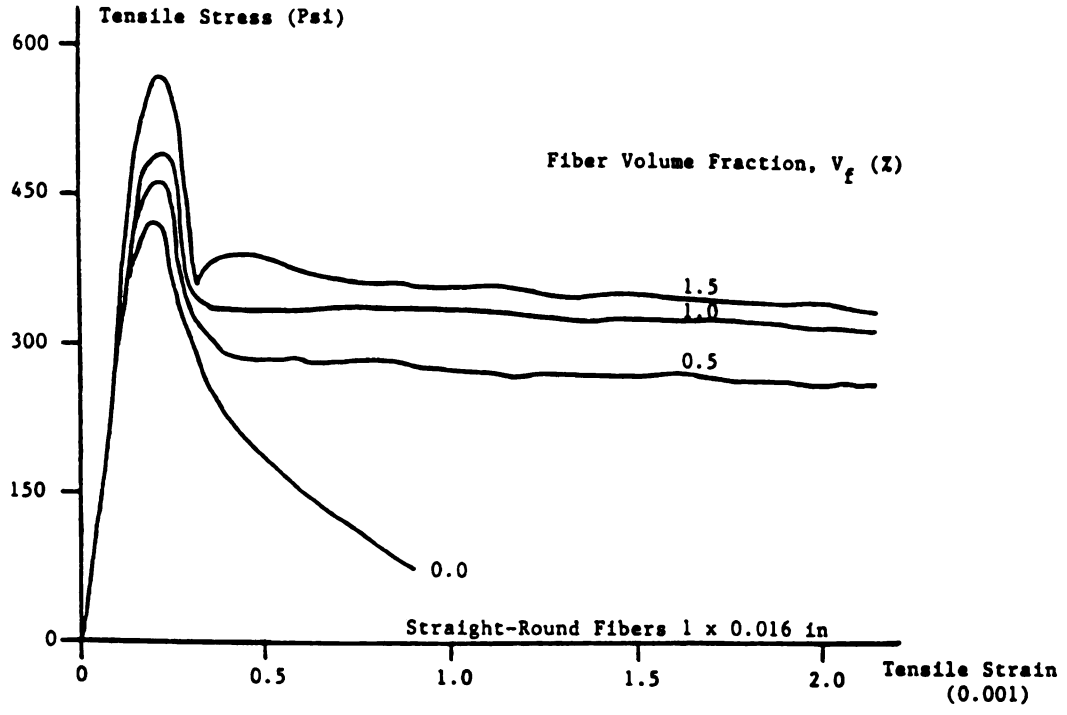

Figure 2.21: Typical stress-strain relationships obtained from direct tension tests on plain and fibrous mortar matrices.[32] (water-cement ratio = 0.5, sand-cement ratio = 2, prismatic specimen's length = 12 in (300 mm) and cross-section = 2 x 3/4 in (50 x 19 mm)) 1 in = 25.4 mm, 1 Ksi = 6.9 N/mm^2

Direct tension test results on plain mortar specimens exhibit a linar elastic behavior up to about 50% of tensile strength. The onset of inelastic behavior prior to the peak load suggests that microcracks start to propagate rather early under tensile loading; although no cracks were detected (optically at a 100 times magnifiacation). Almost immediately after the peak load, deformations become localized and eventually a single crack starts to widen. Unreinforced matrices exhibit some decreasing traction capacity at displacements several times that

observed at peak load.[32]

Direct tensile behavior of steel fiber reinforced mortar is linearly elastic up to about 80% of the matrix tensile strength. Non-linear deformations start to take place beyond this point. This peak stress and the strain associted with it in fibrous composites are larger than the corresponding values in unreinforced matrices (by as much as 25 to 30% at 1.5% volume fraction of steel fibers in mortar matrices).[32] Following the peak stress, the tensile load carrying capacity of steel fiber reinforced concrete rather abruptly to a stress level termed by some investigators as the post cracking strength. One single crack becomes visible at a critical section. Upon further increase in tensile displacement, the load carrying capacity starts to drop almost linearly. A frictional type pull-out resistance is perhaps responsible for the linear door in post-peak tensile resistance with increasing deformations.[32]

The localization of deformations in one crack and the consequent drop in tensile resistance leads to the unloading and reduction of strains outside the cracked zone at the same time the crack is opening and producing major local strains (see Figure 2.22).[32] The formation of a crack at the critical notched section is observed to produce significantly large strains at location 1 in Figure 2.22, and a simultaneous unloading and drop in strain at location 2.[32] The strain reading over a gage length of 3.25 in (83mm) provides values in between the highest one at the crack section and lowest one outside the crack. It should be noted the unloading and drop in strain

at location 2 is slower what could be expected in a plain matrix. This is probably because the fibrous composite develops microcracks prior to the formation of major crack, which are restrained from closing due to the presence of the fibers. Consequently, permanent deformations (strains) are larger at location 2 in steel fiber reinforced concrete than those observed in plain matrices.[32] The major crack at which the tensile fracture of steel fiber reinforced concrete occurs has a more tortuous profile than that of concrete profile than that of plain concrete. The fibrous concrete stiffness also deteriorates less significantly under repeated loading in the post-cracking region (Figure 2.23).[32] This is proposed to result from the interfacial failure of fibers and the irreversible nature of fiber slip across the crack. The residual deformations are thus relatively large (due to the fractional resistance against crack closing provided by fibers.[32]

The absorbtion of tesile fracture energy takes place in steel fiber reinforced concrete through a number of mechanisms, including: (a) work of fracture of the matrix, (b) energy required to debond fibers from the matrix, (c) frictional work required to pull-out fibers from the matrix, and (d) plastic work related to the deforming of fibers that are inclined to the crack face. Prior to the peak stress level, contributions of energy absorbtion mechanisms (a) and (b) are likely to be more significant than mechanisms (c) and (d). Mechanisns (c) and (d) are, however, responsible for most of the post-peak energy absorbtionin steel fiber reinforced concrete.[32]

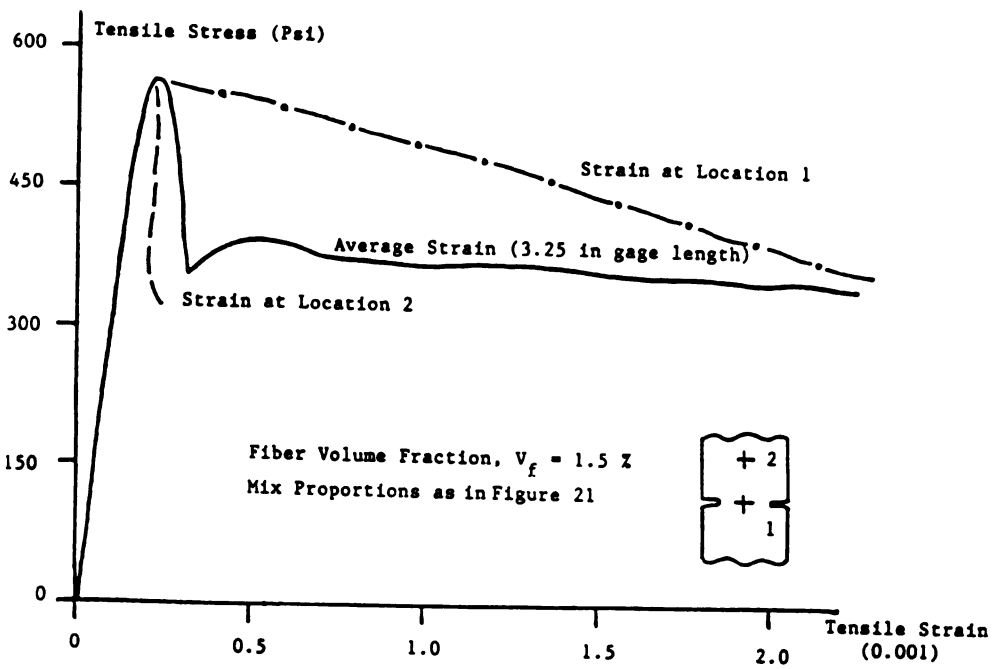

Figure 2.22: Measured tensile strains for steel fiber reinforced mortar at the critical zone and away from it.[32] 1 in = 25.4 mm, 1 Ksi = 6.9 N/mm^2

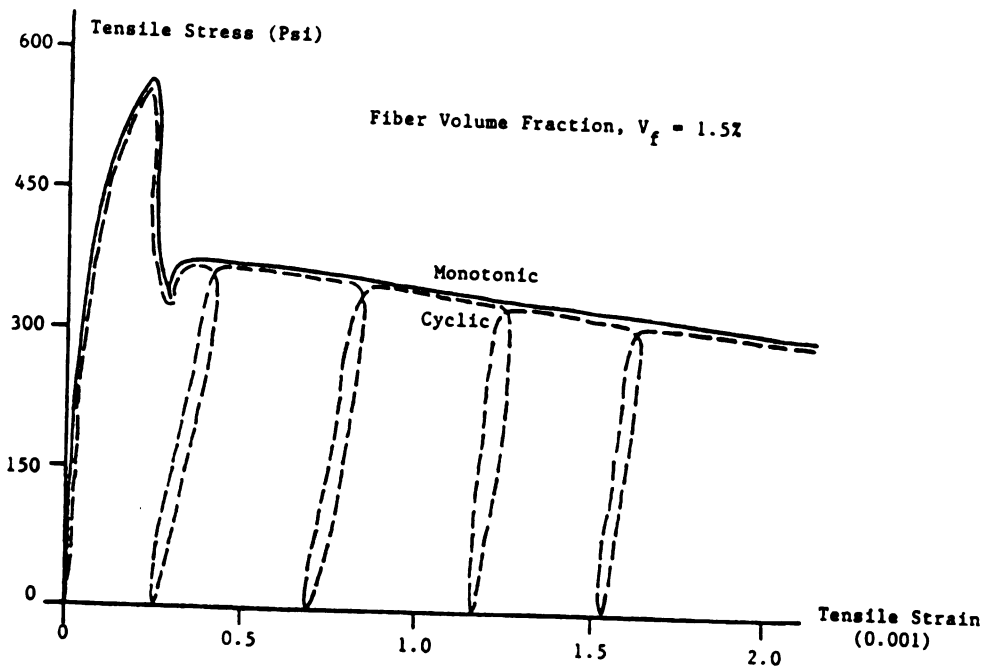

Figure 2.23: Tensile stress-strain relationships under repeated loading. [32]

1 in = 25.4, 1 Ksi = 6.9 N/mm^2

References 32-34 suggest that the tensile strength of steel fiber reinforced concrete increases almost linearly with the increase in fiber content (see Figure 2.24). Reference 32 reports that the post-cracking strength is also linearly related to fiber volume fraction, as far as the fiber aspect ratio is kept constant.

The test data presented in Figure 2.25 suggests that the tensile strength of steel fiber reinforced mortar increases with increasing fiber aspect ratio.[33] The increase in tensile strength does not seem to be directly proportional to aspect ratio, but rather to a power of aspect ratio. For aspect ratio up to 100, a power relationship based on $(l/d)^{3/2}$ is shown in Figure 2.25 to closely apporimate the actual data. At higher aspect ratios, the problems with fiber dispersion and compaction of fresh mix start to damage the tensile strength of the hardened material.[33]

In order to establish a single overall fiber reinforcement parameter to which the percentage increase in tensile strength is closely and simply related, two combinations of the important variables (V_f and l/d) are considered in Reference 33. The first, illustrated in Figure 2.26.a, uses $V_f (l/d)^{3/2}$ as the single variable, while the second, illustrated in Figure 2.26.b, uses the mathematically simple expression V_f l/d. The corresponding correlation coefficients are 0.887 and 0.878, respectively, both of which are well in excess of 0.554 corresponding to a significance level of 10%. Hence, a desireable correlation exists between the

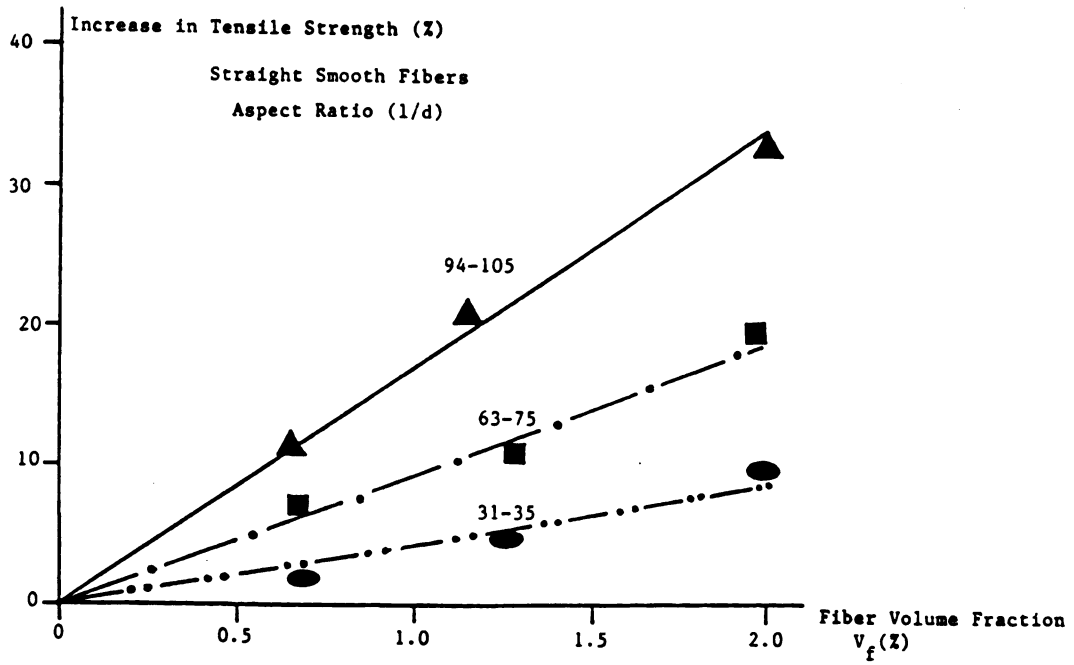

Figure 2.24: Increase in tensile strength of steel fiber reinforced mortar with straight-round fibers.[33] (water-cement ratio = 0.5, sand-cement ratio = 3.0, prismatic specimen's length = 30 in (750 mm) and cross-section = 4 x 4 in (100 x 100 mm)) 1 in = 25.4 mm, 1 Ksi = 6.9 N/mm^2

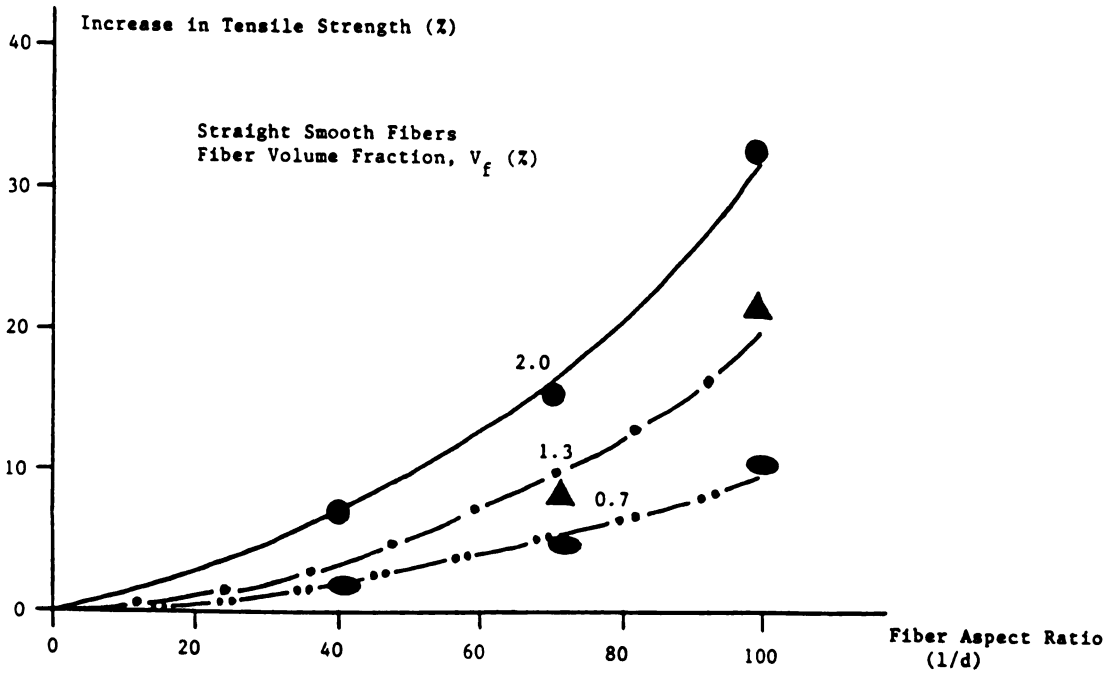

Figure 2.25: Increase in tensile strength of steel fiber reinforced mortar with fiber aspect ratio of straight-round fibers.[33] (water-cement ratio = 0.5, sand-cement ratio = 3.0, prismatic specimen's length = 30 in (750 mm) and cross-section = 4 x 4 in (100 x 100 mm)) 1 in = 25.4 mm, 1 Ksi = 6.9 N/mm^2

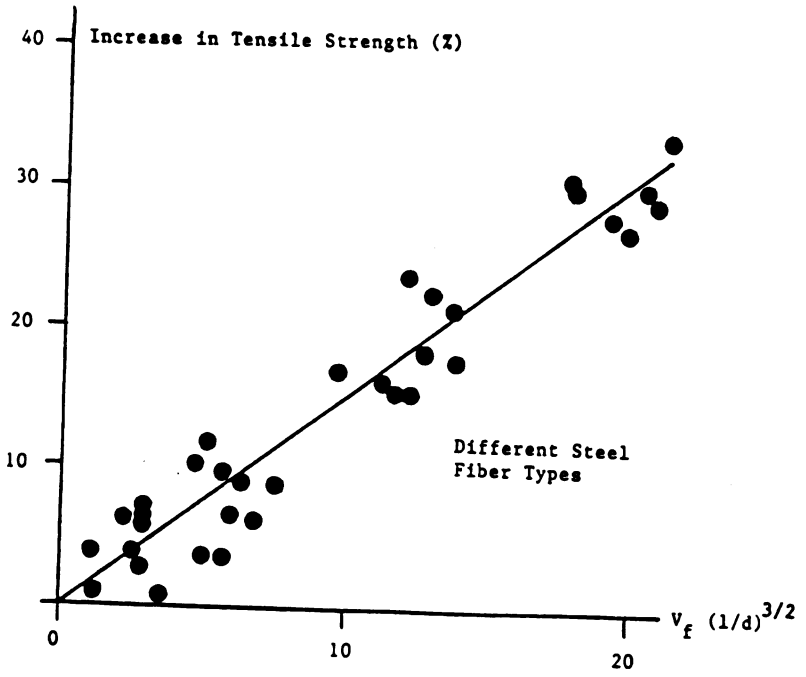

a. $V_f (l/d)^{3/2}$

Figure 2.26: Relationship between the increase in tensile strength and fiber reinforcement parameters.[33] (water-cement ratio = 0.5, sand-cement ratio = 3.0, prismatic specimen's length = 30 in (750 mm) and cross-section = 4 x 4 in (100 x 100 mm)) 1 in = 25.4 mm, 1 Ksi = 6.9 N/mm^2

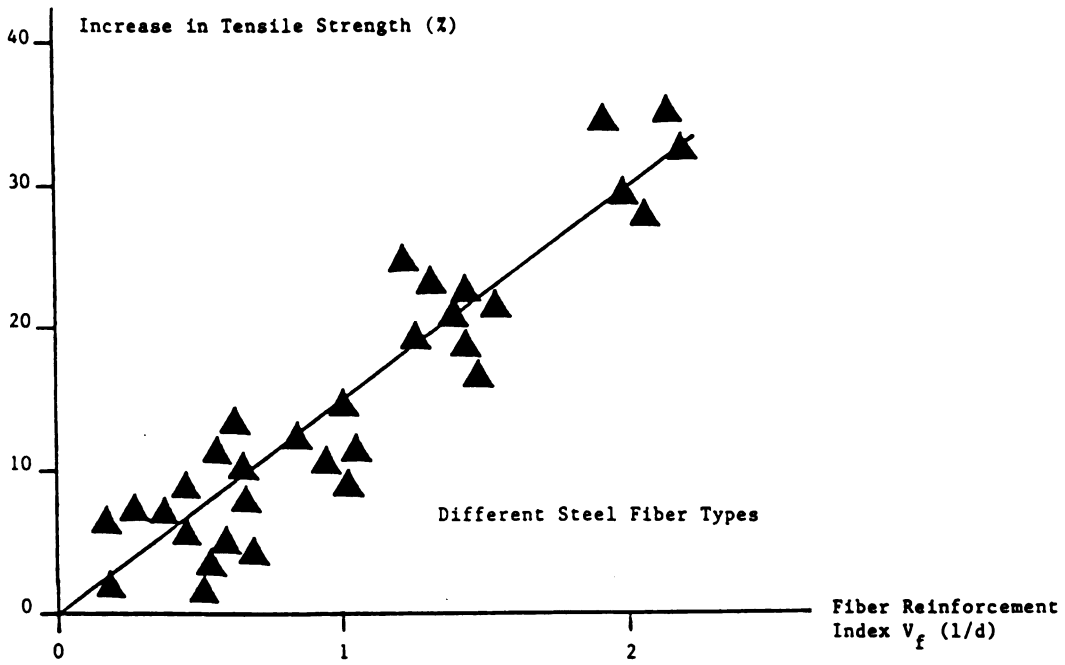
Increase in Tensile Strength (%)
40
30
20
10
0
0
1
2
Different Steel Fiber Types
Fiber Reinforcement
Index V_f (1/d)

b. V_f (l/d)

percentage increase in tensile strength and either of the two proposed fiber reinforcement parameter.[5] In spite of the high degree of similarity of these two parameters, Reference 33 prefers $V_f (l/d)^{3/2}$ over $V_f (l/d)$ as representative of the effectiveness of steei fibers in increasing the tensile strength of mortar. As shown in Figure 2.27, a resonable degree of correlation also exists between the increase in strain at peak tensile stress resulting from steel fiber reinforcement and either of the two alternative fiber reinforcement parameters (correlation coefficient is about 0.7 in both cases).[33] In the evaluation of Figure 2.27, it should be noted that the tensile strain measurements of Reference 33 have exhibited a relatively large scatter.

Reference 35 also has correlated direct tensile strength test results with the fiber reinforcement parameter $V_f (l/d)$ (see Figure 2.28). The results presented in this figure confirm that a resonable degree of correlation exists between the fibrous concrete tesile strength and $V_f (l/d)$.

Reference 36 has studied the effects of l/d, for different fiber types, on the tensile behavior of steel fiber reinforced concrete. The matrix had a water-cement ratio of 0.49, aggregate-cement ratio of 4, fine-to-coarse aggregate ratio of 0.6 and a maximum aggregate size of 3/8 in (10 mm). The specimens were cylinders with a diameter of 3.18 in (79.5 mm) and length of 14.17 in (360 mm). The fiber

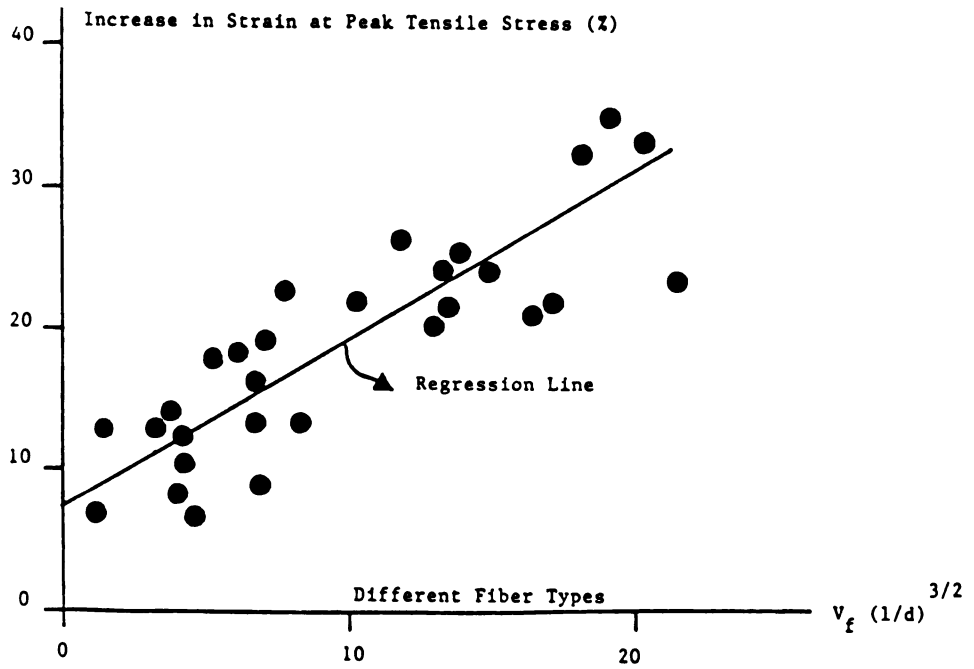

a. $V_f (l/d)^{3/2}$

Figure 2.27: Relationship between the increase in tensile strain at peak tensile stress and different fiber reinforcement parameters.[33] (water-cement ratio = 0.5, sand-cement ratio = 3.0, prismatic specimen's length = 30 in (750 mm) and cross-section = 4 x 4 in (100 x 100 mm)) 1 in = 25.4 mm, 1 Ksi = 6.9 N/mm^2

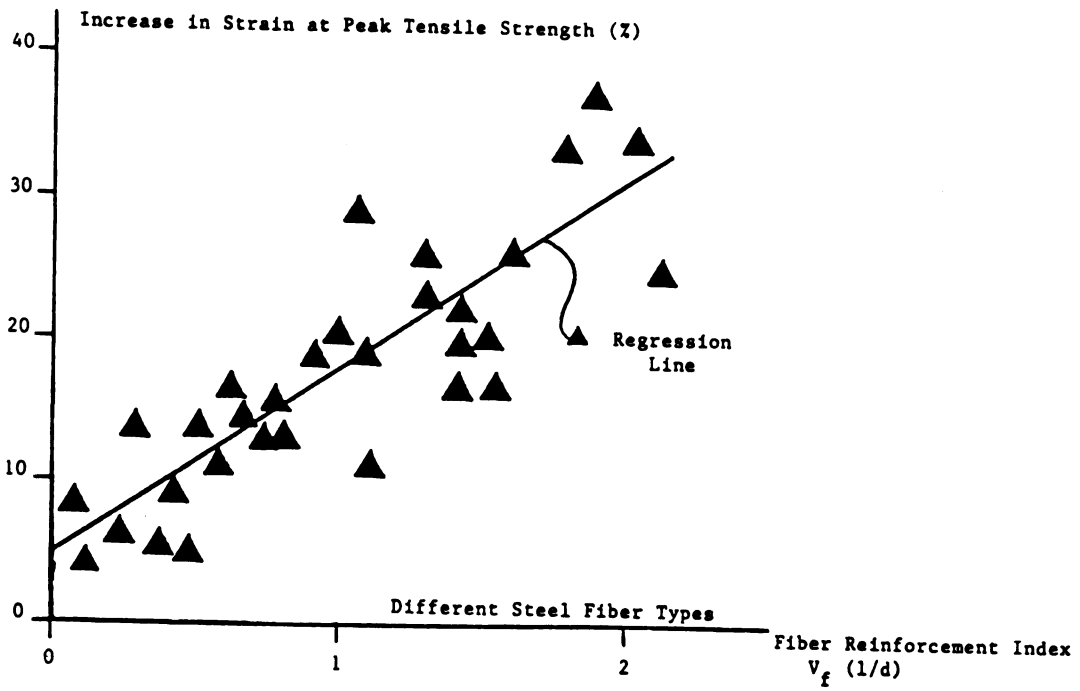
Increase in Strain at Peak Tensile Strength (%)
40
30
20
10
0
Regression Line
Different Steel Fiber Types
0
1
2
Fiber Reinforcement Index
V_f (1/d)

b. V_f (l/d)

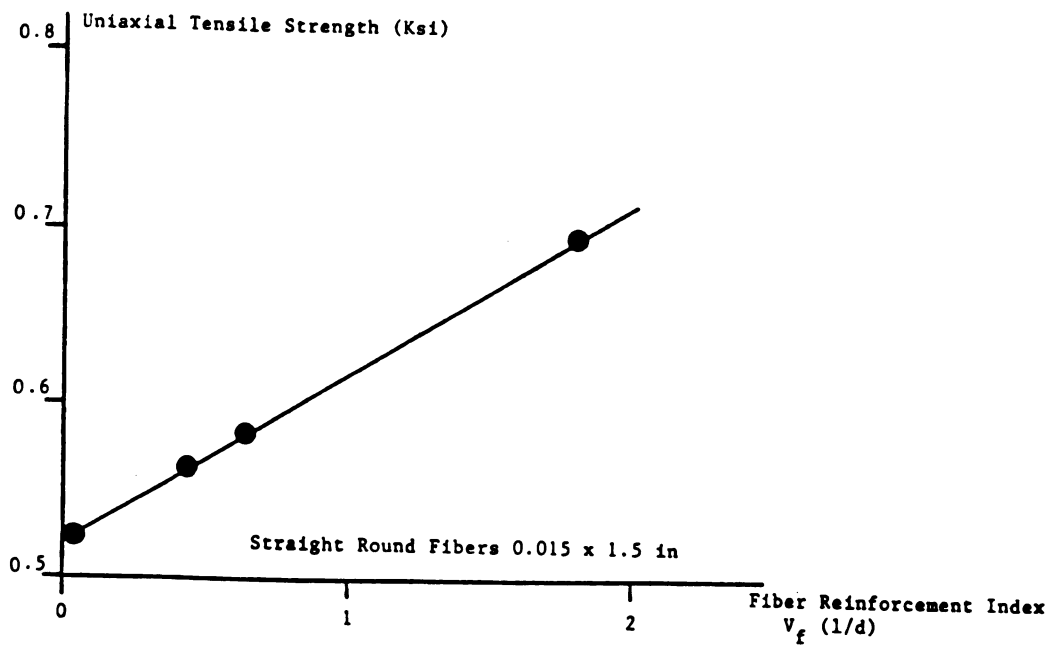

Figure 2.28: Relationship between the direct tensile strength and the fiber reinforcement parameter (V_f l/d).[35] (water-cement ratio = 0.5, sand-cement ratio = 4, prismatic specimen's length = 24 in (600 mm) and cross-section = 4 x 4 in (102 x 102 mm)) 1 in = 25.4 mm, 1 Ksi = 6.9 N/mm^2

volume fraction used in Reference 36 was 1.5%. The differences in the effects of fiber aspect ratio on the tensile strength and post-peak resistance of concretes reinforced with different fiber types seem to be relatively small in Figures 2.29.a and 2.29.b, respectively. A similar conclusion can be derived from the tensile strength test results of Reference 33 produced for mortars reinforced with straight-round and duoform fibers at a volume fraction of 1.3% and different aspect ratios.

2.3 Experimental Program

The program outlined in this section was designed to investigate the effects of fiber length, diameter and volume fraction on the fresh mix and hardened material properties of steel fiber reinforced concrete. The fiber types considered were straight, crimped and hooked. The fresh fiber mix was characterized by its slump and inverted a slump cone time (Figure 2.1),[4,9] and the hardened material properties investigated were compressive and flexural load-deformation relationships.

The steel fiber reinforced concretes included in this program all had a water-binder (cement+fly ash) ratio of 0.4, a fly ash-binder ratio of 0.3, aggregate-binder ratio of 4.0, coarse-to-fine aggregate ratio of 1.0, and superplasticizer-binder ratio of 1.5%. The fly ash-binder ratio was decided, based on the other phases of this project, to be an optimum value for use in steel fiber reinforced concrete. The fly ash used in this study was type F provided by the

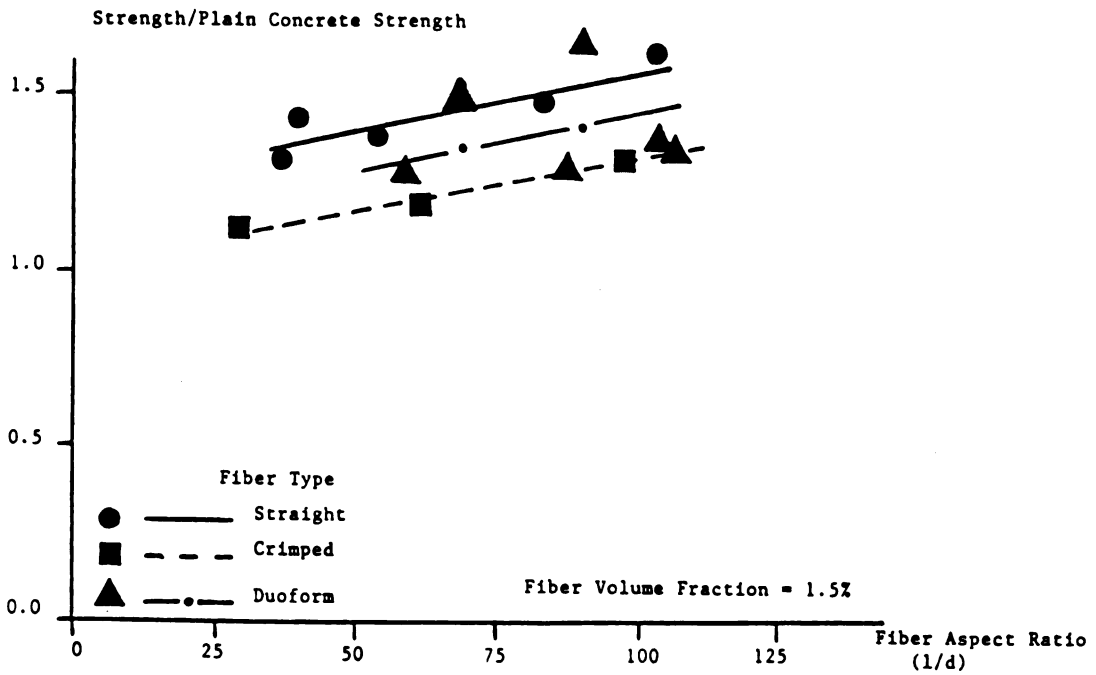

a. Tensile strength of concrete

Figure 2.29: Effects of fiber aspect ratio on the tensile strength and post-peak resistance of concretes reinforced with different steel fiber types.[36]
(water-cement ratio = 0.49, aggregate-cement ratio = 4, fine-to-coarse aggregate ratio = 0.6, maximum aggregate size = 3/8 in (10 mm), cylindrical specimen's length = 14 in (360 mm) and diameter = 3.2 in (80 mm))
1 in = 25.4 mm, 1 Ksi = 6.9 N/mm^2

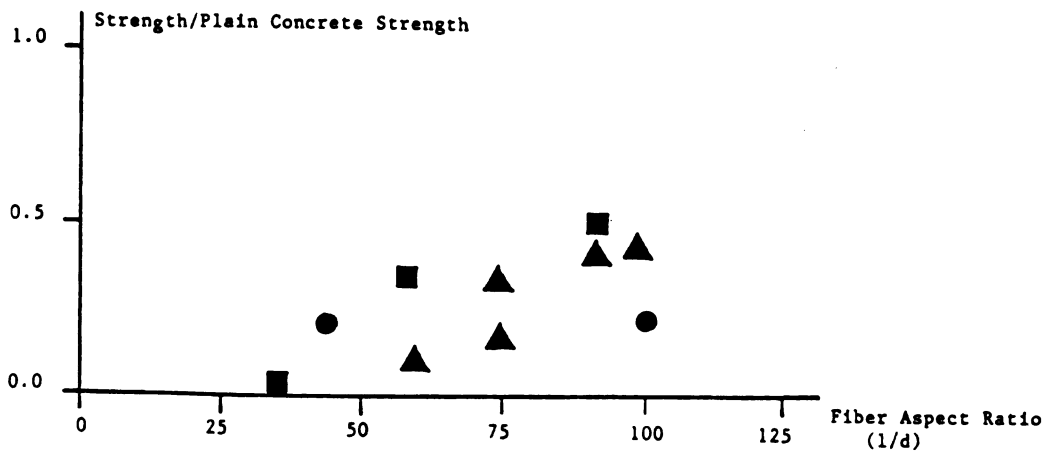

b. Maximum post-peak resistance of concrete.

Lansing Board of Water and Light (see Table 2.1 for the physical and chemical propertiesof fly ash),[37] and the superplasticizer was Daracem 100 (a Naphtalene-Formaldehyde-Sulfonate based superplasticizer with water constituting 60% of its weight) which is capable of maintaining its effectiveness over the relatively long period usually needed for manufcturing and placing of steel fiber reinforced concrete.[38] Cement was regular type I, and the aggregates were natural river sand and gravel, with a maximum coarse aggregate size of 0.75 in. (19 mm).

The variables of this test program were the diameter, length, volume fraction and type of steel fibers. Different combinations of these variables used in the test program are presented in the Table 2.2.

Two cylindrical compression test specimens 6 in (150 mm) in diameter by 12 in (300 mm) in height,[27] and three flexural specimens 6x6x20 in (150x150x500 mm)[27] were made from each mix (which was prepared in a rotary drum mixer). The sequence and rate of addition of different mix ingredients were as follows:

(1) Charge the mixer with all the sand and gravel;

(2) Start the mixer and add 1/3 of the water-superplasticizer mixture;

(3) Add half to 70% of the cementitious materials (cement+fly ash) together with another 1/3 of the water-superplasticizer mixture over a 4-minute period;

(4) Add the fibers to the mix (perferably through a wire mesh basket with an openning size of 1.5x1.5 in) in a gradual manner such that piling up of fibers on

Table 2.1: Major chemical and physical properties of fly ash used in the experiments.[37] 1 in = 25.4 mm

Chemical Composition

Compound	% By Weight
Silica, Si02	47.0
Alumina, Al203	22.1
Iron, Fe203	23.4
Titanium, Ti02	1.1
Calcium, CaO	2.6
Magnesium, MgO	0.7
Potassium, K20	2.0
Carbon, C	4.3

Gradation

Size of Sieve	% Passing
# 30 (0.6mm = 600 micron)	100
#200 (0.074mm = 74 micron)	92
#325 (0.045mm = 45 micron)	84
0.020mm = 20 micron	63
0.010mm = 10 micron	36
0.005mm = 5 micron	17

Specific Gravity = 2.245

Table 2.2: Fiber reinforcement properties in the mixes of the test program. 1 in = 25.4 mm

Fiber type	Length l (in.)	Diameter d (in.)	Volume Fraction (Vf) %	l/d	Vf(l/d)
Straight Round	2	0.035	3	57	171
			2	57	114
			1	57	57
	2.5	0.035	2	72	144
	1.5	0.035	2	43	86
Hooked-Collated	2	0.02	2	100	200
			1	100	100
			0.5	100	50
Crimped Circular	2	0.035	2	57	114
			1	57	57
Hooked-Collated	2.36	0.0315	2	75	150
			1	75	75

the mix is prevented. The addition of fibers usually takes about 3 minutes;
(5) Add the remainder of the water-superplasticizer mixture and the cementitious materials over a 2-minute period; and
(6) Continue mixing for 3 minutes until a homogeneous mix is achieved. Then stop the mixer for 3 minutes, followed by a 2-minute mixing period.

Following mixing, the fresh mix workability is measured by the slump and inverted slump cone testing procedures. Slump is the popular method for measuring the workability of concrete. In the presence of steel fiber and fly ash, however, the slump test results can be misleading in the sense that they do not reflect the flowability of the mix under vibration.[5-26] The inverted slump cone test seems to be more applicable to fibrous mixes containing fly ash. In this technique (see Figure 2.1),[9] the time needed for evacuating an inverted slump cone, filled with the fresh mix, through intervel vibration is used as a measure of the fresh mix workability.[9] Shorter inverted slump cone times are indicative of a better mix workability. Also, a subjective measure of workability was used in the experimental program reported herein. This subjective measure is a representative of the overall workability of the mix and takes into account flowability, mobility, compactibility, placeability, stability, finishability as well as fiber dispersion. The subjective workability measure was performed consistently by the author on a scale of four with four being the best and zero the worst.

The specimens were cast in two layers and vibrated externally (for 30 sec per layer) using a vibration table. The specimens were kept inside their molds under plastic sheets for 24 hours, and were then demolded and cured for 7 days in a moist room (at 72^{o} F = 22^{o} C and 100% relative humidity) and then in air (at regular lab environment) until the test age of 28 days. A compressometer-extensometer was used to measure the values of strain in compression tests (see Figure 2.30.a).[27,39] Two displacement transducers were used to monitor the displacements at the load points in flexural tests (Figure 2.30.b), which were conducted by loading at 1/3 points on a span of 18 in. (450 mm).[27] Both the compression and flexural tests were performed in a quasi static manner.

2.4 Experimental Results

This section describes the results of tests on fresh mix workability and hardened material flexural and compressive performance for different fiber reinforcement conditions.

2.4.a Fresh Mix Workability: Figures 2.31.a, b and c show the measured values of slump, inverted slump cone time and subjective workability of fresh fibrous mixtures vs their fiber reinforcement index (fiber volume fraction times aspect ratio = V_f l/d), for different fiber types. It is obvious in all these figures that the fresh mix workability is damaged by the increase in fiber reinforcement index. The rate of drop in workability with the increase in fiber reinforcement index

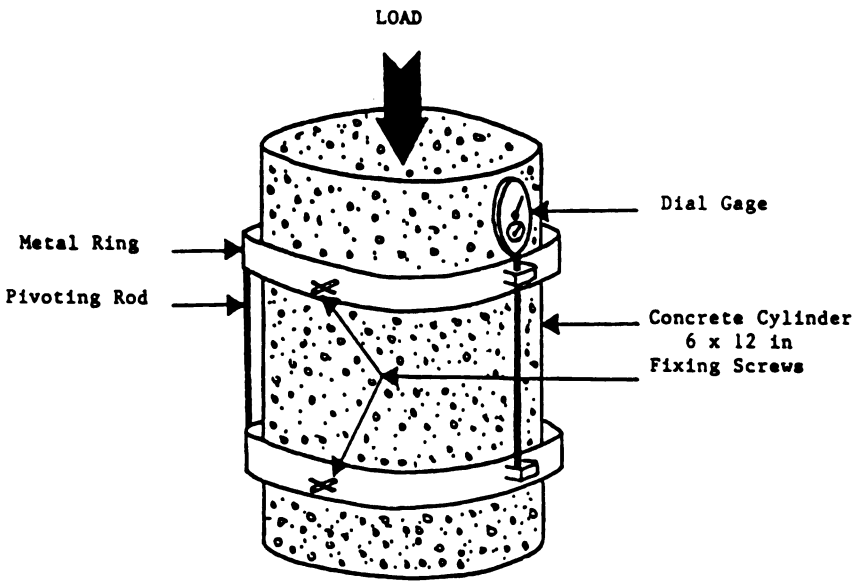

a. Compression

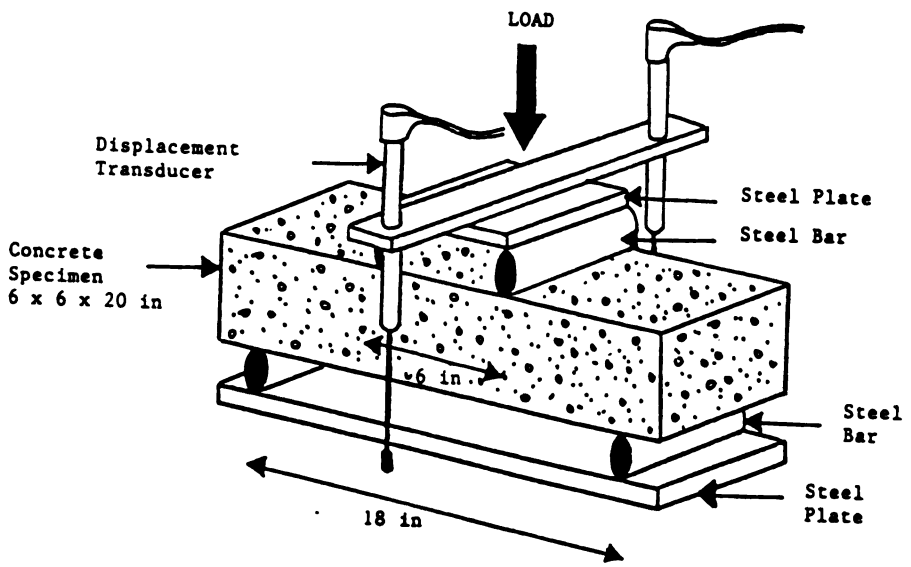

b. Flexure

Figure 2.30: Compression and flexural test set-ups and instrumentations.

1 in = 25.4 mm

seems to be comparable for different fiber types. At a specific fiber reinforcement index, however, crimped fibers seem to give slightly higher slumps (see Figure 2.31.a) while the straight fibers produce fresh fibrous mixtures with slightly lower inverted slump cone times as shown in Figure 2.31.b. Hooked fibers produce slumps comprable with those of straight fibers but their inverted slump cone times tend to be slightly higher than those of both crimped and specially straight fibers. The limited test data on subjective workability (Figure 2.31.c) do not show any significant effects of fiber type on the subjective workability of fresh steel fiber reinforced concrete mixtures, noting that subjective workability is a more comprehensive measure of fresh mix workability but has a lower accuracy than the slump and inverted slump cone measurements.

2.4.b Flexural Performance: The experimental load-deflection relationships for different steel fiber reinforced concrete mixtures are presented in Figures 2.32.a through 2.32.c. Each curve in these figures is the average of three measurements made on similar specimens. The trends observed in the flexural test results shown in Figure 2.32 are summarized in Figures 2.33.a through 2.33.d which present the first crack and ultimate flexural loads, energy absorption capacity, and toughness index of different steel fiber reinforced concretes as a function of the fiber reinforcement index. Energy absorbtion represents the total area underneath the load-deflection curves up to a maximum deflection of 5.5 times the flexural cracking deflection.[27] Toughness index is defined as the ratio of this energy

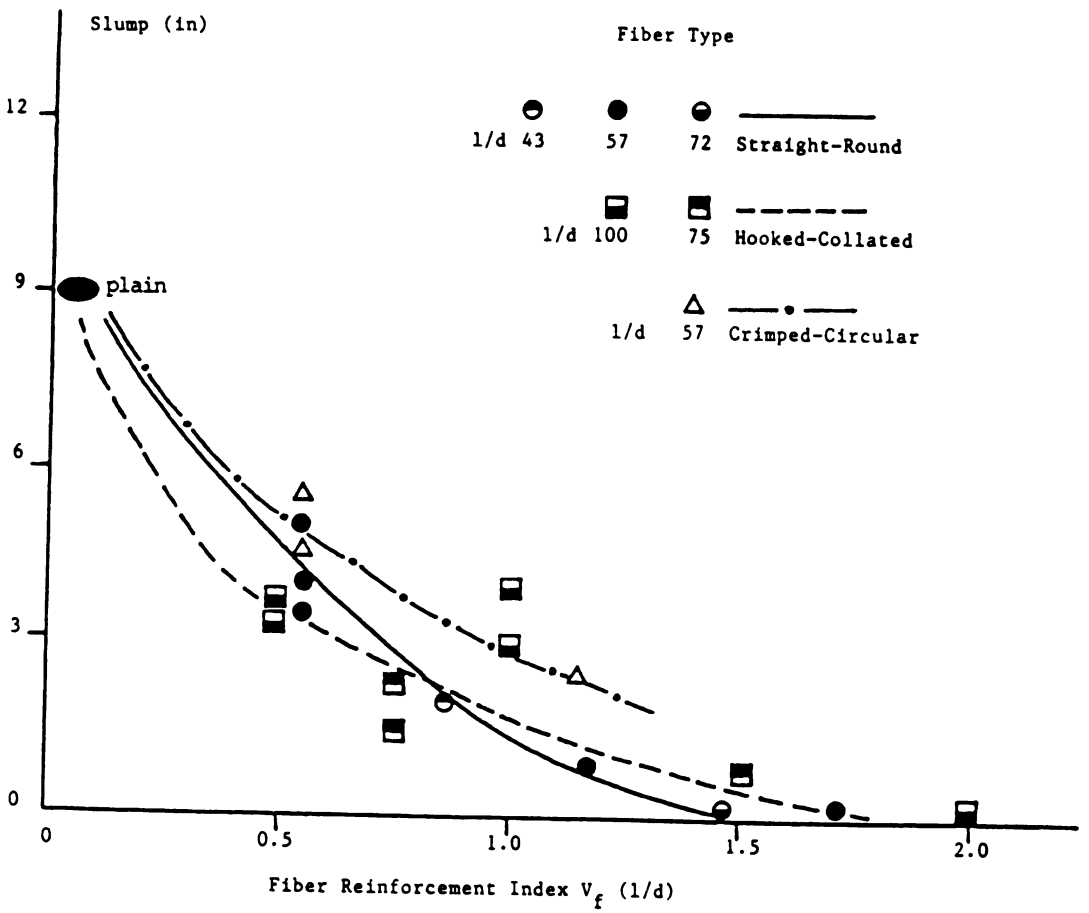

a. Slump. 1 in = 25.4 mm

Figure 2.31: Effects of fiber reinforcement index and fiber type on fresh mix workability.

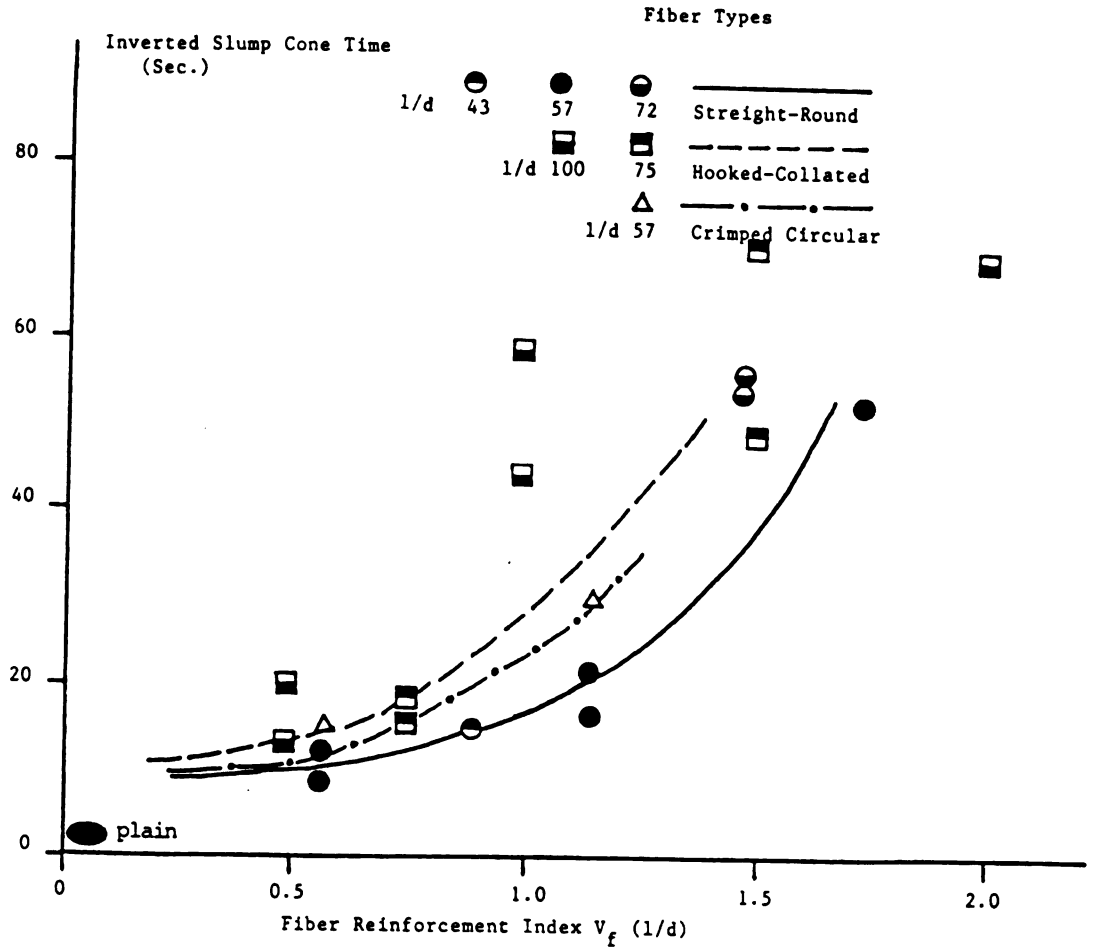

b. Inverted slump cone time

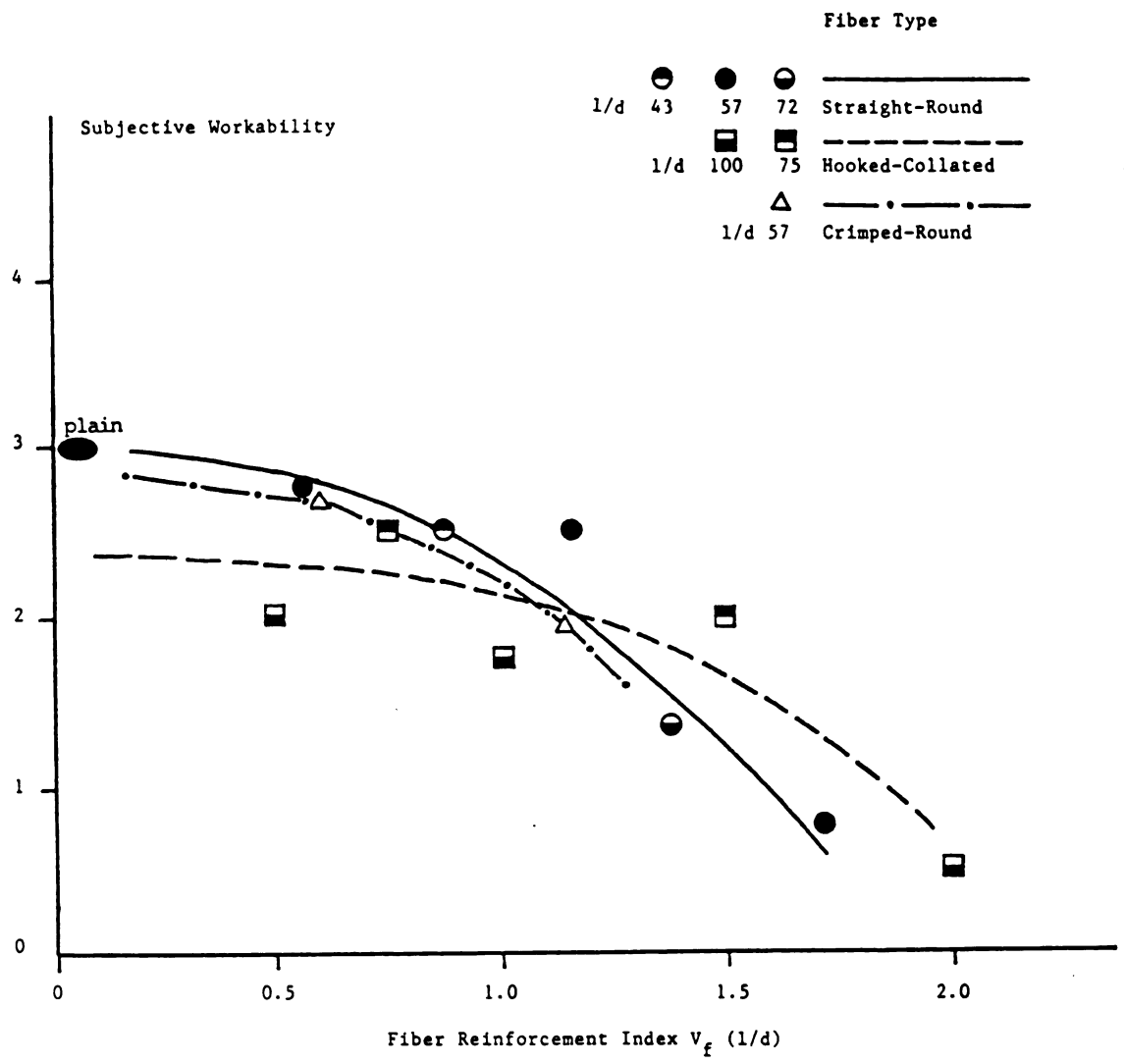

c. Subjective workability

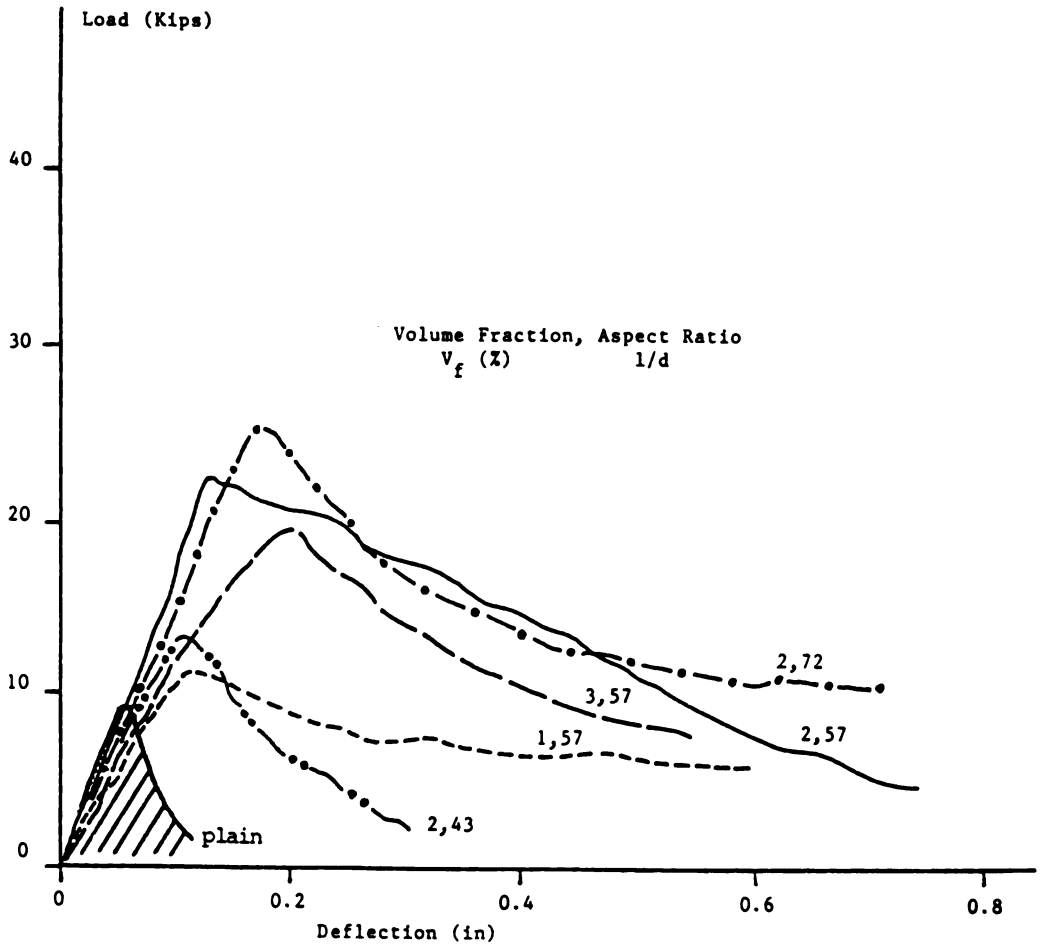

a. Straight fibers

Figure 2.32: Flexural load-deflection relationship. 1 in = 25.4 mm,

1 Ksi = 4.5 KN.

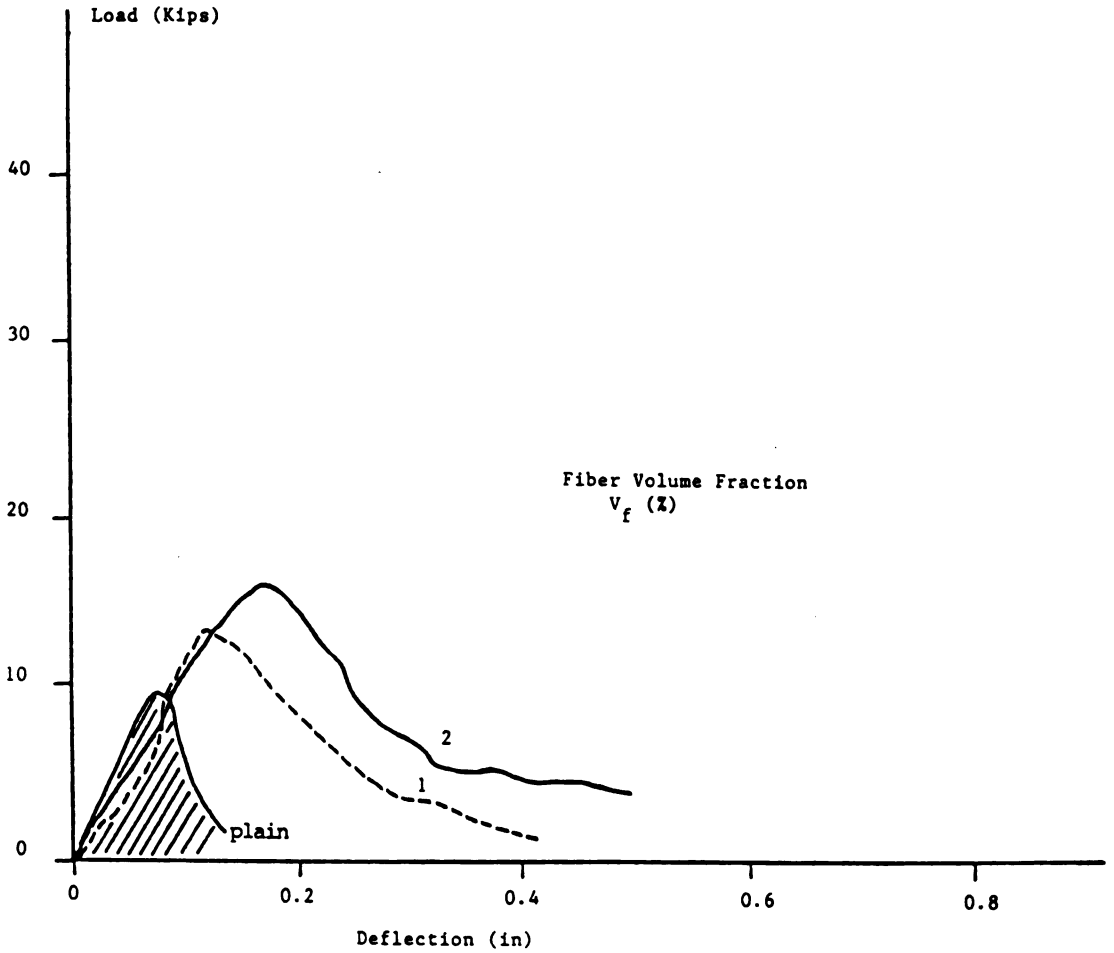

b. Crimped fibers

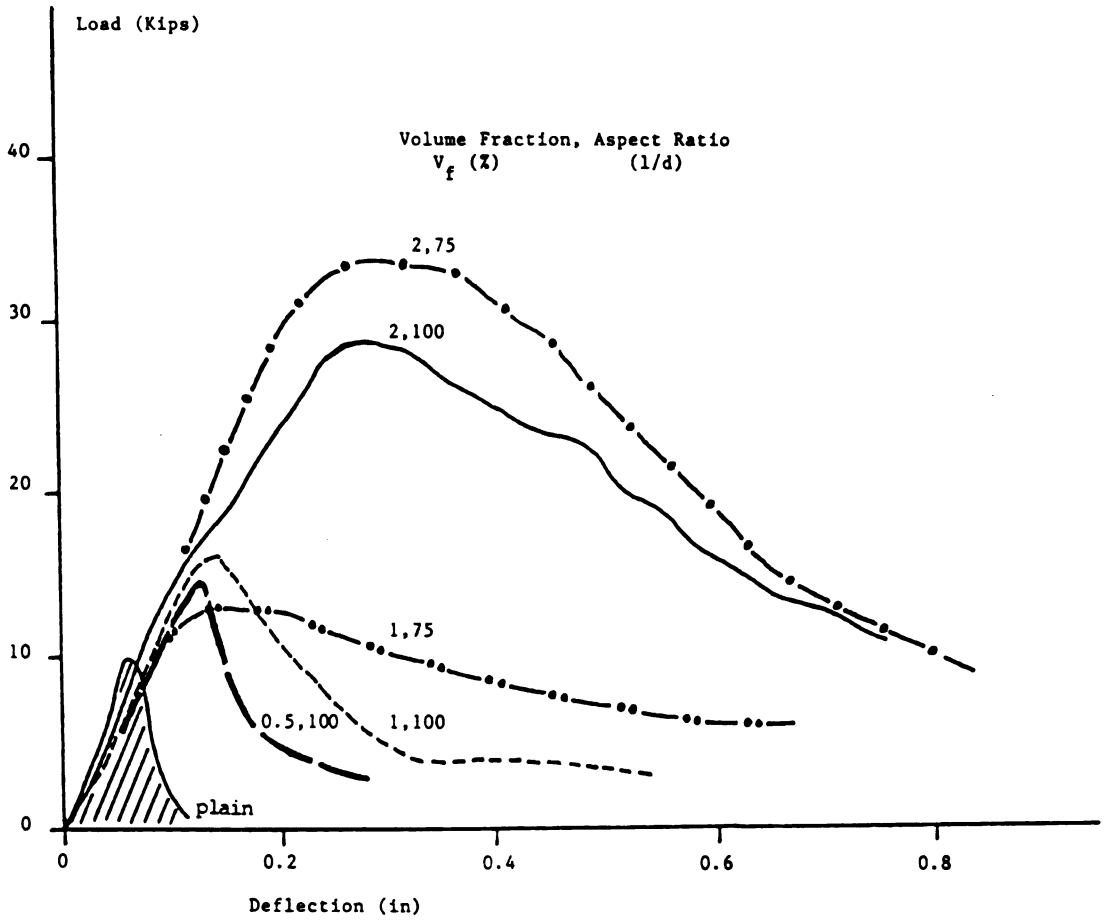

c. Hooked-end fibers

absorbtion capacity to the pre-cracking energy absorption (area underneath the flexural load-deflection curve up to the cracking point). A toughness index of 11 represents an elastic-perfectly plastic type of behavior (with yield point corresponding to the cracking condition).

The first crack and ultimate flexural loads are observed in Figures 2.33.a and 2.33.b to increase with increasing fiber reinforcement index up to about 1.5. At higher fiber reinforcement indices, the problems with workability of fresh mix seem to reverse this trend and cause damage to the hardened material flexural strength. Hooked fibers, especially at higher fiber reinforcement indices, lead to flexural strengths superior to those obtained with straight and specially crimped fibers.

The flexural energy absorbtion capacity of steel fiber reinforced concrete is also observed in Figure 2.33.c to increase with increasing fiber reinforcement index up to an index value of about 1.5, beyond which this trend start to reverse. Hooked fibers, especially at higher fiber reinforcement indices, produce concretes with higher energy absorbtion capacity than straight and especially crimped fibers. The trends in fiber reinforcement effects on the toughness of steel fiber reinforced concrete in Figure 2.33.d are indicative of the simultaneous increase in pre- and post-cracking flexural energy absorbtion of steel fiber reinforced concrete with the increase in fiber reinforced index. In general, crimped fibers seem to give lower toughness indices than other fiber types. Most of the fibrous concretes have

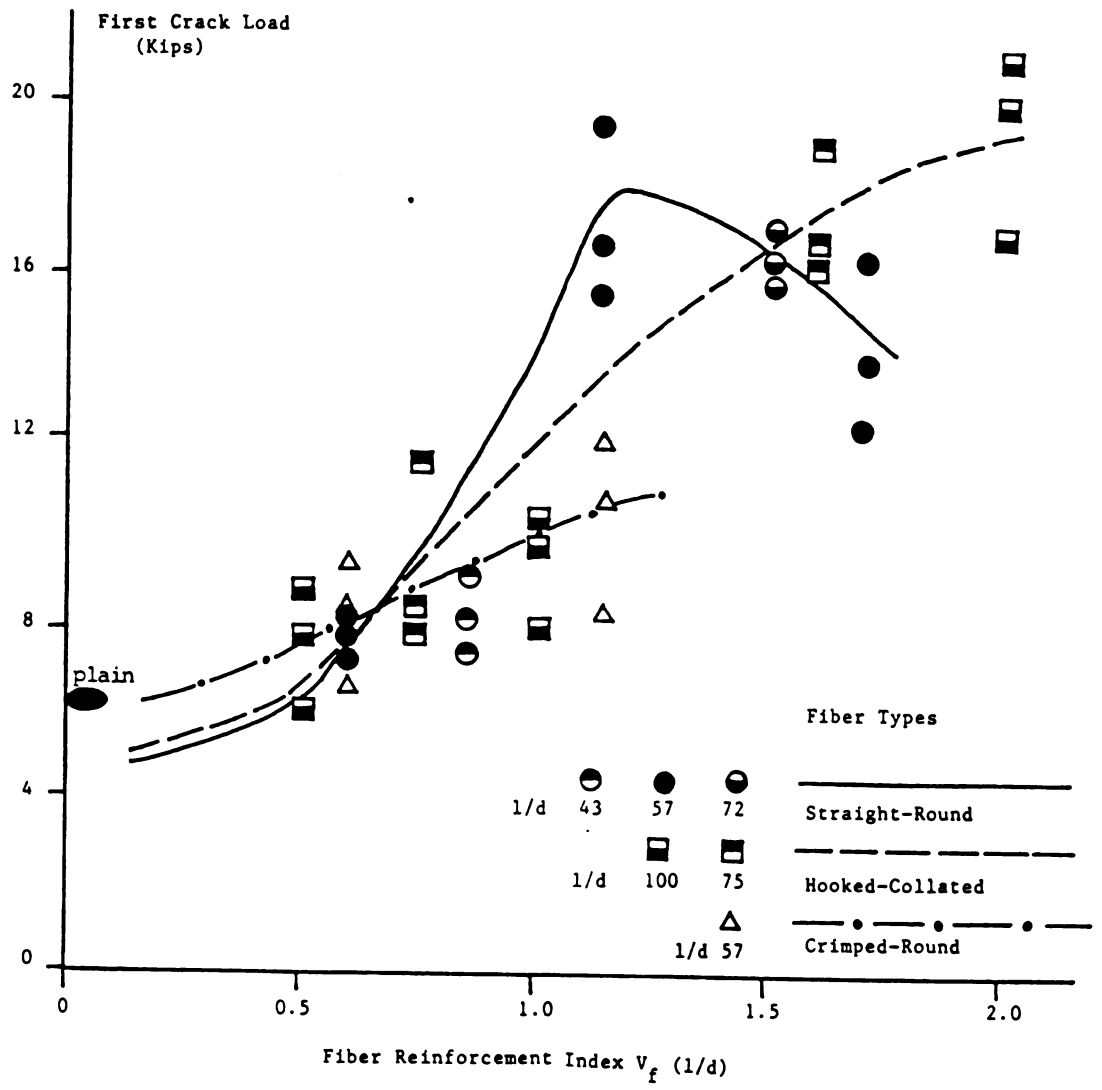

a. First-crack load

Figure 2.33: Effects of fiber reinforcement index and fiber type on different aspects of the flexural performance of steel fiber reinforced concrete.

1 in = 25.4 mm, 1 Ksi = 4.5 KN, 1 lb. in = 115 N.mm

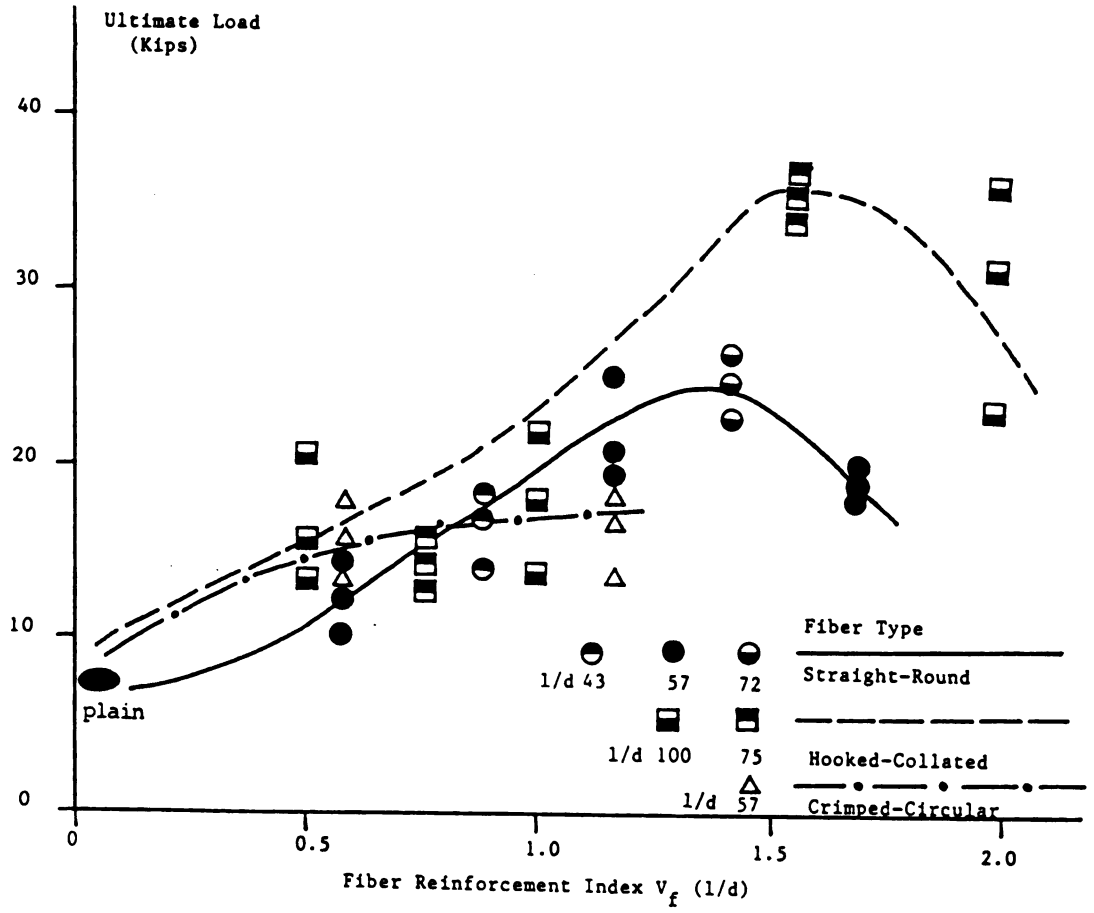

b. Ultimate load

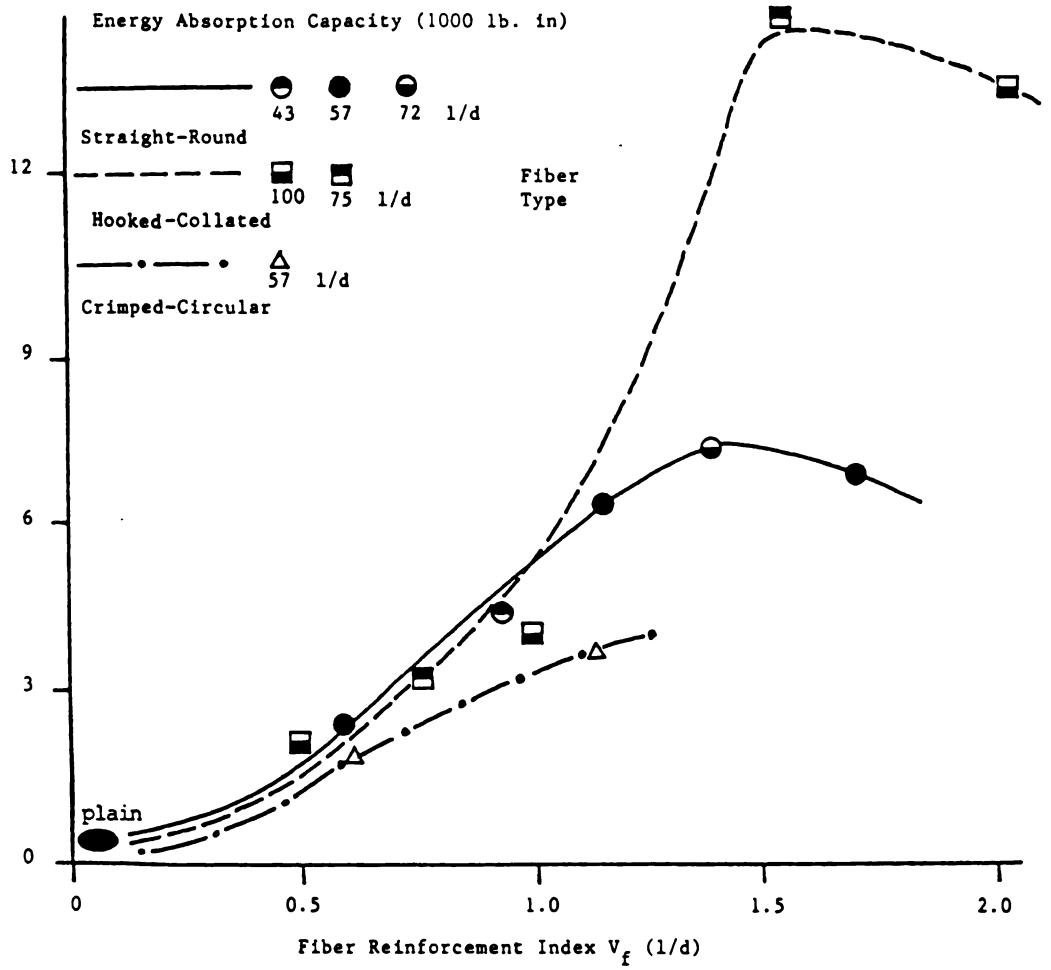

c. Energy absorption capacity

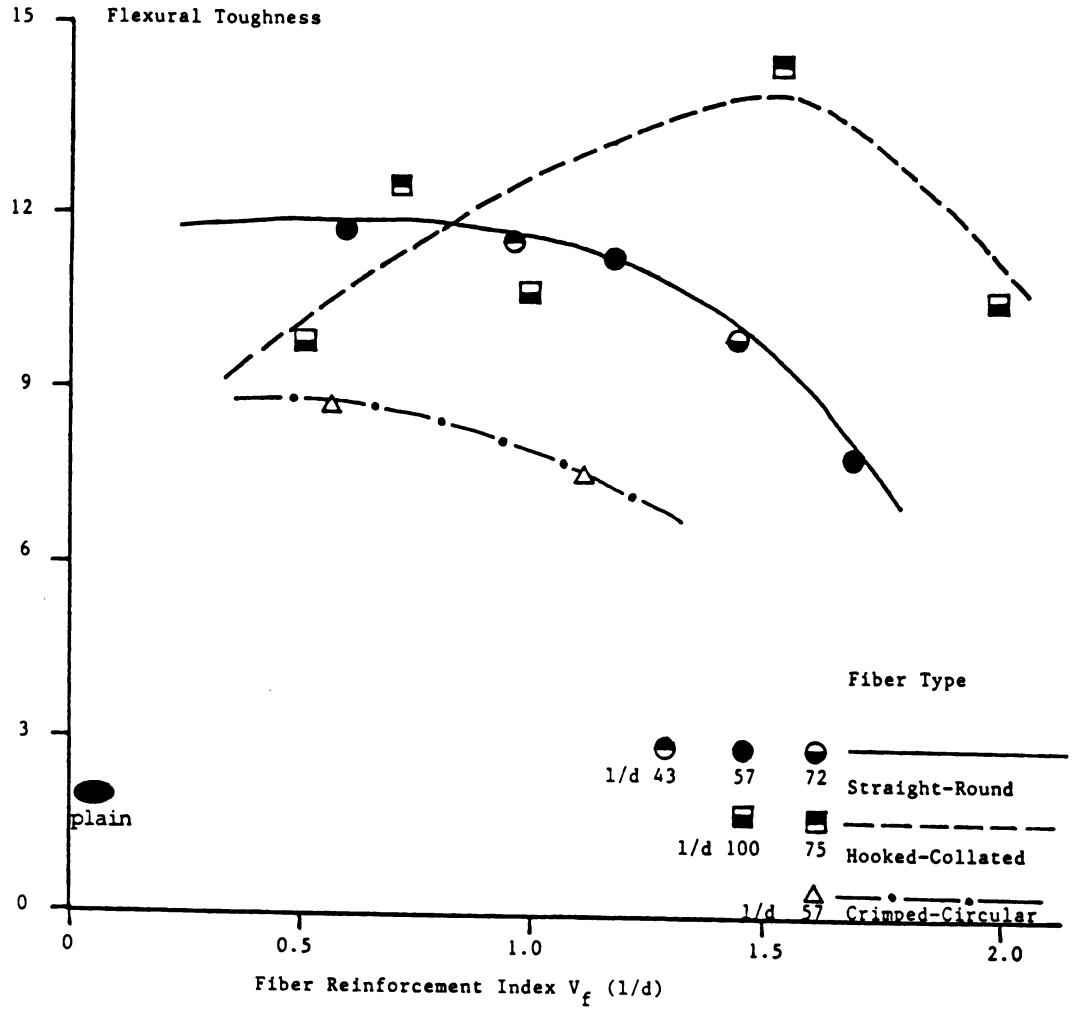

d. Toughness index

toughness index values comparable to that corresponding to an elastic-perfecly plastic behavior,[27] which is indicative of the desirable ductility of the material.

2.4.c Compressive Behavior: Figures 2.34.a, b and c show the compressive stress-strain relationships for straight, crimped and hooked fibers, respectively. The trends observed in different aspects of the compressive performance of steel fiber reinforced concrete at different fiber reinforcement indices and for different fiber types are preseted in Figures 2.35.a through 2.35.d. These figures present the compressive strength, strain at peak stress, energy absorbtion capacity and toughness of the material. Compressive energy absorbtion capacity is defined as the area underneath the stress-strain curves up to a maximum strain of 5.5 times that at peak stress. Compressive toughness was defined as the ratio of energy absorbtion capacity to the pre-peak energy absorption (area underneath the compressive stress-strain curve up to the peak load).

From Figure 2.35.a it may be concluded that steel fiber reinforcement only slightly increases the compressive strength of concrete. This also seems to apply to strain at peak stress (Figure 2.35.b), expect that mixes with least workability (hooked fibers at a fiber reinforcement index of 200), possibly due to the excessive void content resulting from compaction problems, seem to have relatively low stiffnesses and relatively high strains at peak stress. Steel fiber reinforcement effects on compressive energy absorption (Figure 2.35.c) seem to be more pronounced than the corresponding effects on compressive strength.

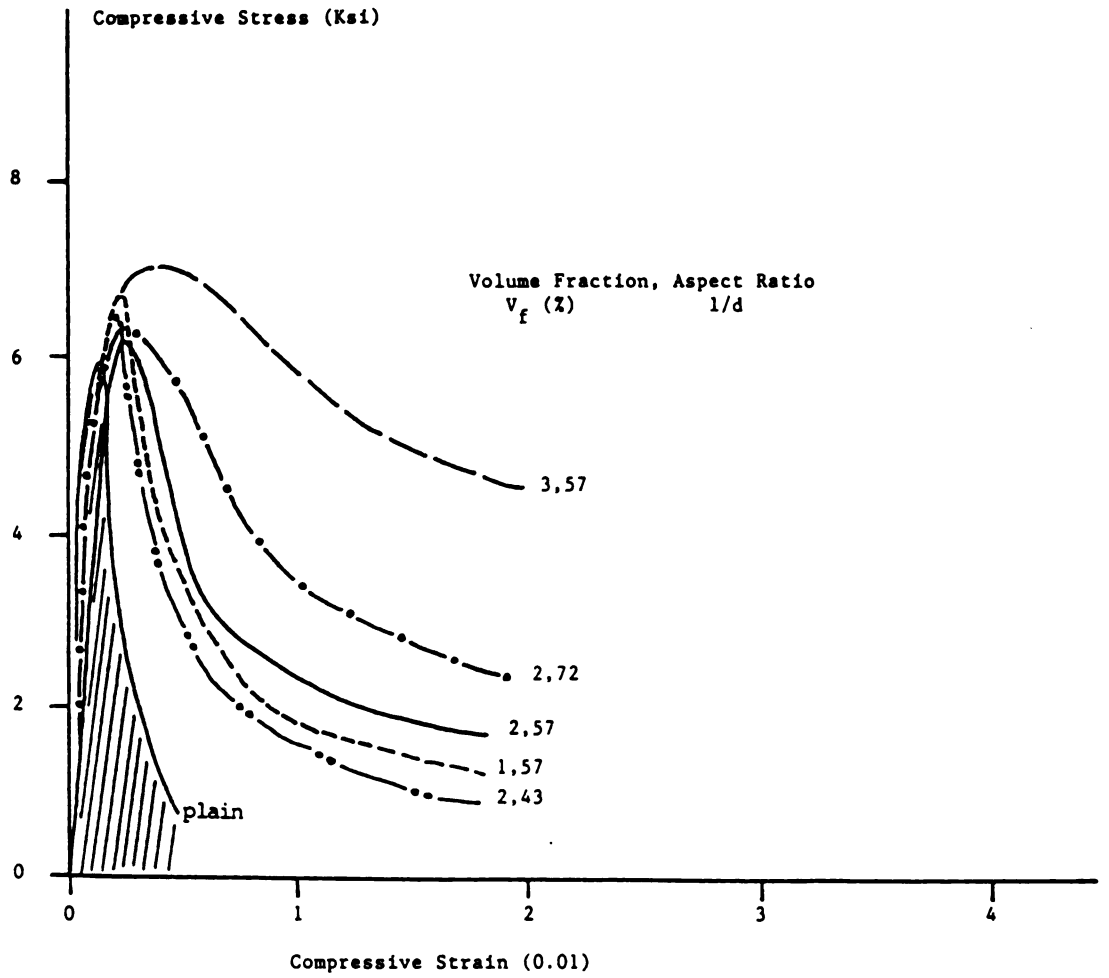

a. Straight fibers

Figure 2.34: Compressive stress-strain relationships of steel fiber reinforced concrete. 1 in = 25.4 mm, 1 Ksi = 6.9 N/mm^2

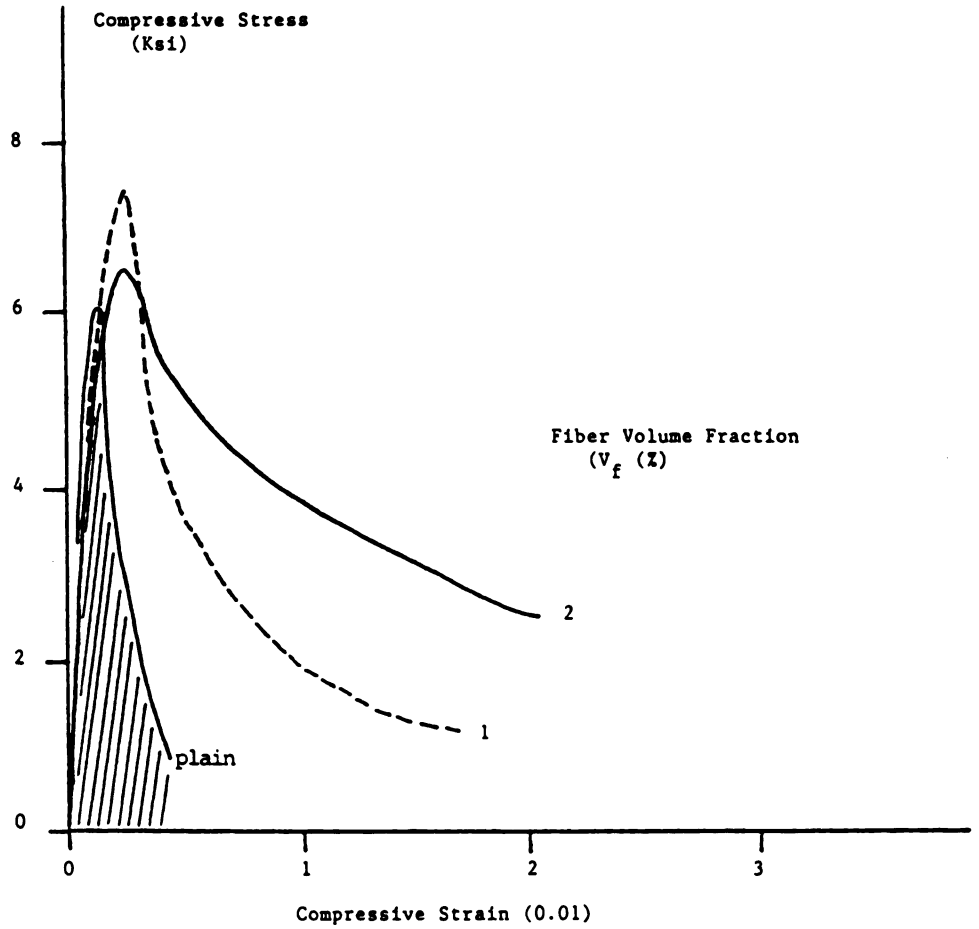

b. Crimped fibers

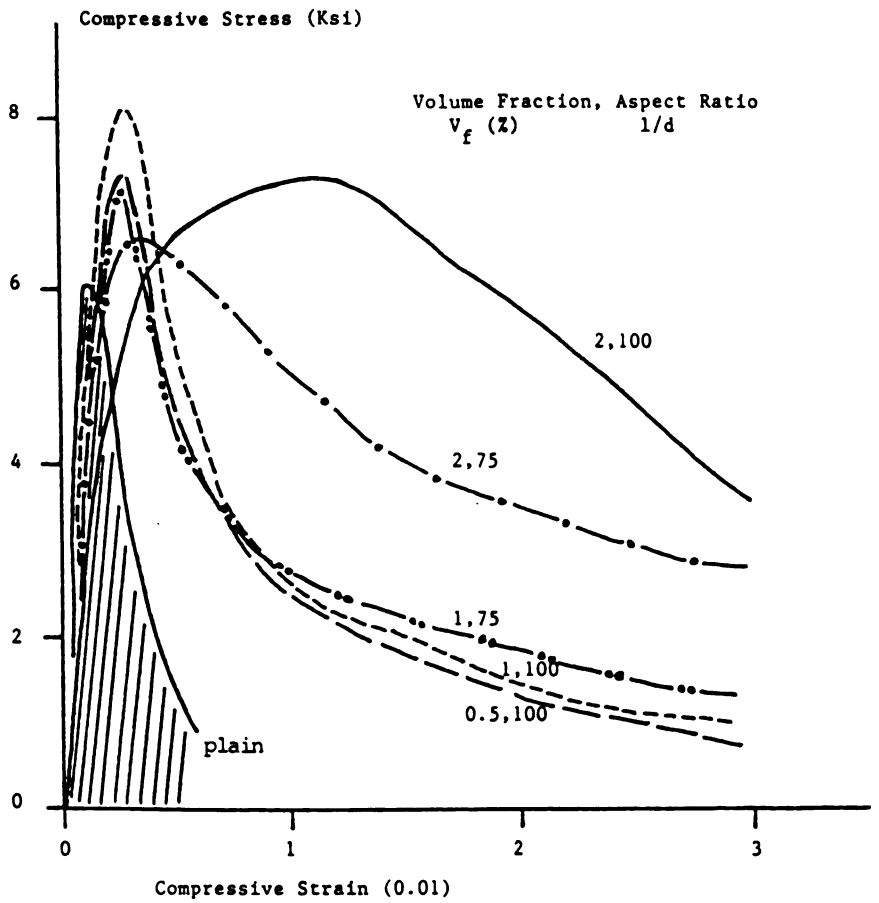

c. Hooked fibers

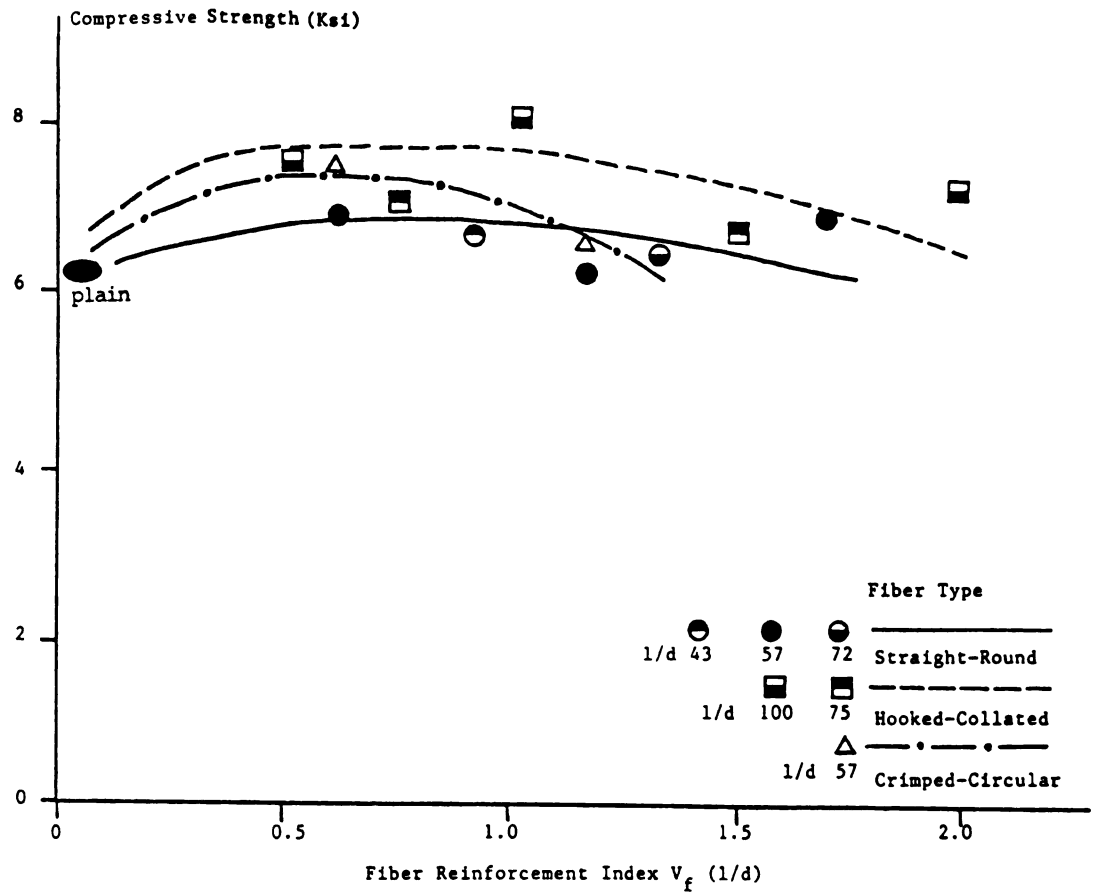

a. Strength

Figure 2.35: Effects of fiber reinforcement index and fiber type on different aspects of the compresive behavior of steel fiber reinforced concrete.

1 in = 25.4 mm, 1 Ksi = 6.9 N/mm^2, 1 lb. in = 115 N.mm

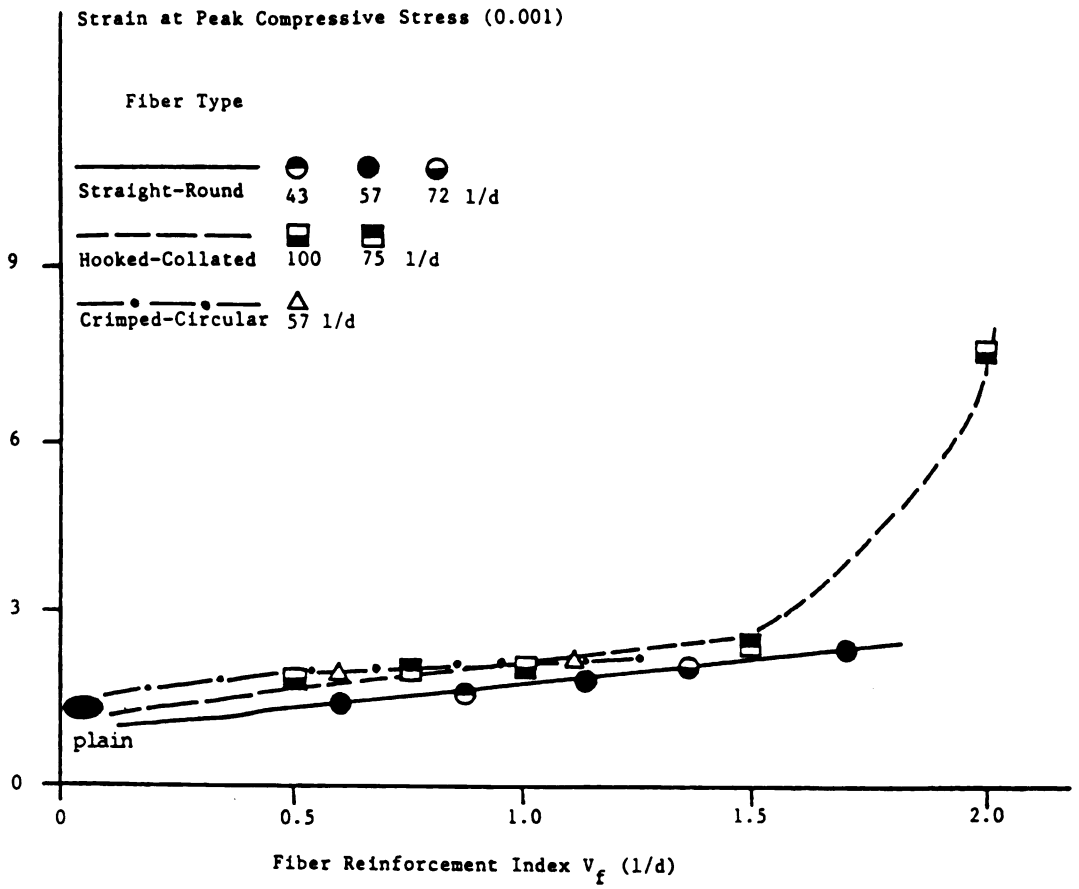

b. Strain at peak stress

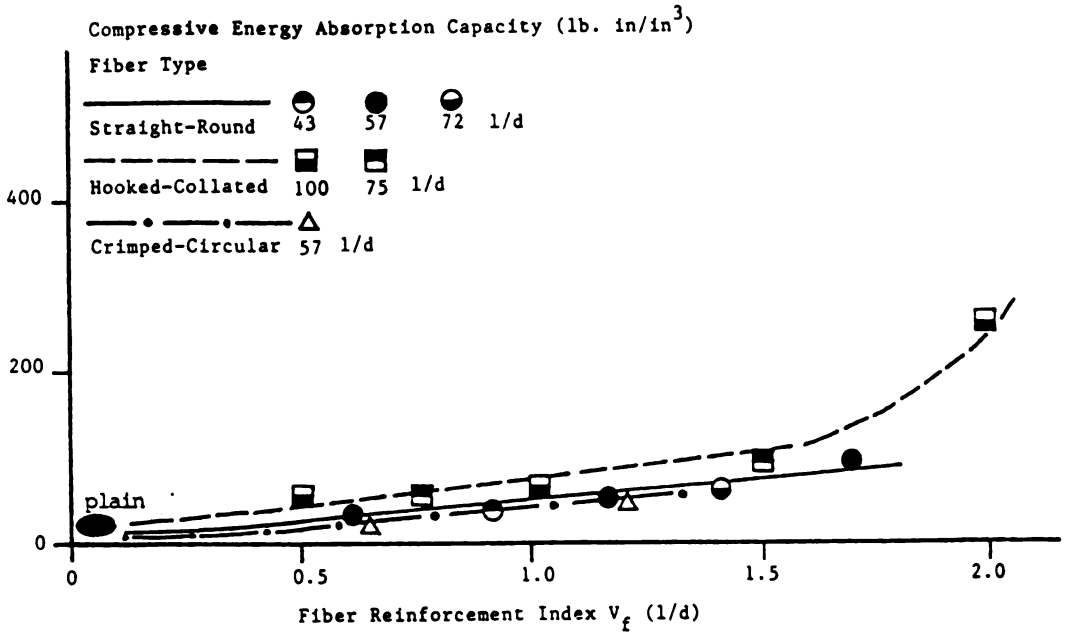

c. Energy absorption capacity

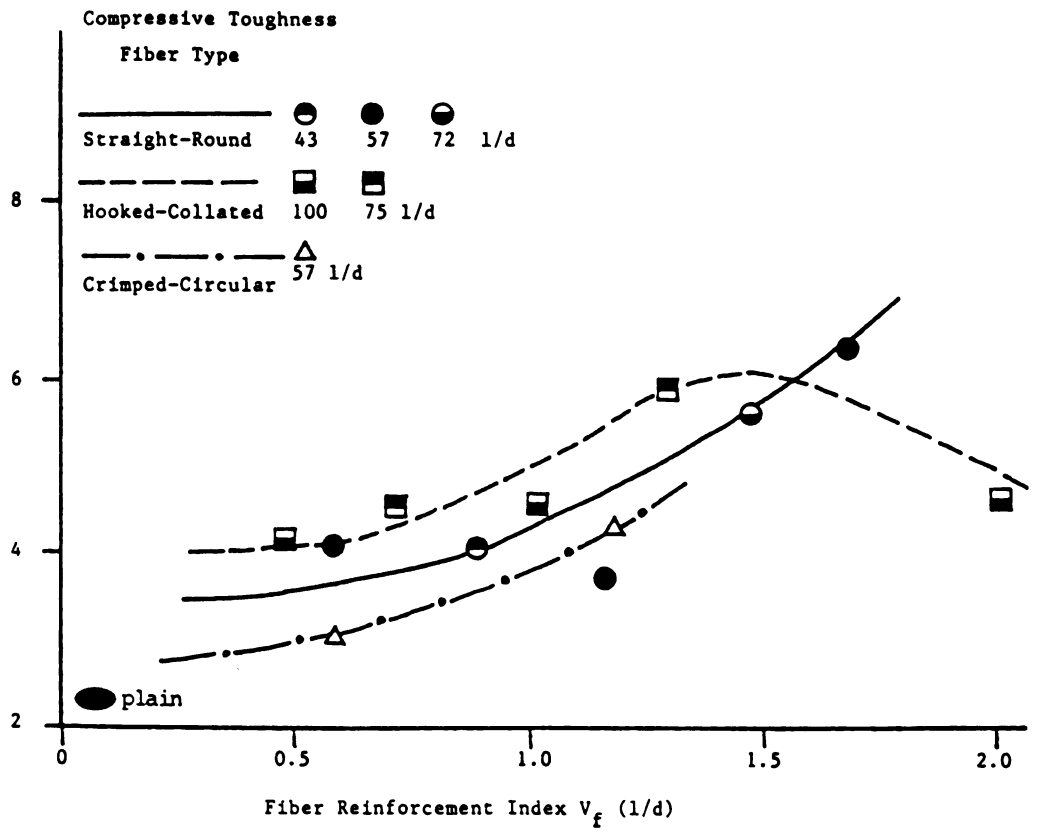

d. Toughness index

Different fiber types, especially the hooked ones at higher fiber reinforcement indices, provide concretes with higher compressive energy absorption characteristics, possibly due to the lower pre-peak stiffness which provides the material with higher pre-peak pre-peak energy absorption and higher strains at peak compressive stress. As shown in Figure 2.35.d, compressive toughness of steel fiber reinforced concrete also increases with fiber reinforcement index, but the damage to workability seems to reduce toughness index of the material at higher fiber reinforcement indices. This confirms that unworkable mixes, due to their lower initial stiffness, have higher pre-peak energy absorption capacities.

2.5 Summary and Conclusions

An experimental program was performed on the effects of the length, diameter, volume fraction and types of steel fibers on material properties of steel fiber reinforced concrete in the fresh and hardened states. The fiber types considered were straight, crimped and hooked, with lengths ranging from 1.5 to 2.5 in (38 to 63 mm), diameters from 0.02 to 0.035 in (0.3 to 0.8 mm) resulting in aspect ratios from 43 to 100, and volume fraction from 0.5 to 3%. The mix proportions had a water-binder ratio pf 0.4, a fly ash-binder ratio of 0.3 (which was decided in other phases of the project to be the optimum fly ash content in steel fiber reinforced concrete), an aggregate-binder ratio 4.0, a coarse-to-fine aggregate ratio of 1.0, a maximum aggregate size of 3/4 in (19 mm), and a superplasticizer (liquid)-binder ratio of 0.015 by weight. The fresh mix was characterized by its slump, inverted slump cone time and subjective workability.

The hardened material, following 7 days of moist curing and 21 days of air drying, was tested in compression and flexure. The following conclusions could be derived from the test data generated in this investigation:

1. The fresh mix workability tends to be damaged by the increase in fiber reinforcement index (fiber volume fraction times fiber aspect ratio), at a rate which is comparable for different fiber types.

2. At a specific fiber reinforcement index, crimped fibers produce concretes with slightly high slumps, while straight fibers generate mixtures with slightly lower inverted slump cone times. Hooked fibers produce slumps coparable with straight fibers, but give inverted slump cone times which are slightly higher than those of straight and crimped fibers.

3. The first crack and ultimate flexural loads, and the flexural energy absorption capacities (pre- and post-peak), of steel fiber reinforced concrete increase with increasing fiber reinforcement index up to a value of about 1.5 and then starts to decrease for higher fiber reinforcement indices due to the fresh mix workability problems.

4. Hooked fibers, especially at higher fiber reinforcement indices, give flexural strengths superior to those obtained with straight and crimped fibers.

5. Steel fiber reinforcement has relatively small effects on the compressive strength of concrete. The effects of steel fibers on energy absorption capacity, however, seem to be more pronounced.

6. High fiber reinforcement indices, due to their damage to the compactibility of fresh mixtures which leads to high entrapped air contents, tend to reduce the pre-peak stiffness of steel fiber reinforced concrete and increase the strain at peak compressive stress.

CHAPTER 3

Evaluation of Steel Fiber Types

3.1 General

Major efforts have been made in the recent years to optimize the shape of steel fibers for achieving improved fiber-matrix bond characteristics, and for enhancing fiber dispersability in the concrete matrix. The steel fibers used today are no more the straight round wires which were simply cut from normal drawn wires.

Steel fibers are now available in many deformed shapes which are claimed to produce better mechanical bonding to concrete matrices than straight round wires (see Figures 3.1.a).[3,5,8,20,40-46]

Wires with a circular cross-section are produced by normal wire drawing techniques which can be relatively expensive. The production method utilizing slit sheet results in rectangular section fibers which may be produced at relatively low costs when supplies of scrap metal sheets are readily available.[5] Another cost effective fiber production technique is the melt extract process. Melt extract fibers differ from drawn wire fibers due to their kidney shaped cross-section. The fiber contour is also irregular resulting in an improved mechanical bond to concrete matrices. The rapid solidification of the fibers also causes a rough texture which improves the adhesion and frictional bond. The melt extract

technique can be applied to chromium steel, stainless steel, as well as carbon steel.[5,43] Figure 3.1.b provides sketches of the round, rectangular and irregular cross-sectional shapes discussed above. It is worth mentioning that some fiber deformations might make them brittle, and some other deformations might produce local stress concentrations in the matrix and actually damage the behavior.[3,5,40] The fresh mix workability and fiber dispersability may also be negatively (or sometimes positively) influenced by fiber deformations.[19,20,44,46] Excessive bond strength resulting from fiber deformations may also lead to fiber rupture (rather than fiber pull-out) dominating failure of the composite material. This could damage some aspects of the material behavior. All these factors sould be considered in selecting an optimum fiber shape for specific applications.[3,5]

Balling of fibers in the fresh mix and reduction of workability in the presence of fibers, especially at higher fiber volume fractions, may complicate the efforts for taking full advantage of fibers in concrete. In an attempt to overcome the fresh mix problems, an approach involving the use of a water-soluble adhesive to glue fibers together in bundles has been developed.[8,21] The idea is to improve workability and eliminate fiber balling by first dispersing the fiber bundles, and then (as the adhesive disolves) dispersing the individual fibers with the mixing action.[8] Figure 3.1.c shows a bundle of hooked fibers glued together with a water soluble adhesive. It should be noted that in addition to mechanically deforming steel fibers, various chemical and physical treatments have also been tried to improve the wire surface bonding to cementitious paste.[4,5] These attempts have led to some

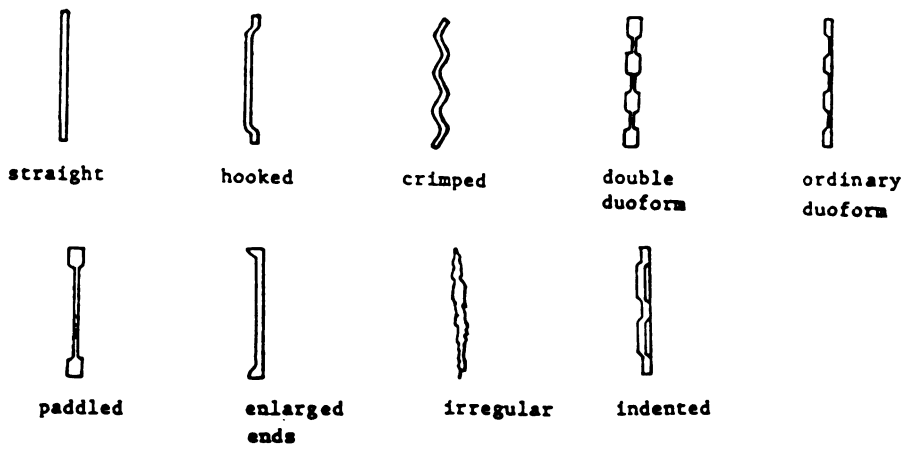

a. Steel fiber shapes

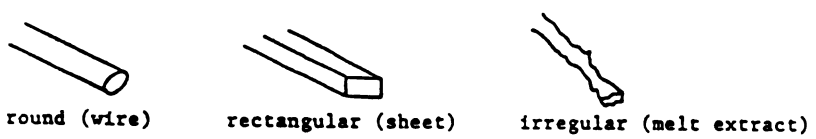

b. Steel fiber cross-sections

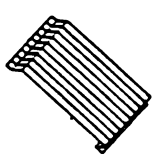

c. Fibers glued together into a bundle

Figure 3.1: Different steel fiber types.

improvements in the pull-out strength of single fibers, but the improvements in the overall performance of fiber reinforced concrete has been much less pronounced.

Measured values of tensile strength for individual fibers have been varied from 40 Ksi (176 MPa) to 350 Ksi (2413 MPa)[1,4,5,40,47] with the lower tensile strength usually belonging to the badly deformed fibers. Steel fibers usually range in length from 0.5 in to 3 in (13mm to 76mm), and in diameter from 0.005 in to 0.04 in (0.13mm to 1 mm).

In the selection of a fiber type for a specific job, due consideration should be given not only to the performance advantages resulting from certain fiber deformations, but also to the possible increase in cost of fibers at a specific job site resulting from the applied deformations. The exact details of cost increase would strongly depend on geographic locations, and they should be justified by the performance improvements which are of interest.

3.2 Background: Fiber Type Effects on Fresh Mix Properties

A fresh fibrous mix may be characterized by its workability and fiber dispersability. Both of these aspects of fresh mix performance are influenced by fiber volume fraction, geometry and type.

Workability is actually a collective term representing some essential properties of

concrete in the plastic condition, including its flowability, compactibility, stability against segregation and finishability. The workability of fresh concrete determines whether satisfactory handling, placing, compaction and finishing of the material is possible in a given situation. The workability of conventional concrete is usually assessed by the simple practical slump test. In the case of fibrous concrete, however, slump is usually close to zero, while material may be compactable to a certain degree which depends on the fiber reinforcement properties.[1,4,5,8,19,21,47] Since the compaction of structural concretes is normally carried out by vibration, the Vebe consistometer and the inverted slump cone tests, [1,4,5,8,9,19,47] which use vibration to remold the fresh material, are more appropriate for assessing the fibrous concrete workability (compatibility) in situations which reasonably simulates the practical conditions. The Vebe and inverted slump cone tests actually provide measures of practical combination of the compactibiity and flowability of vibrated fresh mix.

A collection of long thin fibers with length to diameter ratio (aspect ratio) greater than 100 tends to interlock under shaking and form a mat where it is difficult to dislodge fibers by vibration alone. Short stubby fibers with aspect ratios less than 50, on the other hand, are not able to interlock and it is possible to disperse them by vibration.[5] These effects can also be observed when the fibers are dispersed in mortar or in concrete. The presence of fibers reduces the overall workability of fresh mix and this effect is more pronounced in situations with higher fiber volume fractions, and/or higher fiber aspect ratios. For each aspect ratio, there is

usually a maximum volume fraction of fibers beyond which the workability of fresh mix is unsatisfactory for a specific job.[5] Due to the reduced workability resulting from the presence of fibers, the amount of air left entrapped after compaction is often increased. This fact adversely influences the strength of fiber concrete.[1]

There are only limited test data reported in the literature regarding the effects of steel fiber type on the fresh mix workability. Reference 8 has compared the Vebe and inverted slump cone times, and the slumps of fibrous concretes with straight and hooked-end (glued together into bundles)fibers. The limited test data do not show any consistent difference between the workability of fibrous mixes incorporating straight and hooked end fibers at comparable fiber reinforcement, indexes (V_f l/d). Reference 20 has performed Vebe tests on fibrous mixes incorporating duoform and straight steel fibers. Figure 3.2 presents the measured Vebe times in terms of V_f $(l/d)^2$ for straight and duoform fibers. The test data presented in this figure are very limited and it is hard to see any consistent effects of fiber type (duoform vs. straight).

Reference 19 has reported the results of slump and Vebe tests on straight-round, duoform, crimped and hooked steel fibers of different lengths and diameters at a constant fiber volume fraction of 1.5%. The slumps and Vebe times of Reference 19 are shown in Figures 3.3.a and 3.3.b. These figures indicate that the

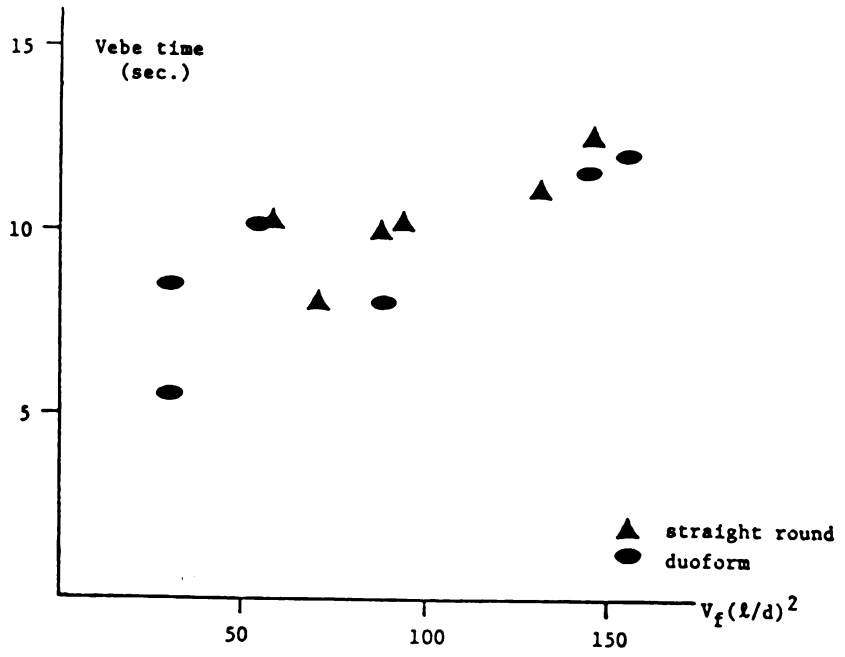

Figure 3.2: Vebe test results for fibrous concrete with duoform and straight fibers.[20] (fiber volume fraction (V_f) = 1.5%, water-cement ratio = 0.49, aggregate-cement ratio = 4.0, fine-to-coarse aggregate ratio = 0.6 and maximum aggregate size = 3/8 in (10 mm))

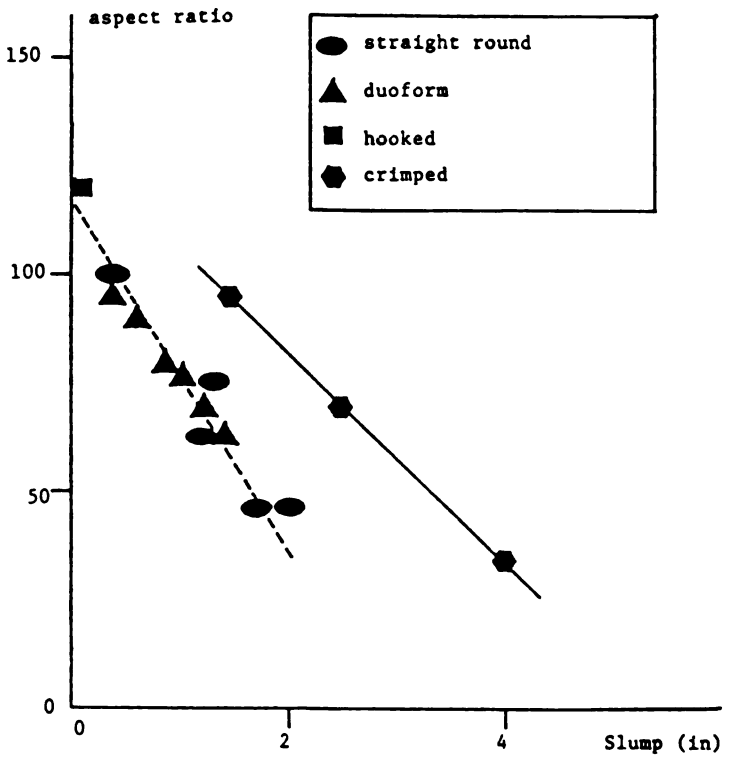

a. Slump. 1 in = 25.4 mm

Figure 3.3: Effect of fiber type on the slump and Vebe time of steel fiber reinforced concrete.[19] (V_f = 1.5%, water-cement ratio = 0.49, aggregate-cement ratio = 4.0, fine-to-coarse aggregate ratio = 0.6 and maximum aggregate size = 3/8 in (10 mm)).

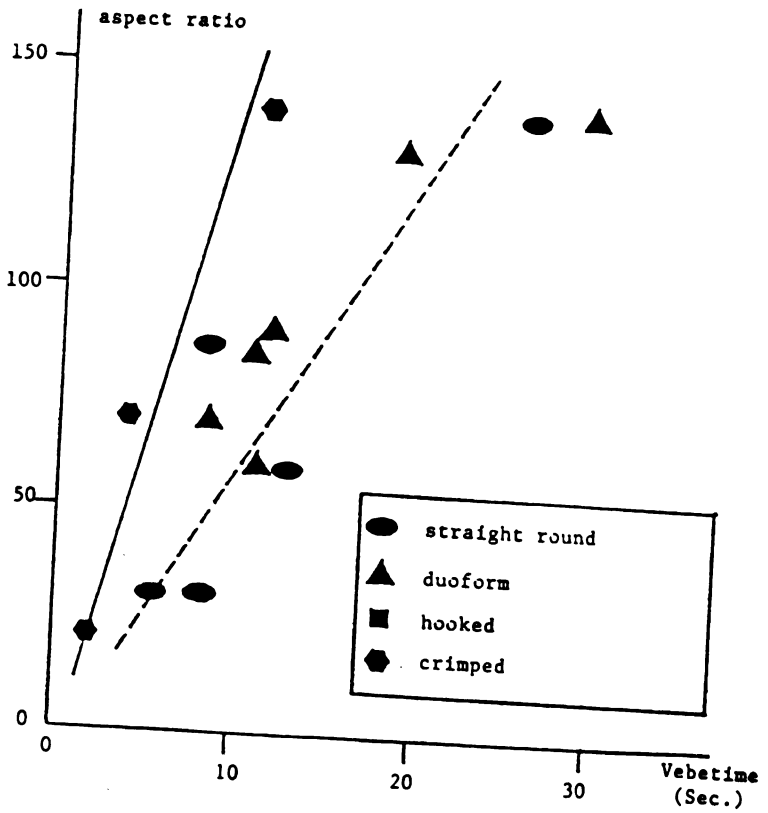
aspect ratio
150
100
50
0
0
10
20
30
Vebetime
(Sec.)
straight round
duoform
hooked
crimped

b. Vebe time

straight-round, duoform and hooked fibers show similar workabilities at comparable fiber aspect ratios and volume fractions. The crimped fibers, however, generally show better workabilities (higher slumps and lower Vebe times).

A tendency toward balling and non-uniform dispersion of fibers is a serious problem in fiber reinforced concrete. Balling during mixing is usually more pronounced when fiber volume fraction and/or fiber aspect ratio increase.[1,4,5,8,9,16,19,21,47] Not much information is available on the effect of fiber type on dispersability (which is a difficult property to measure and is usually assessed subjectively). There is, however, some information available on the effect of bundling the fibers together with a water soluble glue on the dispersability of fibers in concrete mixtures.[4,8,16,21] When such collated fibers are introduced in concrete, they present a fictitiously low aspect ratio, which is the relationship between the length and the fictitious diameter of the fiber bundle. This diameter is obtained considering that the measured perimeter of the bundle corresponds to a circular section.[21] At this fictitious aspect ratio, the bundles disperse rather conveniently inside concrete. The mixing process produces progressive separation of fibers and thus increases their aspect ratio. However, since the bundles are already dispersed, the dispersion of single fibers can also be achieved rather conveniently. Due to their relatively high dispersability, the collated steel fibers do not require special mixing procedure and they can be simply dumped into the mixed concrete matrix and dispersed by

continuation of mixing.[4,5,8,16]

3.3 Background: Fiber Type Effects on the Hardened Material Performance

Experimental data related to the effects of fiber type on the behavior of steel fiber reinforced concrete under direct tension, flexure and compression loading are discussed in this section.

3.3.a Direct Tension: The behavior of steel fiber reinforced concrete under direct tension can provide important information on the mechanism of action of steel fibers in concrete. References 33, 36 and 42 have experimentally investigated the effect of steel fiber deformation on the ultimate strength and stress-strain relationship of steel fiber reinforced concrete under direct tensile loads. Reference 33 has been concerned mainly with the pre-peak behavior of concretes reinforced with straight circular (0.010 in = 0.25 mm and 0.016 in = 0.41 mm diameter), rectangular (0.016 x 0.020 in = 0.25 x 0.50 mm corss-section) and duoform (0.016 in = 0.41mm diameter) steel fibers. The matrix in this investigation was mortar with type I cement. Water-cement ratio was 0.60 and sand-cement ratio was 3.0. No consistent difference could be found in the tensile strength and strain at peak stress of the four fiber types used in this study (see Figure 3.4). Of particular interest is the fact that the duoform fibers, inspite of the higher individual fiber pull-out resistance, are not more effective than comparable circular and rectangular fibers in increasing the direct tensile

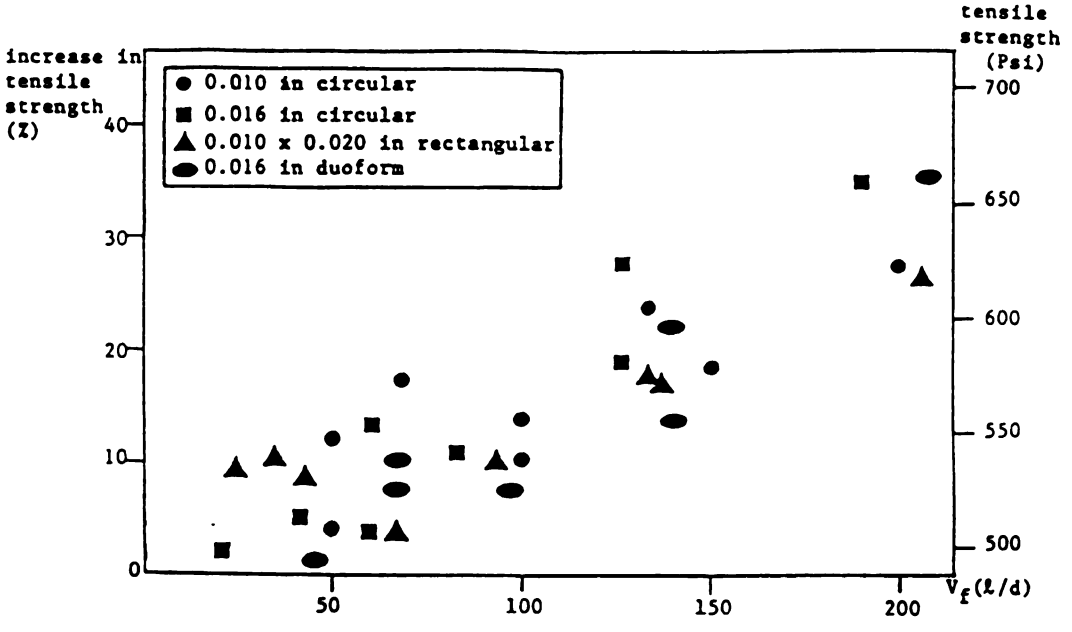

a. Tensile strength

Figure 3.4: Increase in direct tensile strength and strain at peak stress of mortar resulting from reinforcment with different steel fiber types.[33] (water-cement ratio = 0.50, sand-cement ratio = 3.0, prismatic specimen length = 30 in (762 mm) and cross-section = 4 x 4 in (102 x 102 mm)) 1 in = 25.4 mm, 1 Ksi = 6.9 MPa.

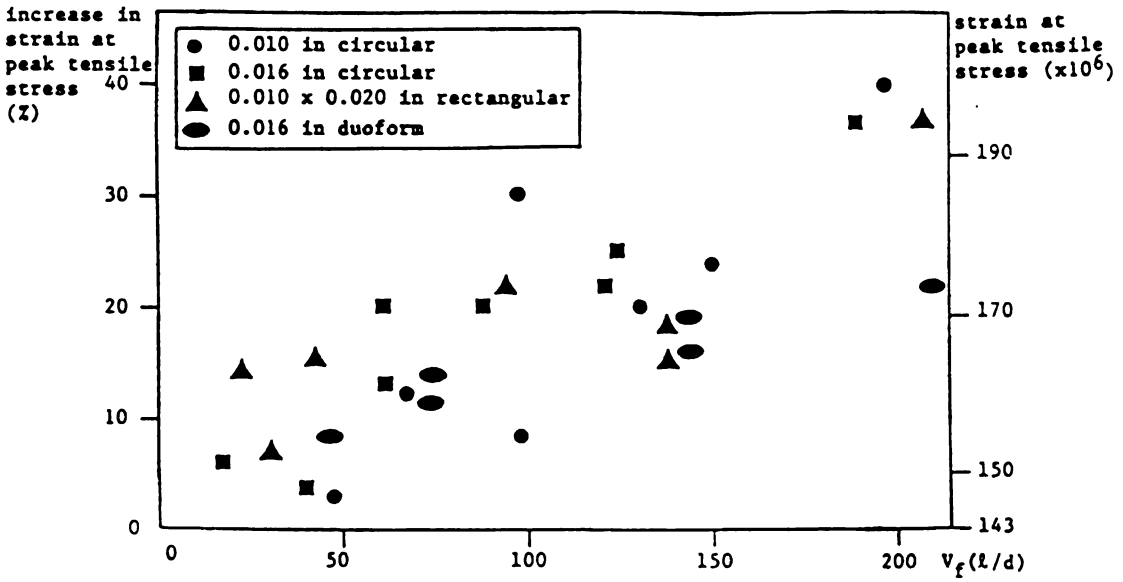

b. Strain at peak tensile stress

strength of concrete.

Reference 36 also has investigated the effects of fiber type on the direct tensile strength of a concrete mixture reinforced with round-straight, duoform, crimped and hooked fibers of different diameters and lengths. The concrete matrix contained portland cement type I, and had a water-cement ratio of 0.49, aggregate-cement ratio of 4.0, and fine aggregate-to-coarse aggregate ratio of 0.6. The coarse aggregate was crushed gravel with a maximum size of 3/8 in (10 mm). Figure 3.5 shows the percentage increase in ultimate strength as a function of fiber reinforcement index (V_f l/d). Here, also, the type of fiber is observed to have no consistent effect on the direct tensile strength of steel fiber reinforced concrete.

An experimental study on the effect of fiber type on the complete stress-strain behavior under direct tension has been reported in Reference 42. Straight-round fibers 1 in (25mm) long x 0.015 in (0.38mm) diameter, hooked fibers 1.2 in (30mm) long x 0.016 in (0.40mm) diameter and paddeled fibers 2 in (50mm) long x 0.030 in (0.75mm) diameter were used in this investigation. The matrix was mortar with a water-cement ratio of 2.5. The complete stress-strain relationships of mortars reinforced with the three fiber types are show in Figure 3.6. In the comparison of the stress-strain relationships of Figure 3.6, it should be considered that the different fiber shapes have different aspect ratios. From the results presented in Figure 3.6, it may be concluded that there is only a slight

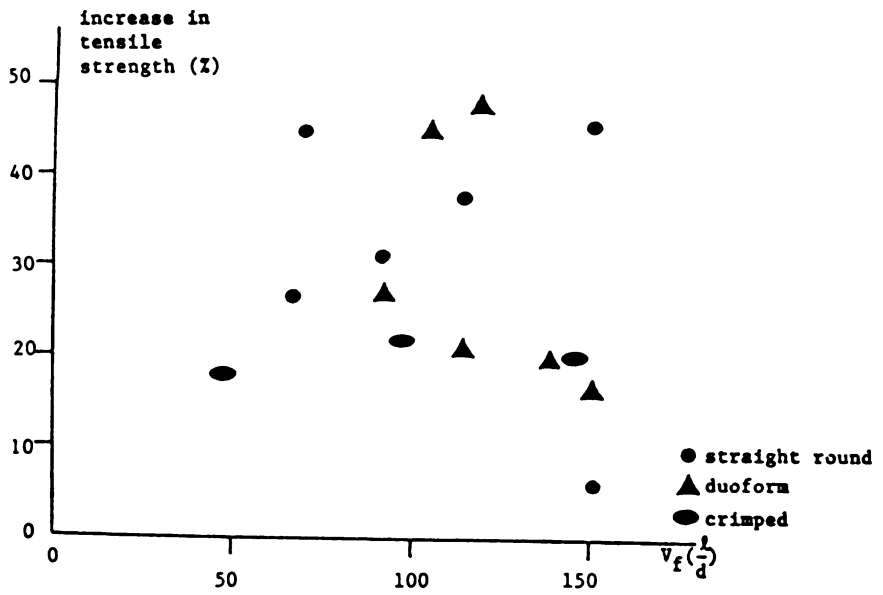

Figure 3.5: Increase in tensile strength of concrete resulting from reinforcement with different steel fiber types.[36] (V_f = 1.5%, water-cement ratio = 0.49, aggregate-cement ratio = 4.0, fine-to-coarse aggregate ratio = 0.6, maximum aggregate size = 3/8 in (10 mm), cylindrical specimen length = 14 in (356 mm) and specimen diameter = 3.12 in (80 mm))

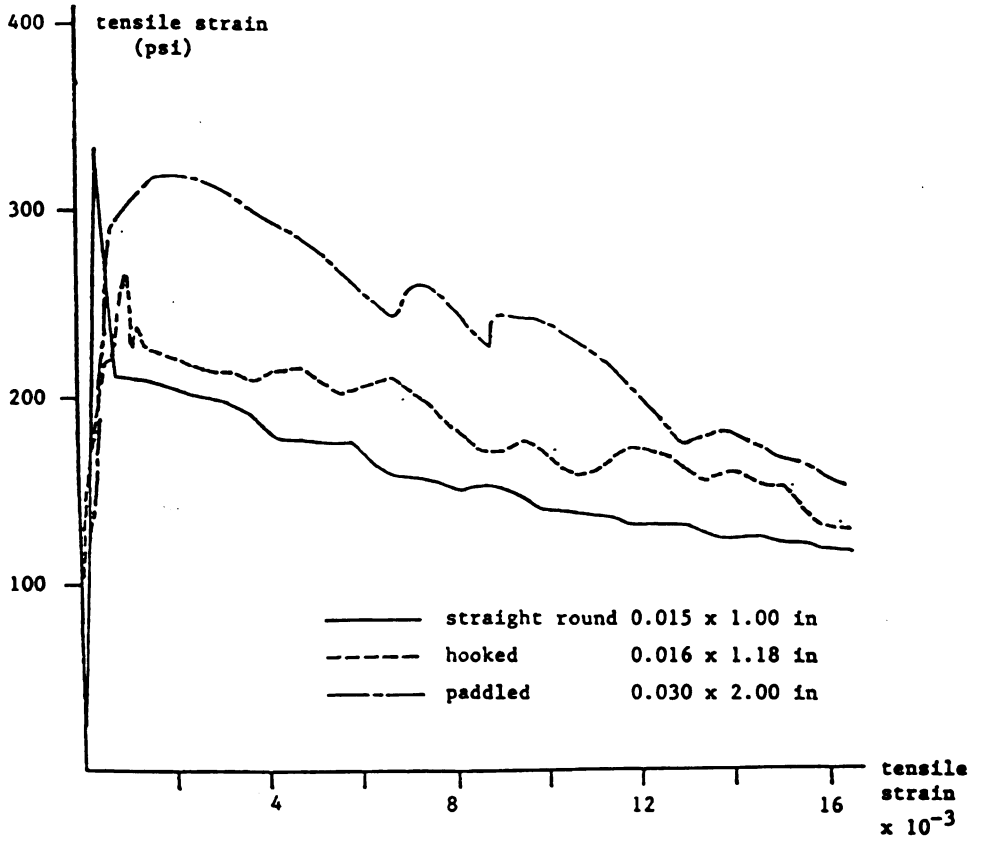

Figure 3.6: Complete direct tensile stress strain relationships of concretes reinforced with different steel fiber types.[42] (V_f = 1.7%, water-cement ratio = 0.45, sand-cement ratio = 2.5, presmatic specimen length = 39.4 in (1000 mm) and specimen cross-section = 7.8 x 2 in (200 x 50 mm)). 1 in = 25.4 mm, 1 Ksi = 6.9 MPa

difference between the overall stress-strain relationship of straight, hooked and paddeled steel fibers. Reference 42 suggests that the observed differences in the direct tensile behavior of steel fiber reinforced concrete are much less than the corresponding differences in the individual fiber pull-out behavior resulting from the use of different steel fiber types.

3.3.b Flexural Behavior: Reference 3 has reported flexural test data on concrete reinforced with straight-round, duoform, hooked and crimped steel fibers. The concrete had a water-cement ratio of 0.49, aggregate-cement ratio of 4.0, fine-to-coarse aggregate ratio of 0.6 and a maximum aggregate size of 3/8 in (10mm). Ordinary portland cement was used and tests were performed on 4 in x 4 in x 20 in (102mm x 102mm x 508mm) beams under center point flexural loading over a span of 16 in (406mm). The specimens were moist cured until the age of 30 days. Figures 3.7.a and 3.7.b compare the flexural load-deflection relationships for concrete beams reinforced with 1.5% volume fraction of different fiber types, having aspect ratios of about 100 and 75, respectively. The results in Figure 3.7 indicate that the flexural strength and especially the post-peak ductility of steel fiber reinforced concrete is dependent on the fiber deformations. Duoform steel fibers seem to be the most efficient followed by hooked fibers. Crimped and straight fibers seem to be the least efficient among the fiber types considered in Figure 3.7. The effects of fiber deformations on flexural strength seem to be more pronounced in the case of fibers of higher aspect ratio. It is interesting to note that crimped fibers, in spite of their seemingly high

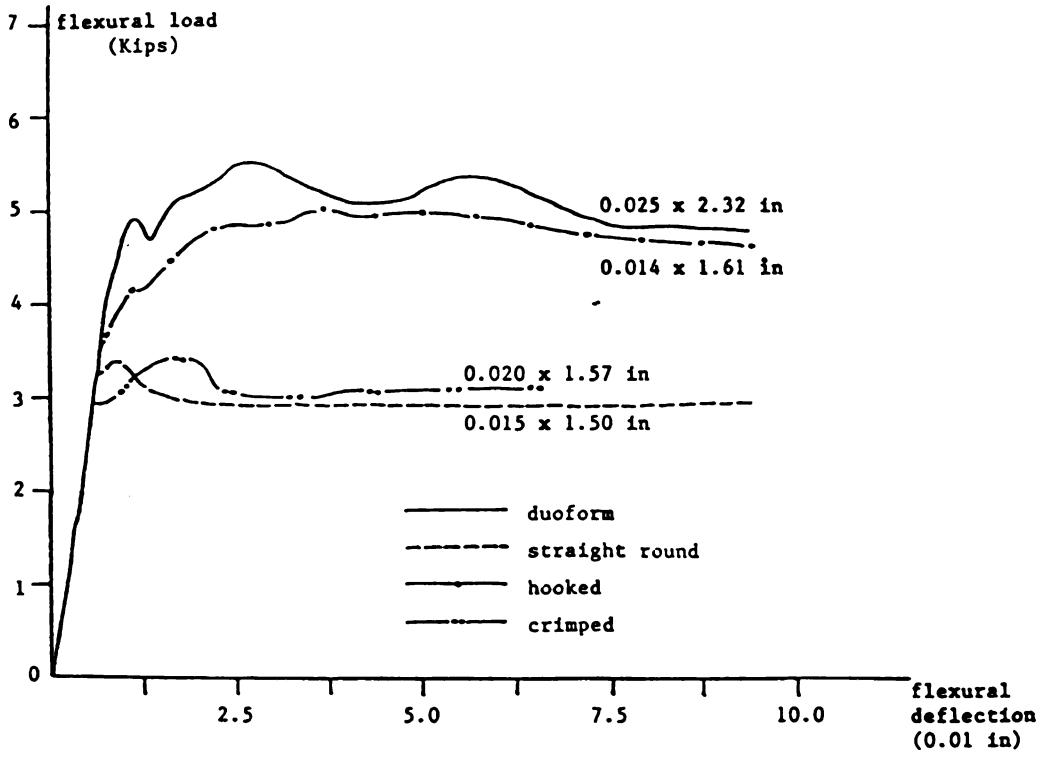

a. l/d = 93 - 107

Figure 3.7: Effects of steel fiber deformations on the felxural behavior of steel fiber reinforced concrete.[3] (V_f = 1.5%, water-cement ratio = 0.49 aggregate-cement ratio = 4.0, fine-to-coarse aggregate = 0.6, maximum aggregate ratio = 3/8 in (10 mm), centrally loaded beams of 4 x 4 x 30 in (102 x 102 x 508 mm) and span length = 16 in (406 mm)). 1 in = 25.4 mm, 1 Kip = 4.5 KN

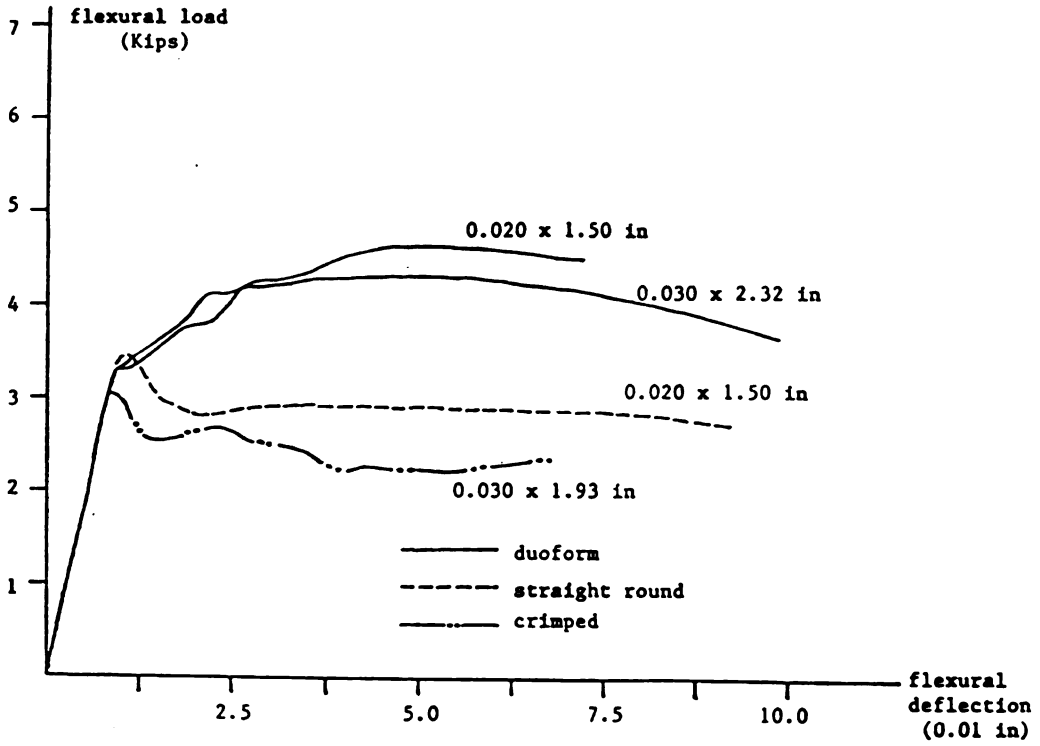
flexural load
(Kips)
7
6
5
4
3
2
1
0.020 x 1.50 in
0.030 x 2.32 in
0.020 x 1.50 in
0.030 x 1.93 in
duoform
straight round
crimped
2.5
5.0
7.5
10.0
flexural
deflection
(0.01 in)

b. l/d = 68 - 82

mechanical bonding capabilities, produce fiber reinforced concretes with relatively low strength and toughness. Reference 3 attributes this observation to the stress concentration generated around the closely spaced corrugations of crimped fibers. Reference 2 suggests that there is still considerable scope for further improvements in the shape of steel fibers.

Reference 8 reported a comparative study on the flexural behavior of hooked-collated and straight-rectangular steel fibers. The concrete matrix has a water-cement ratio of 0.43, aggregate-cement ratio of 4.16, coarse-to-fine aggregate ratio of 0.95 and a maximum aggregate size of 3/4 in (19mm). Air entraining and water-reducing agents were also used. The test specimens were 4 in x 4 in x 14 in(102mm x 102mm x 502mm). The hooked fibers had an aspect ratio of 100, while the equivalent aspect ratio of straight-rectangular fibers was 60. Figure 3.8 presents the flexural load-deformation relationships of the straight and hooked fibers, both at a fiber reinforcement index (V_f l/d) of about 60. Figure 3.8 indicates that the hooked fibers were far more efficient than the straight ones in improving the flexural toughness of concrete. The inefficiency of straight fibers in Figure 3.8 could partially be a result of their relatively short length. The flexural toughness of fibrous specimens reinforced with hooked fibers was on the average 2 to 3 times greater than those reinforced with straight fibers. Reference 8 reported that the failure modes in concretes incorporating straight fibers was strictly a bond failure, while the hooked fibers with higher mechanical

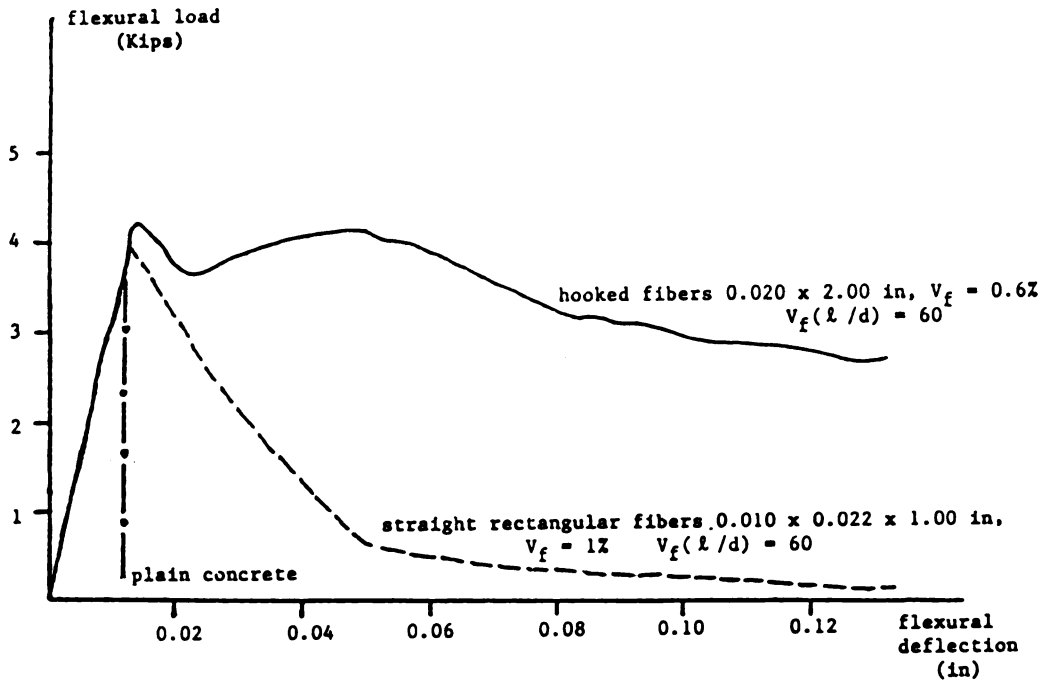

Figure 3.8: Flexural behavior of fibrous concrete reinforced with hooked and straight steel fibers.[8] (water-cement ratio = 0.43, aggregate-cement ratio = 4.16, fine-to-coarse aggregate ratio = 1.05, maximum aggregate size = 3/4 in (19 mm), and specimens were 4 x 4 x 14 in (102 x 102 x 355 mm) loaded at one-third point loading over a span of 12 in (305 mm)). 1 in = 25.4 mm, 1 Kip = 4.5 KN

bonding to the matrix, failed partially by fiber rupture. The variation in flexural strength of steel fiber reinforced concretes incorporating straight fibers was observed in the tests reported in Reference 8 to be smaller than those with hooked fibers. Figure 3.8 also indicates that the flexural toughness of steel fiber reinforced concrete is more sensitive to variations in fiber type than the flexural strength.

Figure 3.9 from Reference 1 summarizes the measured increases (due to fiber reinformcement) in flexural strength of steel fiber reinforced concretes with different steel fiber types reported in the literature. The steel fibers considered in this figure are straight-round, straight-rectangular and duoform. The fibers used had wide ranges of lengths and diameters. No consistent effects of fiber type of flexural strength can be observed in Figure 3.9.

Reference 43 has compared the effects of crimped, straight-round and straight-melt extract steel fibers on the flexural strength of sprayed fiber reinforced concrete. The melt exract fibers have a rough surface texture which is expected to increase the adhesive and frictional bond of fibers to concrete matrices. The limited data on flexural strength of different fiber types reported in Reference 43 does not give any conclusive results regarding the effect of fiber type on flexural strength. The straight-round fibers, however, are observed in Figure 3.10 to give higher strengths than the melt extract and crimped fibers.

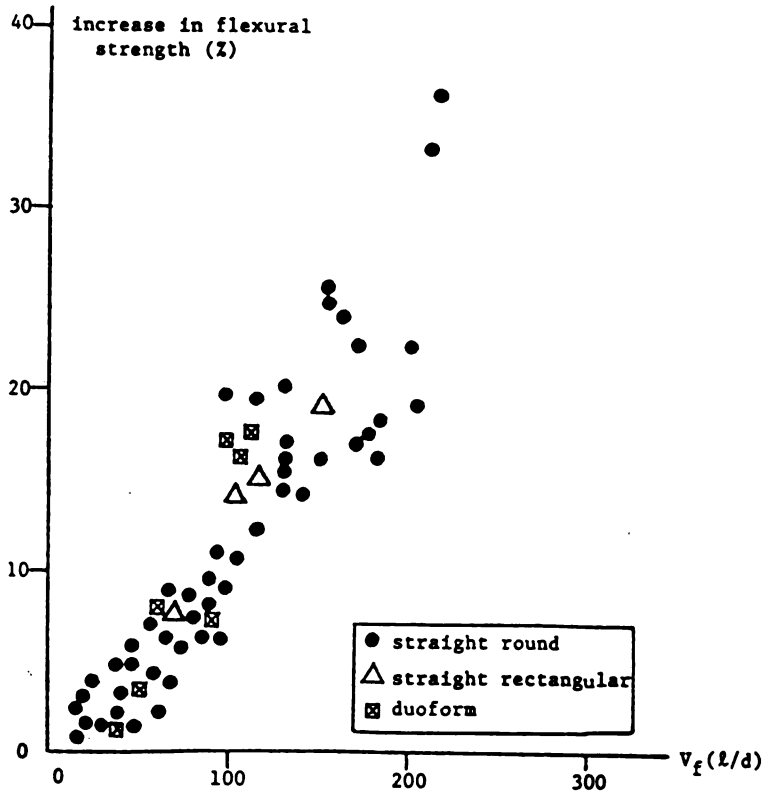

Figure 3.9: Percentage increase in flexural strength of mortars reinforced with different steel fiber types.[1]

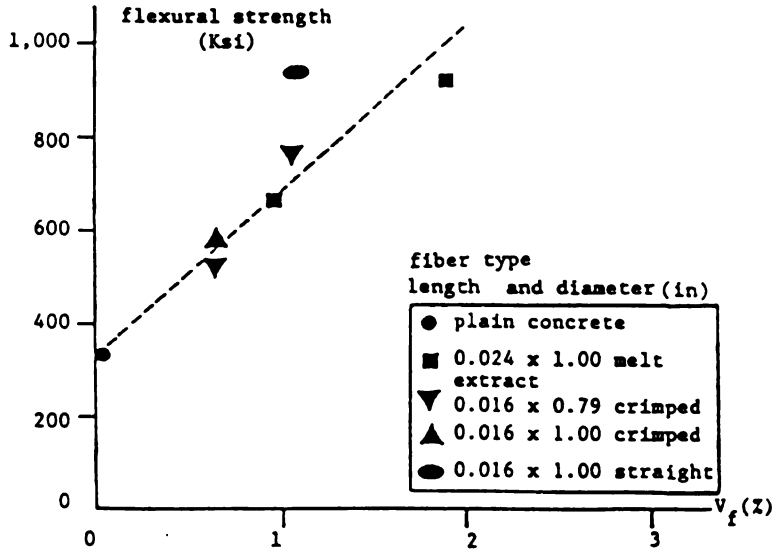

Figure 3.10: Effect of fiber type on flexural strength of steel fiber reinforced mortar.[43] (water-cement ratio = 0.40, sand-cement ratio = 3.0, speciment depth = 3.15 in (80 mm), span length = 12.60 in (360 mm), loading at one-third points and construction by shotcreting). 1 in = 25.4 mm, 1 Ksi = 6.9 MPa

The comparative study of post-crack flexural (tensile) strength of concretes and cement pastes reinforced with 1.5% volume fraction of straight-round, duoform, crimped and hooked steel fibers in Reference 46 (Table 3.1) is indicative of the effectiveness of duoform and hooked fibers and the low efficiency of straight-round and crimped fibers in increasing the flexural strength of concrete.

Table 3.1: Effect of fiber type on the flexural strength of steel fiber reinforced concrete and cement past. [46] (V_f = 1.5%, water cement ratio = 0.49 , aggregate-cement ratio = 4.0, fine-to-coarse aggregate ratio = 0.6, maximum aggregate size = 3/8 in (10 mm), specimen dimensions = 4 x 4 x 20 in (102 x 102 x 508 mm), span = 16 in (406 mm) centrally loaded and test age = 30 days). 1 in = 25.4 mm, 1 Ksi = 6.9 N/mm^2

Fiber diameter x Fiber length (in x in)		Post-Crack Flexural (Tensile) Strength (psi)	
		Concrete	Cement Paste
Round-straight	.020 x 1.50	365	--
Duoform	.025 x 2.36	534	389
Crimped	.021 x 1.96	338	264
Hooked	.014 x 1.65	525	333

An experimental study on the flexural behavior of concrete reinforced with hooked-collated steel fibers reported in Reference 21 has concluded that the flexural strength and toughness of hooked-collated steel fiber reinforced concrete

tend to increase with increasing mixing time (measured after dumping of fibers into the fresh mix), due to the progressive separation of the collated steel fibers by the mixing action of concrete. The overmixed concretes according to Reference 21 continue to have increments in flexural strength with mixing time, indicating no total separation of collated fibers within the regular mixing time.

Reference 23 has reported the results of an experimental investigtion on the flexural energy absorption capacity and toughness of steel fiber reinforced concrete using different fiber types. Test results of Reference 23 indicate that with the same fiber volume fraction and aspect ratio, hooked fibers were more effective than straight, crimped or paddeled rectangular fibers in increasing the flexural toughness and flexural energy absorption capacity of steel fiber reinforced concrete. Due to their relatively short length, duoform fibers used in this study were not as effective as hooked fibers in improving flexural performance. The improvements in flexural toughness and energy absorption capacity tend to be less affected by fiber types at lower volume fractions of steel fibers.

3.3.c Compressive Behavior: Steel fibers, through their confining action and crack arresting properties, improve the ultimate strength and especially the post-peak ductility and energy absorption capacity of concrete under compression. The pre-peak behavior of concrete, however, is not much influenced by the addition of steel fibers.[30] There is a drop in tangent stiffness near the peak and an

increase in strain at peak compressive stress of concrete resulting from steel fiber reinforcement. As the fiber volume fraction and aspect ratio increase, steel fibers tend to be more effective in enhancing the compressive behavior of concrete.

The efficiency of steel fibers in improving concrete behavior under compression can be increased by improving the fiber-matrix bond through deforming the steel fibers. Reference 30 presented test results which indicated that, at the same volume fraction and aspect ratio, hooked fibers were more effective than straight ones in enhancing the compressive behavior of steel fiber reinforced concrete (see Figure 3.11). Reference 8 has also reported test results which indicate that hooked fibers are slightly more effective than straight ones in increasing the compressive strength of concrete.

It is worth mentioning that no previous studies have compared steel fiber reinforced concrete with fibers of the same dimensions but different types. Such comparison can provide valuable information about the effects of fiber type on the behavior of steel fiber concrete.

3.4 Experimental Program

The objective of this phase of the experimental study was to compare the effects of different steel fiber types on fresh mix workability and hardened material flexural and compressive characteristics of concrete. The steel fiber types were straight-round, crimped-round, crimped-rectangular, hooked and

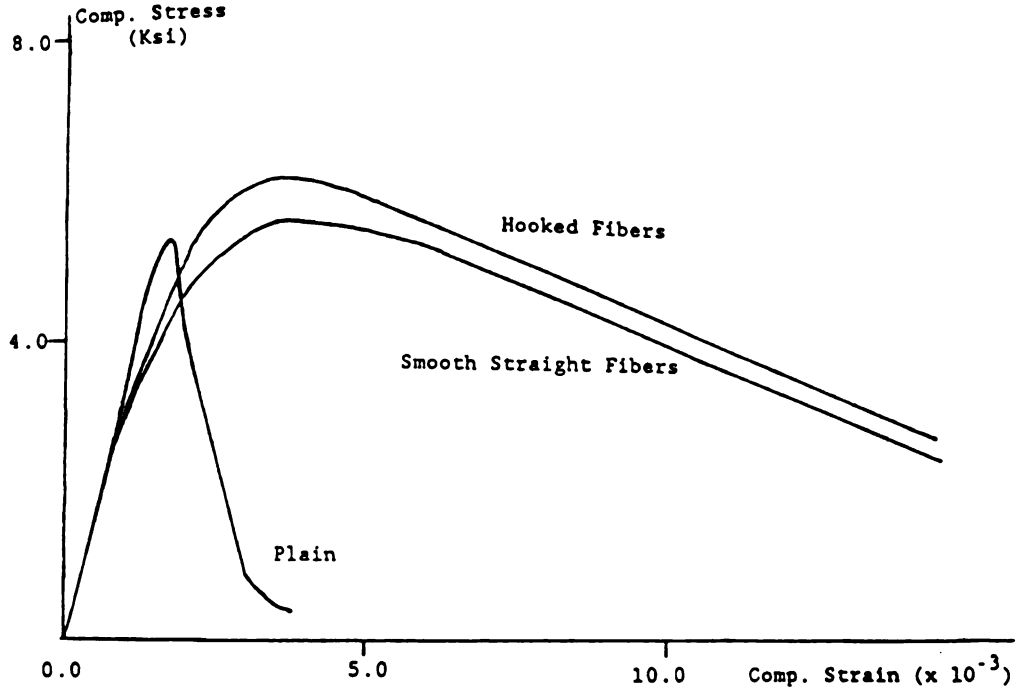

Figure 3.11: Typical compressive stress strain relatioships for concretes reinforced with straight and hooked steel fibers at comparable volume fractions and aspect ratios.[30] 1 Ksi = 6.9 MPa

hooked-collated. Table 3.2 presents the lengths and diameters of the fiber types used in this experimental study. The aspect ratios of different fibers were chosen to be within the two narrow ranges of 57 to 60 and 72 to 75. A constant volume fraction of fibers, 2%, was used throughout this investigation. The fiber reinforcement index (volume fraction x aspect ratio) was thus in the ranges of 114 to 120 and 144 to 150 for the fibrous mixes of this study. Hence, the key factor distinguishing between different fibrous mixes in each fiber reinforcement index group is the fiber type, noting that similar concrete matrices were used for all mixes.

Table 3.2: Geometries of different fiber types. 1 in = 25.4 mm

Fiber Type	Length (in)	Diameter (in)	Aspect Ratio (Length/Diameter)
Straight-round	2	.035	57
Crimped-round	2	.035	57
Crimped-rectangular	2	.035	57
Hooked-collated(ZP 30/50)	1.2	.02	60
Hooked-single(ZL30/50)	1.2	.02	60
Straight-round	2.5	.035	72
Hooked-collated(ZP 60/80)	2.36	.0315	75

The concrete matrices used in this phase of investigation all had a water-binder (cement + fly ash) ratio of 0.4, a fly ash-binder ratio of 0.3, a super placticizer-binder ratio of 0.015, an aggregate-binder ratio of 4.0 and a course-to-fine aggregate ratio of 1.0. The maximum aggregate size was 3/4 in

(19mm). The mixing, curing and testing procedures followed and the materials used were similar to those described in section 2.3 of Chapter 2.

3.5 Experimental Results

The test results and conclusions obtained in this investigation regarding the effects of fiber type on the performance characteristics of steel fiber reinforced concrete in the fresh and hardened states are described in the following sections.

3.5.a Fiber Type Effects on Fresh Mix Workability: The test data generated in this study on the effects of steel fiber type on fresh mix slump, inverted slump cone time and subjective workability are shown in Figures 3.12.a, 3.12.b, and 3.12.c, respectively. Figure 3.12.a indicates that fibrous concretes with crimped fibers have slightly higher slumps than comparable ones with straight or hooked fibers. As far as inverted slump cone (Figure 3.12.b) and subjective workability (Figure 3.12.c) results are concerned, however, the effects of fiber type on fresh mix characteristics seem to be insignificant. The increase in fiber reinformcement index consistently damages fresh mix properties, as shown in Figures 3.12.a through 3.12.c.

3.5.b Fiber Type Effects on Hardened Material Mechanical Properties: The flexural load-deflection characteristics of fiber reinforced concretes with different fiber types at aspect ratios of about 60 and 75 are shown in Figure 3.13.a and 3.13.b, respectively. The curves presented in these figures are

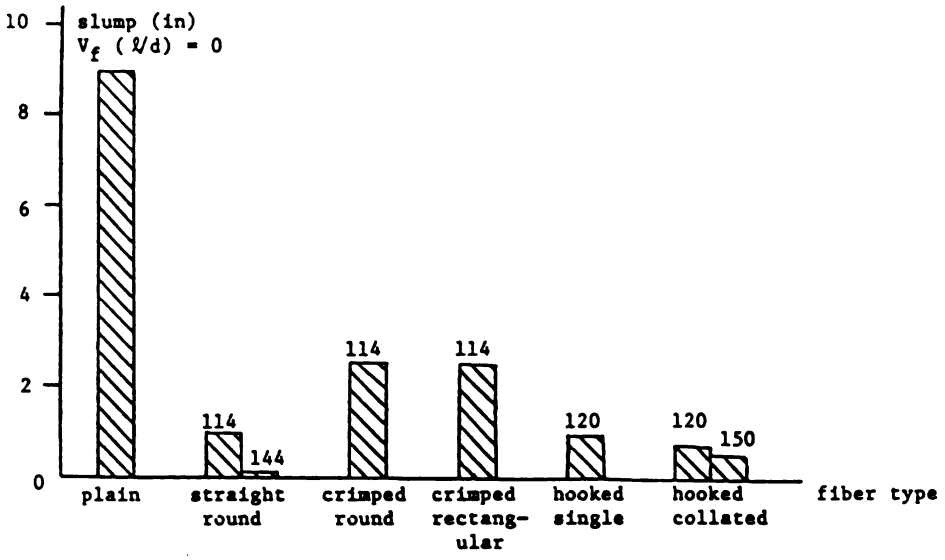

a. Slump. 1 in = 25.4 in

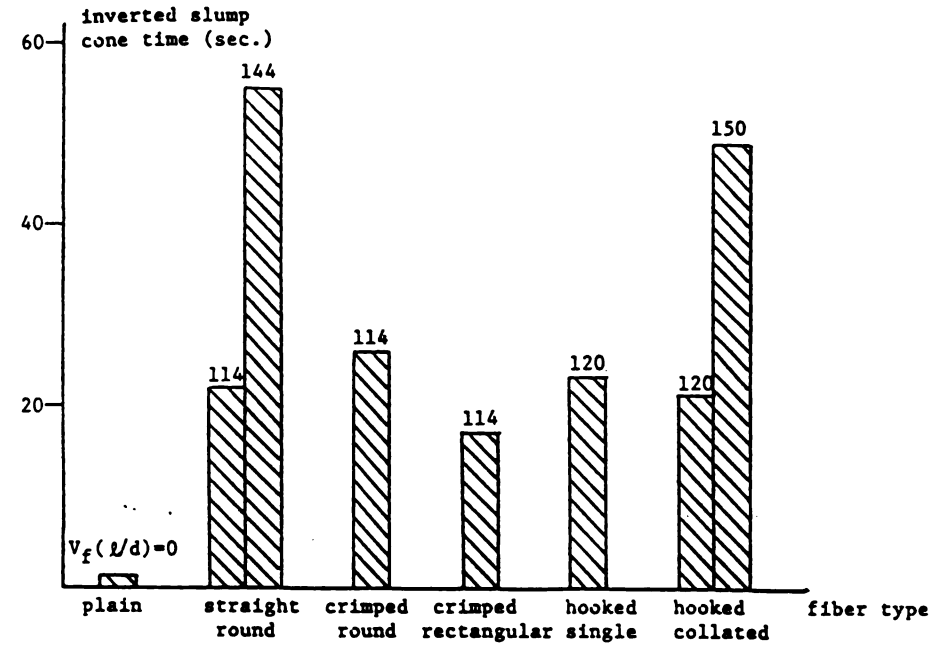

b. Inverted slump cone time

Figure 3.12: Effects of fiber type on fresh mix properties.

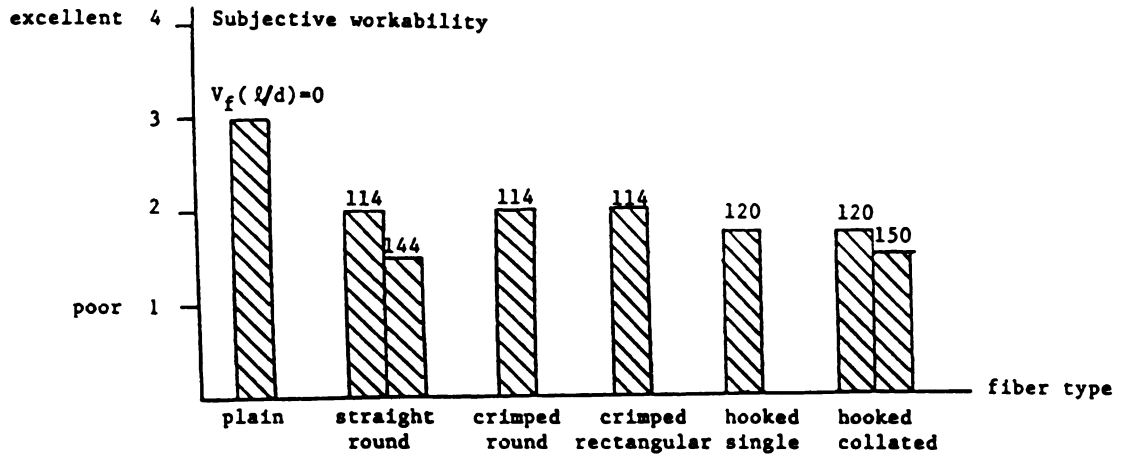

c. Subjective workability

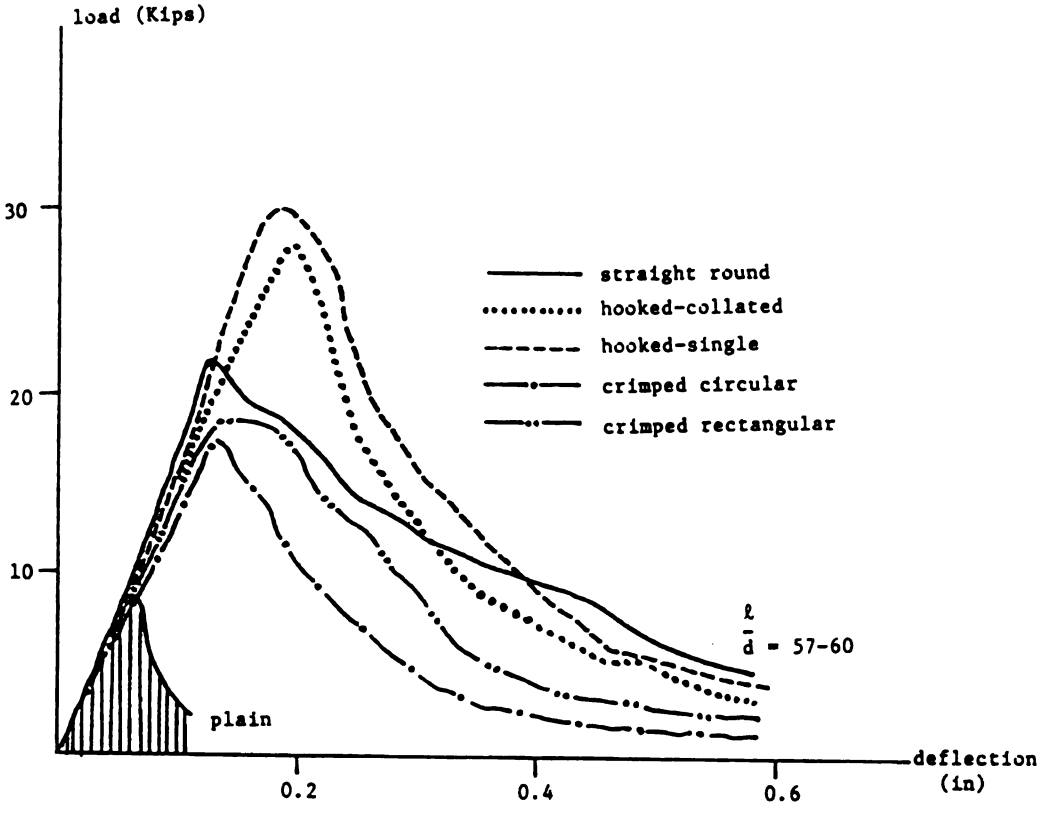

a. Aspect ratio = 57-60

Figure 3.13: Flexural load-deflection charactristics of steel fibrous concrete with different fiber types. 1 in = 25.4 mm, 1 Kip = 4.5 KN.

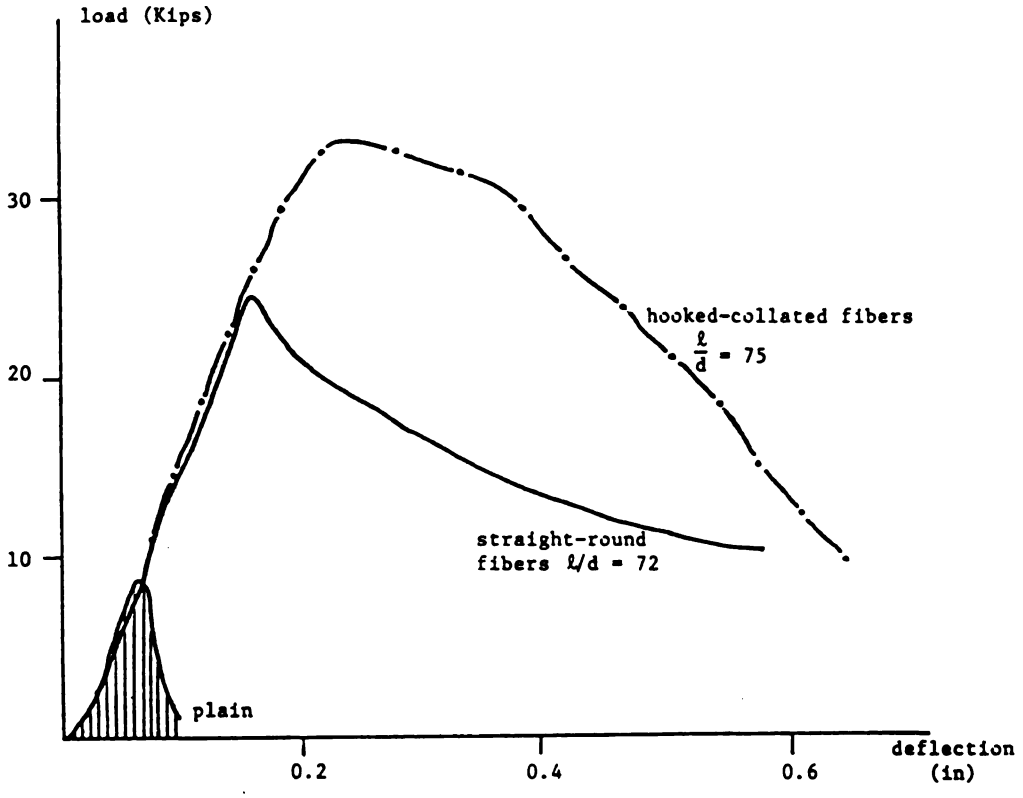

b. Aspect ratio = 72-75

averages of three test results obtained using identical test specimens. Relatively small variations were observed in flexural test results of specimens manufactured from the same mix (the maximum and minimum test results were in the range of 95% to 105% of the average values). From Figure 3.13.a, it may be concluded that the crimped (circular or rectangular) fibers are less effective than the straight ones in improving the ultimate strength and toughness of concrete under flexural loads, at a fiber aspect ratio of about 60 and fiber volume fraction of 2%. At the relatively low aspect ratio of Figure 3.13.a, the use of hooked fibers (collated or single) leads to a higher ultimate strength but a lower post-peak resistance under flexural load when compared with straight fibers. At higher aspect ratios (72 to 75 in Figure 3.13.b), the advantage of hooked fibers in increasing flexural strength of concrete seem to be more pronounced. Although the descending branch of flexural load-deformation relationships is still steeper for hooked fibers when compared with straight ones, the superior flexural strength obtained with hooked fibers of higher aspect ratio results in a desirable post-peak energy absorption capacity when compared with straight fibers having the same aspect ratio.

The total area underneath the flexural load-deformation curve up to 5.5 times the cracking deflection is representative of the total flexural energy absorption capacity of fibrous concrete. The post-cracking energy absorption capacity of fiber reinforced concrete is usually measured by toughness index, defined as the ratio of the total area under the load-deflection relationship up to 5.5 times the

cracking deflection to the area up to the cracking deflection.[27] A toughness index of 10 is indicative of an elastic-perfectly plastic behavior with yielding occurring at the cracking load. Figures 3.14.a and 3.14.b summarize the total energy absorption capacities and toughness indices, respectively, measured using Figures 3.13.a and 3.13.b. From Figure 3.14.a, it may be concluded that at fiber reinforcement indices in the range of 114 to 120, crimped fibers are less effective than the straight and the hooked ones in improving the energy absorption capacity of concrete. At a higher fiber reinforcement index in the range of 144 to 150 (corresponding to fiber with higher apect ratios in Figure 3.13.b), the hooked fibers seem to be superior to the straight ones in enhancing energy absorption capacity. Figure 3.14.b indicates that at fiber reinforcement indices in the range of 114 to 120, there seem to be no significant difference between the toughness indexes of concretes reinforced with different fiber types. At higher fiber reinforcement indexes of 144 to 150 (corresponding to fibers with higher aspect ratio), however, the hooked fibers seem to result in a higher toughness index when compared with straight fibers.

The compressive stress-strain relationships of concretes reinforced with different fiber types at fiber reinforcement indices in the ranges of 114 to 120 and 144 to 150 are shown in Figures 3.15.a and 3.15.b, respectively. Figure 3.16 shows the energy absorption capacities of fibrous mixes with different fiber types and the two ranges of fiber reinforcement index. Energy absorption capacity in compression is defined as the area underneath the compressive stress-strain

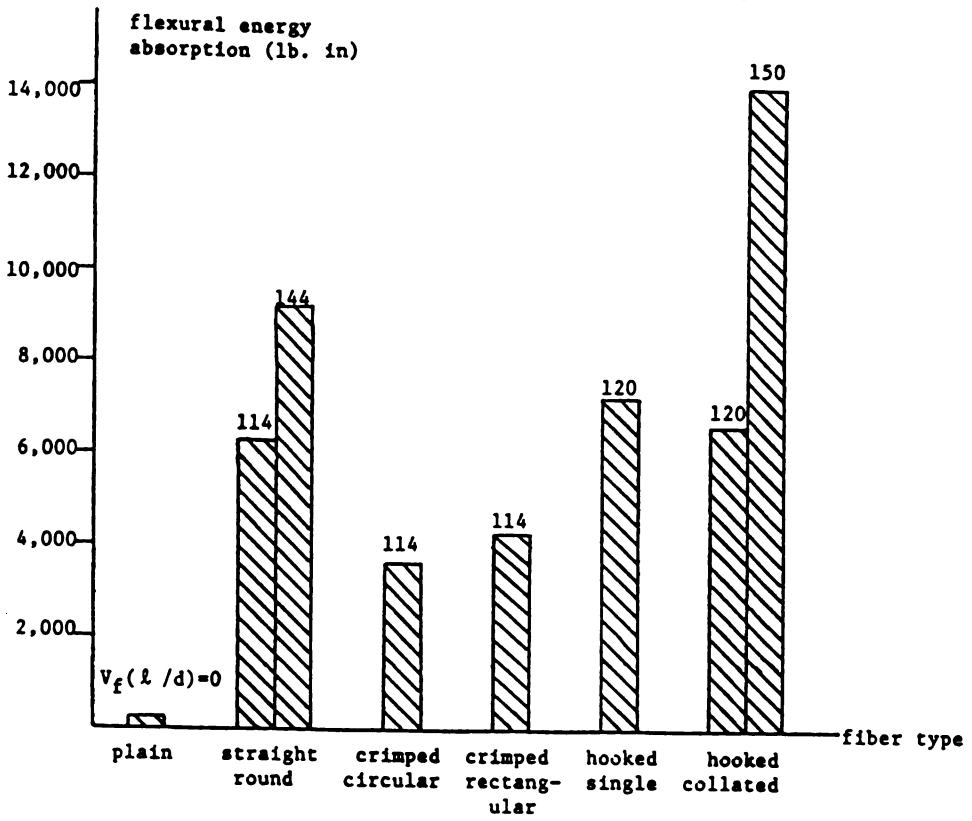

a. Total energy absorption capacity. 1 Kip in = 114 N.m

Figure 3.14: Flexural energy absorption capacity and toughness index of concretes reinforced with different steel fiber types.

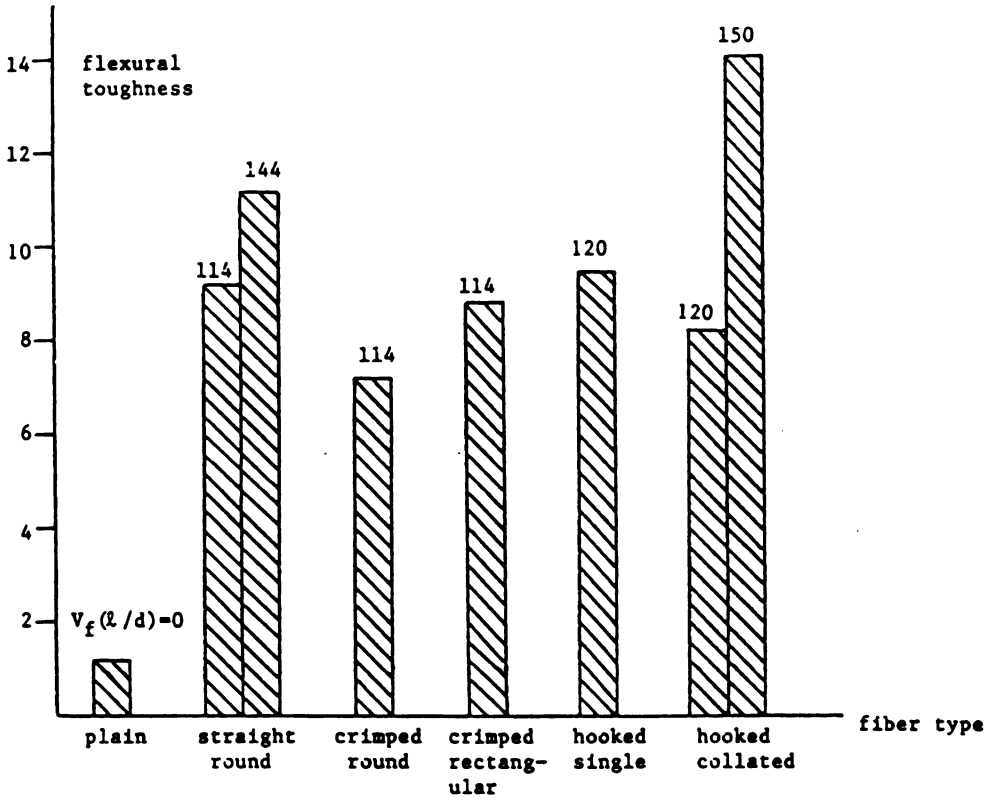

b. Toughness index

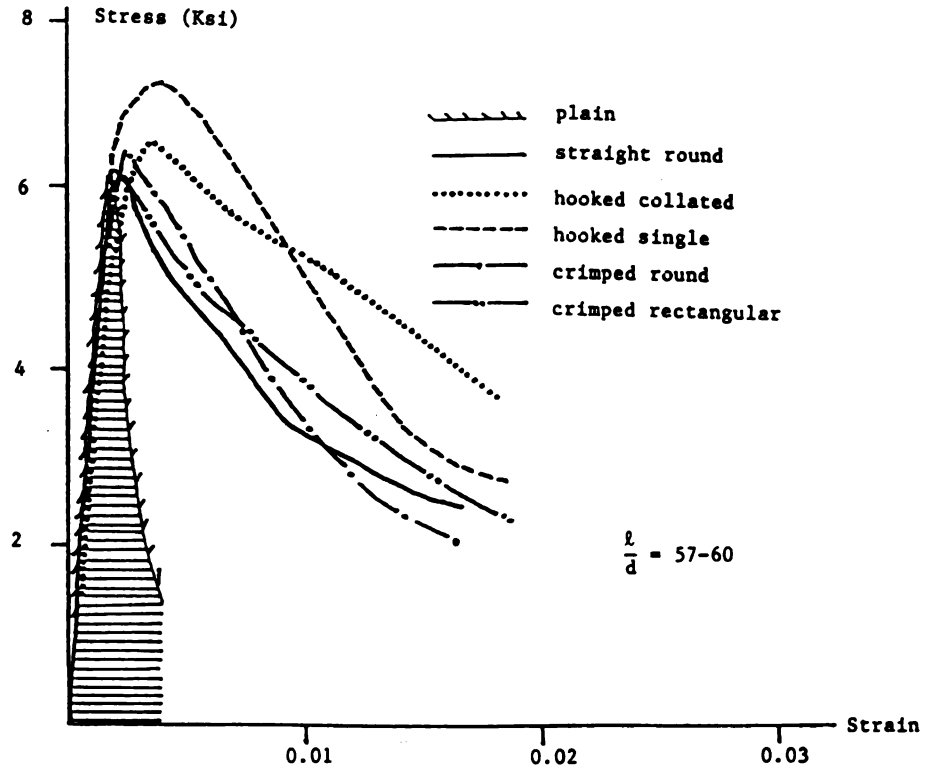

a. Aspect ratio = 57-60

Figure 3.15: Compressive stress-strain relationships of steel fiber concretes with different steel fiber types. 1 Ksi = 6.9 MPa.

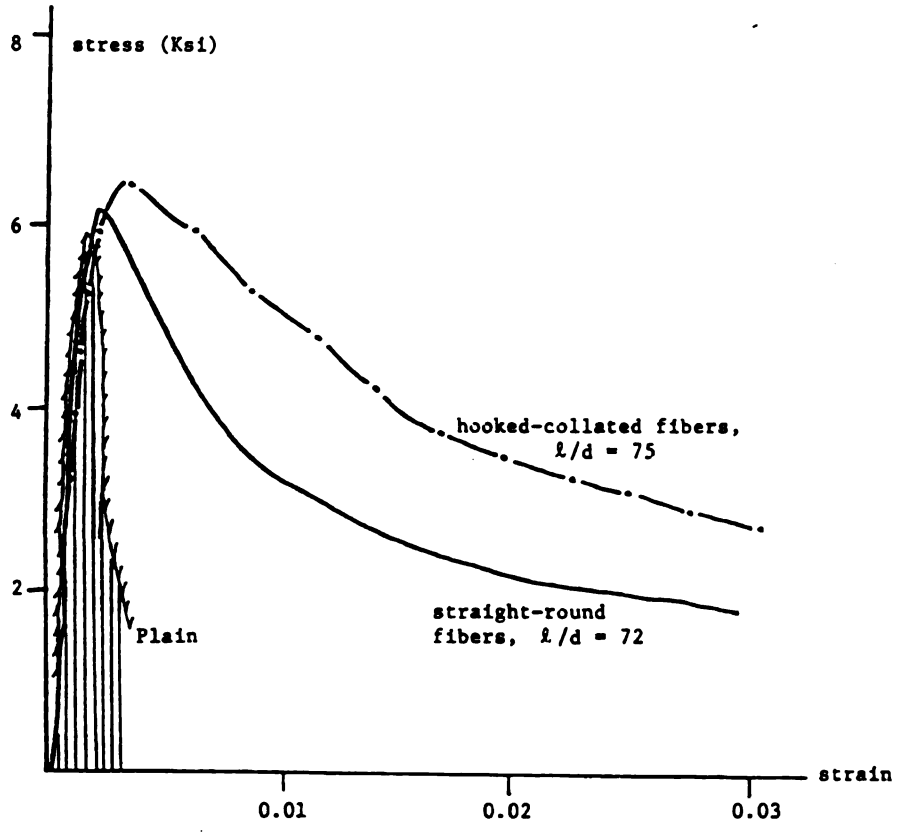

b. Aspect ratio = 72-75

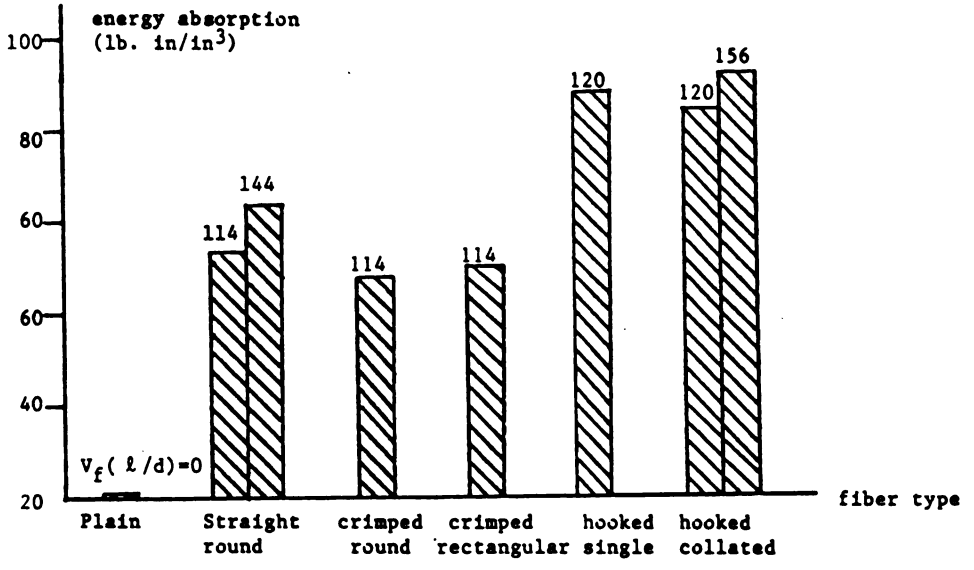

Figure 3.16: Energy absorption capacity of steel fiber reinforced concretes with different steel fiber types. 1 in = 25.4 mm, 1 Kip in = 114 N.m

relationship up to a strain of 5.5 times the strain at peak compressive stress.[27] These figures indicate that fibers increase the post-peak ductility and energy absoprtion capacity of concrete in compression, but have a relatively small effect on the peak compressive stress. Strain at peak compressive stress tends to increase with steel fiber reinforcement, especially when hooked fibers are used. Hooked fibers seem to be more effective than straight and crimped ones in enhancing the energy absorption capacity of concrete under compressive stresses, partially due to the more pronounced effects of hooked fibers on increasing the strain at peak compressive stress of concrete. All fibrous concretes with different fiber types seem to have similar toughness indices (defined as total energy absorption capacity divided by pre-peak energy absorption capacity).

3.6 Summary and Conclusions

An experiment of study was performed to assess the effects of steel fiber type on material properties of steel fiber reinforced concrete in fresh and hardened states. The fresh fibrous concrete was characterized by its slump, inverted slump cone time and subjective workability. For the hardened material, flexural load-deflection curves and compressive stress-strain relationships were used as representative of important mechanical properties of the material. The fibers included in this study were straight-round, crimped-round, crimped-rectangular, hooked single and hooked-collated fibers at aspect ratios ranging from 57 to 60, and straight-round and and hooked-collated fibers at aspect ratios ranging from 72 to 75. All the fibrous mixes incorporated a 2% volume fraction of steel fibers.

The following conclusions could be derived from test results:

1. The inclusion of fibers damages the workability of fresh concrete and this effect is more pronounced for fibers with higher apsect ratios. The effects of fiber types on fresh mix workability, as represented by the inverted slump cone time and the subjective measure, seem to be insignificant. Crimped fibers result in slightly higher slump values than straight and hooked fibers.

2. At an aspect ratio of about 60 and fiber volume fraction of 2%, crimped fibers (circular or rectangular) generate flexural strengths and energy absorption capacities which are inferior to those of straight fibers, but hooked fibers result in higher flexural strengths and similar flexural energy absorption capacities when compared with straight fibers. Hooked fibers are superior to straight ones in enhancing the flexural strength and energy absorption capacity of concrete at fiber aspect ratio of about 75 when added to concrete at 2% volume fraction.

3. Hooked are more effective than straight and crimped fibers in enhancing the total energy absorption capacity under compressive stresses. Strain at peak compressive stress also increases with steel fiber reinforcement, especially when hooked fibers are used. The increase in toughness of concrete resulting from steel fiber reinforcement is not strongly dependent on the fiber type. The effect of fiber reinforcement on compressive strength is relatively small and different fiber types seem to act similarly in this regard.

CHAPTER 4

Effects of Concrete Matrix Mix Proportions on Steel Fiber Reinforced Concrete Properties

4.1 Introduction

Steel fibers when added to compatible concrete mixtures result in important improvements in such properties as toughness, impact resistance, flexural strength, fatigue life and abrasion and cavitation resistance of concrete. To be compatible with steel fibers, the conccrete matrix should: (a) be capable of uniformly dispersing fibers through common mixing techniques; (b) maintain its workability in the presence of steel fibers; (c) provide a stable air-void system in the fibrous composite; (d) coat the fibers with cementitious paste and develop sufficient bonding to the fibers; and (e) reach strength levels adequate to take full advantage of the fiber reinforcement effect. These requirements can best be satisfied through the use of a rich mix with high cement contents which incorporates a suitable system of admixtures. On the other hand, economic considerations would tend to limit the cement content and the complexity of the admixture system. It is thus important to establish the trends in matrix composition effects on steel fiber reinforced concrete properties in fresh and hardened states in order to optimize the concrete mixture incorporating steel fibers for satisfying different job requirements. [4,5,40,48,49]

4.2 Background

The test result reports and elaborations made in the literature on the effects of aggregate (cement) content and maximum aggregate size, water-cement ratio and conrete admixtures on steel fiber reinforced concrete in the fresh and hardened states are reviewed in this section.

4.2.a Aggregate (Cement) Content and Maximum Aggregate Size: Steel fiber reinforced concretes typically have relatively low aggregate content (i.e. high cement content) and small maximum aggregate sizes when compared with conventional plain concrete. These conditions are needed for providing the fibers with a mortar volume in which they can be dispersed (Figure 4.1), maintaining an acceptable level of workability (Figure 4.2, noting that increased Vebe time is an evidence of damage to workability), and for ensuring sufficient coating of the fibers with cement paste.[4,5,40,48,49] Steel fibers, however, once uniformly dispersed inside the mixture, tend to be more effective in concrete matrices (incorporating coarse aggregate) than they are in mortar matrices.[29] The workability of fresh mix may also be damaged by the use of finer aggregate due to increase in surface area. These factors tend to limit the reduction of maximum aggregate size in steel fiber reinforced concrete, which is needed for improving fiber dispersability. There are also limits on cement content (aggregate content) beyond which the rate of improvement in performance with increasing cement content slows down considerably (Figure 4.3).[48] At this limit cement content, Reference 48 suggests that a desirable dense packing of the matrix is achieved and

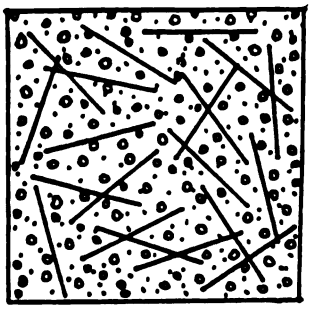

a. Desirable dispersion in mortar (with fine aggregate)

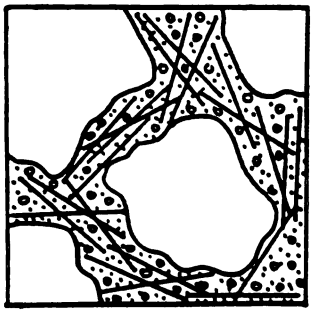

b. Tendency towards balling in concrete (with coarse aggregate)

Figure 4.1: Effect of aggregate size on fiber distribution.[5]

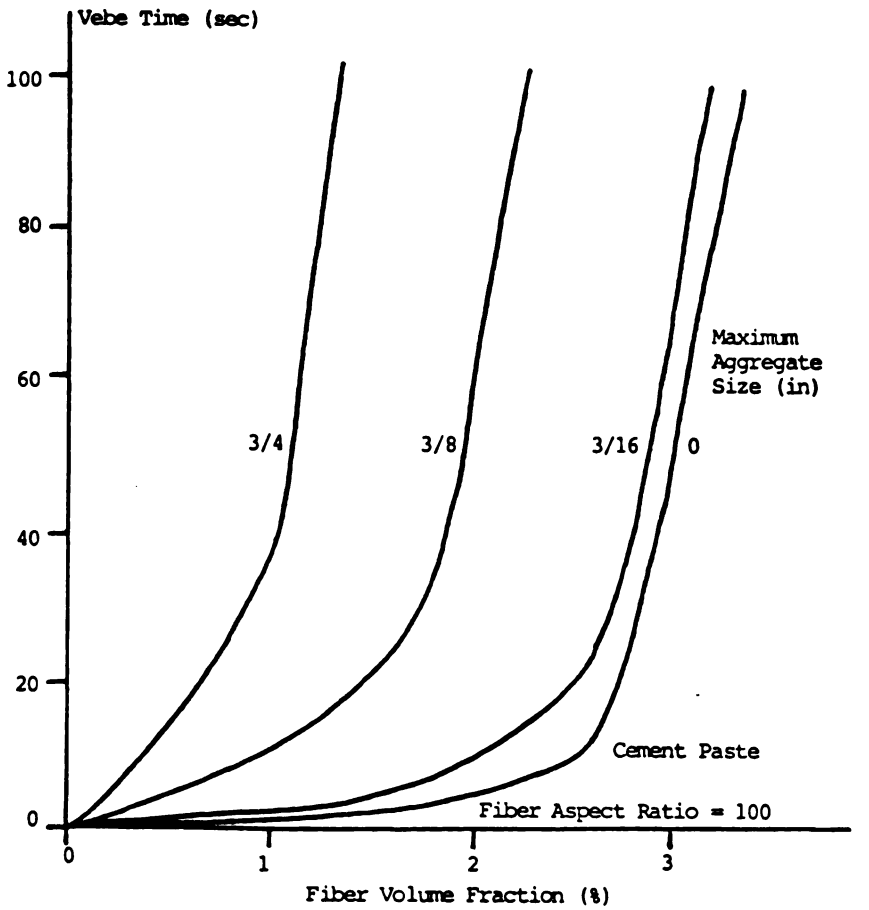

Figure 4.2: Typical effect of aggregate size on fresh steel fiber reinforced concrete workability.[5] 1 in = 25.4 mm

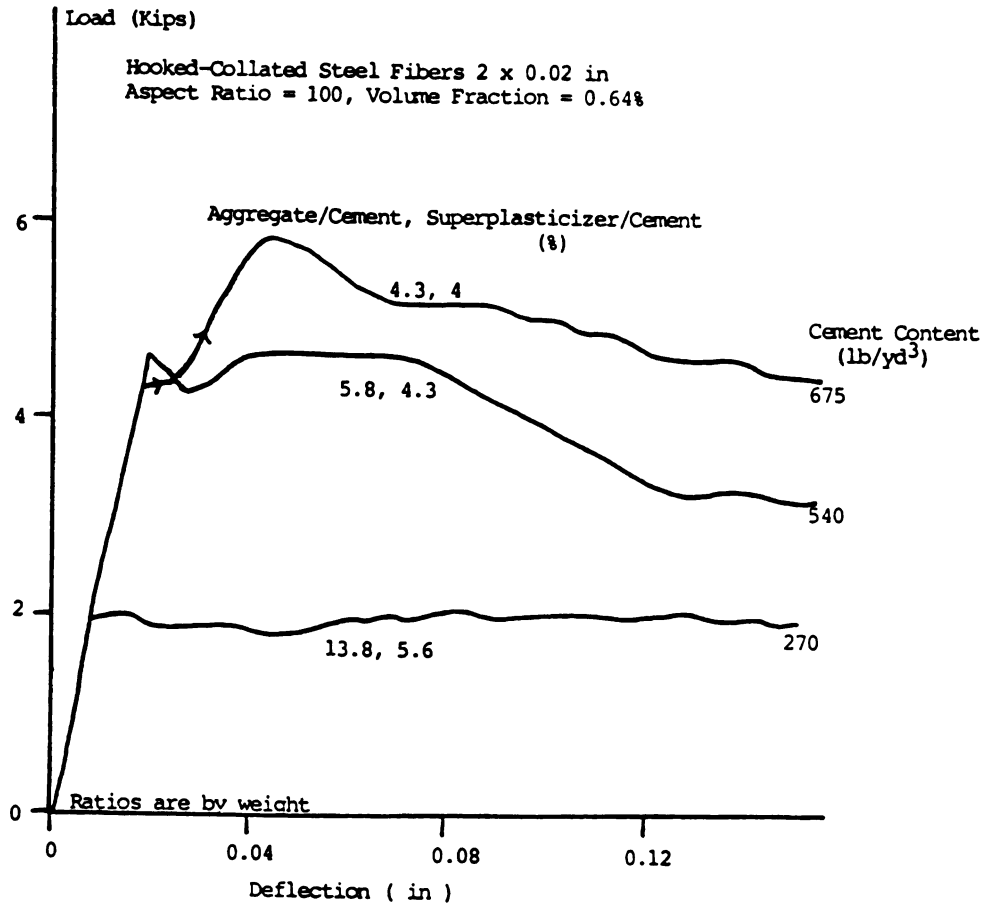

a. Flexural load-deflection relationship (Prismatic specimen dimensions = 4 x 4 x 14 in loaded in four-point loading over a span of 12 in)

Figure 4.3: Improvements in steel fiber reinforced concrete flexural load-deflection reltionship and compressive strength with increasing cement content at a constant water-cement ratio.[48] (water-cement ratio = 0.4, silica fume-cement ratio = 0.2, fine-to-coarse aggregate ratio = 1.0, maximum aggregate size = 1.0 in) 1 in = 25.4 mm, 1 Kip = 4.5 KN, 1 Ksi = 6.9 N/m^2

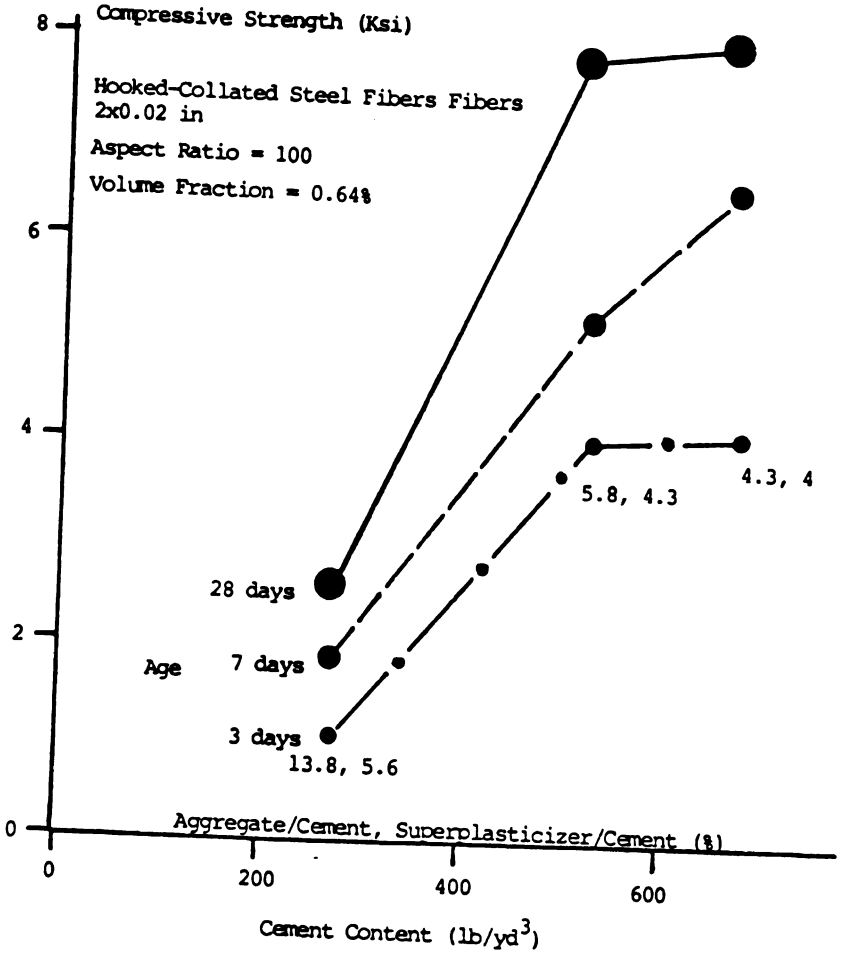

b. Compressive strength (cylindrical specimens of 6 x 12 in)

further increase in cement content hardly improve the packing condition .

4.2.b Water-Cement Ratio: In the presence of fibers, at relatively high volume fractions, the low compactibility of the fresh concrete mixture results in relatively high entrapped air contents and consequently inferior hardened material performance characteristics. The increase in water content up to a certain point enhances the hardened material performance by providing it with a better compaction. Higher water-cement ratios, however, damage the composite material performance through reductions in the matrix and interfacial bond strengths. The trends in water-cement ratio effects on some compressive and flexural characteristics of steel fiber concrete are shown in Figures 4.4.a and 4.4.b, respectively.[48,49]

4.2.c Admixtures: Superplasticizers and air-entraining agents are the two concrete admixtures which are commonly incorporated with steel fiber reinforced concrete mixtures. Considering the damage to workability resulting from fiber reinforcement, superplasticizers have been established as a rather standard constituent of fiber concrete mixtures. Through improving workability, superplasticizers are also partially effective in enhancing the dispersability of steel fibers in fresh concrete mixtures.[5,40,48,50,51] Through improving the fresh mix workability, superplasticizers enhance the effectiveness of air-entraining agents in providing steel fiber reinforced concrete mixtures with a stable air system.[51] Reference 5, however, suggests that the maximum limit on

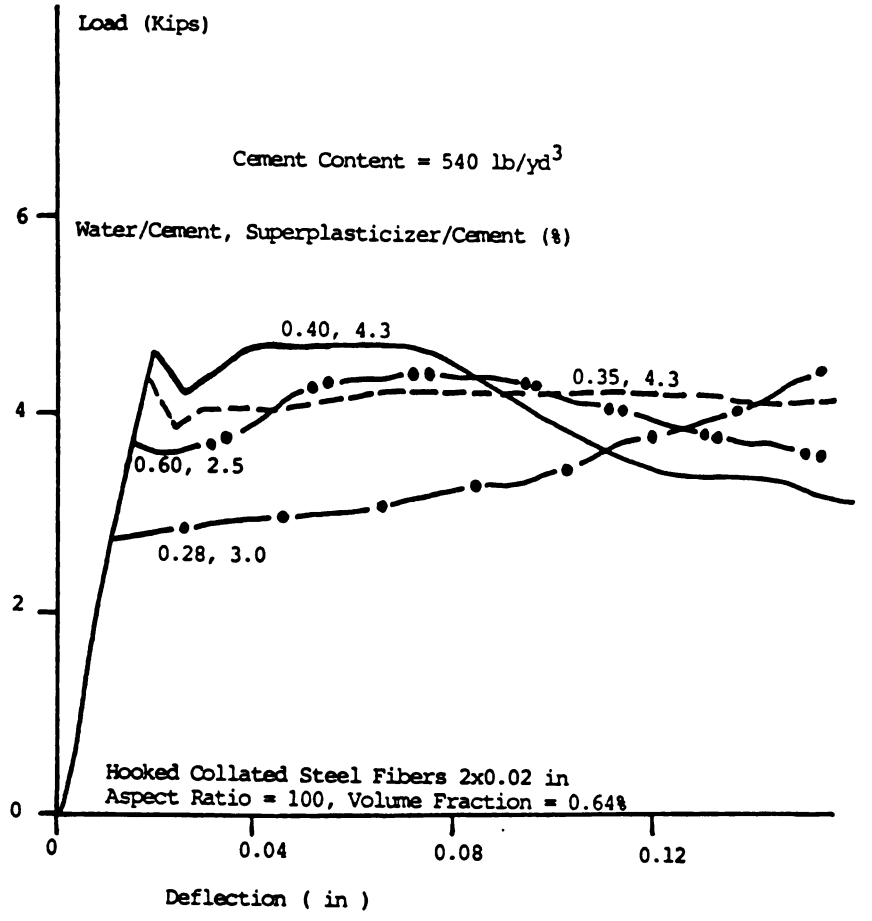

a. Flexural load-deflection relationship (prismatic specimen dimensions = 4 x 4 x 14 in loaded in four-point loading over a span of 12 in)

Figure 4.4: Effects of water-cement ratio on compressive strength and flexural load-deflection relationship of steel fiber reinforced concrete.[48] (silica fume-cement ratio = 0.2, aggregate-cement ratio = 5.4 - 6.0, fine-to-coarse aggregate ratio = 1.0, maximum aggregate size = 1.0 in) 1 in = 25.4 mm, 1 Kip = 4.5 KN, 1 Ksi = 6.9 N/mm^2.

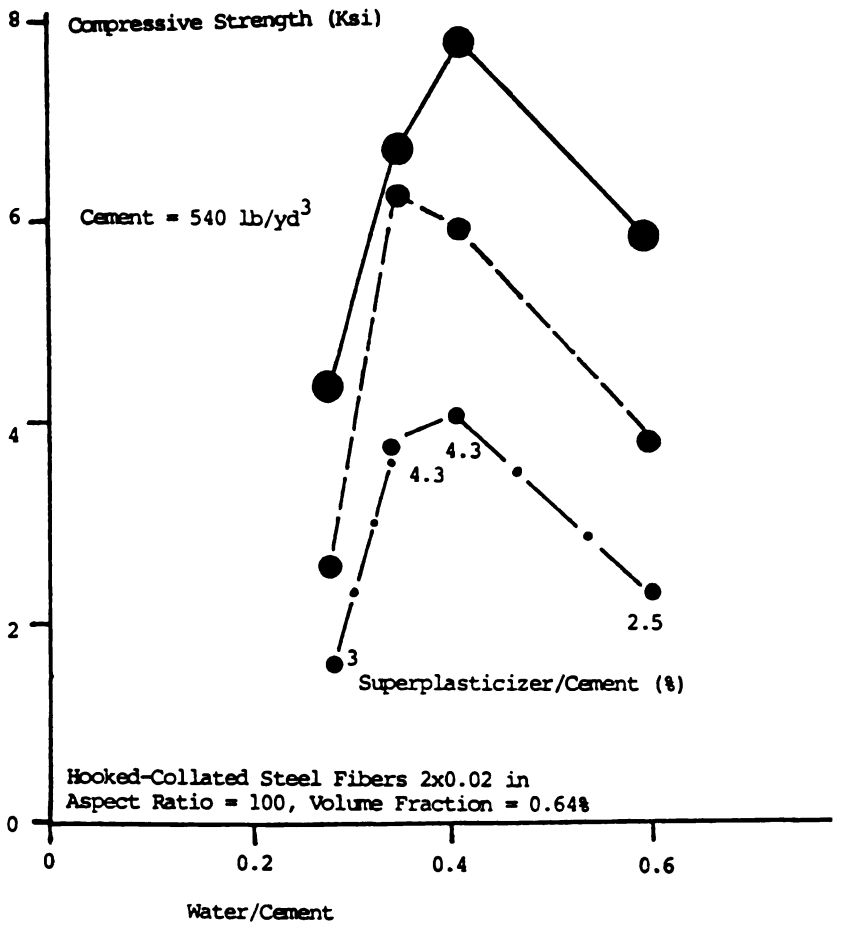

b. Compressive strength (cylindrical specimens of 6 x 12 in)

fiber volume fraction which can be practically incorporated into a specific concrete mixture cannot be necessarily increased through the use of excessive amounts of superplasticizer. According to this reference, the cement paste with relatively high dosage of superplasticizer may become so fluid that it runs out of the fiber clusters as they start to form. Segregation or clumping of fibers, therefore, occurs at about the same fiber volume fraction as for the concrete with low superplasticizer dosage.

Air-entraining agents are used in steel fiber reinforced concrete to provide the material with sufficient air content for resisting freeze-thaw cycles. Air-entraining also has rather positive effects on the workability of fibrous mixtures.[50] The effectiveness of air-entraining agents in fiber reinforced concrete is heavily dependent on the workabiity of fresh mixtures. In tests reported in Reference 51, for steel fiber reinforced concrete with a zero slump, an increase in air-entraining agent from 0.2% to 0.8% by weight of cement caused no appreciable increase in the air content of the composite material. Even very high dosages of air-entraining agent could not provide this fiber concrete mixture (with low workability) of Reference 51 with the target air content of 6%.

As far as the air void characteristics of air-entrained plain and fibrous concretes, Reference 49 suggests that the specific surface of air bubbles is lower in fiber concrete (indicating larger bubble sizes). In general, the air void characteristics are similar in plain and fibrous concretes.

4.2.d Design of Rich Workable Fiber Concret Mixtures: Reference 26 reported a very critical experimental program on steel fiber reinforced concrete. This experimental program was targeted at optimizing the concrete matrix in order to take full advantage of the fiber reinforcement technique. Two methods were used to improve the properties of the concrete matrix in Reference 26 as follows: (a) increasing the cement content of the mixture from 1000 lb/yd^3 to 1150 lb/yd^3. The richer mixes (with higher cement content) have higher cement paste contents and better coating of fibers and aggregates which leads to improved performance characteristics of the mix in the fresh and hardened states, and (b) decreasing the water-cement ratio in order to increase the strength of the hardened concrete. The damaging effect of decreasing water content on fresh mix workability was compensated for (or even overshadowed) by increasing the superplasticizer dosage of the mixture. The increase of superplasticizer content in the experimental program of Reference 26 (although paired with decreasing water-cement ratio) resulted in significant improvements in the fresh mix workability and fiber dispersability. The effects of cement content, water-cement ratio and superplasticizer dosage on the fresh mix workability and hardened material strength of steel fiber reinforced concrete are shown in Figure 4.5.[26]

4.3 Experimental Program

An experimental study was conducted to assess the effects of binder (cement + class F fly ash) content, maximum size and gradation of aggregates, water-binder ratio, and superplasticizer and air entraining agent contents on the fresh mix

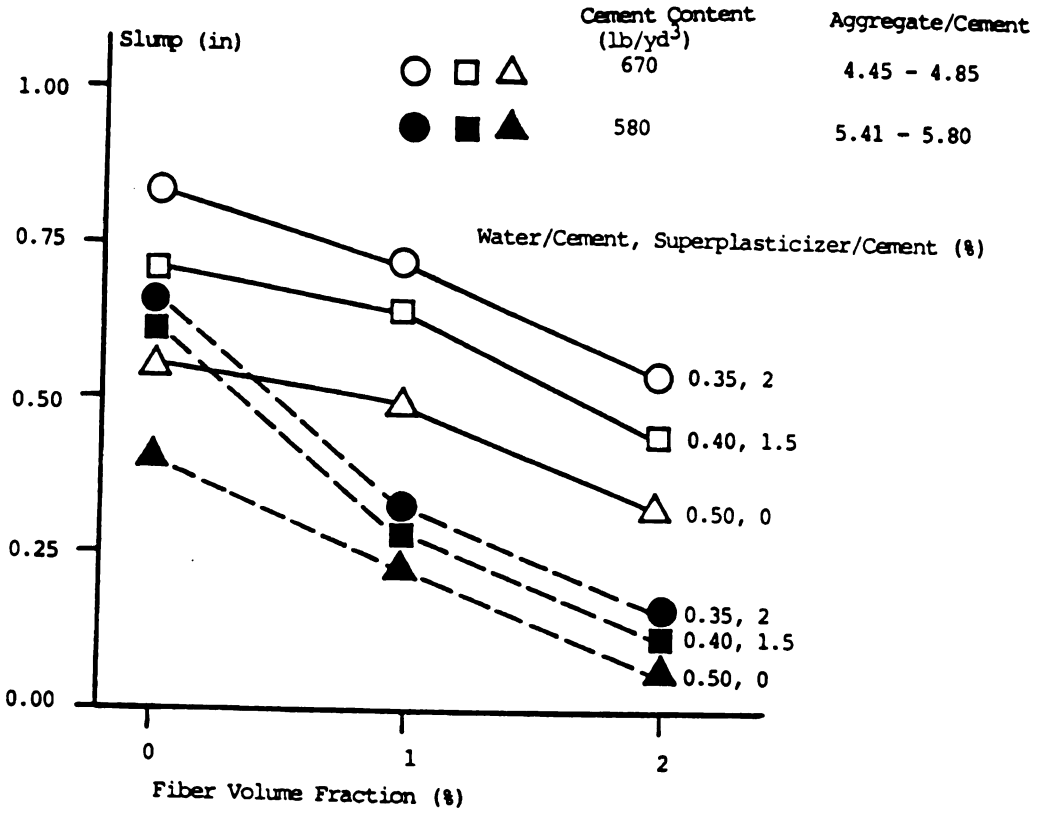

a. Slump

Figure 4.5: Effects of cement content (aggregate content), water-cement and superplasticizer-cement ratios on the characteristics of steel fiber reinforced concrete.[26] (straight round steel fibers with a length = 1.6 in and a diameter = 0.02 in resulting in an aspect ratio = 80) 1 in = 25.4 mm, 1 Ksi = 6.9 Ksi

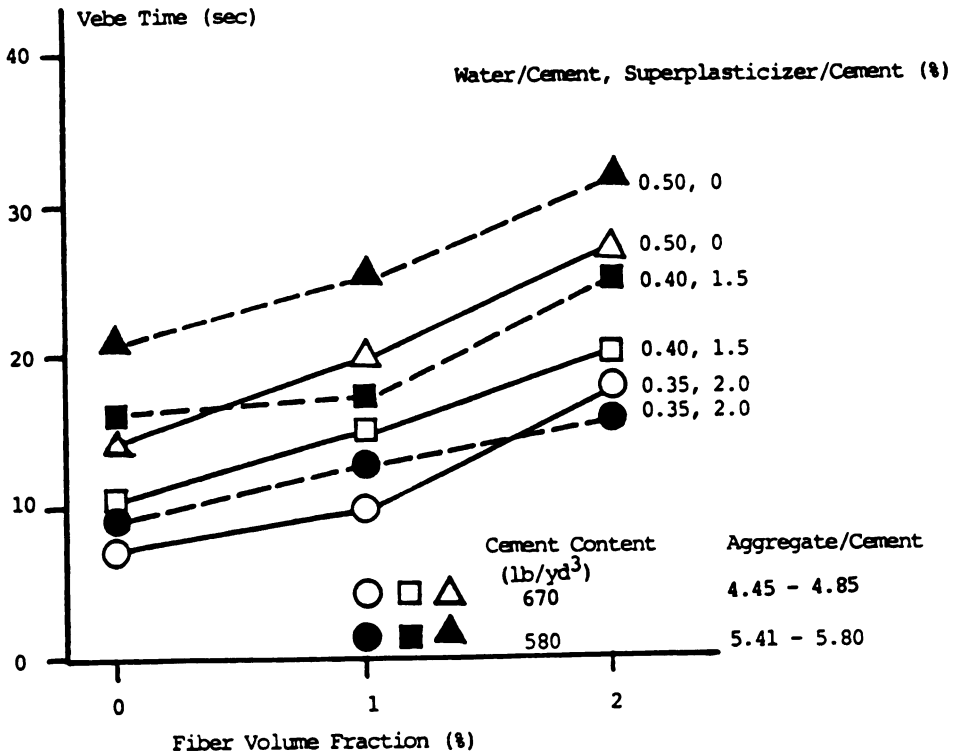
Vebe Time (sec)
40
30
20
10
0
Water/Cement, Superplasticizer/Cement (%)
0.50, 0
0.50, 0
0.40, 1.5
0.40, 1.5
0.35, 2.0
0.35, 2.0
Cement Content (lb/yd3)
670
580
Aggregate/Cement
4.45 - 4.85
5.41 - 5.80
0
1
2
Fiber Volume Fraction (%)

b. Vebe time

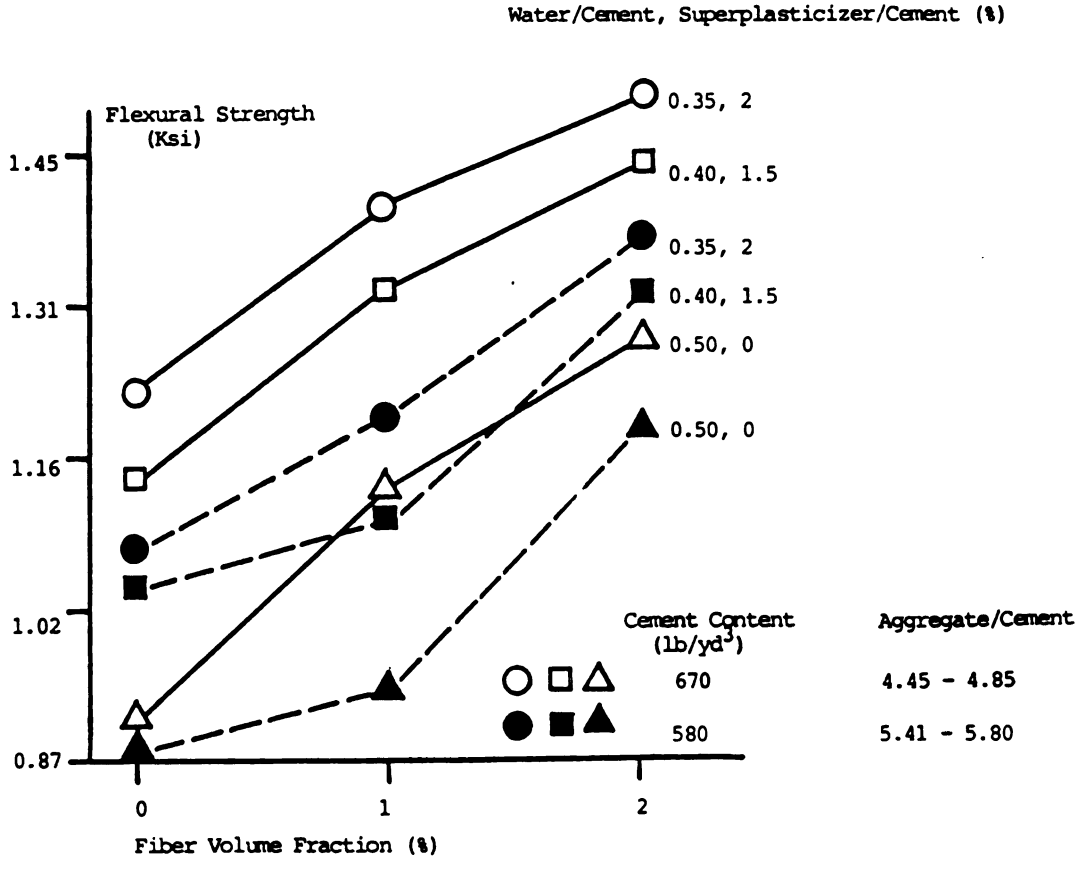

c. Flexural strength

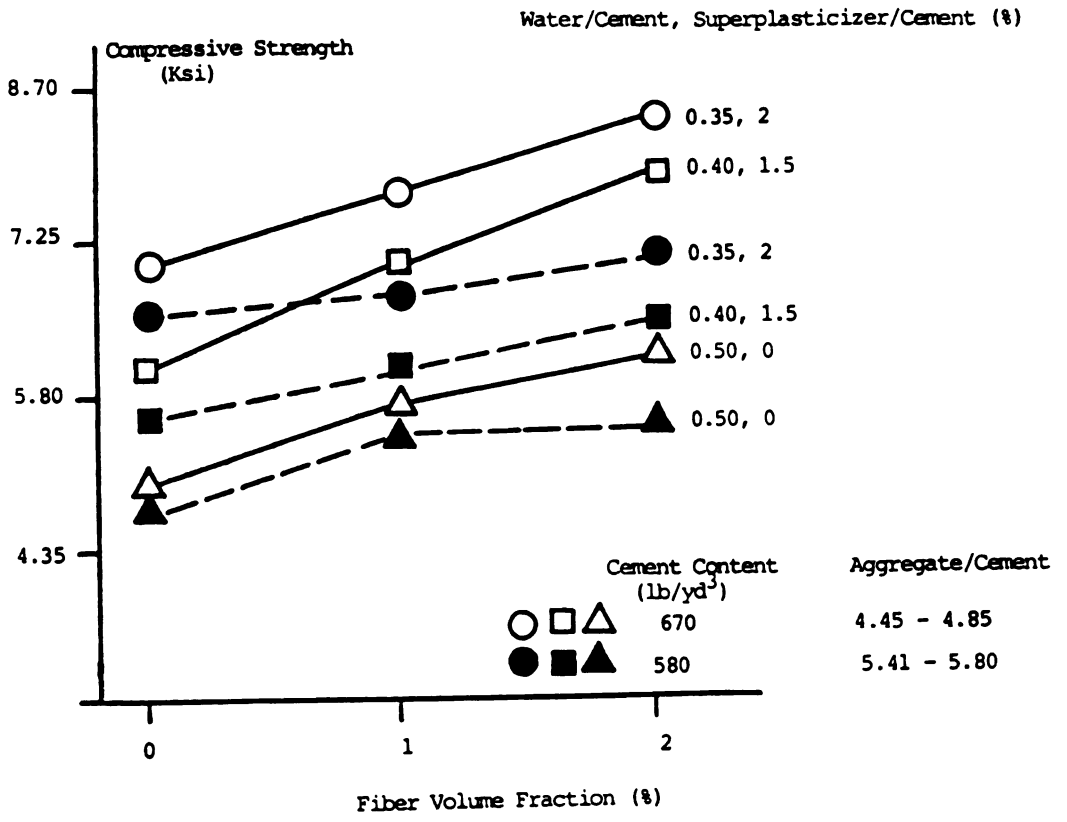

d. Compressive strength

workability and air content, and the flexural and compressive properties of the hardened material. The constants in the mixtures of this experimental study were the fiber volume fraction (at 2%), fiber aspect ratio (at 57, with a length of 2 in = 51 mm and a diameter of 0.035 in = 0.8 mm), and fly ash-binder ratio (at 0.3 by weight). All the fibers used in this experimental study were straight and round with an ultimate tensile strength of about 130 Ksi (900 N/mm^2). The specific values of the matrix mix variables are given in Table 4.1.

The air-entraining agent used in this experimental investigation was Dravair produced by W. R. Grace and Company.[52] Air content of steel fiber reinforced concrete mixtures of this study was measured through the pressure method in accordance to ASTM standards.[27] The remainder of materials (cement, fly ash, superplasticizer, sand, gravel, fibers), manufacturing techniques (mixing and curing) and the remainder of testing techniques (slump, inverted slump cone, subjective workability, compressive and flexural behaviors) were the same as reported in Chapter 2.

4.4 Test Results

This section describes the effects of each mix variable considered in this investigation on the fresh mix workability and air content, and hardened material mechaical properties of steel fiber reinforced concrete.

4.4.a Binder Content: The effects of binder content at a constant water-binder

Table 4.1: Matrix mix variables

Variable	Mix No.	Binder Content (lb/yd^3)	AG/B	S/G	MAS (in)	W/B	SP/B (%)	AE/B (%)
Standard	1	720	4.0	1.0	3/4	0.40	1.5	0
Binder Content	2	860	3.0	1.0	3/4	0.40	1.5	0
	3	780	3.5	1.0	3/4	0.40	1.5	0
	4	660	4.5	1.0	3/4	0.40	1.5	0
	5	610	5.0	1.0	3/4	0.40	1.5	0
	6	560	5.7	1.0	3/4	0.40	1.5	0
Aggregate Gradation	7	720	4.0	1.5	3/4	0.40	1.5	0
	8	720	4.0	0.67	3/4	0.40	1.5	0
Maximum Aggregate Size	9	720	4.0	1.0	3/8	0.40	1.5	0
	10	720	4.0	1.0	3/16 (sand)	0.40	1.5	0
Water/ Binder	11	730	4.0	1.0	3/4	0.35	1.5	0
	12	710	4.0	1.0	3/4	0.42	1.5	0
	13	700	4.0	1.0	3/4	0.45	1.5	0
	14	690	4.0	1.0	3/4	0.50	1.5	0
Superplasticizer/ Binder	15	720	4.0	1.0	3/4	0.40	0	0
	16	720	4.0	1.0	3/4	0.40	0.5	0
	17	720	4.0	1.0	3/4	0.40	1.0	0
Air Entraining Agent/ Binder	18	720	4.0	1.0	3/4	0.40	1.5	0.1
	19	720	4.0	1.0	3/4	0.40	1.5	0.5
	20	720	4.0	1.0	3/4	0.40	1.5	1.0
	21	720	4.0	1.0	3/4	0.40	1.5	1.5

Ratios are by weight
Ag = Aggregate
B = Binder
S = Sand
G = Gravel
MAS= Maximum Aggregate Size
W = Water
SP = Superplasticizer
AE = Air Entraining Agent
1 in = 25.4 mm, 1 lb/yd^3 = 0.6 kg/m^3

ratio on the fresh mix slump, inverted slump cone and subjective workability are shown in Figures 4.6.a, 4.6.b and 4.6.c, respectively. It should be noted that the binder in the mixtures of this study consisted of 70% cement type I and 30% class F fly ash by weight. The increase in binder content is observed in Figure 4.6 to increase slump, decrease inverted slump cone time and increase the subjective workability, all of which are indicative of improvements in workability resulting from the increase in binder content. It seems that there is a limit on binder content below which the workability tends to be unacceptable even though the other mix variables (including the water-binder ratio) are not changed. As a result, the fibrous mixures tend to be richer in binder content when compared with plain concrete mixtures.

Figures 4.7.a and 4.7.b present the flexural load-deflection and the compressive stress-strain relationships, respectively, of steel fiber reinforced concrete mixtures with different binder contents. Figures 4.8 and 4.9 show the trends (derived from Figure 4.7) in some characteristic flexural and compressive properties as influenced by the binder content.

Figure 4.8.a and b indicate that while the first crack strength tends to remain more or less constant, the ultimate flexural strength of steel fiber reinforced concrete tends to increase with increasing binder content. The flexural deflection at first crack in Figure 4.8.c seems to be largely independent of the binder content. The energy absorption capacity (defined as the area under the load-deflection curve up

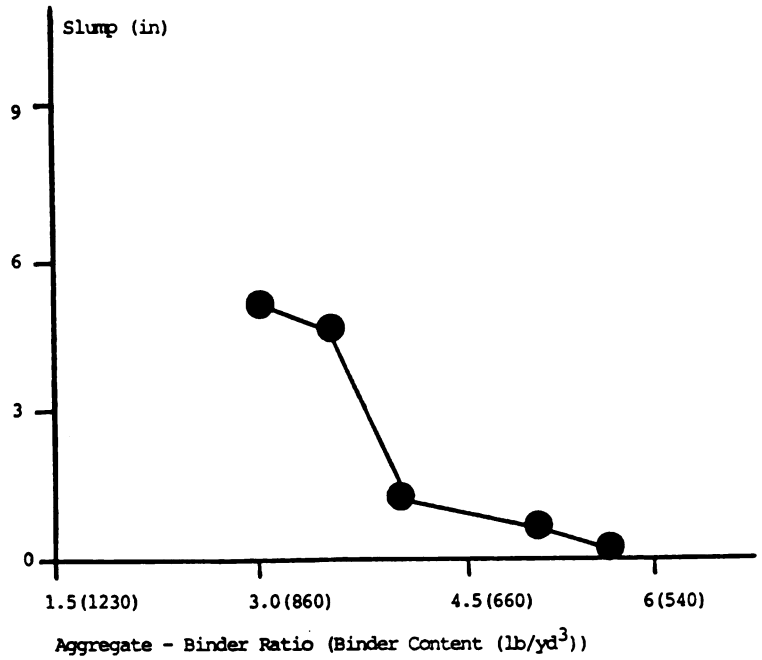

a. Slump. 1 in = 25.4 mm

Figure 4.6: Effects of binder content (aggregate-binder ratio) on fresh mix workability.

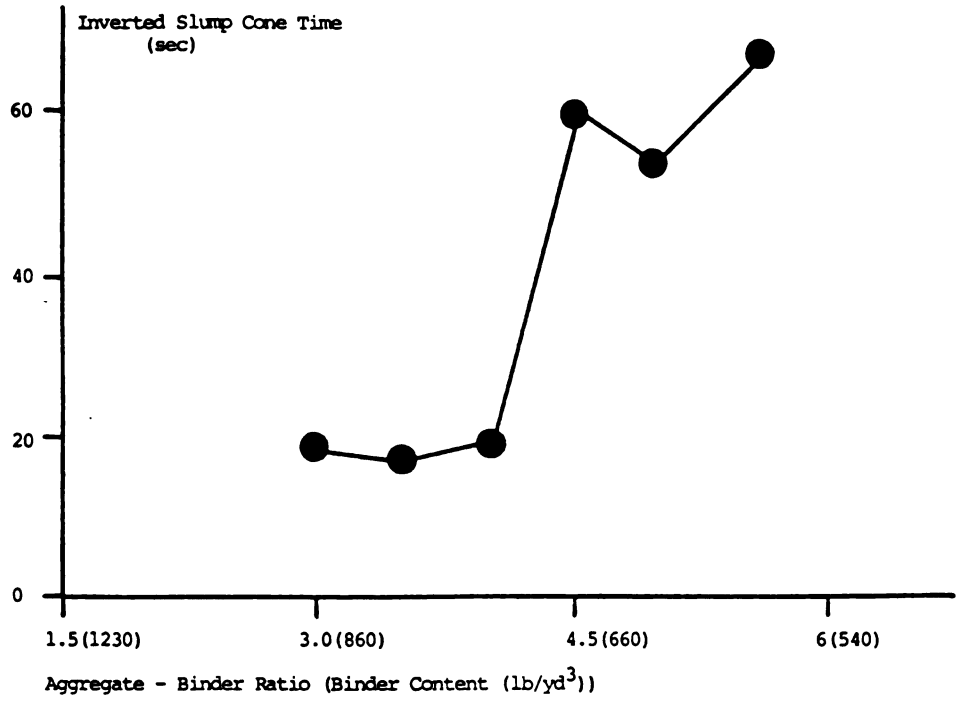

b. Inverted slump cone time

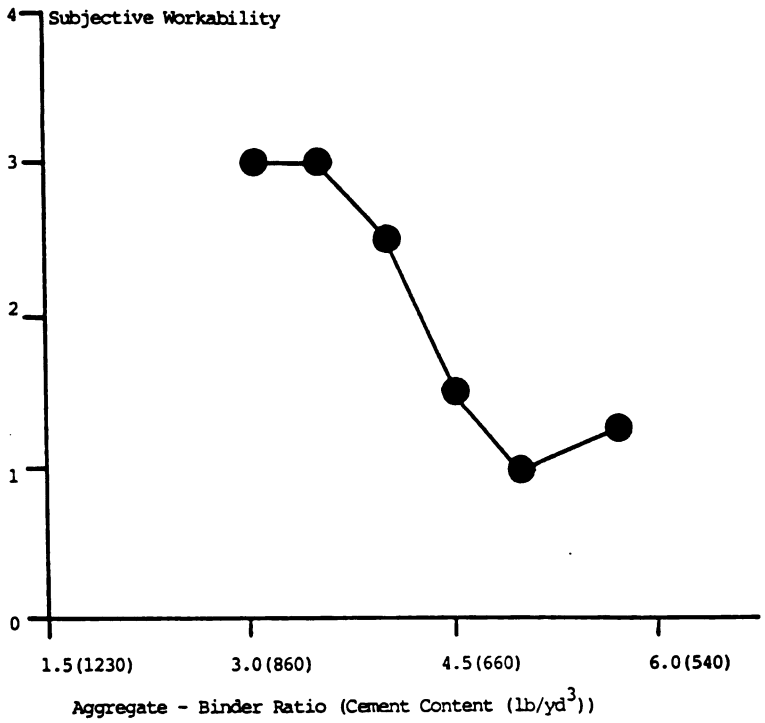

c. Subjective workability

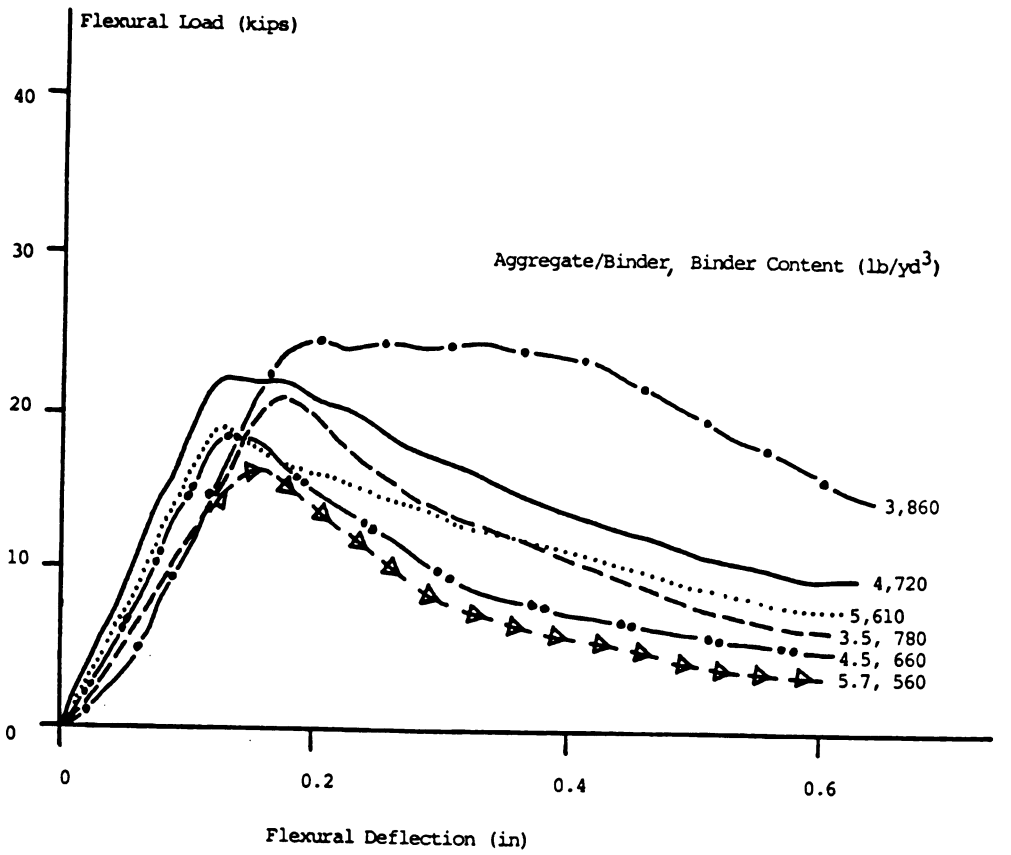

a. Flexural load-deflection relationship

Figure 4.7: Effects of binder content (aggregate-binder ratio) on the flexural and compressive performance of steel fiber feinforced concrete. 1 in = 25.4 mm, 1 Kip = 4.5 KN, 1 Ksi = 6.9 N/mm^2.

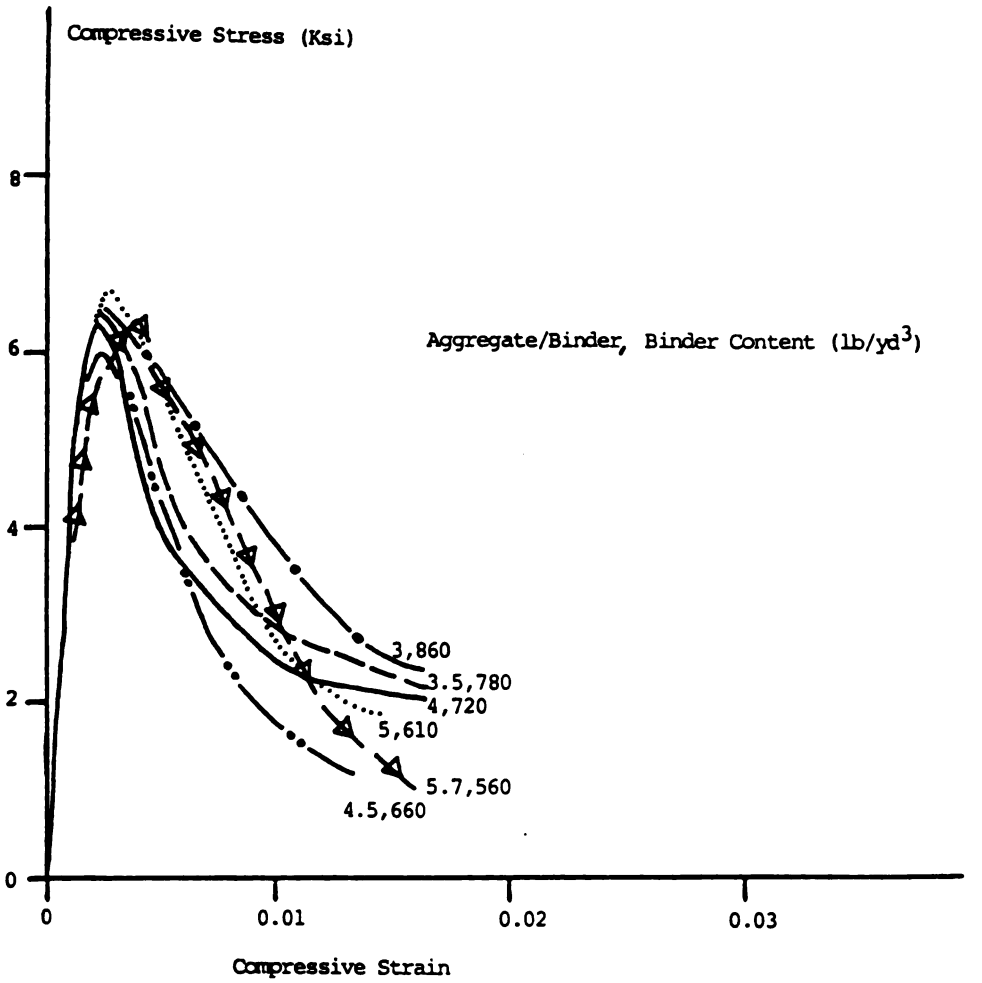

b. Compressive stress-strain curve

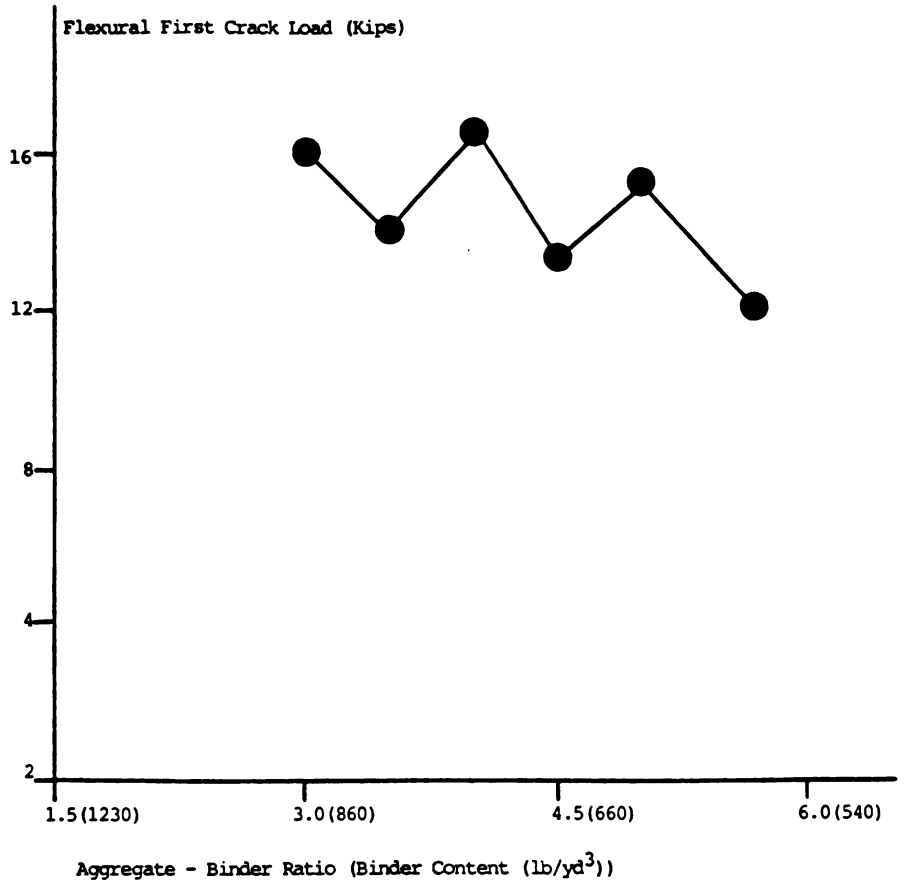

a. First-crack load

Figure 4.8: Effects of binder content (aggregate-binder ratio) on the characteristic flexural properties. 1 in = 25.4 mm, 1 Kip = 4.5 KN, 1 Ksi = 6.9 N/mm^2, 1 Kip in = 114 N.m

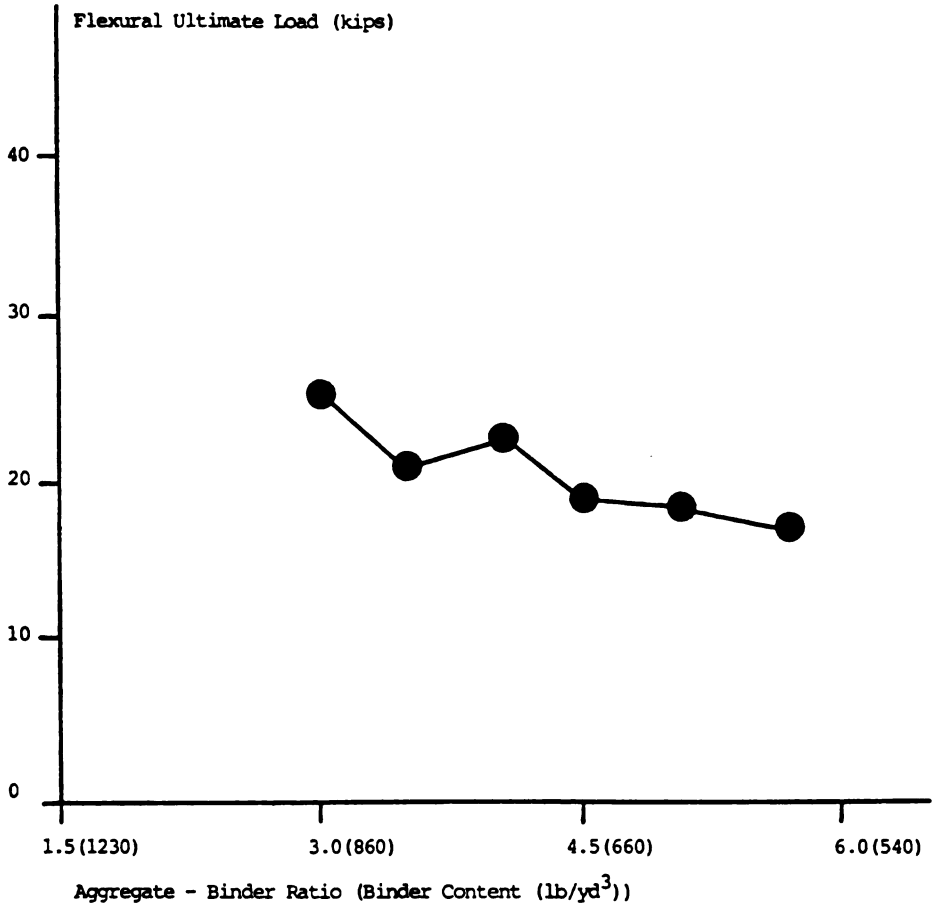

b. Ultimate load

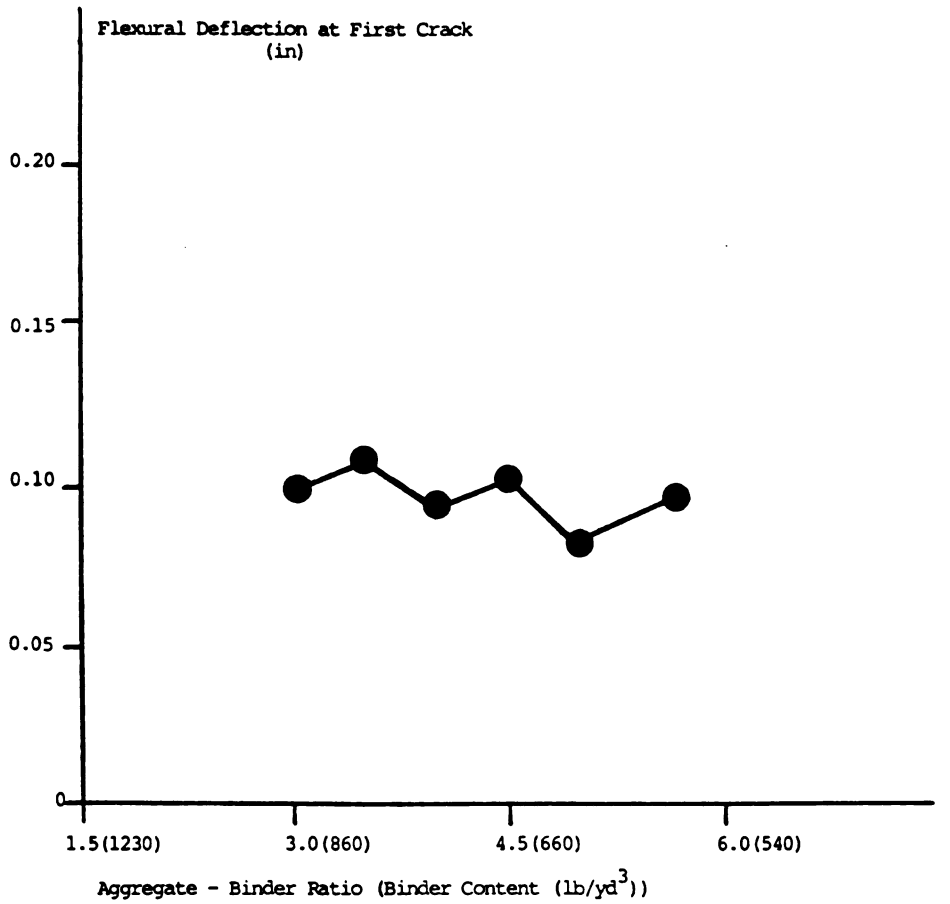

c. Deflection at first crack

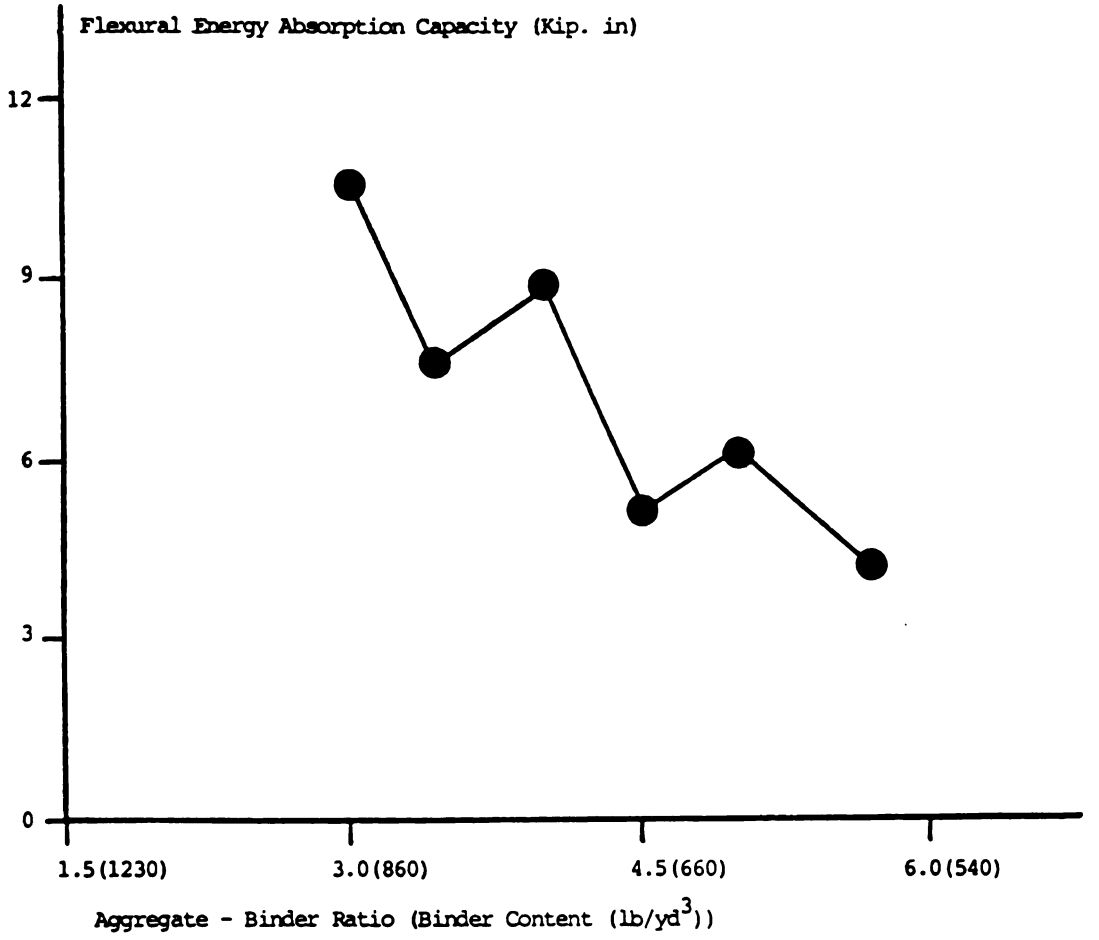

d. Energy absorption capacity

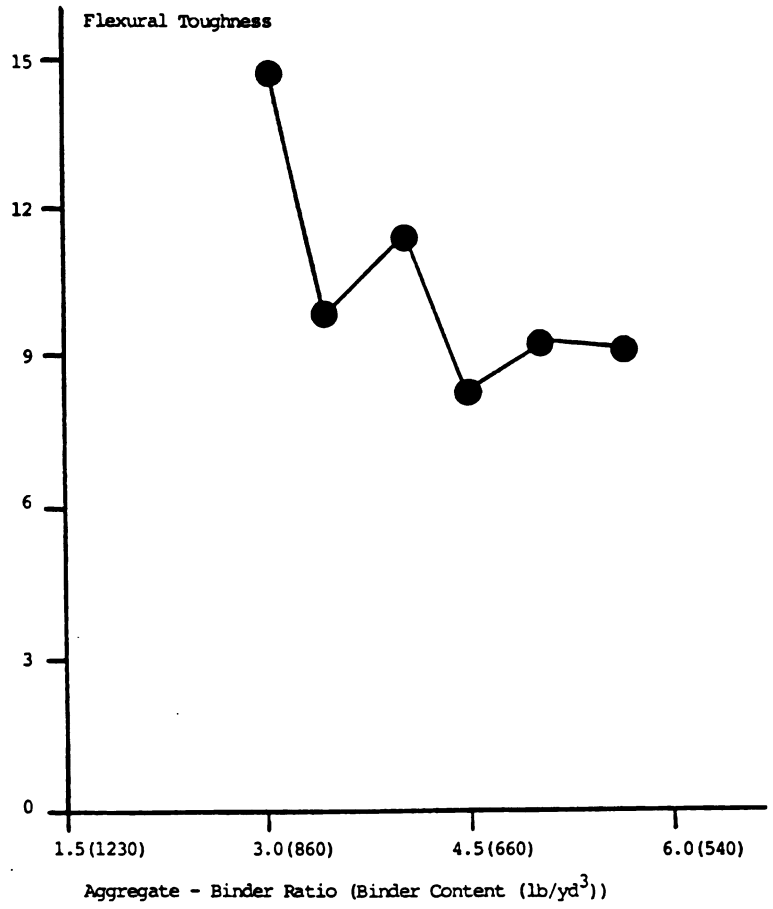

e. Toughness index

to a deflection 5.5 times the deflection at first crack) seems in Figure 4.8.d to generally increase with increasing binder content within the ranges considered in this sutdy. Flexural toughness index (defined as the energy absorption capacity divided by the area underneath the flexural load-deflection curve up to first crack) is observed in Figure 4.8.e to have a tendency, with some exceptions, to increase with increasing binder content. One may conclude from Figure 4.7.a and 4.8 that the flexural strength and toughness characteristics of steel fiber reinforced concrete tend to improve rather significantly with the increase in binder content. Figures 4.7.b and 4.9 present the effects of binder content on the compressive performance characteristics of steel fiber reinforced concrete. The compressive energy absorption capacity in Figure 4.9.c is defined as the area underneath the compressive stress-strain curve up to a strain 5.5 times the strain at peak stress; and the compresive toughness index in Figure 4.9.d is defined as teh energy absorption capacity divided by the pre-peak area underneath the stress-strain curve. It may be concluded from Figures 4.7.b and 4.9 that the compressive performance of steel fiber reinforced concrete is not significantly influenced by the binder content within the range of variables considered in this study.

4.4.b Superplasticizer Content: The effects of superplasticizer content on slump, inverted slump cone and subjective workability of steel fiber reinforced concretes with otherwise comparable mix proportions are shown in Figures 4.10.a, b and c, respectively. While the slump is only slightly increased with the increase in superplasticizer content, there is a consistent drop in inverted slump cone time

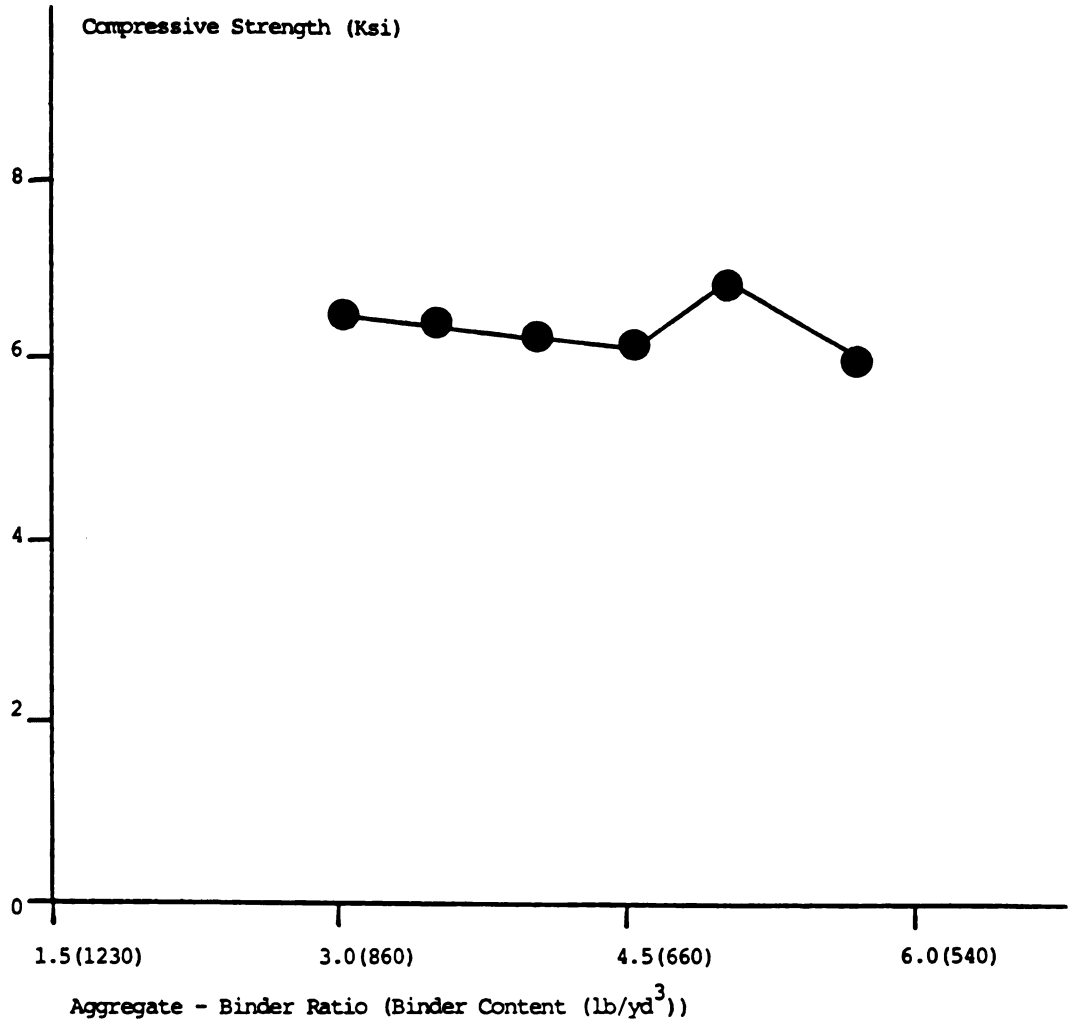

a. Compressive strength

Figure 4.9: Effects of binder content (aggregate-binder ratio) on charactristic compressive properties. 1 in = 25.4 mm, 1 Kip = 4.5 KN, 1 Ksi = 6.9 N/mm^2, 1 Kip in = 114 N.m.

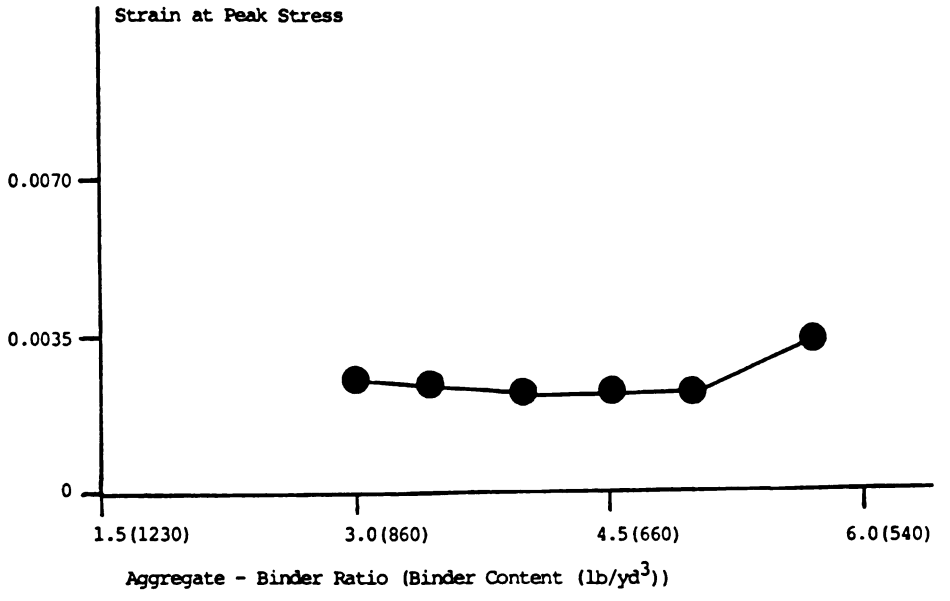

b. Strain at peak compressive stress

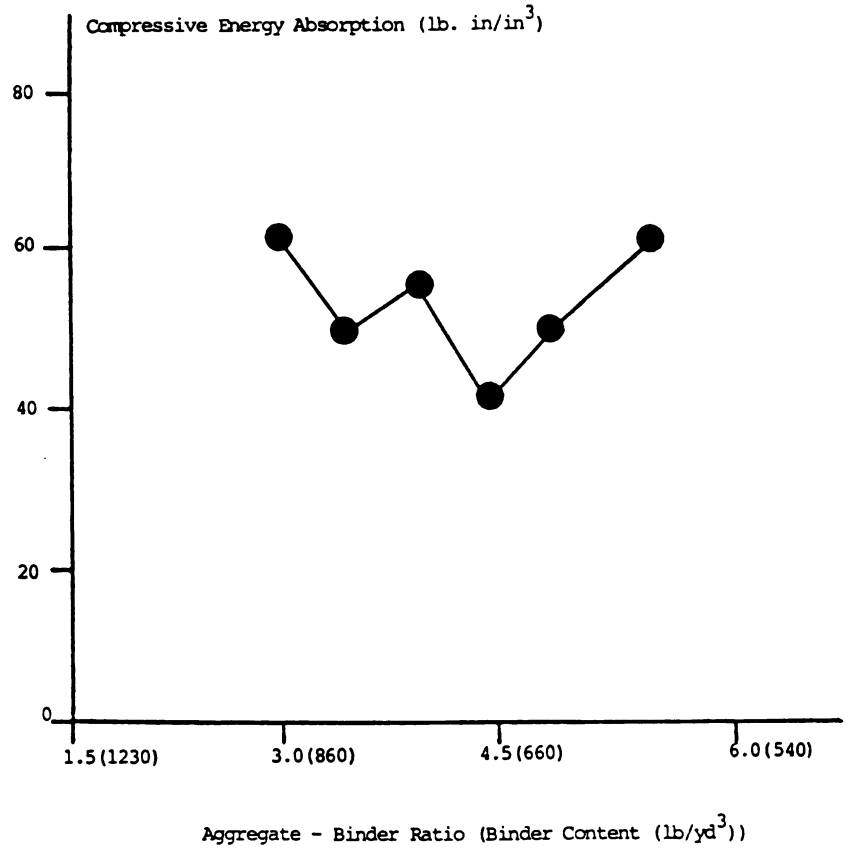

c. Compressive energy absorption capacity

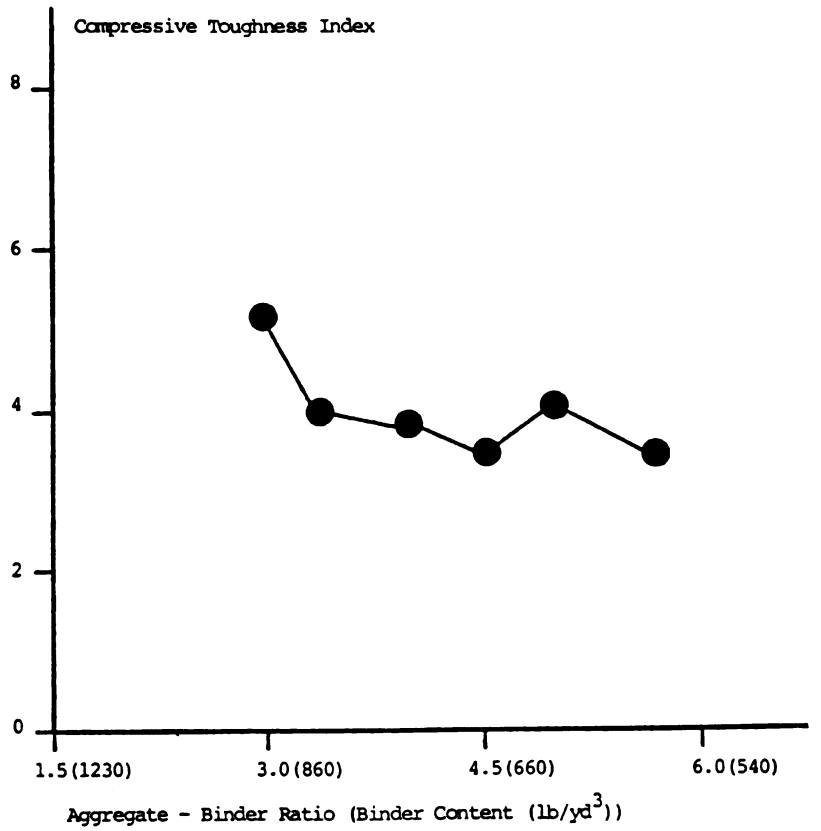

d. Compressive toughness index

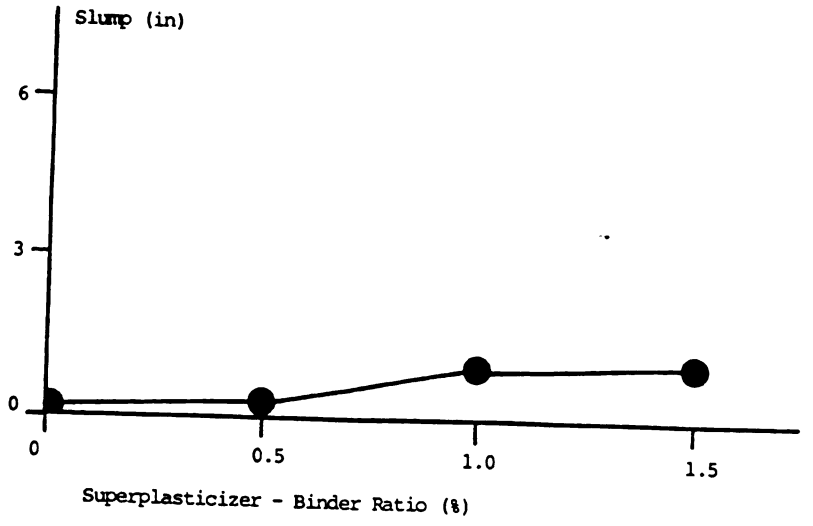

a. Slump 1 in = 25.4 mm

Figure 4.10: Effects of superplasticizer content on fresh mix workability of steel fiber reinforced concrete.

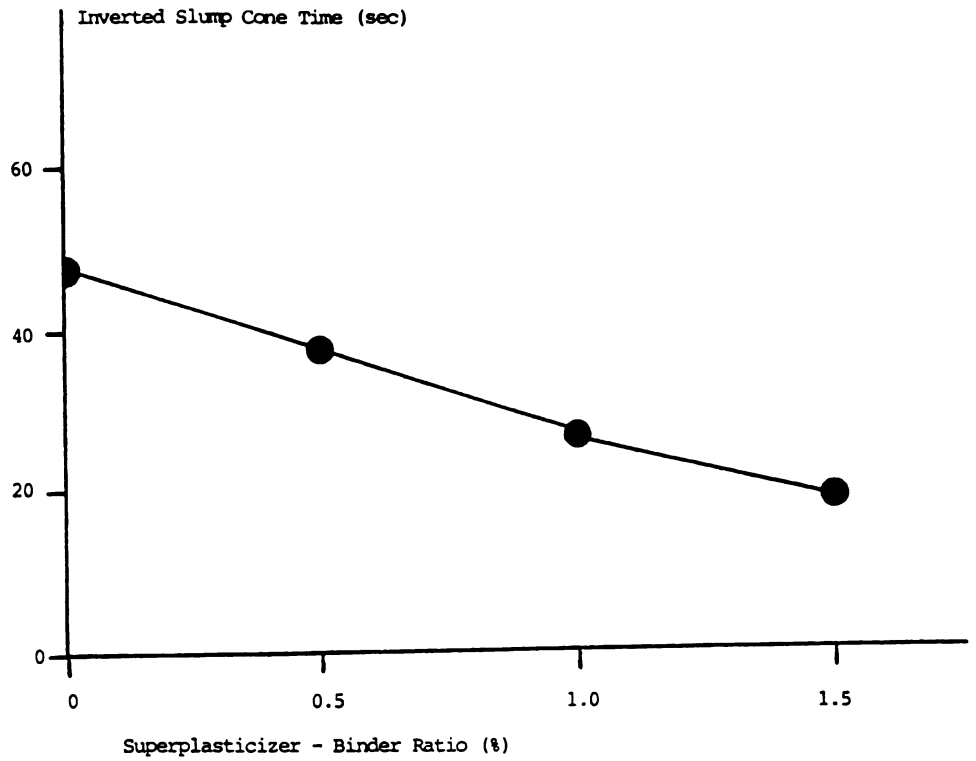

b. Inverted slump cone time

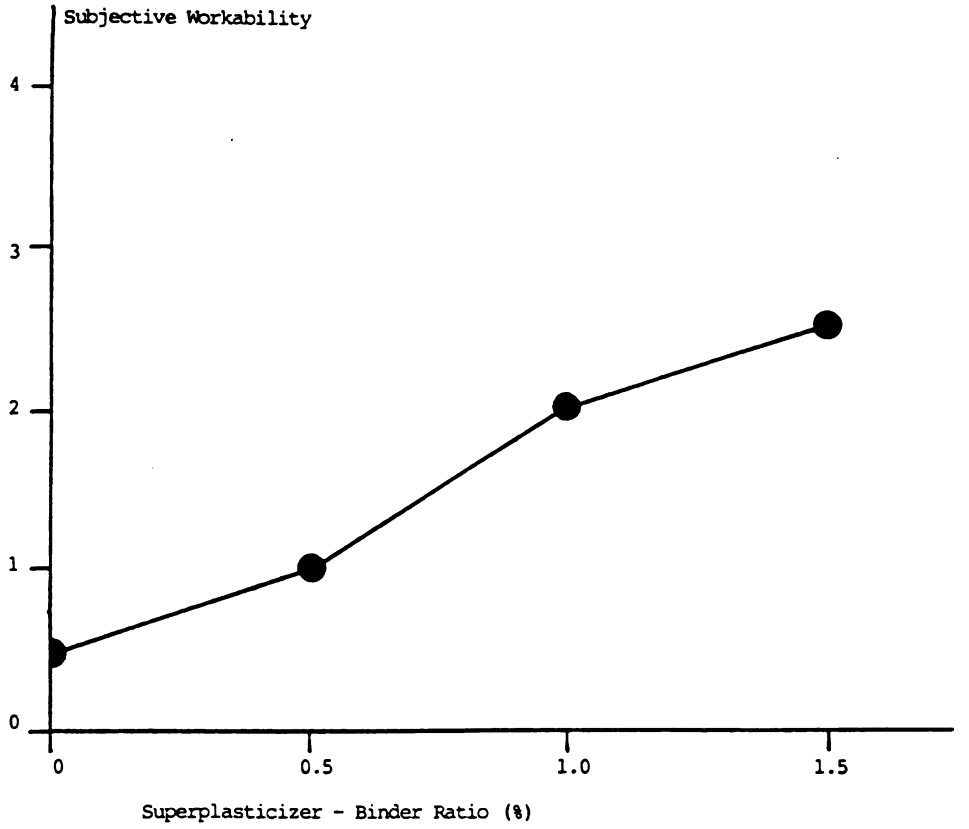

c. Subjective workability

and a consistent increase in subjective workability indicating that the increase in superplasticizer content has positive effects on the compactibility and workability properties of steel fiber reinforced concrete (within the ranges of mix variables considered in this study). There, however, seems to be a maximum superplasticizer content beyond which the fresh mix workability would not be improved significantly.

Figures 4.11.a and 4.11.b present the flexural load-deflection and the compressive stress-strain relationships of comparable steel fiber reinforced concrete mixtures with different superplasticizer content. Characteristic flexural and compressive properties of steel fiber reinforced concrete (as derived from Figure 4.11) are shown in Figures 4.12 and 4.13, respectively, as functions of the superplasticizer content of the mix. The general conclusion that can be derived from Figure 4.11 and 4.12 is that there is a slight improvement in the flexural performance characteristics resulting from the increase in superplasticizer content. Figures 4.11.b and 4.13, however, do not show any significant dependence of the compressive performance of steel fiber reinforced concrete on the superplasticizer content of the mix.

4.4.c Water-Binder Ratio: The increase in water-binder ratio is observed in Figure 4.14 to improve all aspects of the fresh mix workability. It is, however, worth mentioning that excess water-binder ratios may generate concrete matrices with high fluidity in which the steel fibers tend to settle down. The water content

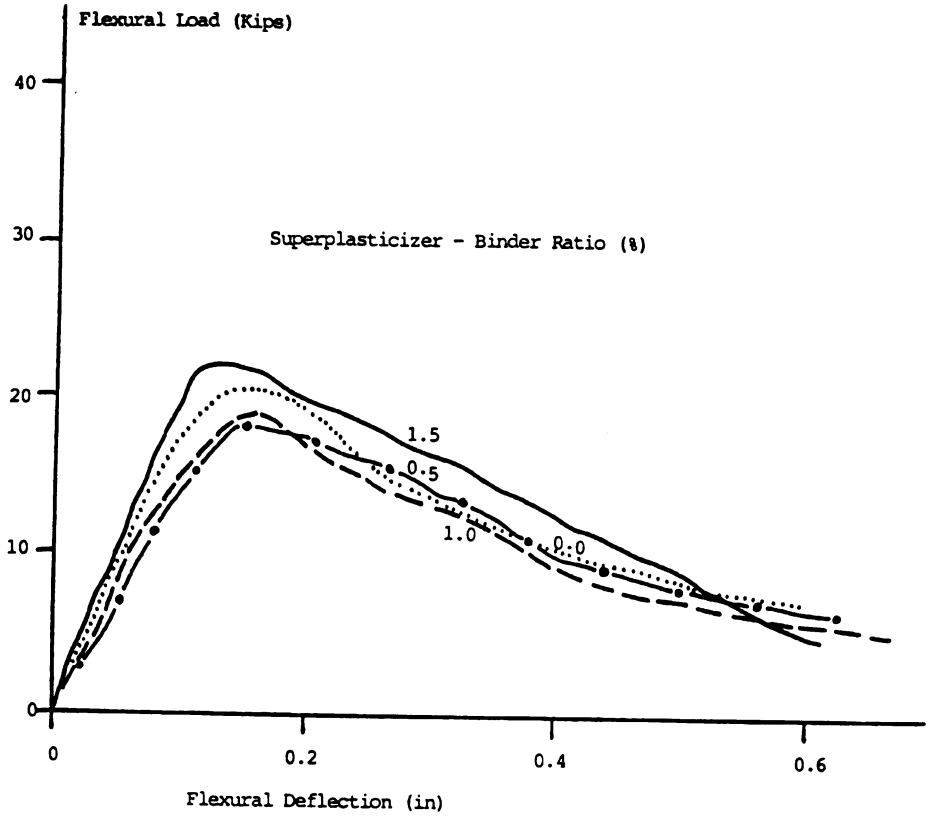

a. Flexural load-deflection relationship

Figure 4.11: Effects of superplasticizer content on flexural and compressive performance of steel fiber reinforced concrete. 1 in = 25.4 mm, 1 Kip = 4.5 KN, 1 Ksi = 6.9 N/mm^2.

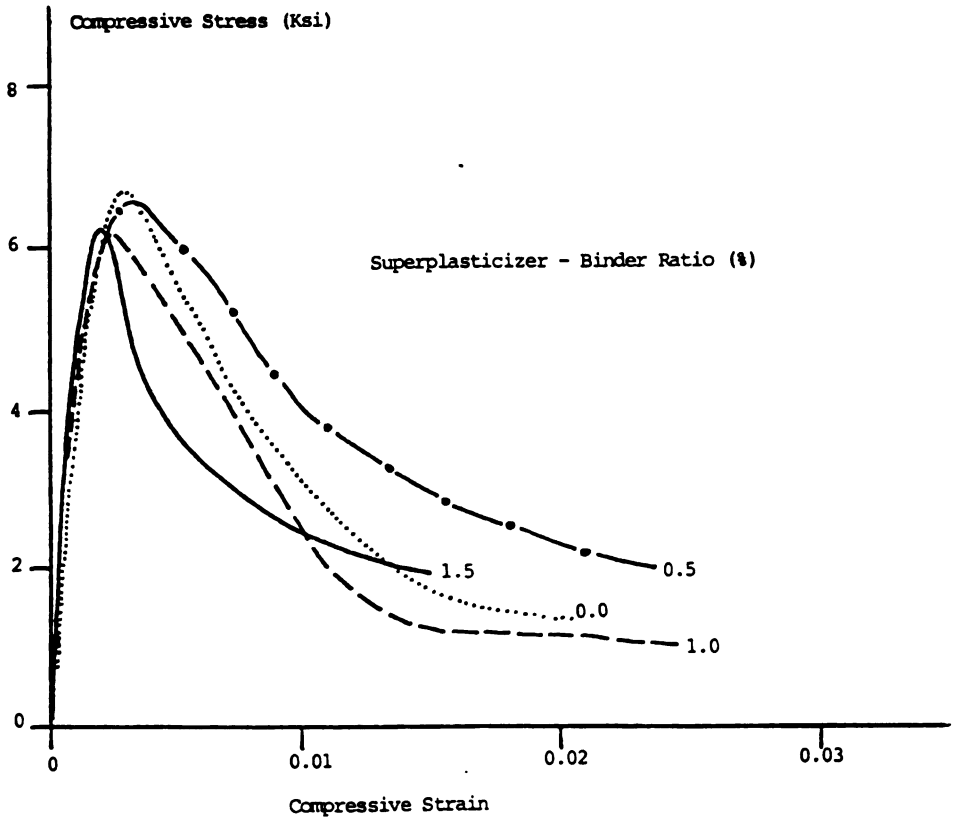

b. Compressive stress-strain relationship

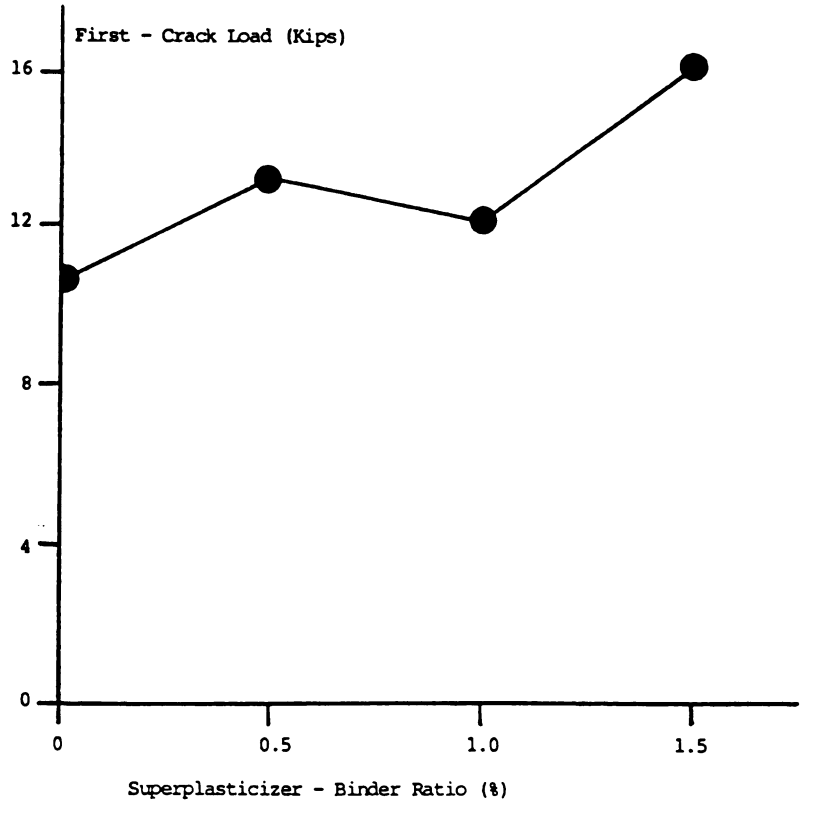

a. First crack load

Figure 4.12: Effects of superplasticizer content on the flexural charactristics of steel fiber reinforced concrete. 1 in = 25.4 mm, 1 Kip = 4.5 KN, 1 Ksi = 6.9 N/mm^2, 1 Kip.in = 114 N.m.

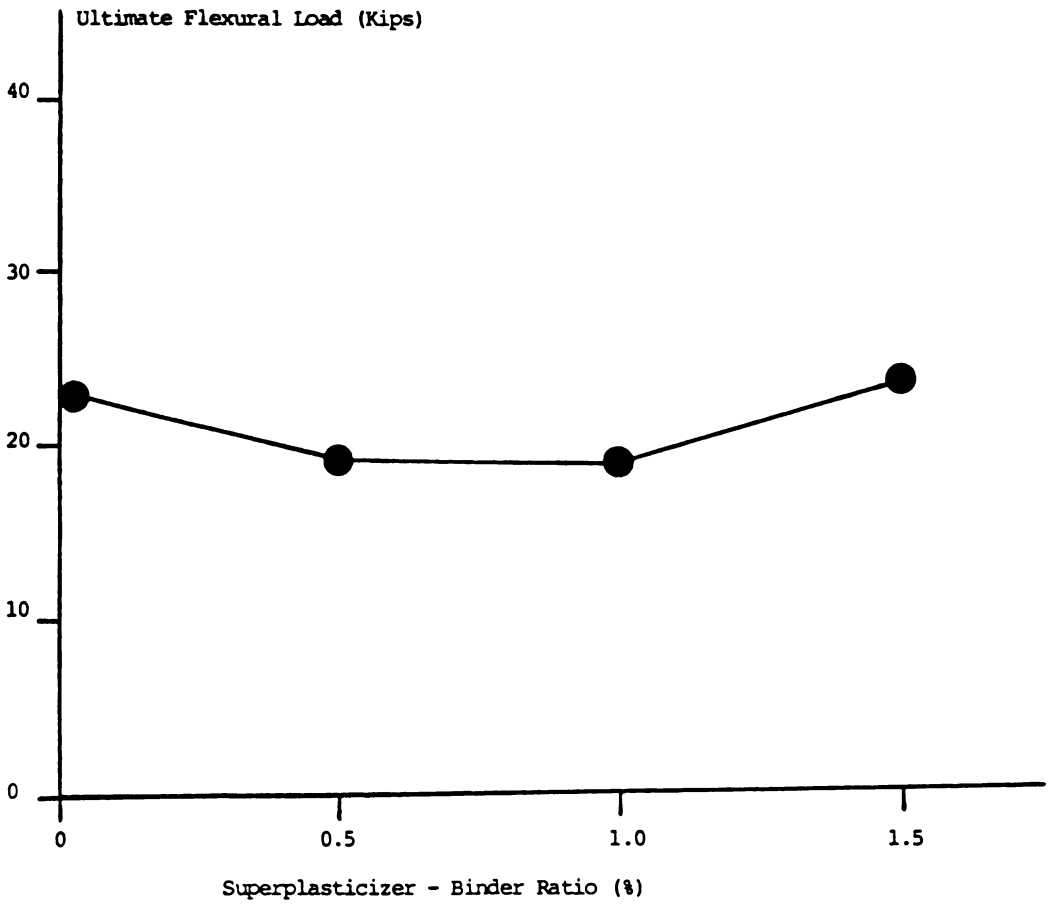

b. Ultimate load

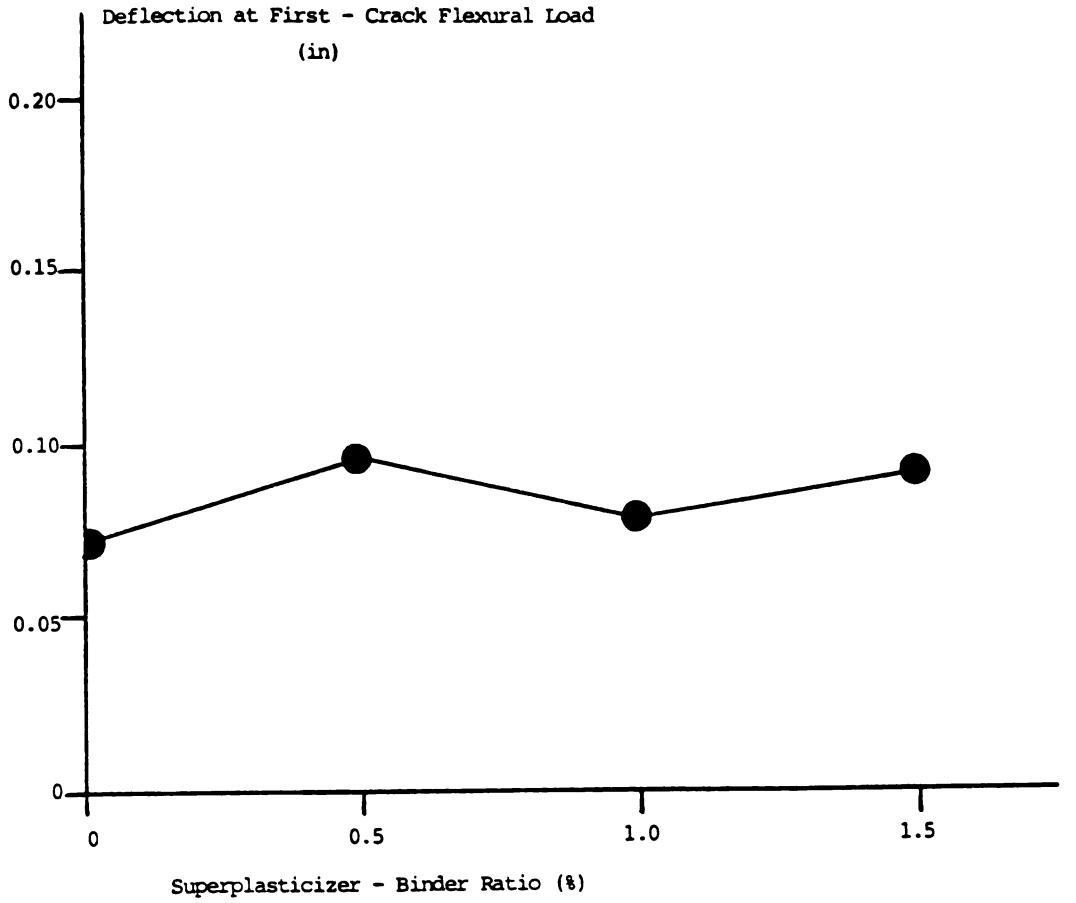

c. Deflection at first crack

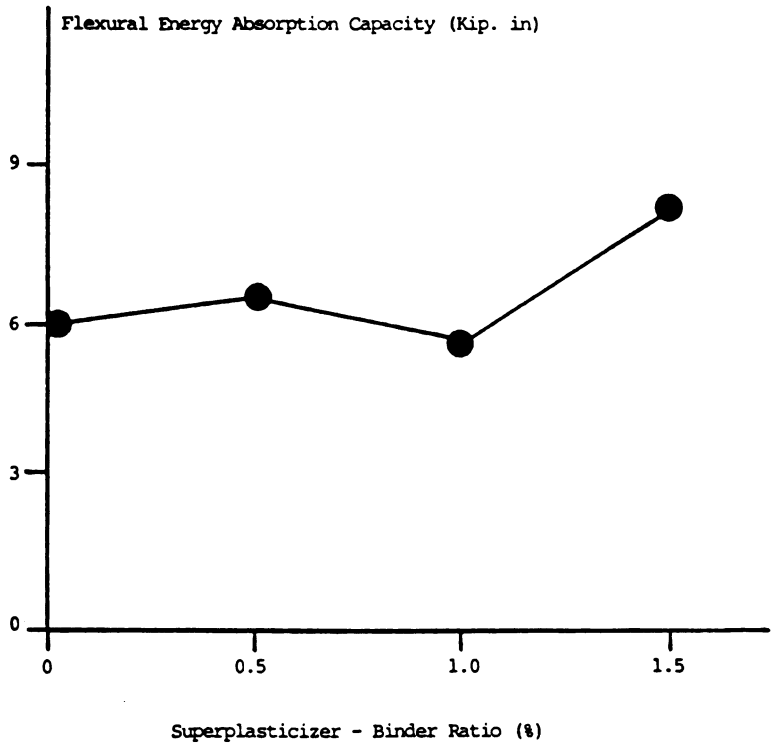

d. Energy absorption capacity

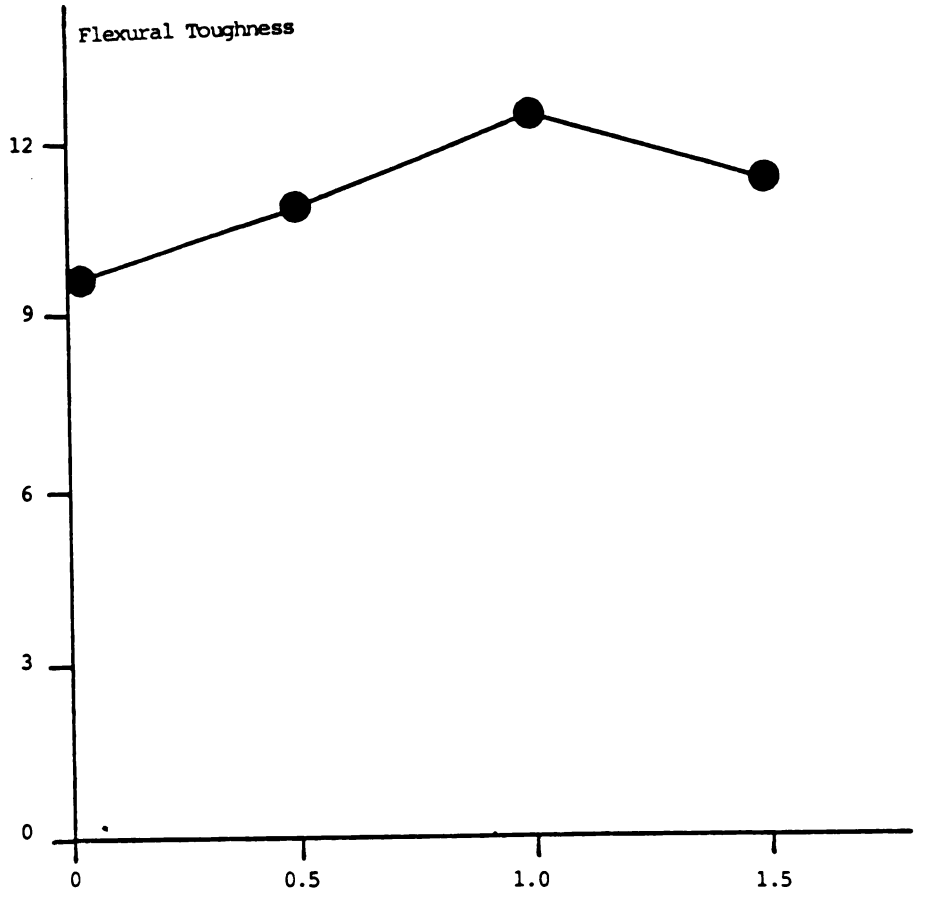

e. Toughness index

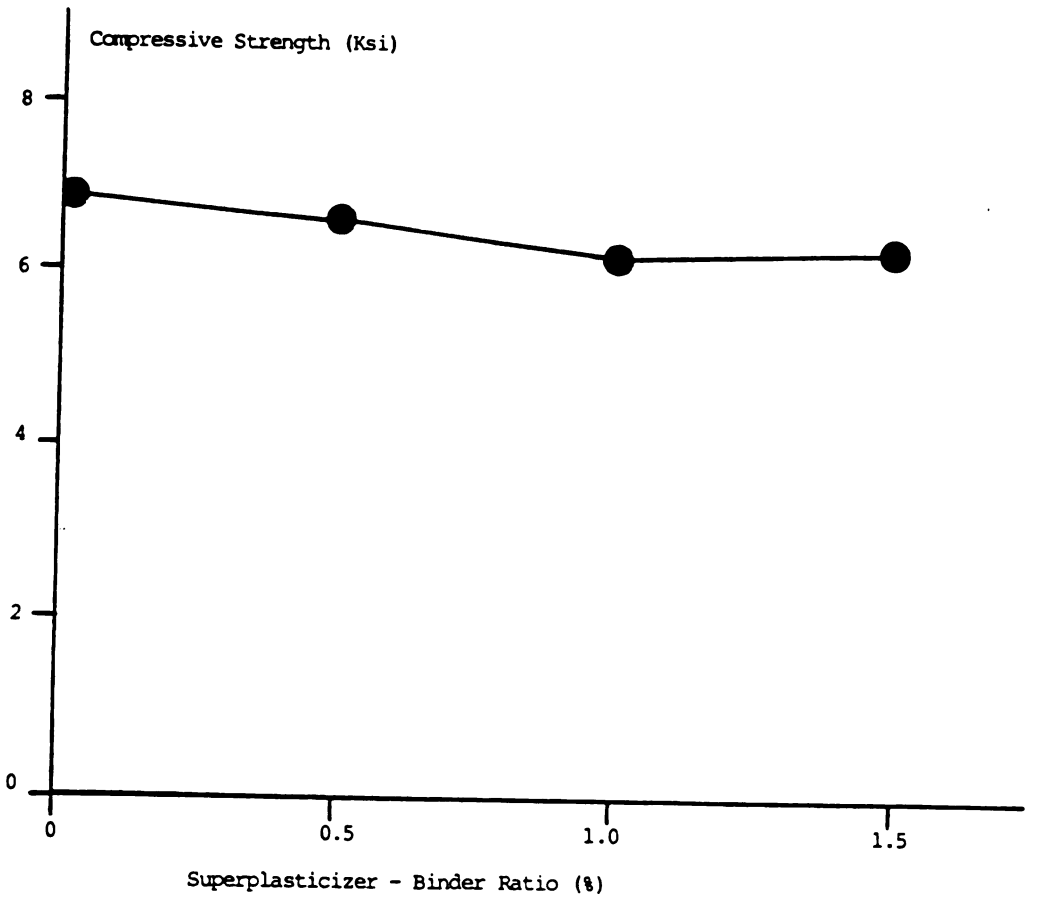

a. Compressive strength

Figure 4.13: Effects of superplasticizer content on the charactristic compressive performance. 1 in = 25.4 mm, 1 Ksi = 6.9 N/mm^2, 1 Kip.in = 114 N.m.

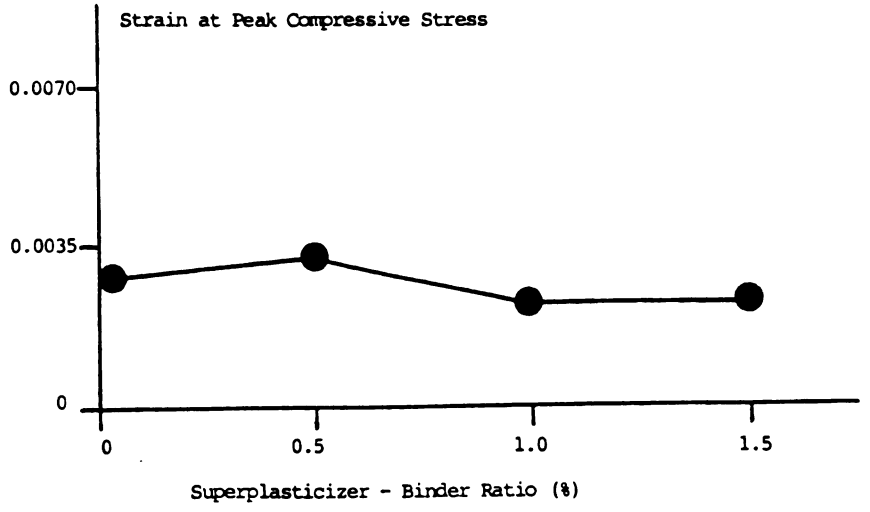

b. Strain at peak compressive stress

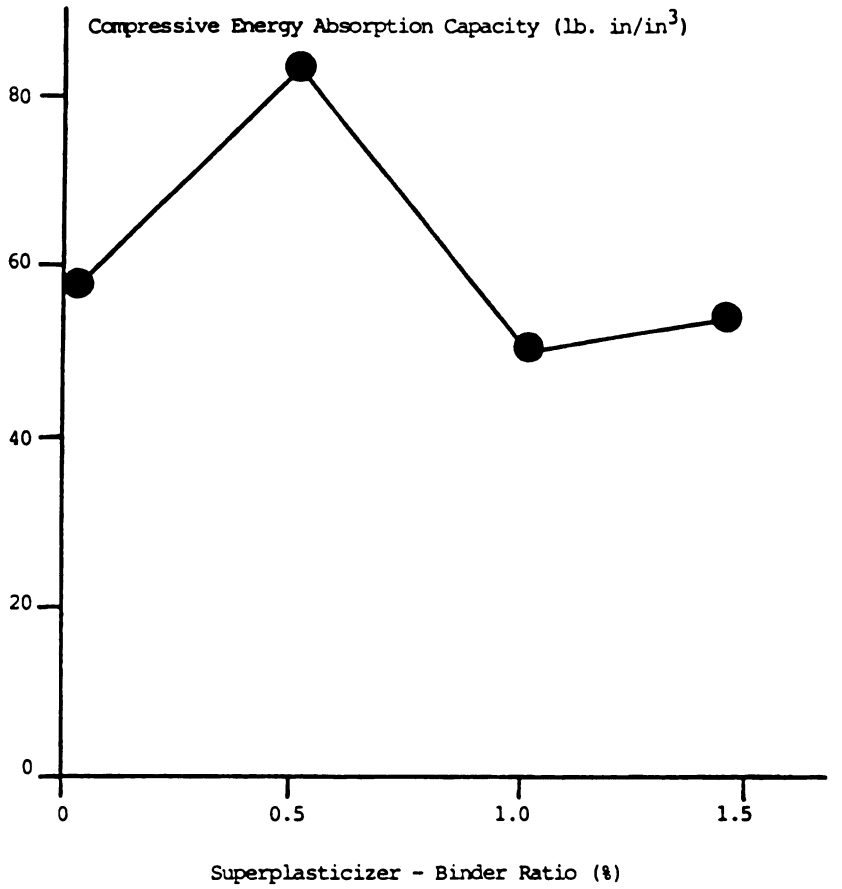

c. Compressive energy absorption capacity

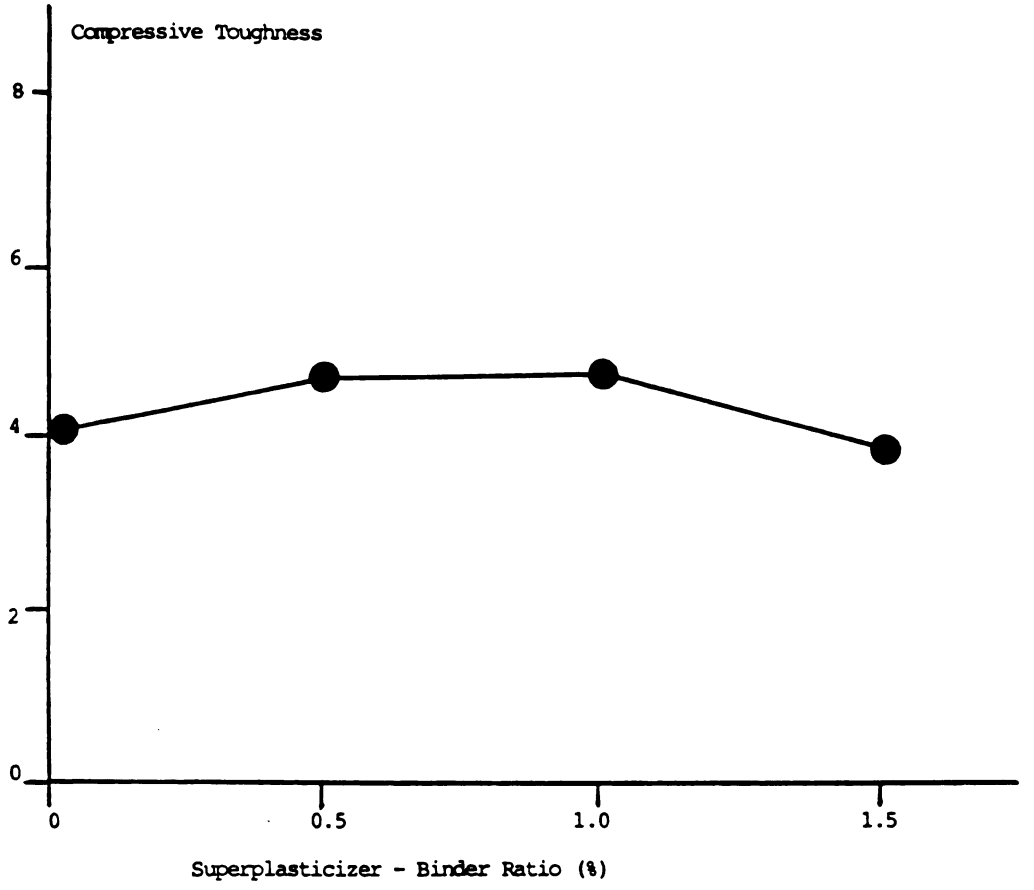

d. Compressive toughness index

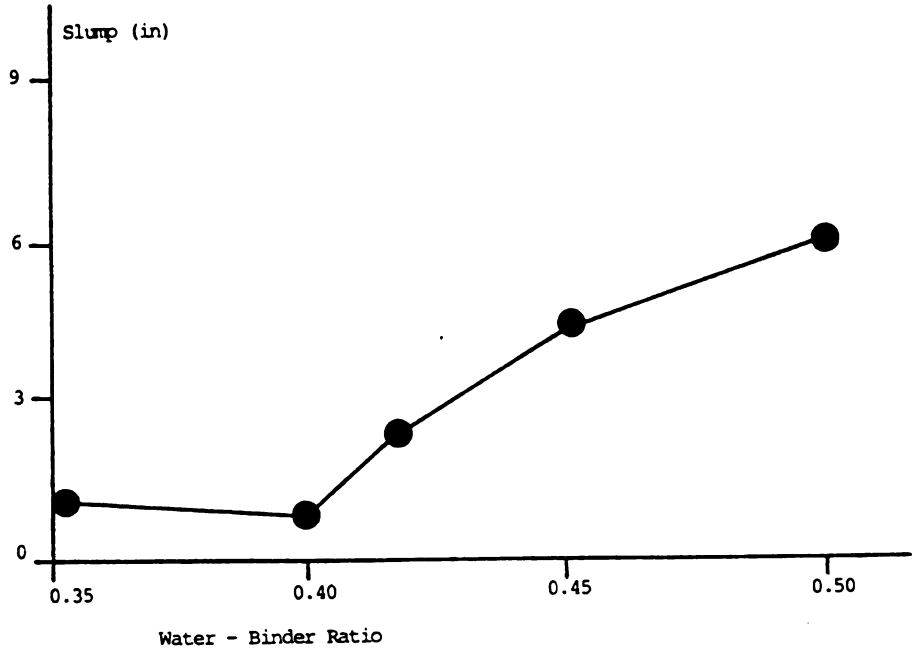

a. Slump. 1 in = 25.4 mm

Figure 4.14: Effects of water content on fresh mix workability.

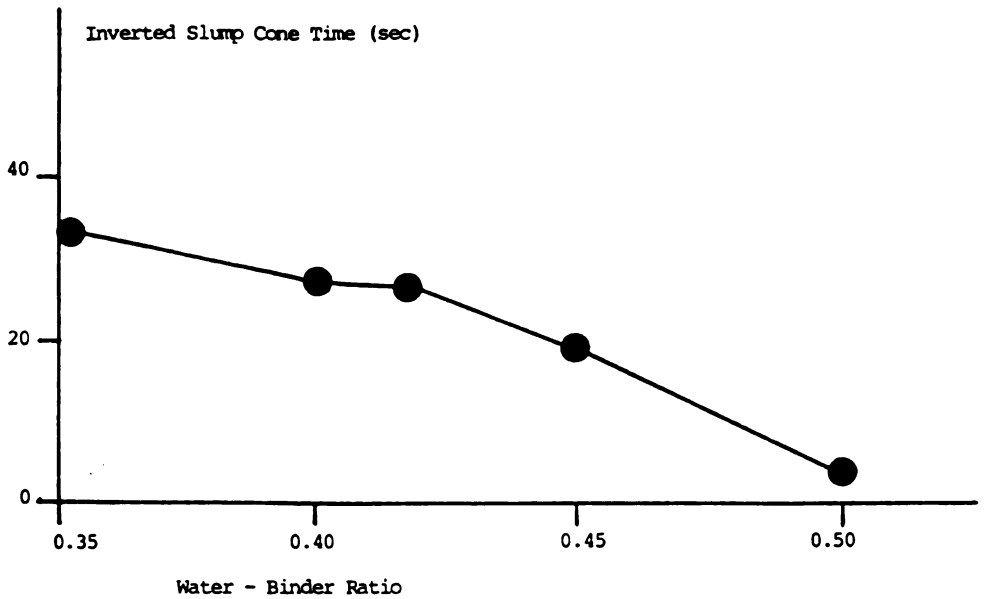

b. Inverted Slump cone time

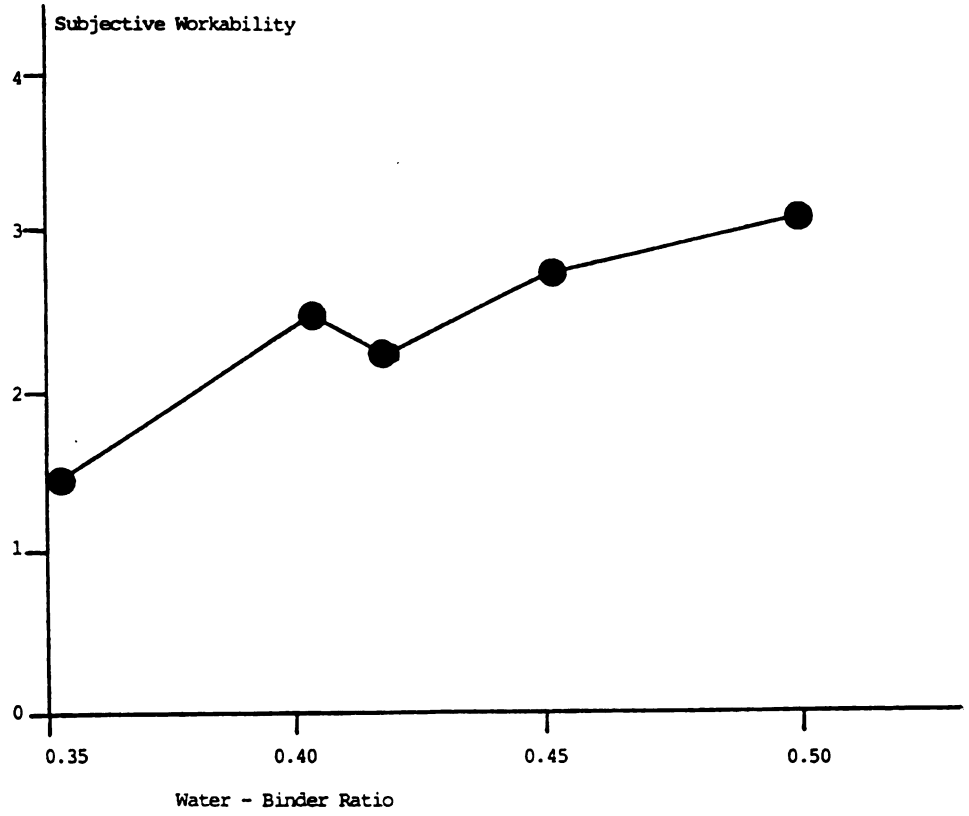

c. Subjective workability

effects of the flexural and compressive performance of otherwise comparable steel fiber reinforced concretes are shown in Figures 4.15, 4.16 and 4.17. Figures 4.15.a and 4.16 indicate that the flexural performance is not significantly influenced by the variations in water-binder ratio within the range considered in this study. There is only some drop in the toughness index (indicating damage to the post-peak performance of steel fiber reinforced concrete under flexural loads) resulting from the decrease in water-cement ratio. Figures 4.15.b and 4.17.a are indicative of the drop in compressive strength resulting from the increase in water-binder ratio in the steel fiber reinforced concrete mixtures of this study. The effects of water-binder ratio on the compressive strain at peak stress, energy absorption capacity and toughness, tend, however, to be relatively small as shown in Figures 4.17.b, c and d, respectively.

4.4.d Maximum Aggregate Size: Figures 4.18.a, b and c present the effects of maximum aggregate size on the slump, inverted slump cone time and subjective workability of steel fiber reinforced concrete. There is a general tendency in workability to improve with increasing maximum aggregate size. This is more obvious in the inverted slump cone and subjective workability (Figures 4.18.b and c) than the slump (Figure 4.18.a). It should be noted that the reduction in maximum aggregate size was achieved in this study by simply eliminating the coarser aggregates from the mix. Hence, mixes with smaller maximum aggregte size tend to have aggregate with a higher degree of fineness. The larger surface area of aggregate in this condition would require higher water and paste contents to

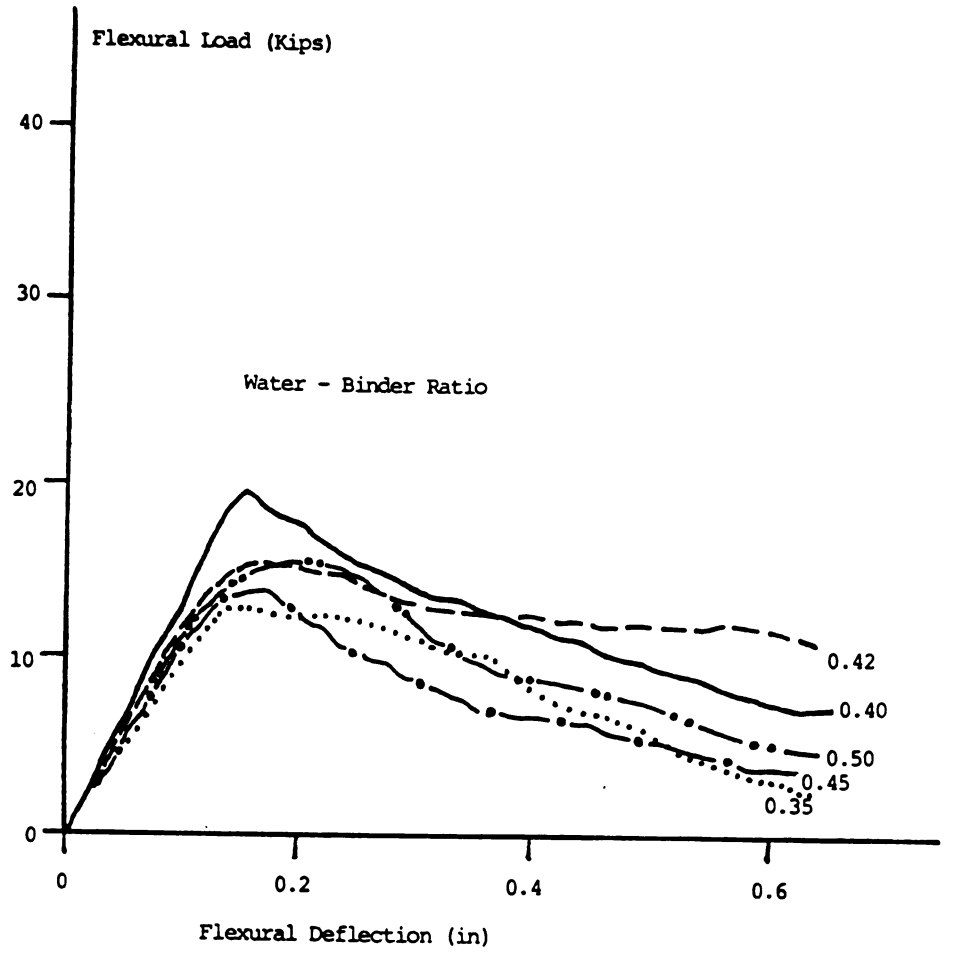

a. Flexural load-deflection relationship

Figure 4.15: Effects of water content on flexural and compressive performance. 1 in = 25.4 mm, 1 Kip = 4.5 KN, 1 Ksi = 6.9 N/mm^2.

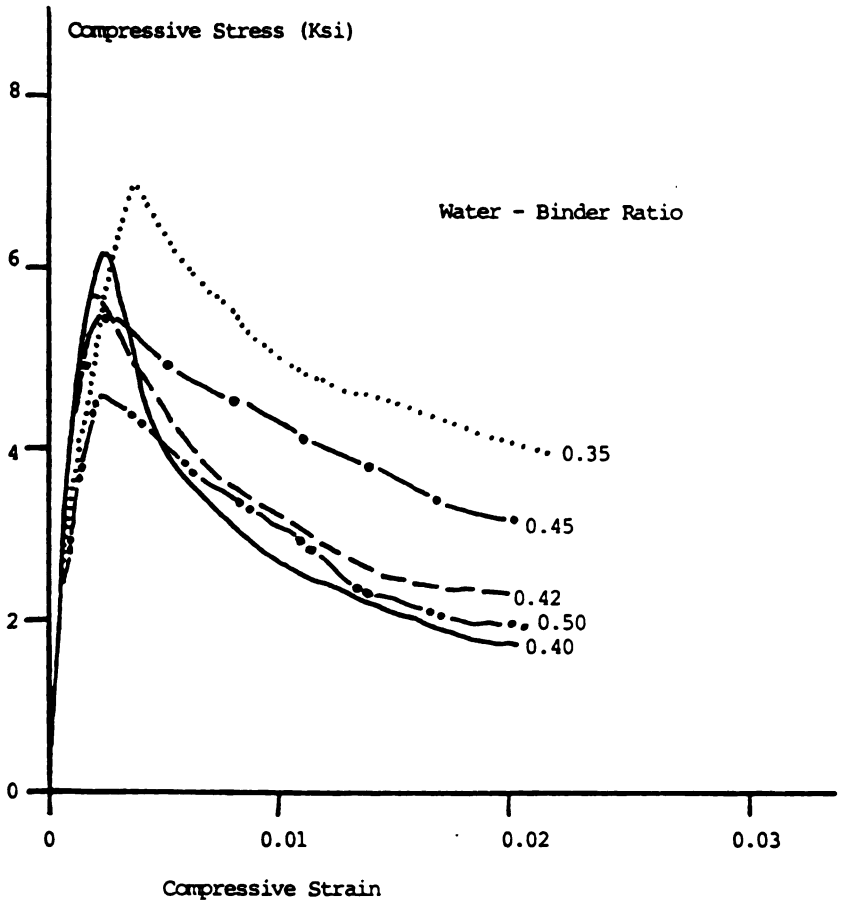

b. Compressive stress-strain curve

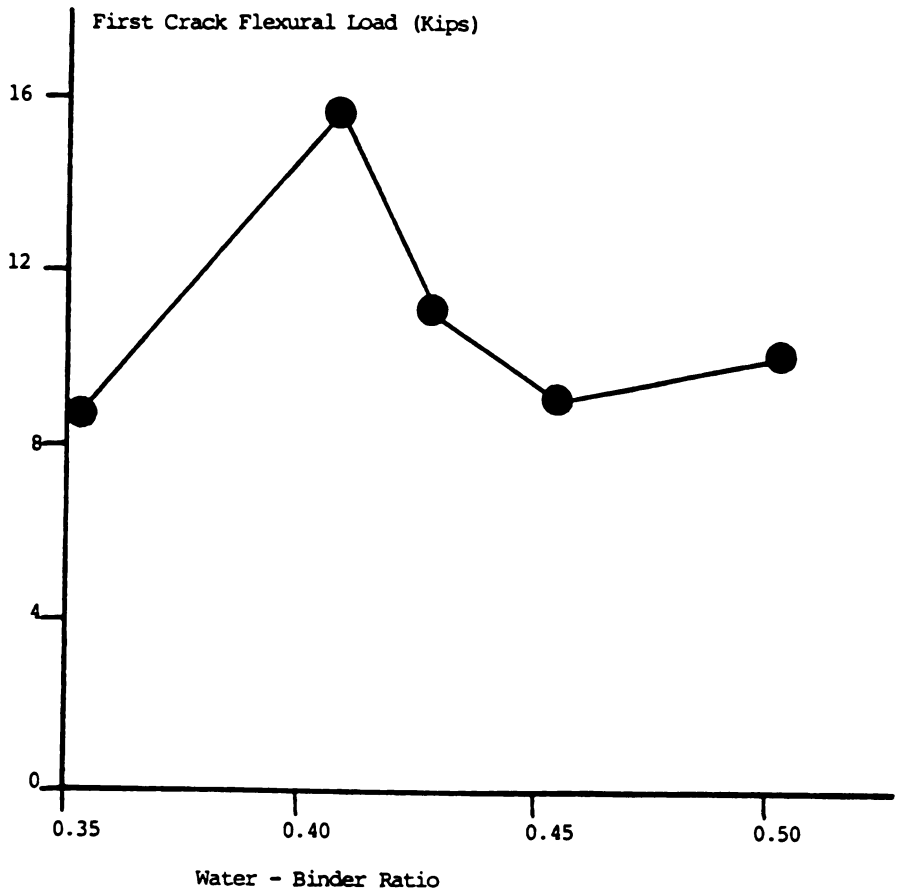

a. First crack load

Figure 4.16: Effects of water content on the flexural performance characteristics.

1 in = 25.4 mm, 1 Kip = 4.5 KN, 1 Ksi = 6.9 N/mm^2, 1 Kip.in = 114 N.m

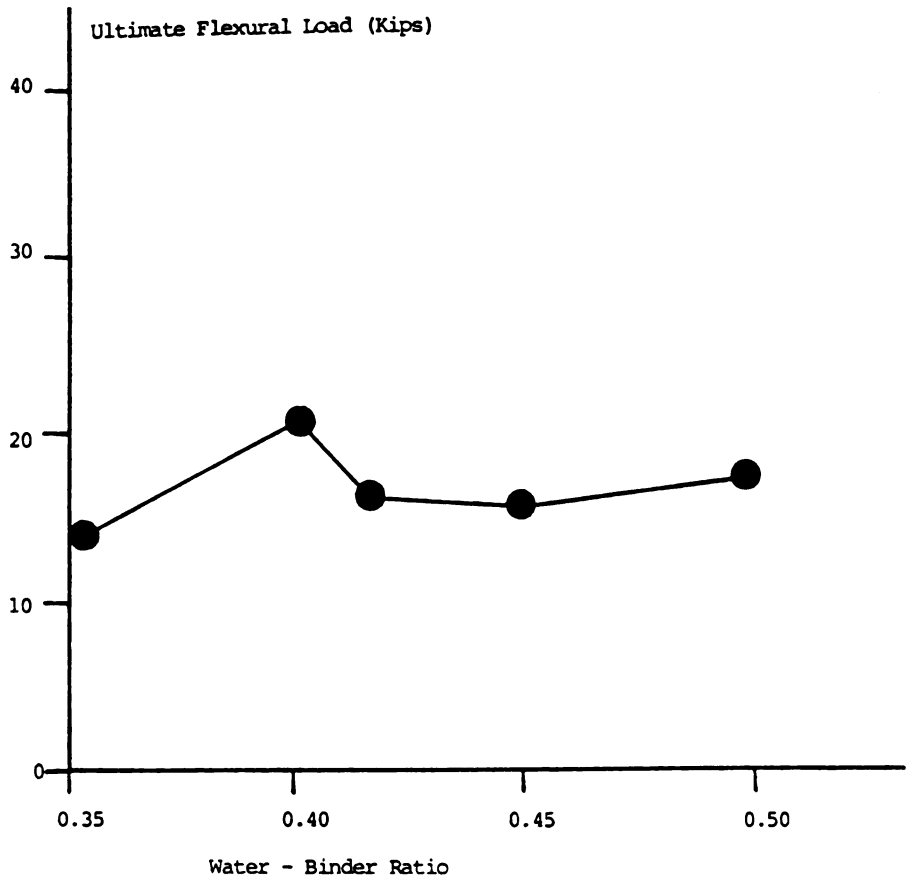

b. Ultimate load

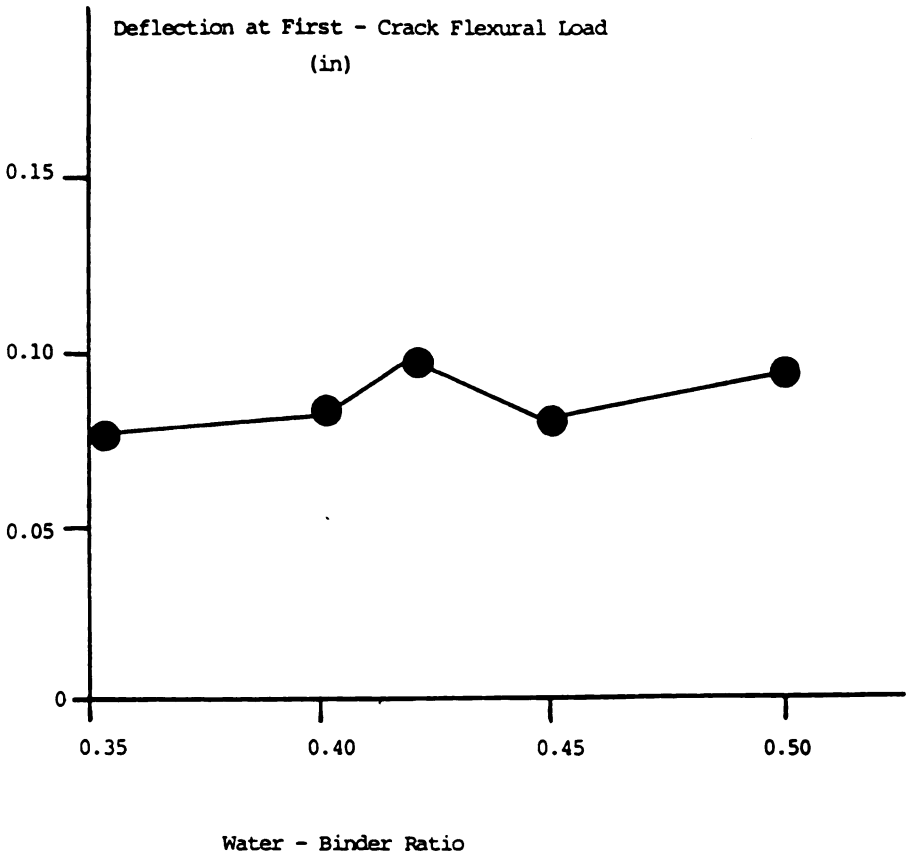

c. Deflection at first crack

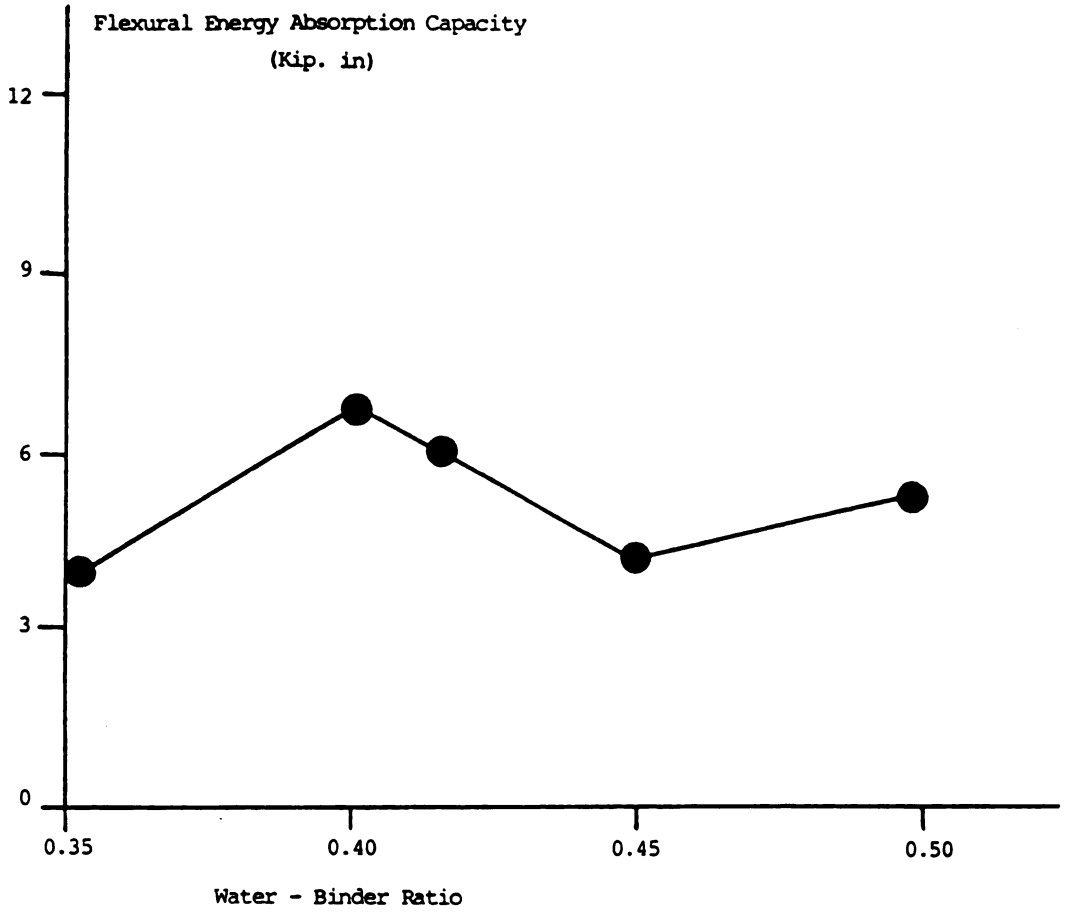

d. Energy absorption capacity

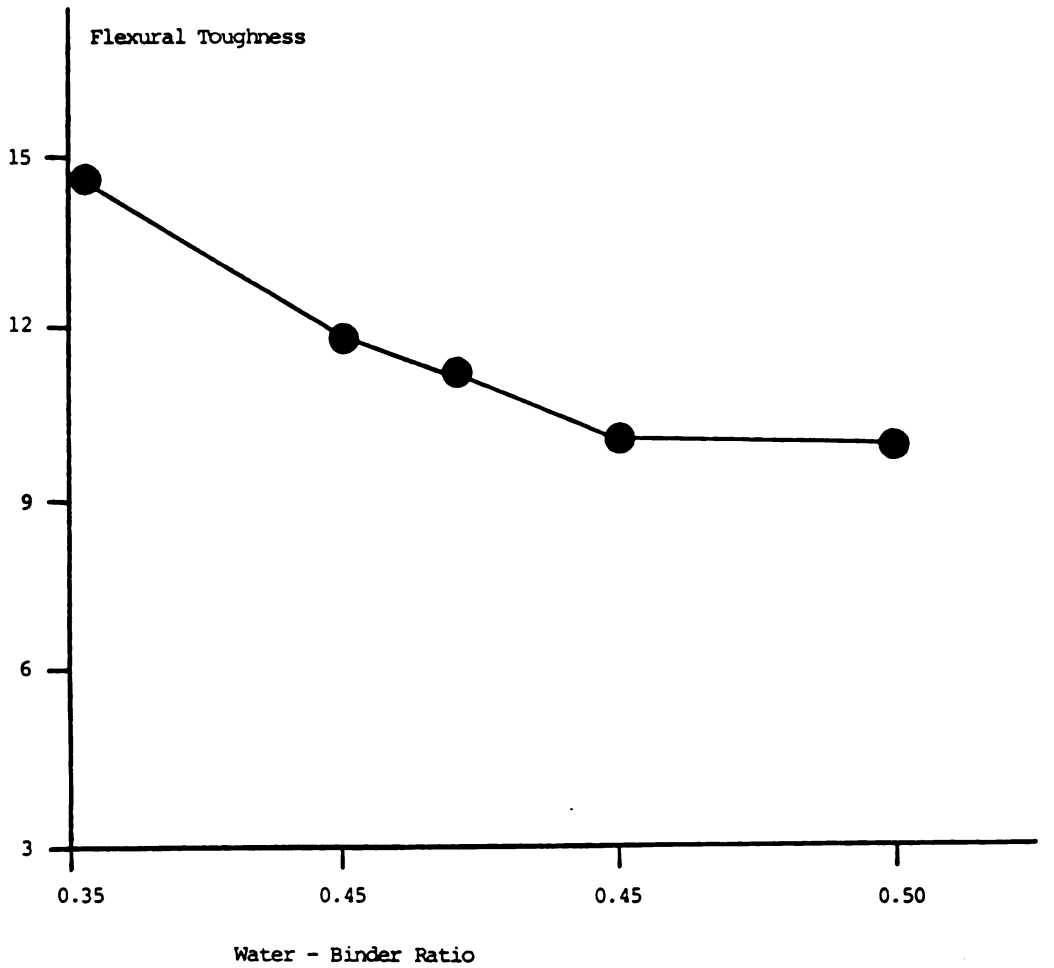

e. Toughness index

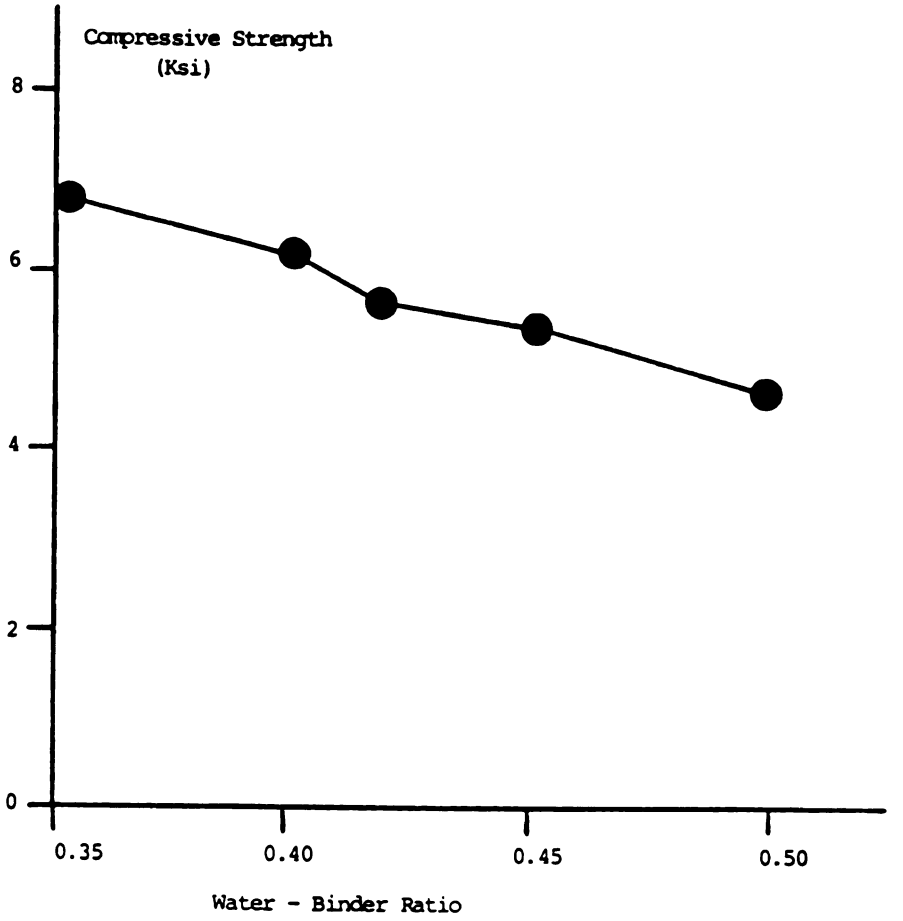

a. Compressive strength

Figure 4.17: Effects of water content on the characteristic compressive performance. 1 in = 25.4 mm, 1 Ksi = 6.9 N/mm^2, 1 Kip.in = 114 N.m.

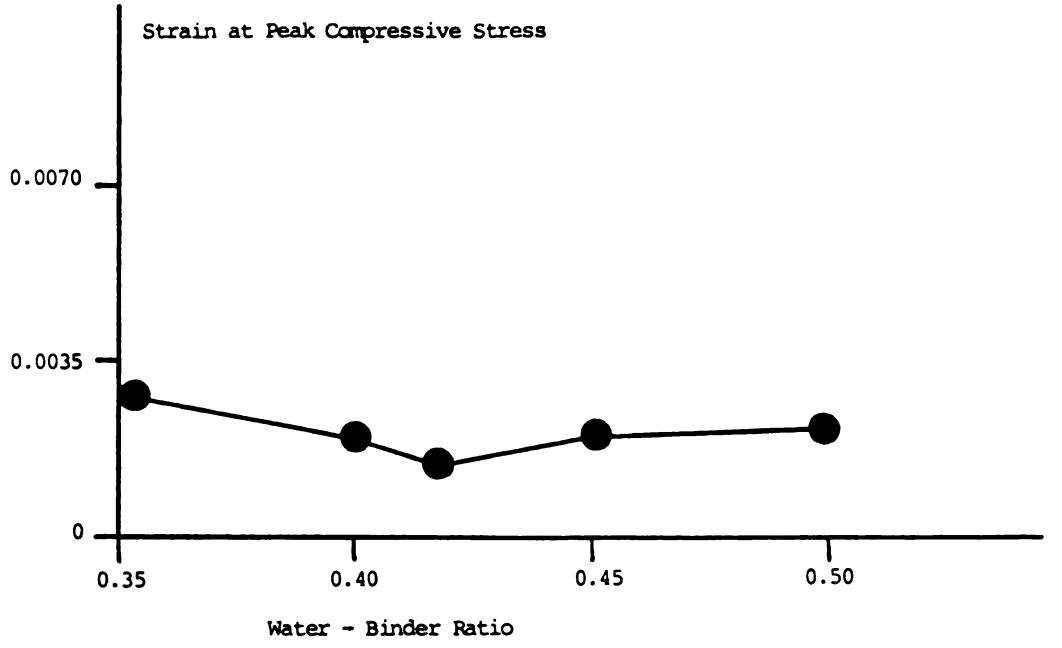

b. Strain at peak compressive stress

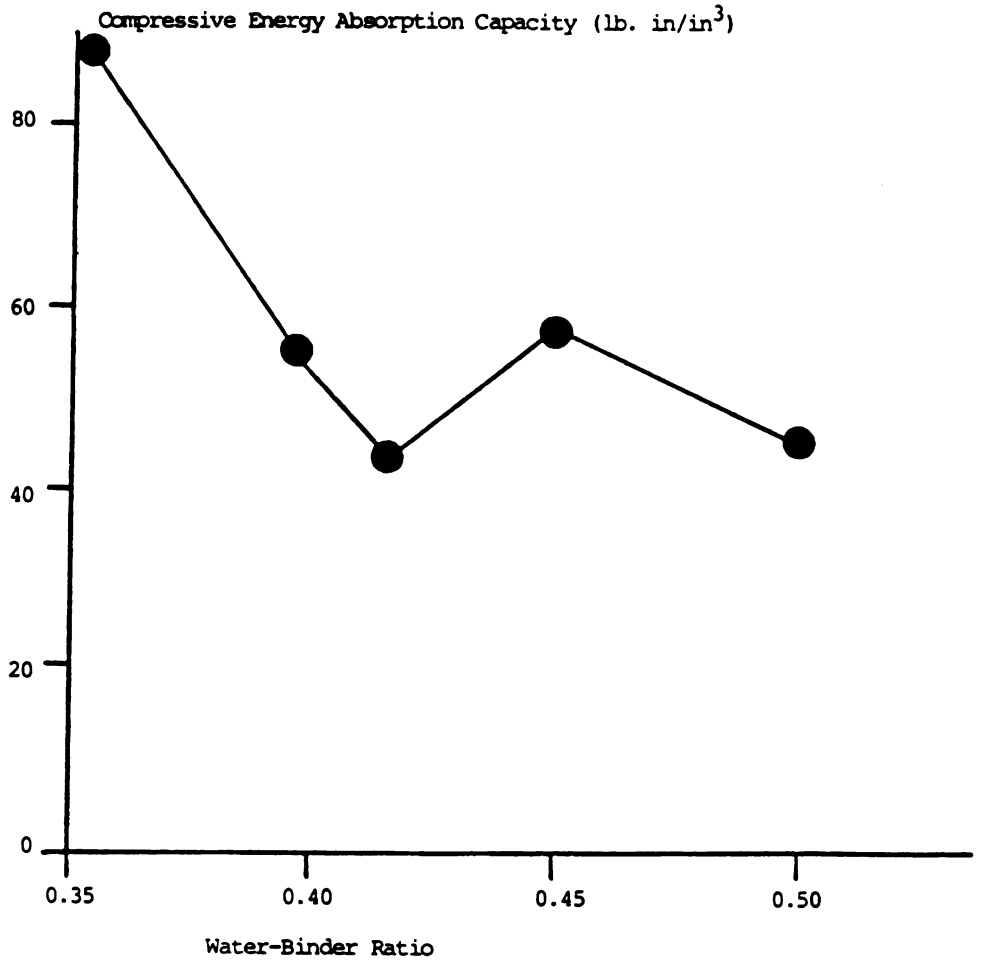

c. Compressive energy absorption capacity

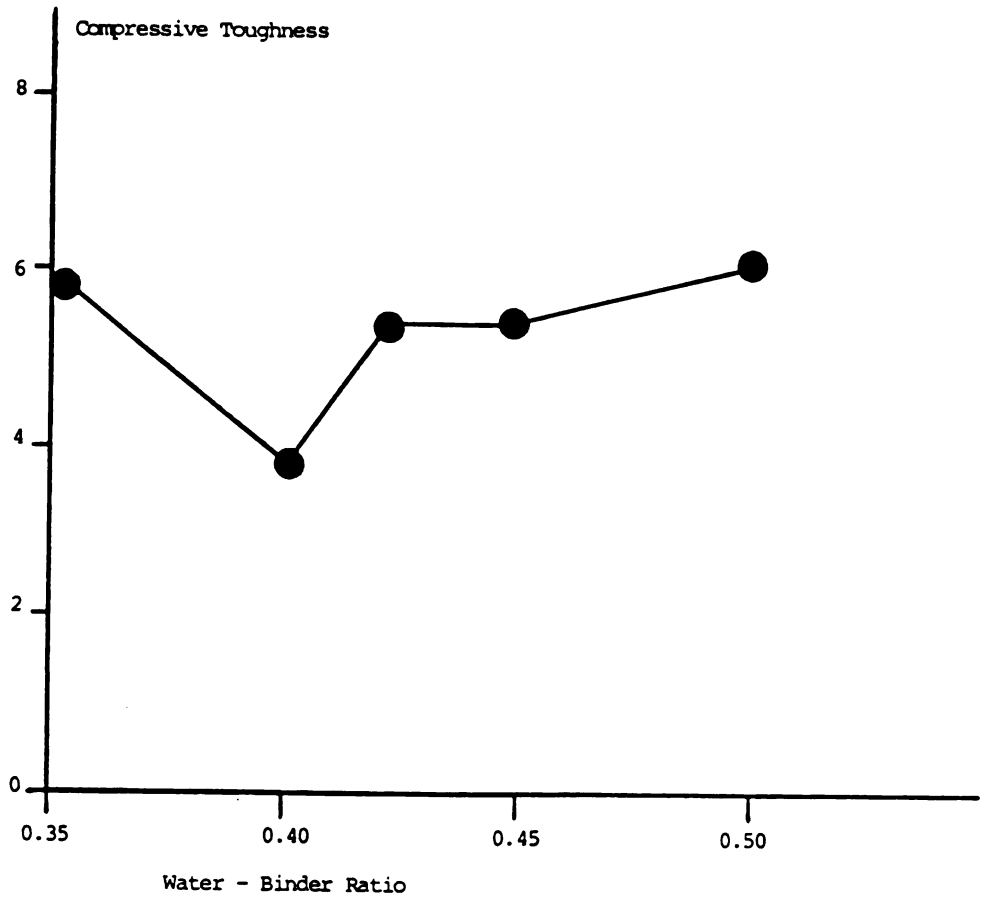

d. Compressive toughness index

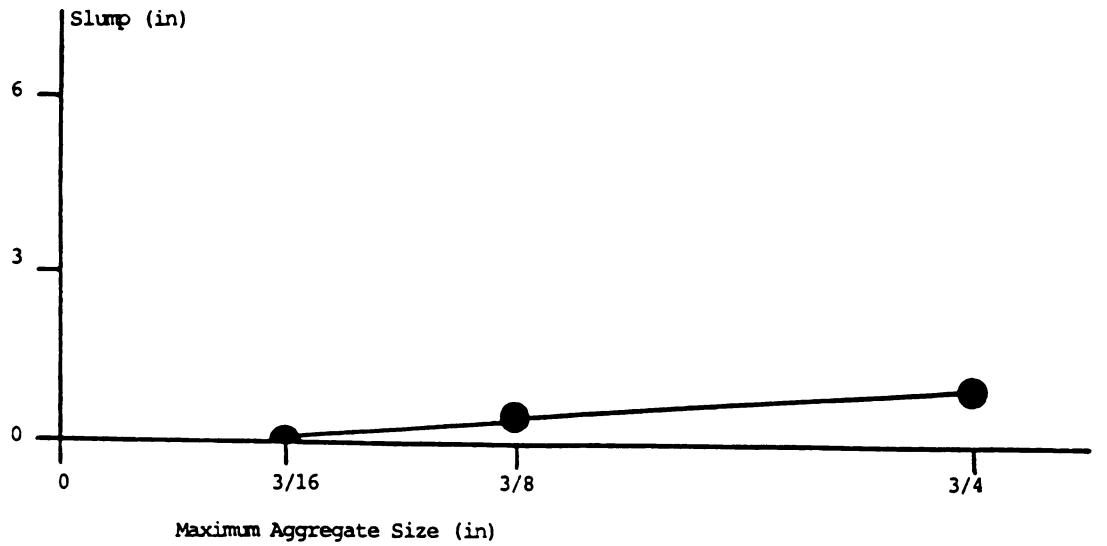

a. Slump. 1 in = 25.4 mm

Figure 4.18: Effects of maximum aggregate size on the fresh mix workability of steel fiber reinforced concrete.

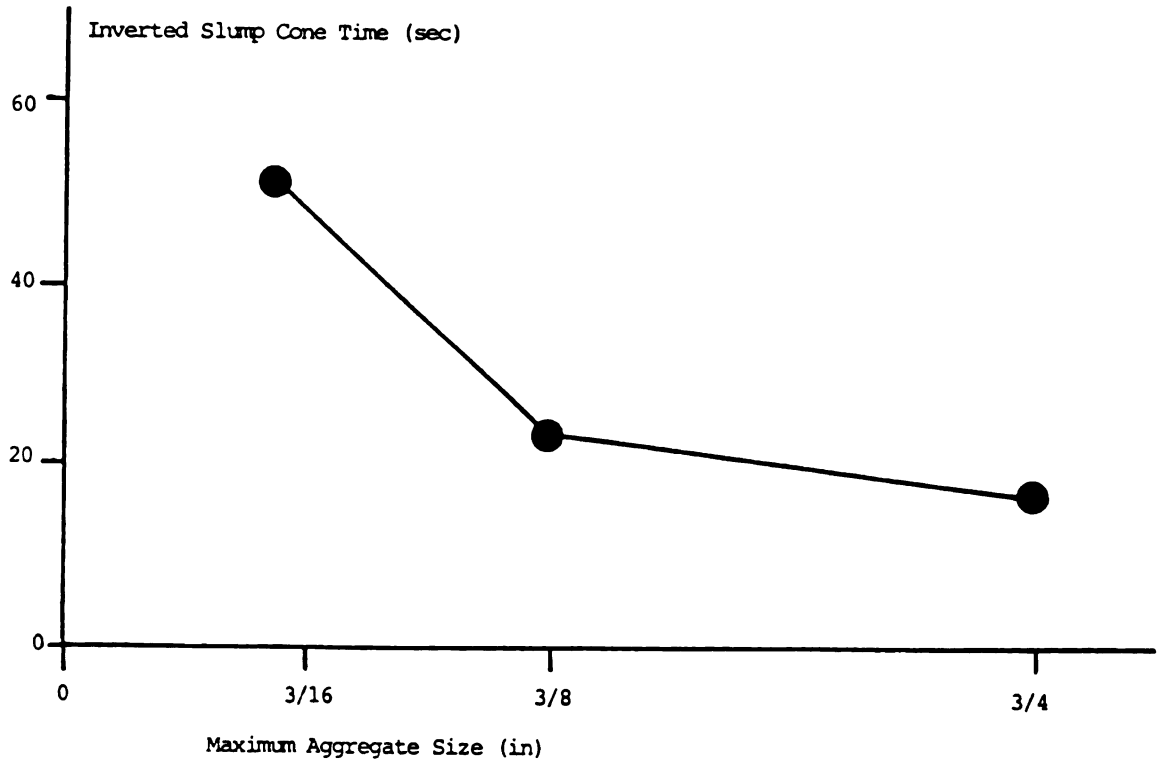

b. Inverted slump cone time

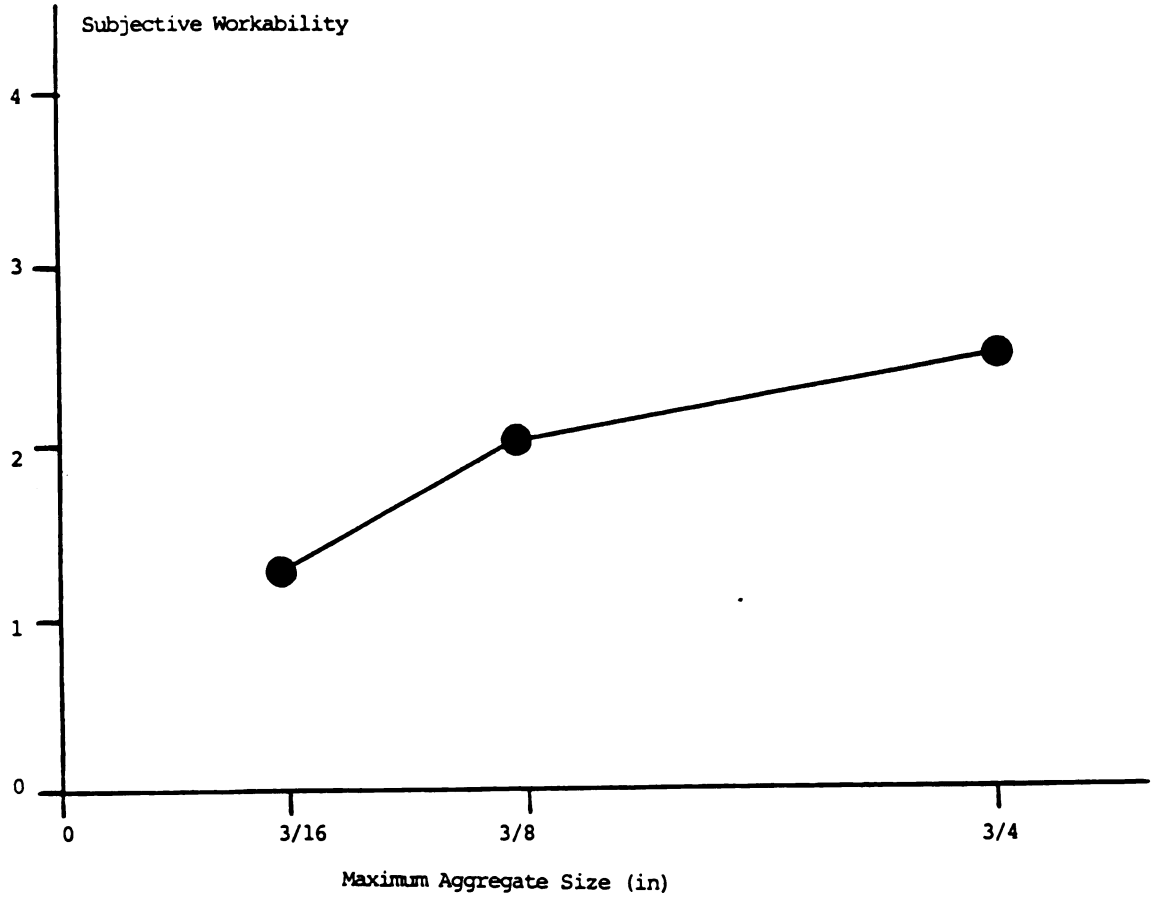

c. Subjective workability

be coated and lubricated. The reduction of maximum aggregate size with no further adjustment of the mix proportions, thus, results in damage to workability.

Figure 4.19, 4.20 and 4.21 summarize the effects of maximum aggregate size on the compressive and flexural performance characteristics of steel fiber reinforced concrete. Figures 4.19.a and 4.20 indicate that the increae in maximum aggregate size results in a slight increase in flexural strength and some more important improvements in the flexural energy absorption capacity and toughness of steel fiber reinforced concrete noting that these conclusions are based on a small set of test data. As far as the compressive behavior is concerned, Figures 4.19.a and 4.21 indicate that the increase in maximum aggregate size does not have major effects on compressive strength of steel fiber reinforced concrete. The limited test data generated does not seem to be sufficient to make further conclusions regarding maximum aggregte size effect on the performance of steel fiber reinforced concrete under compression.

4.4.e Aggregate Gradation: The gradation of aggregates was modified in this study by adjusting the weight ratio of coarse to fine aggregates. Coarser aggregate gradation was obtained by increasing this ratio. The effects of coarse-to-fine aggregate ratio on the slump, inverted slump cone time and subjective workability of fresh steel fiber reinforced concrete mixtures are shown in Figures 4.22.a, b and c, respectively. Slump as a weak representative of steel fiber reinforced concrete workability tends to increase with increasing coarse aggregate content in

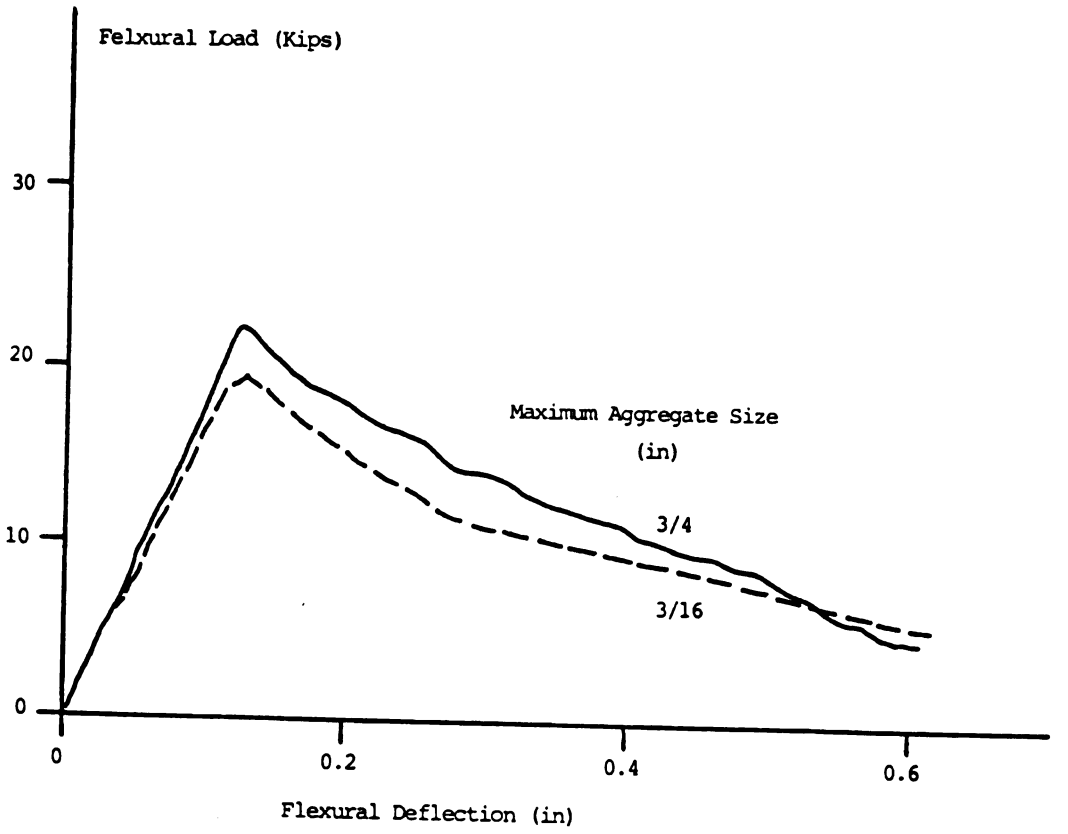

a. Flexural load-deflection relationship

Figure 4.19: Effects of maximum aggregate size on flexural and compressive performance. 1 in = 25.4 mm, 1 Kip = 4.5 KN, 1 Ksi = 6.9 N/mm^2.

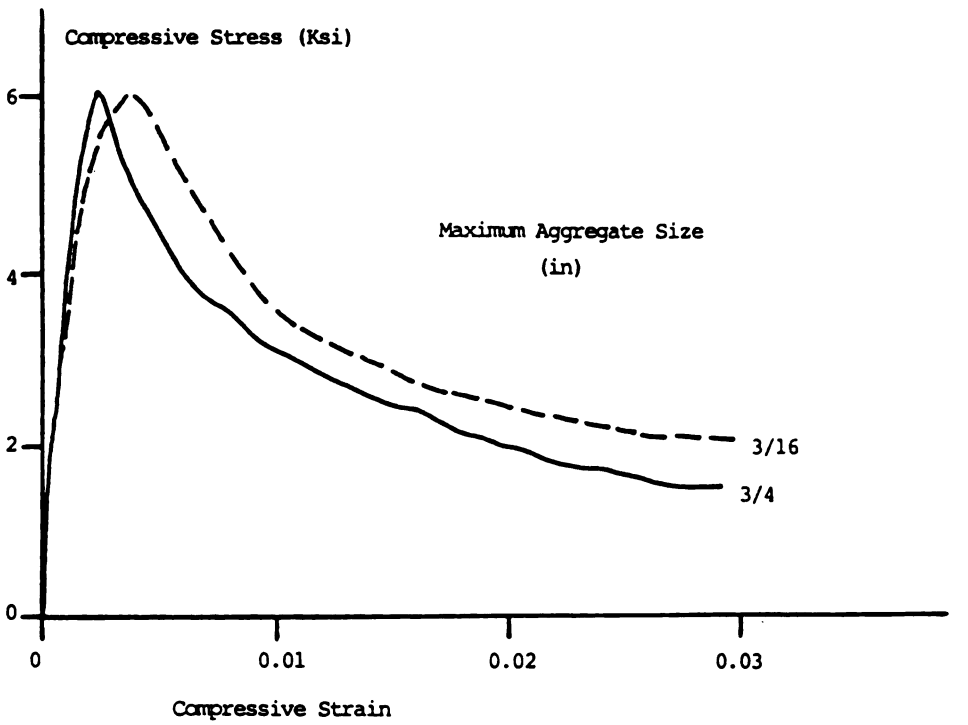

b. Compressive stress-strain curve

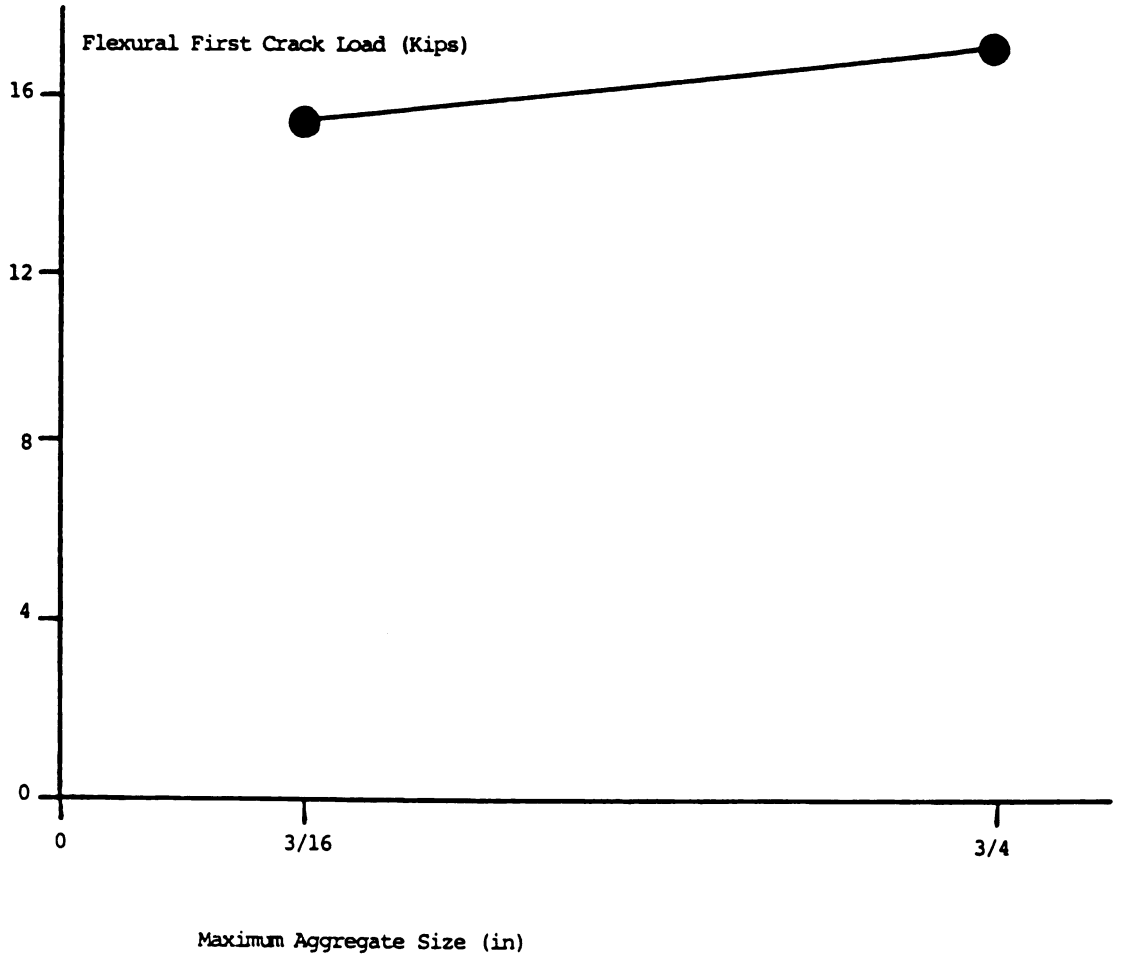

a. First crack load

Figure 4.20: Effects of maximum aggregate size on the flexural performance characteristics. 1 in = 25.4 mm, 1 Kip = 4.5 KN, 1 Ksi = 6.9 N/mm^2, 1 Kip.in = 114 N.m.

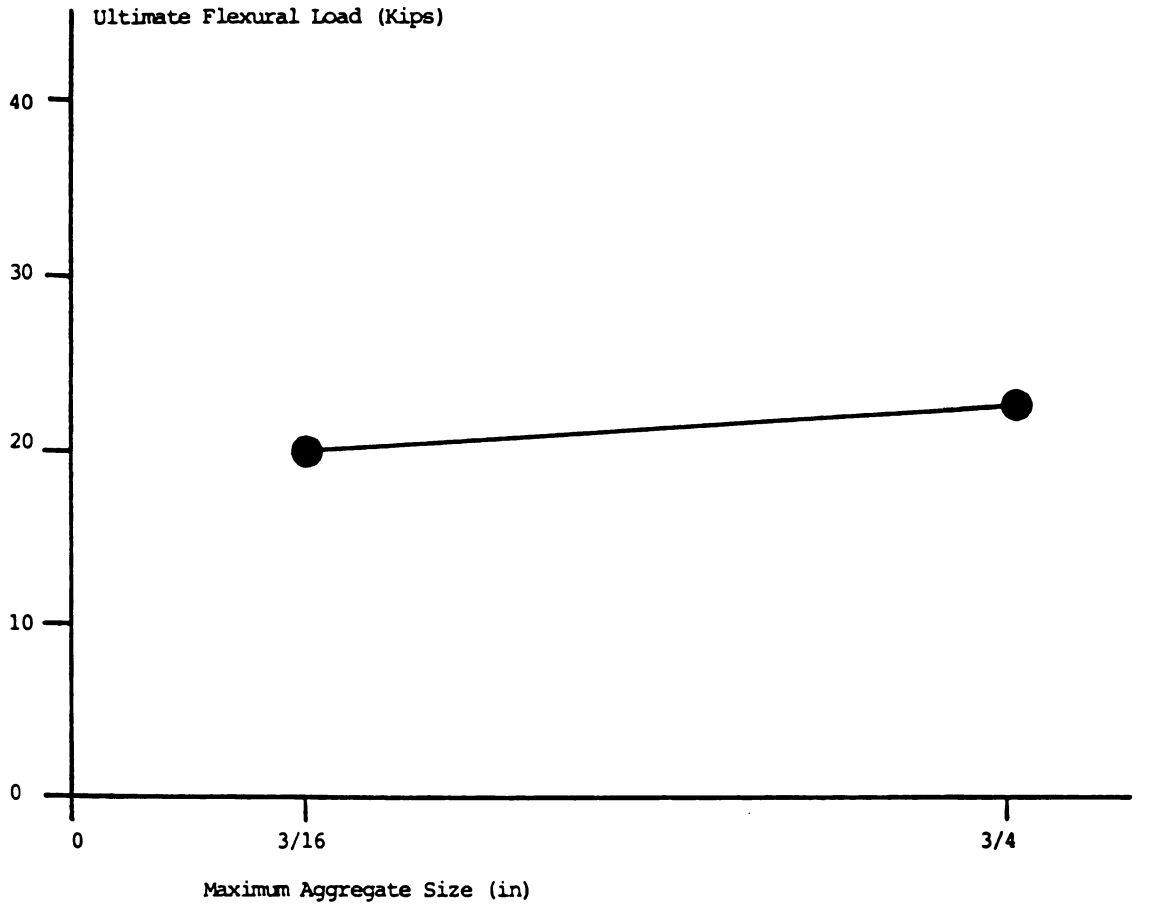

b. Ultimate load

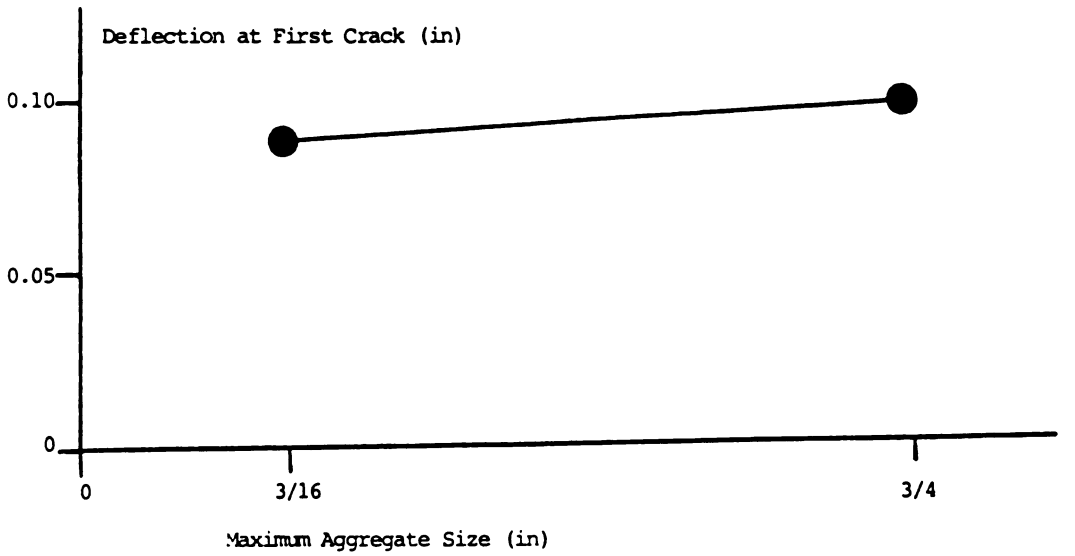

c. Deflection at first crack

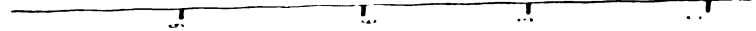

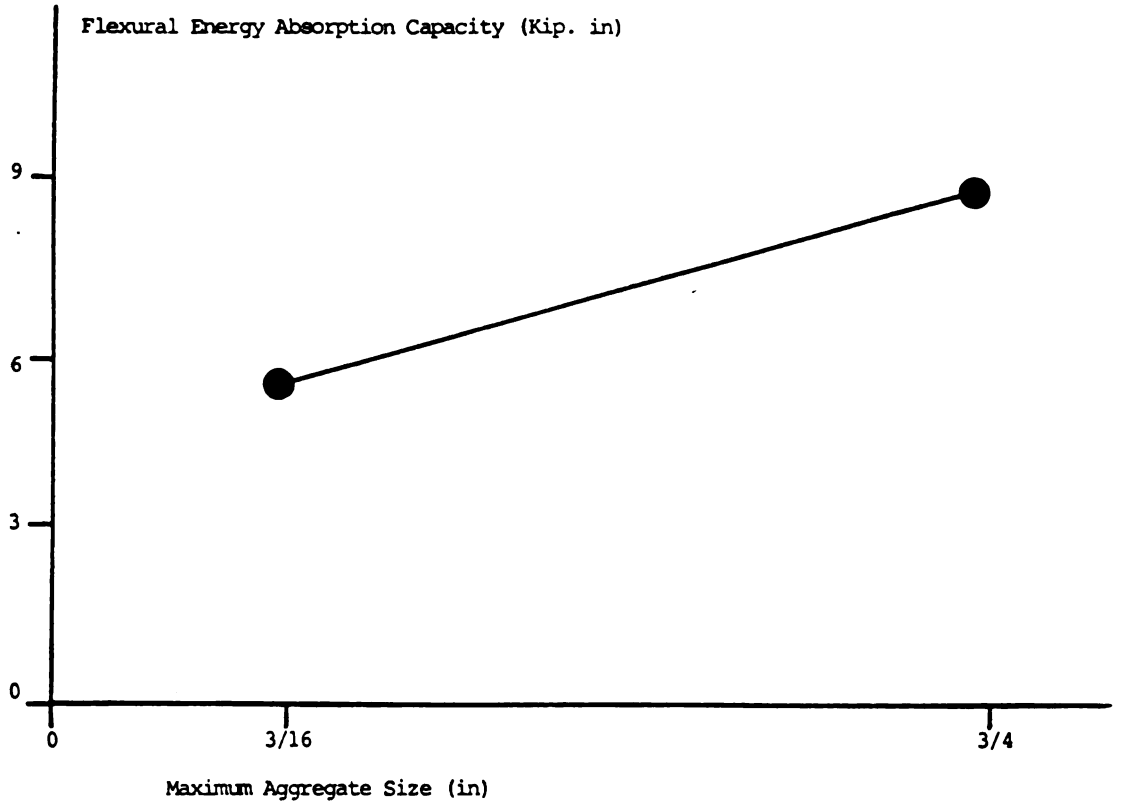

d. Energy absorption capacity

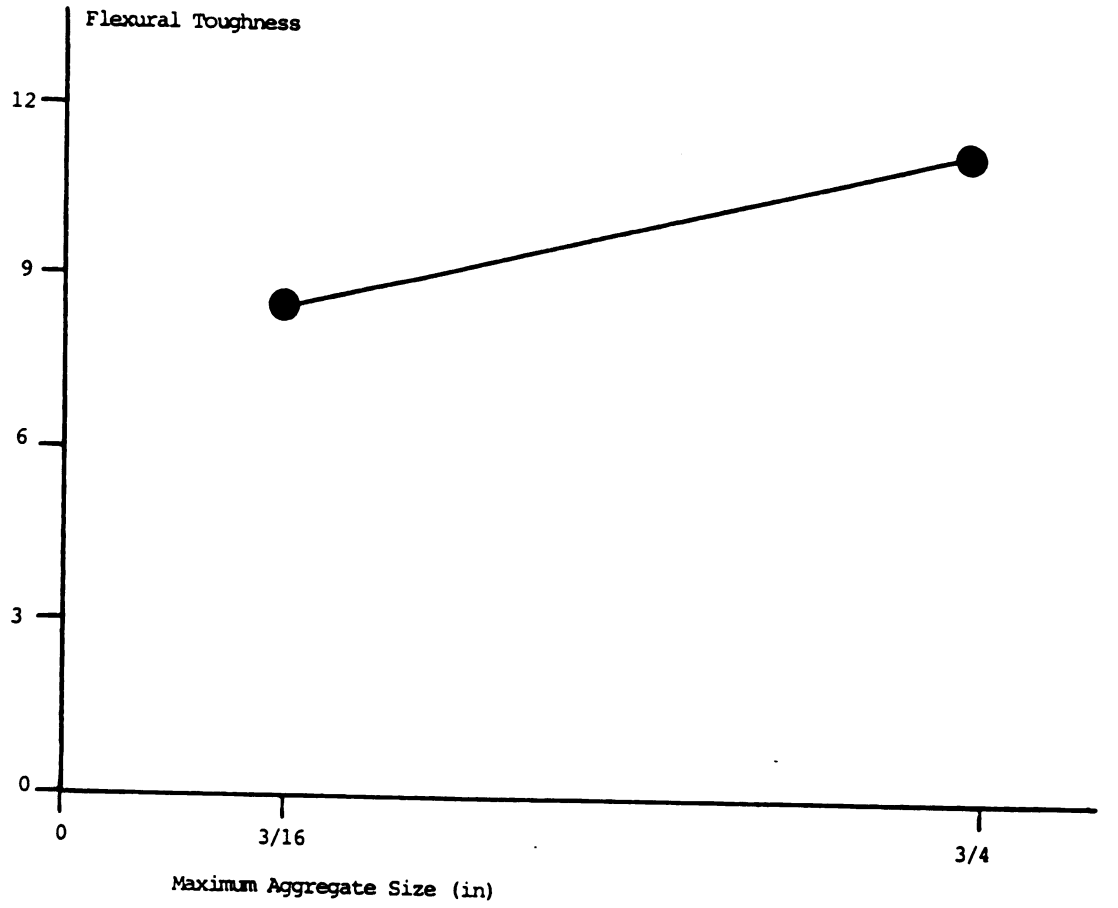

e. Toughness index

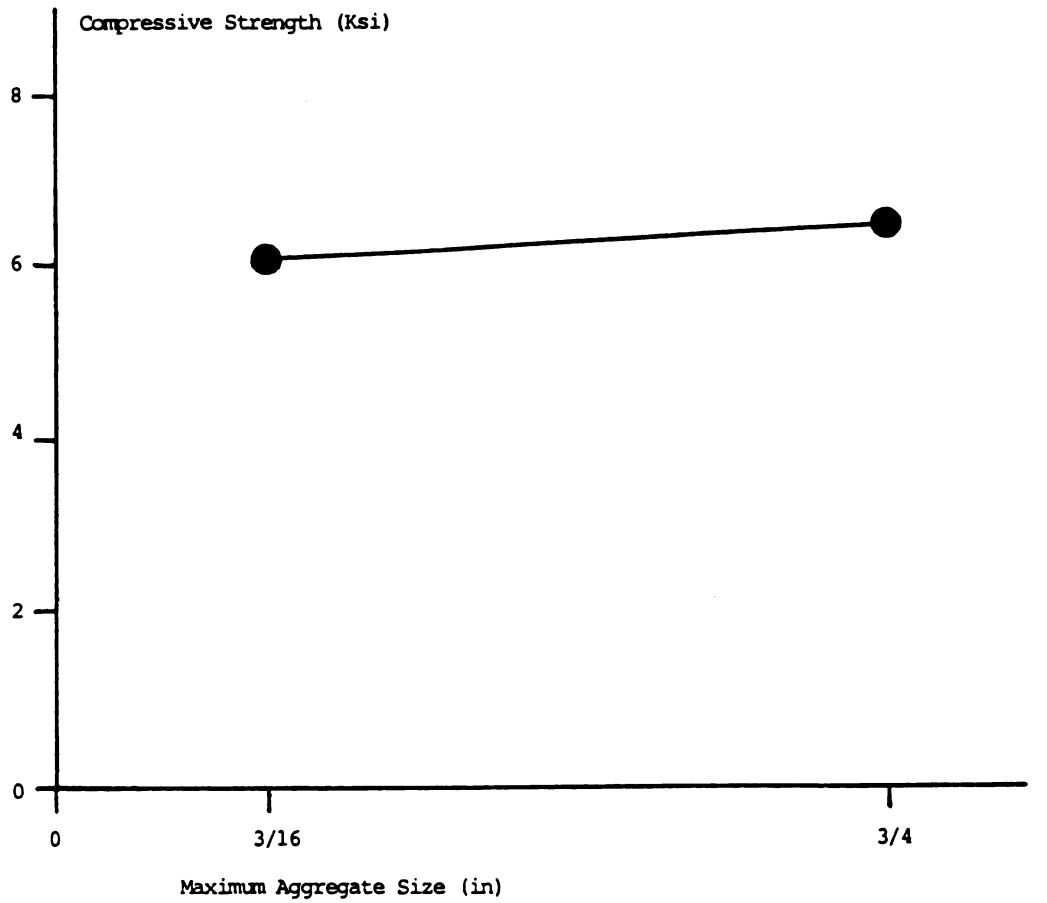

a. Compressive Strength

Figure 4.21: Effects of maximum aggregate size on the characteristic compressive performance. 1 in = 25.4 mm, 1 Ksi = 6.9 N/mm^2, 1 Kip.in = 114 N.m.

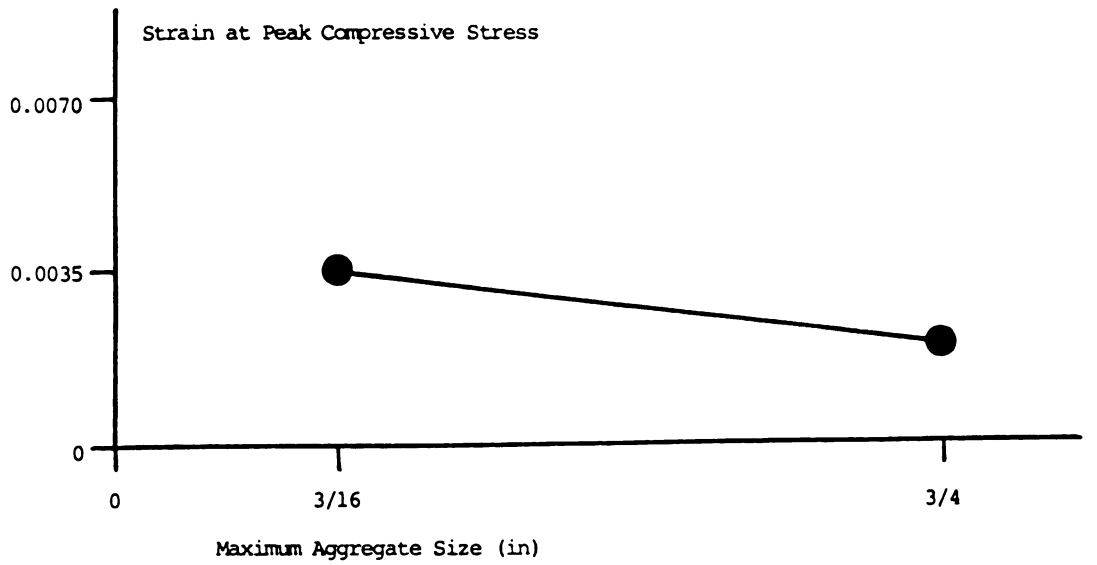

b. Strain at peak compressive stress

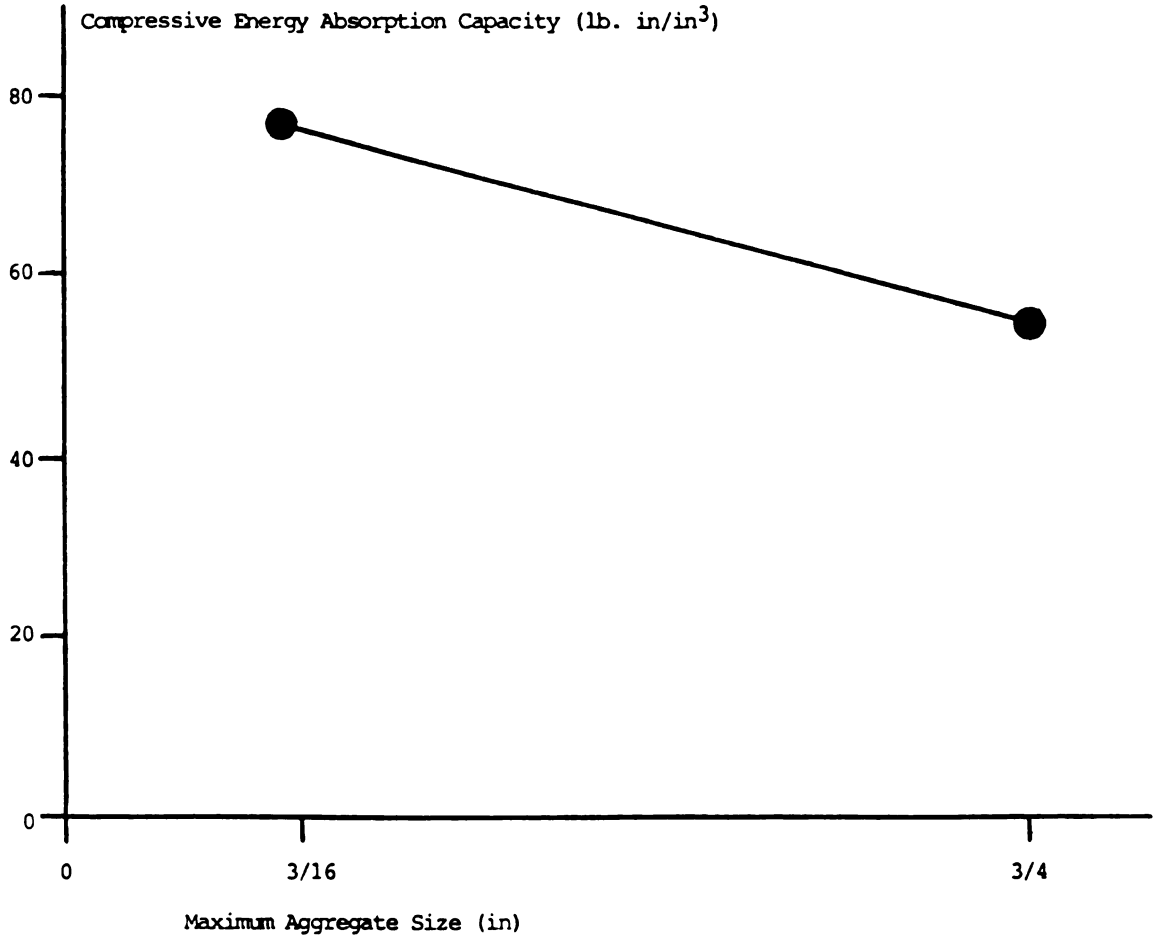

c. Compressive energy absorption capacity

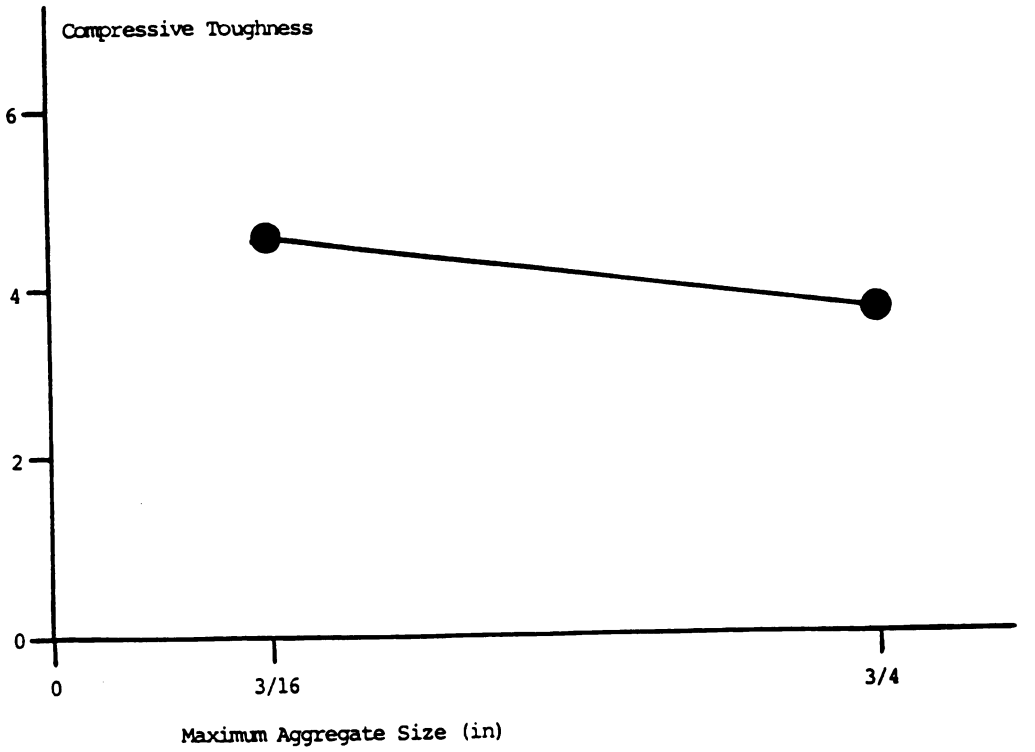

d. Compressive toughness index

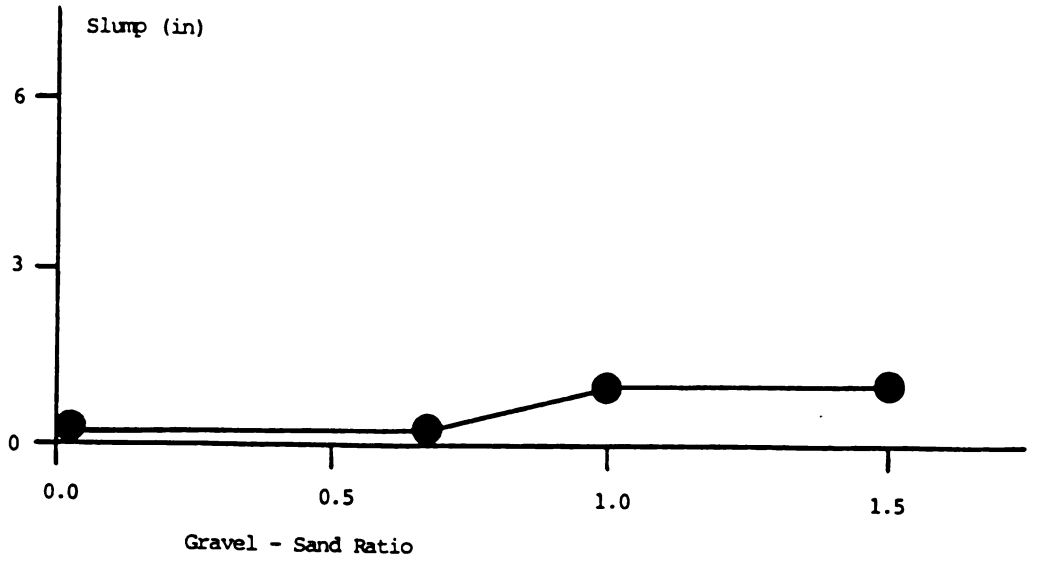

a. Slump. 1 in = 25.4

Figure 4.22: Effects of aggregate gradation (gravel-sand ratio) on fresh mix workability of steel fiber concrete.

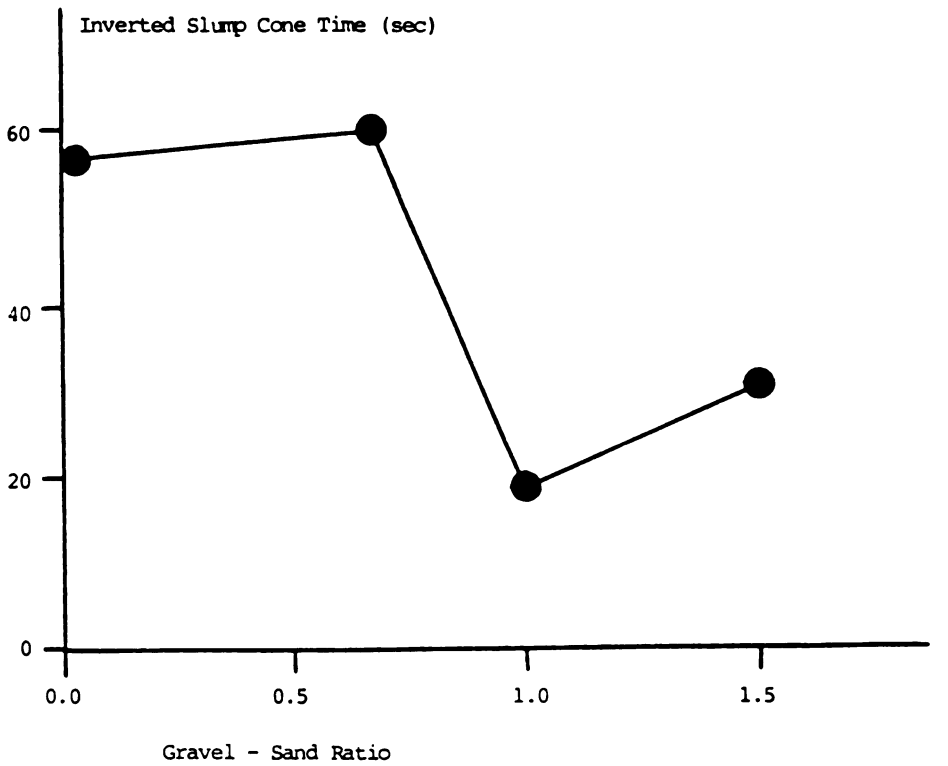

b. Inverted slump cone time

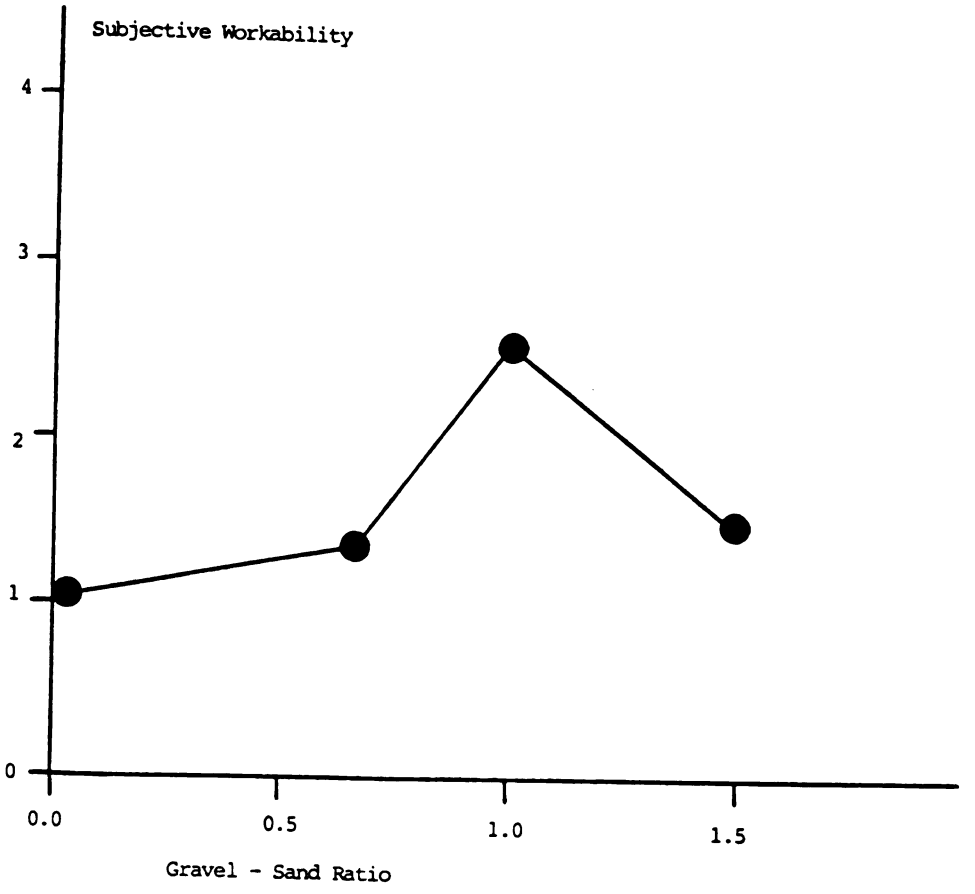

c. Subjective workability

Figure 4.22.a. The inverted slump cone time and subjective workability test results in Figures 4.22.b and c, however, indicate that there is an optimum coarse-to-fine aggregate ratio diviation from which in any direction would tend to damage workability. The damage may occur by tendencies toward fiber balling when coarse aggregate content is increased, and by increasing the surface area of aggregates when higher fine aggregate content is used.

Figures 4.23, 4.24 and 4.25 summarize the test results generated in this study regarding the effects of aggregate gradation on the flexural and compressive performance characteristics of steel fiber reinforced concrete. Form Figures 4.23.a and 4.24, one may conclude that, for specific mix proportions, there is an optimum aggregate gradation (marked in this study by a coarse-to-fine aggregate ratio equal to 1.0) for achieving the best flexural performance of the material. An increase or decreae in coarse aggregate content would result in some damage to the flexural performance of steel fiber reinforced concrete. It is difficult to derive general conclusions regarding the aggregate gradation effect on the compressive performance of steel fiber reinforced concrete from Figures 4.23.b and 4.25. There is, however, a tendency in compressive performance to be damaged by the increase in coarse-to-fine aggregate ratio.

4.4.f Air-Engraining Agent: The effects of the dosage of air-entraining agent on the air content of steel fiber reinforced concrete is presented in Figure 4.26. The air content is observed in this figure to increase, at a decreasing rate, with the

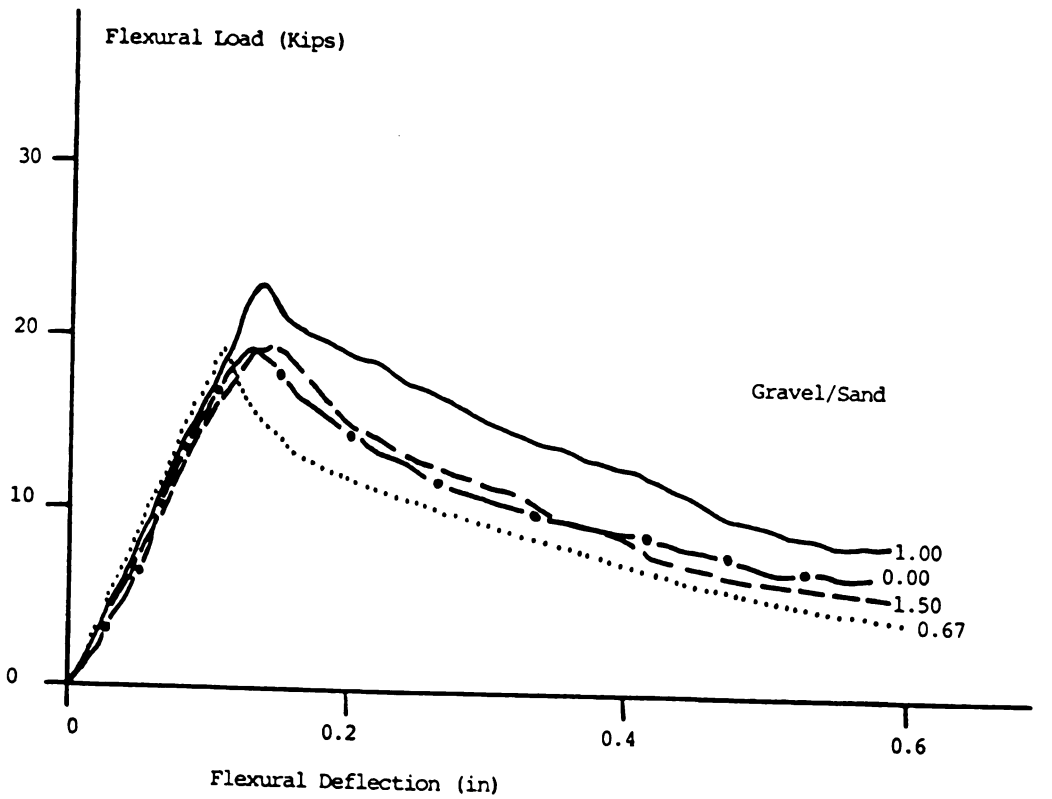

a. Flexural load-deflection relationship

Figure 4.23: Effects of aggregate gradation (gravel-sand ratio) on flexural and compressive load-deformation curves. 1 in = 25.4 mm, 1 Kip = 4.5 KN, 1 Ksi = 6.9 N/mm^2

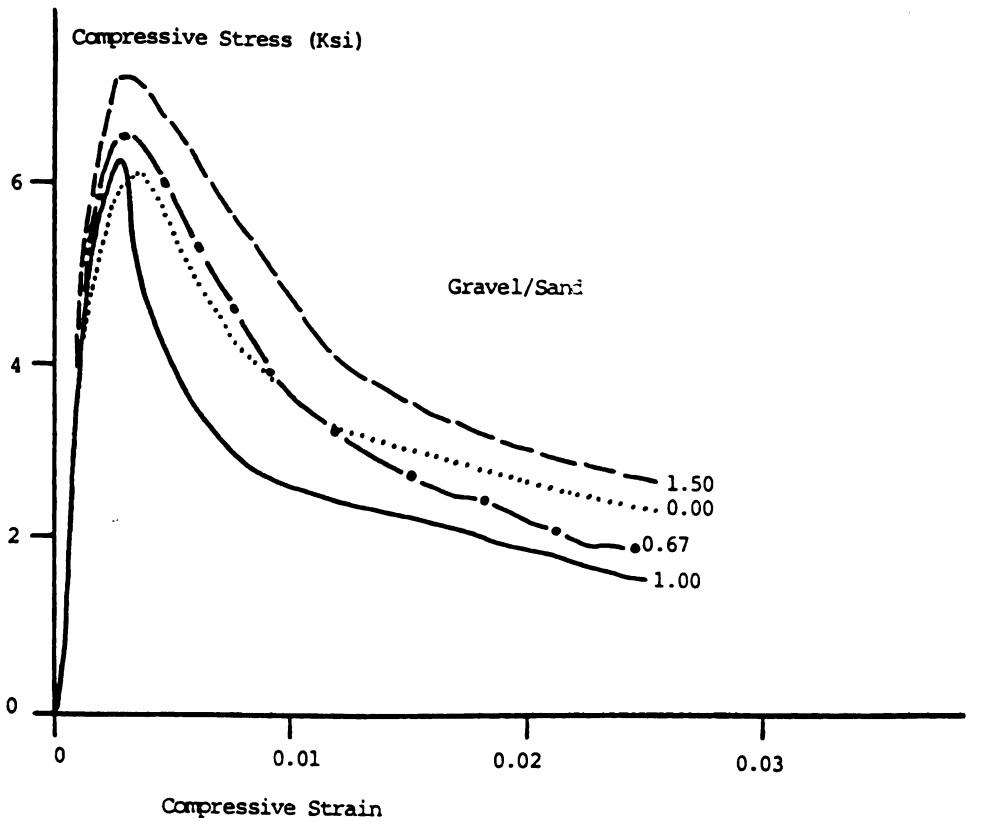

b. Compressive stress-strain relationship

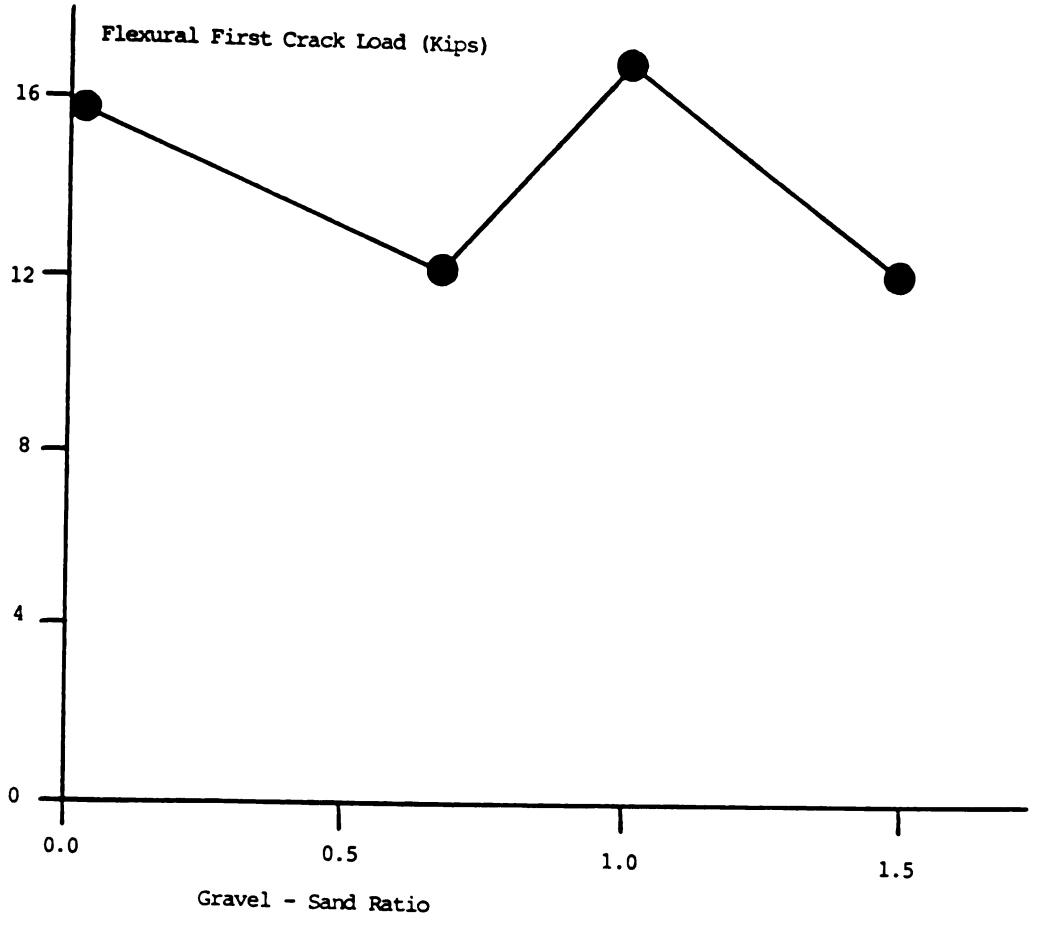

a. First crack load

Figure 4.24: Effects of aggregate gradation (gravel-sand ratio) on flexural performance characteristics. 1 in = 25.4 mm, 1 Kip = 4.5 KN, 1 Kip.in = 114 N.m.

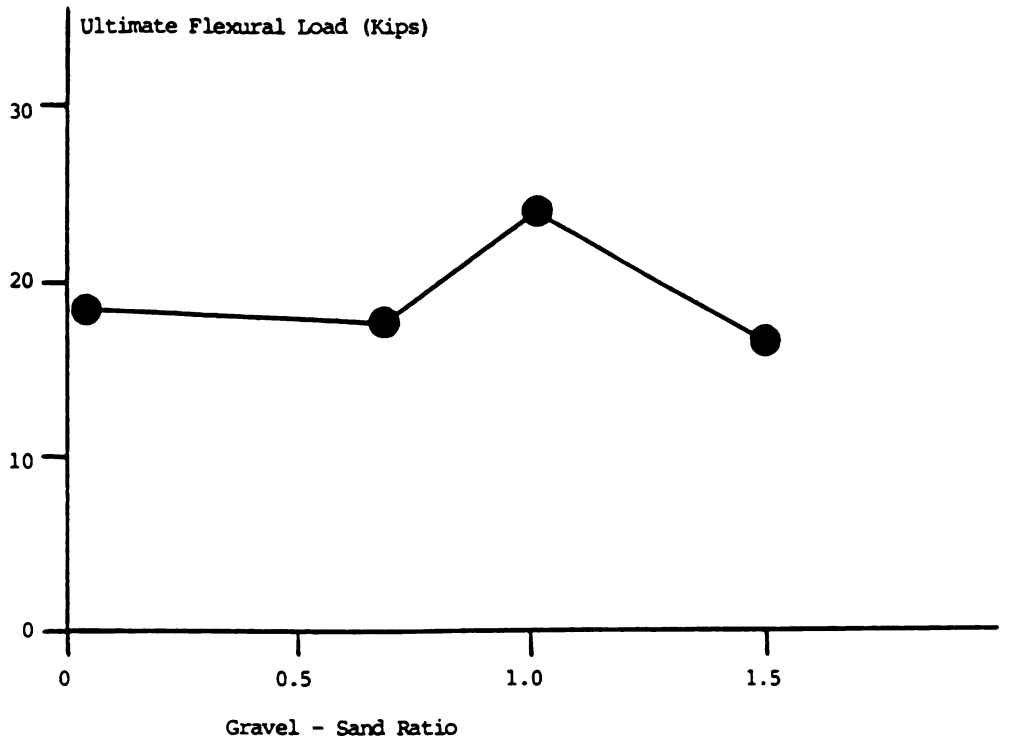

b. Ultimate load

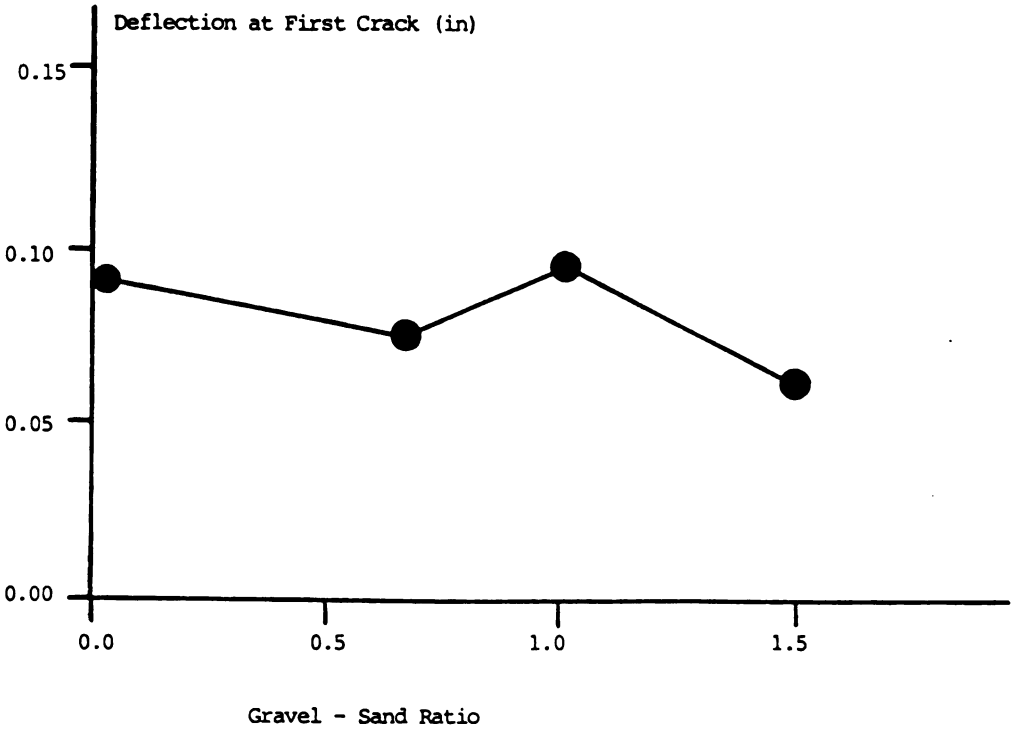

c. Deflection at first crack

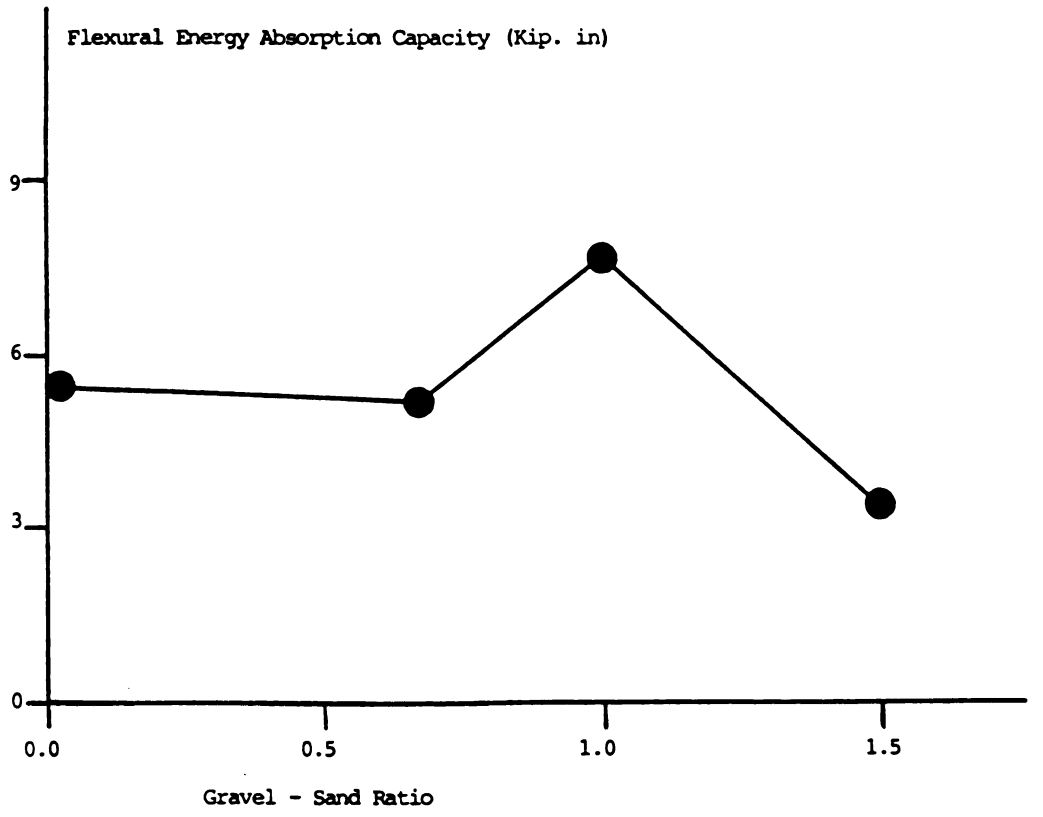

d. Energy absorption capacity

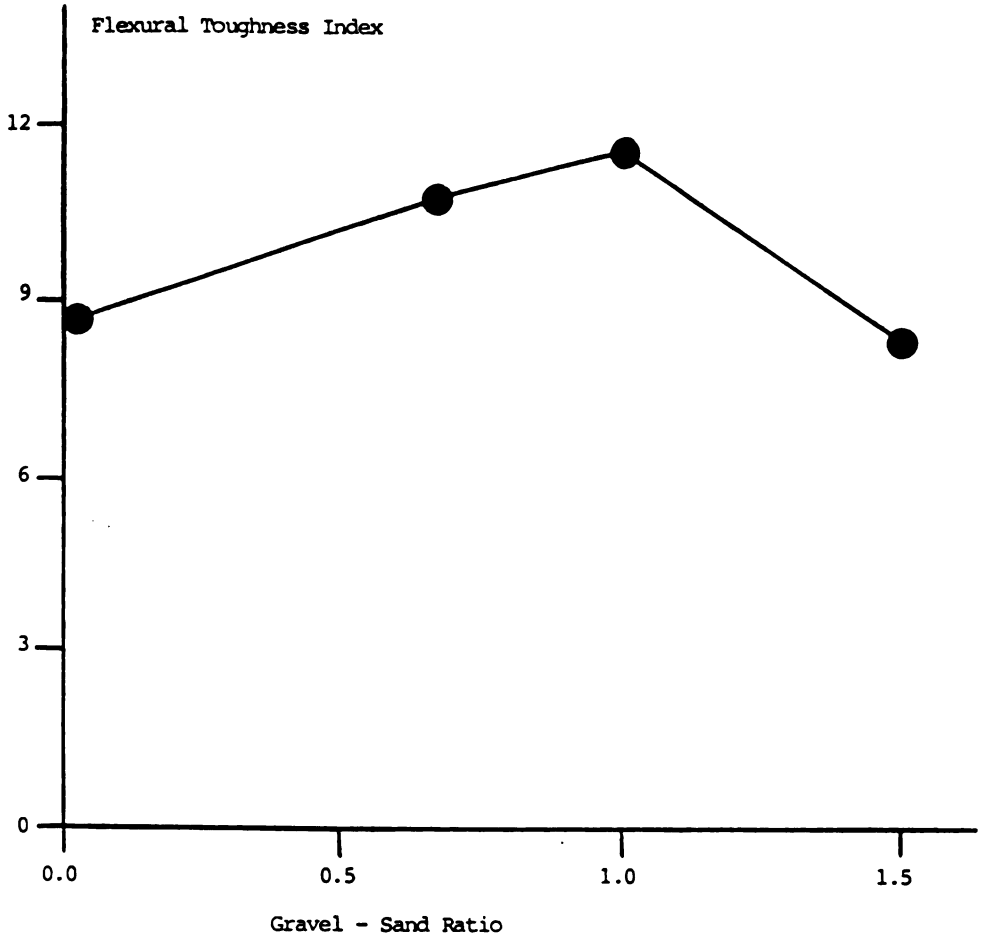

e. Toughness index

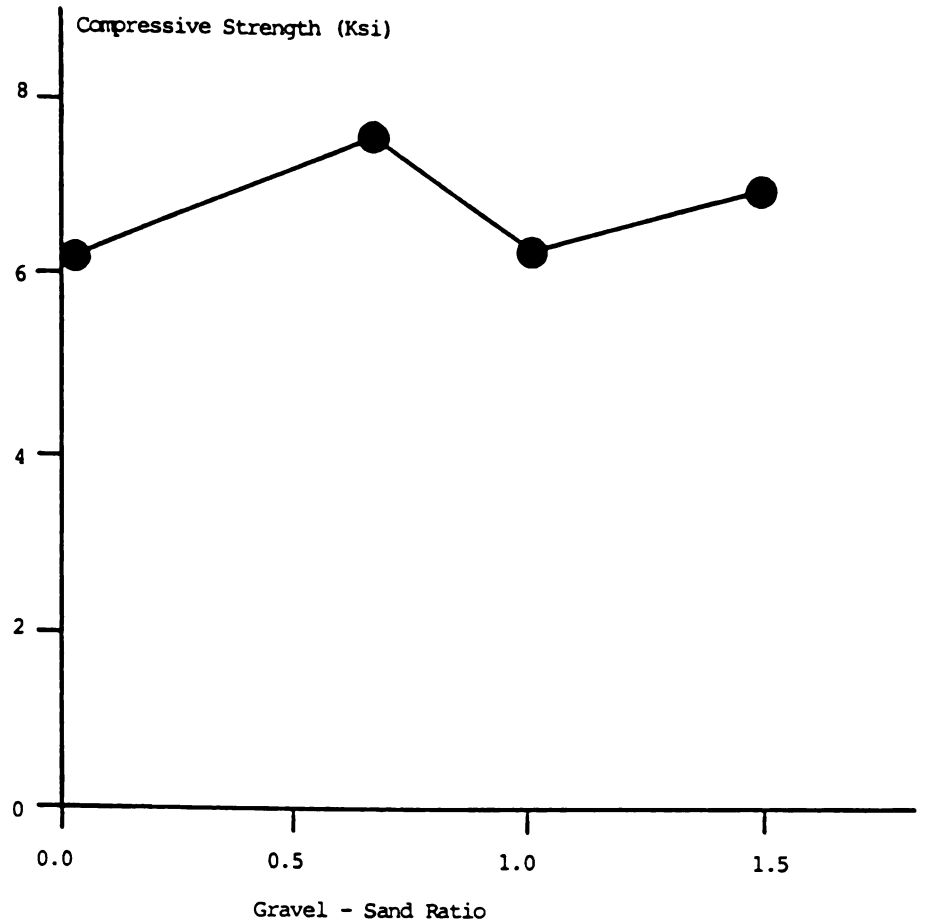

a. Compressive strength

Figure 4.25: Effects of aggregate gradation (gravel-sand ratio) on the characteristics compressive performance. 1 in = 25.4 mm, 1 Ksi = 6.9 N/mm^2, 1 Kip.in = 114 N.m.

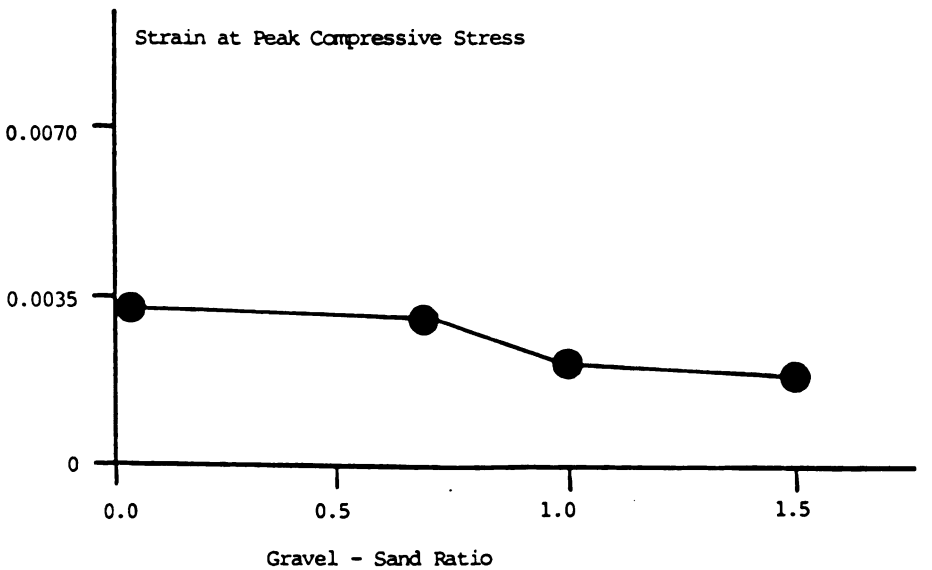

b. Strain at peak compressive stress

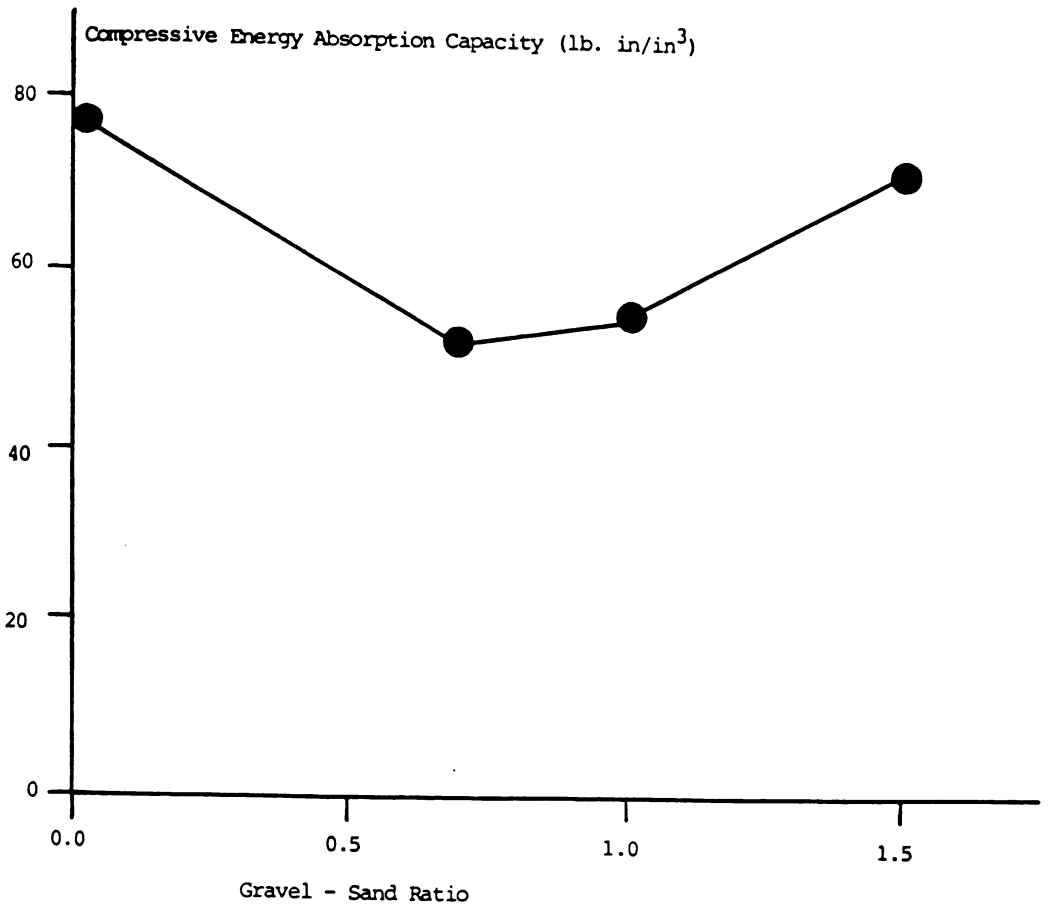

c. Compressive energy absorption capacity

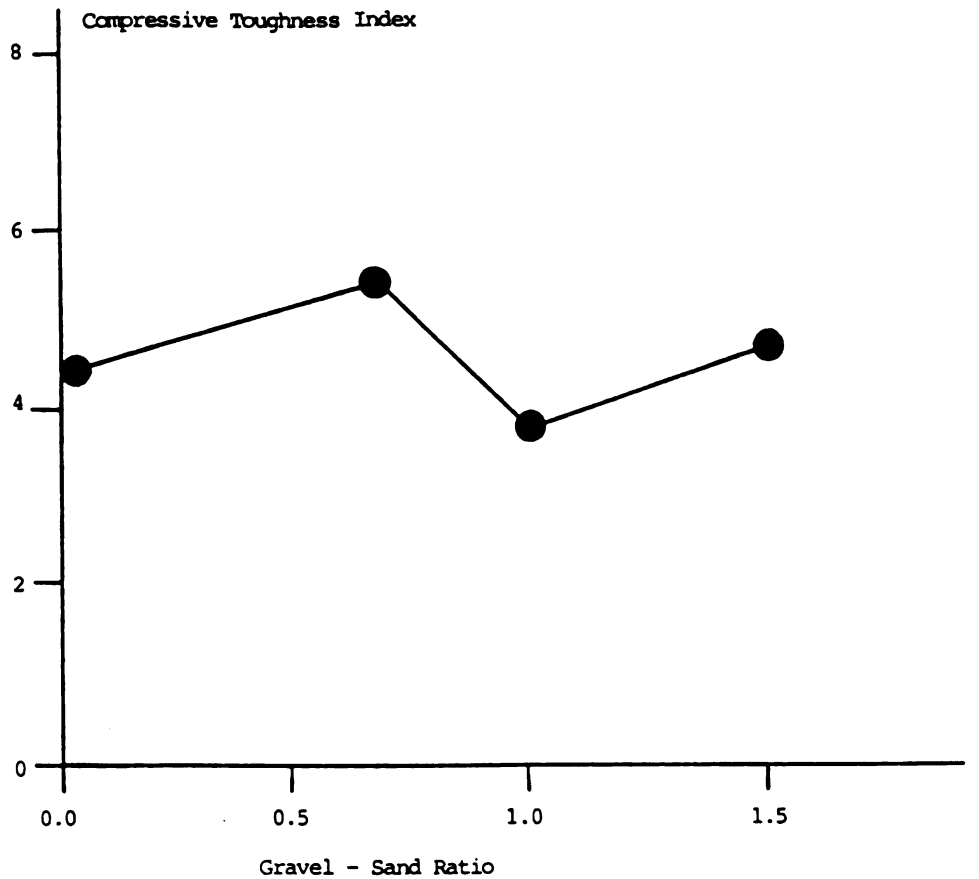

d. Compressive toughness index

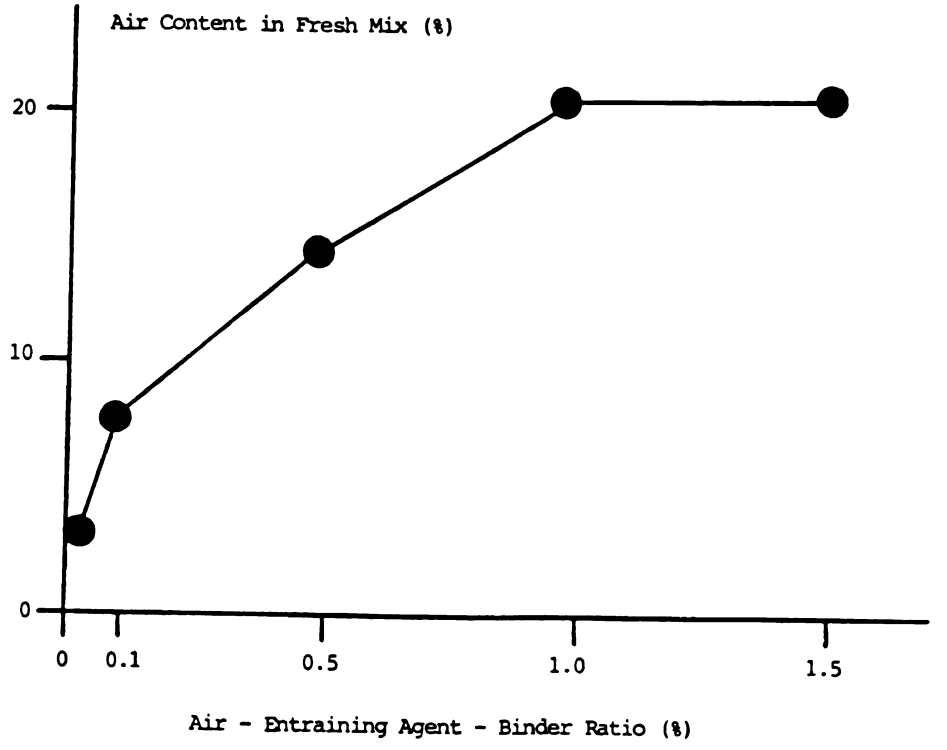

Figure 4.26: Effects of air-entraining agent dosage on the air content of steel fiber reinforced concrete

increase in the air-entraining agent dosage up to a certain point beyond which the effect practically diminishes. An air-entraining agent-binder ratio of 0.1% is observed in Figure 4.26 to generate the entrained air content needed for desirable performance under repeated freeze-thaw cycles.

4.5 Summary and Conclusions

The effects of different matrix mix variables on the fresh mix workabilty and hardened material flexural and compressive performance characteristics of steel fiber reinforced concrete were investigated. A typical fibrous mixture with a relatively high fiber volume fraction was used as a "basic" mix for this investigation. The generated test data indicated that:

1. The workability of fresh steel fiber reinforced concrete tends to improve with the increase in binder (cement: fly ash = 0.7:0.3) content. There are also improvements in the flexural strength and energy absorption characteristics of steel fiber reinforced concrete resulting from the increase in binder content. The compressive performance, however, seems to be largely independent of the binder content.

2. The increase in superplasticizer dosage tends to improve the compactibility and the overall workability of steel fiber reinforced concrete. There is also some tendency in the flexural performance to improve with the increase in superplasticizer dosage. Compressive performance is least influenced by the

change in superplasticizer dosage.

3. The increase in water-binder ratio tends to improve the workability of fresh fibrous mixtures. It should, however, be noted that excessive water contents may produce fluid concrete matrices in which the steel fibers tend to settle down. The increase in water-binder ratio results in a drop in compressive strength of steel fiber reinforced concrete. The corresponding damage to the compressive energy absorption characteristics and the overall flexural performance are, however, less obvious.

4. The workability of steel fiber reinforced concrete improves with increasing aggregate size (within the range of variables considered in this study). The increase in maximum aggregate size also results in a slight increase in flexural strength and some more important improvements in the flexural energy absorption characteristics of steel fiber reinforced concrete. The compressive properties of the material seems to be largely independent of the maximum aggregate size in the mixtures considered in this study.

5. There is an optimum aggregate gradation the deviation from which towards coarser or finer gradation damages the workability and flexural performance of steel fiber reinforced concrete. The optimum gradation was obtained in this study by the use of coarse-to-fine aggregate ratio of 1.0.

6. The entrained air content of steel fiber reinforced concrete mixtures increases at a decreasing rate with the increase in the dosage of air entraining agent. Desirable entrained air contents for resistance against freeze-thaw cycles can be achieved by the use of dosages of air entraining agent which are comparable to those recommended for conventional concrete.

CHAPTER 5

Optimum Use of Pozzolanic Materials in Steel Fiber Reinforced concrete

5.1 General

Fly ash and silica fume are the two pozzolanic materials which have been established in the recent years as commonly used mineral admixtures capable of providing plain and fiber reinforced concrete with distinct performance advantages. Being pozzolanic materials, both silica fume and fly ash react with the alkali calcium hydroxide produced by the hydration of portland cement, leading to the formation of calcium silicate hydrate which has desirable effects on the density and micro structure of concrete materials, espcially at interfaces between cementitious paste and mix inclusions (e.g. aggregate, fiber) where the concentration of calcium hydroxide is generally high. Fly ash and silica fume also have their differences. Silica fume is distinguished from fly ash by its fineness, high pozzolanic reactivity and high silica content. The effects of the two pozzolanic materials on fresh mix workability are also different, while fly ash tends to improve workability, the reverse is genrally true in the case of silica fume. The research reported in this chapter has been concerned with partial substitution of cement with fly ash or silica fume in typical steel fiber reinforced concrete mixes. The trends in the effects of pozzolan contents on fresh mix workability and hardened material mechanical characteristics are established. The optimum pozzolan contents for the specific types of fly ash and silica fume used in the mixes of this study are decided.

5.2 Background

A brief review of the mechanism of action of fly ash and silica fume in concrete together with the outcomes of past investigations on applications to steel fibers reinforced concrete are given below:

5.2.a Fly Ash: Fly ash is the finely divided residue resulting from the combustion of ground or powdered coal.[53] Probably the most important consideration in the use of fly ash in steel fiber reinforced concrete is its ability to improve the fresh mix workability and fiber dispersability.[41,54] The round shape and fineness of fly ash particles improve the flowability of the mix.[55] With fly ash, the volume of cementitious paste in the mix increases (due to the lower specific gravity of fly ash compared to cement, noting that cement is usually replaced with fly ash on an equal mass basis) and thus a more effective coating of fibers and lubrication of the mix inclusions will be achieved.[54] These effects improve the dispersabiity of fibers and workability of the fresh mix. The improvements in fresh mix workability in the presence of fly ash are especially obvious when the fresh material is compacted through vibrtion.[41,54] The improvements in fresh mix workability and fiber dispersability lead to enhanced properties of the composite material in the hardened state.

Application of fly ash to steel fiber reinforced concrete, in addition to improving the fresh mix workability and fiber dispersability, also imparts the following improvements to the material performance:

1. Fly ash contributes to strength of steel fiber reinforced concrete by reducing the water content without damaging workability, by increasing the volume of paste in the mixture, and by its pozzolanic reaction.[56]

2. The increase in cementitious paste volume in the presence of fly ash leads to a better coating of fibers by the matrix material and improved fiber-matrix interacial bond characteristics. This may cause significant improvements in the composite material performance.[41,54]

3. All other advantages of using fly ash in plain concrete (enhanced pore system, reduced permeability and improved durability, reduced alkali-aggregate reactivity, economic and echological advantages, etc.)[53-57] would also apply to steel fiber reinforced concrete.

Certain precautions are needed to take full advantage of fly ash applications in steel fiber reinforced concrete:[41,53-57]

1. The presence of carbon in fly ash results in the reduction of the entrained air content in fly ash concrete materials. Hence, the dosage of air entraining agent used in fly ash concrete should be adjusted according to the carbon content of fly ash.

2. Fly ash generally slows down the rates of setting and hardening of concrete, and fly ash concrete is more sensitive to temperature variation and might need more

favorable curing condition than conventional concrete.

3. Fly ash, being a by-product, has larger variations in chemical and physical properties than portland cement, and approprite quality control measures should be taken depending on the specific job requirements.

5.2.b Silica Fume: Silica fume is a by-product resulting from the reduction of high-purity quartz with coal in electric arc furnaces in the production of silicon and silicon alloys.[58] The fineness and high pozzolanic reactivity of silica fume make it highly effective in enhancing the structural density and adhesion capacity in the bulk of the cement paste and especially within the interface zones between the paste and the mix inclusions including fibers.[48,59,60] Enhanced fiber-matrix bond characteristics have important effects on the strength and ductility of fiber reinforced silica fume concrete under different stress systems.

Steel fiber conretes incorporating silica fume also enjoy those advantages imparted to plain concrete by silica fume including:[58]

1. Increased cohesiveness and reduced segregation tendencies.

2. Reduced permeability resulting from the decrease in the number of coarse pores of the cement paste incorporating silica fume, leading to enhanced durability of the material.

3. Potentials for developing very high strength.

4. Greater sulfate resistance, reduced alkali aggregate reactivity and improved chemical resistance.

Optimum application of silica fume in concrete and fiber reinforced concrete would require certain precautions as described below:

1. The high surface area of silica fume results in an increase in the dosage of air-entraining agent required for producing a certain entrained air content.

2. Silica fume tends to make concrete mixtures rather sticky, and increased water content and/or the use of water reducing agents would be necessary for maintaining the consistency of the mix.

3. Silica fume, mainly due to its high affinity for water, leaves little free water in the mixture and reduces the bleeding of conrete. This reduces the supply of water to the surface and requires adoption of curing procedures which prevent early moisture loss from freshly placed concrete in order to prevent platic shrinkage cracking.

5.3 Experimental Program

Different steel fiber reinforced concrete mixes with variable percentags of cement

substitution with fly ash or silica fume were manufactured, and their characteristics in the fresh and hardened states were assessed.

The mixes with fly ash had a water-binder (cement + fly ash) ratio of 0.42, and those with silica fume had a water-binder (cement + silica fume) ratio of 0.40. The mixes with fly ash incorporated 2% volume fraction of steel fibers, while those with silica fume had a fiber volume fraction of 1.5%. The fraction substitutions of cement with fly ash were 0%, 20%, 30%, and 40% by weight, while in mixes with silica fume 0%, 5%, 10% and 20% of weight of portland cement were substituted by silica fume.

All mixes (with silica fume or fly ash) had an aggregate-binder ratio of 4.0, sand-gravel ratio of 1.0, maximum aggregate size of 3/4 in (19 mm), and a superplasticizer-binder ratio of 0.015 by weight. The steel fibers used in this study were straight-round and had a length of 2 in (51 mm) and a diameter of 0.035 in (0.8 mm), and thus an aspect ratio of 57.

The portalnd cement used in the mixes of thi study was type I, and the superplasticizer was Daracem 100 (a Naphtalene-Formaldahyde-sulfonate based high-range water reducer capable of maintaining its effectiveness over a relatively long time period),[38] The fly ash incorporated into the mixes was type F,[27] and was obtained from the Eckert plant of the Lansing Board of Water and Light. The major physical and chemical properties of fly ash are given in Table 5.1.[37] The

silica fume used in this investigation was a product of Elkem Chemicals, and its chemical and physical properties are given in Table 5.2.[61] The aggregates used in this investigation were natural river gravel and sand.

A rotary drum mixer was used for the manufacture of steel fiber reinforced concretes with silica fume and fly ash. The sequence of the addition of different mix constituents to the mixer was similar to that described in Section 2.3 of Chapter 2.

Following mixing, the fresh mix workability was measured by the inverted slump cone testing procedure.[9] A shorter inverted slump cone time is representative of better workability. For the fresh steel fiber concrete mixtures incorporating fly ash, the air content was also assessed through the pressure method.[27]

Following the experiments on fresh mix, 6 x 12 in (150 x 300 mm) cylindrical specimens for compression test, and 6x6x20 in (150 x 150 x 500 mm) prismatic specimens for flexural test were cast and compacted on a vibration table. All the specimens were demoded after 24 hours, during which they were kept under plastic sheets. The fly ash concrete specimens were then moist cured at 100% relative humidity and 72°F (23°C) for seven days and were then cured in the regular laboratory environment. A total of 6 compression and 3 flexural test specimens were constructed. The three flexural spcimens and two of the compression specimens were tested at an age of 28 days. Two of the compression specimens were tested at an age of 1 day and the other two at 7 days. The silica fume concrete

Table 5.1: Chemical and physical properties of the fly ash used in the experiments.[37] 1 in = 25.4 mm

a. Chemical Composition

Component	SiO2	Al2O3	Fe2o3	TiO2	CaO	MgO	K2O	C
% by weight	47.0	22.1	23.4	1.1	2.6	0.7	2.0	4.3

b. Gradation

Sieve or size	#30 0.6mm (600microns)	#200 0.074mm (74microns)	#325 0.045mm (45microns)	0.020mm (20microns)	0.010mm (10microns)	0.005mm (5microns)
% passing	100	92	84	63	36	17

c. Specific Gravity = 2.245

Table 5.2: Chemical and physical properties of the silica fume used in the experiments.[61]

a. Chemical Composition

Component	SiO_2	C	Fe_2O_3	MgO	Al_2O_3	K_2O	Na_2O
% by weight	96.50	1.40	0.15	0.20	0.15	0.04	0.20

b. Physical Properties

Specific gravity = 2.3

Bulk density = 14 lb/ft^3 = $225Kg/m^3$

Specific Surface = 200,000 am^3/g = $14x\ 10^6 in^2/lb$

Average Particle size = 0.15 micron = $6x10^{-5}$in

Particles Smaller than 45 microns (0.018in) = 99.5%

specimens (2 compressions and 3 flexure) were all moist cured after demolding at 72°F (23°C) and 100% relative humidity until the test age of 28 days.

The flexural tests were performed using the four point loading procedure of a span of 18 in (450 mm) and the load-deflection (at the load point) relationship was monitored throughout the test.[27] In compression tests performed at the age of 28 days, also, the complete stress-strain relationships were obtained using a compressometer.[27,39]

5.4 Experimental Results

The results of tests on the fresh mix and hardened material properties of steel fiber reinforced concretes with different fly ash or silica fume contents are discussed in this section.

5.4. Fresh Mix Workability: The results of inverted slump cone test on fiber reinforced concrete incoroporating fly ash and silica fume are shown in Figures 5.1.a and 5.1.b, respectively, as functions of the pozzolan content. The substitution of increasing fractions of cement with type F fly ash is observed in Figure 5.1.a to reduce the inverted slump cone time of steel fiber reinforced concrete indicating improvements in the compactibility of fresh mix under vibration in the presence of fly ash. It is worth mentioning that, except for the mix without fly ash, all the other steel fiber reinforced concrete mixes with 20% to 40% fly ash-binder ratio have inverted slump cone times within the acceptable limit of 10-30 sec.

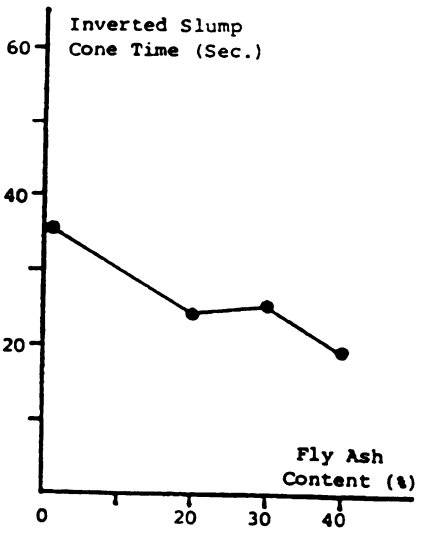

a. Fly ash concrete (V_f = 2%)

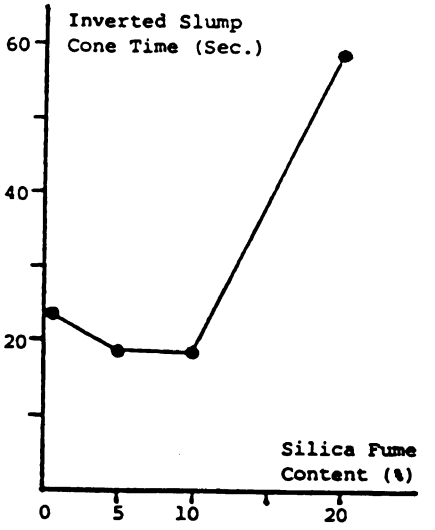

b. Silica fume concrete (V_f = 1.5%)

Figure 5.1: Inverted slump cone test results.

The substitution of portland cement with silica fume up to 10% by weight is observed in Figure 5.1.b to have small effects on the fresh mix workability of steel fiber reinforced concrete. Higher silica fume contents, however, start to damage workability and the mix with 20% silica fume-binder ratio is actually quite unworkable.

5.4.b Flexural Behavior: complete felxural load-deflection relationships are shown in Figures 5.2.a and 5.2.b for mixes with fly ash and silica fume, respectively (each curve represents the average of 3 test results). Figures 5.3.a and 5.3.b summarize the trends observed in Figure 5.2 regarding the fly ash and silica fume effects, respectively, on flexural strength. The trends for flexural energy absorption capacity (the area under the load-deflection diagram up to a deflection 5.5 times the cracking deflection) are shown in Figure 5.4.

The results presented in Figures 5.2.a and 5.3.a indicate that the flexural strength of steel fiber reinforced concrete tends to improve with increasing fly ash content up a fly ash-binder ratio of 0.3. The flexural strength tends to be adversely influenced by further increase in fly ash content. The energy absorption capacity of steel fiber reinforced concrete is observed in Figures 5.2.a and 5.4.a to increase rather substantially as fly ash content increases from 0% to 30%, and to drop at higher fly ash contrents. From Figures 5.2.b and 5.3.b, it may be concluded that the increase in silica fume-binder ratio up to 10% improves the flexural strength of steel fiber reinforced concrete but this trend tends to be reversed for higher silica

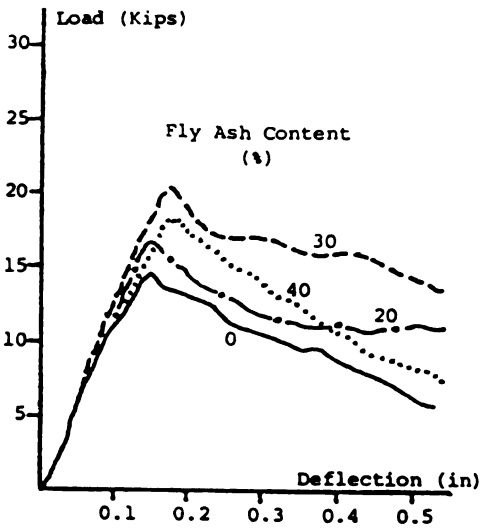

a. Fly ash concrete (V_f = 2%)

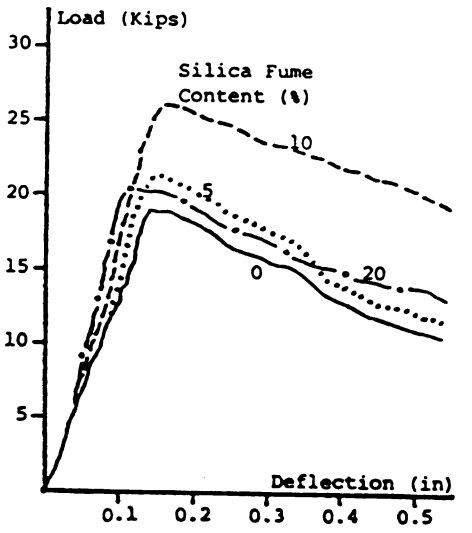

b. Silica fume concrete (V_f = 1.5%)

Figure 5.2: Flexural load deflection relationships. 1 in = 25.4 mm, 1 Kip = 4.5 KN.

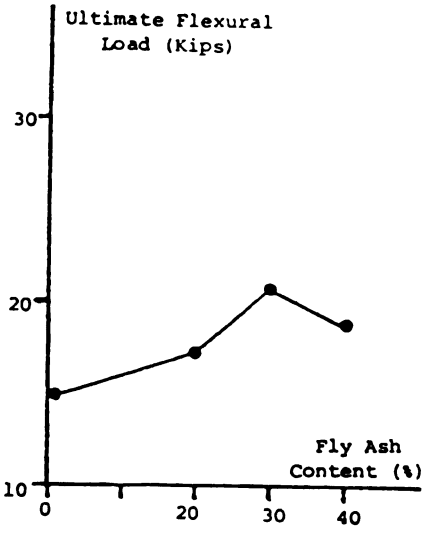

a. Fly ash concrete (V_f = 2%)

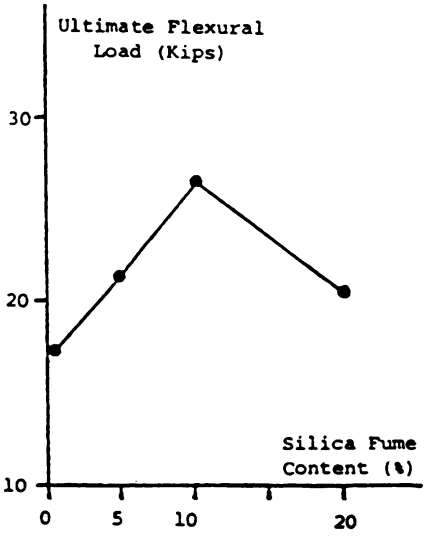

b. Silica fume concrete (V_f = 1.5%)

Figure 5.3: Flexural strength test results. 1 Kip = 4.5 KN.

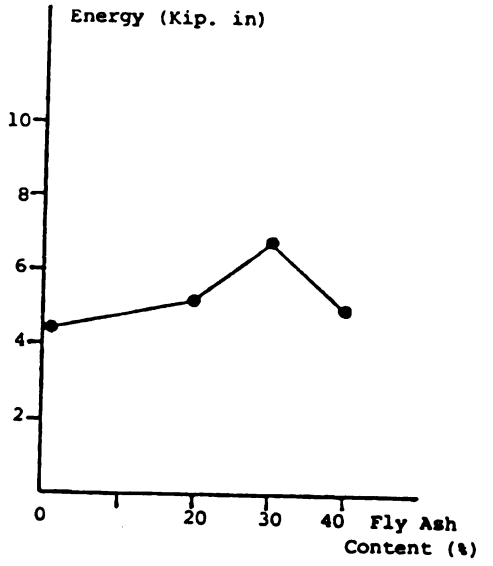

a. Fly ash concrete (V_f = 2%)

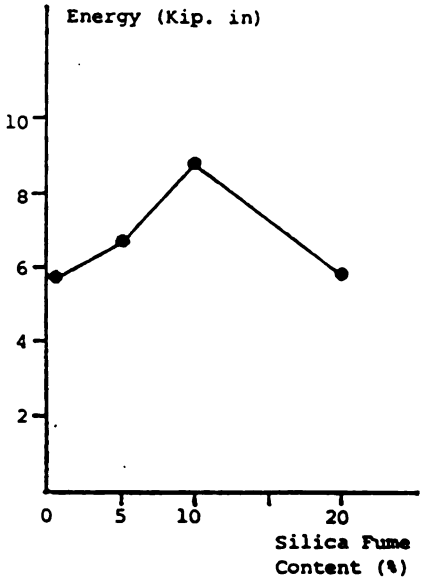

b. Silica fume concrete (V_f = 1.5%)

Figure 5.4: Flexural energy absorption capacities. 1 Kip.in = 114 N.m

fume contents. A similar trend is observed in the effects of silica fume on energy absorption capacity of steel fiber reinforced concrete, as shown in Figures 5.2.b and 5.4.b.

5.4.c Compressive Behavior: The compressive stress-strain relationships, and the compressive strengths and energy absorption capacities derived from test results on steel fiber reinforced fly ash and silica fume concretes are presented in Figures 5.5 through 5.7. The compression energy absorption capacity is defined as the area underneath the compressive stress-strain relationship up to a strain 5.5 times the strain at peak compressive stress.

The test results on steel fiber reinforced fly ash concrete presented in Figures 5.5.a, 5.6.a and 5.7a indicate that an increase in fly ash-binder ratio up to 20% improves the compresssive strength and energy absorption capacity of steel fiber reinforced concrete, but this trend tends to be reversed for higher fly ash contents.

The trends in the effects of silica fume content on the compressive behavior of steel fiber reinforced concrte, shown in Figures 5.5.b, 5.6.b and 5.7.b, indicate that the increase in silica fume-binder ratio up to 10% improves the compressive strength and energy absorption capacity, and the increase in silica fume-binder ratio from 10% to 20% has a relatively small effect on the compressive behavior.

5.4.d Air Content and Development of Strength with Time: For the fly ash concrete

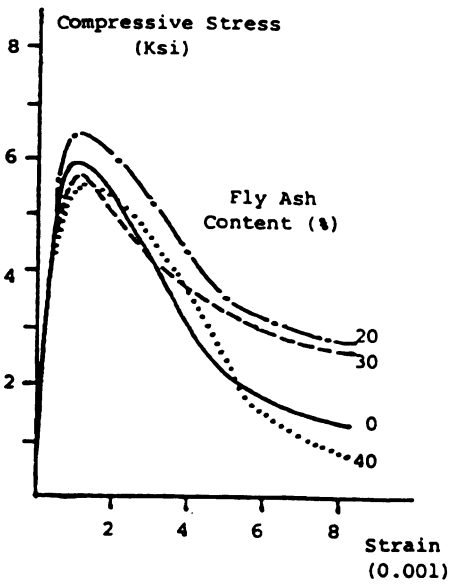

a. Fly ash concrete (V_f = 2%)

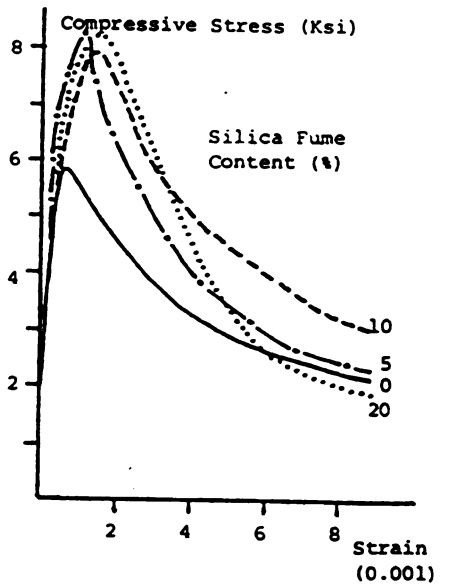

b. Silica fume concrete (V_f = 1.5%)

Figure 5.5: Compressive stress-strain relationships. 1 Ksi = 6.9 MPa.

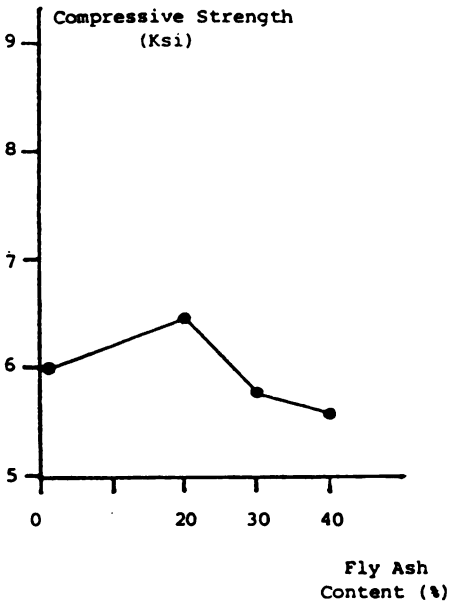

a. Fly ash concrete (V_f = 2%)

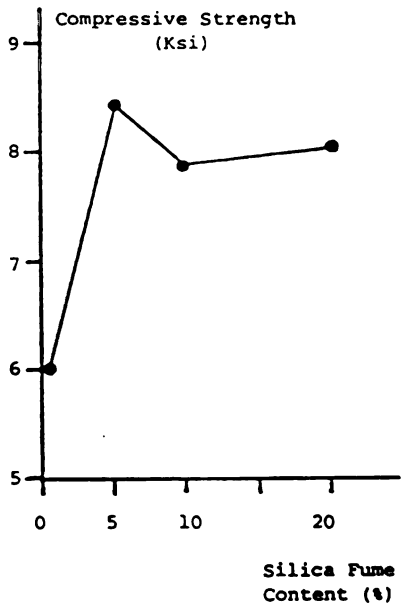

b. Silica fume concrete (V_f = 1.5%)

Figure 5.6: Compressive strength test results. 1 Ksi = 6.9 MPa

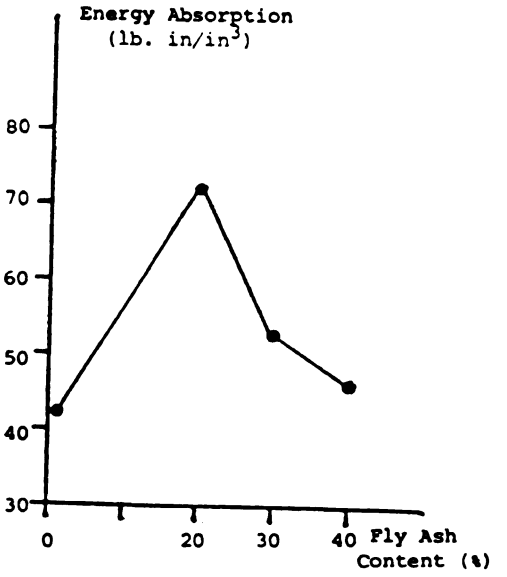

a. Fly ash concrete (V_f = 2%)

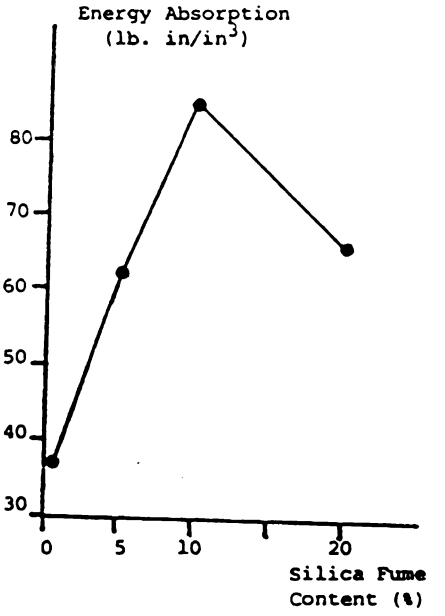

b. Silica fume concrete (V_f = 1.5%)

Figure 5.7: Compressive energy absorption capacities. 1 in = 25.4 mm, 1 Kip.in = 114 N.m

mixtures, the fresh mix air content and the development of hardened material strength with time were assessed. These tests were performed to investigate the possibility of fly ash adversely influencing these aspects of steel fiber reinforced concrete material properties.

The observed trends in fly ash effects on the air content of fresh steel fiber reinforced concrete mixtures are presented in Figure 5.8. Obviously, the increase in fly ash content leads to some reduction of the fresh mix air content. This effect is, however, relatively small and it seems that the use of an air entraining agent can compensate for this effect of fly ash.

The trends in the development of compressive strength with time for steel fiber reinforced concrete incorporating different fly ash content are shown in Figure 5.9. Strength at each age has been normalized in this figure with respect to the corresponding strength of the fibrous mix with 0% fly ash content. One may conclude from Figure 5.9 that the substitution of 20% of cement with fly ash increases the compressive strength of steel fiber reinforced concrete at all ages, when compared with the corresonding mix without fly ash. When 30% or 40% of cement is substituted by fly ash, however, there seems to be a drop in the rate of strength development with time. The 28-day compressive strengths of steel fiber reinforced concrete mixtures with different fly ash contents are, however, not much influenced by the fly ash content.

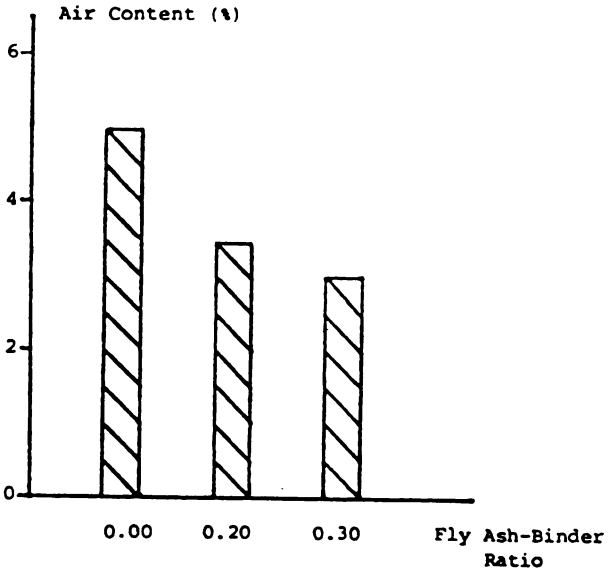

Figure 5.8: Fly ash effects on air content of fresh steel fiber reinforced concrete (V_f = 2%)

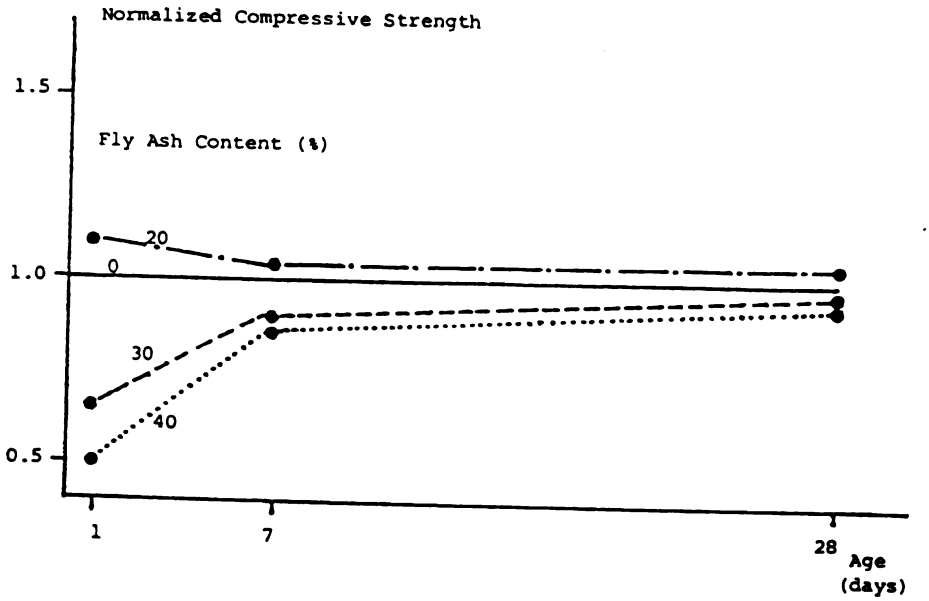

Figure 5.9: Fly ash effects on development of strength with time of steel fiber reinforced concrete

5.5 Summary and Conclusions

The effect of the silica fume and the class F fly ash contents on the properties of steel fiber reinforced concrete in fresh and hardened states were investigated experimentally. From the results it was concluded that:

5.5.a Silica Fume Effects:

1. The compactibility of steel fiber reinforced concrete, as indicated by the inverted slump cone test results, is not much influenced by the increase in silica fume-binder ratio up to a value of about 0.10. Higher silica fume contents, however, adversely influence the workability of fresh mix.

2. The flexural strength and energy absorption capacity of steel fiber reinforced concrete tend to increase with increasing silica fume-binder ratio up to a value of about 0.10; beyond which the effects of silica fume on these aspects of the hardened material behavior tend to be reversed.

3. The compressive strength and energy absorption capacity of steel fiber reinforced concrete tend to increase with increasing silica fume-binder ratio up to silica fume ratio of 0.10. Further increase in silica fume content has relatively small effects on the compressive behavior of steel fiber reinforced concrete.

4. for the steel fiber reinforced concrete mixes used in this study, substitution of 10% of cement with silica fume gave the best results as far as the workability of

fresh mix and the strength and energy absorption capapcity of the hardened material under the action of flexural and compressive loads are concerned.

5.5.b Fly Ash Effects:

5. Substitution of cement with class F fly ash in steel fiber reinforced concrete mixes of this study generally had positive effects on the workability of fresh mix as represented by the inverted slump cone time test results.

6. The 28-day flexural strength and energy absorption capapcity of steel fiber reinforced concretes of this study tend to increase with increasing fly ash-binder ratio up to about 0.3. the increase in fly ash-binder ratio from 0.3 to 0.4, however, adversely influenced the flexural performance of steel fiber reinforced concrete.

7. Substitution of up to 20% of cement with fly ash in steel fiber reinforced concrete mixes of this study resulted in improved 28-day compressive strength and energy absorption capacity of the material. Higher fly ash contents, however, start to have adverse effects on compressive characteristics.

8. The increase in fly ash content led to some reductions in the air content of steel fiber reinforced concrete mixtures.

9. Substitution of more than 20% of cement with fly ash trends to reduce the rate

of compressive strength development in steel fiber reinforced concrete. After 28-days, however, the compresive strengths of mixes with fly ash-binder ratios as high as 0.40 were close to that of the mix with 0% fly ash contents.

10. The optimum fly ash-binder ratio in steel fiber reinforced concrete mixtures of this study, for achieving desirable fresh mix workability and hardened material flexural and compressive properties was in the range of 0.20 to 0.30. Fly ash should be accompanied with an air entraining agent in application to steel fiber reinforced concrete in conditions where freeze-thaw durabiity is of concern. Ths use of more than 20% fly ash-binder ratios lead to a lower rates of strength development in steel fiber reinforced concrete.

CHAPTER 6

Statistical Variation in Steel Fiber Reinforced Concrete Properties

6.1 Introduction

The introduction of steel fibers to concrete adds a number of variables to those deciding the material properties of plain concrete. This factor tends to increase the variations in material properties. On the other hand, steel fiber reinforced concrete is less sensitive than plain concrete to effects such as shrinkage and thermal cracking which are some sources responsible for variations in material properties of concrete. This action of steel fibers tends to reduce the variations in material properties of steel fiber reinforced concrete below those of conventional concrete.

The research reported in this chapter is concerned with the experimental assessments of the variations in fresh mix workability and flexural and compressive properties of hardened material of typical steel fiber reinforced concrete mixtures.

6.2 Background

Reference 62 has reported the results of an experimental study on statistical variations in the flexural and compressive properties of a typical steel fiber reinforced concrete mix with a desirable fresh mix workability incorporating 1% volume fraction of steel fibers with a length of 1.22 in (31 mm) and a diameter of 0.02 in (0.5 mm). The results reported in Reference 62 indicated that the frequency distribution of compressive and flexural strengths of steel fiber reinforced concrete compare reasonably with the theoretical normal distribution. Based on 36 flexural

and compressive tests reported in Reference 62 (on fibrous concretes with compressive strength of 6,423 psi = 44.3 N/mm^2 and modulus of rupture of 1,054 psi = 7.27 N/mm^2), the values of coefficient of variation were found to be 4.7% for compressive strength and 3.2% for flexural strength. These variations are comparable to those reported in Reference 62 for plain concrete mixtures.

The statistical study of Reference 62 has been performed on one steel fiber reinforced concrete mix with a highly desirable fresh mix workability. Therefore, more test results are needed to fully characterize the statistical variations of steel fiber reinforced concrete.

6.3 Experimental Program

The objective of the experimental program was to generate data on the statistical variations in fresh mix workability and also in flexural and compressive performance characteristics of typical steel fiber reinforced concrete mixtures. The fibrous mix used in this statistical investigation has 2% volume fraction of 2 in (51 mm) straight-round steel fibers with a diameter of 0.035 in (0.8 mm). The concrete matrices of all the mixtures had a water-binder (cement + fly ash) ratio of 0.40, a fly ash-binder ratio of 0.30, a superplasticizer-binder ratio of 0.015, an aggregate-binder ratio of 4.0, a sand-to-gravel ratio of 1.0 and a maximum aggregate size of 3/4 in (19 mm). The materials used for the experimental program described in this chapter are the same as described in Chapter 2.

Four batches of the fibrous mix were manufactured in a rotary drum mixer following the procedure presented in Section 2.3. The materials of each batch were used for one inverted slump cone test on the fresh mix (two tests were performed on one of the fresh mixtures), and for the manufacture of three presmatic flexural specimens and two cylindrical specimens for compression test. The flexural specimens were 6 x 6 x 20 in (150 x 150 x 500 mm) and the compression specimens were 6 in (150 mm) in diameter and 12 in (300 mm) high. Both of the compression and the flexural specimens were cast in two layers, and each layer was compacted on a vibration table. The specimens were kept under a plastic sheet inside their molds for 24 hours. They were then demolded and moist cured at 72°F (22°C) and 100% relative humidity for 7 days, and then were air cured in regular laboratory environment until the test age of 28 days.

The flexural tests were performed following ASTM C-1018 (4 point loading on a span of 18 in = 450 mm). Both of the load and load-point deflection were monitored during the test. The compression tests were performed in accordance with ASTM C-469, and a compressometer was used to obtain the stress-strain relationships.

6.4 Experimental Results

Test results on the flexural and compressive strengths and inverted slump cone time of steel fiber reinforced concrete mixtures considered are presented in Table 6.1 together with the means, standard deviations and coefficients of variation of the measurements. Figures 6.1 through 6.3 present the experimental and theoretical

Table 6.1: Experimental results. 1 Ksi = 6.9 MPa

	Flexural Strength (ksi)	Compressive Strength (ksi)	Inverted Slump Cone Time (sec)
	1.320 1.460 1.617 1.621 1.638 1.644 1.678 1.680 1.830 2.123 2.289 2.296	6.086 6.106 6.267 6.482 6.500 6.709 7.015 7.080	16 21 22 31 32
Mean	1.766	6.531	24.4
Standard Diviation	0.312	0.382	6.88
Coefficient of Variation	0.176	0.0584	0.282

(based on normal distribution) frequency and cumulative frequency distributions for the measured values of flexural strength, compressive strength, and inverted slump cone time, respectively.

The coefficient of variation of compressive strength presented in Table 6.1 (5.84%) is comparable to that reported in Reference 62 (4.7%). The variations in flexural strength (coefficient of variation = 17.6%) are, however, far greater than the 3.2% coefficient of variation reported in Reference 62. Noting that the mixtures of this study at 2% volume fraction of steel fibers compared to only 1% volume fraction used in Reference 62, it may be concluded (with caution due to the limited number of test results in this study) that the increase in fiber volume fraction tends to increase the variations in flexural strength test results. The fact that the variations in compressive strength do not seem to strongly depend on fiber volume fraction may result from the fact that compressive strength, unlike flexural strength, is not much dependent on fiber volume fraction. Table 6.1 also shows relatively large variations (coefficient of variation = 28%) in the inverted slump cone test results.

An important conclusion can be derived from the above discussion, again noting the limited test results which are used here, is that the varitions in flexural strength observed in this study exceed the limits used to develop the statistical quality control criteria for conventional concrete (the rage in coefficient of variation from 17.5 to 20.0% represents fair to poor variation conditions in conventional concrete).[62-64] This indicates that some modifications might be needed in the statistical aspects of the

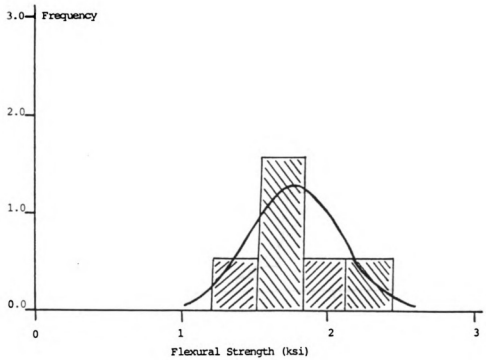

a. Frequency distribution

Figure 6.1: Experimental and theoretical (based on normal distribution) frequency and cumulative frequency distributions for flexural strength test results. 1 Ksi = 6.9 N/mm^2

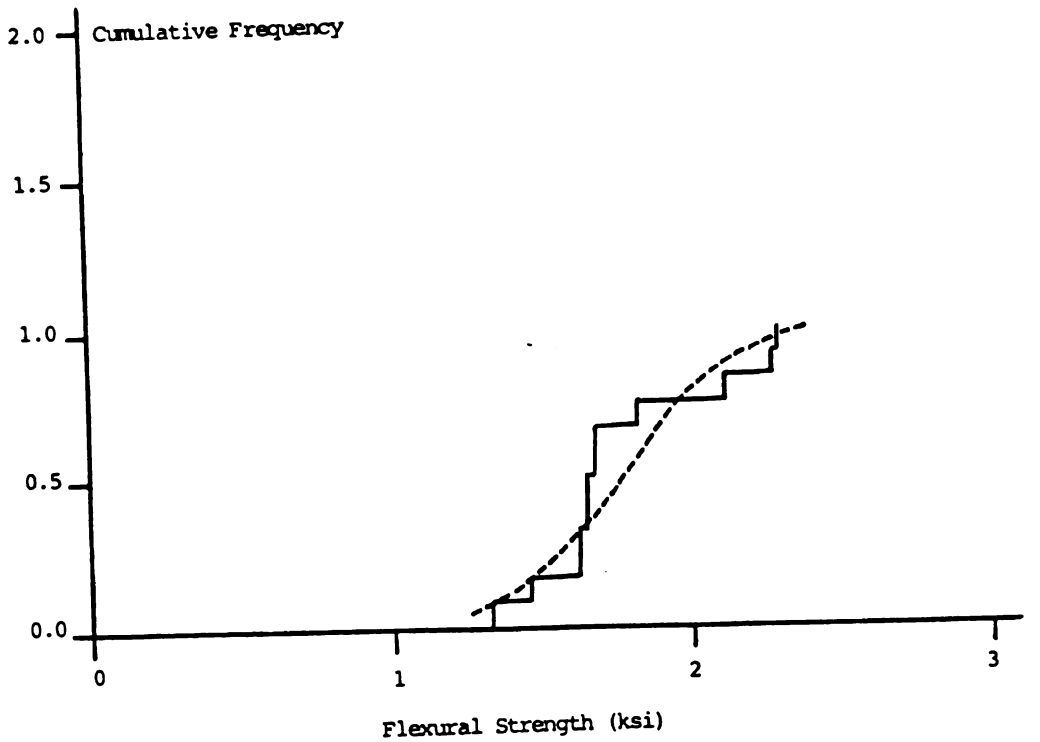

b. Cumulative frequency distribution

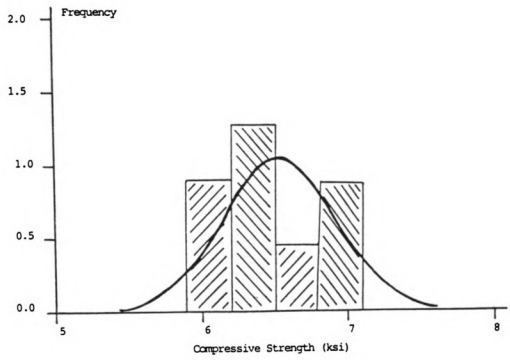

a. Frequency distribution

Figure 6.2: Experimental and theoretical (based on normal distribution) frequency and cumulative frequency distributions for compressive strength test results. 1 Ksi = 6.9 MPa

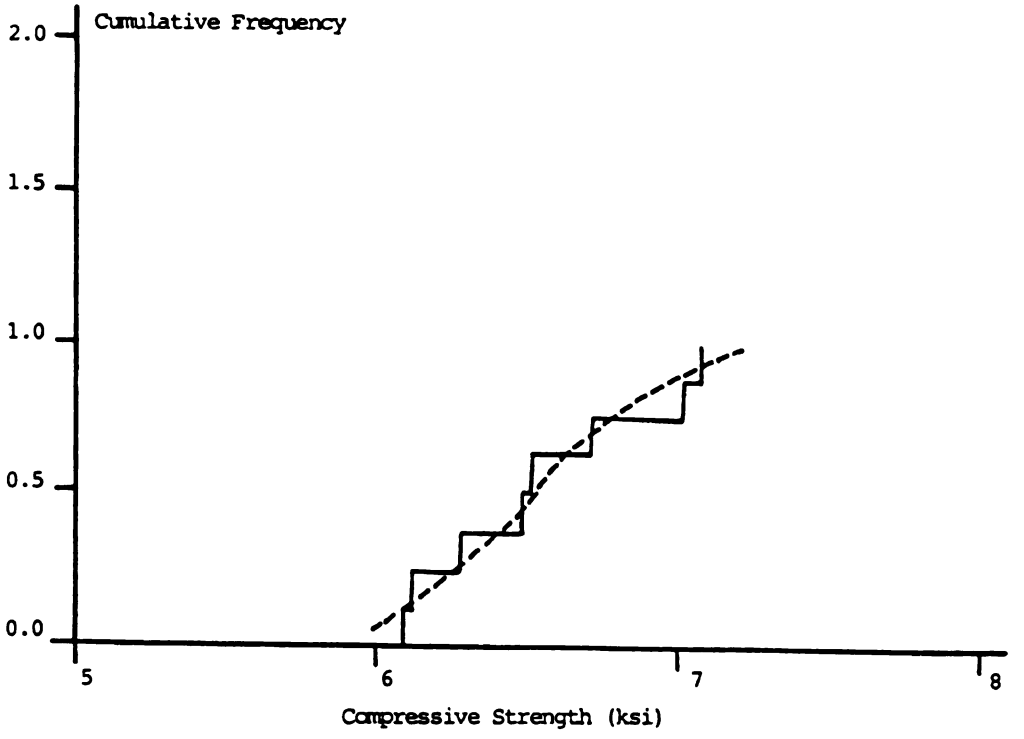

b. Cumulative frequency distribution

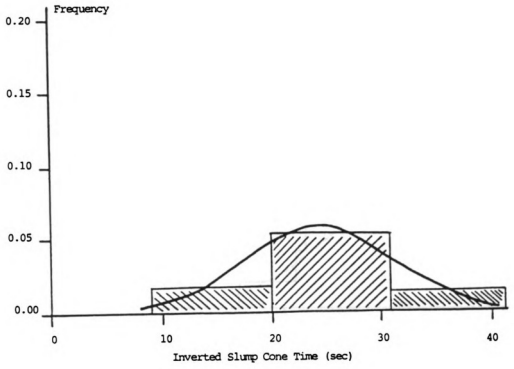

a. Frequency distribution

Figure 6.3: Experimental and theoretical (based on normal distribution) frequency and cumulative frequency distributions for inverted slump cone time test results.

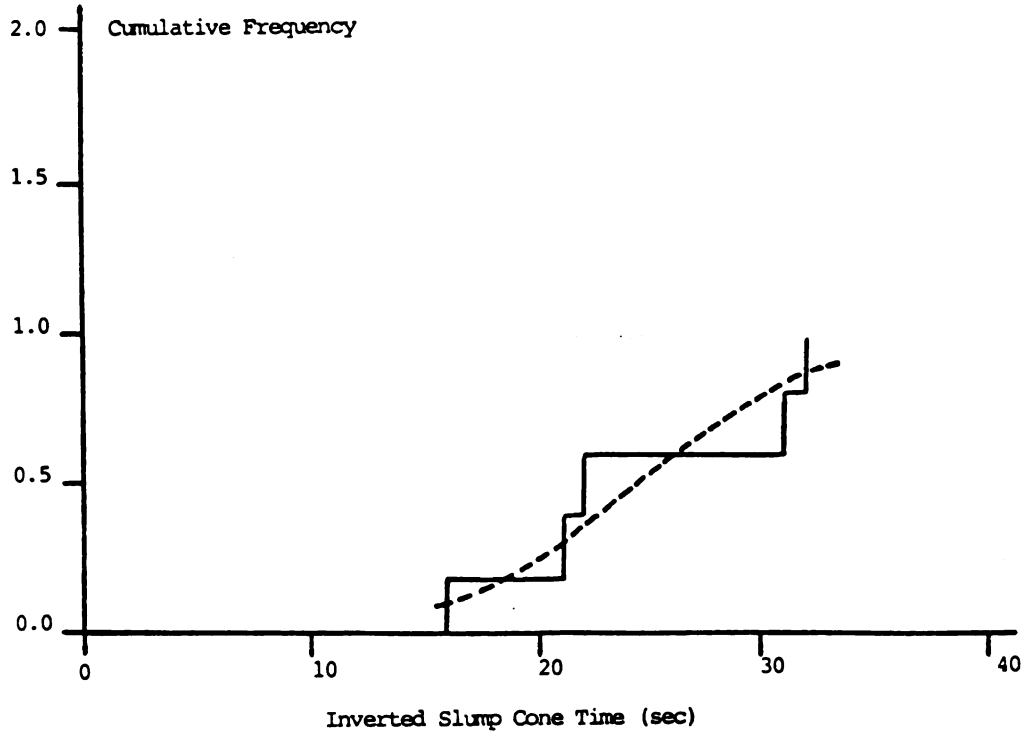

b. Cumulative frequency distribution

quality control procedures for conventional concrete when adopted for steel fiber reinforced concrete (especially with high fiber volume fraction). All this discussion is made based on the fact that flexural strength is a key property of steel fiber reinforced concrete (as is compressive strength in the case of conventional concrete).

The theoretical and experimental frequency and cumulative frequency distributions presented in Figures 6.1 to 6.3 are indicative that the observed variations in steel fiber reinforced concrete material properties follow, to some extent, the normal distribution. A Kolmogorov-Smirnov (K.S.)[65] statistical test was performed to check the goodness of fit of the observed distribution of material properties to the normal distribution. The K.S. statistical test represents the maximim diviation between the measured and the theoretical cumulative distribution curves (see Figures 6.1.b, 6.2.b and 6.3.b). The maximum deviations observed in flexural, compressive and inverted slump cone test results in the K.S. test performed in this study were 0.321, 0.157 and 0.236, respectively. These maximum deviations approve the hypothesis that the variations in compressive strength and inverted slump cone test results follow the normal distribution at a 10% significance level. This conclusion based on the K.S. test, however, does not apply to the flexural test results generated in this test. Further investigations are needed for determining the exact nature of the flexural strength distribution in steel fiber reinforced concrete with high fiber volume fraction (the results of Reference 62 also showed that the fibrous concrete flexural test results diviate more than the fibrous concrete compressive test results from the normal distribution).

Obviously, the number of test results presented in this investigation were rather limited and further studies in this area seem to be warranted.

Finally, based on the observed values of standard diviations presented in Table 6.1 for mixes from different batches, it may be concluded that the performance of 30 tests from different batches will give estimates of the material properties which, with a probability of 1%, diviate from the measurements based on all units in the lot by 160 psi for flexural strength, 179 psi for compressive strength and 3.24 seconds for inverted slump cone time in the mixture of this study.[65]

6.5 Summary and Conclusions

The results of a statistical study on the flexural and compressive strengths, and inverted slump cone time of a typical steel fiber reinforced concrete mix with a relatively high fiber volume fraction were presented. The limited test results generated in this study indicated that:

1. The compressive strength test results showed variations similar to those expected in plain concrete.

2. The flexural strength and inverted slump cone time test results showed relatively high variations indicating that the statistical aspects of the quality control procedures developed for plain concrete may have to be modified for application to steel fiber reinforced concretes with relatively high fiber volume fractions.

3. The observed distributions of compressive and inverted slump cone test results followed rather closely the normal distribution. This conclusion, however, could not be derived for the flexural strength test results.

CHAPTER 7

Application of Steel Fiber Reinforced Concrete to Footings

7.1 General

There are many situations in reinforced concrete structures where large loads are applied to limited areas on the surface of a concrete element. Examples of such localized bearing stresses include: concrete footings (Figure 7.1.a), post-tensioned prestressed members (Figure 7.1.b), and columns in precast concrete structures (Figure 7.1.c). Concrete, when loaded only on a limited fraction of its area by bearing stresses, is capable of resisting stresses in excess of its uniaxial compressive strength.[66,67]

Failure in concrete under bearing stresses occurs by the punching of an inverted cone out of concrete from beneath the loaded area, which is accompanied by the appearance of splitting cracks at the concrete surface (Figure 7.2.a) and their rapid propagation into the concrete depth.[66-74] This penetration of split cracks, depending on the geometric and material properties of the specimen, may take place either vertically towards the bottom of the specimen (Figure 7.2.b),[66,67,69] or in an incluned form (Figure 7.2.c) with the concrete cone trying to tilt over part of the concrete block from the body of the specimen.[68,73] At the ultimate bearing pressure, when split cracking initiates, part of the resistance against bearing load is provided by the splitting tensile strength of concrete. The resistance of concrete against split cracking induces a pressure on the concrete cone and mobilizes a frictional resistance against the punching of the concrete cone under bearing

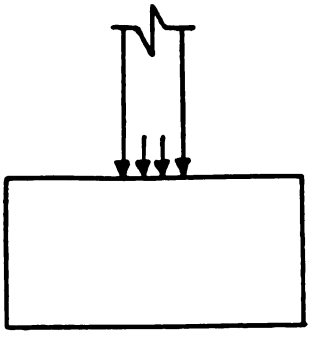

a. Concrete footing

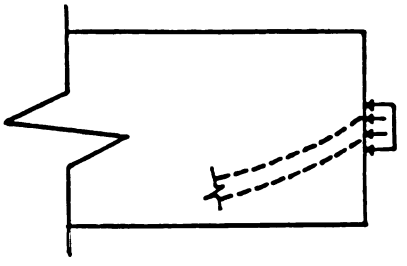

b. Prestressed beam

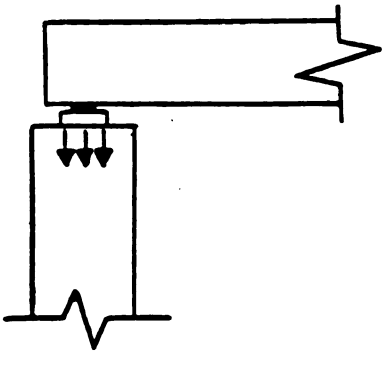

c. Precast element

Figure 7.1: Examples of elements subjected to bearing stresses.

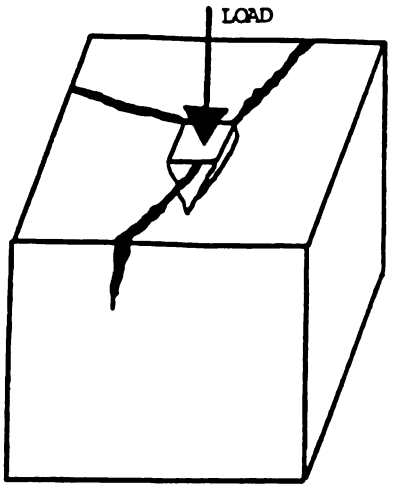

a. Punching out of concrete cone

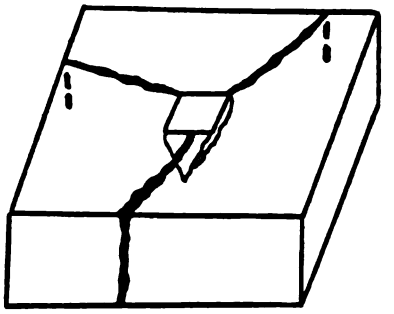

b. Vertical penetration of split cracks

Figure 7.2: Failure mode of concrete under bearing stresses.

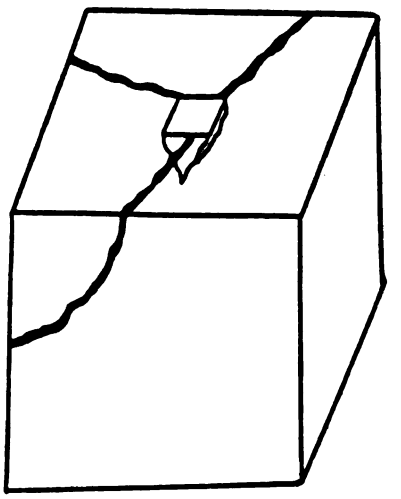

c. Inclind penetration of split cracks

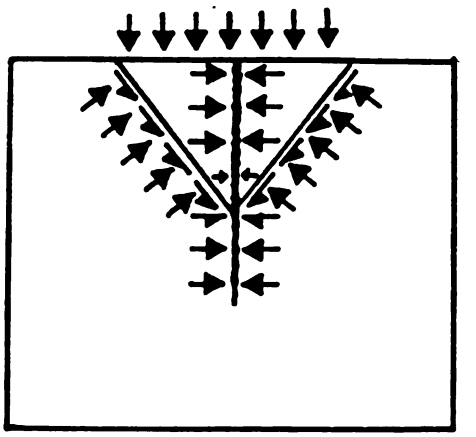

d. Mechanisms resisting bearing stresses

stresses (Figure 7.2.d). This adds to the uniaxial compressive strength which concrete is capable of developing without the confining action provided by the resistance against split cracking.

In order to improve the behavior of concrete under bearing stresses, considering the failure mode described in Figure 7.2, emphasis should be made on increasing the tensile strength, post-cracking tensile resistance and frictional shear strength of concrete. Reinforcement by steel fibers is an effective technique for achieving these objectives.[4,33,36,42,75-80] The research project reported in this chapter has been concerned with the effects of steel fiber reinforcement on the behavior of concrete under bearing stresses with due consideration given to the bearing conditions in concrete footings (Figure 7.1.a).

7.2 Background

Reference 66 has reported the results of an investigation aimed at studying the effects of confining reinforcement resisting split cracking (Figure 7.3.a) on the behavior of concrete under bearing stresses. As shown in Figure 7.3.b, in the presence of restraining steel bars, concrete is capable of maintaining its bearing resistance at large deformations. This indicates that the reinforcing bars provide the concrete with post split cracking tensile resistance. The ultimate bearing strength, however, is not much improved by the restraining bars. This indicates that, at the initiation of failure under bearing stresses, the confining action of reinforcing bars has not been fully mobilized. Larger deformations should occur

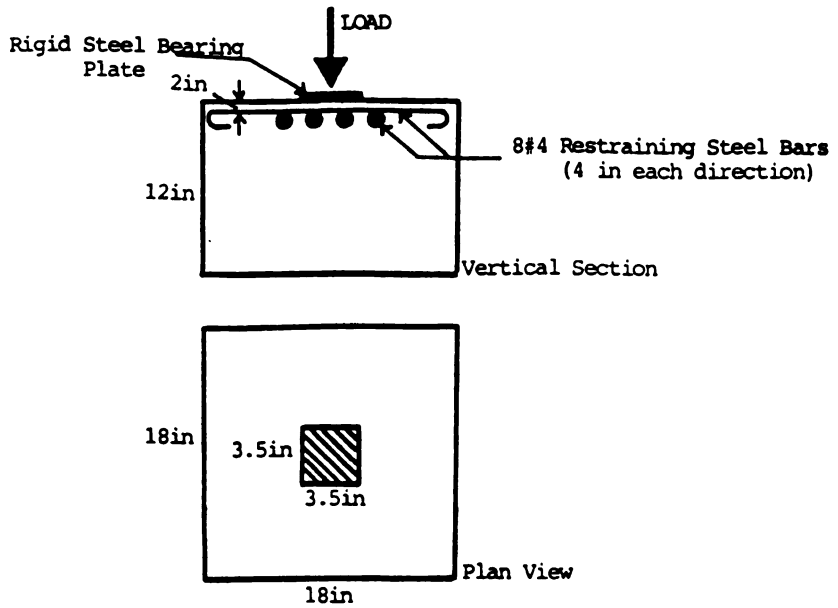

a. Restraining reinforcement

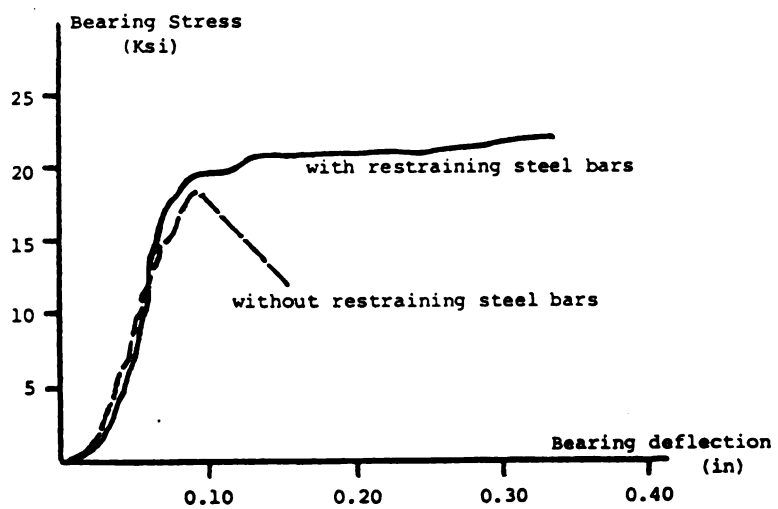

b. Effect of restraining reinforcement

Figure 7.3: Effect of restraining split cracks by rebars on concrete behavior under bearing stresses. 1 in = 25.4 mm, 1 Ksi = 6.9 MPa

before full advantage can be taken of the restraining action of reinforcing bars.

Reference 73 has reported the results of bearing tests on relatively small cylindrical steel fiber reinforced concrete specimens (Figure 7.4.a). The failure mode was always by punching of a concrete cone underneath the bearing area accompanied by split cracking (Figure 7.4.b). The diameter of the specimens and the bearing areas were both constant. The main variables in the test program of Reference 73 were the specimen height and the volume fraction of steel fibers. As shown in Figure 7.4.c, the bearing strength tends to increase with fiber reinforcement and also with increasing the depth of test specimen (the increase in bearing strength with specimen depth takes place at a gradually decreasing rate). Reference 73 does not provide information on the possible improvements in the ductility of failure resulting from fiber reinforcement. Measurements made of stresses and strains in bearing tests of Reference 73 indicated that tensile stresses were higher near the top surface where the bearing stresses are applied, while the compressive stresses tended to increase at depths further away from the bearing surface. This could be expected considering the failure mode under bearing stresses (Figure 7.2.d), where the induced splitting tensile stresses are maximum near the bearing surface, and the transfer of compressive stresses from the small bearing area to the complete corss-section takes place gradually away from the bearing area. An important finding of Reference 73 is that the maximum tensile strains were of the order of 1300 microstrains in plain concrete. This value is approximately 13 times the usual values measured for specimens tested in direct

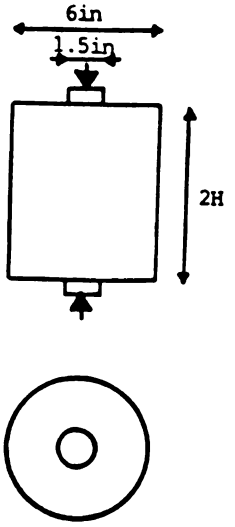

a. Test specimen

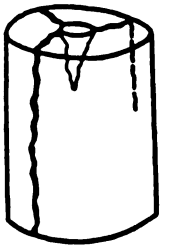

b. Failure mode

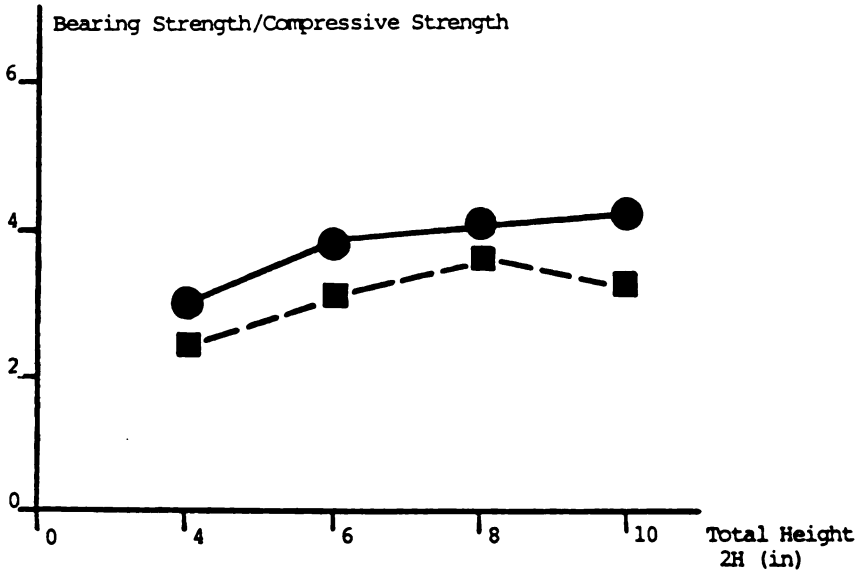

c. Test results

Figure 7.4: Bearing test specimens and test results from Reference 73. 1 in = 25.4mm

tension and roughly twice the values measured in indirect tension.

7.3 Experimental Program

The main objective of the test program performed in this study was to assess the effects of fiber reinforcement of a top layer in concrete footings on the overall footing behavior under bearing stresses. A total of five specimens were tested in this investigation. All of these specimens were designed to ensure that bearing failure precedes the flexural and shear modes of failure. For this pupose, sufficient reinforcement was provided at the bottom layer to resist the applied flexural forces, and the depth was selected to prevent pre-mature shear failure.

Table 7.1 and Figure 7.5 introduce the bearing specimens tested in this study. All the specimens had a 16 x 16 in (406 x 406 mm) square cross-section with a total height of 12 in (305 mm). They were loaded by a 3 x 3 in (76 x 76 mm) square rigid bearing plate locaed at the center of their top surface. Specimen No. 1 (Figure 7.5.a) was basiclly plain (except for the flexural reinforcement). Specimen No. 2 (Figure 7.5.b) was similar to specimen No. 1 except that four #3 (0.375 in = 9.5 mm in diameter) grade 60 (yield strength = 60 Ksi = 420 N/mm^2) vertical dowel bars were placed at the four corners of the bearing plate, and were extended to the bottom of the footing where they were terminated in 90° hooks on the top of the flexural reinforcement. Specimen No. 3 (Figure 7.5.c) was similar to specimen No. 1, but it was reinforced throughout its full depth with 2% volume fraction of straight round steel fibers having an aspect ratio of 57. Specimen No. 4 (Figure

Table 7.1: Bearing test specimens. 1 in = 25.4 mm

Specimen	Fiber Reinforcement		Dowel Bars
	Volume Fraction	Depth	
1	-----	-----	-----
2	-----	-----	4 No. 3
3	2%	12in	-----
4	2%	4in	-----
5	2%	4in	4 No. 3

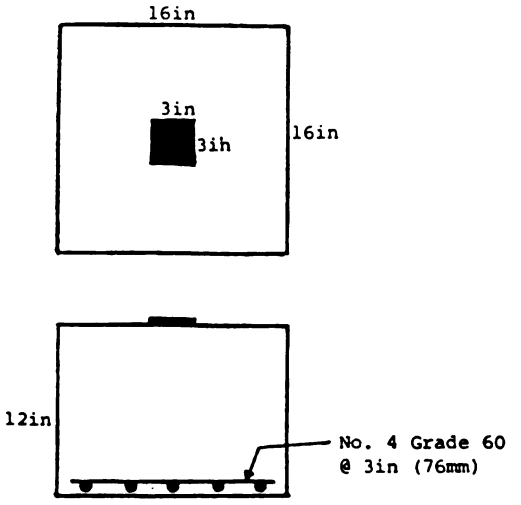

a. Specimen No. 1

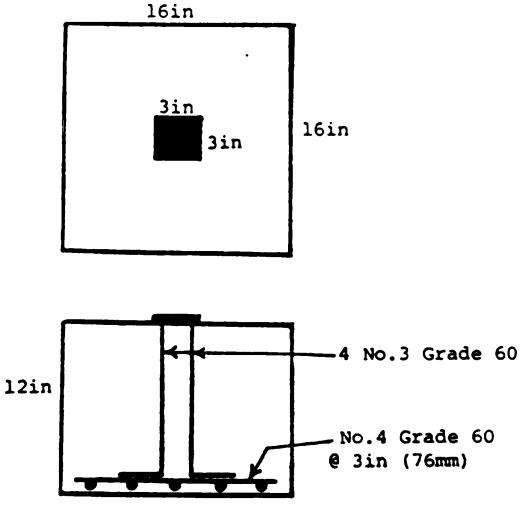

b. Specimen No. 2

Figure 7.5: Bearing test specimens. 1 in = 25.4 mm

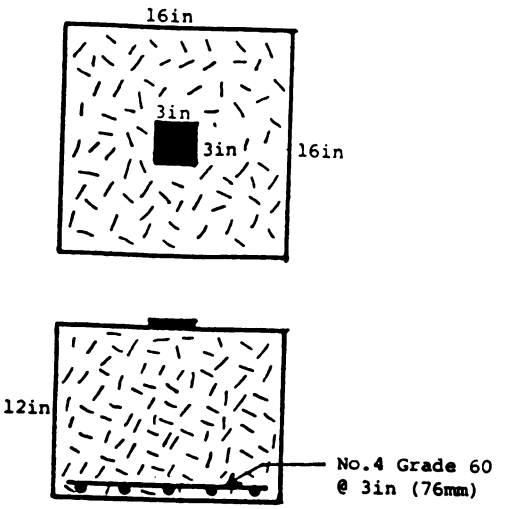

c. Specimen No. 3

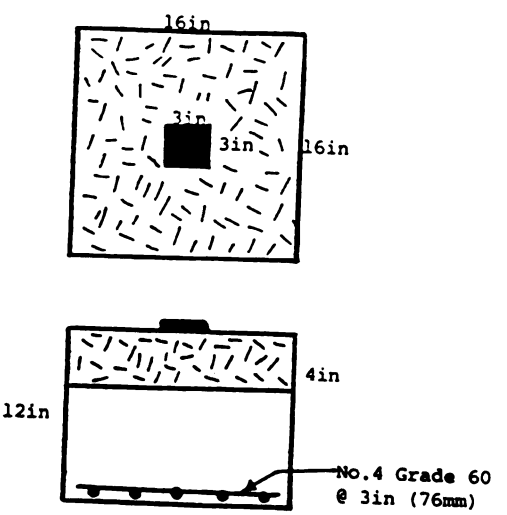

d. Specimen No. 4

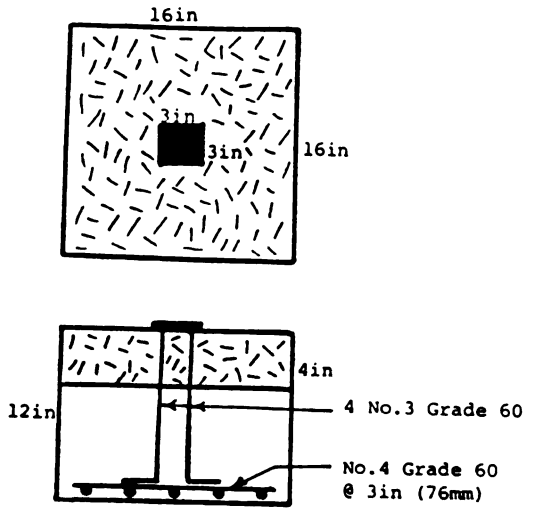

e. Specimen No. 5

7.5.d) was also similar to specimen No. 1 except that it was reinforced with 2% volume fraction of the same steel fibers of specimen No. 3 only through 4 in of its depth at the top surface underneath the bearing area. Specimen No. 5 (Figure 7.5.e) was similar to specimen No. 4, but had four #3 grade 60 vertical dowel bars at the corners of the bearing plate.

The plain concrete used in test specimens had a water-binder (portland cement + fly ash) ratio of 0.45 by weight, fly ash-binder ratio of 0.3, superplasticizer-binder ratio of 0.015 and aggregate-binder ratio of 4.0. The fine-to-coarse aggregate ratio was 1.0 and the maximum aggregate size was 3/4 in (19 mm). The fibrous mixes had a concrete matrix similar to the plain one.

Type I ordinary portland cement and and a class F fly ash (see Table 2.1 in Section 2.3 of Chapter 2 for the fly ash physical and chemical properties)[37] were used, and the superplasticizer was Daracem 100 produced by W.R. Grace and Company.[38] Natural river aggregates were used in the construction of test specimens. The steel fibers used in this study had a diameter of 0.035 (0.89 mm) and a length of 2 in. (50.8 mm). All the steel bars were grade 60.

The plain and fibrous concrete had average compressive strengths of 5,520 psi (38.5 MPa) and 5,650 psi (39.8 MPa), respectively. the complete compressive stress-strain and flexural load-deflection relationships of the plain and fibrous concretes are shown in Figures 7.6.a and 7.6.b. The compression stress-strain

relationships were obtained from testing 6 x 12 in (152 x 305 mm) standard cylindrical specimens, and the flexural load-deflection curves were produced in four-point loading tests on prismatic specimens with a 6 x 6 in (152 x 152 mm) cross-section and a span of 18 in (457 mm). In Figure 7.6.c, the direct tensile stress-strain relationships of the plain and fibrous concretes of this study are derived based on the flexural and compressive load-deformation curves (using a method introduced by Reference 81). The improvements in compressive, tensile and flexural ductilities as well as flexural and tensile strengths of concrete resulting from steel fiber reinforcement are obvious in Figure 7.6.

The five bearing specimens were cast in wooden forms and were vibrated externally on a vibrating table. The specimens were moist-cured inside their forms for seven days, before being demolded and exposed to the regular laboratory environment until the test age of 28 days.

The experiments were performed using a hydraulic compression test machine, with the loading applied at a quasi-static rate. During the test, the specimens were supported on a 1/4 in wooden base which was placed on a rigid steel plate (Figure 7.7). Two electrical displacement transducers were used to measure the penetration of the rigid bearing plate into concrete under bearing stress as shown in Figure 7.8. The transducers had a maximum error equal to 0.4% of the measured value.

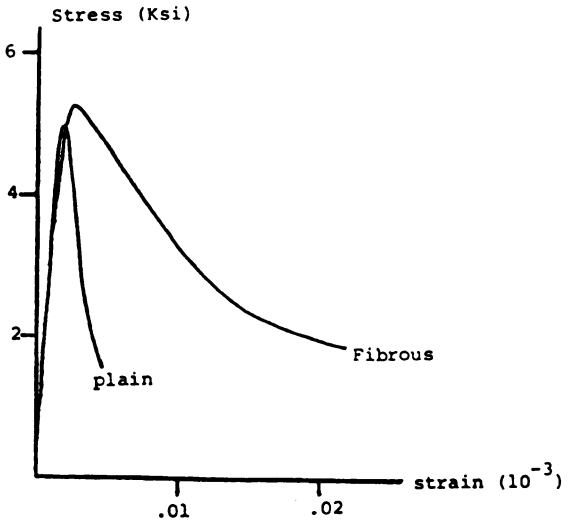

a. Compressive stress-strain relationships

Figure 7.6: Plain and fibrous concrete material properties. 1 in = 25.4 mm, 1 Ksi = 6.9 MPa, 1 Kip = 4.5 KN.

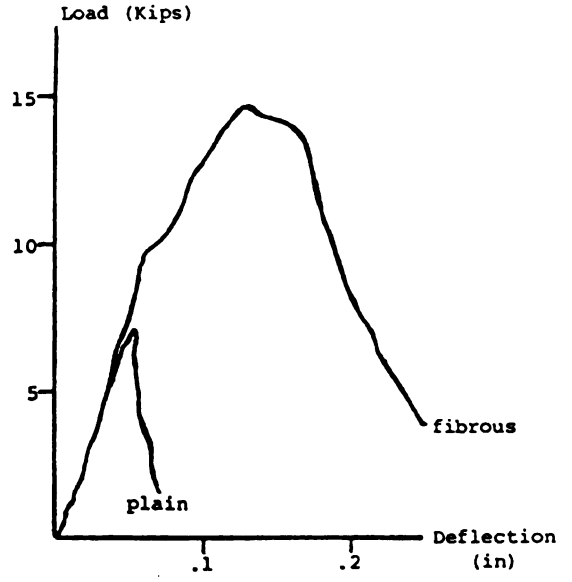

b. Flexural load-deflection relationships

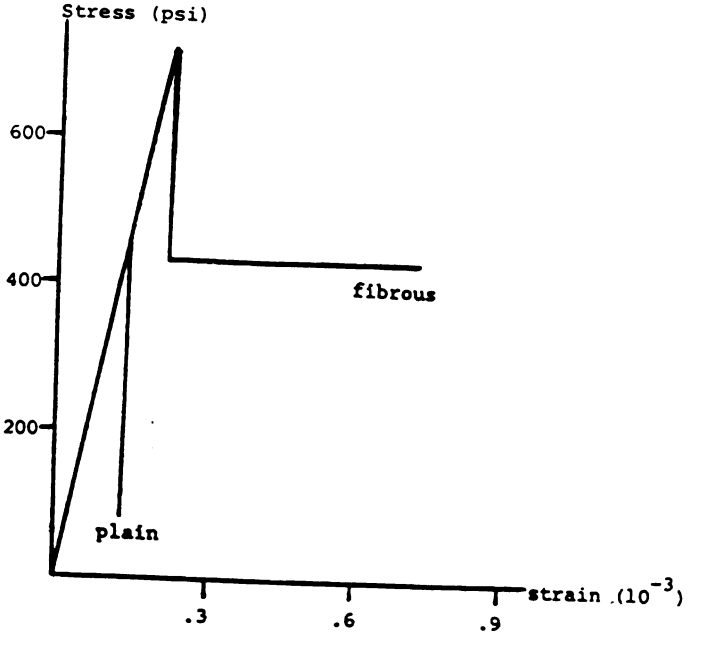

c. Tensile stress-strain relationships

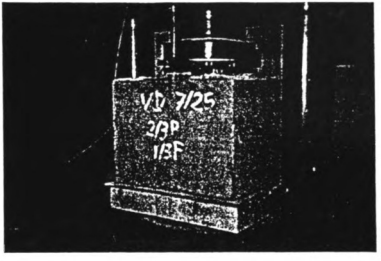

Figure 7.7: Test specimen under load

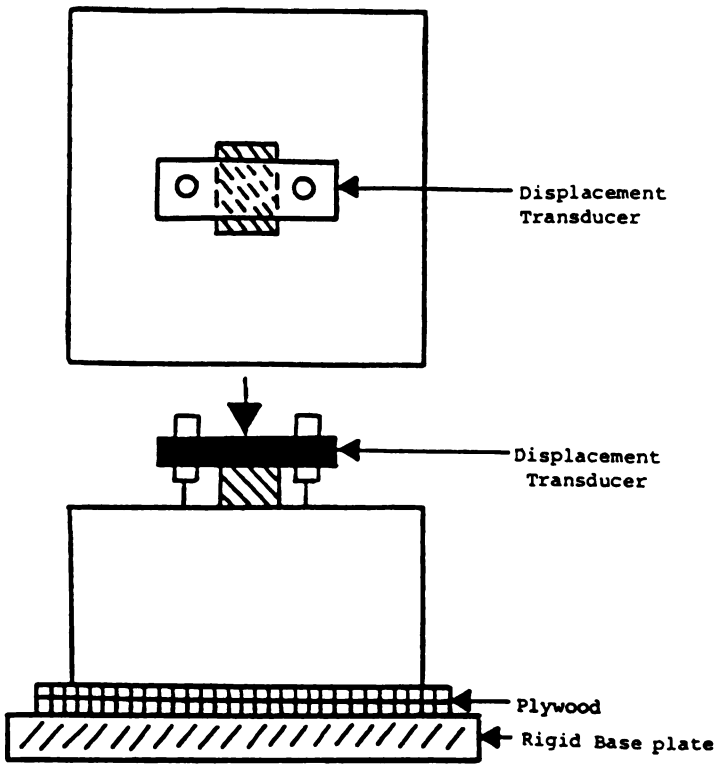

Figure 7.8: Test set-up and instrumentation

7.4 Experimental Results

Failure in the plain and fibrous specimens occured, as expected, by punching of a concrete cone underneath the bearing area into the specimen, leading to the appearance of splitting cracks at the top surface which penetrated into the specimen's depth with continued loading. Typical crack configurtions at the top surface of the plain and fibrous (full or partial depth) specimens are shown in Figures 7.9.a and 7.9.b, respectively. The splitting cracks at the top surface of plain concrete specimens (Figure 7.9.a) were inclined and practically divided the top of the concrete block into four segments. These splitting cracks penetrated into the specimen's depth rather smoothly without much branching, and led to a relatively brittle mode of failure. In the case of specimens reinforced with fibers throughout their full or partial depth, the splitting cracks at the top surface were almost parallel to one of the specimen's sides, and they tended to divide the top of the concrete block into two halves (Figure 7.9.b). The penetration of these splitting cracks into the concrete depth involved branching of the cracks and was rather slow. The failure of all the fibrous specimens took place in a ductile manner.

Figure 7.10.a presents the bearing stress-deflection relationships obtained in tests on plain specimens with and without vertical dowel bars (specimens 1 and 2, respectively, of Table 7.1). The bearing stress-deflection relationships of different fibrous specimens (specimens 3, 4, and 5 of Table 7.1) are given in Figure 7.10.b. From Figure 7.10.a it may be concluded that the vertical dowel bars have a relatively small effect on the overall behavior of concrete under bearing

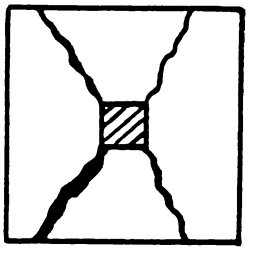

a. Plain concrete

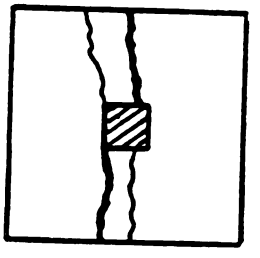

b. Fibrous reinforced concrete (full or partial depth)

Figure 7.9: Typical crack configuration in plain and fibrous specimens.

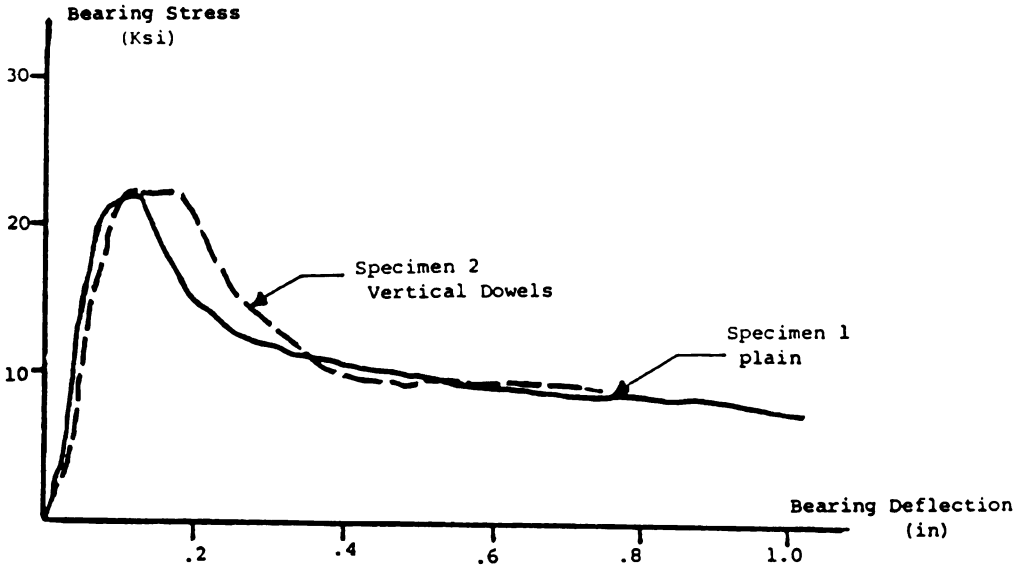

a. Plain specimens

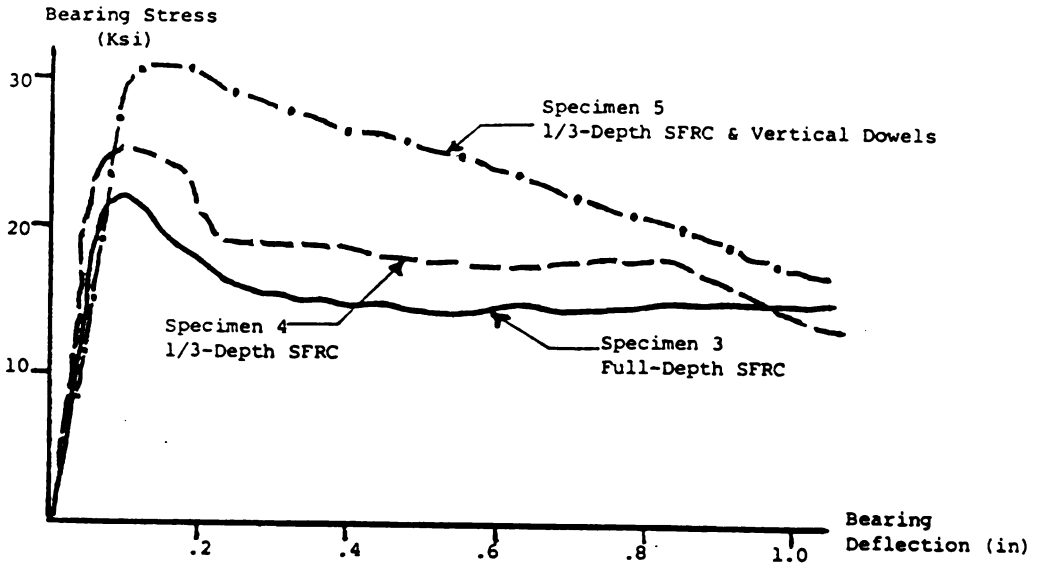

b. Fibrous specimens

Figure 7.10: Experimental bearing stress-deflection relationships. 1 in = 25.4 mm, 1 Ksi = 6.9 MPa.

stresses. This is in agreement with the findings of Reference 66. From the limited test results presented in Figure 7.10.b, it may be concluded that the concrete specimens with fiber reinforcement provided at only 1/3 of their depth underneath the bearing area performed very similarly to the one with full-depth fiber reinforcement. Dowel bars also seem to be more effective in improving the behavior of fibrous concrete, compared to plain concrete, under the action of bearing stresses.

Figures 7.11.a and 7.11.b present normalized bearing stress-deflection relationships for plain and fibrous specimens with and without dowel bars, respectively. The normalization of bearing stresses in these figures has been made with respect to the compressive strength of concrete (or fibrous concrete). Figures 7.11a and 7.11.b clearly demonstrate the effects of fiber reinforcement on the behavior of concrete under bearing stresses. Figure 7.11.a indicates that full-depth or partial-depth steel fiber reinforcement result in an increase in the ultimate bearing strength (also reported by Reference 73) and a significant improvement of the post-peak ductility of concrete under the action of bearing stresses. The more economical method of partial-depth fiber reinforcement seems to be an efficient approach to the improvement of the bearing performance of concrete. The specimen with full-depth fiber reinforcement actually was slightly inferior to the one with only a top layer of fibrous concrete, possibly due to the settlement of fibers to the bottom of specimen under vibration when fiber reinforced concrete was cost in full-depth. Figure 7.11, based on limited results,

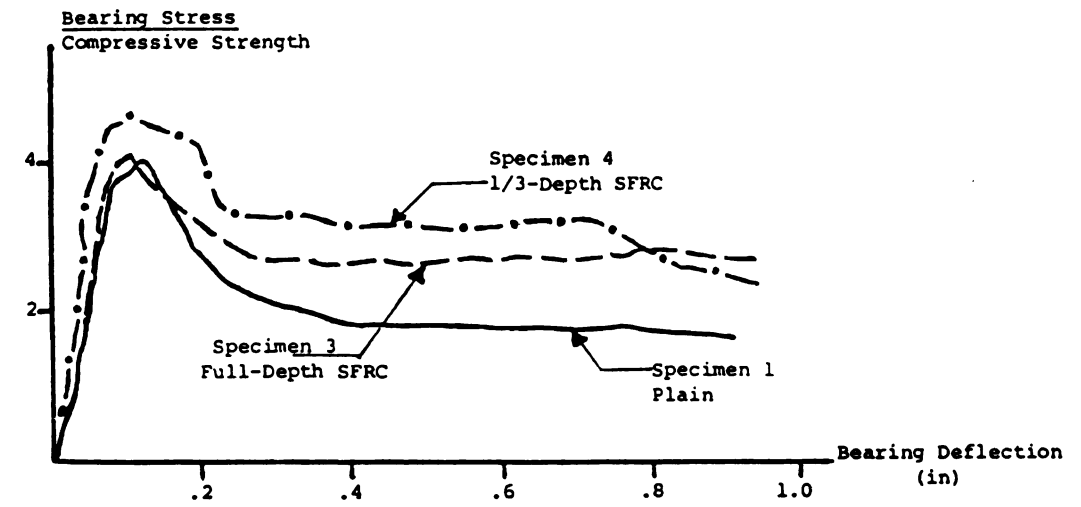

a. Without dowel bars

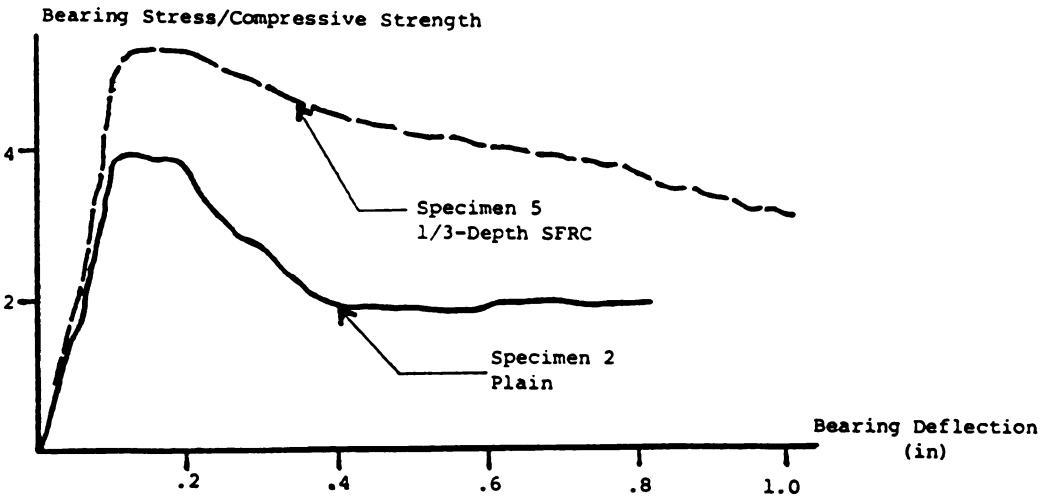

b. With dowel bars

Figure 7.11: Normalized bearing stress vs. bearing deflection relationships. 1 in = 25.4 mm.

is an indication of the increase in the effectiveness of dowel bars under bearing stresses resulting from steel fiber reinforcement. This could be attributed to the better confinement of dowel bars by fibrous concrete which is capable of providing lateral support against buckling of the bars (Reference 79 has shown that steel fibers prevent buckling of compression steel bars in beams).

7.5 Discussion of Results

The bearing test results generated in this study are used in the section to verify the theory presented in Reference 67 for predicting the bearing strength of plain concrete, and also to check the applicability of this theory to steel fiber reinforced concrete. The theory of Reference 67 is based on the failure mode described in Figure 7.12, noting that this model closely simulates the actual behavior of concrete under bearing stresses. Equilibrium conditions require that the edges of the concrete cone punching into the body of the specimen under the bearing area should be inclined at an angle of $45-\phi/2$ from the vertical direction (Figure 7.12.b); where ϕ is the angle of internal friction of concrete. Reference 67 suggests a value of 50° for ϕ in plain concrete with 3/4 in maximum aggregate size. In this model, the punching out of the concrete is suggested to generate an internal pressure against the body of the specimen (Figure 7.12.c) which tends to produce splitting cracks in the specimen. The ultimate bearing stress, according to Reference 67, is reached when this internal pressure reaches a level sufficient for overcoming the tensile resistance of the concrete block at the top surface and initiating the splitting cracks. Based on this failure mode, Reference 67 has derived the following

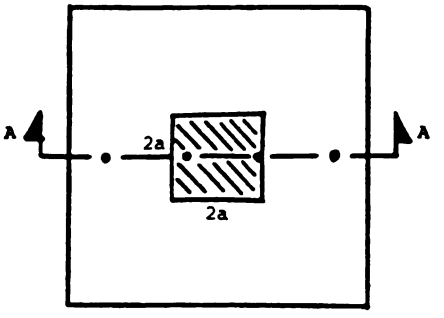

a. Plan

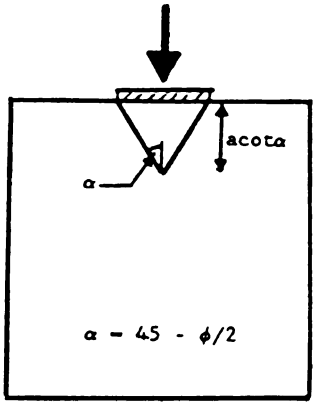

b. Section A-A

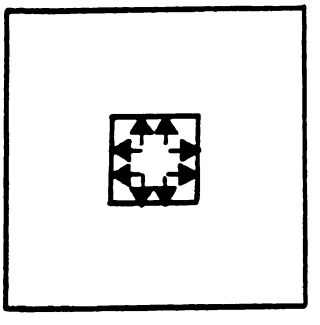

c. Internal presssure causing splitting

Figure 7.12: Failure model of Reference 67.

expression for predicting the bearing strength of concrete in terms of its stensile and compressive strengths and the coefficient of internal friction:

$$f_b = f_c + f_t \cot^2(45 - \phi/2)(\sqrt{A_2/A_1} - 1) \qquad (7.1)$$

where:

f_b = concrete bearing strength;

f_c = concrete compressive strength;

f_t = concrete tensile strength;

ϕ = angle of internal friction;

A_2 = maximum area of the supporting surface that is geometrically similar to and also concentric with the loaded area; and

A_1 = loaded area.

As mentioned earlier, Reference 67 suggests a value of 50° for the angle of internal friction for plain concrete with 3/4 in (19 mm) moximum aggregate size. A value of 47°, for the angle of internal friction of the fibrous concrete mix of this study, produces the best fit between the test results and the prediction of Equation 7.1. Consistent with the observed behavior and the generated test results, the specimens with full and partial depth of fibrous concrete were treated similarly (assuming that, in both cases, the bearing behavior is fully governed by the fiber reinforced

concrete response), and it was assumed that the dowel bars can provide the fibrous specimen with their full yield strength at the peak bearing load. Hence, the contribution of concrete to the bearing strength of the fibrous specimen with dowel bars was assumed to be the peak load minus the yield strength of dowel bars.

Reference 69 has used the following equation for the angle of internal friction of concrete (in terms of the ratio of tensile to compressive strengths of the material):

$$\phi = \arcsin(1 - 2\, f_t/f_c) \qquad (7.2)$$

Values of 48° and 55° can be obtained for the angles of internal friction for the fibrous and plain concretes of this study, respectively, by applying Equation 7.2. This equation provides good estimate for fibrous concrete; however, it can be misleading if used for plain concrete.

Table 7.2 provides a comparison between the bearing test results and the predictions of Reference 67 (with $\phi = 50°$ for plain concrete and $\phi = 47°$ for fibrous concrete).

The American Concrete Institute Design Code 318-83 (Reference 64) suggests the following equation for the beaing strength of concrete:

Table 7.2: Comparison of test results with theoretical predictions of bearing strength

Specimen	Bearing Strength/Compressive Strength		
	Test Results	Equation 7.1 Reference 67	Equation 7.3 Reference 64
1 (plain)	4.03	3.81	1.70
2 (plain+dowels)	3.97* (3.43)**	3.81	1.70
3 (full-depth SFRC)	4.09	4.53	1.70
4 (partial-depth SFRC)	4.60	4.53	1.70
5 (partial-depth SFRC+dowels)	4.89**	4.53	1.70

*Neglecting the resistance of dowel bars
**Considering the yield strength of dowel bars
SFRC=Steel Fiber Reinforced Concrete

$$f_b = 0.85\sqrt{A_2/A_1}\ f_c \leq 1.7\ f_c \qquad (7.3)$$

The Design Code 318-83 of the American Concrete Institute also suggests that the dowel bars in plain concrete can develop their full yield strength at the peak bearing load. The predictions of concrete and fibrous concretes bearing strengths by Equation 7.3 are also given in Table 7.2.

From Table 7.2, it may be concluded that Equation 7.1 (with the assumption that dowel bars are not effective in plain concrete but can develop their full yield strength at ultimate bearing strength in fibrous concrete) can reasonbly predict the test data generated in this study (with the angle of internal friction equal to 50° in plain concrete and 47° in fiber concrete). The predictions of bearing strength by Equation 7.3 are highly conservative. The test results produced in this study and Reference 66 do not agree with the assumption of the American Concrete Institute Design Code 318-83 that dowel bars can develop their yield strength under bearing stresses in plain concrete.

It is worth mentioning that References 68, 69 and 73 have used theorems of limit analysis to predict the bearing strength of concrete. This approach relies on the extensibility of concrete in tension and relates bearing strength to the ratio of specimen height to the planner dimension of the bearing area. References 68 and 73, however, state that the limit theorems can not be applied when the specimen

dimensions are significantly larger than the dimensions of the bearing area, mainly due to the limited local deformability of concrete materials in tension. Test results on plain and fibrous concrete confirm this statement (References 68 and 73).

It should be noted that the available theories emphasize only on the prediction of bearing strength. A major contribution of fiber reinforcement under bearing stresses is, however, related to the improvement of the ductility of concrete behavior. Further studies are needed in order to analytically simulate and quantify this phenomenon and take full advantage of its benefits in design.

7.6 Summary and Conclusions

The results of an experimental study on the behavior of concrete and fiber reinforced concrete under bearing stresses in the condition of concrete footings were presented. A theoretical approach was used to predict the bearing strength of concrete and fiber reinforced concrete, and the results were compared with the generated test data. It was concluded that:

1. The failure mode of concrete and fiber reinforced concrete under bearing stresses results from punching out of a concrete cone from beneath the bearing area, which produces splitting cracks in the concrete block. The splitting crack pattern is different in concrete from fiber concrete, but in both cases, these cracks start from the vicinity of the bearing area.

2. Fiber reinforcement of concrete footings at their full depth and also at a top layer underneath the bearing area, can effectively increase the bearing strength and especially the ductility of failure under bearing stresses. The application of fibers at a top layer can provide results which are comparable to these obtained with full depth fiber reinforcement.

3. Dowel bars do not seem to make a significant contribution to the resistance of plain concrete under bearing pressure. These bars, however, tend to be more effective when a top layer of concrete under the bearing area is reinforced with steel fibers.

4. The failure models and theoretical formulations developed for predicting the bearing strength of concrete can be applied to fiber reinforced concrete when due consideration is given to the changes in concrete tensile and compressive strengths and angle of internal friction resulting from fiber reinforcement. The current theories, however, can not predict the improvements in ductility of behavior under bearing stresses resulting from fiber reinforcement.

CHAPTER 8

Local Bond Behavior of Deformed Bars in Steel Fiber Reinforced Concrete

8.1 Introduction

Application of short randomly distributed steel fibers to beam-column connections results in improved ductility, stiffness, strength and hysteretic performance.[4,82,83] Steel fibers can, thus, partially substitute confining hoops and, consequently, reduce the congestion of steel in seismic-resistant joints. This is a great advantage in construction of beam-column connections in high-risk seismic zones. Fiber reinforcement is also found to reduce the total cost of seismic-resistant joints.

It is generally believed that fibers improve the joint behavior through: (a) improving the confinement of concrete; (b) increasing the shear resistance at the joint; and (c) providing better anchorage of reinforcing bars crossing the joint.[82,83] The test data reported in the literature on fiber reinforced concrete joints are not sufficient to assess the relative significance of these factors. Research is needed on the details of the mechanisms through which fiber reinforcement improves the overall joint behavior.

The improvement in the behavior of anchored bars at reinforced concrete joints resulting from fiber reinforcement is the subject of the investigation reported in this chapter. The local bond behavior of deformed bars at fibrous reinforced

concrete joints is studied experimentally, and the results are compared with the corresponding test results on conventional reinforced concrete joints containing no fibers.

8.2 Behavior of Anchored Bars at Reinforced Concrete Joints

The tendency of anchored bars to slip at beam-column connections under bending moments is resisted by the bond between steel and concrete (Figure 8.1).[84,85] The bond resistance is provided mainly by the mechanical interlocking between bar lugs and concrete (Figure 8.2.a).[86,87] The radial component of the pressure in front of the lugs acts in concrete as an internal pressure and induces tensile stresses which cause a splitting crack (Figure 8.2.b). The presence of reinforcing bars which cross the splitting crack would restrict the widening of the crack (Figure 8.2.c). The confinement provided by such reinforcement will make it possible to increase the pull-out force above the force level corresponding to the appearance of splitting cracks. Loading can be continued in this case, up to complete pull-through of the anchored bar. The effects of confinement on bond stress-slip relationship is shown in Figure 8.2.d.

Effects of steel fiber reinforcement on the interaction between deformed bars and concrete have not been investigated thoroughly. An experimental study reported in Reference 88 has concluded that reinforcement by 2% volume fraction of randomly distributed straight steel fibers with an aspect ratio of 65 can increase the pull-out strength of deformed bars anchored in confined specimens by about 40%. This

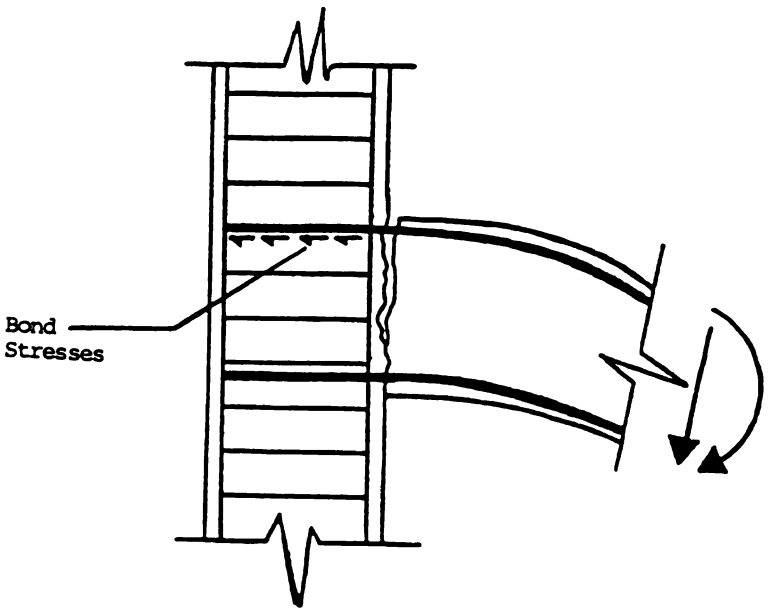

Figure 8.1: Pull-out force on anchored bars

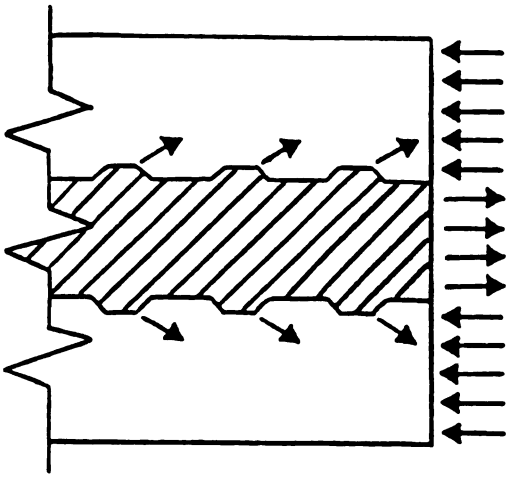

a. Bond resistance

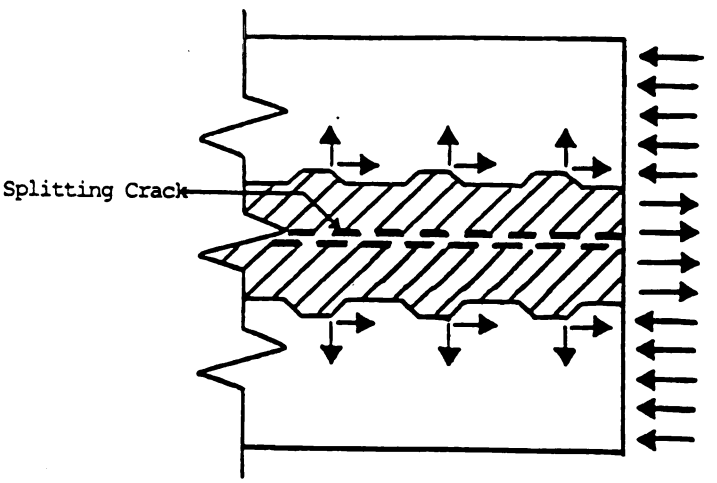

b. Splitting cracks

Figure 8.2: Mechanism of bond resistance under monotinic loading.

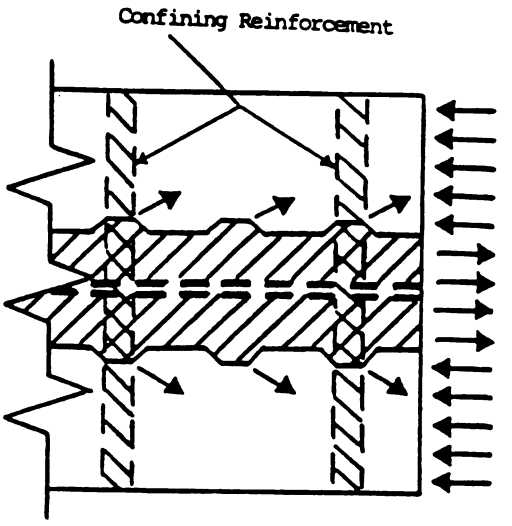

c. Confining reinforcement

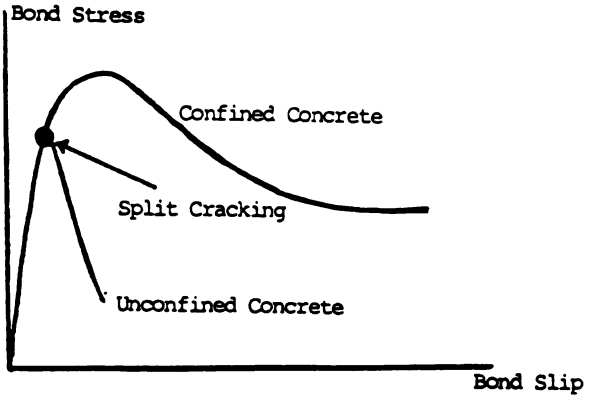

d. Bond stress-slip relationships

reference also reports improvements in bond stiffness and ductility resulting from steel fiber reinforcement.

8.3 Test Program

The specimens tested in this study (Figure 8.3) represent the local bond behavior of deformed bars in the confined region of beam-column connections. In these specimens, a short length of No. 8 (1 in = 25.4 mm nominal diameter) grade 80 (yield strength = 80 Ksi = 550 MPa) deformed bar was embedded in a concrete block confined by vertical and transverse bars (representing column reinforcement). Figure 8.4 shows the reinforcement cage of a specimen inside its wooden form prior to casting concrete. The embedment length was chosen to be $5d_b$, with d_b representing the bonded bar diameter. This embedment length is short enough to result in a fairly uniform bond stress when the bar is being pulled out, but long enough to reduce the scatter of test results usually observed in tests with a very short bonded length.[87]

The bonded length was positioned in the middle of the specimen and a bond-free length of $5d_b$ was provided at either side. This bond-free length was obtained by covering the bar with a thin plastic tube. The embedment length was thus limited to the confined concrete region. Although the splitting cracks are restrained by the column reinforcement, they may still influence the bond behavior. An artificial splitting crack was created in the test specimens by placing a thin plastic sheet

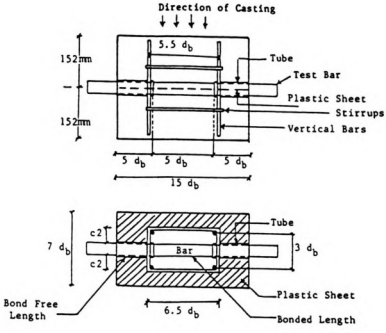

Figure 8.3: Schematic diagram of test specimen

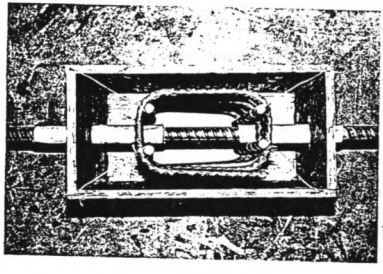

Figure 8.4: Test specimen

during casting in the plane of the longitudinal bar axis as shown in Figure 8.3. This artificial crack represents the splitting cracks caused by the pull-out of the adjacent bars in actual joint conditions.[87,89] The arrangement shown in Figure 8.3 represents the bond behavior when the clear spaing of bars is $4d_b$. The bonded bar was placed in the middle of the specimen (height = 12 in = 305 mm) and casting was in a horizontal position. Therefore, the bond could be expected to be somewhat superior or inferior to top or bottom bars, respectively.

The test set-up is shown in Figure 8.5. The pull-out force was applied by a hydraulic actuator which supported on the specimen's top surface. A greased plastic sheet was provided between the base plate of the actuator and the specimen to reduce the restraining effect of the friction forces. The pull-out force was measured at the loaded end of the bar by a load cell. Assuming that the bond stresses are evenly distributed along the bonded length, they can be calculated by dividing the measured force by the bonded surface area. The bond slip was measured at the unloaded bar end with two displacement transducers. Since the anchored steel bar behaves elastically in these tests, the measured slip valves were assumed to represent the local slip at the middle of the embedment length with sufficient accuracy. The maximum error of the load cell and the displacement transducers used in this experimental study was below 2%.

The deformation pattern of No. 8 deformed bars which were used as bonded bars is

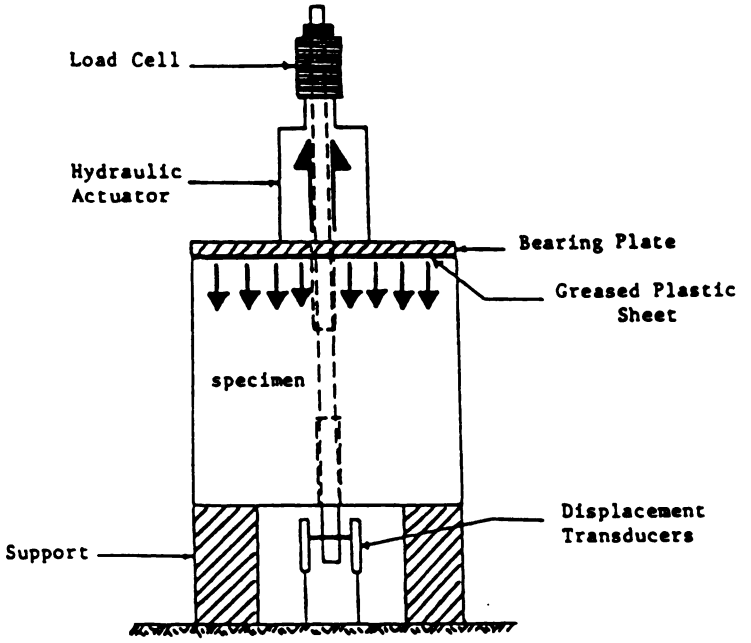

Figure 8.5: Test set-up

shown in Figure 8.6.a. The specimens were constructed with plain or fiber reinforced concretes having a water-binder (cement + fly ash) ratio of 0.4 and a fly ash-binder ratio of 0.3. The cement used in this study was Type I, and the fly ash had a silica content of 47% (see Table 2.1 of Section 2.3 Chapter 2 for the major chemical and physical properties of the fly ash used in this experimental investigation). The mix also contained a superplasticizer-binder ratio of 1.5% by weight, and an aggregate-binder ratio of 4.0, with the sand content being equal to that of gravel (maximum size = 3/4 in = 19 mm). The steel fiber volume fraction in fiber reinforced concrete was 2%, and the round straight fibers used had a diameter of 0.035 in (0.89 mm) and a length of 2 in (51 mm), resulting in an aspect ratio of 57.

The fiber reinforced concrete used in this study had a slump fo 1.2 in (30.5 mm), an inverted slump cone time of 32 seconds, and an air content of 2.7%. The 28-day compressive strengths of fiber and plain concretes were 6,500 psi (44.8 MPa) and 6,000 psi (41.4 MPa), respectively. The flexural strengths were 1,700 psi (11.7 MPa) and 850 psi (5.9 MPa) for steel fiber and plain concretes, respectively. The compression and flexural samples as well as the bond test specimens were moist cured inside their forms for seven days. They were then exposed to the regular lab environment until the test age of 28 days.

The compression specimens were 6 x 12 in (150 x 300 mm) cylinders, and the flexural specimens were 6 x 6 x 20 in (150 x 150 x 500 mm) prisms loaded at

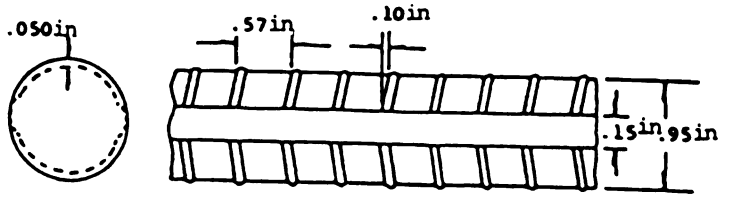

a. Deformation pattern of No. 8 bonded bars

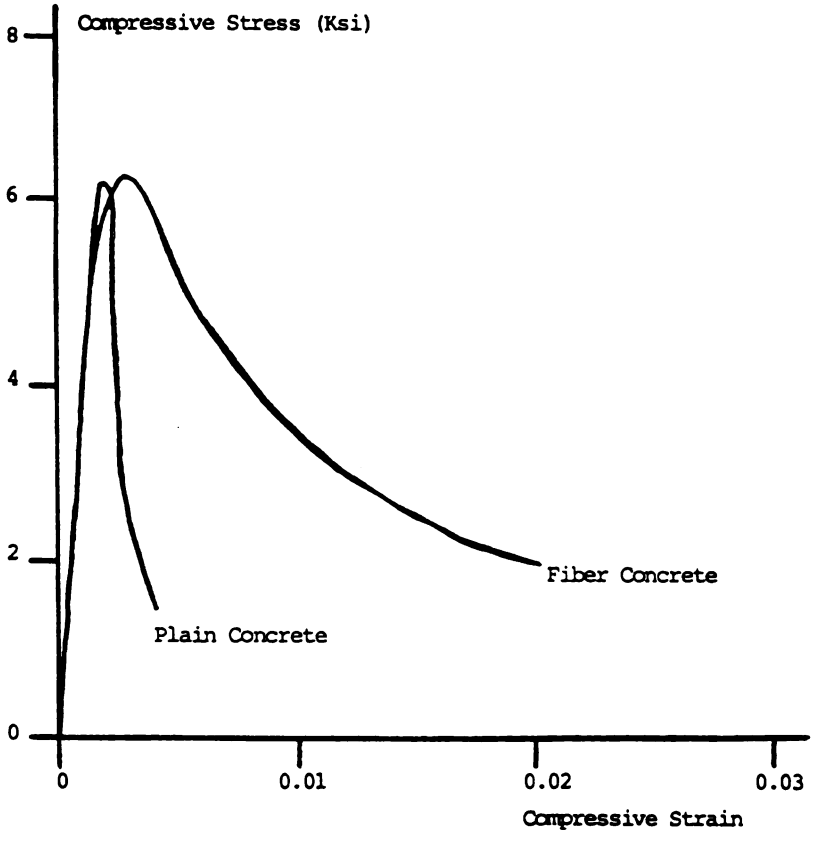

b. Compressive stress-strain relationships of plain-and fiber reinforced concrete

Figure 8.6: Material properties. 1 in = 25.4 mm, 1 Kip = 4.5 KN, 1 Ksi = 6.9 MPa.

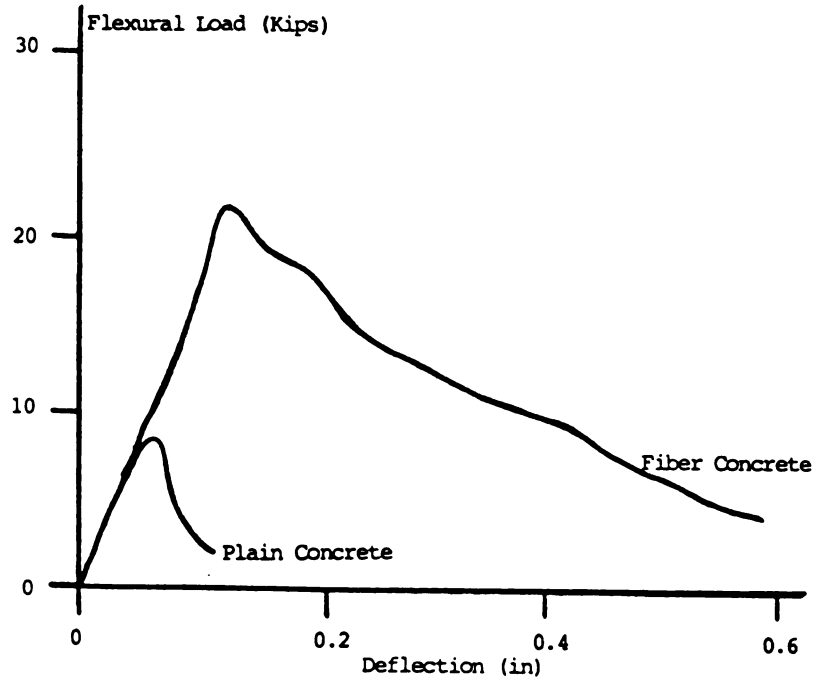

c. Flexural load-deflection relatioships of plain and fiber reinforced concrete

one-third points on a span of 450 mm (18 in). The averages of the compressive stress-strain and flexural load-deflection relationships (obtained from two compressive and three felxural test specimens) for plain and steel fiber reinforced concretes are shown in Figures 8.6.b and 8.6.c, respectively.

Twelve pull-out specimens were constructed in this study (two identical specimens for each condition). The main variables of the test program were the volume fraction of fibers and the amount of grade 60 (yield strength = 60 Ksi = 414 MPs) longitudinal and transverse bars (confining reinforcement) provided in the specimens. Table 8.1 summarizes the test program conducted in this investigation.

8.4 Test Results

From the test results on confined concrete specimens with different fiber contents (specimens 1, 2, and 9, 10 in Table 8.1) presented in Figure 8.7, it may be concluded that the ultimate and post-peak (frictional) bond strengths increase significantly as a result of reinforcement by steel fibers. Each curve in Figure 8.7 represents the average of test results on two specimens, noting that the identical specimens performed very similarly. The ultimate local bond resistance in confined steel fiber concrete was on the average 55% higher than that in confined plain concrete (compared to the 40% increase reported in Reference 88), and the increase in frictional resistance due to the presence of steel fibers was 140%. The contribution of fibers to bond resistance in confined concrete may be attributed to their effects on arresting the cracks, confining the concrete, and maintaining the

Table 8.1: Reinforcement configurations of test specimens (see Figure 8.3) # 4 bar = 0.5 in = 12.7 mm diameter

Specimen No.	V_f (%)	Vertical Steel	Transverse Steel*
1 & 2	2	4 #4	4 #4
3 & 4	2	4 #4	2 #4
5 & 6	2	4 #4	—
7 & 8	2	—	—
9 & 10	0	4 #4	4 #4
11 & 12	0	—	—

* Equally-spaced stirrups.

V_f = Fiber volume fraction

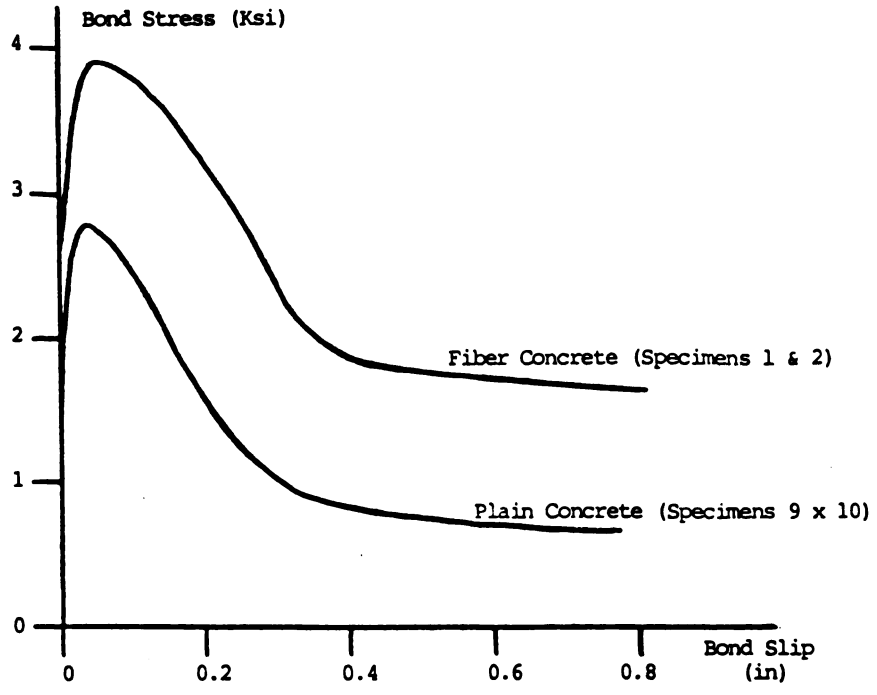

Figure 8.7: Effect of fiber reinforcement on local bond behavior in confined concrete. 1 in = 25.4 mm, 1 Ksi = 6.9 MPa

integrity of concrete in the vicinity of anchored bars after major bond cracking.

In unconfined specimens, with no vertical or transverse reinforcement, failure in plain specimens under pull-out forces was brittle and occurred at relatively low bond stresses when the bond splitting crack appeared. As shown in Figure 8.8, fibers provide more restraint against sudden widening of the splitting crack, and improve the pull-out resistance and post-peak ductility of unconfined specimens.

Figure 8.9 summarizes the average test results presenting the effects of transverse reinforcement, at a constant level of longitudinal reinforcement, on the bond performance of deformed bars in fiber reinforced concrete specimens. The results do not show any consistent effects of transverse reinforcement on the local bond behavior in fiber reinforced concrete, as far as the vertical bars are present to restrict the opening of splitting cracks. It may be concluded from Figure 8.9 that the reduction of transverse confining reinforcement in the presence of steel fibers does not adversely influence the improvements in local bond behavior resulting from steel fiber reinforcement.

8.5 Conclusions

The experimental results reported in this chapter on monotonic local bond behavior is fibrous concrete joints indicated that:

1. The ultimate bond resistance in confined concrete increases by about 55% due to

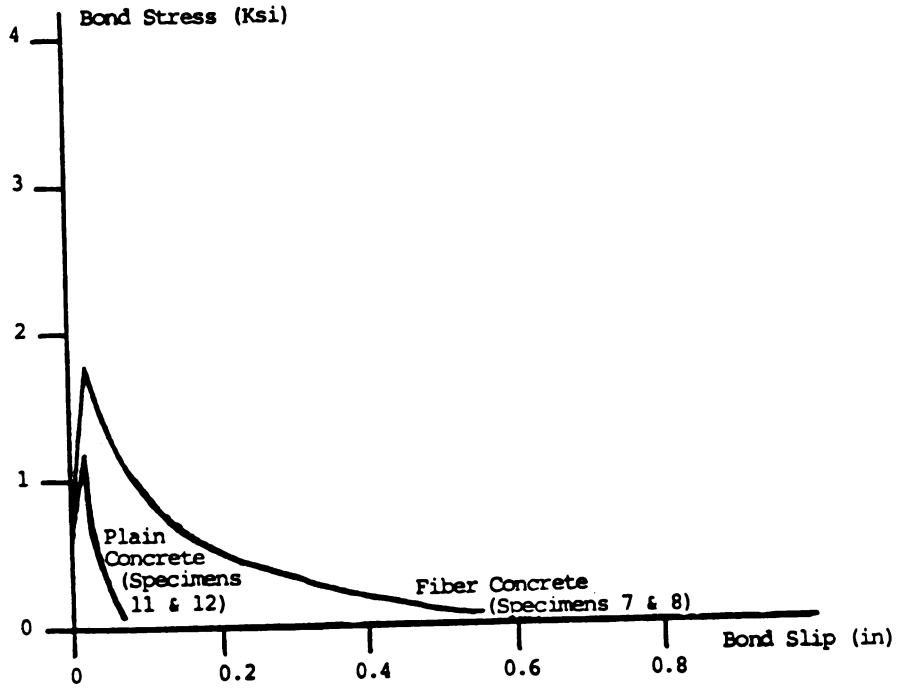

Figure 8.8: Effect of fiber reinforcement on local bond behavior in unconfined concrete. 1 in = 25.4 mm, 1 Ksi = 6.9 MPa

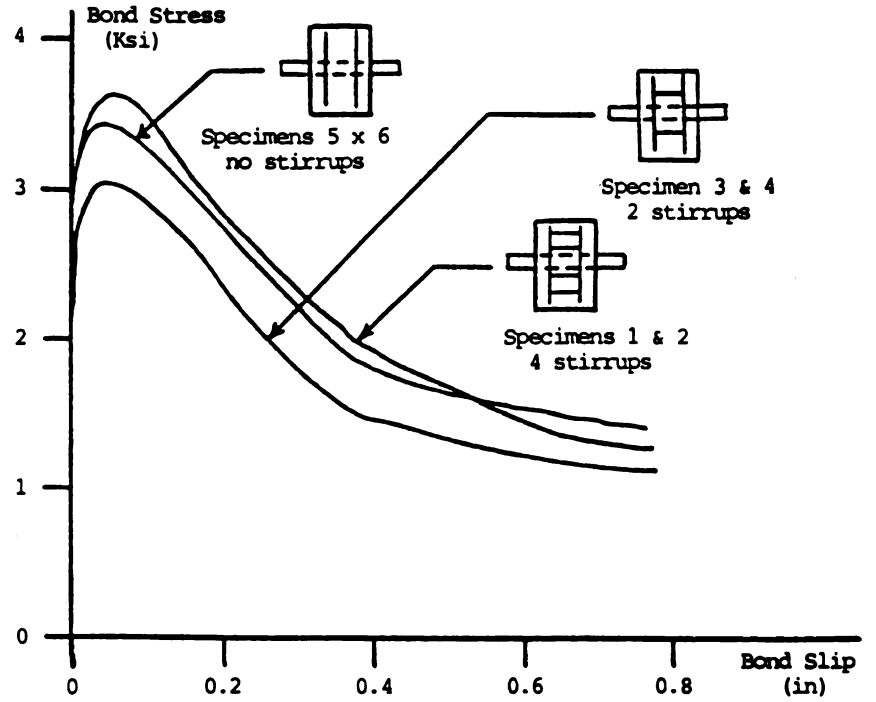

Figure 8.9: Effect of transverse reinforcement on local bond behavior in fiber reinforced concrete with longitudinal reinforcement. 1 in = 25.4 mm, 1 Ksi = 6.9 MPa

reinforcement by 2% volume fraction of straight round steel fibers with an aspect ratio of 57. There also was a 140% increase in the frictional bond resistance resulting from fiber reinforcement.

2. The local bond behavior is not significantly influenced by variations in the amount of transverse reinforcement in fiber reinforced joints, as long as sufficient vertical bars are provided for restraining the bond splitting cracks.

3. In unconfined concrete specimens having no reinforcement for restraining the splitting cracks, the application of fibers increases the local bond ultimate strength (which, like in the case of plain concrete, is the strength reached at split cracking), and provides some post-peak resistance.

CHAPTER 9

A Critical Evaluation of The Composite Material Theories of Steel Fiber Reinforced Concrete

9.1 General

Reinforcement by randomly distributed short fibers in an effective technique for improving toughness, impact resistance and tensile strength of concrete. These enhancements have encouraged the performance of numerous experimental investigations on fiber reinforced concrete in recent years. Analytical simulations of fiber reinforced concrete behavior are, however, just emerging. Currently, such basic problems as modeling of the material constitutive behavior and developing a reliable technique for predicting the tensile strength of fiber reinforced concrete in terms of matrix and fiber properties are yet to be resolved.

This chapter presents a cirtical review of the commonly used composite material concept in its application to predicting the tensile strength of steel fiber reinforced concrete.

9.2 Tensile Behavior of Steel Fiber Reinforced Concrete and the Composite Material Concept

The available direct tension test data have indicated that reinforcement by steel fibers increases tensile strength of concrete and significantly improves the post-peak tensile behavior.[4,5,24,33,35,36,42,80,90] Figure 9.1 presents a critical comparison between the tensile stress-strain diagrams of plain concrete

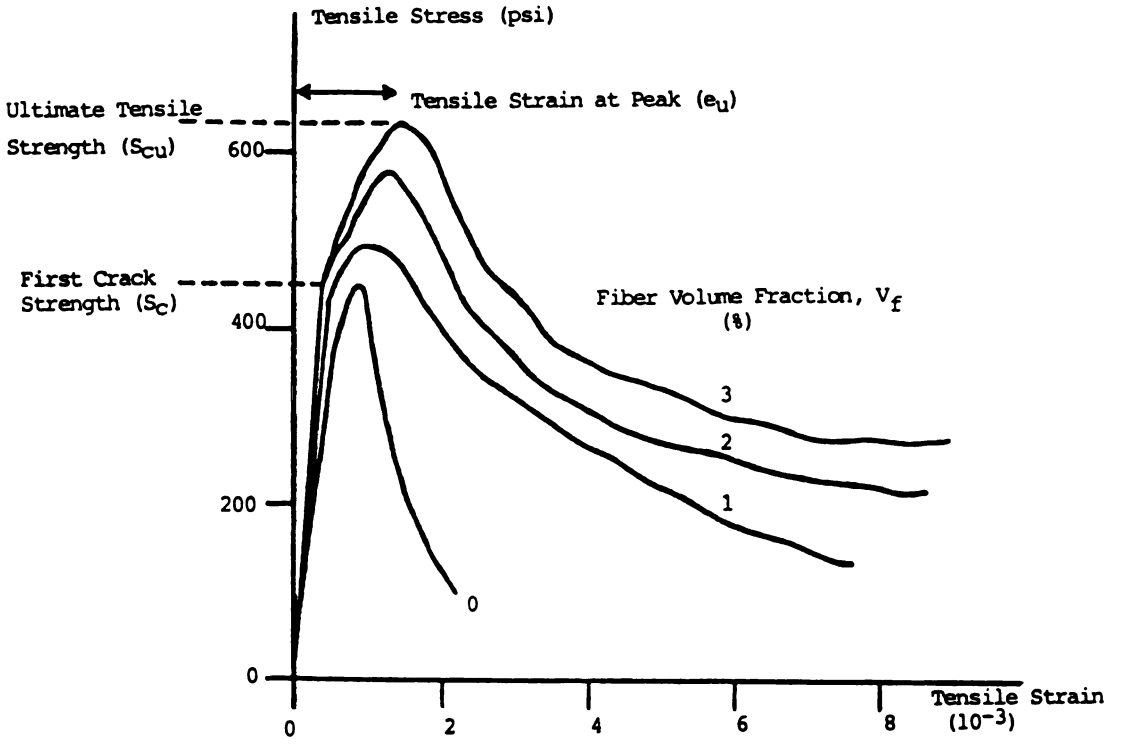

Figure 9.1: Tensile behavior of plain and steel fiber reinforced concretes.[33,35,42,90] 1 Ksi = 6.9 MPa

and fiber reinforced concrete with different fiber volume fractions. In the case of plain concrete, the behavior is linear up to the peak and thereafter the resistance drops at a fast rate.[90] The tensile behavior of fiber reinforced concrete is also linear initially, but there is a drop in stiffness near the peak at a stress usually referred to as the first crack strength. The peak tensile stress of fiber reinforced concrete is higher than plain concrete, and in the post-peak region the drop in tensile resistance is much much slower. Hence, fiber reinforcement considerably improves toughness and energy absorption capacity of concrete. These improvements in tensile behavior of concrete resulting from fiber reinforcement are influenced, as expected, by fiber type (straight, hooked, crimped, etc.) and aspect ratio.

Currently, the composite material concept (sometimes referred to as the law of mixture) is the most popular approach for predicting the tensile strength of fiber reinforced concrete. The analytical technique was basically developed for predicting the first crack strength of composite materials with fully bonded aligned continuous fibers, assuming that poisson's ratio is zero for fiber and matrix. In this case, the first crack strength of the composite, S_c, can be obtained from the following equation:

$$S_c = S_f V_f + S_m (1 - V_f) \qquad (9.1)$$

where:

S_f = fiber tensile stress at matrix rupture;

V_f = fiber volume fraction; and

S_m = matrix tensile strength.

In order to apply the above equation to calculate the ultimate tensile strength of concrete reinforced with randomly distributed fibers, it should be adjusted to account for: (a) random orientation of fibers which reduces their efficiency; (b) imperfect bond and short fiber length that result in fiber slippage during crack opening; and (c) random distribution of cracks which do not necessarily cross fibers at their midlength. With these considerations, the composite material concept, when applied to concrete with short randomly distributed fibers, results in the following equation for the ultimate tensile strength, S_{cu} (References 4,5,17,34,92-95):

$$S_{cu} = 2ab\, T_u\, (l_f/d_f)\, V_f + gS_m\, (1 - V_f) \qquad (9.2)$$

Where:

T_u = average interfacial bond stress at ultimate condition;

l_f = fiber length;

d_f = fiber diameter;

a = efficiency factor accounting for the random orientation of fibers shown in Figure 9.2 (a = 0.41 in References 34,92,94);

b = efficiency factor accounting for the fact that the crack crosses a fiber at a random location along its length, also shown in Figure 9.2. The value of b used by different investigators ranges from 0.41 to 1.0 (References 5,34,92,94); and

g = a factor representing the fraction of the matrix strength contributing to the tensile strength (References 93 and 95 neglect the contribution of the matrix and assume g = 0, while References 17,34,46,92,94 suggest values close to 1.0).

A close examination of Equation 9.2 reveals that the following assumptions have been made for application of the composite material concept to fiber reinforced concrete:

a. Failure occurs by pull-out of fibers (not by fiber rupture), and assuming a uniform interfacial bond distribution, the fiber stress at ultimate condition S_f in Equation 9.2 is replaced by $2\ T_u\ l_f/d_f$ (see Figure 9.3);

b. Adoption of g = 0 (i.e., $S_{cu} = 2ab\ T_u\ l_f/d_f$) by some investigators implies that fiber reinforced concrete reaches its ultimate strength when fibers reach their peak pull-out strength with no contribution from the matrix; and

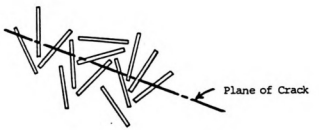

Figure 9.2: Random orientation and location of fibers with respect to crack

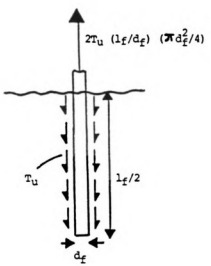

Figure 9.3: Interfacial bond stress at ultimate condition

c. In case of assuming that g is close to 1.0, both of the tensile strength of matrix and pull-out resistance of fibers would be contributing to tensile strength.

9.3 Pull-Out Behavior of Fibers and Tensile Behavior of Fiber Reinforced Concrete

This section presents a brief review of the experimental data that will be used later for an evaluation of the composite material concept as it is currently applied to predict the tensile strength of fiber reinforced concrete.

In studies on the fiber pull-out behavior (References 21,96-104), it should be noticed that due to the random orientation of fibers we are mainly concerned with the pull-out performance of inclined fibers, which is governed by two mechanisms (Figure 9.4): (a) shear at interface; and (b) fiber dowel action (involving inelastic bending of fibers). The contribution of each mechanism to pull-out resistance depends, among other factrors, on fiber angle of inclination. The dowel action of fibers damages the matrix, and thus the behavior of closely-spaced multiple fibers is inferior to that observed in single fiber pull-out tests.

From the above discussion, one may conclude that the actual pull-out behavior of randomly distributed fibers in concrete depends on a set of factors including: (a) interfacial shear between fiber and matrix; (b) matrix properties; (c) fiber rigidity and plastic moment; (d) fiber inclination; (e) number of fibvers per unit area; and (f) fiber aspect ratio.

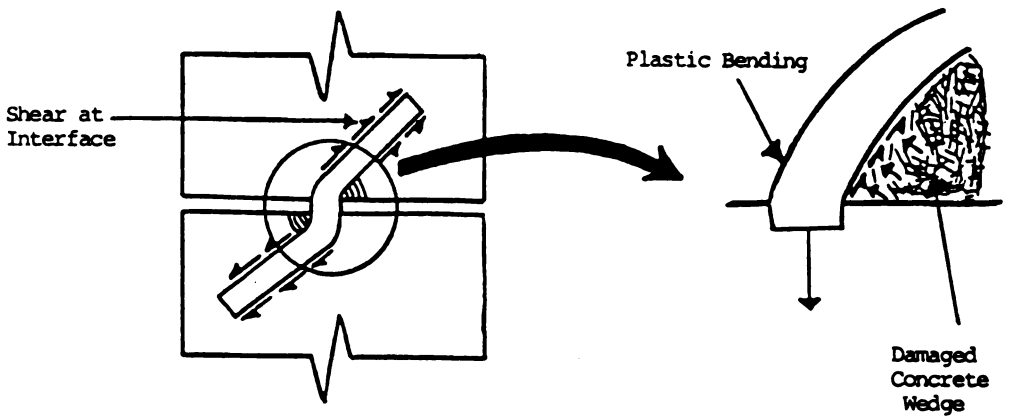

Figure 9.4: Pull-out mechanism of an inclined fiber

In the majority of the reported pull-out tests on fibers (References 21,96-104), a single fiber aligned with the loading direction has been pulled out of unreinforced matrix. A typical pull-out load-slip relationship obtained in such tests is shown in Figure 9.5. Relatively large variations have been observed in fiber pull-out test results. These variations result in large part from different stress disributions in fibers and matrix induced by different pull-out test techniques (see Figure 9.6). Table 9.1 presents a summary of the available pull-out test results on single straight steel fibers aligned with the loading direction. It is worth mentioning that the interfacial bond stresses presented in this chapter are derived assuming a uniform bond stress distribution along the embedment length during pull-out. The main quantities used in this study are, however, pull-out displacement of fibers and opening of cracks. The bond stress values are just used for a qualitative confirmation of the results, and thus a more accurate assessment of the values of interfacial bond stress based on more complex stress distributions (e.g.,

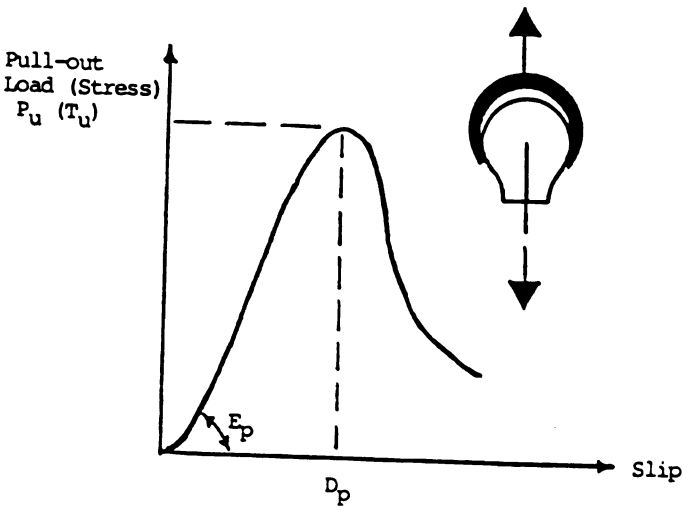

Figure 9.5: A typical fiber pull-out load-slip relationship

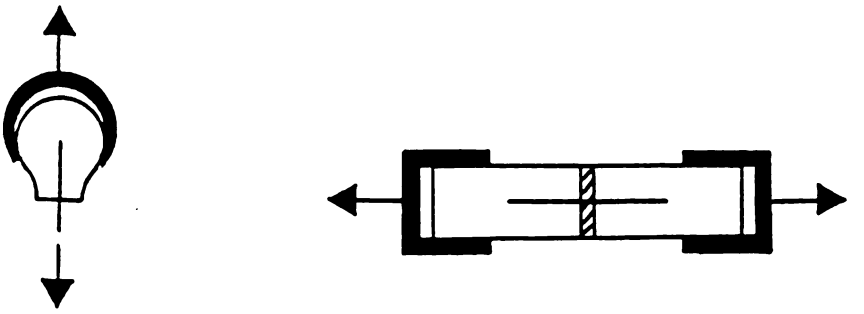

a. References 96, 97 and 99

b. Reference 103

Figure 9.6: Fiber pull-out test techniques.

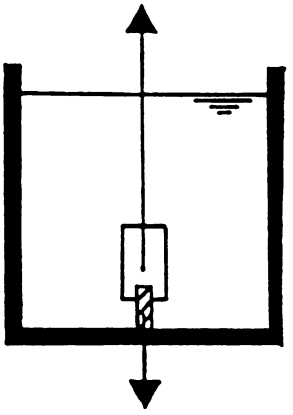

c. Reference 101

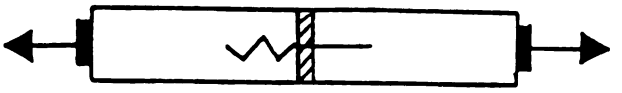

e. Reference 89

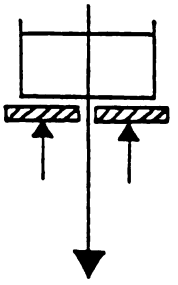

d. Reference 100

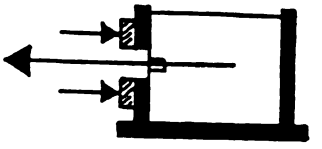

f. Reference 102

Table 9.1: Results of pull-out tests on a single straight steel fiber aligned with the loading with the loading direction

Reference	Test Set-up Figure	MATRIX PROPERTIES			FIBER PROPERTIES			PULL-OUT TEST RESULTS		
		W/C	S/C	Casting Direction with respect to Fiber	Embeded Length in(mm)	Diameter in(mm)	Type	Peak Stress psi(MPa)	Slip at Peak Stress in(mm)	Initial Stiffness psi/in(MPa/mm)
97,99	9.6.a	0.60	2.5	perpendicular	0.50 (12.7)	0.010 (0.25)	brass coated high tensile	380 (2.6)	0.03 (0.76)	11400 (3.10)
96	9.6.a	0.50	3.0	perpendicular	0.47 (12.0)	0.015 (0.38)	**	586 (4.1)	**	**
103	9.6.b	0.31	0.0	perpendicular	1.2 (30.0)	0.029 (0.75)	made of coil wire	250 (1.8)	**	**
101	9.6.c	0.50	2.0	perpendicular	2.0 (50.8)	0.015 (0.38)	brass coated high tensile	194 (1.3)	**	**
101	9.6.c	0.50	2.0	parallel	2.0 (50.8)	0.015 (0.38)	brass coated high tensile	326 (2.3)	**	**
101	9.6.c	0.50	3.0	perpendicular	2.0 (50.8)	0.015 (0.38)	brass coated high tensile	206 (1.4)	**	**
101	9.6.c	0.50	3.0	parallel	2.0 (50.8)	0.015 (0.38)	brass coated high tensile	321 (2.2)	**	**
101	9.6.c	0.50	4.0	perpendicular	2.0 (50.8)	0.015 (0.38)	brass coated high tensile	237 (1.6)	**	**
101	9.6.c	0.50	4.0	parallel	2.0 (50.8)	0.015 (0.38)	brass coated high tensile	260 (1.8)	**	**
100	9.6.d	0.30	0.0	parallel	0.69 (17.5)	0.015 (0.38	low carbon	375 (2.6)	**	**
98	9.6.e	0.60	2.5	perpendicular	0.50 (12.5)	0.015 (0.38)	Arbed	65 (0.45)	0.008 (0.20)	8255 (2.24)
102	9.6.f	0.55	**	perpendicular	0.50 (12.5)	0.015 (0.38)	Arbed	291 (2.0)	0.008 (0.20)	36830 (10.0)
102	9.6.f	0.55	**	perpendicular	1.6 (40.0)	0.028 (0.50)	Arbed	138 (0.95)	0.01 (0.25)	13846 (3.76)

ratios are by weight
W = water
S = sand
C = cement
** = not available

exponential) will not influence the conclusions.

Pull-out tests on fibers inclined with respect to the loading direction (Figure 9.7) (References 97,99,104) have indicated that the peak pull-out load is not much different for aligned and inclined fibers (however, if the pull-out resistance is attributed only to the interfacial bond, as assumed in the composite material concept, the ultimate bond stress would be larger for inclined fibers). There is only a slight decrease in the maximum pull-out distance of inclined fibers, but compared to the aligned ones, the inclined fibers have superior post-peak behavior and larger energy dissipation capacity (Figure 9.7).

Pull-out tests on multiple fibers have shown that increasing the number of fibers per unit area tends to damage the pull-out resistance of inclined fibers much more than aligned ones. Multiple inclined fibers exhibit lower pull-out strength, pull-out work and maximum pull-out distance when compared with the single inclined fibers (Figure 9.8).

Following the composite material concept that assumes that interfacial bond is the only mechanism contributing to pull-out resistance, the ranges below can be deduced from the available pull-out test results (References 21,96-104). Initial pull-out stiffness E_p (shown in Figure 9.5) of single straight steel fibers, algined or inclined, ranges from 8,000 to 37,000 psi/in (2.17 to 10.1 MPa/mm) and the

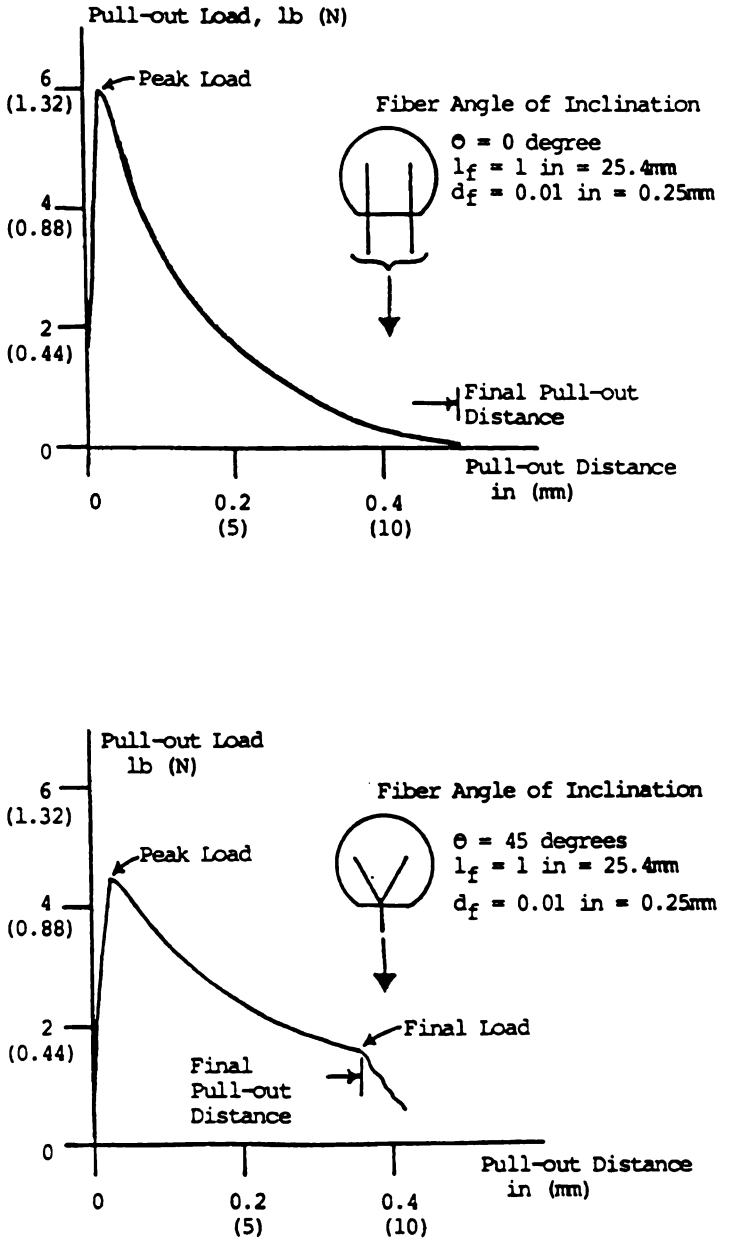

Figure 9.7: Pull-out force-slip relationships of aligned and inclined fibers.[97,99,104]

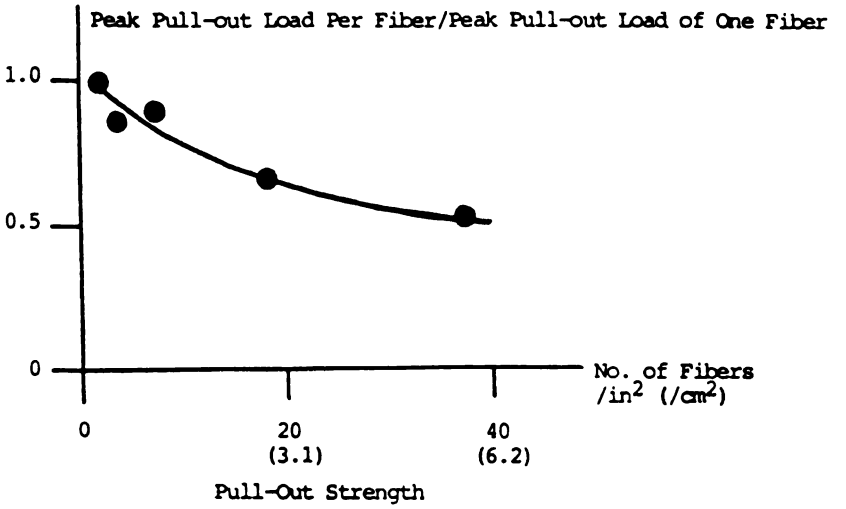

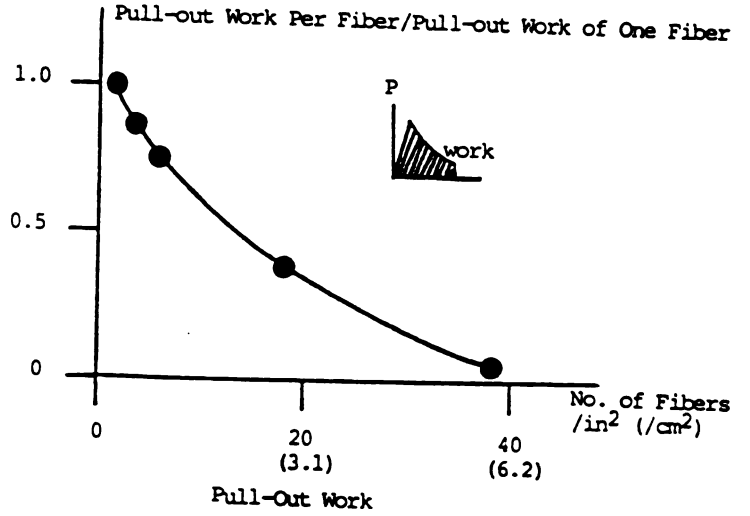

Figure 9.8: Effect of number of incluned fibers on their pull-out behavior. [97,99,104]

slip at peak pull-out stress, D_p, from 0.008 to 0.030 in (0.20 to 0.75 mm). The peak bond stress, T_u, varies between 65 and 600 psi (0.448 and 4.140 MPa) for single aligned fibers, and increases by about 100% for 60° inclined fibers. The available test data are not sufficient for a meaningful quantitative assessment of the effects of the number of fibers per unit area on the above values. It is, however, expected that all these values will be less in pull-out tests on multiple fibers.

In studying the tensile behavior of fiber reinforced concrete (References 4, 5, 24, 33, 35, 36, 42, 80, 90, 91) it should be noticed that, unlike plaine concrete, the post-cracking and post-peak nonlinear behavior of the material in tension are of major importance. Hence, in flexural tests, the tensile stresses can not be accurately obtained using the elastic formulation, and reliance should be made on direct tension test results for assessing the constitutive behavior of fiber reinforced concrete in tension. There are, however, only limited direct tension test data reported in the literature (References 33, 35, 36, 42, 80).

Typical stress-strain relationships obtained in direct tension tests on fiber reinforced mortar are presented in Figure 9.1. Failure in direct tension test specimens is generally due to opening of one crack (References 24, 33, 35, 42, 80). The maximum increase in peak tensile stress resulting from steel fiber reinforcement is about 50%, and the maximum increase in strain at peak, e_u, is about 30% (Reference 5). These increases are functions of volume fraction and

aspect ratio of fibers (Figure 9.9). It should be mentioned that direct tension test results on fiber reinforced concrete show slightly larger strength variations than the corresponding test results on plain concrete (References 33, 35, 42).

9.4 Evaluation of the Composite Material Concept

Direct tension test results discussed in the earlier section have indicated that the increase in concrete strain at peak tensile stress, e_u, resulting from reinforcement by steel fibers is below 30%. This means that the peak stress is reached at a strain of about 150 to 200 microstrains (References 5, 33, 35, 36, 42, 90). Also, fiber reinforced concrete cracks prior to reaching its peak tensile stress, and the crack width represents the degree of mobilization of the pull-out resistance of fibers. Hence, in order to check the validity of the composite material concept, it is important to approximate the crack openings corresponding to the strain at peak stress. Conservatively assuming that in the post-cracking range, the tensile strains are mainly caused by opening of one crack as shown in Figure 9.10 (References 24, 33, 35, 36, 42, 80), the maximum width at peak stress can be approximated as the increase in strain at peak stress resulting from fiber reinforcement (maximum of about 50 microstrains) times the gage length (along which the average strain is measured, typically 4 in or 102mm). This approach gives the upper bound of the crack width, because it neglects the displacements along the gage length caused the strains outside the major crack and assumes that all the displacement are concentrated in this major crack. The pull-out test results

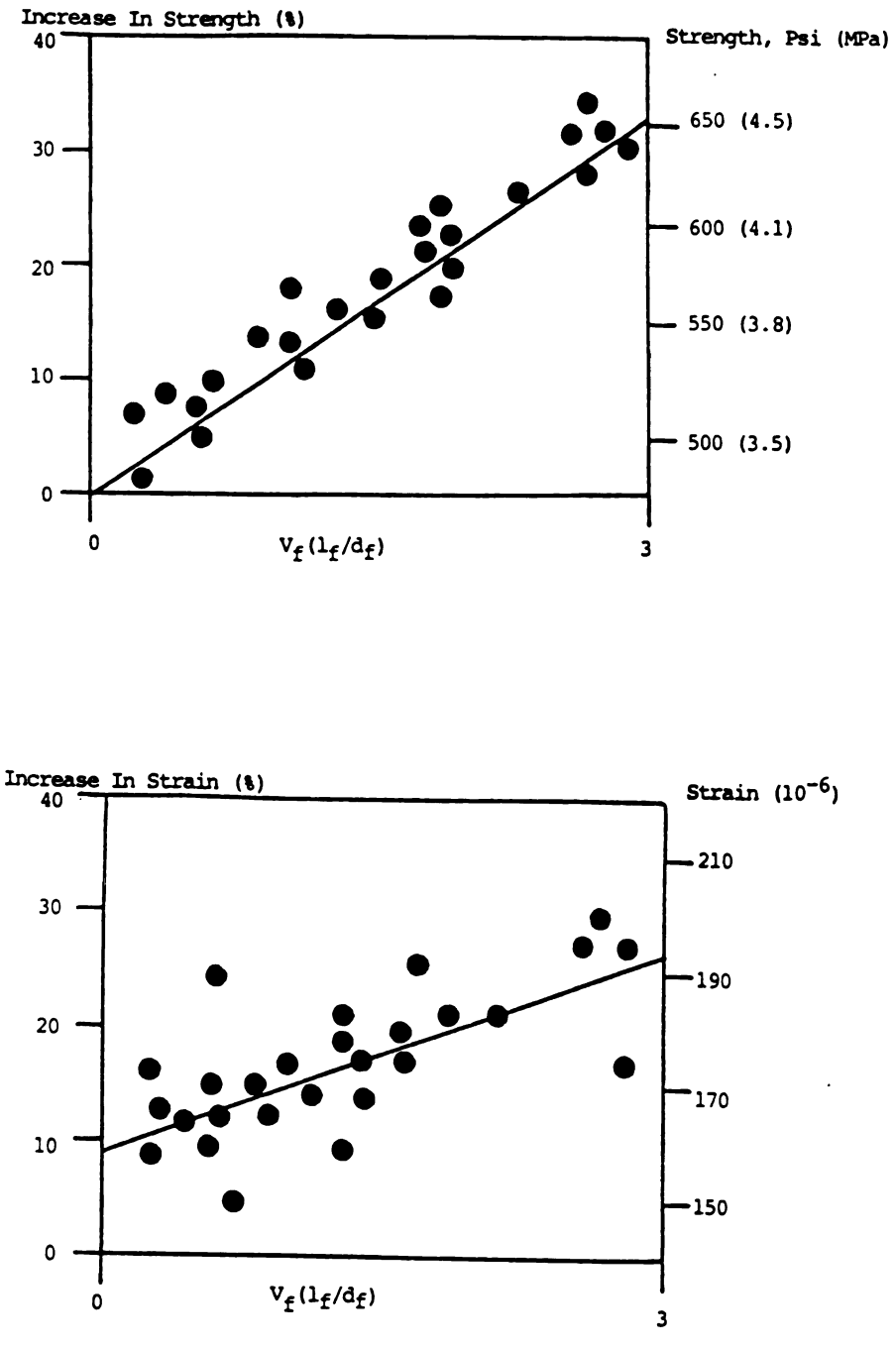

Figure 9.9: Increase in peak tensile stress and strain at peak stress resulting from fiber reinforcement.[33]

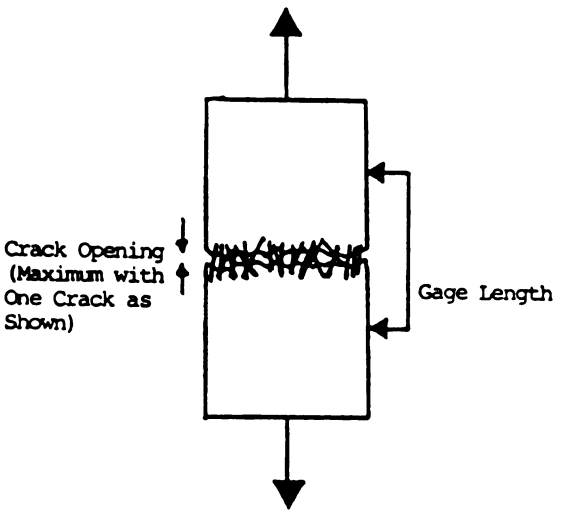

Figure 9.10: Crack opening in direct tension test

presented earlier in conjunction with the above assumption imply that the maximum crack opening when the peak stress is reached is of the order of 0.0002 in (0.005mm), while in fiber pull-out tests, the peak load occurs at a slip of about 0.015 in. (0.38mm) which is two orders of magnitude higher than the maximum crack opening expected at peak stress in direct tension tests. This means that the fiber interfacial bond stresses are far below their peak values, and the fiber pull-out mechanism is practically ineffective when the peak tensile stress of fiber reinforced concrete is reached. For example, for the typical values of fiber pull-out stiffness given earlier, at the estimated 0.0002 in (0.005mm) crack opening obtained when the peak tensile stress is reached (considering the average number of fibers corssing a unit area of a crack, their random orientation and location with respect to the crack as presented in References 10, 93, 105) is only

about 2 psi (0.01 MPa) for a 2% volume fraction of straight steel fibers with a diameter of 0.015 in (0.38mm) and a length of 1.5 in (37.5mm).

The above conclusion contradicts the basic assumptions used in the application of the composite material concept for predicting the tensile strength of fiber reinforced concrete. Applying this concept with g = o (see Equation 9.2) implies that at ultimate tensile stress, fibers reach their peak pull-out stress. With g close to 1.0 also, regression analysis of direct tension test results (References 34, 92, 94) have indicated that the interfacial bond stress in Equation 9.2 should be close to (if not larger than) its ultimate value for this equation to be valid. It was, however, shown that the strain at peak tensile stress of fiber reinforced concrete is far below the values needed to fully mobilize the interfacial bond stress of fibers.

In case that g is assumed to be close to 1.0 in the composite material concept (Equation 9.2), another contradiction arises from the fact that at a crack wide enough to fully activate fiber pull-out mechanism, the opening is too large for concrete to be still effective in resisting tension.

The previous discussion indicates that the nature of bond between fibers and concrete is not a key factor influencing the percentage increase in the concrete tensile strength resulting from fiber reinforcement. At the relatively low strains corresponding to the peak tensile stress of fiber reinforced concrete, fibers seem to act mainly as barriers against propagation of microcracks and other relatively

narrow cracks. This conclusion agrees with the philosophy on the basis of which the spacing concept for prediction of the tensile strength of fiber reinforced concrete is developed. More studies based on the fracture mechanics concept seem to be necessary for achieving an in-depth understanding of the effects of uniformly dispersed and randomly oriented short fibers on the iniatation and propagation of cracks in cementitious matrices (Reference 106). Application of the surface energy rather than the shear-bond strength approach to interpretation of the pull-out test results also warrants consideration in this regard (Reference 107).

9.5 Summary and Conclusions

Application of the commonly used composite material concept for predicting the tensile strength of fiber reinforced concrete implies that the fiber pull-out resistance is mobilized to a large extent when the material reaches its peak stress. For this to happen, according to the reported pull-out test results on steel fibers, bond slippages of the order of 0.015 in (0.38 mm) need to take place. Direct tension test results on steel fiber reinforced concrete, however, indicate that the maximum crack openings at peak stress are of the order of 0.0002 in (0.005 mm), which is far below the values needed for a meaningful mobilization of the pull-out resistance of fibers. This questions the applicability of the composite material concept to the ultimate tensile strength of fiber reinfoced concrete, and indicates that the pull-out behavior of fibers does not play a major rate when the peak tensile stress is reached.

CHAPTER 10

Summary and Conclusions

A comprehensive experimental study was conducted on the performance characteristics of steel fiber reinforced concrete. The effects of different fiber reinforcement properties and matrix mix variables on fresh mix performance and hardened material mechanical properties of steel fiber reinforced concrete were assessed. The statistical variations in material properties were also established.

An investigation was performed on the applications of steel fiber reinforced concree to load bearing structural elements. The advantages of steel fibers in improving the performance of concrete footings under bearing pressure were examined. The increases in strength and ductility of the bond behavior between deformed reinforcing bars and concrete resulting from steel fiber reinforcement were evaluated.

Some popular techniques for analytical simulation for steel fiber reinforced concrete performance under tensile stress systems were critically investigated based on experimental results reported in the literature. Suggestions were made for the development of more representative models for the mechanism of action of steel fibers in concrete.

The research was performed in 8 phases: (a) effects of fiber volume fraction and geometry on material performance; (2) effects of fiber type on material

performance; (3) properties of steel fiber reinforced concrete with different matrix mix proportions; (4) applications of pozzolanic materials to steel fiber reinforced concrete; (5) statistical varitions of steel fiber reinforced concrete properties; (6) steel fiber effects on concrete footing performance under bearing pressure; (7) bond between reinforcing bars and steel fiber reinforced concrete; and (8) analytical simulation of steel fiber action in concrete.

A summary of the activities undertaken in each phase of the research together with the conclusions derived from the outcomes are presented below.

10.1 Effects of Fiber Volume Fraction and Geometry on Material Performance

An experimental program was performed on the effects of the length, diameter, volume fraction and types of steel fibers on material properties of steel fiber reinforced concrete in the fresh and hardened states. The fiber types considered were straight, crimped and hooked, with lengths ranging from 1.5 to 2.5 in (38 to 63 mm), diameters from 0.02 to 0.035 in (0.3 to 0.8 mm) resulting in aspect ratios from 43 to 100, and volume fraction from 0.5 to 3%. The mix proportions had a water-binder ratio pf 0.4, a fly ash-binder ratio of 0.3 (which was decided in other phases of the project to be the optimum fly ash content in steel fiber reinforced concrete), an aggregate-binder ratio 4.0, a coarse-to-fine aggregate ratio of 1.0, a maximum aggregate size of 3/4 in (19 mm), and a superplasticizer (liquid)-binder ratio of 0.015 by weight. The fresh mix was characterized by its

slump, inverted slump cone time and subjective workability. The hardened material, following 7 days of moist curing and 21 days of air drying, was tested in compression and flexure. The following conclusions could be derived from the test data generated in this investigation:

1. The fresh mix workability tends to be damaged by the increase in fiber reinforcement index (fiber volume fraction times fiber aspect ratio), at a rate which is comparable for different fiber types.

2. At a specific fiber reinforcement index, crimped fibers produce concretes with slightly high slumps, while straight fibers generate mixtures with slightly lower inverted slump cone times. Hooked fibers produce slumps coparable with straight fibers, but give inverted slump cone times which are slightly higher than those of straight and crimped fibers.

3. The first crack and ultimate flexural loads, and the flexural energy absorption capacities (pre- and post-peak), of steel fiber reinforced concrete increase with increasing fiber reinforcement index up to a value of about 1.5 and then starts to decrease for higher fiber reinforcement indices due to the fresh mix workability problems.

4. Hooked fibers, especially at higher fiber reinforcement indices, give flexural strengths superior to those obtained with straight and crimped fibers.

5. Steel fiber reinforcement has relatively small effects on the compressive strength of concrete. The effects of steel fibers on energy absorption capacity, however, seem to be more pronounced.

6. High fiber reinforcement indices, due to their damage to the compactibility of fresh mixtures which leads to high entrapped air contents, tend to reduce the pre-peak stiffness of steel fiber reinforced concrete and increase the strain at peak compressive stress.

10.2 Effects of Fiber Type on Material Performance

An experimental study was performed to assess the effects of steel fiber type on material properties of steel fiber reinforced concrete in fresh and hardened states. The fresh fibrous concrete was characterized by its slump, inverted slump cone time and subjective workability. For the hardened material, flexural load-deflection curves and compressive stress-strain relationships were used as representative of important mechanical properties of the material. The fibers included in this study were straight-round, crimped-round, crimped-rectangular, hooked single and hooked-collated fibers at aspect ratios ranging from 57 to 60, and straight-round and and hooked-collated fibers at aspect ratios ranging from 72 to 75. All the fibrous mixes incorporated a 2% volume fraction of steel fibers. The following conclusions could be derived from test results:

1. The inclusion of fibers damages the workability of fresh concrete and this effect

is more pronounced for fibers with higher apsect ratios. The effects of fiber types on fresh mix workability, as represented by the inverted slump cone time and the subjective measure, seem to be insignificant. Crimped fibers result in slightly higher slump values than straight and hooked fibers.

2. At an aspect ratio of about 60 and fiber volume fraction of 2%, crimped fibers (circular or rectangular) generate flexural strengths and energy absorption capacities which are inferior to those of straight fibers, but hooked fibers result in higher flexural strengths and similar flexural energy absorption capacities when compared with straight fibers. Hooked fibers are superior to straight ones in enhancing the flexural strength and energy absorption capacity of concrete at fiber aspect ratio of about 75 when added to concrete at 2% volume fraction.

3. Hooked are more effective than straight and crimped fibers in enhancing the total energy absorption capacity under compressive stresses. Strain at peak compressive stress also increases with steel fiber reinforcement, especially when hooked fibers are used. The increase in toughness of concrete resulting from steel fiber reinforcement is not strongly dependent on the fiber type. The effect of fiber reinforcement on compressive strength is relatively small and different fiber types seem to act similarly in this regard.

10.3 Properties of Steel Fiber Reinforced Concrete with Different Matrix Mix Properties

The effects of different matrix mix variables on the fresh mix workabilty and hardened material flexural and compressive performance characteristics of steel fiber reinforced concrete were investigated. A typical fibrous mixture with a relatively high fiber volume fraction was used as a "basic" mix for this investigation. The generated test data indicated that:

1. The workability of fresh steel fiber reinforced concrete tends to improve with the increase in binder (cement: fly ash = 0.7:0.3) content. There are also improvements in the flexural strength and energy absorption characteristics of steel fiber reinforced concrete resulting from the increase in binder content. The compressive performance, however, seems to be largely independent of the binder content.

2. The increase in superplasticizer dosage tends to improve the compactibility and the overall workability of steel fiber reinforced concrete. There is also some tendency in the flexural performance to improve with the increase in superplasticizer dosage. Compressive performance is least influenced by the change in superplasticizer dosage.

3. The increase in water-binder ratio tends to improve the workability of fresh fibrous mixtures. It should, however, be noted that excessive water contents may produce fluid concrete matrices in which the steel fibers tend to settle down. The increase in water-binder ratio results in a drop in compressive strength of steel

fiber reinforced concrete. The corresponding damage to the compressive energy absorption characteristics and the overall flexural performance are, however, less obvious.

4. The workability of steel fiber reinforced concrete improves with increasing aggregate size (within the range of variables considered in this study). The increase in maximum aggregate size also results in a slight increase in flexural strength and some more important improvements in the flexural energy absorption characteristics of steel fiber reinforced concrete. The compressive properties of the material seems to be largely independent of the maximum aggregate size in the mixtures considered in this study.

5. There is an optimum aggregate gradation the deviation from which towards coarser or finer gradation damages the workability and flexural performance of steel fiber reinforced concrete. The optimum gradation was obtained in this study by the use of coarse-to-fine aggregate ratio of 1.0.

6. The entrained air content of steel fiber reinforced concrete mixtures increases at a decreasing rate with the increase in the dosage of air entraining agent. Desirable entrained air contents for resistance against freeze-thaw cycles can be achieved by the use of dosages of air entraining agent which are comparable to those recommended for conventional concrete.

10.4 Applications of Pozzolanic Materials to Steel Fiber Reinforced Concrete

The effect of the silica fume and the class F fly ash contents on the properties of steel fiber reinforced concrete in fresh and hardened states were investigated experimentally. From the results it was concluded that:

1. The compactibility of steel fiber reinforced concrete, as indicated by the inverted slump cone test results, is not much influenced by the increase in silica fume-binder ratio up to a value of about 0.10. Higher silica fume contents, however, adversely influence the workability of fresh mix.

2. The flexural strength and energy absorption capacity of steel fiber reinforced concrete tend to increase with increasing silica fume-binder ratio up to a value of about 0.10; beyond which the effects of silica fume on these aspects of the hardened material behavior tend to be reversed.

3. The compressive strength and energy absorption capacity of steel fiber reinforced concrete tend to increase with increasing silica fume-binder ratio up to silica fume ratio of 0.10. Further increase in silica fume content has relatively small effects on the compressive behavior of steel fiber reinforced concrete.

4. For the steel fiber reinforced concrete mixes used in this study, substitution of 10% of cement with silica fume gave the best results as far as the workability of

fresh mix and the strength and energy absorption capapcity of the hardened material under the action of flexural and compressive loads are concerned.

5. Substitution of cement with class F fly ash in steel fiber reinforced concrete mixes of this study generally had positive effects on the workability of fresh mix as represented by the inverted slump cone time test results.

6. The 28-day flexural strength and energy absorption capapcity of steel fiber reinforced concretes of this study tend to increase with increasing fly ash-binder ratio up to about 0.3. the increase in fly ash-binder ratio from 0.3 to 0.4, however, adversely influenced the flexural performance of steel fiber reinforced concrete.

7. Substitution of up to 20% of cement with fly ash in steel fiber reinforced concrete mixes of this study resulted in improved 28-day compressive strength and energy absorption capacity of the material. Higher fly ash contents, however, start to have adverse effects on compressive characteristics.

8. The increase in fly ash content led to some reductions in the air content of steel fiber reinforced concrete mixtures.

9. Substitution of more than 20% of cement with fly ash trends to reduce the rate of compressive strength development in steel fiber reinforced concrete. After

28-days, however, the compresive strengths of mixes with fly ash-binder ratios as high as 0.40 were close to that of the mix with 0% fly ash contents.

10. The optimum fly ash-binder ratio in steel fiber reinforced concrete mixtures of this study, for achieving desirable fresh mix workability and hardened material flexural and compressive properties was in the range of 0.20 to 0.30. Fly ash should be accompanied with an air entraining agent in application to steel fiber reinforced concrete in conditions where freeze-thaw durabiity is of concern. Ths use of more than 20% fly ash-binder ratios lead to a lower rates of strength development in steel fiber reinforced concrete.

10.5 Statistical Variations in Steel Fiber Reinforced Concrete Properties

The results of a statistical study on the flexural and compressive strengths, and inverted slump cone time of a typical steel fiber reinforced concrete mix with a relatively high fiber volume fraction were presented. The limited test results generated in this study indicated that:

1. The compressive strength test results showed variations similar to those expected in plain concrete.

2. The flexural strength and inverted slump cone time test results showed relatively high variations indicating that the statistical aspects of the quality

control procedures developed for plain concrete may have to be modified for application to steel fiber reinforced concretes with relatively high fiber volume fractions.

3. The observed distributions of compressive and inverted slump cone test results followed rather closely the normal distribution. This conclusion, however, could not be derived for the flexural strength test results.

10.6 Steel Fiber Effects on Concrete Footing Performance under Bearing Pressure

The results of an experimental study on the behavior of concrete and fiber reinforced concrete under bearing stresses in the condition of concrete footings were presented. A theoretical approach was used to predict the bearing strength of concrete and fiber reinforced concrete, and the results were compared with the generated test data. It was concluded that:

1. The failure mode of concrete and fiber reinforced concrete under bearing stresses results from punching out of a concrete cone from beneath the bearing area, which produces splitting cracks in the concrete block. The splitting crack pattern is different in concrete from fiber concrete, but in both cases, these cracks start from the vicinity of the bearing area.

2. Fiber reinforcement of concrete footings at their full depth and also at a top

layer underneath the bearing area, can effectively increase the bearing strength and especially the ductility of failure under bearing stresses. The application of fibers at a top layer can provide results which are comparable to these obtained with full depth fiber reinforcement.

3. Dowel bars do not seem to make a significant contribution to the resistance of plain concrete under bearing pressure. These bars, however, tend to be more effective when a top layer of concrete under the bearing area is reinforced with steel fibers.

4. The failure models and theoretical formulations developed for predicting the bearing strength of concrete can be applied to fiber reinforced concrete when due consideration is given to the changes in concrete tensile and compressive strengths and angle of internal friction resulting from fiber reinforcement. The current theories, however, can not predict the improvements in ductility of behavior under bearing stresses resulting from fiber reinforcement.

10.7 Bond Between Reinforcing Bars and Steel Fiber Reinforced Concrete

The experimental results reported in this chapter on monotonic local bond behavior is fibrous concrete joints indicated that:

1. The ultimate bond resistance in confined concrete increases by about 55% due

to reinforcement by 2% volume fraction of straight round steel fibers with an aspect ratio of 57. There also was a 140% increase in the frictional bond resistance resulting from fiber reinforcement.

2. The local bond behavior is not significantly influenced by variations in the amount of transverse reinforcement in fiber reinforced joints, as long as sufficient vertical bars are provided for restraining the bond splitting cracks.

3. In unconfined concrete specimens having no reinforcement for restraining the splitting cracks, the application of fibers increases the local bond ultimate strength (which, like in the case of plain concrete, is the strength reached at split cracking), and provides some post-peak resistance.

10.8 Analytical Simulation of Steel Fiber Action in Concrete

Application of the commonly used composite material concept for predicting the tensile strength of fiber reinforced concrete implies that the fiber pull-out resistance is mobilized to a large extent when the material reaches its peak stress. For this to happen, according to the reported pull-out test results on steel fibers, bond slippages of the order of 0.015 in (0.38 mm) need to take place. Direct tension test results on steel fiber reinforced concrete, however, indicate that the maximum crack openings at peak stress are of the order of 0.0002 in (0.005 mm), which is far below the values needed for a meaningful mobilization of the pull-out resistance of fibers. This questions the applicability of the composite

material concept to the ultimate tensile strength of fiber reinfoced concrete, and indicates that the pull-out behavior of fibers does not play a major rate when the peak tensile stress is reached.

REFERENCES

1. Johnston, C., "Steel Fiber Reinforced Mortar and Concrete: A Review of Mechanical Properties," ACI Publication SP-44: Fiber Reinforced Concrete, 1974, pp. 127-142.

2. Fanella, D. and Naaman, A., "Stress-Strain Properties of Fiber Reinforced Mortar in Compression," ACI Journal, Vol. 82, No. 4, July-August, 1985, pp. 475-483.

3. Hughes, B. and Fattuhi, N., "Load-Deflection Curves for Fiber Reinforced Concrete Beams in Flexure," Magazine of Concrete Research, Vol. 29, No. 101, December, 1977, pp. 199-206.

4. ACI Committee 544, "State-of-the-Art Report on Fiber Reinforced Concrete," Report: ACI 544.1R-82, American Concrete Institute, May, 1982, 16 pp.

5. Hannant, D.J., "Fiber Cements and Fiber Concretes," John Wiley & Sons, Ltd., 1978, 219 pp.

6. Nishioka, K., Kakimi, N., Yamakawa, S. and Shirakawa, K., "Effective Applications of Steel Fiber Reinforced Concrete," Proceedings, RILEM Symposium on Fiber Reinforced Cement and Concrete (London), Vol. 1, 1975, pp. 425-433.

7. Ramakrishnan, V., Coyle, W., Kulandaisamy, V., and Schrader, E., "Performance Characteristics of Fiber Reinforced Concretes with Low Fiber Contents," ACI Journal, Vol. 78, No. 5, September-October, 1981, pp. 388-394.

8. Ramakrishnan, V., Brandshaug, T., Coyle, W. and Schrader, E., "A Comparative Evaluation of Concrete Reinforced with Straight Steel Fibers and Fibers with Deformed Ends Glued Together into Bundles," ACI Journal, Vol. 77, No. 3, May-June, 1980, pp. 135-143.

9. ACI Committee 544, "Measurement of the Properties of Fiber Reinforced Concrete," ACI Journal, Vol. 75, No. 7, July, 1978, pp. 283-289.

10. Ramauldi, J. and Mandel, J., "Tensile Strength of Concrete Affected by Uniformly Distributed and Closely Spaced Short Lengths of Wire Reinforcement," ACI Journal, Vol. 61, No. 6, June, 1964, pp. 657-670.

11. Lankard, D., "Opening Paper: Fiber Concrete Applications," Proceedings, RILEM Symposium on Fiber Reinforced Cement and Concrete (London), Vol. 1, 1975, pp. 3-19.

12. Nagamj, T., and Dwarakanath, H., "Structural Response of Partially Fibrous Concrete Beams," ASCE Journal of Structural Engineering Division, Vol. 110, No. ST11, November, 1984, pp. 2798-2812.

13. Dave, N., O'Leary, D. and Saunders, J., "Structural Use of Fibrous Cement in Composite Concrete Construction," ACI Publication SP-44: Fiber Reinforced Concrete, 1974, pp. 511-532.

14. Malmberg, B. and Skarendahl, A., "Method of Studying the Cracking of Fiber Concrete Under Restrained Shrinkage," Proceedings, RILEM Symposium on Testing and Test Methods of Fiber Cement Composites (Sheffield), 1978, pp. 173-179.

15. Swamy, R., and Stravrides, H., "Influence of Fiber Reinforcement on Restrained Shrinkage and Cracking," ACI Journal, Vol. 76, No. 3, March, 1979, pp. 443-460.

16. ACI Committee 544, "Guide for Specifying, Mixing, Placing, and Finishing Steel Fiber Reinforced Concrete," ACI Journal, Vol. 81, No. 2, March-April, 1984, pp. 140-148.

17. Swamy, R., and Mangat, P., "Influence of Fiber Geometry on the Properties of Steel Fiber Reinforced Concrete," Cement and Concrete Research, Vol. 4, No. 3, March, 1974, pp. 451-465.

18. Swamy, R., Mangat, P. and Rao, C., "The Mechanics of Fiber Reinforcement of Cement Matrices," ACI Publication SP-44: Fiber Reinforced Concrete, 1974, pp. 1-28.

19. Hughes, B. and Fattuhi, N., "The Workability of Steel Fiber Reinforced Concrete," Magazine of Concrete Research, Vol. 28, No. 96, September, 1976, pp. 157-161.

20. Hughes, B. and Fattuhi, N., "Assessing the Workability of Steel Fiber Reinforced Concrete," Proceedings, RILEM Symposium on Testing and Test Methods of Fiber Cement Composites (Sheffield), 1978, pp. 57-60.

21. Giaccio, G., Giovambattista, A. and Zerbino, R., "Concrete Reinforced with Collated Steel Fibers: Influence of Separation," ACI Journal, Vol. 83, No. 2, March-April, 1986, pp. 232-235.

22. Moens, J. and Nemegeer, D., "Flexural Strength of Fiber Reinforced Concrete Test Beams," Proceedings, RILEM Symposium on Testing and Test Methods of Fiber Cement Composites (Sheffield), 1978, pp. 389-397.

23. Johnston, C., "Toughness of Steel Fiber Reinforced Concrete," Proceedings, U.S. - Sweden Joint Seminar on Fiber Reinforced Concrete (Stockholm), June 3-5, 1985, pp. 333-360.

24. Shah, S. and Rangan, B., "Fiber Reinfroced Concrete Properties," ACI Journal, Vol. 68, No. 2, February, 1971, pp. 126-135.

25. "Vee-Bee Consistometer Type VBR," Operation Instructions, Soil Test, Inc., 1986, 3 pp.

26. El-Refai, F., and Morsey, E., "Some Properties of Fiber Reinforced Concrete with Superplasticizer," Proceedings, RILEM Symposium on Developments in Fiber Reinforced Cement and Concrete (Sheffield), July 13-17, 1986, Vol. 1, No. 3.2, 9 pp.

27. "1987 Annual Book of ASTM Standards," Section 4: Construction, Vol. 4.02: Concrete and Mineral Aggregates, ASTM, 1987, 912 pp.

28. Naaman, A., "Fiber Reinforcement for Concrete," Concrete International, Vol. 7, No. 3, March, 1985, pp. 21-25.

29. Otter, D. and Naaman, A. "Steel Fiber Reinforced Concrete Under Static and Cyclic Compressive Loading," Proceedings, RILEM Symposium on Developments in Fiber Reinforced Cement and Concrete (Sheffield), July 13-17, 1986, Vol. 1, No. 3.10, 8 pp.

30. Soroushian, P. and Lee, C., "Steel Fiber Reinforced Concrete under Compression: Performance Characteristics and Constitutive Modeling," Technical Article Submitted for Publication to the ACI Materials Journal.

31. Williamson, G., "Effect of Steel Fibers on the Compressive Strength of Concrete," ACI Publication SP-44: Fiber Reinforced Concrete, 1974, pp. 195-208.

32. Gopalaratnam, V., and Shah, S., "Micromechanical Model for the Tensile Fracture of Steel Fiber Reinforced Concrete," Proceedings, RILEM Symposium on Developments in Fiber Reinforced Cement and Concrete (Sheffield), July 13-17, 1986, Vol. 1, No. 1.3, 10 pp.

33. Johnston, C. and Coleman, R., "Properties of Fiber Reinforced Mortar in Uniaxial Tension," ACI Publication SP-44 : Fiber Reinforced Concrete, 1974, pp. 177-193.

34. Mangat, P., "Tensile Strength of Steel Fiber Reinforced Concrete," Cement and Concrete Research, Vol. 6, No. 2, April, 1976, pp. 245-252.

35. Johnston, C. and Gary, R., "Uniaxial Tensile Testing of Steel Fiber Reinfroced Cementitious Composites," Proceedings, RILEM Symposium on Testing and Test Methods of Fiber Cement Composites (Sheffield), 1978, pp. 451-461.

36. Hughes, B. and Fattuhi, N., "Fiber Reinfroced Concrete Under Direct Tension," Proceedings, ICE Conference on Fiber Reinforced Materials: Design and Engineering Applications (London), March 23-24, 1977, pp. 127-133.

37. Tons, E., Goetz, R. and Razi, M., "Fly Ash as Asphalt Reducer in Bituminous Base Coarses," Project Report, Division of Research Development and Administration, University of Michigan, June, 1983, 61 pp.

38. "The Daracem Advantage," Product Information Brochure, Grace Construction Products, 1986, 6 pp.

39. "Concrete Cylinder Compressometer-Extensometer: Model CT-167," Operation and Service Instructions, Soil Test, In., 1986, 9 pp.

40. Snyder, M. and Lankard, D., "Factors Affecting the Flexural Strength of Steel Fibrous Concrete," ACI Journal, Vol. 69, No. 2, February, 1972, pp. 96-100.

41. Swamy, R., "Steel Fiber Concrete for Bridge Deck and Building Floor Applications," U.S.-Sweden Joint Seminar on Fiber Reinforced Concrete (Stockholm), June 3-5, 1985, pp. 443-478.

42. Shah, S., Stroeven, P., Dalhuisen, D. and Stekelenburg, P., "Complete Stress-Strain Curves for Steel Fiber Reinforced Concrete in Uniaxial Tension and Compression," Proceedings, RILEM Symposium on Testing and Test Methods of Fiber Cement Composites (Sheffield), 1978, pp. 399-408.

43. Robins, P. and Austin, S., "Melt Extract Fiber-A New Impetus for Steel Fiber

Sprayed Concrete," Proceedings, RILEM Symposium on Developments in Fiber Reinforced Cement and Concrete (Sheffield), July 13-17, 1986, Vol. 1, No. 3.7, 8 pp.

44. Sakai, M. and Nakamura, N., "Analysis of Flexural Behavior of Steel Fiber Reinforced Concrete," Proceedings, RILEM Symposium on Developments in Fiber Reinforced Cement and Concrete (Sheffield), July 13-17, 1986, Vol. 1, No. 1.4, 8 pp.

45. Narayanan, R. and Kareem-Palanjian, A., "Factors Influencing the Strength of Steel Fiber Reinforced Concrete," Proceedings, RILEM Symposium on Developments in Fiber Reinforced Cement and Concrete (Sheffield), July 13-17, 1986, Vol. 1, No. 3.1, 8 pp.

46. Hughes, B., "Design of Prestresssed Fiber Reinforced Concrete Beams for Impact," ACI Journal, Vol. 78, No. 4, July-August, 1981, pp. 276-281.

47. Tatro, S., "The Effect of Steel Fibers on the Toughness Properties of Large Aggregate Concrete," M.S. Thesis, Purdue University, December, 1985, 113 pp.

48. Ramakrishnan, V. and Srinivasan, V., "Silica Fume in Fiber Reinforced Concrete," The Indian Concrete Journal, Vol. 56, No. 12, December, 1982, pp. 326-334.

49. Balaguru, P. and Ramakrishnan, V., "Properties of Fiber Reinforced Concrete: Workability, Behavior Under Long-Term Loading, and Air-Void Characteristics," ACI Materials Journal, Vol. 85, No. 3, May-June 1988, pp. 189-196.

50. Balaguru, P. and Ramakrishnan, V., "Freeze-Thaw Durability of Fiber Reinforced Concrete," ACI Journal, Vol. 83, No. 3, May-June 1986, pp. 374-382.

51. Ramakrishnan, V., Coyle, W., Kopac, P. and Parko, T., "Performance Characteristics of Steel Fiber Reinforced Superplasticized Concrete," ACI Publication SP-68: Developments in the Use of Superplasticizers, 1981, pp. 515-534.

52. "Darex Concrete Admixtures: Daravair," Product Information Brochure, Grace Construction Products, 1980, 1 pp.

53. ACI Committee 226, "Use of Fly Ash in Concrete," ACI Materials Journal, Vol. 84, No. 5, September-October 1987, pp. 381-409.

54. Swamy, R., Ali, S. and Theodorakopoulos, D., "Engineering Properties of Concrete Composite Materials Incorporating Fly Ash and Steel Fibers," ACI Publication SP-79: Fly Ash, Silica Fume, Slag and Other Mineral By-Products in Concrete, Vol. 1, 1983, pp. 559-588.

55. Virtanen, J., "Freeze-Thaw Resistance of Concrete Containing Blast-Furnace Slag, Fly Ash or Condensed Silica Fume," ACI Publication SP-79: Fly Ash, Silica Fume, Slag and Other Mineral By-Products in Concrete, Vol. 2, 1983, pp. 923-942.

56. Popovics, S., "Strength Relationships for Fly Ash Concrete," ACI Journal, Vol. 79, No. 1, January-February 1982, pp. 43-49.

57. Bordonado, G. and Nissoux, J., "Road Building Concretes Incorporating Fly Ash or Slag," ACI Publication SP-79: Fly Ash, Silica Fume, Slag and Other Mineral By-Products in Concrete, Vol. 1, 1983, pp. 471-493.

58. ACI Committee 226, "Silica Fume in Concrete," ACI Materials Journal, Vol. 84, No. 2, March-April 1987, pp. 158-166.

59. Mehta, P., "Concrete Structure, Properties and Materials," Prentice-Hall, Inc., 1986, 450 pp.

60. Robins, P. and Austiņs, S., "Bond of Light-Weight Aggregate Concrete Incorporating Condensed Silica Fume," ACI Publication SP-91: Fly Ash, Silica Fume, Slag and Natural Possolans in Concrete, Vol. 2, 1986, pp. 941-948.

61. "Microsilica-Typical Analysis," Product Information Sheets, Elkem

Chemicals, 1984, 2 pp.

62. Swamy, R. and Stavrides, H., "Some Statistical Considerations of Steel Fiber Composites," Cement and Concrete Research, Vol. 6, No. 2, February 1976, pp. 201-216.

63. Taylor, W., "Concrete Technology and Practice," American Elsevier Publishing Company, Inc., 1965, 667 pp.

64. ACI Committee 318, "Building Code Requiremetns for Reinforced Concrete (ACI 318-83)," American Concrete Institute, 1983, 111 pp.

65. Scheaffer, R. and McClave, J., "Statistics for Engineers," Duxbury Press, 1982, 475 pp.

66. Soroushian, P., Ahmadi, P., Navas, F. and Haji, M., "Transfer of Column Pressure to Concrete Footings," Concrete International, Vol. 8, No. 12, December 1986, pp. 38-42.

67. Hawkins, N., "The Bearing Strength of Concrete Loaded Through Rigid Plates," Magazine of Concrete Research, Vol. 20, No. 62, March 1968, pp. 31-40.

68. Chen, W. and Drucker, D., "Bearing Capacity of Concrete Blocks or Rocks,"

ASCE Journal of Engineering Mechanics Division, Vol. 95, No. EM4, August 1969, pp. 955-978.

69. Bortolotti, L., "Double-Punch Test for Tensile and Compressive Strengths in Concrete," ACI Materials Journal, Vol. 85, No. 1, January-February, 1988, pp. 26-32.

70. Hawkins, N., "The Bearing Strength of Concrete Loaded Through Flexible Plates," Magazine of Concrete Research, Vol. 20, No. 63, June 1968, pp. 95-102.

71. Soroushian, P., Obaseki, K. and Rojas, M., "Bearing Strength and Stiffness of Concrete Under Reinforcing Bars," ACI Materials Journal, Vol. 84, No. 3, May-June, 1987, pp. 179-184.

72. Hawkins, N., "The Bearing Strength of Concrete for Strip Loading," Magazine of Concrete Research, Vol. 22, No. 71, June 1970, pp. 87-98.

73. Chen, W. and Carson, J., "Bearing Capacity of Fiber Reinforced Concrete," ACI Publication SP-44: Fiber Reinforced Concrete, 1974, pp. 209-220.

74. Murray, D., Chitnuyanondh, L., Rajub-Agha, K. and Wong, C., "Concrete Plasticity Theory for Biaxial Stress Analysis," ASCE Journal of Engineering Mechanics Division, Vol. 105, No. EM6, December, 1979, pp. 989-1006.

75. Niyogi, S. and Dwarakanathan, G., "Fiber Reinforced Concrete Under Moment and Shear," ASCE Journal of Structural Engineering Division, Vol. 111, ST3, March 1985, pp. 516-527.

76. Jindal, R., "Shear and Moment Capactities of Steel Fiber Reinforced Concrete Beams," ACI Publication SP-81: Fiber Reinforced Concrete, 1984, pp. 1-16.

77. Swamy, R. and Bahia, H., "The Effectiveness of Steel Fibers as Shear Reinforcement," Concrete International Journal, Vol. 7, No. 3, March 1985, pp. 35-40.

78. Batson, G., Jenkins, E. and Spatney, R., "Steel Fibers as Shear Reinforcement in Beams," ACI Journal, Vol. 69, No. 10, October 1972, pp. 640-644.

79. Parameswaran, V., Krishnamoorthy, T., Balasubramanian, K. and Lakshmanan, N., "Behavior of Fiber Reinforced Concrete Beams with Equal Tension and Compression Reinforcement," Proceedings, International Symposium on Fiber Reinforced Concrete, (Madras), December 1987, pp. 1.57-1.67.

80. Walkus, B., Januszkiewicz, A. and Jeruzal, J., "Concrete Composites with Cut Steel Fiber Reinforcement Subjected to Uniaxial Tension," ACI Journal, Vol. 76, No. 10, October 1979, pp. 1079-1092.

81. Laws, V. and Walton, P., "The Tensile-Bending Relationship for Fiber Reinforced Brittle Matrices," Proceedings, RILEM Symposium on Testing and Test Methods of Fiber Cement Composites (Sheffield), 1978, pp. 429-438.

82. Craig, R. Mahadev, S., Patel, C., Viteri, M. and Kertesz, C., "Behavior of Joints Using Reinforced Fibrous Concrete," ACI Publication SP-81: Fiber Reinforced Concrete, 1984, pp. 125-167.

83. Henager, C., "Steel Fibrous Ductile Joint for Seismic-Resistant Structures," ACI Publication SP-53: Reinforced Concrete Structures in Seismic Zones, 1977, pp. 371-386.

84. Filippou, F., Popov, E. and Bertero, V., "Effect of Bond Deterioration on Hysteretic Behavior of Reinforced Concrete Joint," Report No. UBC/EERC-83/19, Earthquake Engineering Research Center, University of California at Berkeley, August 1983, 184 pp.

85. Viwathanatepa, S., Popov, E. and Bertero, V., "Effects of Generalized Loadings on Bond of Reinforcing Bars Embedded in Confined Concrete Blocks," Report No. UBC/EERC-79/22, Earthquake Engineering Research Center, University of California at Berekely, August 1979, 293 pp.

86. Obaseki, K., "Cyclic Dowel Action and Pull-out Behavior of Beam

Reinforcement at Reinforced Concrete Joints," Ph.D. Thesis, Department of Civil and Environmental Engineering, Michigan State University, 1985, 208 pp.

87. Eligehausen, R., Popov, E. and Bertero, V., "Local Bond Stress-Slip Relationships of Deformed Bars Under Generalized Excitations," Report No. UCB/EERC-83/23, Earthquake Engineering Research Center, University of California at Berkeley, October 1983, 169pp.

88. Swamy, R. and Al-Noori, K., "Bond Strength of Steel Fiber Reinforced Concrete," Concrete, Vol. 8, No. 8, August 1974, pp. 36-37.

89. Choi, K., "Anchorage of Beam Reinforcement at Conventional and Fibrous Beam-Column Connections," Ph.D. Dissertation, Department of Civil and Environmental Engineering, Michigan State University, 1988, 174 pp.

90. Gopalaratnam, V. and Shah, S., "Softening Response of Plain Concrete in Direct Tension," ACI Journal, Vol. 82, No. 3, May-June 1985, pp. 310-323.

91. Pakotiprapha, B., Pama, R., and Lee, S., "Mechanical Properties of Cement Mortar with Randomly Oriented Short Steel Wires," Magazine of Concrete Research, Vol. 26, No. 86, March 1974, pp. 3-15.

92. Swamy, R. and Mangat, P., "A Theory for the Flexural Strength of Steel Fiber

Reinforced Concrete," Cement and Concrete Research, Vol. 4, No. 2, 1974, pp. 313-325.

93. Swamy, R. and Al-Taan, S., "Deformation and Ultimate Strength in Flexure of Reinforced Concrete Beams Made with Steel Fiber Concrete," ACI Journal, Vol. 78, No. 5, September-October 1981, pp. 395-405.

94. Swamy, R. and Mangat, P., "The Interfacial Bond Stress in Steel Fiber Reinforced Cement Composites," Cement and Concrete Research, Vol. 6, No. 5, September 1976, pp. 641-650.

95. Henager, C. and Doherty, T., "Analysis of Reinforced Fibrous Concrete Beams," ASCE Journal of Structural Engineering Division, Vol. 102, No. ST1, January 1976, pp. 177-188.

96. Maage, M., "Fiber Bond and Friction in Cement and Concrete," Proceedings, RILEM Symposium on Testing and Test Methods of Fiber Cement Composites (Sheffield), 1978, pp. 329-336.

97. Naaman, A. and Shah, S., "Bond Studies on Oriented and Aligned Steel Fibers," Proceedings, RILEM Symposium on Fiber Reinforced Cement and Concrete (London), Vol. 1, 1975, pp. 171-178.

98. Stroeven, P. Haan, Y., Bouter, C. and Shah, S., "Pull-out Tests of Steel Fibers," Proceedings, RILEM Symposium on Testing and Test Methods of Fiber Cement Composites (Sheffield), 1978, pp. 345-353.

99. Naaman, A. and Shah, S., "Pull-out Mehcanism in Steel Fiber-Reinforced Concrete," ASCE Journal of Structural Engineering Division, Vol. 102, No. ST8, August 1976, pp. 1537-1548.

100. Tattersall, G. and Urbanowicz, C., "Bond Strength in Steel-Fiber-Reinforced Concrete," Magazine of Concrete Research, Vol. 26, No. 87, June 1974, pp. 105-113.

101. Gray, R. and Johnston, C., "The Measurement of Fiber-Matrix Interfacial Bond Strength in Steel Fiber-Reinforced Cementitious Composites," Proceedings, RILEM Symposium on Testing and Test Methods of Fiber Cement Composites (Sheffield), 1978, pp. 317-328.

102. Burakiewicz, A., "Testing of Fiber Bond Strength in Cement Matrix," Proceedings, RILEM Symposium on Testing and Test Methods of Fiber Cement Composites (Sheffield), 1978, pp. 355-365.

103. Hughes, B. and Fattuhi, N., "Fiber Bond Strengths in Cement and Concrete," Magazine of Concrete Research, Vol. 27, No. 92, September 1975, pp. 161-166.

104. Maage, M., "Steel Fiber bond Strengths in Cement Based Matrixes Influenced by Surface Treatments," Cement and Concrete Research, Vol. 7, No. 11, November 1977, pp. 703-710.

105. Rahimi, M. and Kesler, C., "Partially Steel-Fiber Reinforced Mortar," ASCE Journal of Structural Engineering Division, Vol. 105, No. ST1, January 1979, pp. 101-109.

106. Jeng, Y. and Shah, S., "Crack Propagation in Fiber Reinforced Concrete," ASCE Journal of Structural Engineering Division, Vol. 112, No. 1, January, 1986, pp. 19-34.

107. Stang, H. and Shah, S., "Failure of Fiber Reinforced Composites by Pull-Out Fracture," Journal of Material Science, Vol. 21, No. 3, March 1986, pp. 953-957.